TID-7654

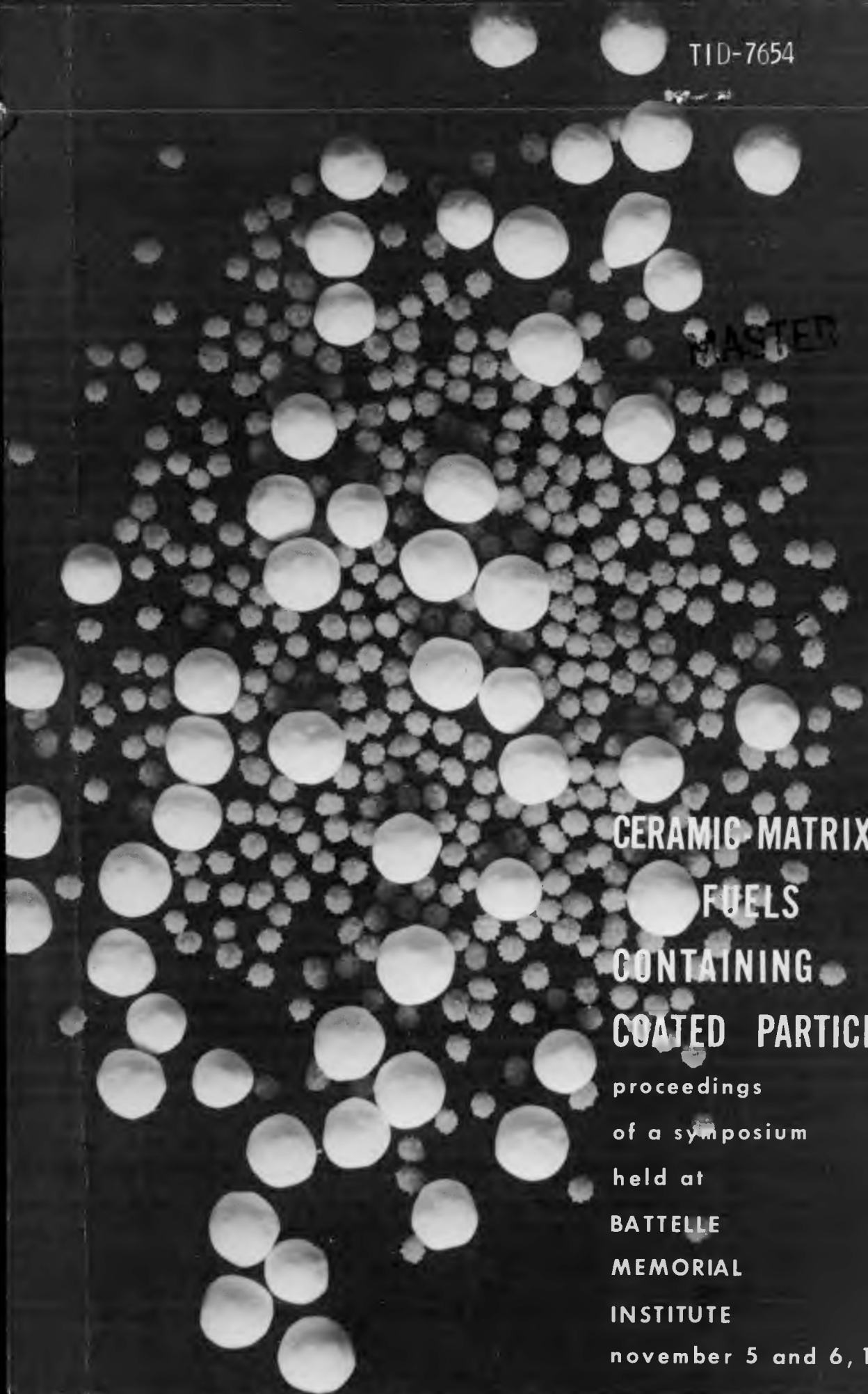

CERAMIC MATRIX FUELS CONTAINING COATED PARTICLES

proceedings
of a symposium
held at
BATTELLE
MEMORIAL
INSTITUTE
november 5 and 6, 1962

LEGAL NOTICE

Printed in USA. Price $6.00. Available from the Office of Technical Services, Department of Commerce, Washington 25, D. C.

USAEC Division of Technical Information Extension, Oak Ridge, Tennessee

CERAMIC-MATRIX FUELS CONTAINING COATED PARTICLES

Proceedings of a Symposium Held at
Battelle Memorial Institute
November 5 and 6, 1962

UNITED STATES ATOMIC ENERGY COMMISSION
DIVISION OF TECHNICAL INFORMATION

FOREWORD

The AEC-sponsored Symposium on Ceramic-Matrix Fuels Containing Coated Particles, held at Battelle on November 5 and 6, 1962, was highly successful. Under the able Chairmanships of Merrill Whitman and Bill Larkin, some 25 scheduled papers, including 10 describing the capabilities of U.S. commercial suppliers in this field, were presented and discussed in the 2-day meeting. Attending were 125 scientific and technical representatives of 38 organizations and six countries actively interested in coated-particle fuels. A substantial volume of good information of wide interest was made available in a very short time.

All available formal presentations at the Symposium are collected here. In the instances where manuscripts were not used by the speakers summaries of the presentations based on notes of attendees are provided. In compiling this collection every effort was made to burst into print as quickly as possible. Editorial and typographical niceties were cold-bloodedly sacrificed for an earlier publication date. No one was allowed any second thoughts. Only the gist of the discussion was recorded.

Our sole task involved getting reproducible copy to the TIS people at Oak Ridge, who very kindly initiated printing operations immediately. As a consequence, workers in this field may expect to find this volume a document of more than merely historical interest. Adding to this interest is a bibliography at the end which includes every reference on ceramic coated particles which could be located in the standard sources of information on atomic-energy literature, or could be supplied by workers in this field.

Organizing this symposium was no small task, and its success was due to the talented assistance of many individuals. R. F. Kirkpatrick, M. J. Whitman, and J. Conner, of the Division of Reactor Development, Atomic Energy Commission, initiated the concept of the Symposium and directed its planning. Many of the Battelle staff lent valuable assistance in arranging features of the Symposium, especially A. W. Hare and C. A. Snavely. The success of the conference was due in large measure to the assistance of these and many other people, and their help is gratefully acknowledged. Above all, however, the conference was successful because of the high technical quality of the papers and the subsequent discussions.

R. W. Dayton
J. H. Oxley
C. W. Townley

ABBREVIATIONS FOR ORGANIZATIONS REPRESENTED

AAEC	Australian Atomic Energy Commission
AC	Allis-Chalmers Manufacturing Company
AGN	Aerojet-General Nucleonics, General Tire and Rubber Company
AMP	American Metal Products Company, Research Division
ANL	Argonne National Laboratory
BBK	Brown Boveri/Krupp Reaktorbau G.m.b.H.
BMI	Battelle Memorial Institute
BNL	Brookhaven National Laboratory
BrEm	British Embassy, Washington, D. C.
CE	Combustion Engineering, Inc., Nuclear Division
DAC	Diamond Alkali Company
Dav	W. R. Grace & Co., Davison Chemical Division
DrgP	Dragon Project, O.E.C.D. High Temperature Reactor Project
GA	General Atomic Division, General Dynamics Corporation
GEAPD	General Electric Company, Atomic Products Division
HAPO	General Electric Company, Hanford Atomic Products Operation
LASL	Los Alamos Scientific Laboratory
LRC	Lewis Research Center, Space Nuclear Propulsion Office
M&C	Metals and Controls Inc., Division of Texas Instruments, Inc.
ML	Mound Laboratory, Monsanto Research Corporation
MMM	Minnesota Mining and Manufacturing Co.
MND	The Martin Co., Nuclear Division
Mtsb	Mitsubishi Metal Mining Co., Ltd.
NCC	National Carbon Company, Union Carbide Corporation
Nkm	Nukem, Nuklear-Chemie und -Metallurgie G.m.b.H.
NMPO	General Electric Nuclear Materials and Propulsion Operation
NpnC	Nippon Carbon Co., Ltd.
NUMEC	Nuclear Materials and Equipment Corporation
ORNL	Oak Ridge National Laboratory
Ray	Raytheon Company, Research Division
SpC	Speer Carbon Company
UCN	Union Carbide Nuclear Company, Division of Union Carbide Corporation
UKAEA	United Kingdom Atomic Energy Authority
UNC	United Nuclear Corporation, Chemicals Division
USAEC	United States Atomic Energy Commission
WAFD	Westinghouse Electric Corporation, Atomic Fuel Division
WAL	Westinghouse Electric Corporation, Astronuclear Laboratory
WRG	W. R. Grace & Company, Research Division

NAMES OF ATTENDEES

BMI	ALEXANDER, Dr. C. A.
AAEC	BAILLIE, Mr. M. G.
LASL	BARD, Dr. R. J.
BMI	BARNES, Mr. R. H.
MND	BARR, Mr. H. N.
ANL	BEALS, Dr. R. J.
DrgP	BEUTLER, Mr. H.
BMI	BLOCHER, Dr. J. M.
WAL	BOLTAX, Dr. A.
BMI	BROCKWAY, Mr. M. C.
NMPO	BROWNE, Dr. C. C.
BMI	BROWNING, Mr. M. F.
WAFD	BRYANT, Mr. W. A.
BMI	BURIAN, Mr. R. J.
ORNL	CARLSEN, Mr. F. L.
BMI	CARLSON, Mr. R. J.
BMI	CARMICHAEL, Mr. D. C.
BMI	CHASTAIN, Mr. J. W.
CE	CHERNOCK, Mr. W. P.
BMI	CLEGG, Dr. J. W.
ORNL	COOBS, Mr. J. H.
BMI	CUNNINGHAM, Dr. G. W.
BMI	DAYTON, Dr. R. W.
BMI	DEEM, Mr. H. W.
BMI	DICKERSON, Mr. R. F.
BMI	DINGEE, Mr. D. A.
BMI	DUCKWORTH, Mr. W. H.
BMI	EPSTEIN, Mr. H. M.
BMI	FACKELMANN, Mr. J. M.
BMI	FARKAS, Mr. M. S.
BMI	FAWCETT, Dr. S. L.
USAEC	FELDMAN, Mr. B. C.
WRG	FITCH, Dr. F. T.
M&C	FLANDERS, Mr. R. B.
BMI	FOSTER, Mr. E. L.
AGN	FUNK, Mr. C. W.
BMI	GATES, Mr. J. E.
GA	GOEDDEL, Mr. W. V.
BMI	GOLDTHWAITE, Mr. W. H.
DrgP	GOUGH, Mr. J. R. C.
UKAEA	GREENOUGH, Dr. G. B.
BNL	GURINSKY, Dr. D. H.
UCN	HAMRIN, Mr. C. E.
BMI	HARE, Mr. A. W.
ORNL	HARMS, Dr. W. O.
BMI	HODGE, Mr. E. S.
AMP	JAMESON, Mr. T. A.
BMI	KELLER, Mr. D. L.
USAEC	KIRKPATRICK, Mr. R. F.
BMI	KIZER, Mr. D. E.
BMI	KNORR, Dr. T. G.
UNC	KUHLMAN, Mr. C. W.
USAEC	LARKIN, Mr. W. J.
NMPO	LATTA, Mr. R. E.
Ray	LEPIE, Dr. M. P.
ANL	LEVITZ, Mr. N. M.
BMI	LEVY, Mr. A.
USAEC	LOSCALZO, Mr. J. J.
BMI	LUCKS, Mr. C. F.
LASL	LYON, Mr. L. L., Jr.
UCN	McWHORTER, Mr. W. C.
ORNL	MANLY, Mr. W. D.
UCN	MARROW, Mr. G. B.
NpnC	MASUYAMA, Mr. T.
GA	MATHESON, Dr. A. R.
BMI	MILLER, Mr. N. E.
BMI	MORRISON, Dr. D. L.
UKAEA	MURRAY, Dr. P.
NpnC	NAGAOKI, Mr. T.
GEAPD	OGAWA, Mr. S. Y.
AC	O'LEARY, Dr. W. J.
BMI	OXLEY, Dr. J. H.
USAEC	PAHLER, Mr. R. E.
BMI	PAPROCKI, Mr. S. J.
BMI	PARDUE, Mr. W. M.
SpC	PARKER, Dr. W. E.
NUMEC	PEPKOWITZ, Dr. L. P.
DAC	PERRIN, Dr. T. S.
BMI	POREMBKA, Mr. S. W.
BMI	RAINES, Mr. G. E.
NCC	REUTER, Mr. R. A.
BMI	RHODES, Mr. D. E.
BMI	RITZMAN, Dr. R. L.
BMI	ROSENBERG, Mr. H. S.
ORNL	ROSENTHAL, Dr. M. W.
BMI	ROUGH, Mr. F. A.
BMI	RUSSELL, Dr. H. W.
WRG	SANCHEZ, Dr. M. G.
DrgP	SAUNDERS, Mr. R. A.
UKAEA	SAVAGE, Dr. D. W.
Nkm	SCHÄFER, Dr. L. F.
BMI	SECREST, Mr. A. C.
BMI	SECREST, Mrs. V. S.
DrgP	SHEPHERD, Dr. L. R.
BMI	SHERWOOD, Dr. E. M.
Dav	SHORT, Mr. L. E.
BMI	SMALLEY, Mr. A. K.
BMI	SNAVELY, Dr. C. A.
MMM	SOWMAN, Dr. H. G.
BMI	STANG, Mr. J. H.
BrEm	STEPHENSON, Mr. J.
NCC	STOUGHTON, Mr. L. D.
BMI	SUNDERMAN, Dr. D. N.
Mtsb	SUZUKI, Mr. T.
UKAEA	TAYLOR, Dr. H. A.
WAL	THEIS, Mr. D. E.
LRC	THIELKE, Mr. N. R.
BMI	THOMAS, Dr. B. D.
WAL	THOMAS, Dr. D. E.
AGN	TITUS, Mr. G. W.
BMI	TOWNLEY, Dr. C. W.
ML	TUCKER, Mr. P. A.
AAEC	TURNER, Mr. K. S.
BMI	VAUGHAN, Mr. D. A.
BMI	VEIGEL, Mr. N. D.
BBK	von der DECKEN, Dr. C. B.
UKAEA	WAINE, Mr. P.
ORNL	WATSON, Mr. G. M.
USAEC	WHITMAN, Mr. M. J.
AC	WICK, Mr. E. A.
BMI	WILSON, Mr. W. J.
HAPO	YOSHIKAWA, Dr. H. H.
BMI	ZIELENBACH, Mr. W. J.
GA	ZUMWALT, Dr. L. R.

TABLE OF CONTENTS

TABLE OF CONTENTS
(Continued)

Third Session, November 6, 1962
PROGRAMS UNDER WAY IN OTHER COUNTRIES
Chairman: W. J. Larkin, USAEC

TABLE OF CONTENTS
(Continued)

GCR

COATED-PARTICLE FUELS FOR CIVILIAN GAS-COOLED REACTORS

By R. E. Pahler

Division of Reactor Development
United States Atomic Energy Commission

I appreciate this opportunity to discuss the AEC's program on coated-particle fuel and the various applications we consider interesting for this fuel in gas-cooled reactors.

Ceramic coated-particle fuels have been of great interest for use in the gas-cooled reactor program since initial irradiations of Al_2O_3-coated UO_2 particles were made in 1960 as part of the Sanderson & Porter-Battelle Memorial Institute program on pebble-bed reactor fuel development. Shortly thereafter, the General Atomic-AEC research and development program for the Peach Bottom HTGR and the gas-cooled reactor development program at Oak Ridge National Laboratory began major investigations of ceramic coated-particle fuels. The Battelle program was subsequently broadened to include a basic investigation of ceramic coated fuels for gas-cooled and possibly superheat applications. These three organizations currently conduct the main AEC-sponsored development efforts on this fuel. Work being done at each of these sites will be fully described during this meeting. This AEC-sponsored effort has been supplemented by commercial fuel suppliers who have manufactured fuel samples for AEC testing.

As the versatility and capability of coated-particle fuel have been demonstrated in capsule and loop tests, our interest has grown until the majority of our fuel development work for civilian gas-cooled reactors is now concentrated on this fuel type. The ultimate objective in the AEC's civilian gas-cooled reactor program is the development of high-temperature, high-conversion-ratio systems with long fuel lifetimes. In these characteristics, coated particles are unexcelled as fuel material for gas-cooled reactors.

Gas-cooled reactors have advantages and limitations different from our more fully developed saturated-water systems and therefore are a very complimentary system for future development. This is illustrated in Chart 1.

A very basic difference is the outlet coolant temperature as shown on the first graph. Water reactors are currently limited to a modest top temperature of 600 F with increases up to about 1000 F possible with nuclear superheat. Certain gas-cooled reactor types are currently capable of 1400 F, and by modifications to the fuel design, while remaining with the same basic materials, coolant temperatures in the 2000 F range appear feasible. These two distinctly different temperature ranges do, of course, broaden the possible applications of nuclear power, and each type of reactor system should receive fresh consideration as to its best application.

A second difference is fuel burnup capability and fuel fabrication cost as shown in the second graph. Coated-particle gas-cooled reactor fuel has the fortunate combination of very good irradiation stability and near unity conversion ratio on U-Th fuel, because of the fuel's excellent nuclear properties. This means that reactivity is maintained for the very high burnup that the fuel is metallurgically capable of reaching. This long fuel-lifetime advantage of coated-particle fuel is partially counterbalanced by high fabrication costs which, at present, are quite uncertain. The burnup-fabrication cost characteristic however imposes limitations on some gas reactor types. For example, reactors which have a low converstion ratio, such as small plants with high neutron leakage, or plants operated on a U-Pu fuel cycle, cannot maintain reactivity for long burnup and therefore cannot spread the high fuel fabrication cost over as many kwhr.

The third major area of comparison is size-range capability as shown in the third graph. Water reactors are relatively simple, have small neutron leakage, and, therefore, even in small plant sizes, are practical for certain applications. There is, of course, the pressure-vessel problem, which limits the upper size to approximately 500 MW(e) per unit for a shop-fabricated vessel. By comparison, graphite fueled, gas-cooled reactors in small size units pay a severe penalty in neutron leakage and capital costs. However, very large plants are practical because the pressure vessels can be readily field fabricated from unclad carbon steel of moderate thickness, and thus can be scaled up to almost any desired size. For example, if a coated-particle fuel element core with its relatively high power density were fitted into the 60 to 70 ft pressure vessels now being built in England for their natural uranium plants, the output of such a reactor would be several million killowatts electric.

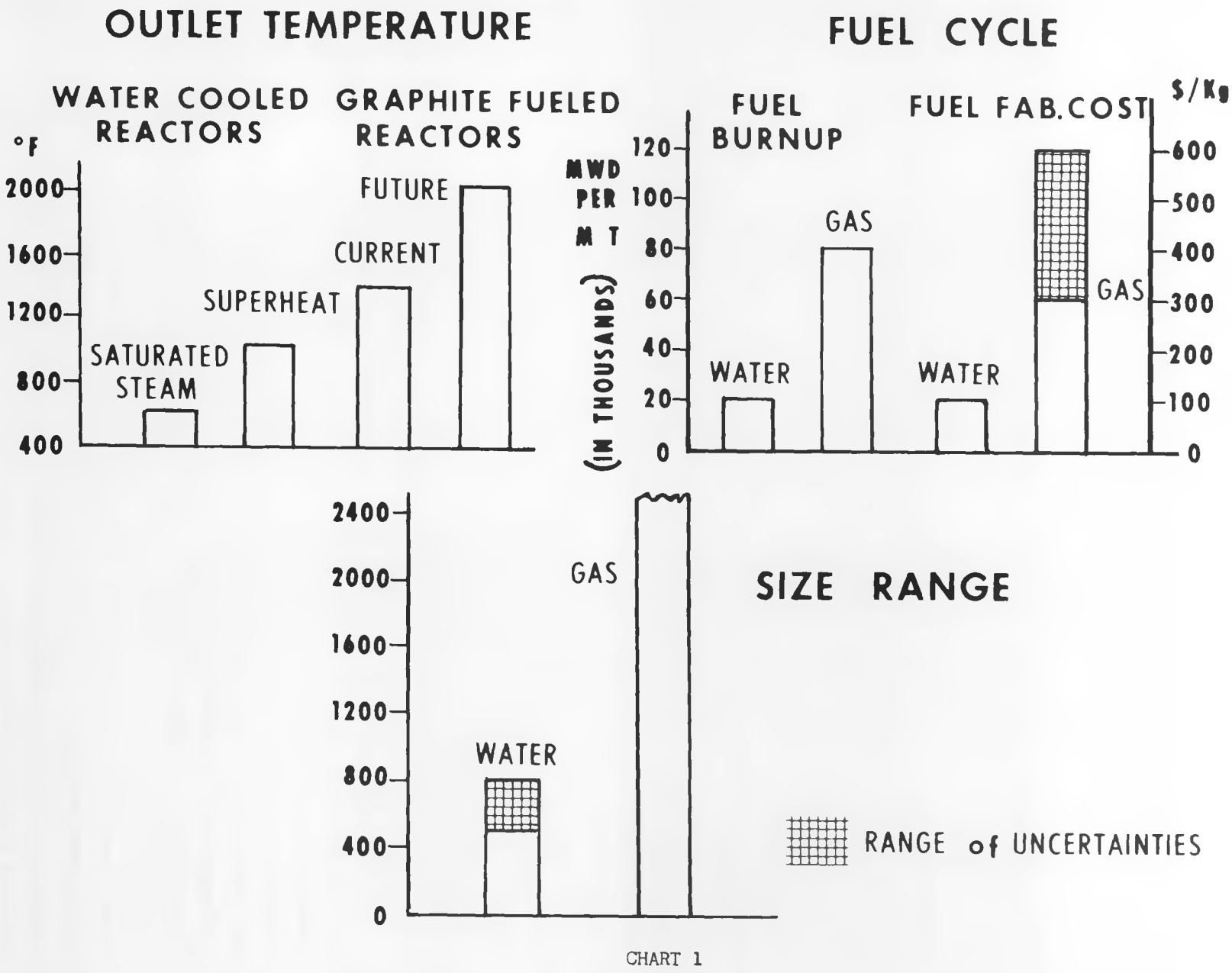
OUTLET TEMPERATURE
WATER COOLED REACTORS
GRAPHITE FUELED REACTORS
°F
2000
1600
1200
800
400
SATURATED STEAM
SUPERHEAT
CURRENT
FUTURE
FUEL CYCLE
FUEL BURNUP
FUEL FAB. COST
$/Kg
MWD PER M T (IN THOUSANDS)
120
100
80
60
40
20
0
600
500
400
300
200
100
0
WATER
GAS
WATER
GAS
SIZE RANGE
2400
2000
1600
1200
800
400
0
WATER
GAS
RANGE of UNCERTAINTIES

CHART 1

I would now like to discuss some of the possible applications for the unique characteristics of gas-cooled reactors using coated-particle fuel. Chart 2 illustrates what is expected to be the natural evolution of high-efficiency gas-steam cycle power plants. The first schematic illustrates a "first generation" plant which would utilize a modern high-temperature, high-pressure reheat steam system and electric or steam-driven circulators. The second schematic illustrates a similar reactor and steam plant but utilizes a gas turbine driving a gas circulator. In this scheme, the substantial electric power normally required for motor-driven gas circulators would be available for distribution, resulting in higher net efficiency and lower cost per electrical kilowatt. The last schematic illustrates the effect of increasing the gas temperature up to the limit of the fuel elements or turbine blading. The energy output of the turbine would be substantially greater than that required to operate the compressor so electric energy could be generated by the gas turbine in addition to that generated by the steam plant.

We expect a straightforward evolution of the gas-cooled reactor concept, along the lines illustrated, to permit steady, long-term improvement in plant efficiency and power cost until the full potential and capability of coated-particle fuel is realized. The present plant designs are merely the beginning.

Other applications for coated-particle fuel and the gas-cooled reactor system are shown on Chart 3. The first application illustrated is the straight gas-turbine, Brayton-cycle power plant. It, of course, has a lower net plant efficiency than the previously described combined cycles, but it has the virtue of greater simplicity which could result in lower capital cost. The Brayton cycle also can have a high temperature rise in the heat-rejection fluid unlike the steam cycle which is designed for a low ΔT in the heat-rejection fluid unlike the steam cycle which is designed for a low ΔT in the condenser cooling water. Thus air cooling or water cooling with a high ΔT (which reduces the required flow) is practical. The Brayton-cycle system would be especially attractive in areas where cooling water is at a premium. With our projected power-requirement growth curve, cooling-water problems in highly industrialized areas are certain to increase in the future.

Another possible application is a plant for the production of electricity and high-temperature process steam. In this application, steam is generated to modern conditions and fed to a standard turbogenerator. However, the reheat steam is heated to 1500 to 2000 F for use as process heat instead

EVOLUTION OF GAS - STEAM CYCLE POWER PLANTS

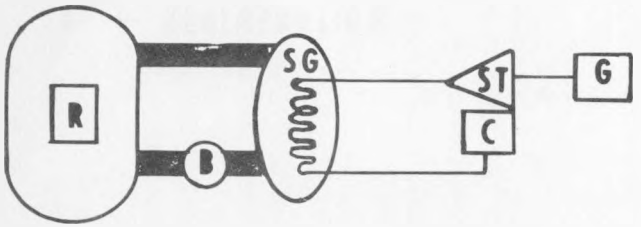

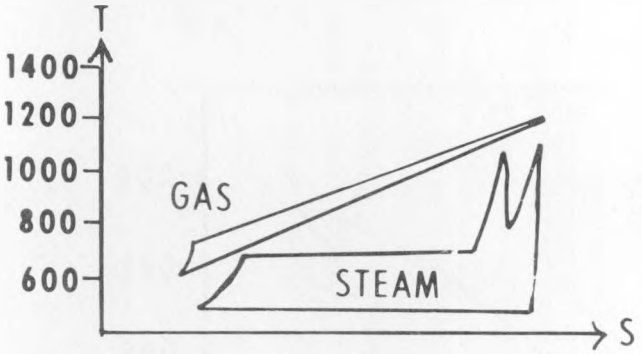

$\eta = 42\%$

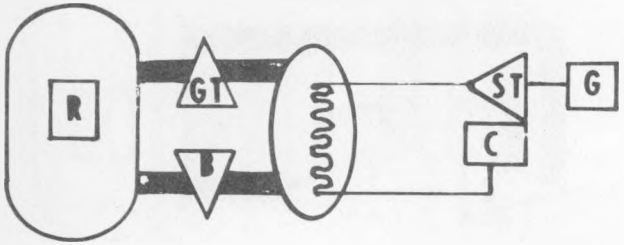

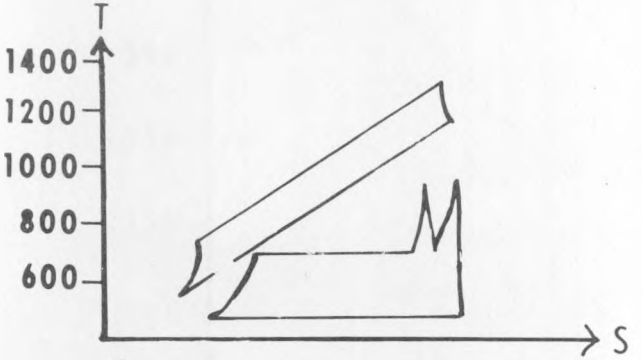

$\eta = 45\%$

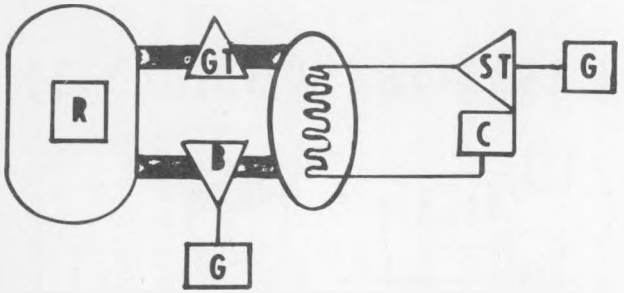

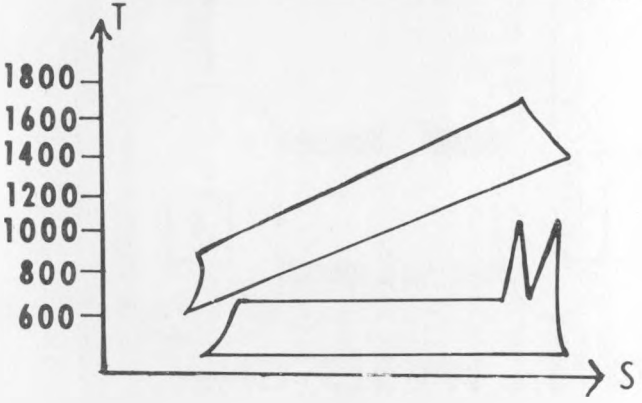

$\eta = 50\%$

SG – STEAM GENERATOR
ST – STEAM TURBINE
G – GENERATOR
C – CONDENSER
B – BLOWER
GT – GAS TURBINE

CHART 2

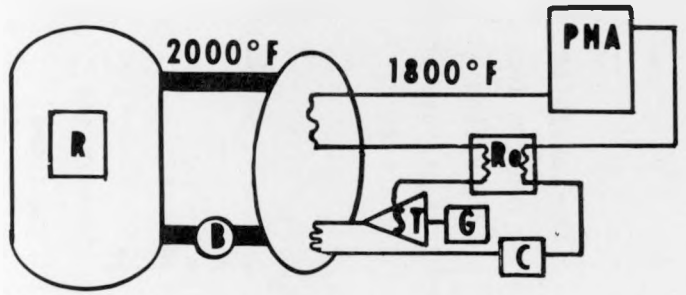

ELECTRICITY–PROCESS HEAT

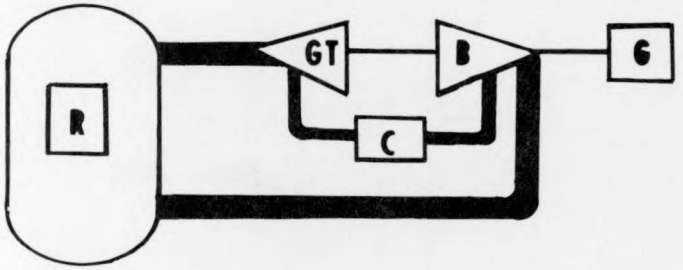

BRAYTON CYCLE

MHD–STEAM PLANT

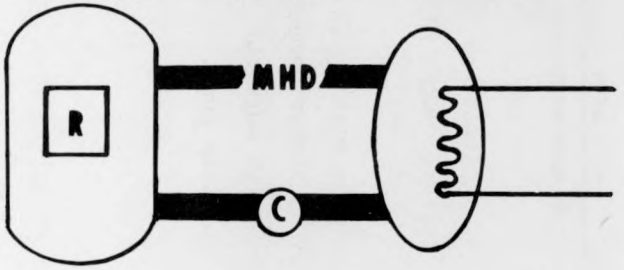

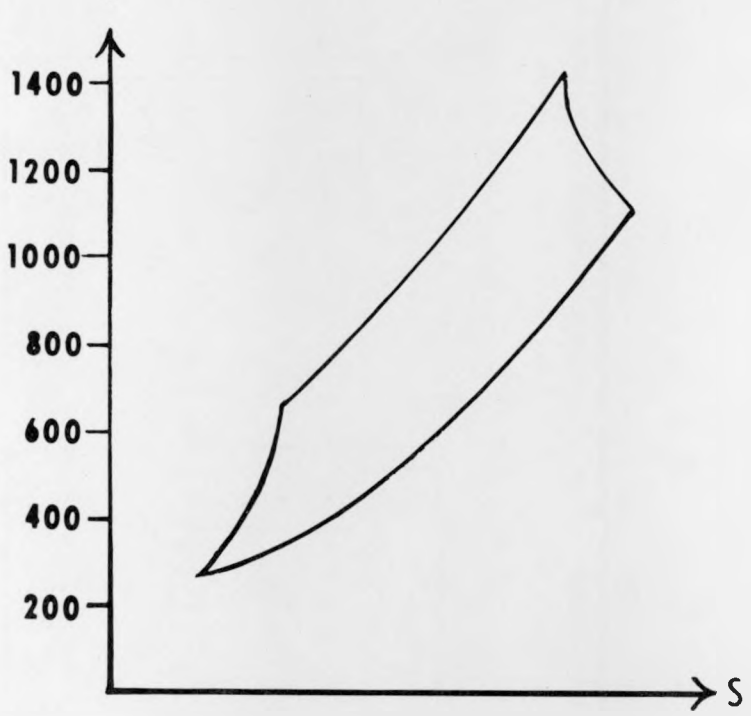

Re — REGENERATION
MHD — MAGNETOHYDRODYNAMIC PHA—PROCESS HEAT APPLICATION

of the normal 1000 F for return to the turbine. It is practical to generate these high steam temperatures because the steam and reactor-coolant pressures are balanced (about 300-500 psi) resulting in minimum stress on the very hot heat exchanger tubes. This is a situation in which a nuclear plant can produce energy in a form that would be difficult if not impossible to duplicate with conventional equipment. Various applications for high-temperature process heat could be considered, including coal gasification.

The final application is a magnetohydrodynamic-steam turbine plant. This is a step beyond a gas-steam turbine power plant because of the higher temperature requirements, but if recent theories on nonthermal ionization work out, this concept may be within the temperature capability of coated-particle fuel.

In addition to the new power-plant concepts made feasible by coated-particle fuel, new fuel-element designs have also evolved. These fuel-element designs are illustrated in Chart 4. The fuel concepts most fully developed are the standard vented fuel with a separate graphite can, as used in the Peach Bottom HTGR plant, and the nonvented design such as would be used in a pebble-bed reactor. Other possibilities are coextrusion of the fuel matrix and outer sleeve. Coextrusion would eliminate the gap between matrix and can and eliminate the substantial temperature drop involved. This coextrusion design might also be cheaper to fabricate.

The "composite" fuel design suggests that other materials might be used in the fuel elements if their nuclear properties were suitable. One possibility is BeO, which has a desirable n-2n reaction and which would reduce neutron leakage. Coextruded and composite fuel-element designs in the vented configuration use a relatively permeable graphite which permits the helium coolant to diffuse to the lower pressure zone in the center of the element and thus restrict back diffusion of fission gases into the bulk coolant.

The final illustration suggests the use of coated-particle fuel in an "advanced EGCR" type reactor. This heterogeneous core could use flat plates of graphite containing coated-particle fuel and be located inside the fuel sleeves.

Many of the ideas presented here require substantial advancement in reactor componentry, but the key requirement for advanced applications—that is, a practical, high-temperature fuel--appears to be obtainable with the coated-particle fuel concept. The irradiation program has demonstrated acceptable fission-product-retention characteristics in the 1500 to 2700 F temperature range, and some irradiations have already been successfully carried to over 100,000 MWD/ton. Commercial coated-particle fuel fabrication plants have been constructed. The basic feasibility and practicality of gas-

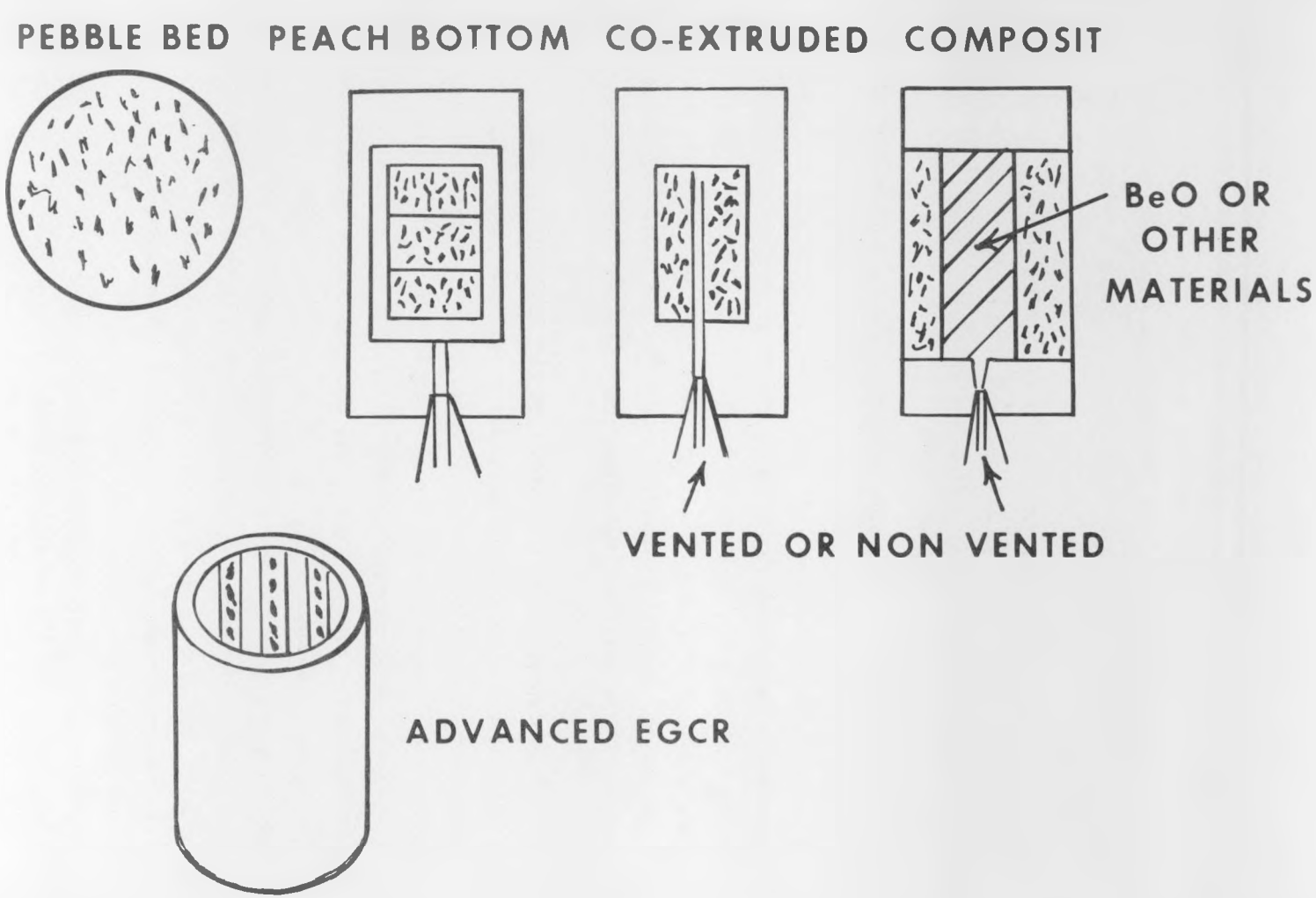
PEBBLE BED
PEACH BOTTOM
CO-EXTRUDED COMPOSIT
BeO OR
OTHER
MATERIALS
VENTED OR NON VENTED
ADVANCED EGCR
UNFUELED GRAPHITE
COATED PARTICLES
IN GRAPHITE

CHART 4

cooled reactors have been demonstrated by the large United Kingdom and French programs, and the US's helium-cooled EGCR and HTGR are well in the construction phases.

We would welcome ideas for commercial exploitation of the substantial technical and industrial base which has been developed. Certainly what has been mentioned in this paper is not the limit of the possibilities. I would welcome the opportunity to discuss any additional thoughts you may have.

We have a basic development program at Hanford and ORNL which specializes in in-pile tests of fuels and materials, and we attempt to direct this work to the areas of greatest interest and need. Those industrial organizations interested in the commercial application of coated-particle fuel in gas-cooled reactors should make their requirements known, and we will take them into consideration in planning our program.

BATTELLE STUDIES OF CERAMIC-COATED PARTICLE FUELS*

By R. W. Dayton, J. H. Oxley, and C. W. Townley

Battelle Memorial Institute
Columbus 1, Ohio

INTRODUCTION

Fission-product retention has been difficult to achieve for otherwise optimum gas-cooled reactor fuel materials. The reason is that ceramic materials, which normally would be preferred, are usually permeable and allow excessive amounts of volatile fission products to escape. Attempts to solve this problem by using impermeable ceramic coatings on ceramic fuel elements have been unsuccessful because the coatings crack owing to thermal or other stress, and the fuel then releases essentially as large a quantity of fission products as uncoated fuel. While metal jacketing can be used to retain fission products, its use usually sets an undesirably low limit to allowable reactor operating temperature, places stringent requirements on the coolant composition, and degrades the neutron economy of the reactor.

A new type of ceramic fuel which solved the problem of cracking from thermal stress was tested in a radiation experiment a few years ago at Battelle as one part of the Sanderson & Porter Pebble-Bed Reactor project. This fuel material consisted of spherical UO_2 particles 100 to 140 μ in diameter clad by a vapor-phase method with a 40-μ layer of impermeable alumina. These fuel particles were dispersed in graphite matrix and fabricated into a ball about 1-1/2 in. in diameter by the National Carbon Company.

Irradiation was carried on in a core position of the Battelle reactor for several months, at temperatures in the range of 950 to 1350 F. Fission-product loss was determined at intervals throughout the run with the results shown in Figure 1. As can be seen in this graph, fission-product retention was initially excellent, the rate of release of fission gases being less than 1 ppm of the rate of production. (This ratio is called R/B.) Performance deteriorated somewhat at the test proceeded as a consequence of cracking of some of the coatings. At 1 per cent burnup, R/B for the fission gas had increased to only 0.1 to 10 ppm, so only a small fraction of the particles contained in the graphite ball could have been cracked. Cracking continued as the run proceeded, until at the end about 10 per cent of the particle coatings had cracked. Photomicrographs of cracked and uncracked coatings at the end of the run are shown in Figures 2 and 3.

Even at the end of the run, the loss of fission products was not really extreme, being 100 ppm or less for all isotopes except xenon-133. This degree of fission-product retention is far better than can be obtained from a graphite-matrix fuel containing uncoated fuel particles, for which releases of 10 to 50 per cent of the fission gases have been observed.

This experiment created great interest in coated-particle fuels because it seemed likely that good fission-product retention, far better than that demonstrated in this first test, might be achieved. This optimism was justifiable because most fission-gas release is caused by cracking of the particle coatings, and such cracking is not

*Work performed under Contract W-7405-eng-92.

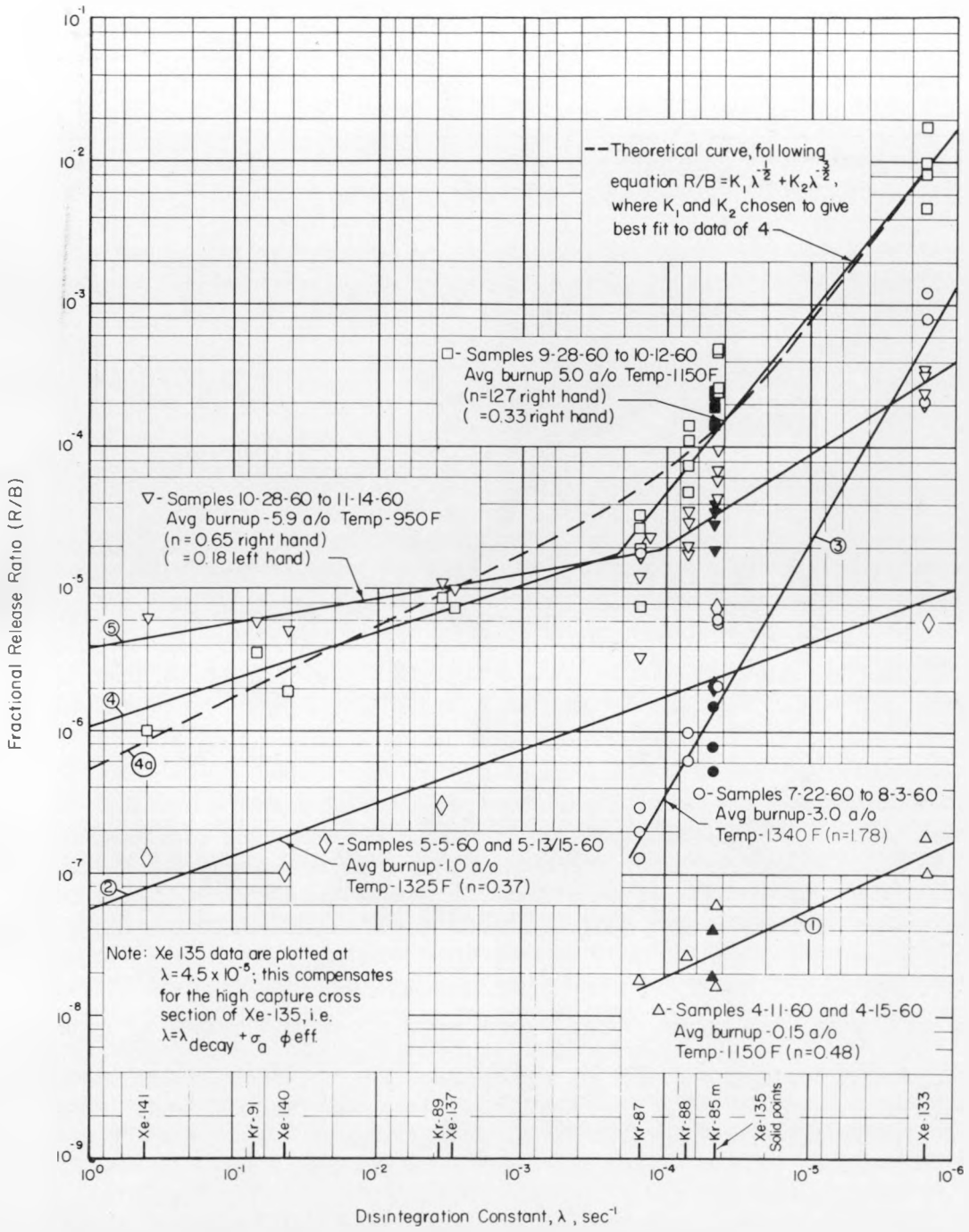

FIGURE 1. FISSION-GAS-RELEASE CHARACTERISTICS OF COATED-PARTICLE FUEL

Note: The straight lines follow the relation $R/B = K\lambda^{-n}$. The experimental values for "n" are given in the curve descriptions.

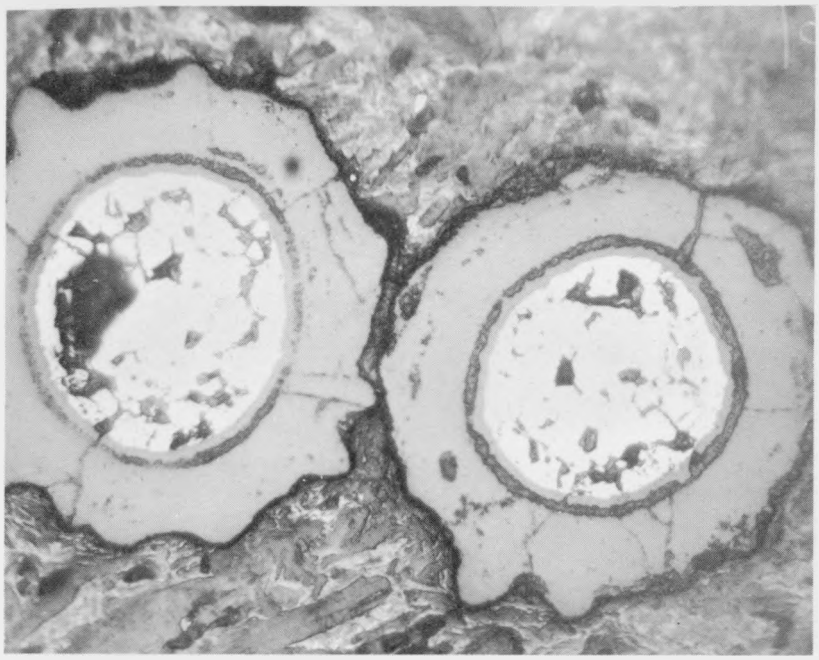

250X HC6768

FIGURE 2. TYPICAL IRRADIATED PARTICLES WITH CRACKED COATINGS EXAMINED IN SITU IN GRAPHITE

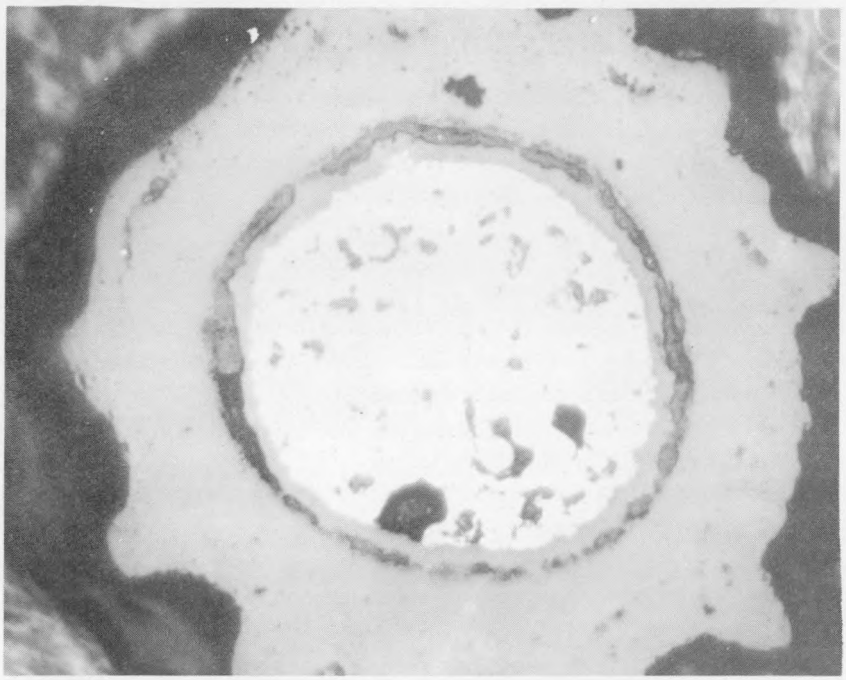

500X HC6770

FIGURE 3. TYPICAL IRRADIATED PARTICLE WITH INTACT COATING EXAMINED IN SITU IN GRAPHITE

Particles examined after separation from the graphite matrix were similar in appearance.

inevitable since 90 per cent of the coatings did not crack in this first test. Interest in this fuel material was heightened because it seemed probable that good retention of fission products could be achieved without compromising either the high-temperature capability of gas-cooled reactors through the use of metal cladding or degrading their good neutron economy through the use of materials having a high neutron capture cross section.

SCOPE OF BATTELLE RESEARCH PROGRAM ON COATED-PARTICLE FUEL MATERIALS

Owing to the potential of these materials, a number of investigations of ceramic coated-particle fuel materials were authorized by the AEC; the Battelle study is one of these. This Battelle study is a general one, unrelated to any specific gas-cooled reactor project. A wide variety of materials, under a considerable range of experimental conditions, are being examined in an effort to realize the full potential of coated-particle fuels through identifying the factors which limit their usefulness and learning how to design and fabricate them in the best way.

There are three major parts of the Battelle program:

(1) A materials-selection program, in which materials are chosen for more extensive study on the basis of an evaluation of those of their properties that affect fission-gas retention

(2) A materials-fabrication program, in which coated particles, and dispersions of these in a ceramic matrix, are fabricated so as to have desired characteristics

(3) A radiation program, in which the best materials are irradiated, under conditions like those of service, to determine when failures occur, and why.

The work in each of these three programs is discussed in this paper.

MATERIALS-SELECTION PROGRAM

The fission-product retention of coated-particle fuel materials is the focus of attention of the Battelle program. The goal of this program is the development of all-ceramic fuel materials which will retain fission products nearly completely (R/B of 1 ppm or less) to high burnup of the fuel, can be operated at high temperature, and have a low neutron-absorption cross section.

Some of the characteristics of the fuel materials which affect fission-product retention are controlled by the manner of making the materials. Thus, impermeable coatings are required, and this property is controlled by the conditions of coating.

Coatings may be cracked in fabricating a ceramic dispersion, so it is important to learn now to make dispersions while minimizing this difficulty. Coatings may crack in use from internal fission-gas pressure if they are weak or have too little internal void space for fission-gas accumulation. They may be prevented from cracking if support from the matrix can be provided. These characteristics, too, are controlled by the fabrication process.

Other characteristics of the fuel materials which affect not only fission-product retention but also maximum operating temperature and neutron economy are controlled by the selection of the coating material. The important properties of coating materials for use in gas-cooled reactors, and consequently those which have been made the basis for selecting materials for thorough study, are the following:

(1) Neutron-absorption cross section below 1 barn

(2) Melting point over 2000 C

(3) Low fission-gas-diffusion rates

(4) Resistance to radiation damage

(5) Chemical inertness against solid-solid and solid-gas phase reactions.

Neutron-Absorption and Melting-Point Criteria

The first requirement eliminates three-quarters of the elements from consideration, the second eliminates compounds made from the metallic elements bismuth, lead, rubidium, sodium, and tin and from the nonmetallic elements fluorine, phosphorus, and sulfur. As a result of this process of elimination*, it is found that only the eight ceramic coating materials listed in Table 1 need to be considered in an experimental study.

The three uranium fuel materials given in Table 1 appear to be the best ones for fuel particles; it might be noted that the equivalent thorium and plutonium compounds have somewhat similar and useful properties. Also given in Table 1 are some of the properties of the coating materials which are significant for their use in coated-particle fuel materials.

These eight coating materials and three fuel materials are the ones most suitable for coated-particle fuels from the standpoints of neutron economy and melting point, and therefore are the ones being studied experimentally to determine their suitability in other respects. The results of studies of some of their other pertinent properties are given in the following sections.

---

*CaO has been eliminated because it is not a good ceramic material, and CeO_2 has been eliminated because it is too readily reduced to Ce_2O_3.

TABLE 1. REPRESENTATIVE PROPERTIES OF POTENTIALLY USEFUL COATED-PARTICLE MATERIALS

Material	Macroscopic Neutron Absorption Cross Section, cm^{-1}	Melting Point, C	Crystal Structure	Thermal Conductivity, w/(cm)(C)	Thermal Expansivity, 10^{-6} per C	Youngs Modulus, 10^6 psi
			Coatings			
C[a]	0.36×10^{-3}	3650 (sublimes)	Hexagonal (turbostratic)[a]	a: 4.3; c: 0.031 (0C) 2.9; 0.012 (500 C) 1.8; 0.008 (1000 C) 0.8; 0.004 (2000 C)	a: -1.5; c: -- (0-100 C) a: 1.8; c: 24 (100-1000 C)	a = 3-4
BeO	0.74×10^{-3}	2547	Hexagonal (zincite)	2.6 (100 C)[b] 0.21 (1000 C) 0.14 (2000 C)	8.8 (α_a 9-12% > α_c)	56
Be_2C	1.1×10^{-3}	2150 (dissociates)	Cubic (antifluorite)	0.09 (0 C)[b] 0.16 (500 C) 0.24 (1000 C)	10.5 (25-600 C)	22
MgO	3.4×10^{-3}	2800	Cubic (NaCl)	0.46 (0 C)[b] 0.066 (1000 C) 0.14 (2000 C)	13.8 (0-1000 C) 15.7 (0-1500 C)	30
ZrO_2[c]	5.5×10^{-3}[c]	2715	Cubic (fluorite)	0.016 (0 C) 0.020 (1000 C) 0.023 (1500 C)	7.5 (0-1000 C) 20 (0-2000 C)	24
SiC	6.4×10^{-3}	2200 (dissociates)	Hexagonal	1.21 (500 C)[d] 0.49 (1000 C) 0.14 (1500 C)	4.8 (0-1000 C) 10.2 (0-1800 C)	68.5
ZrC	7.2×10^{-3}	3530	Cubic (NaCl)	0.25 (0 C) 0.42 (2000 C)	6.7 (20-600 C)	
Al_2O_3	11×10^{-3}	2035	Rhombohedral (oxygen ions nearly HCP)	0.39 (0 C) 0.11 (500 C) 0.06 (1000 C) 0.09 (2000 C)	a: 7.1; c: 6.0 (100 C) a: 9.7; c: 8.9 (500 C) a: 14.2; c: 13.8 (1000 C)	60
			Fuels			
UO_2	190×10^{-3}[e]	2760	Cubic (fluorite)	0.090 (100 C) 0.028 (1000 C) 0.025 (2000 C) 0.040 (2800 C)	10.0 (0-1000 C) 17.2 (0-2000 C) 25.4 (0-2800 C)	27
UC	250×10^{-3}[e]	2475	Cubic (NaCl)	0.25 (100 C) 0.20 (1000 C)	9.5 (0-1000 C)	31.5
UC_2	210×10^{-3}[e]	2375	Tetragonal (CaC_2) cubic (fluorite) over 1820 C	0.29 (100 C)[f] 0.21 (250 C)[f]	14.3 (0-1000 C)	

(a) Pyrolytic graphite.
(b) Sintered.
(c) Stabilized in cubic structure. Stabilizing addition will increase neutron cross section above the value shown.
(d) Self-bonded.
(e) Containing natural uranium.
(f) Sintered to a density 85 per cent of theoretical.

Fission-Product Diffusion in Ceramic Materials

In coated-particle fuel materials 5 to 10 per cent of the fission recoils will come to rest in the coating and can escape from it and from the fuel material by a diffusional process. If the coatings do not crack, the fission products must diffuse through the thickness of the coating, and, in this case, the diffusion coefficients may be rather large without release becoming excessive. Thus, a diffusion coefficient in the range of 10^{-11} to 10^{-13} cm^2 per sec is permissible for fission products having half-lives in the range of 10^4 to 10^6 sec.

If coatings are cracked, diffusional release is possible from the interior surface of the coating in which recoils have been lodged, and from the surface of the fuel. In this case, release is very much greater, so that, even with a fairly low diffusion coefficient, 10^{-16} cm^2 per sec., R/B for Xe^{133} will be 10^{-3} for a typical coated particle. If the diffusion coefficient is larger, loss will be correspondingly higher, increasing as $\sqrt{D}$.

It is clear that the primary factor in preventing fission-product loss from coated particles is preventing cracking of the coatings. However, since complete freedom from cracking cannot be expected, a low value of D is nevertheless desirable.

Studies of the diffusion of fission products in the ceramic materials listed in Table 1 are being made. The experimental procedure is to bombard the materials with fission recoils, which lodge in the surface. The samples are then heated, and the gaseous fission products released are trapped and analyzed.

These studies show that the loss of gaseous fission products does not follow simple solid-phase diffusion laws. Instead, fission gas is lost more rapidly than expected at first, giving rise to the phenomenon known as a "burst". Such behavior is thought to occur probably because of such complicating factors as interaction with radiation-produced defects, or a clustering of the diffusing materials with themselves or other lattice defects. However, the diffusion process is so complicated that it has not yet been possible to understand it, and, consequently, it is now possible only to analyze the data crudely, in terms of an apparent diffusion coefficient.

Some of the data obtained from this study are shown in the following graphs. Figure 4 shows release in two crystallographic directions from a rather perfect sample of recrystallized pyrolytic graphite. As would be expected from the crystal structure of graphite, diffusion is far more rapid along the crystal planes than across them. In fact, the carbon atoms are so close packed in the crystal planes that diffusion of rare-gas atoms across them must depend to a great extent on the presence of lattice defects, and one consequently would expect that diffusion in this direction would be very sensitive to crystal perfection. This may be the explanation for the data shown in Figure 5, where release from two types of pyrolytic carbon coatings is shown. In both of these types, the c-axis is radial, but the laminar type is deposited more rapidly than the columnar type, and would be expected to contain a greater number of lattice defects. As expected, radial diffusion is far more rapid in the laminar type.

Data on apparent diffusion coefficients for single-crystal alpha-alumina and pyrolytic-carbon coatings are shown in Figure 6. Here, it can be seen that release from

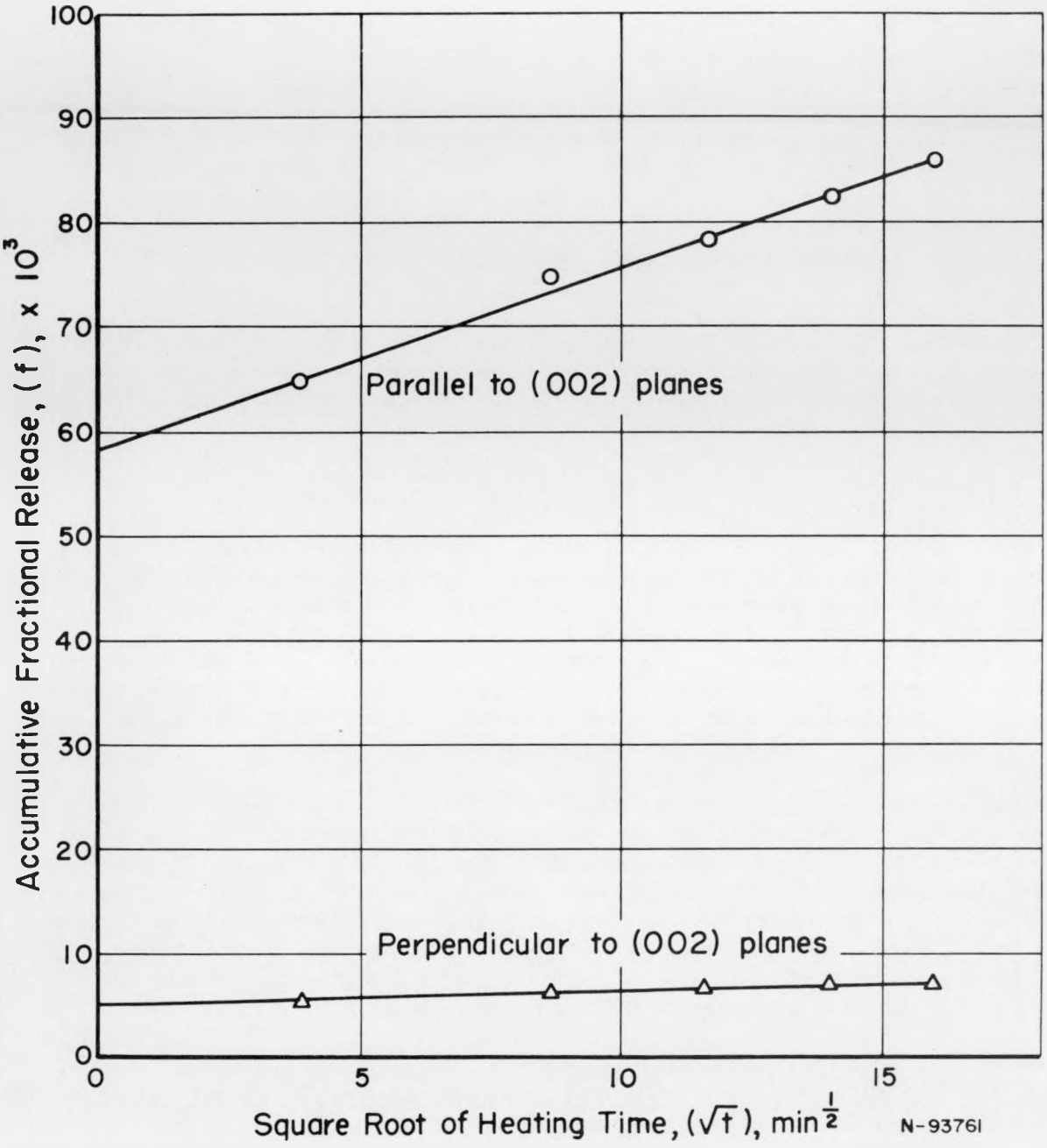

FIGURE 4. XENON-133 RELEASE FROM RECRYSTALLIZED PYROLYTIC CARBON AT 1200 C

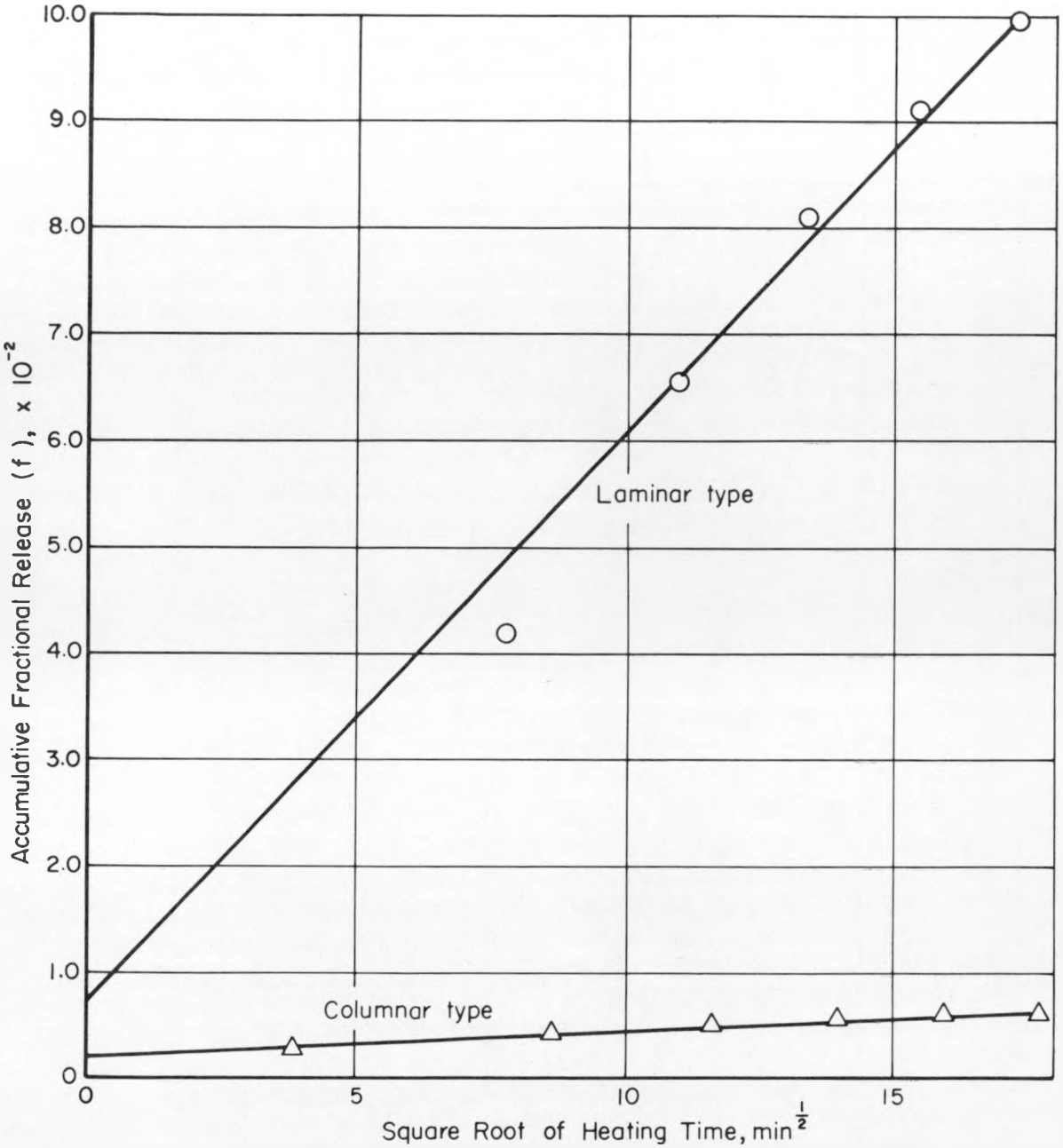

FIGURE 5. XENON-133 RELEASE FROM PYROLYTIC CARBON AT 1200 C

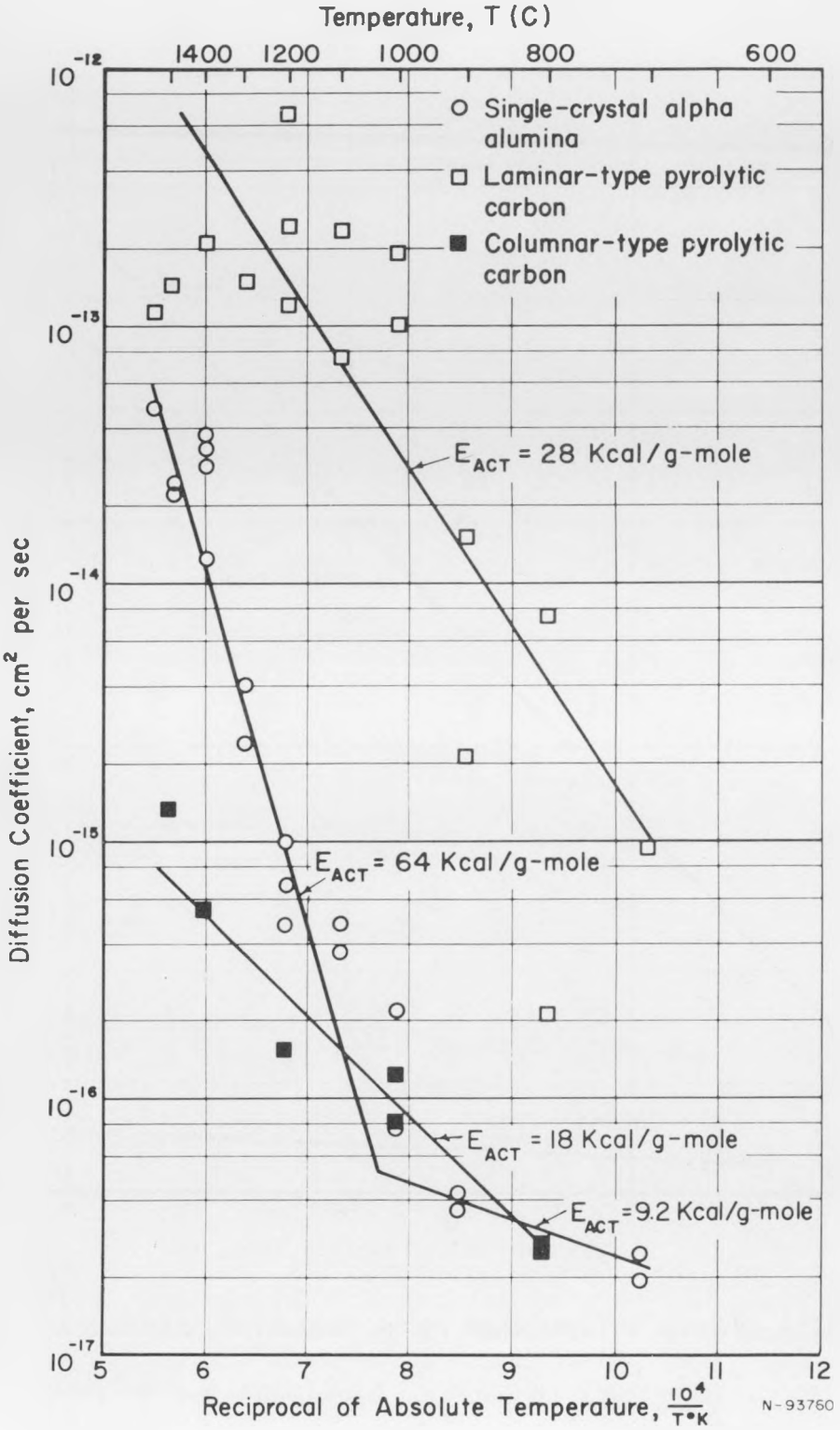

FIGURE 6. DIFFUSION COEFFICIENTS FOR XENON-133 IN ALPHA ALUMINA AND PYROLYTIC CARBON AS A FUNCTION OF TEMPERATURE

the laminar type of pyrolytic carbon is one to three orders of magnitude more rapid than from alumina, while that for the columnar type is about the same as for alumina.

Figure 7 is a composite for all the materials so far studied. Here it is apparent that for all oxides D is approximately the same.

The present indications from these studies are the following:

(1) Significant release of fission gas through uncracked coatings is unlikely to occur for any coating material except laminar PyC, and then only for temperatures above 1200 C.

(2) None of the oxide materials appears to be significantly better or worse than the others.

(3) It may be desirable to deposit a layer of oxide below a pyrolytic-carbon coating to minimize fission-gas release from cracked coated particles when the reactor operating temperature is low enough so that the carbon-oxide reaction does not occur to a significant extent.

Radiation Damage

As will be described in detail in the later discussion of radiation testing, rapid failures are being experienced in testing Al_2O_3 coatings at low temperatures but not at temperatures above 500 C. The behavior indicates that the effect is probably one of strain produced by radiation damage in which the damage is annealed out at temperatures above 500 C.

Such behavior can be explained, on the following basis. Irradiation of ceramic materials leads to the creation of point defects, and normally causes a density decrease. In coated-particle fuels, the inner surface of the coating is the only part radiated by fission recoils, so density changes are nonuniform and stresses are produced. At elevated temperatures, mobility of the point defects will cause them to anneal out, reducing the stresses.

This radiation effect is being studied in some detail, since rapid low-temperature failure would be a serious handicap for coated-particle fuels. The first experiment was an exploratory one, to determine whether significant strains were developed in a pre-post type of experiment. For this purpose thin sapphire wafers were exposed to fission recoils on one surface, and the radiation-induced strain was deduced from the warpage produced in these plates during the radiation. It was found that the maximum compressive strain in the recoil-catching layer was about 10^{-3}. In a coated particle this would lead to a maximum comprehensive stress of 80,000 psi, a maximum tensile stress of about 11,000 psi, and a maximum shear stress of about 40,000 psi, as shown in Figure 8. The strain annealed out to a considerable extent at relatively low temperatures, up to 700 C. These stresses seem high enough to be a likely cause of failure, and the stress may, of course, have been even higher in-pile.

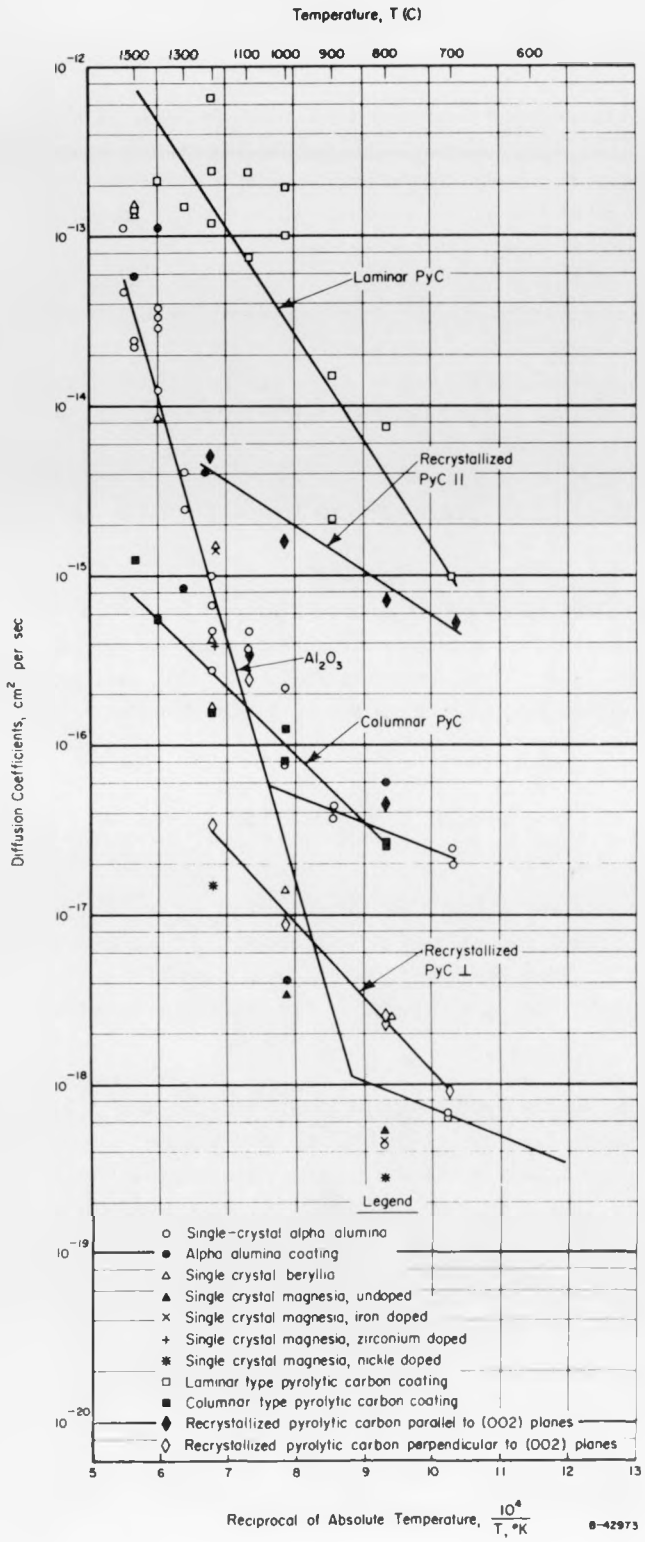

FIGURE 7. DIFFUSION COEFFICIENTS FOR XENON-133 IN CERAMICS AND PYROLYTIC CARBON AS A FUNCTION OF TEMPERATURE

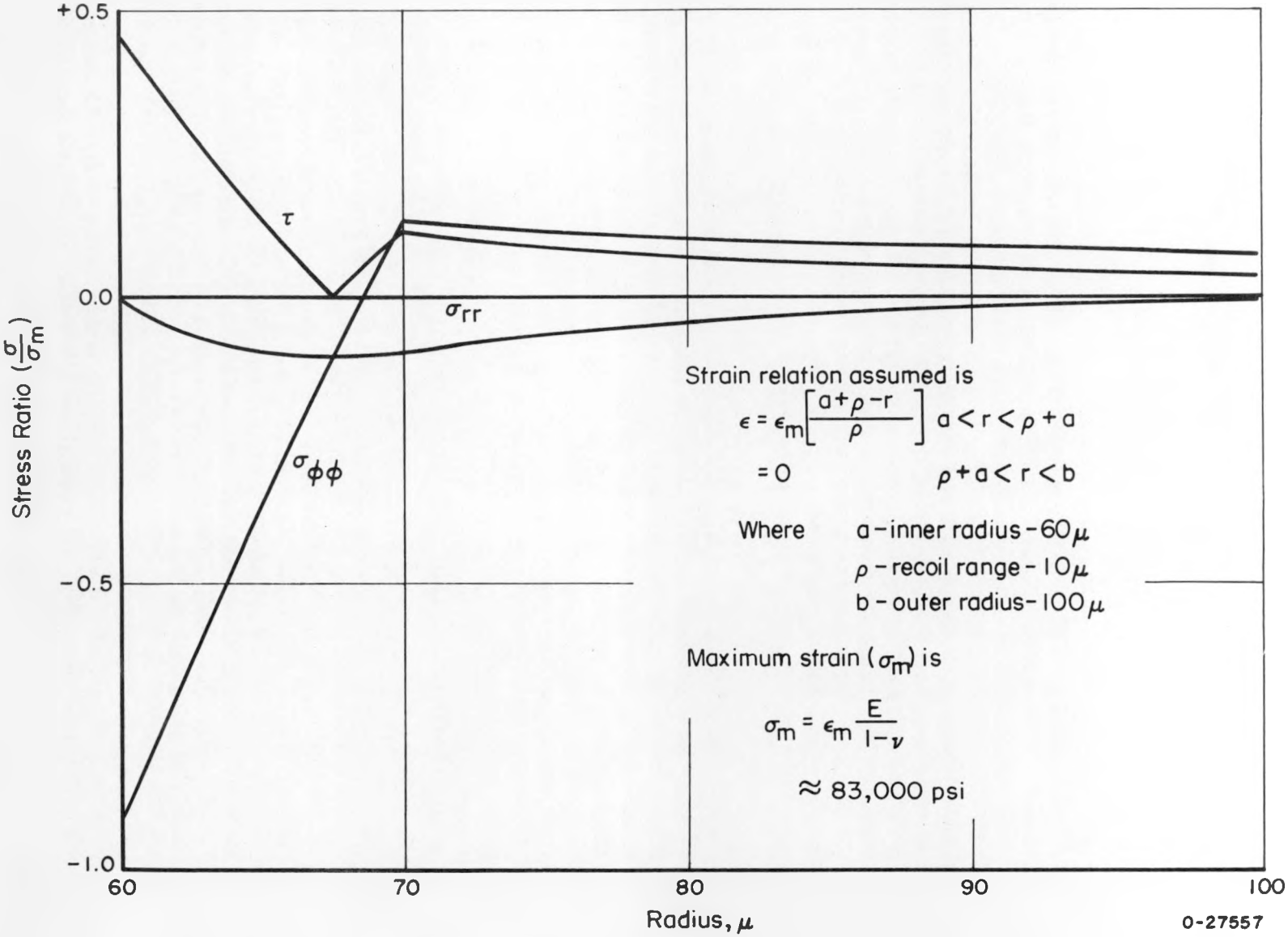

FIGURE 8. STRESSES PRODUCED BY RADIATION-INDUCED STRAIN

The program is now continuing, with a more extensive pre-post study of many of the materials in Table 1 and the design of in-pile apparatus to determine whether in-pile effects are greater than those observed in the pre-post experiments.

Solid-Phase Chemical Reactions

Various solid-phase chemical reactions may occur at high temperatures and cause coating deterioration. These limit operating temperature, and are being studied for that reason. Some of the types of reaction which are being studied are as follows:

(1) Oxygen Diffusion. It has been found that oxygen diffuses through alumina coatings, allowing oxidation of the underlying UO_2. The results shown in Figure 9, obtained on two different types of coatings, show that rate of diffusion depends markedly on the type of the coating, being far more rapid in alumina deposited at low-temperature than at high. These data suggests that oxygen diffusion through coatings will limit the maximum operating temperature of coated-particle fuels containing UO_2 to 1000 to 1200 C, when the atmosphere contains enough oxygen to oxidize UO_2.

(2) Carbon Diffusion. Studies of the diffusion of uranium in pyrolytic carbon are in progress. The technique being used is to perform a diffusion heat treatment of PyC-coated UO_2, section the particles, place the section in contact with photographic film for a period of time, develop the film, and then count the alpha tracks in the film to compute the uranium concentration. A typical photomicrograph showing alpha tracks is shown in Figure 10.

The results are not as consistent as desired, and it is thought that this is partly a consequence of nonuniform diffusion in the pyrolytic carbon. Present indications are that the diffusion coefficient is not over 5×10^{-10} cm^2 per sec at 1600 C in laminar PyC, that diffusion is more rapid in columnar PyC, and that 1600 C is too high a temperature to use or deposit PyC and UC_2, for minimum surface contamination.

Fuel migration in the UC_2-carbon system, observed at GA, is also to be studied, with primary attention being given to the role of contaminants in accelerating migration.

(3) Carbon-Oxide Reactions. Still another type of chemical reaction which limits performance of coated particles is the reaction between oxide-coated particles and a graphite matrix. This is important where oxide-coated particles are dispersed in a graphite matrix. From available thermodynamic data,[1,2] one can compute the maximum allowable operating temperature at which no reaction will occur. The results for several CO pressures are shown in Table 2.

There are also some kinetic data[2], which have been extrapolated to long periods of time to permit an estimate of a maximum operating temperature when it is assumed that little or no CO will be present in the coolant gas, but that a 3-μ-thick layer of the oxide coating can be reacted without affecting the performance of the coated particle. These data suggest that for 10,000-hr operation the maximum temperatures will be 1550 C for BeO-coated particles; 1340 C for Al_2O_3-coated particles, and 910 C for MgO-coated particles. Long-time compatibility tests are in progress for these oxides in graphite.

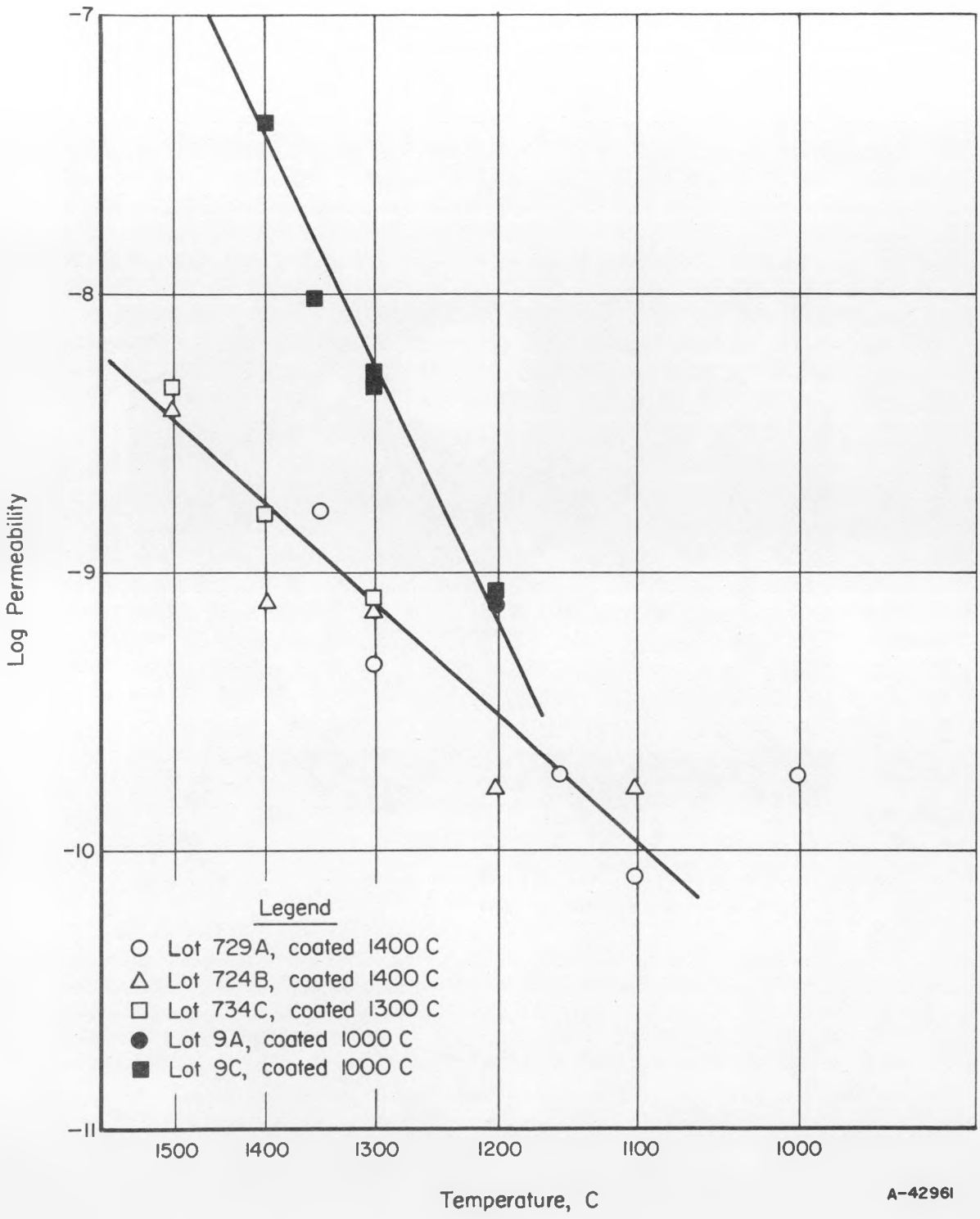

FIGURE 9. PERMEABILITY OF OXYGEN THROUGH Al_2O_3 COATINGS

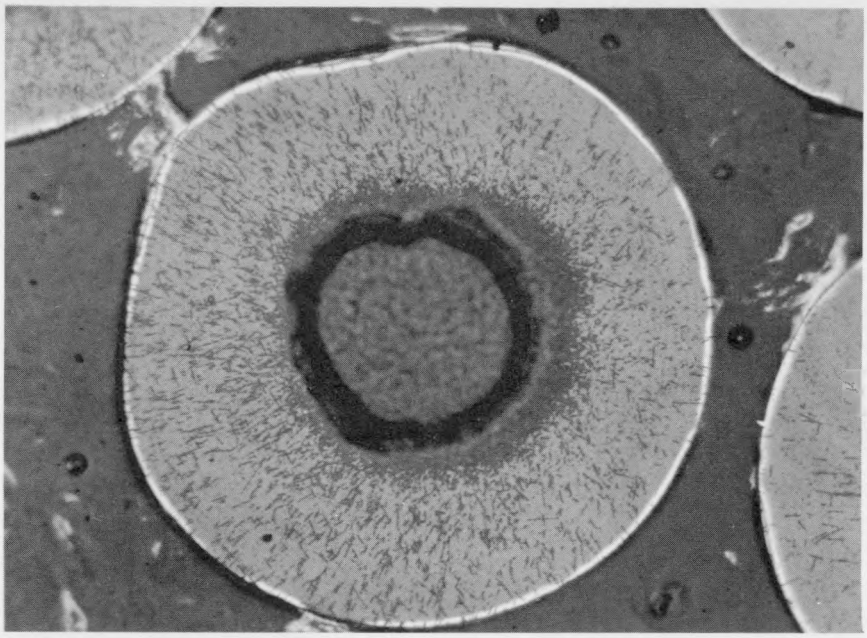

250X N87631

FIGURE 10. AUTORADIOGRAPH OF UC_2 PARTICLE COATED WITH LAMINAR-TYPE PYROCARBON AND HEAT TREATED 2 HR AT 1600 C

TABLE 2. REACTION TEMPERATURE FOR OXIDE-GRAPHITE MIXTURES

Reaction	Operating Temperature, C, at Which Some Reaction Will Occur Below CO Pressure Indicated (Mm of Mercury) 0.001	1	10
1. $MgO + C \rightarrow Mg(g) + CO(g)$	920	1280	1420
2. $ZrO_2 + 3C \rightarrow ZrC + 2CO(g)$	870	1200	1350
3. $Al_2O_3 + 9/2C \rightarrow 1/2\ Al_4C_3 + 3CO(g)$	1120	1440	1540
4. $Al_2O_3 + 2C \rightarrow Al_2O(g) + 2CO(g)$	1150	1480	1640
5. $2BeO + 3C \rightarrow Be_2C + 2CO(g)$	1220	1600	1770

As indicated above this reaction can be held back by small CO pressures. Thus, Al_2O_3-coated particles have been overcoated with an impervious PyC coating and heated to 2000 C without signs of reaction, because the PyC coating allowed a sufficient back-pressure of CO to be maintained to stop the reaction. Particles of this type may have useful characteristics and are being studied.

Solid-Gas Chemical Reactions

The use of ceramic fuel materials may allow greater flexibility in the choice of gas coolants than would otherwise be possible. A thermodynamic analysis was made of the behavior of various coating materials in a variety of gaseous coolants. On the basis of this analysis, it was possible to compute an allowable operating temperature at which the various coating materials could be used in each of the coolants. The results for oxide materials are shown in Table 3 and those for carbon-containing materials in Table 4. These data are considered to be moderately satisfactory for most of the coolants – the major exception being the case for steam. Here some doubt exists about the validity of the computations. For that reason, experimental studies in low-pressure steam have been undertaken with the results shown in Figure 11. These data are thought to be quite satisfactory assuming only that different volatile species do not become important in high-pressure steam.

TABLE 3. MAXIMUM OPERATING TEMPERATURES[a] FOR SEVERAL OXIDES

Coolant (or Impurity)	Pressure, atm	Maximum Operating Temperature for Solid-Phase[b] Oxide Shown, C					
		Al_2O_3	BeO	MgO	Nb_2O_5	UO_2	ZrO_2
H_2O	0.001	1200	700	1200	700	700	>1200
	80	1100	370	800	600	500	1200
Hydrogen	0.001	1000	600	600	(c)	>1200	1200
	100	700	400	500	(c)	>1200	1000
CO_2	100	>1200	>1200	>1200	>1200	600	>1200
Oxygen	100	>1200	>1200	>1200	>1200	500	>1200
Nitrogen	100	>1200	>1200	1100	>1200	1200	>1200

(a) Temperature at which the vapor pressure of volatile species results in a loss rate of oxide of approximately 10 μ per year.

(b) Volatile species:

Al_2O	$Be(OH)_2$	$Mg(OH)_2$	NbO	UO_3	ZrO
Al_2O_2	BeH_2	Mg			Zr
AlO	BeOH				
$AlHO_2$	BeC_2				
Al	Be				

(c) Incompatible even with trace amounts of reducing atmosphere.

TABLE 4. MAXIMUM OPERATING TEMPERATURES FOR GRAPHITE AND SOLID CARBIDES WITH VARIOUS GASEOUS COOLANTS

Gas-Phase Impurity or Coolant	Pressure, atm	Maximum Operating Temperature[a] for Solid-Phase Carbide Shown, C			
		Carbon	SiC		ZrC
Nitrogen	100	760	>1200		1200
CO_2	100	m	m		m
H_2O	1	~300	i		i
Oxygen	100	u	~800	SiO_2	a
	1	u	~800	SiO_2	a
	0.0001	u	~500	SiO	a
Hydrogen	100	m	u		u

(a) Code:

m, mixed gas required
i, insufficient information to select a probable mechanism of reaction
u, unsatisfactory
a, limits probably similar to SiC.

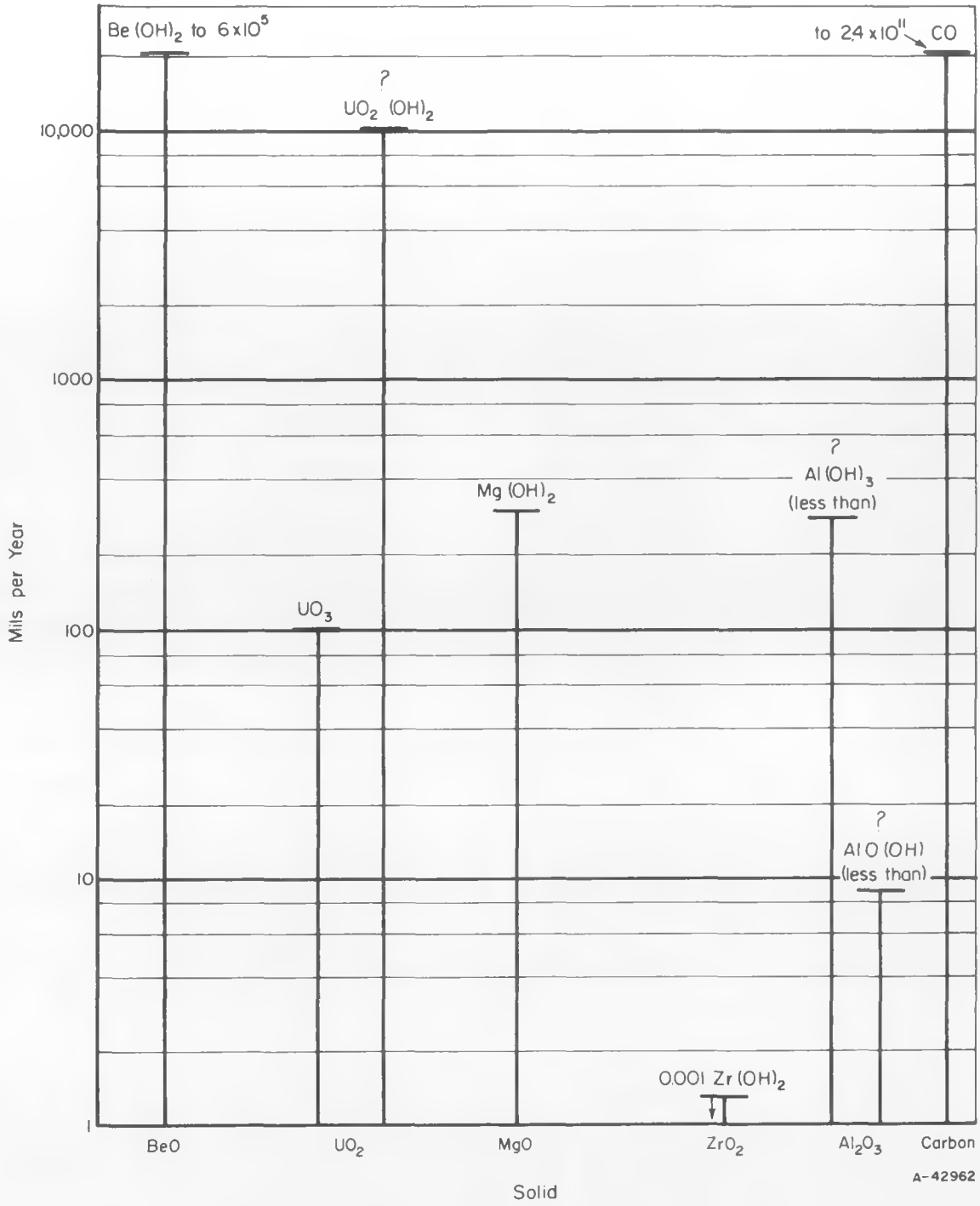

FIGURE 11. CALCULATED EROSION RATES AT 1500 K AND 80 ATM STEAM (2250 F AND 1200 PSIA)

MATERIALS FABRICATION PROGRAM

Fuel Materials

Of the three most promising fuel materials – uranium dioxide, uranium monocarbide, and uranium dicarbide – only the first and last have been readily available as small spherical particles suitable for coated-particle fuels. Consequently, studies of uranium monocarbide have been deferred, and only the dicarbide and the dioxide have been employed.

Having a choice of fuel material and assuming costs were comparable, one would use the material most resistant to radiation damage. While the effect of irradiation on uranium dioxide is relatively well established, extensive data for the carbides are not as yet available.

Figure 12 shows the results of a Bettis study on the effect of irradiation on the expansion of fully enriched 97 per cent dense uranium dioxide.[3] These experiments were carried out with the uranium dioxide sheathed in Zircaloy containers and subjected to an external pressure of 2000 psi on the metal jacket. Since the UO_2 was initially under considerable compression, the unrestrained irradiation-induced expansion of fully dense oxide should be more severe than indicated by these data. The difference for the two curves representing constant fissioning rate is assumed to be the result of the difference in restraint offered by the jackets on the specimens.

Among the results of the few studies reported for carbide fuels it has been shown that the monocarbide exhibits no gross dimensional changes at 0.7 a/o uranium burnup at temperatures below 700 C and that it exhibits a 3.4 to 4.4 volume per cent expansion at 500 C at a burnup of 2.7 a/o uranium. The sesquicarbide shows no density changes at 0.6 a/o burnup at about 700 C. Data on the dicarbide are unavailable.

The net conclusion from these data is that relatively dense fuel, whether it be the oxide or one of the carbides can be expected to tend toward appreciable expansion at burnups of a few atom per cent, and may exert appreciable stress against a tightly fitting, nonyielding ceramic coating.

It is not yet known what fuel-particle density is desired. The fully dense particles should release the least amount of fission products, since the release of fission products by diffusion is essentially directly proportional to exposed surface area, and the fully dense particles should provide the most compact type of reactor core. However, if the fuel is run to very high burnups, the fuel may swell or the pressure of fission gas accumulated within the coated particle may rupture the coating. It may, therefore, be desirable to use porous fuel particles to accommondate fuel expansion or fission-gas buildup. Unfortunately, it is now fairly clear that the properties of the core material can have a considerable effect on the structure of the oxide coatings. Therefore, it may be difficult to independently vary core density and still obtain high-quality coatings.

With regard to the shape of the particles, it is intuitively believed that smooth, spherical nonagglomerated particles are best. It is believed that a smooth spherical surface should minimize regions of stress concentration. Such a spherical, symmetrical geometry should also avoid difficulties associated with the expansion of an irregular core into a coating with an irregular inner surface during subsequent processing

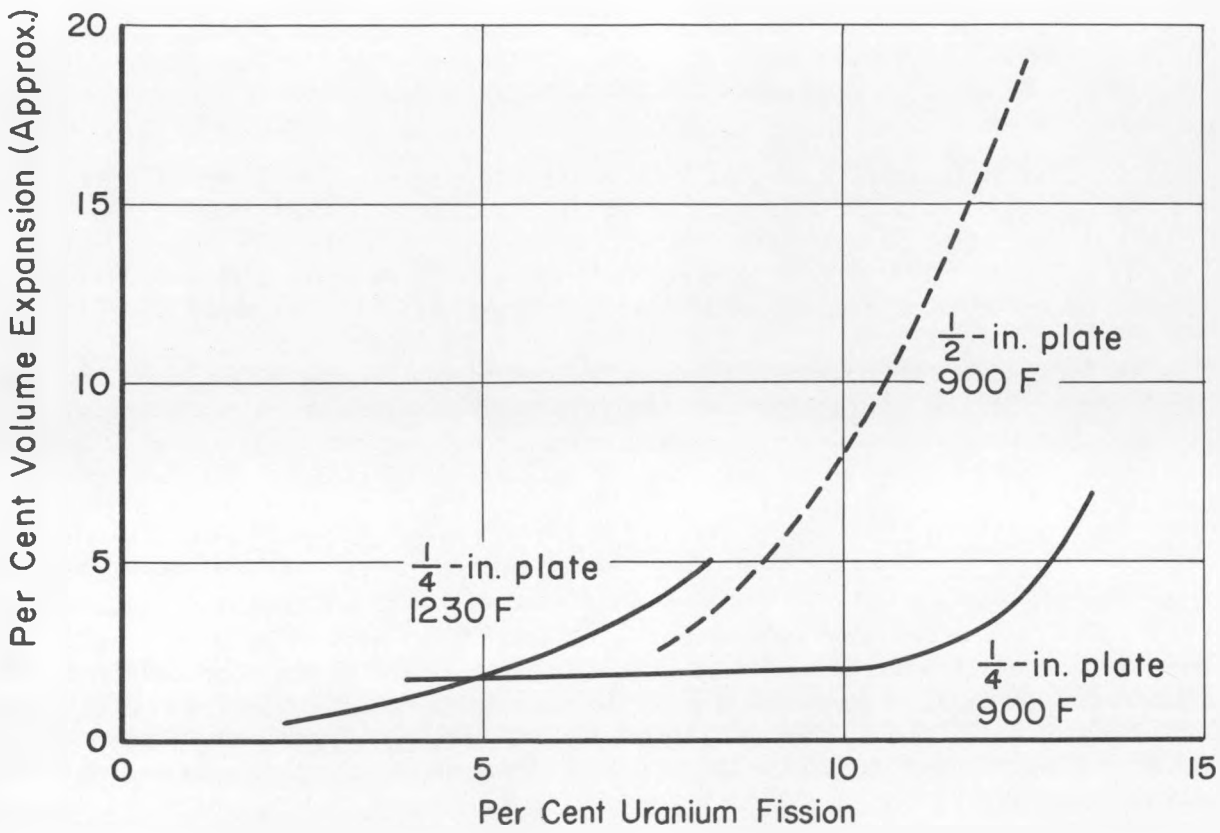

FIGURE 12. RADIATION-INDUCED EXPANSION OF URANIUM DIOXIDE[3]

operations. The presence of doublets or more severely agglomerated particles is also thought to be undesirable for essentially the same reasons.

The stoichiometry of UO_2 fuel is also known to be an important consideration. For example, the diffusion coefficient of the fission product Xe^{133} is strongly dependent on the oxygen/uranium ratio, as shown in Figure 13.[4] Thus, in order to minimize release of the fission products from the core, it is desirable to have essentially stoichiometric UO_2. For this reason, a hydrogen atmosphere is used in the alumina-coating process, so that the oxygen-to-uranium ratio of the fuel is reduced from an as-received value as high as 2.039 to a value of 2.002. No data are available on the effects of composition on the performance of carbide fuels, but it is expected to be a signficant variable.

Particle Coatings

The four coating materials studied most extensively to date are alumina, beryllia, magnesia, and pyrolytic carbon. As mentioned earlier (Table 1), beryllium carbide, silicon carbide, and zirconium carbide, as well as zirconium oxide, are also possible candidates as coatings. The effects of minor additions to these materials may also be studied in the future in an attempt to optimize the properties of the coatings.

It is known that fast neutrons will generally lead to swelling of all ceramic materials at low temperatures, and the percentage expansion is considerably different along the different crystallographic axes. Thus, an oriented coating can be stressed at low temperatures by neutron damage alone. In addition, fission-recoil damage to ceramic materials is usually more severe than neutron damage. Since in the case of coatings on particles, a nonuniform fission-damaged region will result to the distance to which fission recoils penetrate (Table 5), additional stress will be set up. At high temperatures, this damage may anneal. At low temperatures, it may cause failure, so ways to control the stress are necessary and are being sought. In general then, the thickness of the coating on a particle must probably be considerably more than the recoil distance, if it to resist radiation-induced stresses, retain fission-gas pressures, and prevent diffusion of fission products out of the coated particles. Unfortunately it is not possible to calculate this optimum thickness due to the lack of data on strength, elasticity and diffusivity of irradiated materials.

TABLE 5. COMPUTED RECOIL RANGES IN VARIOUS COMPOUNDS AT THEORETICAL DENSITY

Material	Maximum Fission Recoil Range, μ
C	14
BeO	10
MgO	10
Al_2O_3	9
ZrO_2	9
SiC	11
ZrC	9

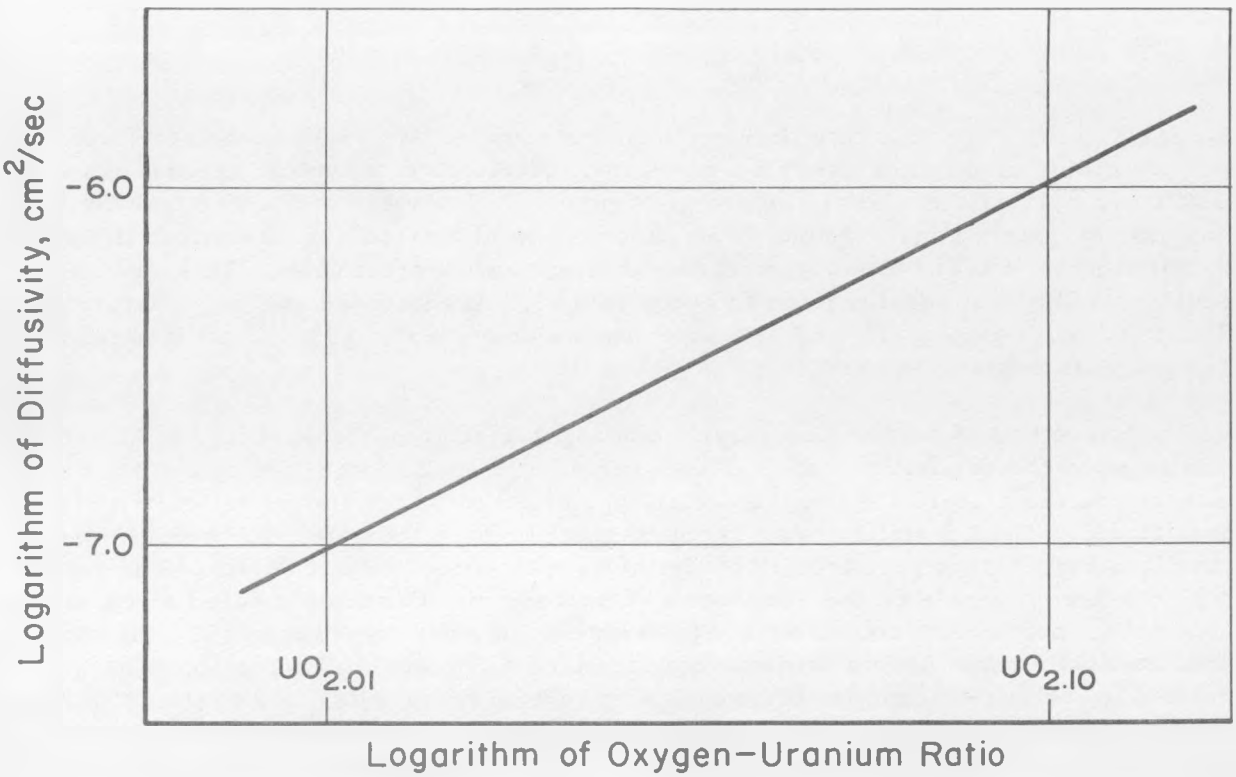

FIGURE 13. VARIATION OF XENON-133 DIFFUSION IN UO_{2+X} WITH OXYGEN CONTENT[4]

These are some of the considerations that have lead to the following coating studies.

Pyrolytic-Carbon Coatings

Both UO_2 and UC_2 particles have been coated with pyrolytic carbon at temperatures from 950 to 2000°C by the decomposition of hydrocarbon gases in a fluidized-bed reactor. The two reactions shown below have been extensively used to deposit pyrolytic-carbon coatings:[5]

$$CH_4 \rightarrow C + 2H_2$$

$$C_2H_2 \rightarrow 2C + H_2$$

These involve the pyrolysis of either methane or acetylene to yield carbon and hydrogen as well as minor amounts of other by-products. A sketch of a typical apparatus for the deposition of pyrolytic carbon is shown in Figure 14. It consists of a vertical cylindrical reactor of quartz construction. The particles to be coated are suspended in turbulent motion by an upward-flowing stream of helium and hydrocarbon. This type of apparatus is used at temperatures up to about 1200 C. At intermediate temperatures, a Mullite reactor is employed, and at temperatures above about 1400 C, an induction-heated graphite reactor is used.

The structure of a 1400 C pyrolytic coating varies from "columnar" to "laminar", depending upon the deposition rate. These terms are applied because of the microscopic appearance of the material – the columnar type appears to consist of radially oriented grains (although the crystallite size is much smaller than the appearance would indicate), and the laminar coating appears to consist of concentric spherical shells. The type of coating obtained depends on the conditions of deposition. Coatings applied at rates of less than 10 μ per hr are columnar in appearance, as shown in Figure 15, while those applied at higher rates have a laminar appearance, as shown in Figure 16. The crystallite size of pyrolytic-carbon coatings also varies with temperature and rate. The c-axis crystallite size of a laminar coating deposited at 1400 C and below is about 25 A, and increases to 150 A at a coating temperature of 1800 C. Columnar coatings prepared at about 1400 C have a crystallite size of approximately 40 A. As noted by many observers, the pyrolytic-carbon deposits are highly oriented, the c-axis being radial. Owing to the extreme anisotropy of thermal expansion in this material and the curvature of the deposits, this orientation leads to both transient and steady thermal stresses as a result of temperature changes.

The apparent density of the coatings is strongly affected by the deposition conditions. Figure 17 shows the effect of coating temperature and deposition rate on the coating density. These curves are drawn from relatively few data points and should be used with caution. However, they do indicate the general trend of the density as a function of process variables.

It has been found that if pyrolytic carbon is deposited on UC_2 at temperatures above 1600 C, the coatings become severely contaminated with uranium, as shown by alpha-particle counts for samples of the particles and measurements of xenon release from neutron-activated samples. If proper precautions are taken in the coating process, it is possible to minimize contamination, and it is essential to do so when maximum

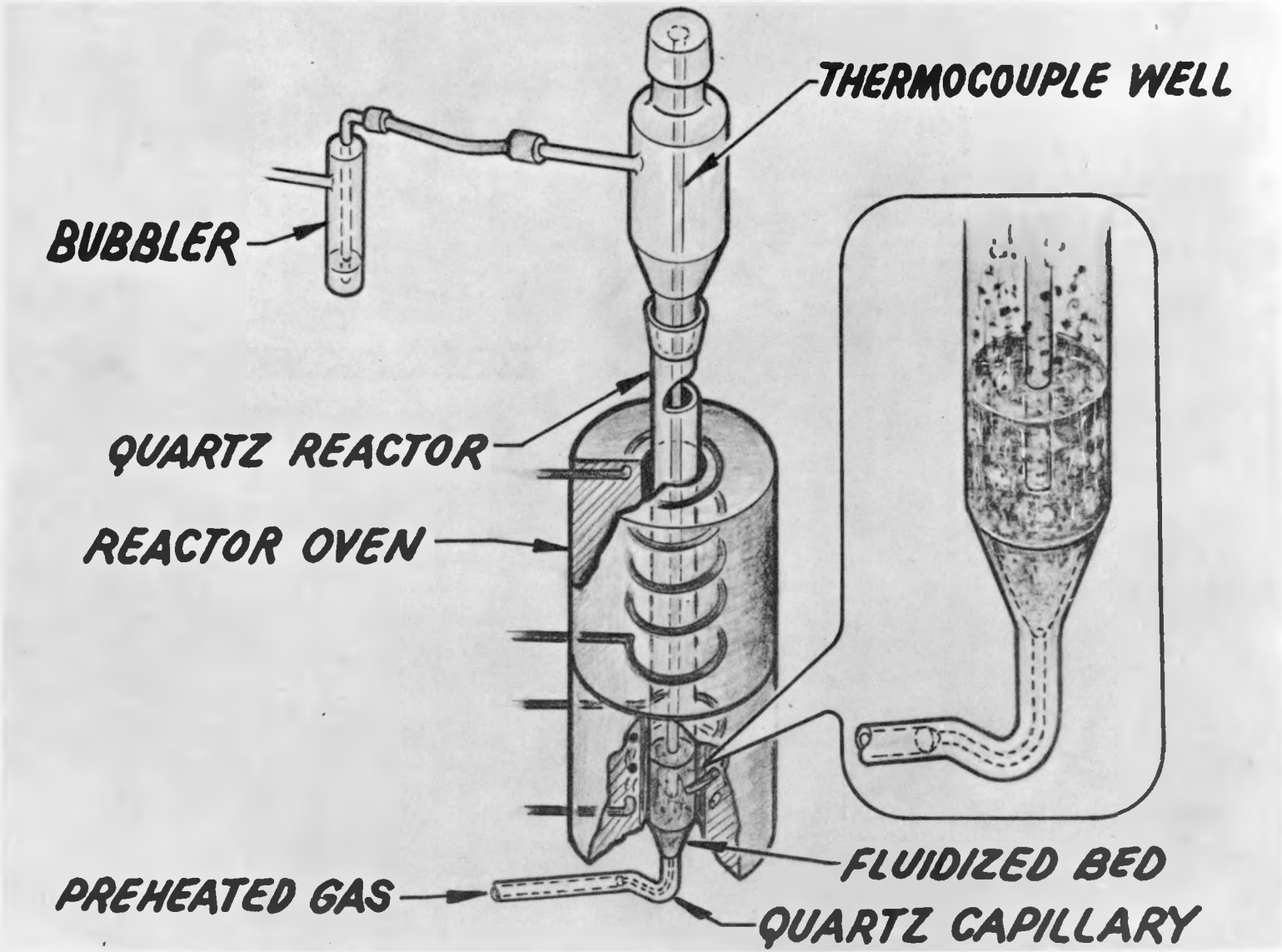

FIGURE 14. APPARATUS FOR COATING POWDERS WITH CARBON

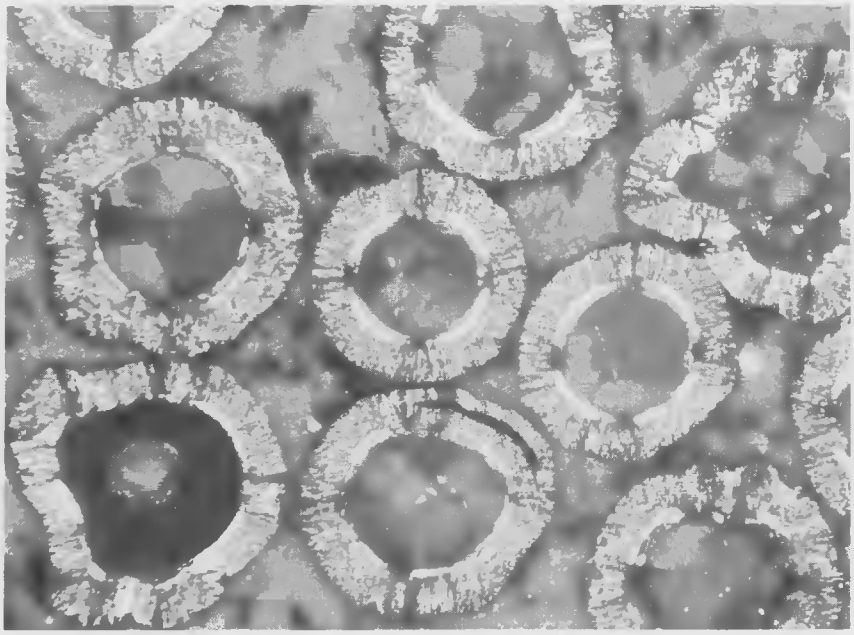

N78860

FIGURE 15. COLUMNAR PYROLYTIC-CARBON COATINGS ON DICARBIDE PARTICLES

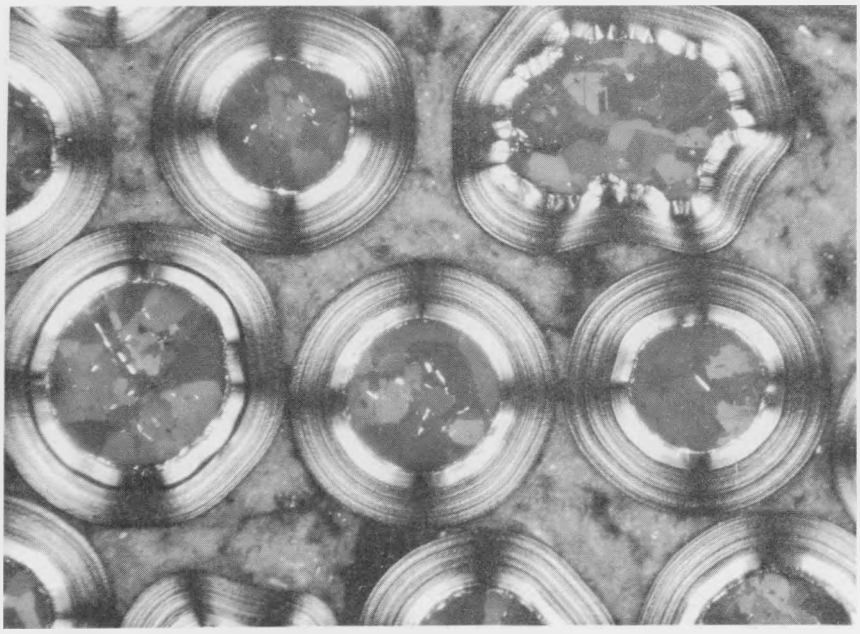

N78862

FIGURE 16. LAMINAR PYROLYTIC-CARBON COATINGS ON DICARBIDE PARTICLES

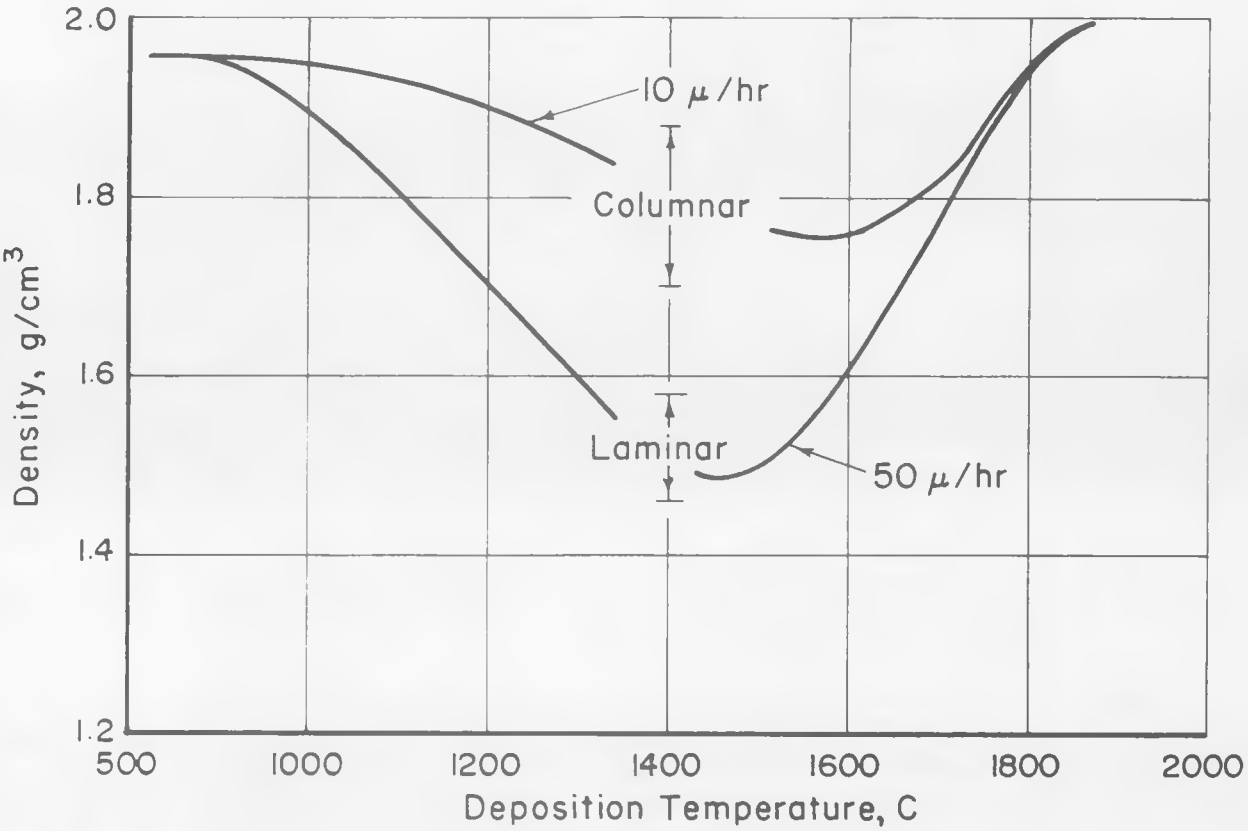

FIGURE 17. DENSITY OF PYROLYTIC CARBON AS A FUNCTION OF PROCESSING CONDITIONS

fission-product containment is desired. In the present study all samples are checked for contamination before irradiation. The standard procedure for carbon-coated particles involves a heat treatment in helium for 48 hr at 1250 C followed by leaching in hot nitric acid, and checking for Xe^{133} leakage at 1300 C after neutron activation. After this treatment, satisfactory lots will show alpha-particle counts indicating that 1 to 5 ppm of the uranium is within alpha range, and xenon-release values of 0.01 to 1 ppm of the amount contained after activation.

Oxide Coatings

Al_2O_3, BeO, and MgO are deposited by the hydrolysis of a volatile halide.[6, 7] The presently preferred reactions for the deposition of each are shown below:

$$2AlCl_3 + 3H_2O \rightarrow Al_2O_3 + 6HCl$$

$$BeCl_2 + H_2O \rightarrow BeO + 2HCl$$

$$MgI_2 + H_2O \rightarrow MgO + 2HI \ .$$

The precise conditions necessary to produce dense, impermeable coatings in fluidized-bed deposition differ for the various oxides. In general, porous coatings are deposited at the lowest temperature, perhaps because the oxide nucleates in the gas phase and subsequently attaches itself to the surface of the fuel particles, or possibly owing to the deposition of intermediate products such as the oxyhalides or hydrated oxides which are subsequently converted to the oxide with corresponding density changes. At higher temperatures, either the intermediates do not form, the nucleation tendency of the system is reduced as a result of a shift in the reaction equilibrium, or the material recrystallizes quickly, so that dense material is obtained. At still higher temperatures rapid grain growth occurs, and the deposits are generally weaker and have an integrity inferior to that of coatings deposited at lower temperatures.

Alumina Coatings. Alumina coatings deposited at temperatures from 500 to 700 C are porous and of low density, and X-ray diffraction examination indicates they are completely amorphous. However, the coatings become crystalline on heating at temperatures of about 1000 C and above. Alumina coatings of near theoretical density are deposited at 1000 C. These are impermeable and consist of small crystallites of alpha alumina with an average size of 0.3 μ dispersed in what appears to be an amorphous matrix. Coatings deposited at higher temperatures become more crystalline. Those deposited at 1400 C are highly crystalline and have an average crystallite size of about 25 μ, but exhibit a coating integrity inferior to that of 1000 C coatings. A photomicrograph of a coarse-grained Al_2O_3 coating prepared at a temperature of 1400 C is shown in Figure 18. The hardness of the coatings prepared at 1000 C and above is equal to or higher than that of sapphire (2200-2500 KHN, 50-g load).

Beryllia Coatings. Beryllia coatings must apparently be deposited at higher temperatures than alumina coatings to obtain equivalent properties. Thus, coatings deposited at temperatures between 800 and 1100 C are not obviously crystalline, and they are porous. However, at deposition temperatures of 1400 C, the coatings are impervious. Beryllia coatings prepared at 1400 C are of near theoretical density, are very crystalline, and have good integrity. A photomicrograph of a typical beryllia coating

deposited at a temperature of 1400 C is shown in Figure 19. The average crystallite size in the BeO coatings increases as a function of temperature. As temperatures below about 1100 C, the crystallites are of submicron size, but increase to about seven microns at temperatures of about 1400 C. The hardness of the 1400 C coating is essentially equal to that of single-crystal BeO (1200 to 1400 KHN, 50-g load).

Magnesia Coatings. Magnesia coatings, an example of which is shown by the photomicrograph in Figure 20, are relatively transparent, dense, and void-free when deposited at 1400 C. Coatings prepared at 1100 and 800 C are less transparent and appear to contain submicron pores. The hardness of the coatings is not significantly affected by coating temperature, and the hardness is slightly less than fused MgO (925 to 975 KHN, 50-g load). The crystallite size is about 1 μ for coatings deposited at 800 C and about 14 μ for coatings deposited at 1400 C. After heat treatment of these coatings at 1400 C for 24 hr in helium, the average crystallite size increases to 16 μ and 36 μ, respectively. Upon cooling from the coating temperature, since MgO has a higher thermal expansion than UO_2, the MgO coatings crack unless a porous UO_2 is employed or a spherical void is incorporated between the coating and core. All MgO coatings have failed to withstand oxidation at 1100 C. Since cracks in the coatings cannot be found, it is believed that oxygen diffusion through the coating is the major source of difficulty. All of these oxide-coated particles are evaluated before irradiation in the same manner as the carbon-coated particles, except, in addition, they are tested for oxidation resistance in air at temperatures of 1100 C for 20 hr.

Coatings Designed for Special Purposes

Most of the simpler types of coatings which have been described are now being or have been irradiated and the results will be summarized later in this paper. Some of these materials have shown quite remarkable performance under certain conditions, but in other cases they have not been as satisfactory. The current materials effort is now being directed toward the development of coatings to minimize the effects of irradiation and temperature on the coated particles. These modifications include incorporation of interlayers of materials to absorb and retain fission recoils without damaging the outer coating and use of void regions within the coating or fuel to permit dimensional changes, promote reduction in fission-gas pressure, or serve as barriers to crack propagation.

As an example of these newer types of structures, Figure 21 shows a photomicrograph of a pyrolytic-carbon coating over an inner layer of Al_2O_3. The purpose of the Al_2O_3 is to protect the pyrolytic carbon from direct fission-recoil damage and also to provide a material in which the fission products will lodge and through which they will diffuse slowly. As has been pointed out previously, the diffusion rate of some fission products in Al_2O_3 may be much lower than in pyrolytic carbon. An example of an advanced type of all-oxide structure is shown in Figure 22. Here a complete void has been developed within the coating between an intermediate porous layer of Al_2O_3 and in inner layer of dense Al_2O_3. The purpose of the void is to provide space for irradiation-induced expansion of fuel and, possibly, the coating, as well as space for accumulation of fission-product gases. The purpose of the porous Al_2O_3 is to protect the outer coating from recoil damage.

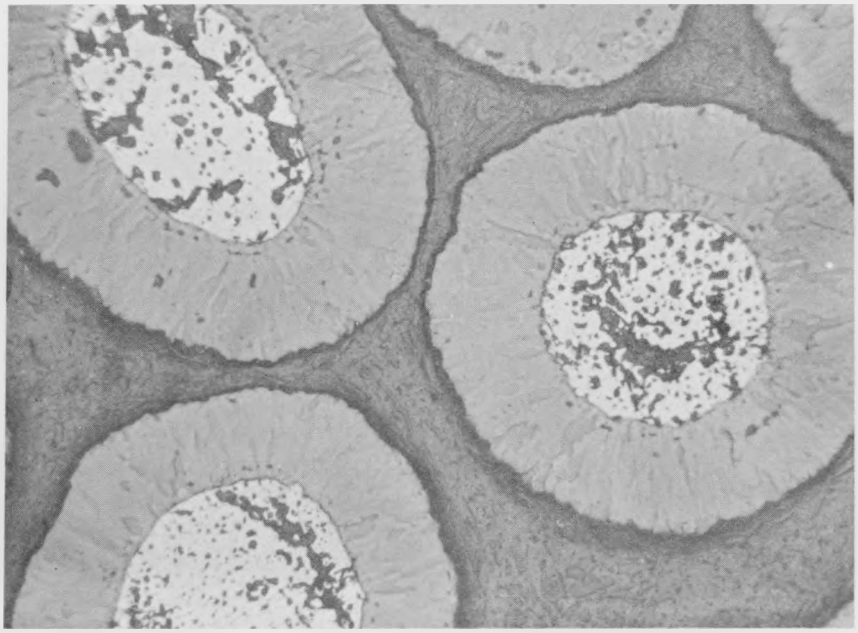

N84360

FIGURE 18. PHOTOMICROGRAPH OF 1400 C ALUMINA COATING ON URANIUM DIOXIDE

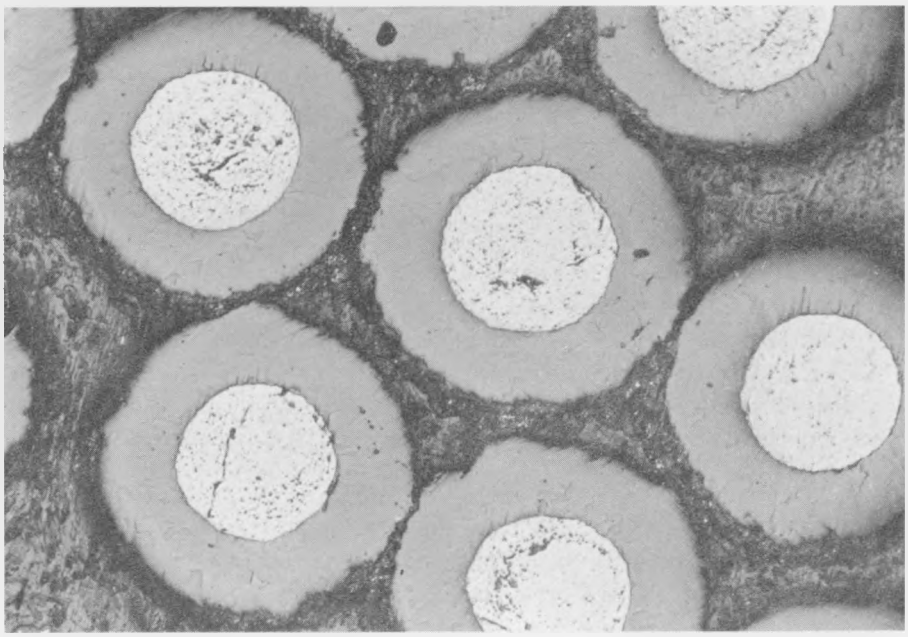

N93507

FIGURE 19. PHOTOMICROGRAPH OF 1400 C BERYLLIA COATING ON URANIUM DIOXIDE

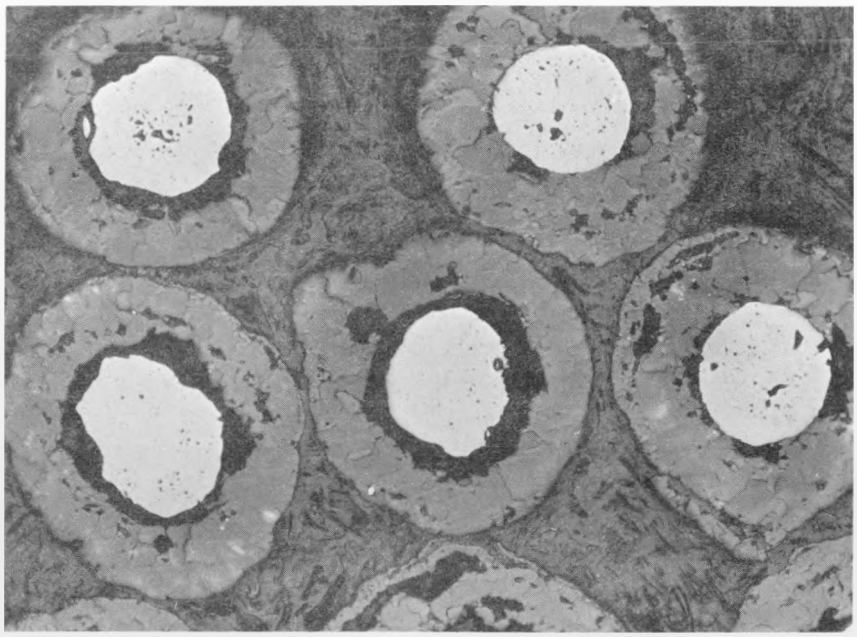

N93921

FIGURE 20. PHOTOMICROGRAPH OF 1400 C MAGNESIA COATING ON URANIUM DIOXIDE

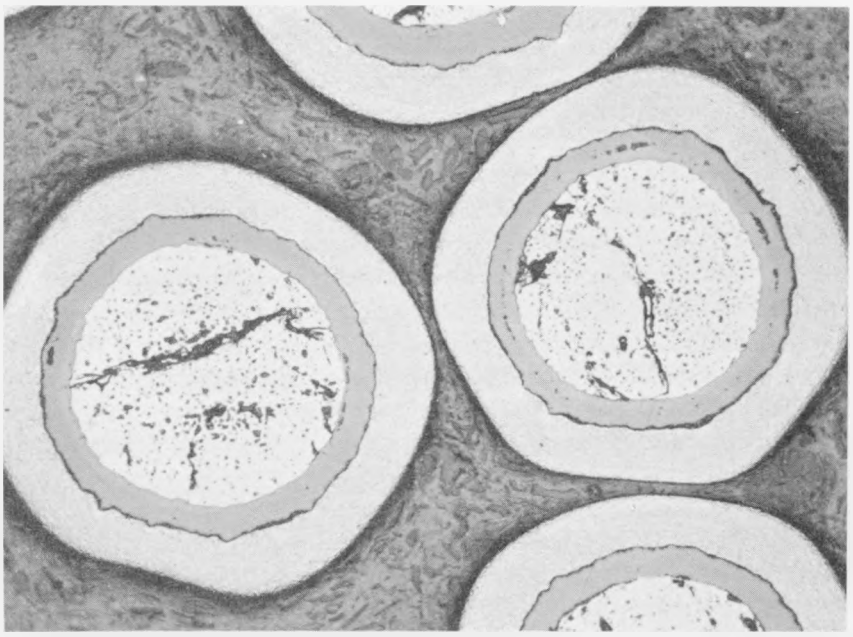

N88514

FIGURE 21. PYROLYTIC-CARBON COATING PROTECTED BY INNER LAYER OF ALUMINA

Matrix Bodies

To be useful, ceramic-coated particles will normally be dispersed either in graphite or BeO. Special problems are introduced into ceramic technology through the use of coated particles. These problems are:

(1) Normal mixing methods may crack particle coatings.

(2) Particle coatings may crack when random mixtures of particles and matrix are pressed at conventional pressures.

(3) Dense, unsinterable coated particles hinder the sintering of oxide bodies, giving unsatisfactory products.

(4) Cracks in an oxide matrix containing oxide-coated particles will penetrate particle coatings unless special precautions are taken to prevent this.

These problems have required that conventional methods be modified and have encouraged the development of new methods for dispersing coated particles. Pelletizing techniques, whereby the coated particles are coated with the required amount of finely powdered matrix material, and whereby intermediate layers of burnout agents can also be introduced, have been particularly promising. (8)

Graphite Dispersions

In the case of dispersions of coated particles in a graphite matrix, adequate random dispersions can be made using gentle mixing methods, and by avoiding excessive pressures during molding or baking.

A technique found satisfactory was as follows: A master batch of coated particles, 40 μ graphite or carbon flour, coal-tar pitch binder, and a liquid vehicle of benzene was carefully mixed. Aliquot samples were withdrawn and molded into irradiation specimens using pressures of about 2000 psi. These samples were finally baked at a maximum temperature of 1250 C, using a very low heating rate over a period of about 1 week. This solvent batch-mixing procedure did provide the means for preparing initial sets of enriched fuel specimens for irradiation testing, but the product left much to be desired. The matrix density and strength were not high, and consistent freedom from fuel damage was not realized.

In order to more effectively meet the particular needs of this program, particularly the processing of very small quantities of many different fuel types, less conventional procedures of dispersion and processing were developed. Specimen quantities of the matrix materials and fuel in a benzene solvent were micromixed with a magnetically driven rod which limited the force on any given fuel particle to a value less then the previously determined crushing strength of the particle. The partially desolvented sample was then molded and the balance of the solvent removed under vacuum. The sample was then pressure baked, using a procedure developed by General Atomic, at 5000 psi at a maximum temperature of 1250 C. A very rapid heating cycle of an hour or so was employed. It was found on the basis of Xe^{133} release measurement during postirradiation

heating at temperatures of 1150 C for several hours that the coated fuel particles in these dispersion specimens were consistently free of damage. The specimens had matrix densities of 1.75 g per cm^3, crushing strengths of 9000 psi, and tensile strengths of 1450 psi. These values are all quite acceptable. Precise specimen fuel loading and dimensioning were also achieved, as was a completely random dispersion of the fuel, as can be seen in Figure 23.

It was possible to get a nearly ideal instead of a random dispersion and to press at higher pressures so as to get a stronger, denser matrix by using a pelletizing technique. With this technique, graphite flour and binder are caused to adhere to the coated fuel particles in a coating drum. While the coated particles are tumbled in the rotating drum, a benzene solvent for the binder and containing the graphite flour in suspension is intermittently sprayed from an air-driven atomizer onto the particles. The benzene solvent is continuously evaporated. The pelletized particles are then molded into shape. Higher pressures can be employed without damage to the coated particles, and thus improved matrix properties can be obtained. An example of the ideal dispersion made from pelletized particles is shown in Figure 24. The final element has excellent fuel distribution, and no particles are exposed at the surface. Some control of the orientation of the graphite crystallites around each coated particle can also be achieved. With this improved technique, matrix densities of 1.80 g per cm^3, tensile strengths of 2200 psi, and crushing strengths of 14,000 psi have been realized.

Other ways of making dispersions from coated particles also are possible. One is chemical sintering. A sample made by a chemical-sintering approach is shown in Figure 25. In this application, the coated particles were overcoated with sufficient pyrolytic carbon so that the desired distance between fuel particles was obtained when the overcoated particles were loosely packed into an expendable form of the same shape as the final fuel element. Hydrocarbon gas was then passed slowly through this packed bed at elevated temperatures, and the over-coated particles were cemented together by the deposition of carbon in the intersticies between the particles.

Oxide Dispersions

Pelletizing methods have also proved useful in making oxide ceramics and, in fact, the original studies were concerned with oxide systems.[9] Most of the work to date has been done with Al_2O_3-coated particles in an Al_2O_3 matrix. One modification is desirable for oxide ceramics owing to shrinkage during sintering – a burnout layer should be applied to the coated particle before the matrix material is applied. Then, after pressing, the burnout layer is dissipated during heating, giving room for matrix shrinkage. Pyrolytic carbon, removed by oxidizing, and ammonium alum, which decomposes to gases with a small amount of alumina residue, have been found to be satisfactory burnout layers. Al_2O_3-coated and pelletized particles are shown in Figure 26, and a polished cross section of a sintered sample is shown in Figure 27.

Studies of BeO-matrix materials are in progress. $Be(OH)_2$ has been found to be a satisfactory burnout layer in this case. A major problem is that severe grain growth occurs in the vapor-deposited coatings during sintering of the matrix, and the coatings loose their integrity.

Other methods of making oxide ceramics containing coated particles have been considered, and some study of them has been carried on. The chemical-sintering

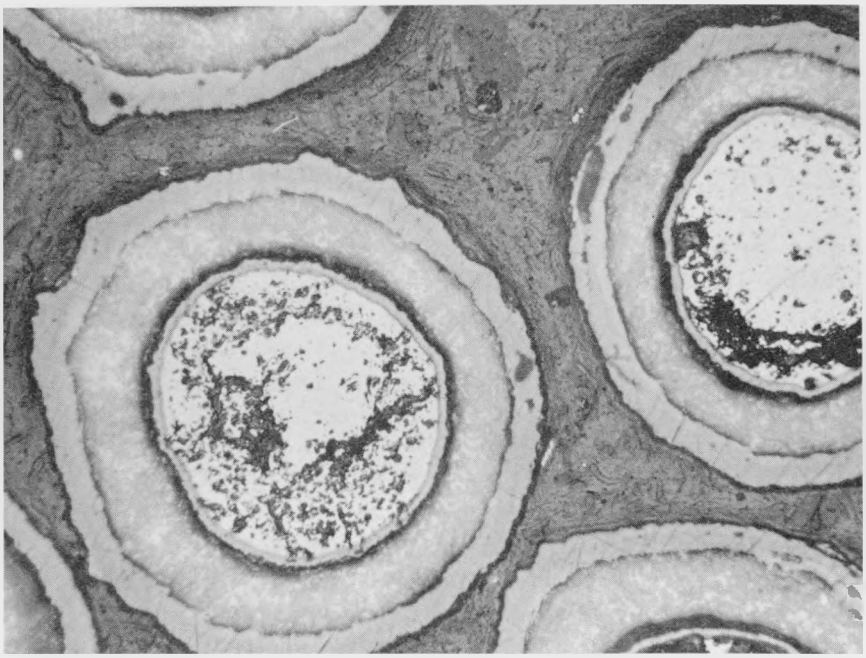

N88512

FIGURE 22. COMPOSITE ALL-ALUMINA COATING ON URANIUM DIOXIDE

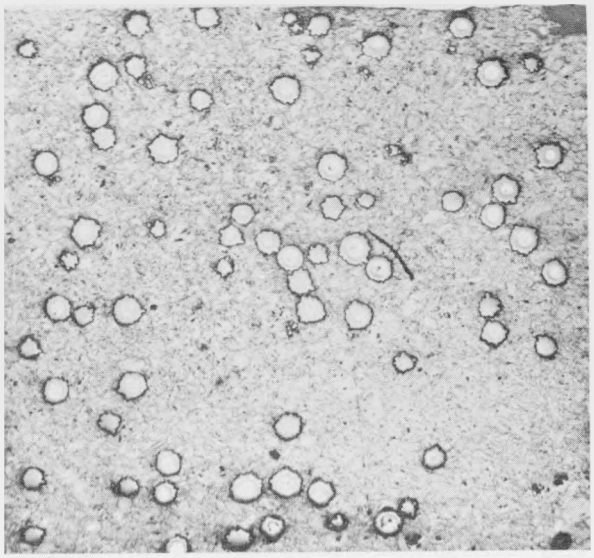

RM19426

FIGURE 23. RANDOM DISPERSION OF COATED-PARTICLE FUEL ON A GRAPHITE MATRIX

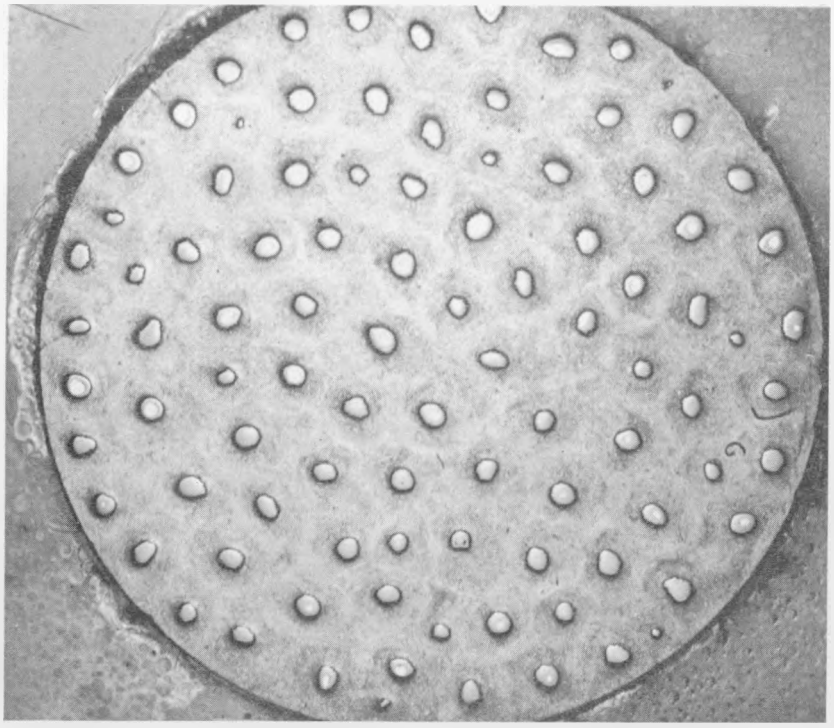

RM20429

FIGURE 24. DISPERSION OF COATED-PARTICLE FUEL IN GRAPHITE-MATRIX BODY

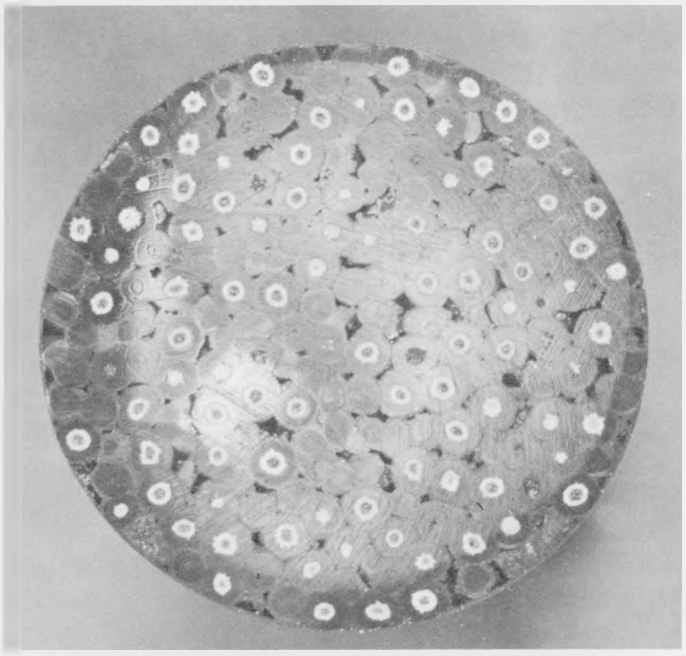

N79964

FIGURE 25. DISPERSON OF COATED-PARTICLE FUEL IN CARBON-MATRIX BODY PREPARED BY CHEMICAL SINTERING

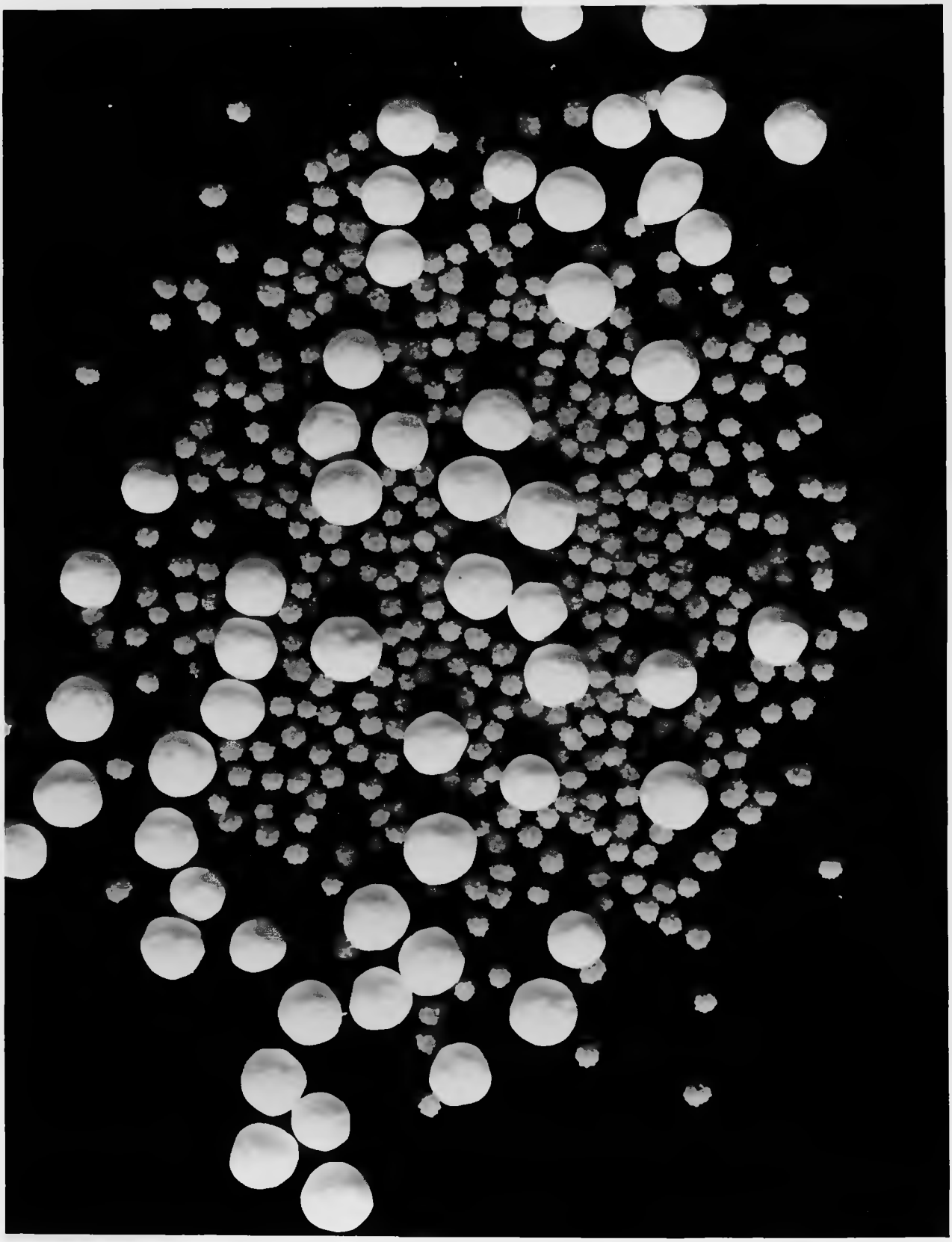

N86854

FIGURE 26. ALUMINA-COATED URANIUM DIOXIDE PARTICLES AND OXIDE-PELLETIZED PRODUCT

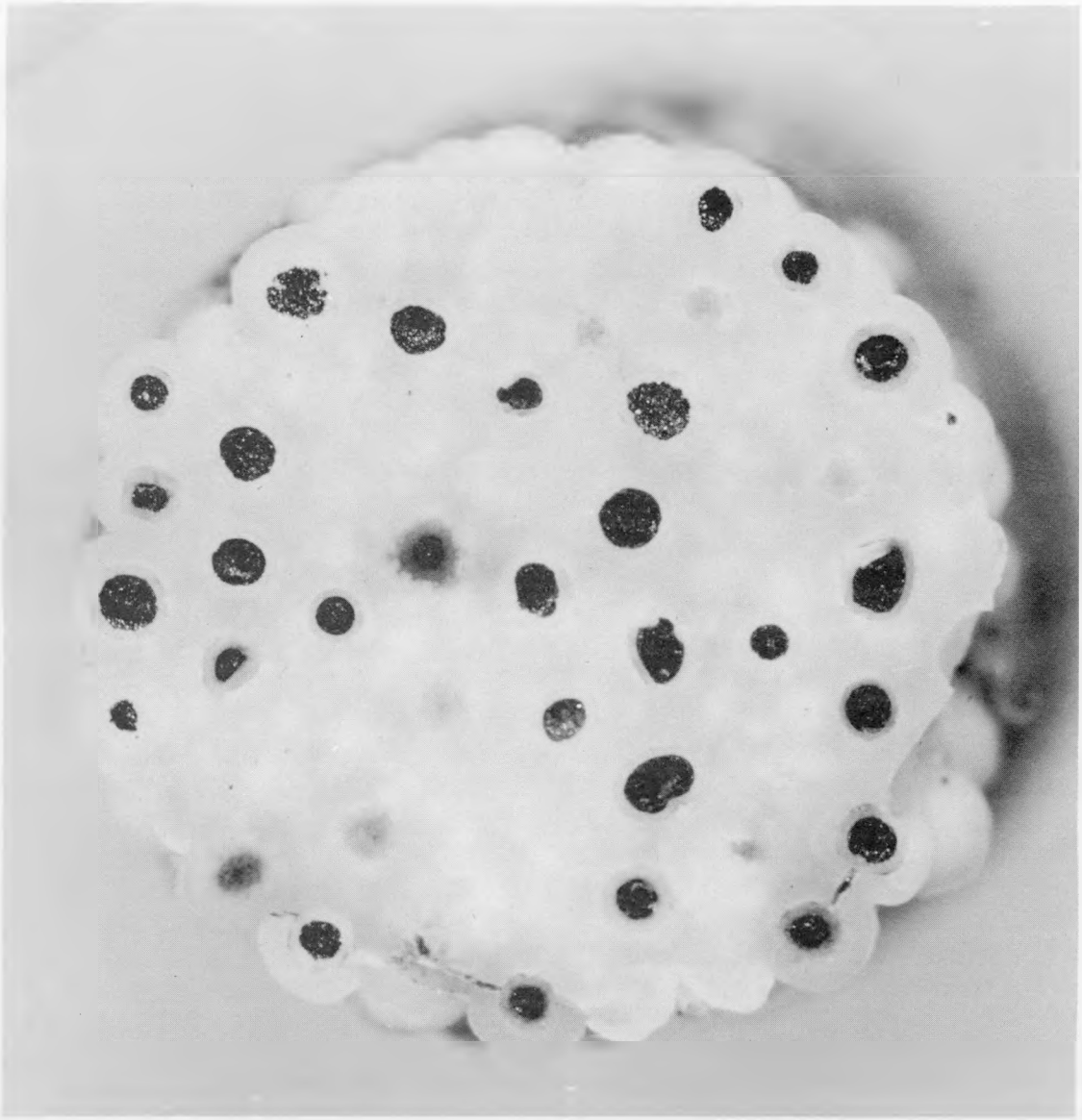

N84273

FIGURE 27. POLISHED SECTION OF ALUMINA-MATRIX BODY PREPARED FROM PELLETIZED FUEL

approach has been considered. It would probably work on a laboratory scale, but difficulties are foreseen during scale-up, and therefore the process has not been studied to date. However, this position may be revised at some time in the future. Hot isostatic pressing of the oxide-coated particles is being attempted, and dense bodies can be fabricated, but hairline cracks are evidently present in the coatings after bonding.[10] Nevertheless, efforts in this area are continuing.

RADIATION TESTING PROGRAM

In-pile irradiation studies of alumina, beryllia, and pyrolytic carbon-coated fuel particles have been performed in the Battelle Research Reactor. The testing procedures employed were designed to evaluate the performance of the coated particles in a reactor environment and to achieve sufficient understanding of their behavior that new particles can be designed to overcome any deficiencies in fission-product retention. The effects on coating integrity of factors such as fuel burnup, temperature of irradiation, and support from a matrix have been investigated.

These studies were performed by irradiating the specimens in either a static or a dynamic helium atmosphere. In the static system the materials were irradiated at constant temperatures to various degrees of burnup, and their performance was evaluated by postirradiation examinations. The integrity of a number of specimens could be studied simultaneously in the static experiments. The dynamic or sweep system provided information on the behavior of the fuel materials during irradiation. In the sweep experiments, fission-gas release was monitored during the irradiation, thus enabling one to correlate changes in the integrity of the coatings with such factors as accumulated irradiation time or burnup and specimen-temperature variations. All tests were performed at thermal-neutron fluxes of 1 to 2 x 10^{13} nv.

Studies of Alumina-Coated Fuel Particles

A variety of types of alumina-coated particles have been tested. These include dense UO_2 particles coated with dense Al_2O_3 at 1000 C (Lot 715A), at 1025 C (Lot 733B), or at 1225 C (Lot 725D), porous UO_2 coated with dense Al_2O_3 at 1000 C (Lot 717B), dense UO_2 coated with dense Al_2O_3 at 1000 C and heat treated at 1250 C (Lot 715A-HT), dense UO_2 coated with alternating dense, porous, and dense Al_2O_3 coatings (Lots 4E and 721C), and porous UO_2 coated first with laminar pyrolytic carbon and then with dense Al_2O_3 (Lot 736B). The tests included static-capsule and sweep-capsule irradiations at 100 C and at 1070 C and sweep-capsule irradiations at variable temperatures. Both unsupported-particle specimens and matrix specimens were tested.

Static-Capsule Irradiations

The results of static-capsule irradiations of alumina-coated UO_2 are given in Table 6. The postirradiation data include: (1) the fraction of the Xe^{133} released, which is determined by puncturing the specimen cans, collecting the gas, and analyzing the gas by gamma-ray spectrometry, and (2) the fraction of the uranium removed from the particles by dissolution with nitric acid.

The significant feature of these data is the fact that, at 100 C, a large fraction of the alumina coatings cracked some time during the irradiation to a fuel burnup of 3 to 5 per cent. This was not the case, however, when the irradiations were performed at 1070 C. At 1070 C the release of Xe^{133} was low, and the leach data indicated failure of

TABLE 6. RADIATION-TEST RESULTS

Sample	Fuel Material	Coating Description	Tests of Particles Alone[a]			
			Tested at 100 C			
			Burnup, per cent	Xe^{133} Release, ppm	Uranium Removed in Leach, per cent	Burnup, per cent
715A	d. UO_2	42 μ of 1000 C Al_2O_3	3.0	120	>7[c]	1.7
			3.3	120	54	3.2
			3.9	60	5[c]	--
			4.0	10-430*	>82	--
			4.7	140	39	--
715A-HT	d. UO_2	42 μ of 1000 C Al_2O_3 plus 48-hr 1250 C anneal	3.9	--	95	--
			Nil	140*	--	--
717B	p. UO_2	43 μ of 1000 C Al_2O_3	3.9	--	1.5[c]	--
725D	d. UO_2	56 μ of 1225 C Al_2O_3	3.9	20	0.3[c]	3 est.
733B	d. UO_2	47 μ of 1025 C Al_2O_3	3.9	--	3[c]	4 est.
4E	d. UO_2	8 μ of d. Al_2O_3, 6 μ of p. Al_2O_3, and 28 μ of d. Al_2O_3	2.9	10	28	--
721C	d. UO_2	8 μ of d. Al_2O_3, 18 μ of p. Al_2O_3, and 28 μ of d. Al_2O_3	3.1	30	95	1.7
			3.4	2	88	3.2
			4.6	20	5[c]	--
736B	p. UO_2	14 μ of laminar PyC, 1400 C, and 29 μ of 1025 C Al_2O_3	--	--	--	--

(a) The asterisks denote sweep-capsule irradiations.

(b) The letter G indicates a graphite matrix and C indicates a carbon matrix.

(c) These results are very uncertain, since only a small fraction of the particles were recovered from each capsule for leaching. In some cases the Xe^{133} data indicate a higher degree of failure than the leach data.

(d) The temperature did not remain at 1070 C throughout these irradiations. The capsules operated at 1070 C for 4 days, at 440 C for 3 days, and at 750 C for the remaining 37 days.

FOR Al_2O_3-COATED PARTICLES

Tested at 1070 C		Tests of Particles in Matrix[a][b]					
		Tested at 100 C			Tested at 1070 C		
Xe^{133} Release, ppm	Uranium Removed in Leach, per cent	Burnup, per cent	Xe^{133} Release, ppm	Uranium Removed in Leach, per cent	Burnup, per cent	Xe^{133} Release, ppm	Uranium Removed in Leach, per cent
0.1	0.9	3.5	2(G)	≥33	1.7	-(G)	0.007
0.02	0.2	5.0	0.8(G)	≥40	3.3	<4(G)	--
--	--	--	--	--	--	--	--
--	--	--	--	--	--	--	--
--	--	--	--	--	--	--	--
--	--	3.6	0.5(G)	93	4 est.	-(G)	0.3
--	--	--	--	--	--	--	--
--	--	--	--	--	--	--	--
700[d]	--	--	--	--	3 est.	30(G)	2.4[d]
					3 est.	1-12*(G)	1.9[d]
30	--	--	--	--	--	--	--
--	--	--	--	--	3.9	0.3(G)	0.65
					3.8	-(G)*	--
20	3	3.0	2(C)	≥33	1.6	≤2(C)	0.5
4	0.5	3.4	≤18(G)	≥44	1.7	≤36(G)	0.004
--	--	4.8	2(G)	≥30	3.3	≤60(C)	0.094
		4.9	4(C)	≥43	3.4	150(G)	--
--	--	--	--	--	6 est.	14-90(G)*	≥34

only a small fraction of the particles. These observations apply, in general, to all of the types of alumina coatings tested, both when unsupported and when supported in a matrix. The leach data suggest that unsupported particles from Lots 717B, 725D, and 733B performed well at 100 C, but these data have not been confirmed. As mentioned in a footnote to the table, difficulties in recovering particles from the capsules have caused these data to be uncertain.

The xenon release data for the matrix specimens, tested at 100 C, suggest a much lower degree of particle failure than the leach data indicate. This is believed to be due to retention of fission gas by the matrices at low temperature. Supporting evidence for this is the fact that 270 ppm of Kr^{85} was released from one specimen when it was heated to 815 C after the irradiation. The Xe^{133} release from this specimen (determined by puncturing the capsule at room temperature) was only 0.8 ppm, although the leach data indicated that over 40 per cent of the particles were cracked.

Sweep-Capsule Irradiations

Sweep-capsule irradiations of alumina-coated particles were conducted to provide additional information on the problem of low-temperature failure. A specimen of unsupported Lot 715A particles was tested at 100 C (see Table 7). The R/B values (ratio of release rate to production rate) determined from the first fission-gas sample were on the order of 10^{-4} after only 8 hr of irradiation. No increase in the release was observed in an additional 38 days, indicating that all of the failure occurred in the first 8 hr. Over 82 per cent of the particles were found to be cracked when they were leached at the end of the irradiation.

A heat-treated specimen of Lot 715A particles (715A-HT) was tested in the same manner, and again failure was essentially complete in only 8 hr at 100 C. The R/B for Xe^{133} was on the order of 10^{-4} (see Table 2). In these tests an R/B of only 10^{-9} to 10^{-8} is caused by uranium contamination in the coatings. Total failure of the particles gives an R/B of about 2×10^{-4}.

A sweep-capsule irradiation of a graphite-matrix specimen of Lot 725D particles was performed at elevated temperatures. The results of this experiment are given in Table 8. During the first 4 days at 1050 C, the R/B values for all species remained below 10^{-8}, indicating little, if any, failure. After this time, an electrical-heater failure caused a temperature drop to 775 C, and operation of the reactor at reduced power caused an additional drop to 440 C for a period of about 3 days. A gas sample taken at 440 C showed a large increase in the release, suggesting that the decrease in temperature had caused coating failure. Little change in the release was observed during the remaining 37 days of irradiation at 750 C. The R/B for Xe^{133} remained at about 2×10^{-6}, indicating that some failure had occurred but that it was probably not total failure.

To further investigate the temperature dependence of coating failure, a variable-temperature sweep-capsule experiment was performed with unsupported alumina-coated particles from Lot 715A. The data are given in Table 9 and are shown graphically in

TABLE 7. LOW-TEMPERATURE (100 C) SWEEP-CAPSULE IRRADIATIONS OF ALUMINA-COATED UO_2

Sample	Time, days	R/B					Uranium Removed in Leach, per cent
		Kr^{87}	Kr^{88}	Xe^{135}	Kr^{85m}	Xe^{133}	
715A	1/3	--	--	3×10^{-4}	--	2×10^{-4}	--
	3	3.7×10^{-5}	4.3×10^{-5}	9.1×10^{-5}	7.1×10^{-5}	4.3×10^{-4}	--
	3	--	--	7.8×10^{-5}	--	1.6×10^{-4}	--
	7	4.7×10^{-5}	4.4×10^{-5}	5.1×10^{-5}	7.5×10^{-5}	1.5×10^{-5}	--
	7	--	--	2×10^{-5}	2×10^{-5}	1×10^{-4}	--
	10[a]	--	--	1.7×10^{-5}	--	5.1×10^{-5}	--
	16	7.6×10^{-5}	4.4×10^{-5}	2.2×10^{-5}	1.3×10^{-4}	7.8×10^{-5}	--
	16	--	--	1.1×10^{-4}	--	1.0×10^{-4}	--
	17	2.6×10^{-5}	3.6×10^{-5}	3.7×10^{-5}	6.8×10^{-5}	1.9×10^{-4}	--
	28	3.9×10^{-5}	1.9×10^{-5}	6.1×10^{-5}	5.1×10^{-5}	2.3×10^{-4}	--
	28	--	--	3.5×10^{-6}	--	1.0×10^{-5}	--
	35	2.2×10^{-5}	1.3×10^{-5}	2.8×10^{-5}	5.0×10^{-5}	8.0×10^{-5}	--
	38	--	--	3.4×10^{-5}	--	9.3×10^{-5}	>82
715A-HT	1/3	--	--	--	--	1.4×10^{-4}	--

(a) This sample was taken 1 hr after a reactor shutdown. No krypton isotopes were detected.

TABLE 8. ELEVATED-TEMPERATURE SWEEP-CAPSULE IRRADIATION OF LOT 725D ALUMINA-COATED UO_2 PARTICLES IN A GRAPHITE MATRIX

Time, days	Temperature C	R/B				
		Kr^{87}	Kr^{88}	Xe^{135}	Kr^{85m}	Xe^{133}
1/12	1050	1.8×10^{-8}	4.3×10^{-9}	2.8×10^{-9}	9.5×10^{-9}	--
1/6	1050	1.5×10^{-8}	4.8×10^{-9}	4.0×10^{-9}	1.0×10^{-8}	--
1	1050	1×10^{-8}	5.0×10^{-9}	5.8×10^{-9}	1.0×10^{-8}	--
2	1050	--	--	6.1×10^{-9}	8.3×10^{-9}	4.7×10^{-9}
4	1050	--	--	5.8×10^{-9}	1.1×10^{-8}	1.2×10^{-8}
4	1050	--	--	5.5×10^{-9}	8.8×10^{-9}	1.0×10^{-8}
4	1050	--	--	3.3×10^{-9}	9.8×10^{-9}	7.0×10^{-9}
4.2	775	Heater failure				
5.3	440	Reactor at reduced power				
8.6	440	--	--	3.0×10^{-6}	--	1.4×10^{-4}
8.7	750	2.4×10^{-6}	1.2×10^{-6}	2.2×10^{-7}	3.0×10^{-6}	1.5×10^{-6}
9	750	4.1×10^{-6}	4.5×10^{-6}	9.9×10^{-6}	1.3×10^{-5}	7.5×10^{-6}
13	750	--	3.5×10^{-6}	4.9×10^{-6}	1.1×10^{-5}	1.2×10^{-5}
16	750	1.5×10^{-6}	1.2×10^{-6}	2.8×10^{-6}	4.5×10^{-6}	1.1×10^{-6}
26	750	6.0×10^{-7}	4.3×10^{-7}	1.5×10^{-6}	2.0×10^{-6}	4.1×10^{-6}
36	750	6.7×10^{-7}	4.0×10^{-7}	5.2×10^{-7}	1.8×10^{-6}	1.9×10^{-6}
46	750	5.0×10^{-7}	4.0×10^{-7}	5.9×10^{-7}	1.1×10^{-6}	2.8×10^{-6}

TABLE 9. VARIABLE-TEMPERATURE SWEEP-CAPSULE IRRADIATION OF UNSUPPORTED LOT 715A ALUMINA-COATED UO_2 PARTICLES

Time, days	Temperature C	R/B				
		Kr^{87}	Kr^{88}	Xe^{135}	Kr^{85m}	Xe^{133}
1/12	815					
3/4	815					
2	645	All species about 4×10^{-9}				
3	645					
4	645					
4.1	470					
5.0	470	3.7×10^{-7}	3.0×10^{-7}	3.1×10^{-7}	1.1×10^{-6}	4.2×10^{-6}
6	470	1.5×10^{-6}	1.1×10^{-6}	2.3×10^{-6}	3.3×10^{-6}	1.4×10^{-4}
7	470	2.7×10^{-6}	1.8×10^{-6}	1.8×10^{-6}	7.4×10^{-6}	1.0×10^{-4}
8	645	1.9×10^{-6}	1.3×10^{-6}	2.0×10^{-6}	4.1×10^{-6}	2.0×10^{-5}
9	645	2.1×10^{-6}	1.4×10^{-6}	2.7×10^{-6}	5.0×10^{-6}	1.5×10^{-5}
9	645	4.3×10^{-6}	2.1×10^{-6}	1.5×10^{-6}	8.0×10^{-6}	4.1×10^{-5}
10	645	1.6×10^{-6}	7.7×10^{-7}	4.4×10^{-6}	3.0×10^{-6}	7.3×10^{-6}
12.5	645	1.0×10^{-6}	7.1×10^{-7}	3.0×10^{-6}	2.7×10^{-6}	1.2×10^{-5}
12.7	470	1.1×10^{-6}	7.2×10^{-7}	2.2×10^{-6}	3.0×10^{-6}	5.9×10^{-6}
14	470	3.0×10^{-6}	1.9×10^{-6}	9.0×10^{-6}	7.1×10^{-6}	1.8×10^{-4}
14.5	470(a)	--	--	6.8×10^{-6}	--	1.1×10^{-4}
14.6	295	9.9×10^{-6}	5.2×10^{-5}	5.4×10^{-5}	2.3×10^{-5}	4.0×10^{-3}
17.6	295	5.1×10^{-5}	2.8×10^{-5}	1.3×10^{-4}	1.3×10^{-4}	3.0×10^{-4}
18.5	815	7.6×10^{-5}	5.2×10^{-5}	1.2×10^{-4}	1.7×10^{-4}	5.8×10^{-4}
23	815	1.2×10^{-4}	5.7×10^{-5}	1.0×10^{-4}	1.8×10^{-4}	5.7×10^{-4}
25	815	3.8×10^{-5}	2.3×10^{-5}	6.2×10^{-5}	8.3×10^{-5}	3.3×10^{-4}

(a) Taken 5.2 hr after shutdown. The presence of krypton isotopes was doubtful.

Figure 28. The capsule was operated at 815 C for 2 days and then at 645 C for 2 days. The R/B values remained at about 4×10^{-9} during this period, indicating little, if any, failure. The temperature was then reduced to 470 C, and a gas sample taken about 2 hr after the temperature change still gave R/B values of about 4×10^{-9}. It was not until 24 hr later that the continuous line monitors began to show an increase in release, which appeared as discrete bursts occurring at 1 to 2-hr intervals. These bursts are believed to have resulted from the release of stored fission gas as the coatings failed on individual particles. An adsorption sample taken at this time showed an increase of two orders of magnitude in the release of all species. The release continued to increase throughout the 4 days of operation at 470 C, until an average R/B of about 3×10^{-6} was reached for xenon-135 and the three kryptons. Xenon-133 is not a good indicator of the fraction of particles failed during periods when failure is occurring, for release of stored gas from the particles results in unusually high R/B values for xenon-133. The shorter lived xenon-135 and the krypton species are not influenced to as large a degree by stored-gas release; so these gases are a better measure of particle integrity during these nonequilibrium periods.

After the 4 days at 470 C, the temperature was raised to 645 C again and maintained at that level for 5 days. No additional failure occurred during this period. The R/B values at this point indicated that 90 per cent or more of the particles were still intact. The temperature was then reduced to 470 C, and, after 2 days at 470 C, the temperature was dropped to 295 C. An immediate increase in release was detected on the line monitors, and an adsorption sample taken about 3 hr after the temperature change showed a large increase in the R/B values. After 4 days at 295 C, the temperature was raised to 815 C and maintained at that level for 1 week. No increase in release was observed during operation at 815 C, and the equilibrium R/B values obtained at this temperature were indicative of total specimen failure. It is apparent that low-temperature failure becomes important below about 500 C, and it appears that the rate of failure increases as the temperature decreases.

A sweep-capsule test was also performed on the dense-porous-dense alumina-coated UO_2 material (4E) in a graphite matrix. This is the same material as that studied in the Sanderson & Porter Pebble-Bed Reactor project. The results of this sweep-capsule irradiation at 1070 C are given in Table 10. The R/B values throughout the 8 days of this test were on the order of 10^{-6}, except for the initially high release of Xe^{133} which is indicative of particles failing. These data suggest that the dense-porous-dense type coating does not perform as well at high temperature as the fully dense alumina coatings.

A graphite-matrix specimen of UO_2 particles coated first with 14 μ of laminar pyrolytic carbon and then with 29 μ of dense alumina (736B) was also tested in an elevated-temperature sweep capsule. The results of this experiment are given in Table 11. At the beginning of the irradiation at 1050 C the R/B values were on the order of 10^{-8}, and they remained at this level for the first 2 weeks. An electrical-heater failure in the first week, which caused a temperature drop to 800 C, did not noticeably affect the specimen. At the end of the first 2 weeks the release went up by over two orders of magnitude, and it continued to increase over a period of about 3 weeks. After the irradiation, the specimen was leached and 34 per cent or more of the particles were found to be cracked. This specimen did not exhibit the high-temperature integrity of dense alumina coatings. Its behavior was characteristic of pyrolytic-carbon coatings, as will be discussed in a later section.

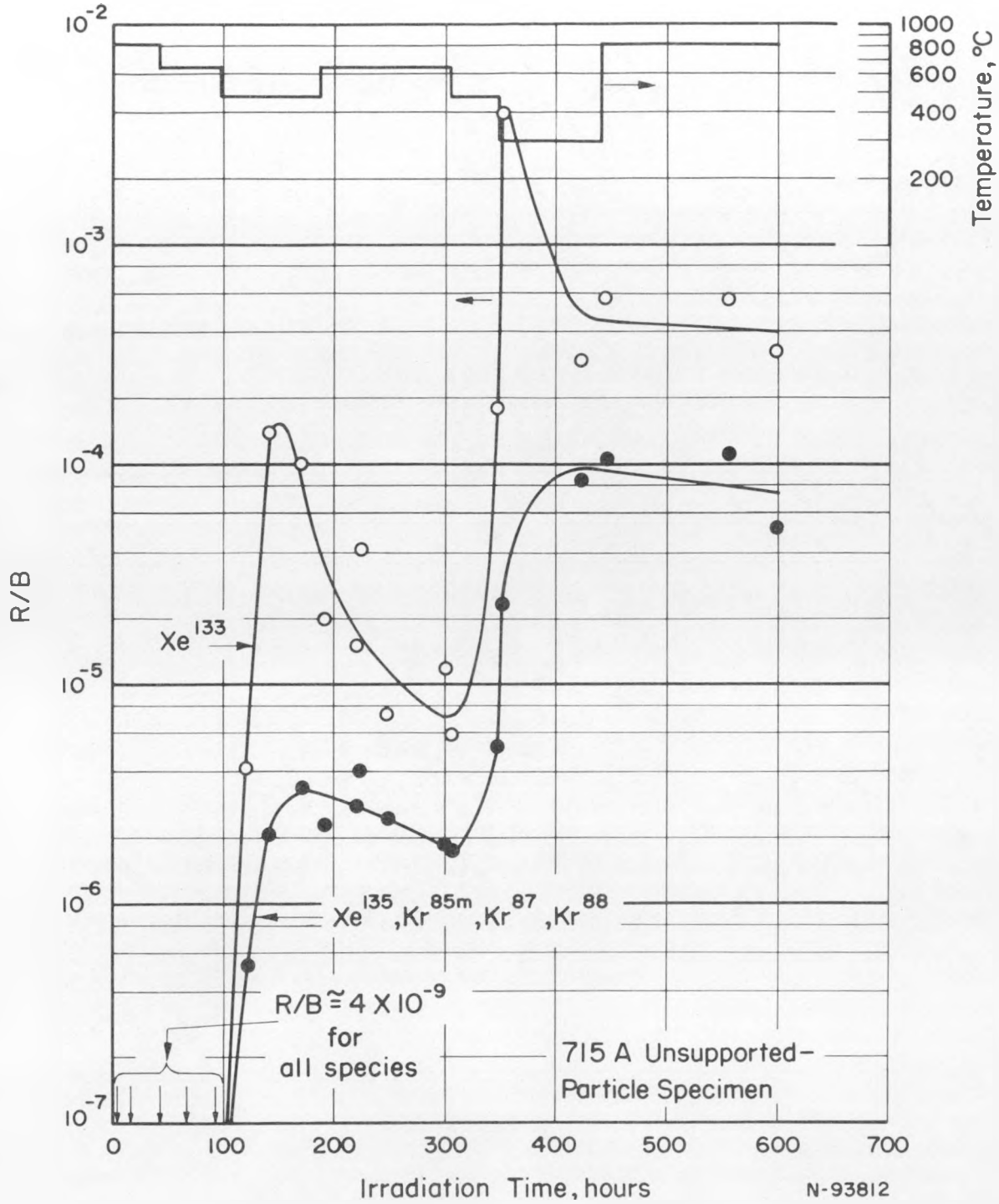

FIGURE 28. VARIABLE-TEMPERATURE SWEEP-CAPSULE IRRADIATION OF ALUMINA-COATED UO_2

TABLE 10. ELEVATED-TEMPERATURE SWEEP-CAPSULE IRRADIATION AT 1070 C OF LOT 4E DENSE-POROUS-DENSE ALUMINA-COATED UO_2 PARTICLES IN A GRAPHITE MATRIX

Time, days	R/B				
	Kr^{87}	Kr^{88}	Xe^{135}	Kr^{85m}	Xe^{133}
1/12	--	--	--	1.4×10^{-6}	4.1×10^{-5}
1/2	2.9×10^{-6}	3.6×10^{-6}	2.4×10^{-6}	6.4×10^{-6}	4.7×10^{-5}
2	1.2×10^{-6}	2.7×10^{-6}	2.9×10^{-6}	5.5×10^{-6}	1.3×10^{-5}
3	2.4×10^{-6}	3.5×10^{-6}	1.1×10^{-6}	6.0×10^{-6}	4.9×10^{-6}
4	4.8×10^{-7}	6.0×10^{-6}	2.5×10^{-6}	6.5×10^{-6}	9.4×10^{-6}
5	2.1×10^{-6}	4.2×10^{-6}	1.8×10^{-6}	7.7×10^{-6}	6.7×10^{-6}
6	6.4×10^{-6}	2.9×10^{-6}	1.7×10^{-6}	1.2×10^{-6}	6.7×10^{-6}
7	4.4×10^{-6}	6.7×10^{-6}	3.7×10^{-6}	1.2×10^{-6}	1.7×10^{-6}
8	--	--	1.6×10^{-6}	--	7.5×10^{-6}

TABLE 11. ELEVATED-TEMPERATURE SWEEP-CAPSULE IRRADIATION OF LOT 736B COMPOSITE PyC-Al_2O_3-COATED UO_2 PARTICLES IN A GRAPHITE MATRIX

Time, days	Temperature C	R/B					Uranium Removed in Leach, per cent
		Kr^{87}	Kr^{88}	Xe^{135}	Kr^{85m}	Xe^{133}	
1/24	1050	--	--	3.3×10^{-9}	7.6×10^{-8}	--	--
2	1050	3.2×10^{-8}	2.1×10^{-8}	2.5×10^{-8}	5.5×10^{-8}	5.6×10^{-8}	--
5	800	--	1.5×10^{-8}	1.1×10^{-8}	3.1×10^{-8}	3.1×10^{-8}	--
7	800	--	--	2.7×10^{-8}	2.5×10^{-8}	5.6×10^{-8}	--
11[a]	800	--	--	--	--	--	--
12	800	--	--	2.6×10^{-8}	1.8×10^{-8}	3.2×10^{-8}	--
15	800	4.2×10^{-6}	2.6×10^{-6}	5.4×10^{-6}	8.0×10^{-6}	4.5×10^{-5}	--
15.5	800	1.2×10^{-5}	5.0×10^{-6}	9.3×10^{-6}	1.5×10^{-5}	4.2×10^{-5}	--
18	800	6.9×10^{-6}	3.7×10^{-6}	2.3×10^{-5}	1.4×10^{-5}	4.4×10^{-4}	--
19	800	1.4×10^{-5}	6.7×10^{-6}	1.7×10^{-5}	2.3×10^{-5}	1.6×10^{-4}	--
22	800	4.8×10^{-5}	2.9×10^{-5}	5.1×10^{-5}	5.4×10^{-5}	1.3×10^{-4}	--
22[b]	800	--	--	4.2×10^{-6}	--	5.3×10^{-6}	--
34	800	--	3.0×10^{-4}	1.2×10^{-3}	8.7×10^{-4}	3.6×10^{-3}	--
34	800	1.1×10^{-3}	3.3×10^{-4}	5.2×10^{-4}	6.3×10^{-4}	1.5×10^{-3}	--
38	800	1.0×10^{-3}	4.1×10^{-4}	1.2×10^{-3}	3.2×10^{-4}	5.4×10^{-3}	--
39	800	6.1×10^{-4}	3.9×10^{-4}	1.0×10^{-3}	3.9×10^{-4}	4.4×10^{-3}	--
42	800	1.2×10^{-4}	9.0×10^{-5}	1.6×10^{-4}	2.1×10^{-4}	1.2×10^{-3}	--
53	800	--	--	5.8×10^{-3}	2.4×10^{-3}	3.0×10^{-2}	--
63	800	5.9×10^{-5}	2.4×10^{-5}	4.0×10^{-5}	8.3×10^{-5}	1.4×10^{-4}	--
69	320-400	Temperature dropped to 320-400 C for about 18 hr					
76	600	--	--	2.1×10^{-4}	--	9.0×10^{-4}	>34

(a) Taken 1.5 hr after shutdown. No fission gases were detected.
(b) Taken 1.5 hr after shutdown. The presence of krypton activity was possible.

A sweep-capsule experiment is in progress in which heat-treated alumina-coated UO_2 particles (715A-HT) in a pelletized graphite matrix are being irradiated at about 850 C. This specimen is still exhibiting excellent fission-product retention after about 2 per cent burnup or 6 weeks of irradiation. The R/B values have been on the order of 10^{-8} for all species. This irradiation will be continued to a burnup of 10 to 12 per cent.

Discussion of Results

The results of radiation testing of alumina-coated UO_2 particles can be summarized as follows:

(1) Dense, as-deposited Al_2O_3 coatings fail rapidly during low-temperature (100 C) irradiation. Essentially complete failure occurs in just a few hours.

(2) The same materials do not fail appreciably at 1070 C, at 3 per cent uranium burnup.

(3) A variable-temperature sweep test showed that some coating failure occurs at 470 C but not at 645 C. At 295 C failure is more complete and more rapid than at 470 C.

(4) Annealing of dense alumina coatings does not improve their low-temperature behavior.

(5) Intervening porous layers do not significantly reduce the low-temperature failure, and they do not appear to provide the high degree of containment possible at elevated temperatures with fully dense alumina coatings.

(6) Alumina-overcoated, pyrolytic-carbon-coated UO_2 particles exhibit poor behavior at elevated temperatures.

(7) Graphite matrices do not reduce coating failure, but they may retain fission gas at low temperatures.

The cause of the low-temperature failure of alumina-coated UO_2 particles is believed, at this time, to be radiation damage. Damage produced by the fission recoils is believed to cause an expansion of the interior of the Al_2O_3 coatings, which places this region in compression and causes a tensile stress to be exerted on the outer portion of the coatings. Above 500 C, annealing of the damage is apparently sufficiently rapid to prevent cracking.

Studies of Beryllia-Coated Fuel Particles

Radiation testing of UO_2 particles coated with 60 μ of dense BeO has just recently been initiated. Two sweep-capsule irradiations at 100 C have been performed, and the results are given in Table 12. In the first experiment, the R/B values were on the

TABLE 12. LOW-TEMPERATURE (100 C) SWEEP-CAPSULE IRRADIATIONS OF BeO-COATED UO_2

Test	Time, days	R/B				
		Kr^{87}	Kr^{88}	Xe^{135}	Kr^{85m}	Xe^{133}
1	1/24	--	2.0×10^{-5}	5.0×10^{-6}	3.8×10^{-5}	--
	1/6	5.3×10^{-5}	2.6×10^{-5}	2.0×10^{-5}	6.9×10^{-5}	5.5×10^{-6}
	2/3	3.7×10^{-6}	2.2×10^{-6}	1.2×10^{-5}	8.8×10^{-6}	3.3×10^{-6}
	8	4.0×10^{-6}	3.7×10^{-6}	2.1×10^{-5}	1.1×10^{-5}	6.7×10^{-5}
	18	5.1×10^{-6}	2.7×10^{-6}	9.2×10^{-6}	1.1×10^{-5}	4.5×10^{-5}
	32	1.7×10^{-5}	7.2×10^{-6}	4.2×10^{-5}	2.6×10^{-5}	2.5×10^{-4}
2	1/10(a)	--	2.0×10^{-5}	3.8×10^{-5}	5.0×10^{-6}	--
	1-1/2	--	--	1.8×10^{-5}	--	1.6×10^{-5}

(a) This sample was taken 30 min after the reactor reached full power (2 megawatts). Prior to this the reactor operated for about 2 hr at reduced power (<1 megawatt).

order of 10^{-5} after only 1 hr of irradiation, and they remained at this level throughout the experiment. Leach data are not yet available, so the fraction of the particles failed is not known. The fission-gas release, however, indicates that greater than 10 per cent and possibly as much as 50 per cent of the particles failed. The release from failed BeO-coated particles would be expected to be about the same as the release from failed Al_2O_3-coated particles, on the basis of fission-gas-diffusion studies reported earlier.

A second low-temperature test was performed with another specimen of particles from the same lot, but this specimen was upgraded by preirradiation oxidation and leaching and by removing particles that appeared to be of poor quality. The results were the same, however, high release being observed just after starting the irradiation. Beryllia-coated particles apparently behave in a manner similar to alumina-coated ones, at least at low temperature.

Studies of Pyrolytic-Carbon-Coated Fuel Particles

The pyrolytic-carbon-coated particles tested have included UC_2 coated at 1400 C with either columnar (Lot 918A) or laminar PyC (Lot 919A), UO_2 coated at 1400 C with laminar PyC (Lot 920A), UO_2 coated at 1300 C with 11 μ of laminar PyC and overcoated at 1600 C with 55 μ of laminar PyC (1010A), and UO_2 coated first with dense Al_2O_3 and then with mixed laminar and columnar PyC (Lot 921). As in the case of the alumina particles, the tests included both static- and sweep-capsule irradiations of both unsupported-particle specimens and matrix specimens.

Static-Capsule Irradiations

Static-capsule irradiations of pyrolytic-carbon-coated particles have been carried out at 100 C and at 1070 C to uranium burnups of about 4 per cent. The results of these tests are summarized in Table 13. These data indicate that the behavior of pyrolytic-carbon coatings is significantly different from that observed for alumina coatings. Considerable failure occurred at both high and low temperatures. This was true of both laminar and columnar coatings and of both UO_2 and UC_2 fuel particles. The particles with the composite coatings (Lot 921) exhibited good integrity at 1070 C, compared to the other materials. The Al_2O_3 undercoatings on these particles were cracked in fabrication and would thus not retain fission gases, but they apparently inhibited failure of the pyrolytic carbon, at least at high temperature.

The xenon-133 release was, in general, higher for pyrolytic-carbon-coated particles than for alumina-coated ones. This can be explained by the higher diffusion coefficients for fission gases in pyrolytic carbon. Because of this, back-diffusion of xenon recoils out of the inside surface of the carbon coatings and through the cracks in the particles is more rapid than in the case of alumina coatings.

TABLE 13. RADIATION-TEST RESULTS FOR PYROLYTIC-CARBON-COATED PARTICLES

Sample	Fuel Material	Coating Description	Tests of Particles Alone						Tests of Particles in Matrix[a, b]					
			Tested at 100 C			Tested at 1070 C			Tested at 100 C			Tested at 1070 C		
			Burnup, per cent	Xe^{133} Release, ppm	Uranium Removed in Leach, per cent	Burnup, per cent	Xe^{133} Release, ppm	Uranium Removed in Leach, per cent	Burnup, per cent	Xe^{133} Release, ppm	Uranium Removed in Leach, per cent	Burnup, per cent	Xe^{133} Release, ppm	Uranium Removed in Leach, per cent
918A	UC_2	55 μ of columnar PyC, 1400 C	3.1	250	93	3.8	6200	>21	--	--	--	1.8	5300(G)*	--
919A	UC_2	70 μ of laminar PyC, 1400 C	3.2	18	--	3.7	9000	>55	--	--	--	3 est.	30(G)[c]	5.6
920A	d. UO_2	45 μ of laminar PyC, 1400 C	3.4	290	30	3.8	2100	66	--	--	--	3 est.	400(G)[c]	90
			3.7	84	3[d]	--	--	--	--	--	--	--	--	--
1010A	d. UO_2	66 μ of laminar PyC 11 μ at 1300 C, 55 μ at 1600 C	3.6	--	0.1[d]	4 est.	15,000	--	--	--	--	4 est.	50-940(G)*	--
921	d. UO_2	48 μ of 1000 C Al_2O_3 and	3.1	60	46	1.6	0.2	7.2	--	--	--	--	--	--
		32 μ of mixed 1400 C PyC	4.9	20	2.2[d]	3.3	0.02	3.0	--	--	--	--	--	--

(a) The asterisks denote sweep-capsule irradiation.

(b) The letter G indicates a graphite matrix.

(c) The temperature did not remain at 1070 C throughout these irradiations. The capsule operated at 1070 C for 4 days, at 440 C for 3 days, and at 750 C for the remaining 37 days.

(d) These data are uncertain, since only a small fraction of the particles were recovered from each capsule for leaching and foreign material was observed in the specimens.

Sweep-Capsule Irradiations

Sweep-capsule experiments at elevated temperatures were performed to provide an understanding of the rate of coating failure. A graphite-matrix specimen of columnar PyC-coated UC_2 particles (Lot 918A) was irradiated for 2 weeks at 1070 C. The release for the first 5 days was on the order of 10^{-9} to 10^{-8} (R/B values), indicating little, if any, failure (see Table 14). On the sixth day, however, a large increase in release was observed. This occurred when the reactor was started up after a 28-hr shutdown. At the same time a large pressure drop through the sweep system began to build up, with a resulting decrease in the flow of sweep gas. This caused large uncertainties in the R/B determinations and necessitated termination of the experiment after 14 days. It was apparent, however, that failure of the specimen did occur and not until after at least 5 days of irradiation.

Another specimen of 918A particles were irradiated unsupported in a sweep capsule operated at variable temperature. The temperature was maintained at 815 C the first two days, at 645 C for 2 days, at 470 C for 4 days, and at 645 C again for the last 3 days. The data for this test are given in Table 14. Little failure occurred until about the ninth day of irradiation, and on that day the R/B values increased by approximately four orders of magnitude. The failure did not appear to be related to any of the temperature changes. It may or may not be significant, but as in the preceding test, a reactor shutdown immediately preceded the initiation of failure.

A graphite-matrix specimen of laminar PyC-coated UO_2 particles (1010A) was also tested at elevated temperature in a sweep capsule. The results of this experiment are given in Table 15, and they show that the behavior of this material was essentially the same as that observed for the columnar PyC-coated UC_2 particles. At 1070 C the coatings remained intact through the first week of irradiation, but began to fail on about the tenth day. The release continued to increase for another 10 days, after which time a large fraction of the particles were apparently failed. Leach data are not yet available to confirm the degree of failure.

Discussion of Results

The results of radiation testing of pyrolytic-carbon-coated fuel particles can be summarized as follows:

(1) 1400 C pyrolytic carbon coatings fail severely when irradiated at both 100 C and 1070 C to burnups of 3 to 4 per cent.

(2) Failure of pyrolytic-carbon coatings at elevated temperature is much slower than the low-temperature failure of alumina coatings. It does not begin until after about 1 week of irradiation, and it continues over a period of at least 10 days.

(3) Release of fission gas from failed carbon coatings is higher than from failed alumina coatings.

TABLE 14. ELEVATED-TEMPERATURE SWEEP-CAPSULE IRRADIATIONS OF PYROLYTIC-CARBON-COATED UC_2

Sample	Time, days	Temperature, C	R/B				
			Kr^{87}	Kr^{88}	Xe^{135}	Kr^{85m}	Xe^{133}
918A(G)	1/12	1070	--	--	--	4.6×10^{-10}	--
	1/6	1070	--	--	--	4.3×10^{-9}	--
	1	1070	9.2×10^{-9}	--	1.2×10^{-8}	6.9×10^{-9}	--
	2	1070	1.4×10^{-8}	1.1×10^{-8}	3.3×10^{-9}	2.9×10^{-8}	--
	3	1070	3.4×10^{-9}	6.4×10^{-9}	7.9×10^{-9}	8.2×10^{-9}	--
	4	1070	7.4×10^{-9}	1.7×10^{-8}	1.1×10^{-8}	3.1×10^{-8}	1.1×10^{-8}
	5	1070	6.2×10^{-9}	1.7×10^{-8}	1.3×10^{-8}	3.1×10^{-8}	2.1×10^{-8}
	5-1/2	1070	6.0×10^{-9}	1.3×10^{-8}	1.6×10^{-8}	2.5×10^{-8}	3.2×10^{-8}
	6	1070	--	--	1.1×10^{-4}	1.6×10^{-4}	3.2×10^{-3}
	7	1070	2.9×10^{-6}	--	1.7×10^{-5}	3.6×10^{-6}	1.1×10^{-3}
	7	1070	--	--	3.3×10^{-5}	4.7×10^{-5}	2.5×10^{-4}
	7-1/2	1070	6.3×10^{-8}	9.7×10^{-7}	6.2×10^{-6}	3.5×10^{-6}	3.2×10^{-5}
	14	1070	--	6.6×10^{-3}	5.3×10^{-4}	5.0×10^{-3}	5.3×10^{-3}
918A	1/2	815					
	1	815					
	2	645					
	3	645					
	4	645		All species about 3×10^{-9}			
	4	470					
	5	470					
	6	470					
	7	470					
	8	645	3.1×10^{-8}	1.8×10^{-8}	--	3.8×10^{-8}	--
	9	645	2.6×10^{-6}	2.4×10^{-6}	1.9×10^{-6}	3.9×10^{-6}	2.3×10^{-5}
	9.5	645	1.1×10^{-4}	7.7×10^{-5}	3.2×10^{-5}	2.0×10^{-4}	2.9×10^{-4}
	10	645	9.6×10^{-5}	6.1×10^{-5}	7.1×10^{-5}	2.1×10^{-4}	3.9×10^{-4}

TABLE 15. ELEVATED-TEMPERATURE SWEEP-CAPSULE IRRADIATION OF LOT 1010A PYROLYTIC-CARBON-COATED UO_2 IN A GRAPHITE MATRIX

Time, days	Temperature, C	R/B				
		Kr^{87}	Kr^{88}	Xe^{135}	Kr^{85m}	Xe^{133}
1	1070	--	1.8×10^{-8}	3.7×10^{-8}	3.3×10^{-8}	5.4×10^{-8}
2	1070	1.9×10^{-8}	1.0×10^{-8}	1.9×10^{-8}	2.1×10^{-8}	5.3×10^{-8}
4	1070	--	--	3.7×10^{-8}	2.6×10^{-8}	1.1×10^{-7}
6	1070	1.0×10^{-8}	1.4×10^{-8}	1.4×10^{-8}	2.2×10^{-8}	5.9×10^{-8}
10	1070	2.4×10^{-6}	1.4×10^{-6}	2.0×10^{-6}	3.9×10^{-6}	9.8×10^{-6}
15	1070	1.8×10^{-5}	1.0×10^{-5}	1.0×10^{-5}	2.3×10^{-5}	3.8×10^{-5}
18	1070	1.8×10^{-5}	1.0×10^{-5}	6.9×10^{-6}	3.0×10^{-5}	2.5×10^{-5}
20	1070	--	--	6.1×10^{-6}	1.0×10^{-4}	6.5×10^{-4}
20	1070	1.3×10^{-4}	4.1×10^{-5}	6.6×10^{-5}	1.1×10^{-4}	3.9×10^{-4}
23	1070	1.4×10^{-4}	5.5×10^{-5}	7.9×10^{-5}	1.7×10^{-4}	3.4×10^{-4}
26	960	2.9×10^{-5}	1.8×10^{-5}	1.3×10^{-5}	6.2×10^{-5}	5.3×10^{-5}
30[a]	960	2.5×10^{-7}	1.7×10^{-7}	3.0×10^{-5}	9.4×10^{-7}	6.8×10^{-5}
32	960	1.9×10^{-5}	1.1×10^{-5}	2.8×10^{-5}	4.9×10^{-5}	1.4×10^{-4}
38	960	2.3×10^{-5}	1.2×10^{-5}	3.6×10^{-5}	4.7×10^{-5}	2.3×10^{-4}
44	960	5.3×10^{-5}	3.2×10^{-5}	8.1×10^{-5}	1.1×10^{-4}	6.7×10^{-4}
54	960	5.7×10^{-5}	3.6×10^{-5}	1.2×10^{-4}	1.2×10^{-4}	9.4×10^{-4}
59[b]	960	1.2×10^{-5}	2.1×10^{-5}	4.6×10^{-5}	5.6×10^{-5}	2.8×10^{-4}

(a) Sample taken 1 hr after shutdown.

(b) Sample taken 1.5 hr after shutdown.

(4) A composite coated particle, with a layer of dense alumina under a layer of mixed laminar and columnar pyrolytic carbon retains fission gas well at 1070 C, even though the alumina coatings are cracked before irradiation. Protecting the pyrolytic carbon from fission recoils may reduce cracking of the PyC layer.

The cause of the failure of pyrolytic-carbon coatings may be due to fission-gas pressure, fission-fragment damage, fast-neutron damage, or swelling of the fuel core, to mention a few possibilities. It is not clear, at this time, which mechanism actually causes the failure, although some type of radiation damage to the coatings is suspected. This might be damage caused by the fission recoils, similar to that believed to be occurring in the alumina coatings, or it might be neutron damage. Future experiments will have the objective of clarifying the situation.

SUMMARY

Progress is being made towards the objectives of the BMI program for studying coated particle fuel materials, in identifying the principles governing the performance of these materials, and in determining combinations of material giving optimum performance.

Methods have been found for depositing impermeable alumina, beryllia, and magnesia and pyrolytic carbon coatings on particles of fuel materials. Methods for making ideal dispersions of these in graphite and oxide matrices also have been developed.

In radiation studies it has been found that the oxide coated materials retain their imperviousness to fission products if used at an elevated temperature, but fail almost instantly at low temperatures owing to cracking from radiation-induced strain. Ways to prevent this type of failure are being sought. Carbon coated materials are able to resist cracking for a longer time, but then fail at either high or low temperatures. The reasons for this are not yet understood but it is thought to be a consequence of fuel swelling or coating shrinkage. The effects of adding void space within the coated particle is being studied to determine whether this prevents failure.

The program is continuing with emphasis on designing coated particles so that failure in radiation will not occur in long times under practical conditions of gas cooled reactor operation.

ACKNOWLEDGMENT

Development of coated-particle fuel materials involves to various extents the efforts of a great many Battelle scientists. Their cooperation in furnishing data for this review of the program is gratefully acknowledged.

REFERENCES

(1) Elliot, J. F., and Gleiser, M., Thermochemistry for Steelmaking, Addison-Wesley Publishing Company, Reading, Mass. (1960), Vol 1.

(2) Klinger, W., Coucoulas, A., Komarek, K. L., "Study of the Reaction Rates Between Refractory Oxides and Graphite", New York University Report on Contract AF 33(616)-6082, Project 7022, Task 70634.

(3) Bleiberg, M. L., Maskarinec, G., Clark, D., and Yeniscavich, W., "Burnup Limitations of Bulk UO_2 Prototype Fuel Elements – An Interim Examination of the CR-V-n Experiment", Bettis Technical Review, USAEC Report WAPD-BT-18 (April 1960), pp 107-134.

(4) Lindner, R., and Matzke, H. J., "Diffusion of Xe^{133} in Uranium Oxide of Different Oxygen Contents", Z. Naturforsch., 14A, 582-584 (1959).

(5) Oxley, J. H., Secrest, A. C., Landrigan, R. B., Powell, C. F., and Blocher, J. M., Jr., "Coating and Preparation of Uranium and Thorium Carbides", USAEC Report BMI-X-160 (August 2, 1960).

(6) Browning, M. F., Cook, T. E., Veigel, N. D., Diethorn, W. S., and Blocher, J. M., Jr., "Alumina Coating of UO_2 Shot by Hydrolysis of Aluminum Chloride Vapors", USAEC Report BMI-1471 (October 25, 1960).

(7) Blocher, J. M., Jr., Browning, M. F., Secrest, A. C., Secrest, V. M., and Oxley, J. H., "Preparation of Ceramic-Coated Nuclear-Fuel Particles", in USAEC Report TID-7622 (May 22, 1962), pp 57-73.

(8) Smalley, A. K., Brockway, M. C., and Duckworth, W. H., "Improved Techniques for Dispersing Fuel Particles in Ceramic Bodies", USAEC Report BMI-1579 (May 22, 1962).

(9) Smalley, A. K., Riley, W. C., and Duckworth, W. H., "Alumina-Clad UO_2 for Fuel Applications", USAEC Report BMI-1321 (February 18, 1959).

(10) Paprocki, S. J., Keller, D. L., and Pardue, W. M., "Study of Experimental Fuel Bodies Made from Alumina-Coated UO_2 Particles", USAEC Report BMI-1586 (July 16, 1962).

DISCUSSION

Question, N. M. Levitz (ANL): "Have you investigated variations in the core materials in the coated particles, i.e., different types of UO_2?"

Reply, G. W. Cunningham (BMI): "Not much. Primarily spherical, dense, commercially available UO_2 particles have been used."

Question, C. W. Funk (AGN): "How were the matrix specimens prepared in the early part of the program, when particles were damaged?"

Reply, M. C. Brockway (BMI): "By planetary mixing."

Question, W. P. Chernock (CE): "What burnup do you have in mind for coated-particle fuels, and will the ceramic coatings survive the radiation damage?"

Reply, R. W. Dayton (BMI): "Our program is not directed toward any specific reactor concept; so we have no set burnup objective. We are trying to find how to achieve the highest possible burnup."

Question, L. R. Zumwalt (GA): "In discussing the diffusion of fission products from materials, was the time effect considered; i.e., a permeation time?"

Reply, R. W. Dayton (BMI): "We do not interpret our data in terms of permeation time, but in terms of fractional release ratio, R/B."

Question, L. R. Zumwalt (GA): "Perhaps xenon does not go through the coating because it is not soluble in the coating material."

Reply, R. W. Dayton (BMI): "Since you drive xenon into the lattice by recoil, it can essentially be said to be in solution."

Question, M. W. Rosenthal (ORNL): "What are the temperature limitations placed on the fuel by the Al_2O_3-C or PyC-UO_2 reactions?"

Reply, G. W. Cunningham (BMI): "The Al_2O_3-C reaction goes rapidly at 1100 C in vacuum. Fortunately, when a flowing gas such as the coolant is used, the removal of reactants such as CO is decreased and the maximum allowable temperature is increased. If CO can leave the pyrolytic-carbon coatings on UO_2 the carbon-UO_2 reaction will proceed; if held in the reaction will not continue. Thick pyrolytic-carbon coatings may be useful to 1700 C while thin coatings may be limited to 1400 C."

Question, G. B. Greenough (UKAEA): "Does the $BeCl_2$ react with the UO_2 or the fluidized-bed reactor material?"

Reply, J. M. Blocher (BMI): "There was no apparent effect on the fuel. There was with the reactor, but since precoating the reactor with BeO, contamination of the particle coatings by reactor materials has been minimized."

Comment, L. P. Pepkowitz (NUMEC): "I agree, there is no effect on the fuel."

Question, L. P. Pepkowitz (NUMEC): "Is the BMI program going to be extended to include evaluations of coated particles prepared by industrial firms?"

Reply, R. W. Dayton (BMI): "When the program was set up initially, we requested commercial vendors to supply test specimens of coated particles. Although interest was shown initially, we received only one specimen for test. The request is still open, and we hope commercial vendors will send us specimens for evaluation."

Question, D. W. Savage (UKAEA): "What is your interpretation of the decrease in density of pyrolytic-carbon coatings as the coating rate is increased?"

Reply, J. H. Oxley (BMI): "One interpretation proposed by British investigators is that sootlike particles are trapped in the coating at the higher rates. I believe this is the primary factor involved."

COATED-PARTICLE FUEL DEVELOPMENT AT OAK RIDGE NATIONAL LABORATORY

Compiled by W. O. Harms

Metals and Ceramics Division, Oak Ridge National Laboratory*
Oak Ridge, Tennessee

INTRODUCTION

The research program on coated-particle nuclear fuel elements at the Oak Ridge National Laboratory (ORNL) has been concerned in large measure with the broad evaluation of materials for gas-cooled, fueled-graphite systems involving pyrolytic-carbon-coated carbide fuel particles. The major emphasis in this connection has been on investigation of the behavior of these materials under simulated power reactor conditions, particularly with regard to fission-product retention. The test conditions have included high burnups, partially oxidizing environments, and a wide range of temperatures. The results of these investigations, in conjunction with those from more specialized supporting studies, have served to elucidate those properties and phenomena governing the performance of the materials under consideration. In addition, they have served to delineate those problem areas requiring further research effort for exploitation of this coated-particle concept.

A less extensive part of the program at ORNL has consisted of determining the potential of coated-particle fuel materials, involving both oxide- and pyrolytic-carbon-coated particles, in a variety of liquid coolants. Compatibility studies have been carried out in pressurized water, organic-moderator coolants, and molten fluoride salts, and the effects of gamma irradiation have been investigated.

Methods for chemical processing of graphite-matrix fuels containing both carbon- and alumina-coated particles have been investigated on a laboratory scale. The methods include "grind-leach," combustion-dissolution, the hot 90% nitric acid process, anodic disintegration, and

*Operated for the U. S. Atomic Energy Commission by the Union Carbide Corporation.

chloride volatility.

This paper describes the techniques used and the significant results and implications that have evolved in the three general problem areas comprising the ORNL Coated-Particle Fuel Element Development Program.

FUELED GRAPHITE, GAS-COOLED REACTOR APPLICATIONS

(F. L. Carlsen, Jr.)

EVALUATION AND IRRADIATION TESTING

The evaluation and irradiation testing program has been concerned primarily with vendor-supplied coated-particle materials. Materials have been supplied by the Minnesota Mining and Manufacturing Company (3M), National Carbon Company (NCC), High Temperature Materials, Incorporated (HTM), General Atomic (GA), Nuclear Materials and Equipment Company (NUMEC), and Speer Carbon Company (SCC).

This portion of the program is conveniently divided into two sections: (1) tests on unsupported pyrolytic-carbon-coated carbide particles; and (2) tests on graphite-matrix elements containing coated particles. Detailed descriptions and results of the evaluation and irradiation tests have appeared in ORNL Gas-Cooled Reactor Program Progress Reports.[1-6]

Unsupported Coated Particles

Unsupported coated particles have been studied in considerable detail and some 50 different batches have been examined. The fuel particles have for the most part been uranium carbide, although recently uranium-thorium carbide particles have been included.

---

[1] GCR Quar. Prog. Rep. Mar. 31, 1961, ORNL-3102, pp. 104–7.

[2] GCR Quar. Prog. Rep. June 30, 1961, ORNL-3166, pp. 84–8.

[3] GCR Quar. Prog. Rep. Sept. 30, 1961, ORNL-3210, pp. 133–46.

[4] GCR Quar. Prog. Rep. Dec. 31, 1961, ORNL-3254, pp. 137–65.

[5] GCR Quar. Prog. Rep. Mar. 31, 1962, ORNL-3302, pp. 165–222.

[6] GCRP Semiann. Sept. 30, 1962, ORNL-3372 (in press).

Preirradiation Evaluation (E. S. Bomar, J. L. Cook, R. J. Gray, R. W. McClung, Metals and Ceramics Division)

Unsupported coated particles are subjected to rigorous evaluation testing prior to in-reactor testing. The evaluation includes determination of the structure, shape, and dimensions of the coatings and particles, the amount of exposed fuel, the impurity content, the density, the crushing strength, and the effects of heat treatments.

Structure, Shape, and Dimensions. The structure of coated particles is determined by metallography, microradiography, and x-ray diffraction analysis. Photomicrographs showing the three principal types of pyrolytic-carbon coatings studied are shown in Figs. 1–3. The coating microstructure shown in Fig. 1 is termed laminar, because of its layer-like appearance. The structure shown in Fig. 2 is distinguished by its large, radially oriented grains and is described as columnar. Figure 3 shows the structure described as duplex because of the inner laminar coating, adjacent to the fuel particle, and the outer, fine-grained columnar coating. The uranium carbide particles generally are composed of UC_2, as the major phase, with minor amounts of UC and graphite flakes.[7] Generally there is a more or less continuous layer of graphite, which is present on the particles prior to coating, at the interface between the uranium carbide particle and the pyrolytic-carbon coating. Similar descriptions apply to uranium-thorium carbide particles.

X-ray diffraction analyses have been performed to determine the interlayer spacing and crystallite size of several coatings. The observed interlayer spacings range from 3.42 A to values greater than that for "turbostratic" carbon. (The interlayer spacing is thought to reflect the degree of stacking order in the graphite crystal structure. For ideal crystalline graphite this spacing is 3.354 A and for the completely disordered "turbostratic" carbon it is 3.440 A.[8]) The crystallite sizes of the coatings, as determined by x-ray diffraction

---

[7]C. K. H. DuBose and R. J. Gray, Metallography of Pyrolytic Carbon Coated and Uncoated Uranium Carbide Spheres, ORNL-TM-91 (Mar. 21, 1962).

[8]J. Biscoe and B. E. Warren, J. Appl. Phys. 13, 364 (1942).

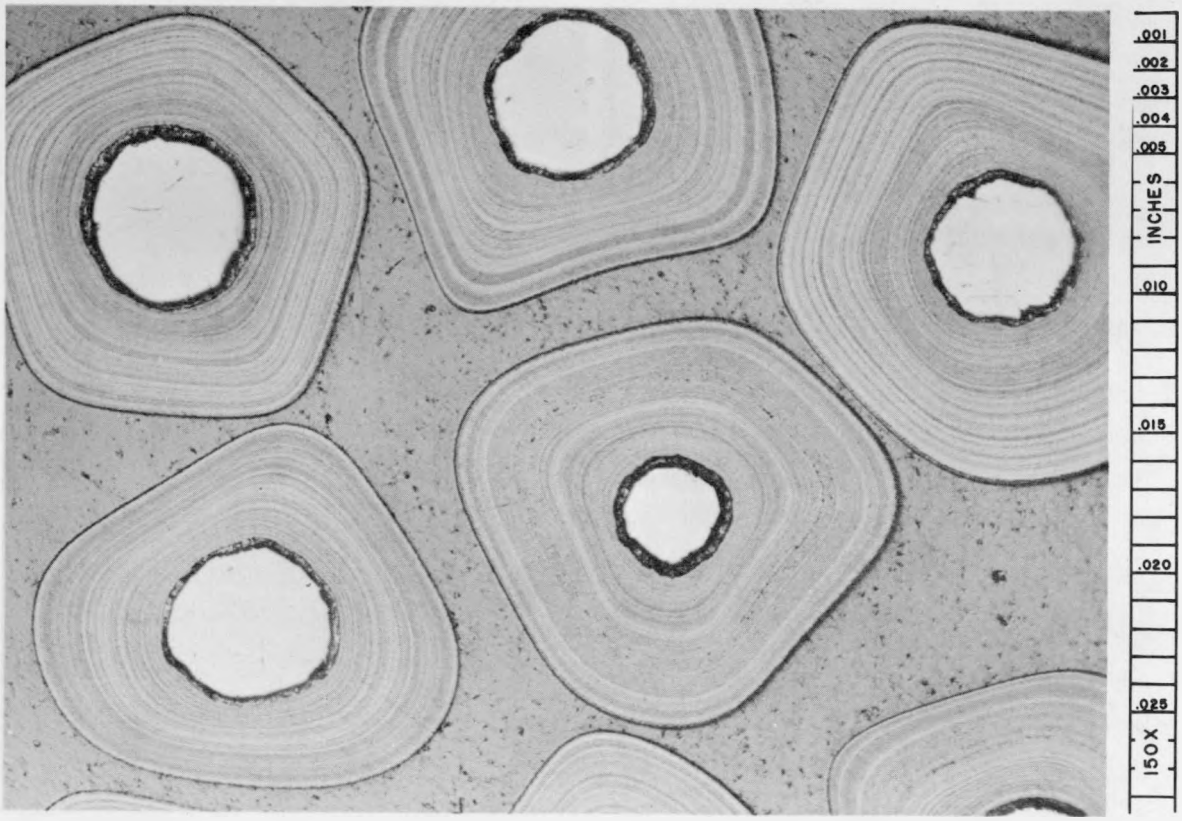

Fig. 1. Photomicrograph of Laminar-Pyrolytic-Carbon-Coated Uranium Carbide Particles from Batch 3M-SP-2. Bright-field. As-polished.

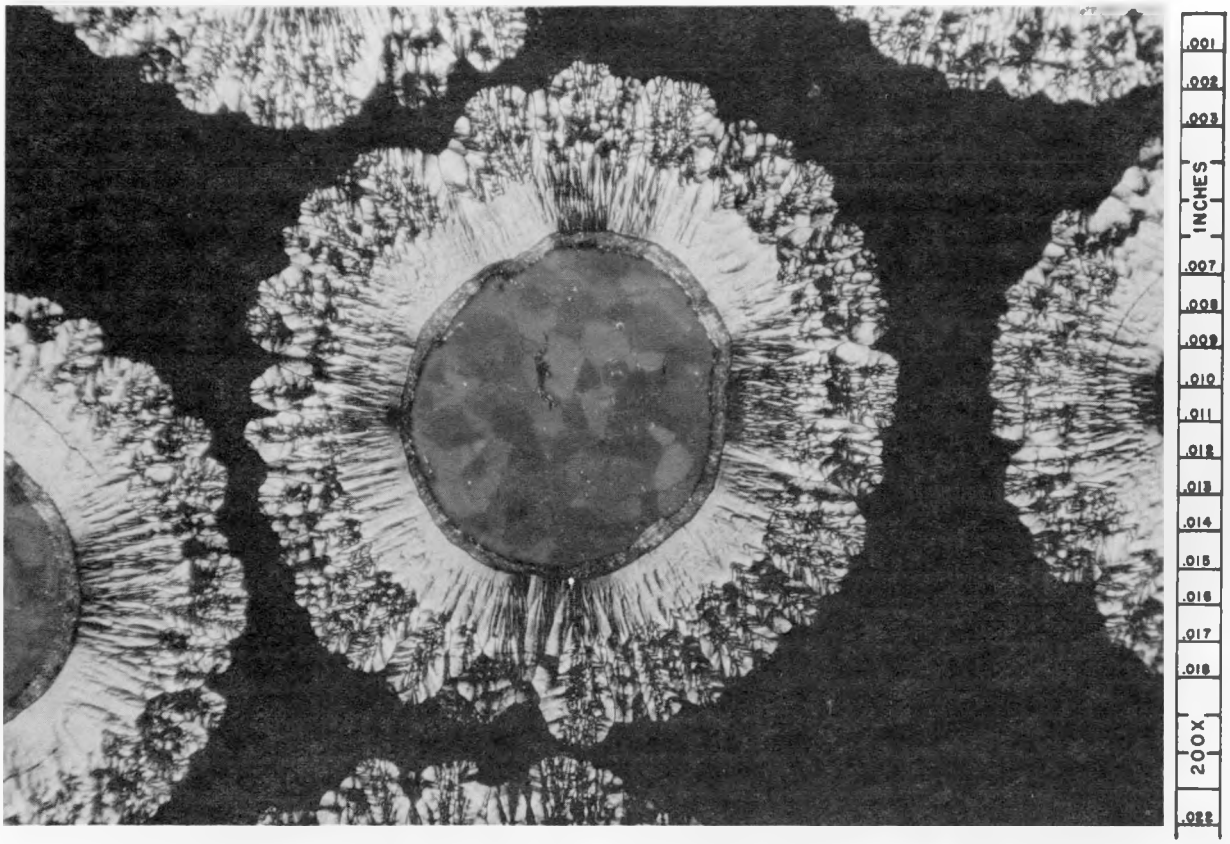

Fig. 2. Photomicrograph of Columnar-Pyrolytic-Carbon-Coated Uranium Carbide Particles from Batch HTM-1. Polarized light. Etchant: HAC, HNO_3, H_2O 1:1:1.

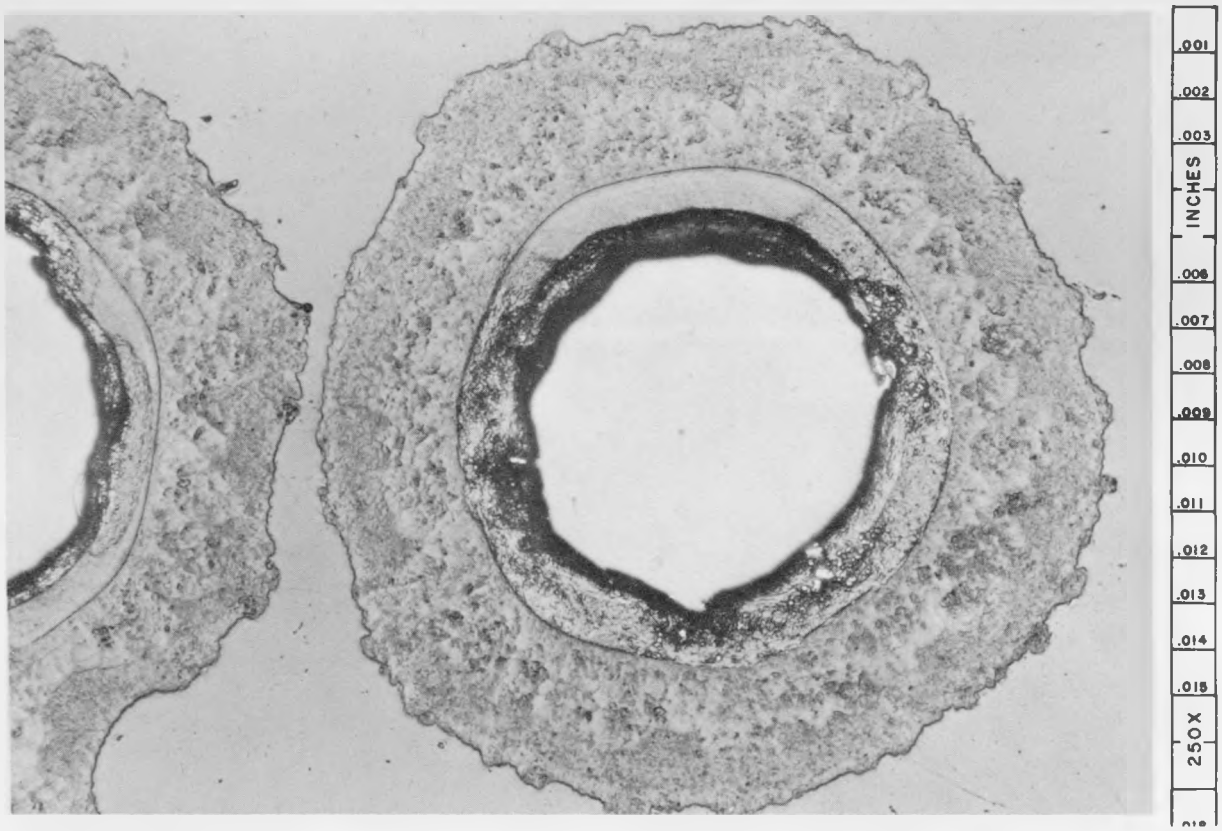

Fig. 3. Photomicrograph of Duplex-Pyrolytic-Carbon-Coated Uranium Carbide Particles from Batch NCC-AD. Bright-field. As-polished.

line broadening, range from 25 to 70 A for laminar coatings to 85 to 95 A for duplex coatings. In general, neither the c-spacing nor crystallite size correlate well with the type of coating microstructure.

Microradiographic examination gives additional information about the structure of coated particles.[5,9] It is particularly useful in determining the extent of uranium migration in the pyrolytic carbon coatings (see, for example, Figs. 4 and 11) and the presence of void space between the coating and particle. This nondestructive technique also allows the accurate determination of the dimensions and shape of coated particles. Coating thickness is very accurately determined by this technique because the coating thickness at the midplane of a coated particle is very well defined in the microradiographs. The dimensions are determined from 50-particle samples selected at random. For a typical batch of coated particles, with an average particle diameter of approx 200μ and average coating thickness of approx 100μ, the standard deviations for these dimensions are 25 and 13μ, respectively. The shape of the fuel particles in a given lot often ranges from nearly spherical to irregular with major-to-minor diameter ratios of 3:1.

Exposed Fuel. The amount of exposed fuel in a sample of coated particles is determined from measurements of the alpha activity and the amount of uranium removed by leaching in 8 M HNO_3 at 95°C for 8 hr. The alpha activity is proportional to the amount of uranium within approx 20μ of the surfaces of the coated particles. The uranium removed by leaching comes both from particles with cracked coatings as well as from the surface of the coatings on sound particles. In general, the amount of exposed fuel is less than 5×10^{-3}% of that contained in the coated particles.

Impurity Content. Chemical analyses are used to determine the amount of uranium in the coated particles as well as the impurity content. The nature and quantity of the analytical data obtained, however, are such that no positive statement regarding impurity levels can be made at the present time.

---

[9]R. W. McClung, Techniques for Low-Voltage Radiography, ORNL-3252 (Feb. 14, 1962).

Density. Several methods have been evaluated for determining the density of both uncoated and coated particles. A technique employing a helium pycnometer is felt to be the most satisfactory.[10] The density of the uncoated uranium carbide particles is generally between 10.0 and 11.0 g/cm^3. The density of the coated particles depends upon the ratio of coating thickness to particle diameter and ranges between 2.5 and 6.5 g/cm^3.

The density of the coatings is determined by a sink-float method on fragments obtained by crushing the coated particles with impact loading, followed by leaching in HNO_3 to remove the uranium carbide. By this method a range of density values is obtained for coatings in a given lot. For example, the densities of 89% of the fragments from a sample of duplex coatings were found to be in the range 1.86 to 1.92 g/cm^3 and those for the remaining fragments were equally distributed above and below this range. The density of the laminar coatings examined has ranged between 1.95 and 2.01 g/cm^3. The density of large-grained columnar coatings has not been determined.

Crushing Strength. Crushing-strength tests are performed by crushing individual coated particles from a randomly selected sample of 50 particles from each batch.[6] For a typical batch of coated particles with an average crushing load of approx 1500 g, the standard deviations range from 200 to 300 g. The load at failure has been found to increase as the coating thickness increases; it is less dependent upon the structure of the coating.

Effects of Heat Treatments. The routine evaluation of a lot of coated particles includes a thermal-cycling test in which a sample from a given lot of particles, previously leached in 8 M HNO_3, is subjected to three thermal cycles between approx 200 and 1500°C with a one-hour exposure at the temperature extremes in each cycle. The sample is heated in a small induction furnace which allows very rapid heating and cooling. The effect of the thermal cycling is determined by measuring the amount of exposed uranium by the acid-leaching and alpha-counting techniques. In general, the alpha activity is slightly increased

---

[10] P. Hidnert, Density of Solids and Liquids, NBS Circular 487, p. 24 (Mar. 15, 1950).

and the exposure to nitric acid results in the removal of quantities of uranium equal to or slightly greater than that for the as-received particles.

Extended heat treatments are employed to determine the long-time stability of coated particles, particularly with regard to uranium migration. In some tests the thermal conditions are selected to match those experienced by samples in irradiation experiments. In tests of several hundred hours it has been demonstrated that some uranium migration can occur[6] at temperatures up to 1400°C; however, complete penetration of 100μ-thick coatings has not been observed under these conditions. Heat treatments at higher temperatures result in an acceleration of the uranium migration. At 1900°C, for example, uranium migration is observed in only five minutes; complete penetration at 1900°C, however, requires exposure times greater than 100 hr.

The effect of heat-treatment temperature on uranium migration in laminar-coated particles is shown in the microradiographs of Fig. 4. Figure 4a shows the as-received material (no uranium apparent in the coatings). Figure 4b was taken after a heat treatment at 1750°C for 3 hr and shows that substantial uranium migration occurred. Figure 4c indicates that the effect of heat treatment for 5 min at 1950°C is similar to that after 3 hr at 1750°C.

Irradiation Tests (R. R. Sellers, Reactor Division; P. E. Reagan, R. M. Carroll, D. F. Toner, Reactor Chemistry Division; J. L. Scott, E. L. Long, Metals and Ceramics Division)

Neutron-Activation Tests. The irradiation testing of coated-particle materials begins with neutron-activation tests. These tests involve short-time exposures of samples at low temperatures in the ORNL Graphite Reactor followed by out-of-reactor heat treatments during which the fission-product release behavior is determined.[11] Irradiation times and fluxes are selected to give about 10^{15} fissions per sample. The resulting sensitivity for the detection of Xe^{133} is approx $3 \times 10^{-5}\%$ of the Xe^{133} present. For screening-type tests designed to evaluate coating integrity, the postirradiation heat treatments are conducted at 1400°C for approx 3 hr. Other heat treatment conditions are used in studies

[11] GCR Quar. Prog. Rep. Dec. 31, 1959, ORNL-2888, p. 68.

a.

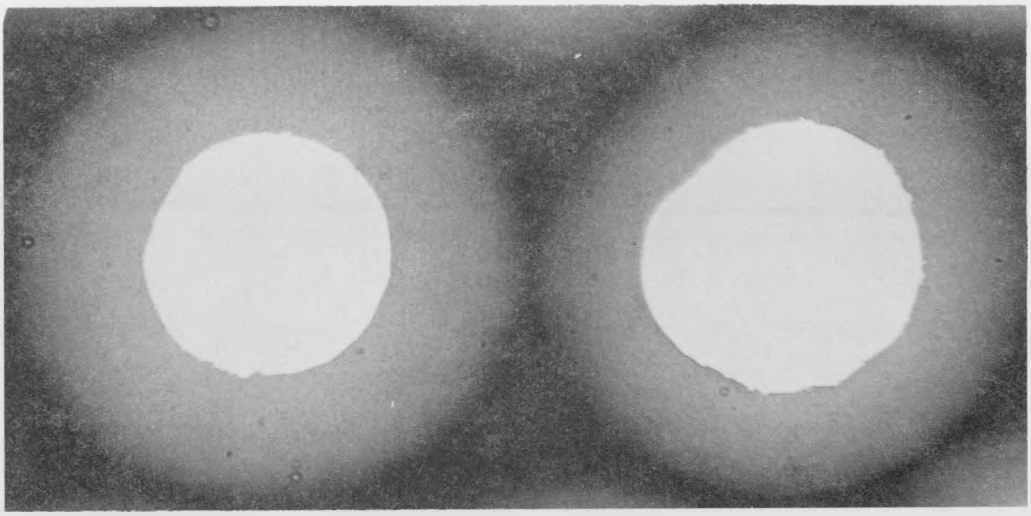

b.

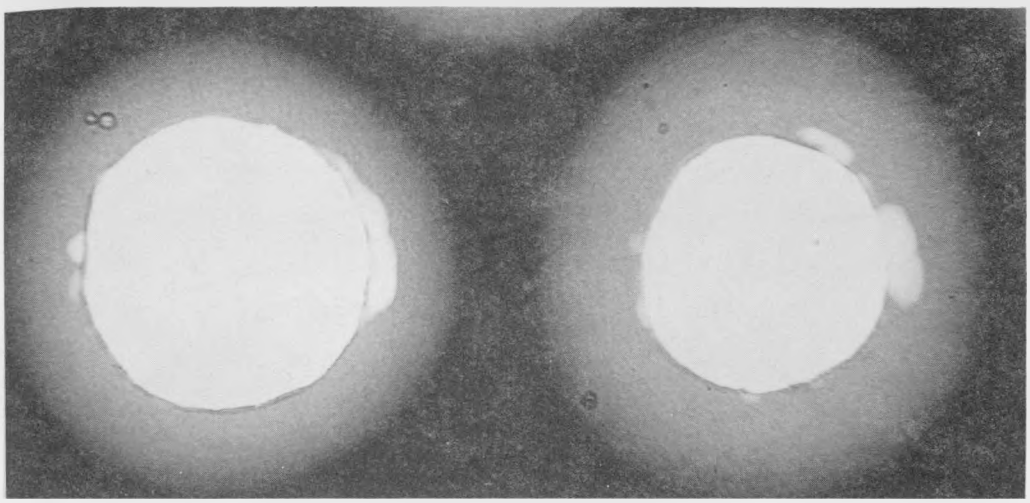

c.

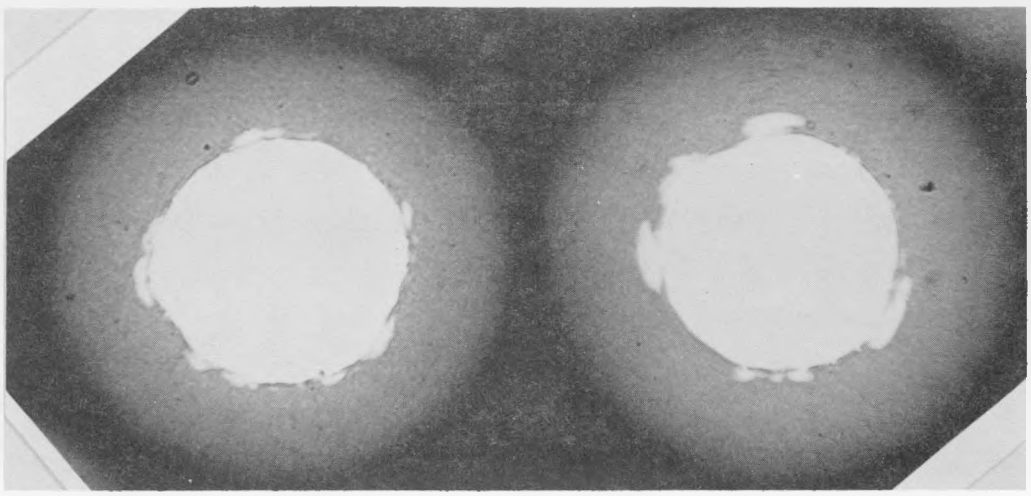

Fig. 4. Microradiographs of As-Received and of Heat-Treated Samples of Laminar-Pyrolytic-Carbon-Coated Particles from Batch 3M-102-B. a. As-received; b. heat treated at 1750°C for 3 hr; c. heat treated at 1950°C for 5 min. 200X.

designed to provide data on the mechanism of fission-product release and to establish the ultimate limitations of coated-particle fuels.

The neutron-activation experiments have shown that for coated particles having low amounts of exposed fuel ($< 10^{-2}\%$), less than $2 \times 10^{-4}\%$ of the contained Xe^{133} is released after heating for 3 hr at 1400°C. The large majority of the samples tested exhibit these very low release rates. For samples having amounts of exposed uranium exceeding 0.1% the fission-gas release is essentially proportional to the amount of exposed uranium. For samples with less than about 0.1% of exposed uranium, the detectable fission-gas release seems to be independent of the amount of exposed uranium.

Neutron-activated coated-particle samples have been heat treated to temperatures much higher than 1400°C with very interesting results. Thermal treatments at 1960°C for 140 hr did not cause increased fission-gas release for uranium carbide particles with approx 100μ-thick laminar pyrolytic-carbon coatings. Heat treatments to temperatures of 2050°C for 103 hr, however, resulted in fission-gas-release bursts characteristic of rupture of the particle coatings as shown in Fig. 5. The first burst was observed after 37 hr and the second after approx 42 hr; at the end of the 103-hr test period the number of recorded bursts indicated that approx 53 particles in the 100-particle sample had ruptured. Subsequent examination of the particles revealed that coatings on this number of particles had indeed ruptured.

In other experiments[2], where the Xe^{133} release was less than $3 \times 10^{-3}\%$, significant amounts of Ba^{140} were detected on heating at temperatures between 1400 and 1900°C. Release of iodine, tellurium, and silver has been observed at temperatures as low as 1000°C. At 1000°C the fractional release of silver was four thousand times that of Xe^{133}.

Static Capsule Tests. Unsupported coated particles are irradiated in static capsules in the Low Intensity Test Reactor (LITR). Each capsule consists of two containers, of the type shown in Fig. 6, which are encapsulated in an atmosphere of helium and hermetically sealed in a compartmented Inconel tube. Tantalum-sheathed tungsten-rhenium thermocouples are used to measure the central temperature in each container.

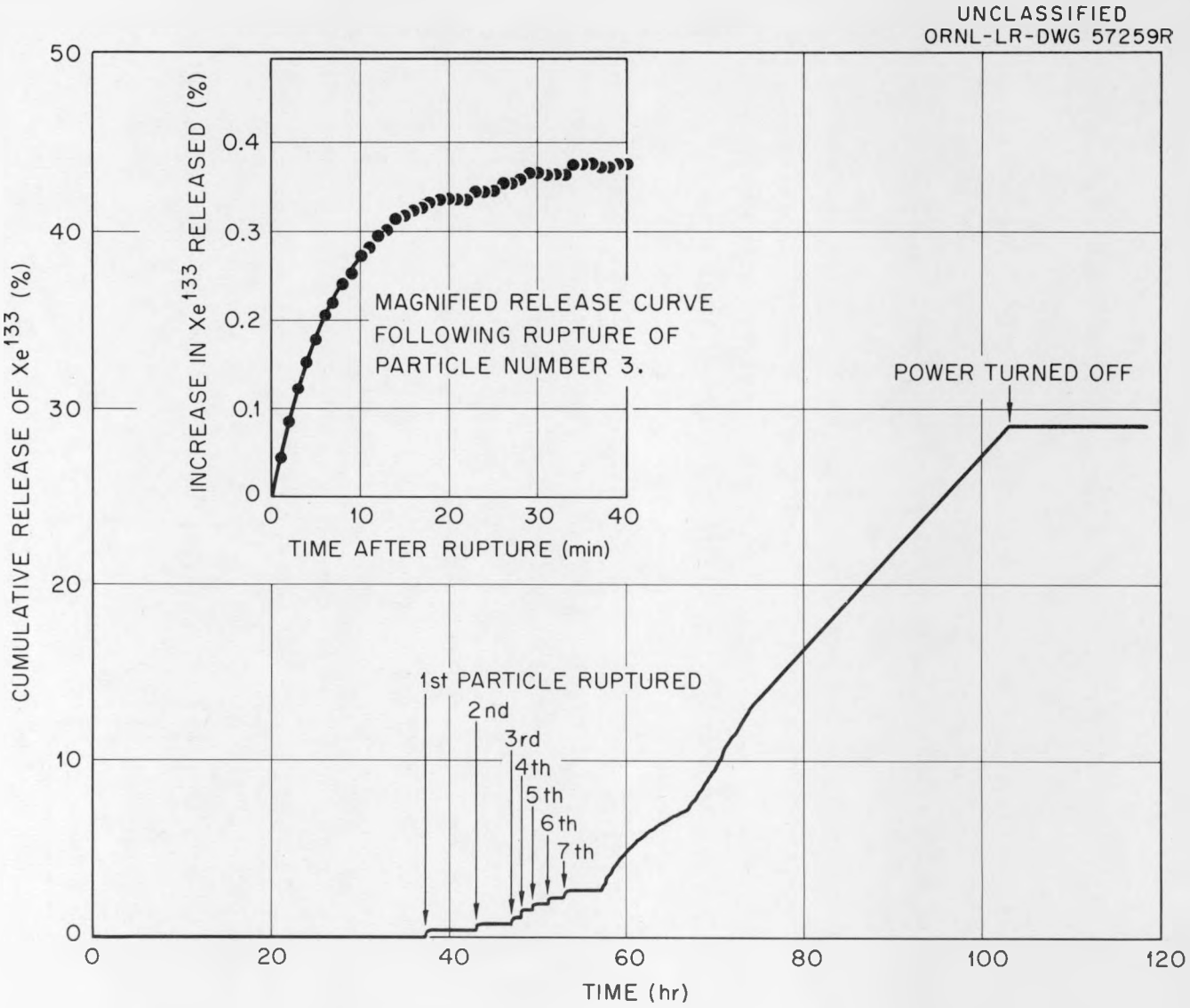

Fig. 5. Release of Xe^{133} from Irradiated Pyrolytic-Carbon-Coated Uranium Carbide Particles During Heating at 2050°C After Neutron Activation.

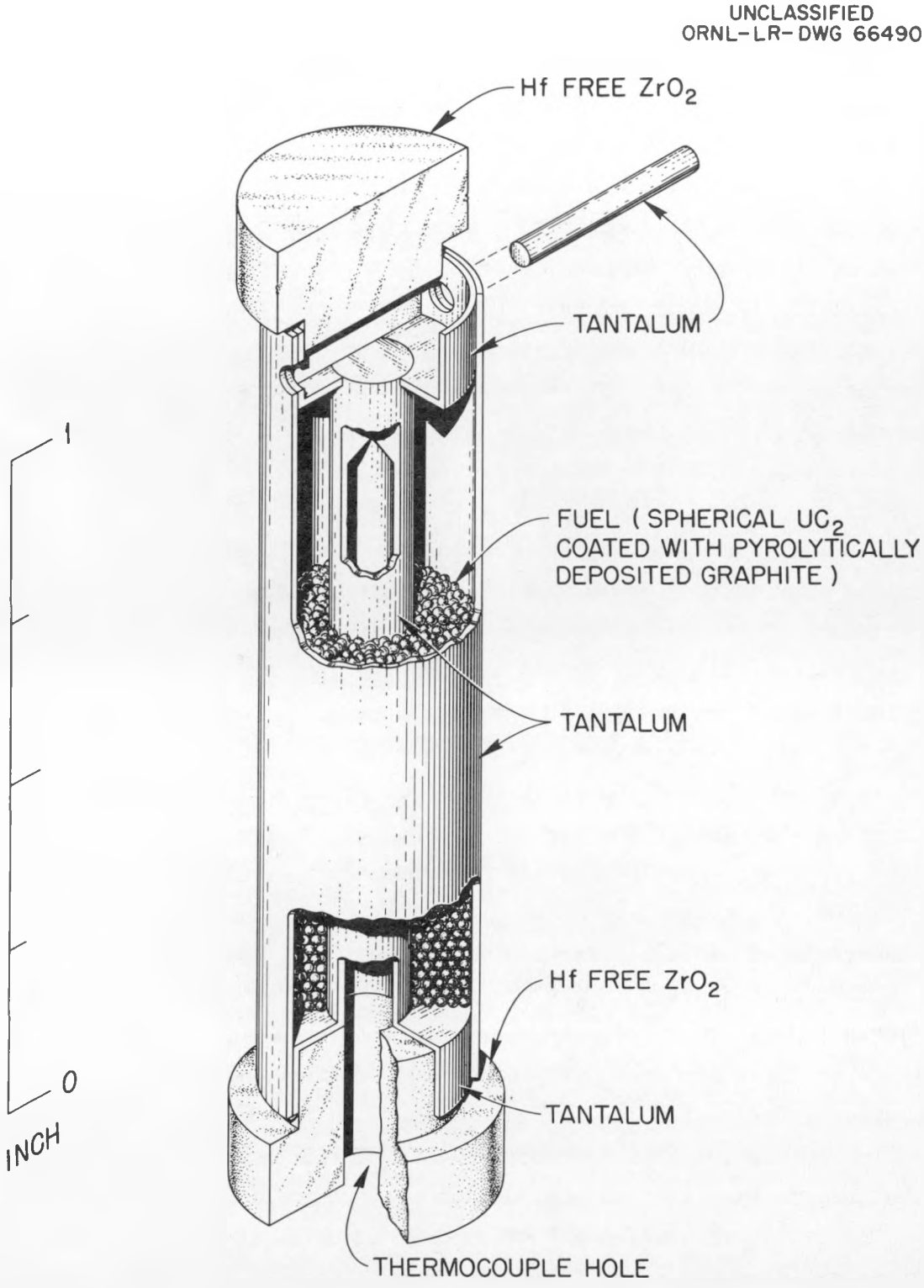

Fig. 6. Container Used in Static Capsule Tests of Coated Particles in the LITR.

The results of four static capsule tests that have been completed are summarized in Table 1.[2-6] The purpose of these tests was to assess the role of coating microstructure and of coating thickness on the irradiation stability of the coated particles at 2000 to 2500°F after burnups of 5 to 6 at. % of total uranium. Cracked coatings were found in all of the samples and the fraction that was cracked depended upon the microstructure and thickness of the coatings. The 100μ-thick coatings with the duplex microstructure were the most stable under the irradiation conditions employed, whereas, the columnar coatings that were only 50μ in thickness were badly damaged.

A photograph of the laminar-coated particles showing cracked coatings after irradiation is presented in Fig. 7. A cross section of a particle with a cracked laminar coating is shown in Fig. 8 and is to be compared with that of duplex-coated particles in Fig. 9. The superior performance of the duplex coatings may be associated with the presence of the discontinuity that exists between the laminar and columnar portions of the coating and to the fact that fission recoil damage, at least initially, is confined to the inner layer.

Several additional observations of interest have been made in connection with these experiments. The first is that dumbbell-shaped coated particles (doublets) crack more readily than the spherical particles. In the postirradiation examination of the 100μ-thick columnar-coated particles irradiated in the LCP-1 experiment, it was noted that the majority of the cracked-coated particles were doublets, as shown in Fig. 10. Secondly, the effect of an impure environment was noted when air leaked into the LCP-1a and LCP-2a compartments. As noted in Table 1, the number of cracked coatings and the amount of exposed uranium for particles in the compartments containing air were several times greater than that in the compartments containing pure helium.

The extent of uranium migration that occurred in the laminar-coated particles under the irradiation conditions of the LCP-2b experiment was determined by microradiography. As shown in Fig. 11, the uranium migrated to a depth of approx 25μ or approx 1/4 of the coating thickness.

Table 1. Results of Static Capsule Irradiation Experiments on Unsupported Pyrolytic-Carbon-Coated Uranium Carbide Particles

Experiment Number	Coating Structure	Average Coating Thickness (μ)	Approximate Temperature (°F)	Approximate Burnup (at. % of Total U)	Cracked Coatings[a] (%)	Exposed Uranium[b] (%)	Kr^{85} Release[c] (%)
LCP-2a	Laminar	100	2350	6	17[d]	10[d]	d
LCP-2b	Laminar	100	2500	6	2–4	0.6	0.4
LCP-1a	Columnar	100	1950	5	3[d]	20[d]	d
LCP-1b	Columnar	100	2100	5	1–2	2	0.2
LCP-4a	Columnar	50	2500	6	52	96	e
LCP-4b	Columnar	50	2500	6	45	48	e
LCP-3a	Duplex	100	1950	5	0.3	0.04	e
LCP-3b	Duplex	100	2100	5	0.3	0.18	e

[a]Determined by visual examination at approx 30X, and by metallographic examinations at higher magnifications.

[b]Determined by leaching in 8 M HNO_3 at 95°C for 8 hr; expressed as per cent of total uranium.

[c]Based on analysis of gas released on puncturing the container.

[d]Compartment failed with subsequent air inleakage.

[e]Not determined.

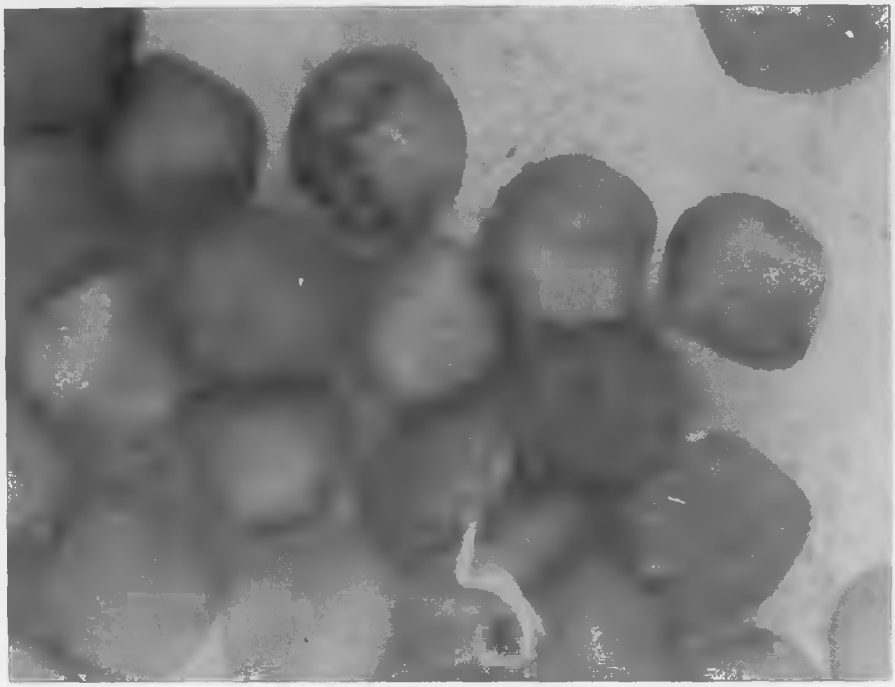

Fig. 7. Photograph of Pyrolytic-Carbon-Coated Uranium Carbide Particles from Batch 3M-SP-2 after Irradiation in Static Capsule LCP-2a at Approximately 2350°F to a Burnup of Approximately 6 at. % of the Total Uranium. Unmounted, oblique lighting. 60X.

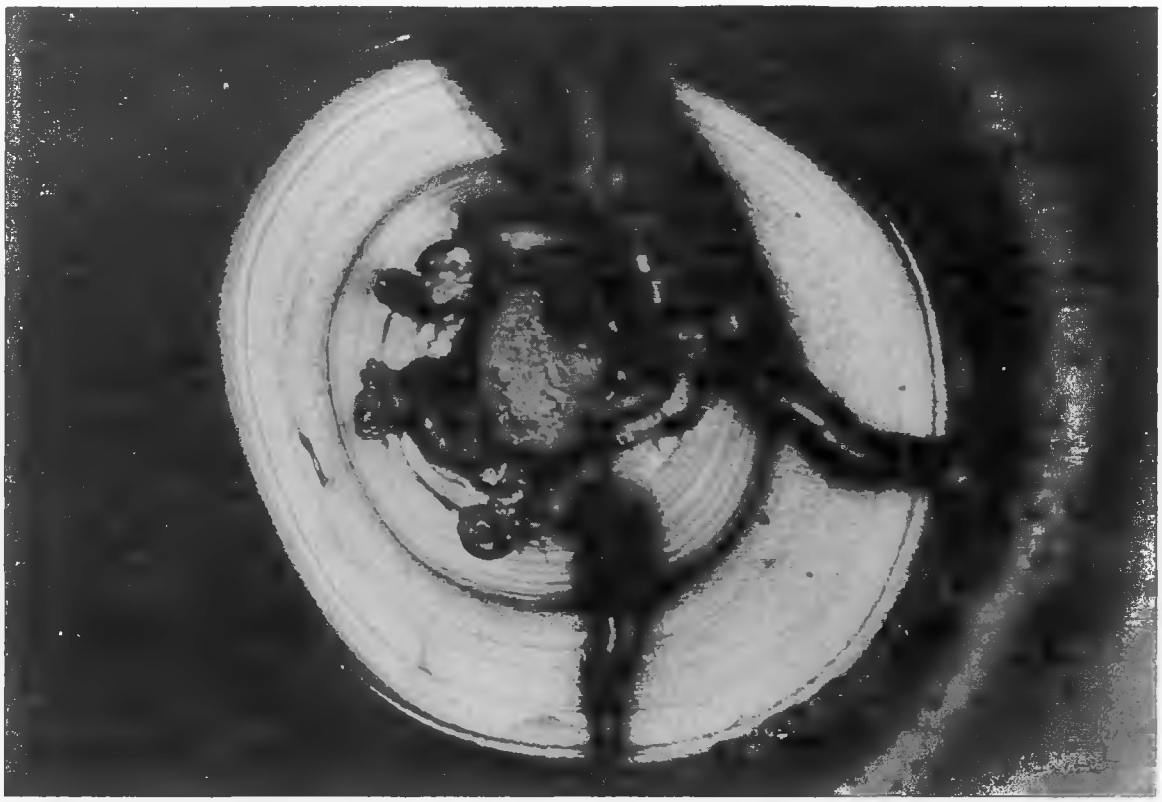

Fig. 8. Photomicrograph of a Cracked Laminar-Coated Particle from Batch 3M-SP-2 After Irradiation in Static Capsule LCP-2b at Approximately 2500°F to a Burnup of Approximately 6 at. % of the Total Uranium. Bright-field. Etchant: HAC, HNO_3, H_2O 1:1:1. 250X.

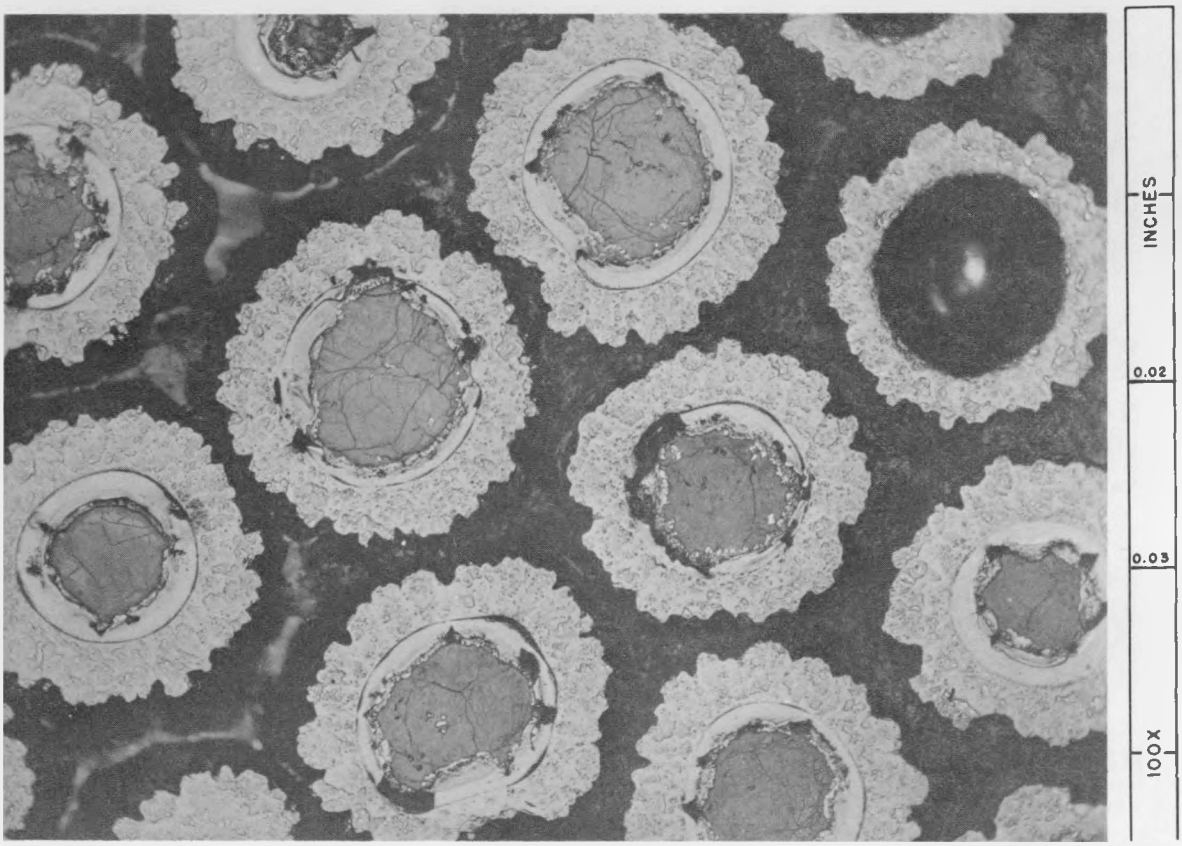

Fig. 9. Photomicrograph of Duplex-Coated Particles from Batch NCC-BE After Irradiation in Static Capsule LCP-3 at 2100°F to a Burnup of Approximately 5 at. % of the Total Uranium. Bright-field. Etchant: HAC, HNO_3, H_2O 1:1:1.

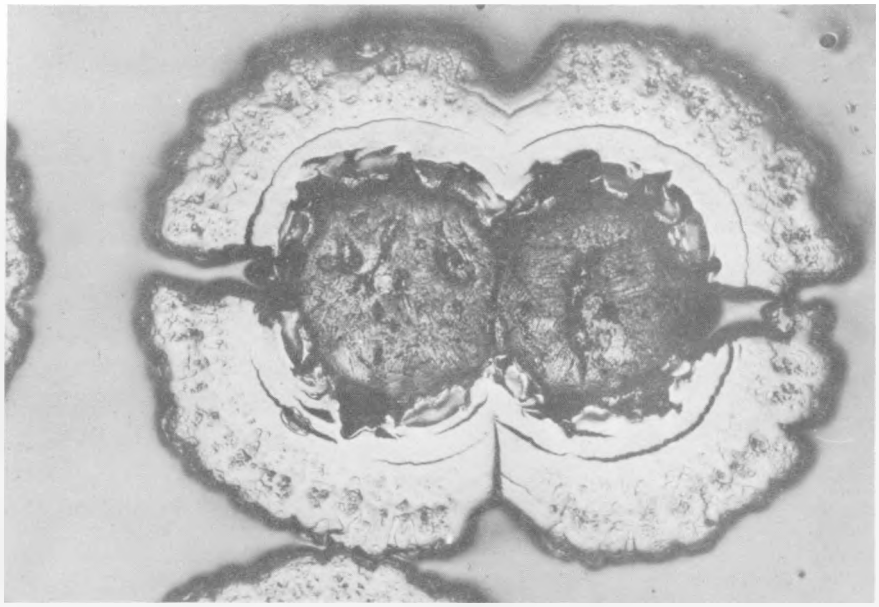

Fig. 10. Photomicrograph of a Columnar-Coated Particle from Batch HTM-1, Irradiated in Capsule LCP-1b at 2100°F to a Burnup of Approximately 5 at. % of Total Uranium. Bright-field. Etchant: HAC, HNO_3, H_2O 1:1:1. 150X.

a. As-Received

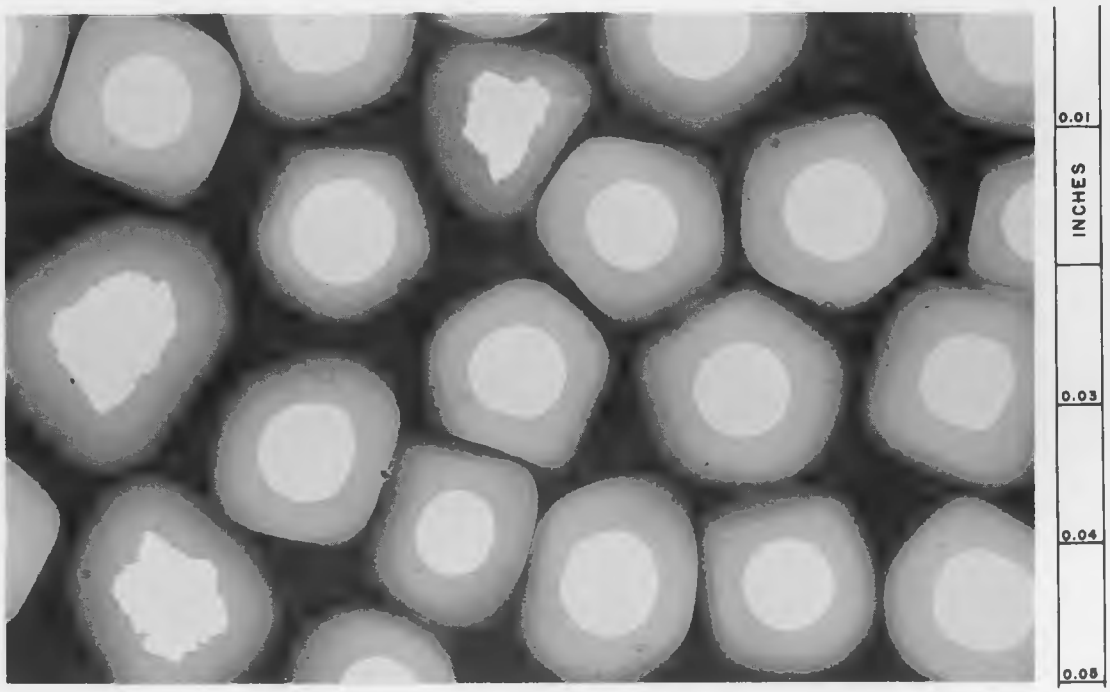

b. Irradiated

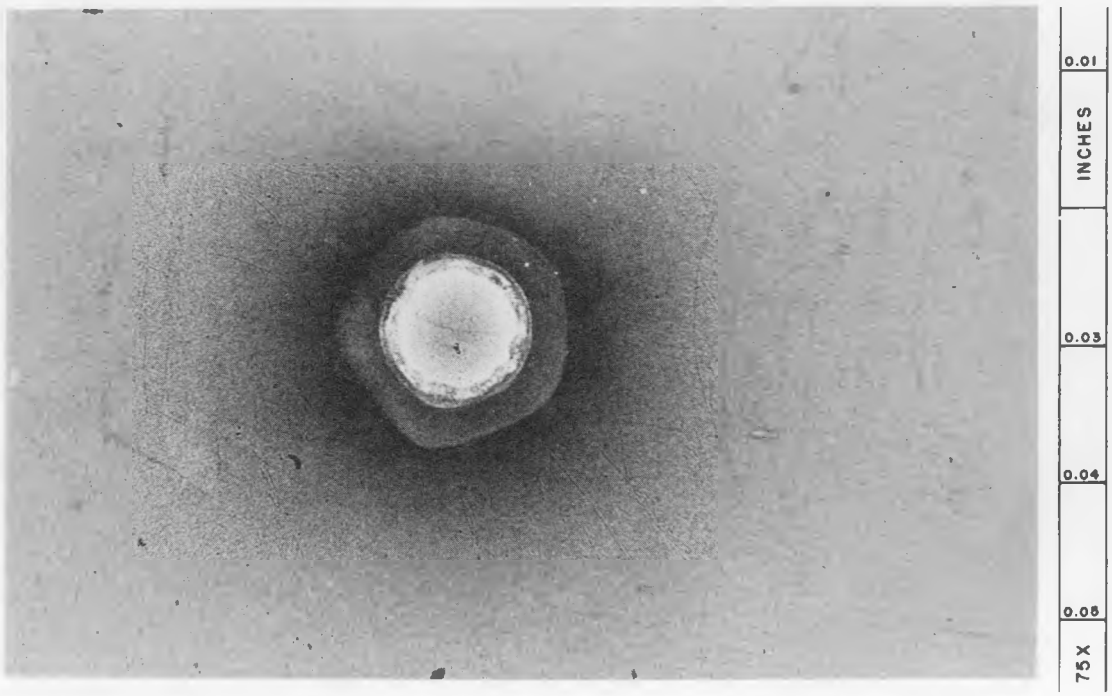

Fig. 11. Microradiograph of Laminar-Coated Particles from Batch 3M-SP-2. a. As-received; b. irradiated in Capsule LCP-2b at 2500°F to a burnup of approximately 6 at. %. 75X.

Sweep Capsule Tests. Sweep capsule irradiation experiments are performed on unsupported coated particles in the B9 and C1 core positions of the Oak Ridge Research Reactor (ORR).[5,6] In these experiments, fuel assemblies of the type shown in Fig. 12 are continuously purged with helium and the gas stream is continuously monitored for gamma activity. Samples of the gas are withdrawn periodically for analysis of fission gases by gamma-ray spectrometry. The neutron flux and the operating temperature can be independently varied over wide ranges in these facilities. Neutron fluxes up to approx 1×10^{14} neutrons/cm^2·sec are obtainable and the flux can be determined at any time by introducing argon into the sweep gas and measuring the Ar^{41} activity.

Uranium carbide particles with each of the three types of pyrolytic-carbon coatings – that is, laminar, columnar, and duplex – and one sample of uncoated uranium carbide particles have been irradiated in these facilities. The average coating thickness was approx 100μ and the fuel particle diameters ranged between 175 and 250μ. The results are summarized in Table 2. Fission-gas-release rates from the duplex-coated particles were substantially lower than those from the other two types of coated particles tested, a result which is consistent with that for the static capsule tests.

In experiment B9-8, bursts of fission gas were observed during the early stages of the 1700°F exposure and the release rates were essentially constant for the remainder of the 13 at. % burnup at this temperature. This observation and the fact that during subsequent irradiation at 800 and at 600°F the release rates were higher than those during the initial exposure for 15 at. % at 1500°F indicate that cracking of coatings occurred as the result of the increase in temperature to 1700°F in this experiment. In all tests, primarily during the early stages, activity bursts were frequently observed and the gas samples withdrawn shortly after these bursts were found to contain inordinately large amounts of the long-lived Xe^{133} isotope. These observations suggest that the bursts, which occurred more frequently from the laminar-coated particles than from the other two types, were caused by the rupturing of individual particle coatings.

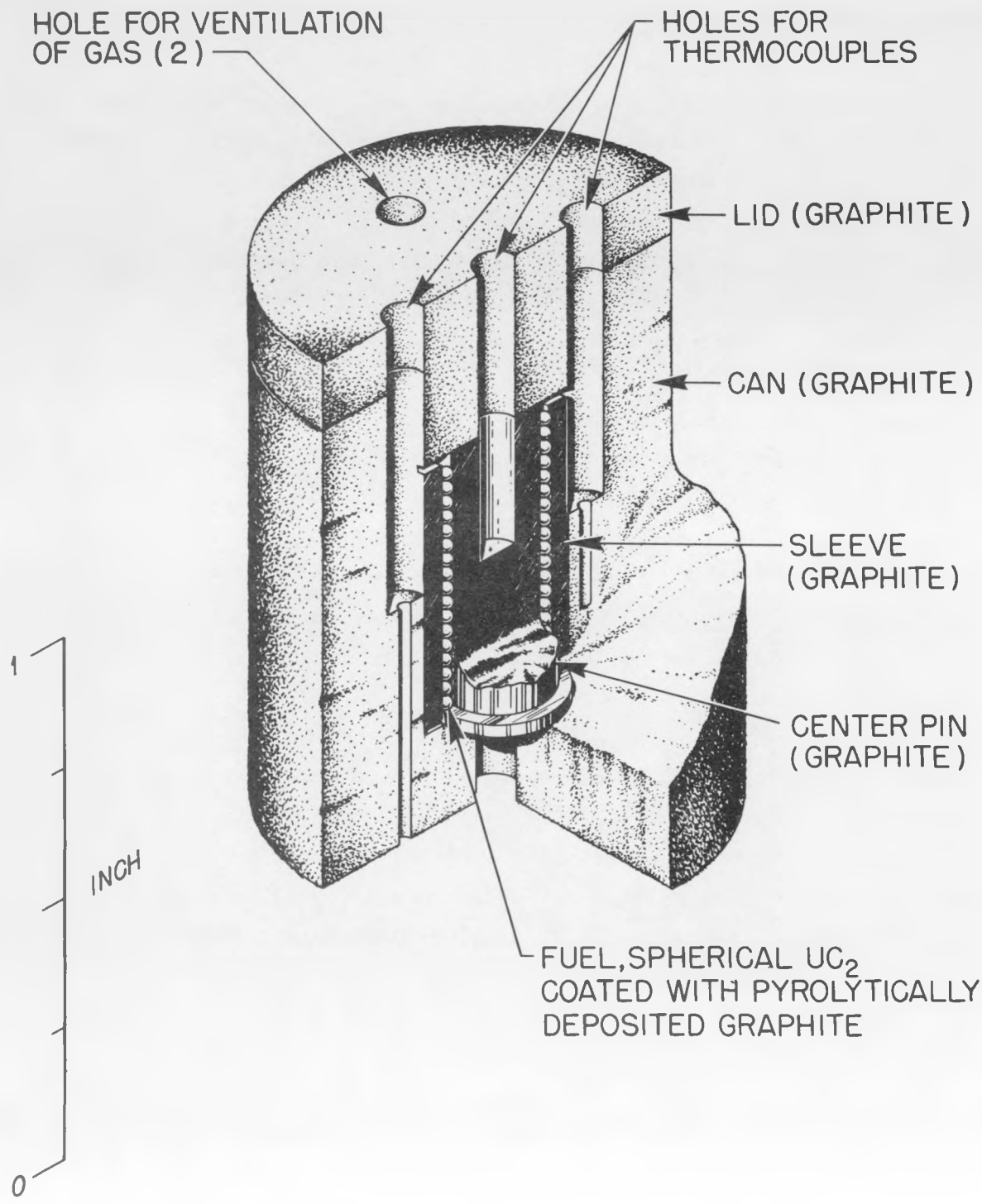

Fig. 12. Capsule for Irradiation of Coated Particles in the ORR-B9 and ORR-C1 Sweep Gas Facilities.

Table 2. Results of Sweep Gas Irradiation Experiments on Unsupported Pyrolytic-Carbon-Coated Uranium Carbide Particles

Experiment No.	Coating Structure	Approximate Temperature (°F)	Burnup Range (at. % of Total U)	R/B[a] for Kr^{88}	Cracked Coatings (%)
				$\times 10^{-5}$	
C1-8	(Uncoated)	1500	0 – 4.3	530	[b]
C1-7	Laminar	1500	0 – 15	18	5
B9-7	Columnar	1500	0 – 8	2.7	
		1650	8 – 12	10	2
B9-8	Duplex	1500	0 – 14.7	0.4	
		1700	14.7 – 27.8	2.1	
		800	27.8 – 28.9	1.0	
		600	28.9 – 29.7	0.9	< 0.5
B9-9	Duplex	800	0 – 4	0.8	[c]

[a] R/B is the average value at steady state of the ratio of the release rate to the birth rate.

[b] Not applicable.

[c] Not determined (experiment in progress).

The half-life dependence of the fission-gas-release rates at 1500°F is given in Fig. 13. The half-life dependency for release from columnar- and duplex-coated particles is about the same as that for the uncoated particles, indicating that the mechanism of release from cracked coatings in these tests was similar to that from uncoated particles. (The dashed line labeled "Selected PBRE Criterion" in Fig. 13 represents an improvement in performance by a factor of 50 relative to uncoated particles.)

Summary and Discussion

The results of these tests have demonstrated that a high level of performance with respect to fission-gas retention, and, therefore, irradiation stability, can be achieved in gas-cooled reactor fuels containing pyrolytic-carbon-coated carbide particles. Steady-state R/B values in the range 10^{-6} to 10^{-5} have been obtained at 1500–1700°F after burnups as high as 28 at. % of total uranium. The performance of the pyrolytic-carbon-coated particles studied depends primarily upon the structure and thickness of the coatings and to some extent on the shape of the carbide particles. The performance of coatings with the duplex structure has been superior to that of coatings with either the laminar or the columnar structures.

The curious fact that only a small percentage of the coatings with average thickness of approx 100μ have failed during extended irradiations indicates that there are "weak sisters" which have passed the preirradiation evaluation tests. Microradiographic examinations have shown that coating thickness is quite variable within given batches of coated particles. A comparison of the coating-thickness data with irradiation test results indicates that there is a good correlation between minimum coating thickness for a population and either the fission-gas release or the percentage of coatings cracked during irradiation. A similar correlation exists between minimum crushing strength and irradiation performance. These correlations suggest that the "weak sisters" may simply be those coated particles with thin and, therefore, weak coatings. In this connection, it is in order to note that more than 50% of the coatings failed by cracking in a single test on particles with an average coating thickness of approx 50μ.

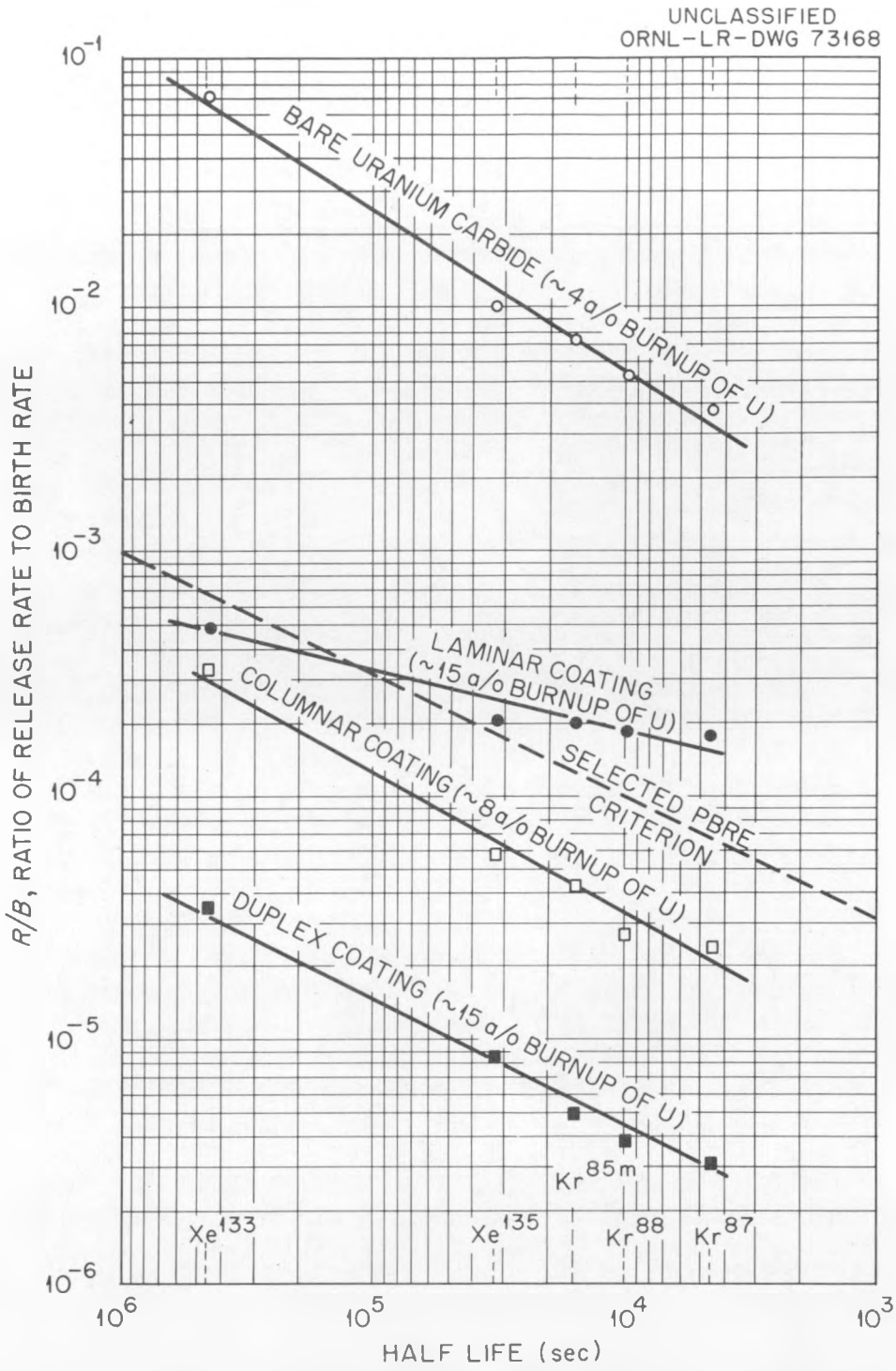

Fig. 13. Relationship Between R/B and Half-Life for Release of Inert Gases from Pyrolytic-Carbon-Coated and Uncoated Uranium Carbide Particles at 1500°F. (Calculation of R/B for Kr^{85m} is based on fission yield of 2.0%.)

Fueled Graphite Elements Containing Coated Particles

Preirradiation Evaluation (E. S. Bomar, R. W. McClung, R. J. Gray, Metals and Ceramics Division)

Graphite-matrix elements containing pyrolytic-carbon-coated particles and having geometries ranging from small, right-cylindrical pellets to 1 1/2-in.-diam spheres, both with and without unfueled shells, have been evaluated. The evaluation procedure includes visual and dimensional inspections, density determinations, determination of the distribution of coated particles, measurements of exposed fuel and fuel loading, structure determinations, and measurements of fracture strength.[3,4,6]

Visual Examination and Dimensions. Visual examinations have shown that the surface condition of the graphite-matrix elements is quite variable. Cylindrical elements with unfueled shells generally are smooth, although sharp corners are often chipped. Coated particles, sometimes in aggregates of three to six particles, are frequently visible on or as slight protrusions from the surface of elements without unfueled shells. Spherical elements frequently exhibit die marks and seams or molding flashes.

Dimensional variations, defined as the difference between maximum and minimum dimensions of elements within a lot divided by the average for the lot, have ranged from 0.001 to 0.07, depending upon the shape and size of the elements. For 1 1/2-in.-diam spheres the dimensional variation has not exceeded 0.02. The thickness and quality of unfueled shells are determined by radiographic and metallographic examinations. The shells on cylindrical and bushing-shaped elements have been quite variable in thickness. In some places the shells are twice the nominal thickness and in others essentially no shell is apparent. The 1/4-in.-thick shells on spherical elements, on the other hand, have been very uniform in thickness. The shells appear to be well bonded to the fueled regions, with no apparent change in the microstructure of the graphite matrix at the interface.

Density. The bulk densities are determined from dimensional and weight measurements and have ranged from 1.54 to 2.10 g/cm^3, depending upon the fuel loading and manufacturing techniques used by the vendors.

The average net carbon density is determined by analyzing several elements from a lot and subtracting the weight of uranium and thorium before calculating the density. Average net carbon densities have ranged from 1.44 g/cm^3 to 1.93 g/cm^3. With a few exceptions, all elements have exceeded the minimum bulk density of 1.70 g/cm^3 and net carbon density of 1.65 g/cm^3 as presently specified.

Distribution of Coated Particles. The uniformity of distribution of coated fuel particles within graphite-matrix fuel elements, as determined by radiographic and metallographic examinations, has been quite variable. The distribution in bushing-shaped elements has ranged from very uniform in some cases to very nonuniform in others. In extreme cases the fuel particles are concentrated near the inside surface, leaving low-density areas near the outside surface. Metallographic examinations have shown that, in general, the distributions in spherical elements are quite uniform. The uniformity of distribution is difficult to assess in radiographs of spherical elements.

Exposed Fuel and Fuel Loading. A measure of the exposed fuel is provided by alpha counting and by the amount of uranium removed by leaching in 8 M HNO_3. Exposed fuel in some of the graphite-matrix elements received early in the program corresponded to as much as 2% of the contained uranium; for elements received more recently, however, less than 0.05% exposed fuel has been detected. The total amount of fuel is determined by chemical analysis. The vendors' control of the fuel loading in a given element has been adequate (±5%).

Structure. Microstructures representative of bushing-shaped elements from three different vendors are shown in Figs. 14, 15, and 16. The obvious differences in these microstructures indicate that the manufacturing processes used in preparing the elements were significantly different. The quantity of binder residue (light-gray material) is greatest in the matrix shown in Fig. 16. The coated particles shown in Figs. 15 and 16 are apparently well bonded to the matrix, whereas, those in Fig. 14 are surrounded by small void regions.

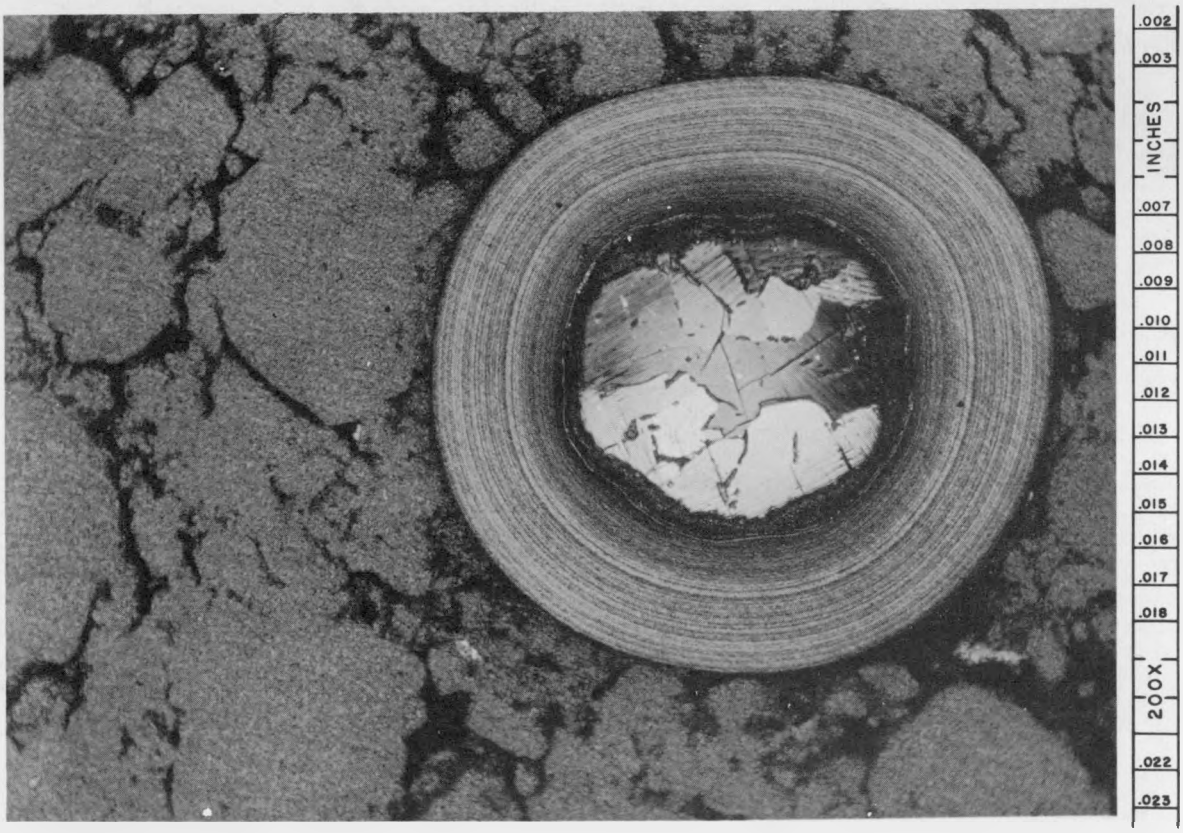

Fig. 14. Photomicrograph of Fueled-Graphite Element Containing Laminar-Coated Particles from Lot 3M-B1. Bright-field. Etchant: HAC, HNO_3, H_2O, 1:1:1.

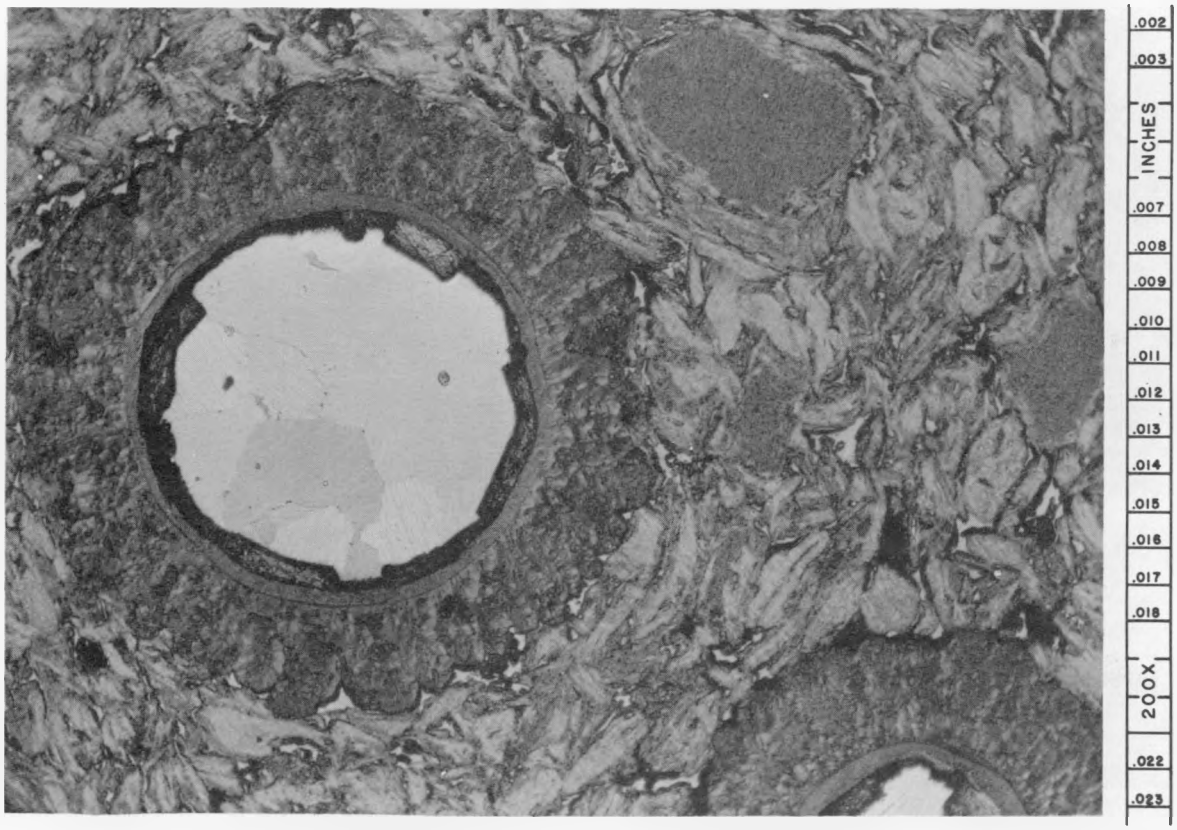

Fig. 15. Photomicrograph of Fueled-Graphite Element Containing Duplex-Coated Particles from Lot NC-B1. Bright-field.
Etchant: HAC, HNO_3, H_2O, 1:1:1.

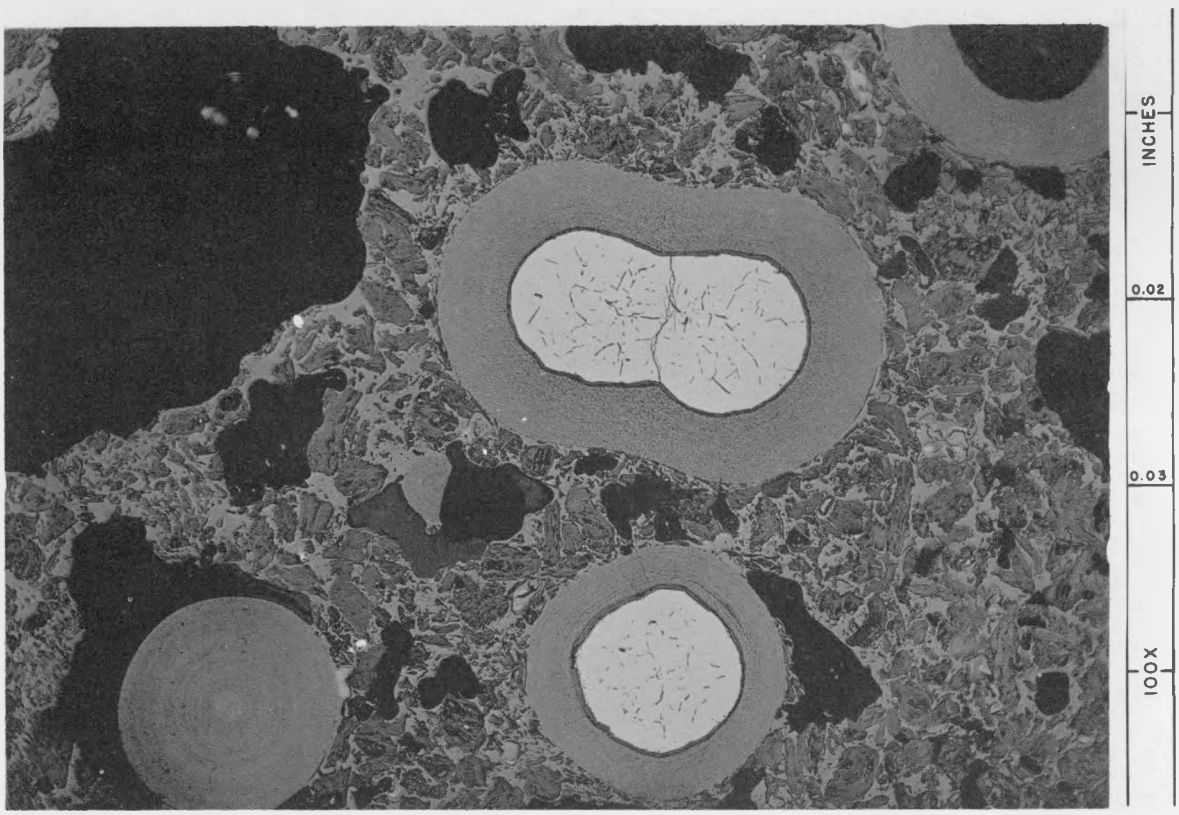

Fig. 16. Photomicrograph of Fueled-Graphite Element Containing Laminar-Coated Particles from Lot SC-B1. Bright-field. As-polished.

Fracture Strength. The fracture strengths of bushing-shaped elements, as determined in brittle ring tests, have ranged from 2000 to 4000 psi. The strength of elements with microstructures as shown in Fig. 14 was the lowest and that for elements with microstructures as shown in Fig. 16 was the highest. The mode of fracture in elements typified by the structure shown in Fig. 16 differed from the others in that the fracture path went through, not around, the coated particles.

Irradiation Tests (V. A. DeCarlo, C. W. Cunningham, Reactor Division; D. F. Toner, M. F. Osborne, Reactor Chemistry Division; R. E. Adams, E. L. Long, Metals and Ceramics Division)

Neutron-Activation Tests. Fission-gas release from neutron-activated elements is measured routinely at 1000°C for 24 hr. Under these conditions the release of Xe^{133} has ranged from 5×10^{-5} to 8×10^{-2}%, the higher values being associated with specimens containing approx 2% exposed fuel.[3-5] Typical Xe^{133} release values range from 10^{-3} to 10^{-2}% or 10 to 100 times those from unsupported-coated particles.

It has been observed that heat treatments of 24 to 100 hr at 2000°C prior to neutron activation increase the Xe^{133} release at 1000°C by factors of 2 to 10. In addition, bursts of fission gas have been detected when specimens heat treated in this manner after neutron activation have been exposed to moist helium at room temperature. This behavior is thought to be caused by uranium migration through the coatings at 2000°C followed by precipitation locally, possibly as UC_2, on cooling to room temperature where subsequent reaction with moisture damages the coatings and releases Xe^{133}.

Sweep Capsule Tests. Fueled-graphite elements containing coated particles have been irradiated in flowing helium in the MTR-48 and ORR poolside sweep gas facilities.

Two experiments, each involving cylindrical specimens approx 1 in. in diameter by 1 1/2 in. long, have been performed in the MTR-48 facility. In the MTR-48-5 experiment the test element contained a 1/8-in.-thick unfueled shell and was fueled with laminar-coated, spherical uranium carbide particles.[3,4] It was irradiated initially at a central temperature of approx 2500°F to a burnup of approx 7 at. % of the total

uranium. Radiochemical analyses of the helium sweep gas showed that the fission-gas-release rates increased continuously during this period until apparently all of the particle coatings had failed. The test was continued at lower temperatures (1600–2000°F) to a final burnup of 17 at. % of total uranium. The fission-gas-release rates were temperature dependent during this period and were steady during each constant-temperature exposure. Postirradiation examination revealed that all of the particle coatings had failed and that the unfueled shell had developed a small crack during the irradiation. It also was noted that a tantalum-sheathed thermocouple had become severely oxidized during the experiment, indicating that the sweep gas contained oxidizing impurities. Thus, the failures observed may not have been due to irradiation effects alone.

In the MTR-48-6 experiment the test element had no unfueled shell and contained laminar-coated, angular particles of thorium-uranium carbide (Th:U = 2.2:1).[5] This element was irradiated in the temperature range 1300–2000°F to a burnup of 1.6 at. % of Th + U. It was observed that the coatings were particularly susceptible to damage during temperature changes, and postirradiation examination showed that 10% of the particle coatings were cracked. As noted in the previous test, metal components in the assembly were partially oxidized.

Twelve bushing-shaped elements, 0.6-in.-OD × 0.25-in.-ID × 0.5-in. long, have been irradiated in each of three ORR poolside sweep capsule tests.[4-6] Two types of elements have been tested, the first characterized as containing laminar-coated particles in a matrix of the type shown in Fig. 14, and the second as containing duplex-coated particles in a matrix such as that shown in Fig. 15. Two capsules, each containing one of the types of elements described, were irradiated with nominal central-fuel temperatures of 1700°F, and the third, containing laminar-coated particles, was operated at 2400°F. It was observed that the fission-gas-release rates in all three capsules were very sensitive to temperature changes. The elements in the third capsule were inadvertently thermally cycled from 2400 to 3210°F in 4 min. After this thermal cycle, a 100-fold increase

in the fission-gas-release rates was observed at 2400°F. A second capsule, also containing elements fueled with laminar-coated particles, was thermally cycled at the same time from 1700 to 2450°F with similar results.

The capsule containing elements with the duplex-coated particles was irradiated in the temperature range 1560–1760°F, with an average temperature of approx 1700°F, to a burnup of 9 at. % of the total uranium. The fission-gas release rates for these elements were 20 to 30 times higher than those for the unsupported duplex-coated particles irradiated at 1700°F in the ORR B9-8 experiment. It is important to note that because of differences in deposition conditions, these two batches of particles were not identical. For the unsupported particles, for example, the nominal thickness of the inner laminar layer, which is exposed to fission recoils, was 25μ. For those in the fuel elements, however, this thickness was only 12μ. In addition, more temperature changes and cycles were experienced by the graphite fuel elements than by the unsupported particles.

Postirradiation examination of these capsules is not complete. The capsule in which the elements containing laminar-coated particles were tested at 1700°F has been visually examined. Four of the twelve elements were found to be cracked, a result which was unexpected in view of the fact that graphite-matrix elements have been irradiated without failure at much higher power density conditions [1,2,3] than those used in these tests. The cracking may be the result of the relatively low strength of this particular type of element. It should be noted that these elements received a rapid thermal shock from 1700 to 2400°F and back to 1700°F during the irradiation test.

Summary and Discussion

Evaluation studies on fueled-graphite specimens have shown that coated-particle fuel elements can be fabricated without excessive damage to the particle coatings and that they meet acceptable specifications with respect to dimensions, fuel loading, bulk- and net-carbon density, and rupture strengths. The performance of the fueled-graphite elements has not been as outstanding as that of the unsupported particles tested in this program. In this regard the following points are felt to be

significant: (1) duplex-coated particles of the exact type which showed superior performance in the unsupported condition have not been used in the fueled-graphite specimens; (2) temperature variations and cycles have been more numerous in the experiments on fueled-graphite specimens; and (3) there is evidence that the level of gaseous oxidizing impurities has been higher in tests on the fueled-graphite specimens.

SUPPORTING RESEARCH

Diffusion of Uranium in Pyrolytic Carbon

(C. M. Blood and R. B. Evans III, Reactor Chemistry Division)

There are several mechanisms by which solid reactor fuel materials can diffuse through carbon or graphite matrices at high temperatures. However, only solid-state diffusion mechanisms need be considered for the special case represented by acceptable pyrolytic-carbon coatings on carbide fuel particles. Such coatings should exhibit an extremely low gas-permeability coefficient even after considerable fuel burnup has occurred. The results of the present studies should be most applicable to situations wherein the coating integrity is maintained, a solid-state diffusion mechanism controls fuel migration, and migration is contained within the coating. Particles with cracked (or otherwise violated) coatings are excluded by this characterization.

The objective of this section is to review the progress attained to date on an experimental investigation of the diffusion of uranium into massive columnar-pyrolytic carbon from an intimately contacted uranium carbide source.

Basic Considerations

Applicable Diffusion Equations. For ease and brevity of discussion, one might consider first the various diffusion relationships which describe the experimental results and also enable one to utilize the experimentally determined parameters for estimation of the migration rates. A rather general boundary condition has been selected for migration in both experimental and actual cases; namely, that the diffusion takes place as it would in a semi-infinite medium. This means that slow migrations have been anticipated for acceptable coatings and that the uranium concentration at the external surface will be zero for long periods of time for specified boundary conditions.

There are three types of equations to be considered. One gives the uranium concentration profile, a second gives the instantaneous rate of migration, and a third gives the total amount of uranium present in the pyrolytic carbon. The second is of little interest because transient conditions prevail; only the first and third equations are needed to describe experiments that are restricted to isothermal and unidirectional flow conditions. Under the conditions cited, the concentration, C, at any time, t, and position, x, takes the form

$$C(x,t) = C_c F(x,Dt), \tag{1}$$

where C_c is a parameter determined by the method of uranium placement at x = 0, and D, in cm^2/sec, is a diffusion coefficient. Sometimes experimental limitations preclude measurements of C(x,t) at a point and one must utilize an integrated form of Eq. (1) which gives the total amount of diffused material within a finite interval, Δx or (x_2-x_1), after a particular exposure time, t′. This relationship is

$$M(t') = A\int_{x_1}^{x_2} C(x,Dt')dx\ , \tag{2}$$

where M(t′) is the amount of diffused material, in grams, within Δx, and A, in cm^2, is the area normal to flow. Classical solutions to Eqs. (1) and (2) are common knowledge. It is not immediately clear, however, whether these solutions apply in fact to the diffusion of uranium in pyrolytic carbon, or whether there exists a set of boundary conditions suitable for both the experiments on massive specimens and the conditions within a pyrolytic-carbon-coated uranium carbide particle.

Diffusion Coefficients (D). Frequently, the only results required from the experiments are a set of diffusion coefficients at different temperatures. Such would be the case if one were interested in impurity atom diffusion as represented, for example, by fission-product migration where the usual procedure is to assume that self-diffusion behavior is approximated and that a trace-layer technique may be employed. This technique is characterized by the placement of a small amount of material, $Q_o(g/cm^2)$, on the surface at x = 0 whereby C_c takes the form $(Q_o)/(\pi Dt)^{1/2}$, and F(x,Dt) becomes exp $[(x)^2/(4Dt)]$. Equation (2) is

given by various forms of the error function [erf(u) or erfc(u)] with the argument u given by $(x)/[2(Dt)^{1/2}]$. The attractive feature of this method is that direct determinations of C(x,t), M(t), and, particularly, Q_o are not required, because D can be obtained from the slope of a semilog plot of various quantities [directly proportional to C(x,t)] vs x^2.

But this is not the case when it is desirable to align the experimental conditions according to those which might exist within coated particles, where at least one of the coating surfaces is always in contact with uranium carbide. An applicable boundary condition for an analogous experiment would be maintenance of a constant potential at x = 0, that is, $C_c = C_o \neq f(t)$. This quantity appears in both Eqs. (1) and (2). In this case, F(x,t) is given by erfc(u). The important point is that one must have values of C_c to define migration rates within particle coatings; thus two parameters must be determined by experimentation.

Diffusion Potential (C_o). The relative importance of the C_o term may be established by comparing the present investigation with conventional diffusion studies (for example, either self-diffusion in single crystals or the interdiffusion of two unlike gases). The conventional studies involve well-characterized systems for which C_o may be readily defined. For example, the state of the diffusing material is known, equilibrium phase relationships are generally available, and the potentials for diffusion are well defined. In these cases, most of the applicable equilibrium phenomena will have been worked out before hand. In the present investigation, however, one is forced to proceed (perhaps prematurely) without the basic information related to C_o. Thus, the present study is, of necessity, a pseudophase study coupled with a determination of diffusion rates. The determination of C_o poses a most difficult problem and recognition of this fact is strongly reflected in the experimental procedures adopted. The present approach is to consider C_o as being of primary importance with D taking a secondary role.

At present, C_o is envisioned as being associated with some sort of saturation value of uranium in carbons or graphites that are contacted by uranium carbide. This saturation value or "apparent solubility" will

probably depend heavily on both temperature and structure. An experimental determination of C_o is the primary objective of this investigation because this parameter represents the driving potential for the uranium diffusion process within particle coatings.

Materials and Experimental Procedure

Pyrolytic-Carbon Specimens. The pyrolytic carbon utilized was obtained from High Temperature Materials, Inc. The deposition conditions used in preparing the pyrolytic-carbon specimens are not precisely known; however, the structure and properties of these specimens are comparable to those for pyrolytic carbon deposited at 2000°C in methane at a total pressure of 20 mm Hg. The overall properties of the material are very similar to those of the large conical or columnar grains which constitute its microstructure. The crystallographic "c" directions in the columnar grains are essentially perpendicular to the (planar) deposition surface used in the manufacturing process; the "a" directions, therefore, are parallel to this surface. The vertices of the conical or columnar grains are situated at or near the deposition surface. The material is very dense with essentially zero open porosity.

In the columnar-type particle coatings, uranium diffusion proceeds from the initial layers (or cone vertices) and through the coating in the "c" direction. The diffusion specimens are fabricated with this orientation in mind. This is an important point since the results obtained elsewhere[12] indicate that migration in the "c" direction takes place along the conical surfaces or grain boundaries. It is also important to note that the structure in the massive specimens utilized in the present (or similar) investigations is not necessarily closely related to the structures that exist in coatings on fuel particles. For example, several coated particles may be placed in the cross section of a single cone of a massive specimen.

Fabrication of Diffusion Couples. The experimental procedures are based on several requirements mentioned in the previous sections. In review, it is desirable that (1) the pyrolytic carbon contacts a large source of uranium carbide during the diffusion heat treatments, (2) the diffusion is unidirectional, and (3) the specimen is of convenient size and shape for subsequent examination and analysis.

---

[12] J. R. Wolfe et al., "Self Diffusion of Uranium, Nickel, and Silver in Pyrolytic Graphite," March 15, 1962 (work performed under USAEC auspices) UCRL-6827T, -6828T.

The starting materials for couple fabrication consist of two plates or coupons of pyrolytic carbon, 0.2 in. × 0.2 in. × 1.5 in., and a strip of uranium metal approximately 0.001 in. thick. The metal is placed between the graphite coupons and is converted to UC by heating at 1300°C under vacuum for 2 hr in a graphite-resistance furnace. In order to effect a rapid conversion from UC to UC_2, the temperature is then raised to 2100°C for periods not greater than 2 hr. The amount of uranium diffusion into the pyrolytic carbon is negligible from the standpoint of detection; it is not zero, however, because the two coupons are firmly joined by the carbide layer, which indicates that some small amount of diffusion must have occurred. After fabrication, all exposed surfaces are subjected to a cleaning operation to minimize effects of contamination during fabrication. The couple is carefully dimensioned after cleaning.

Diffusion Heat Treatments. For the diffusion heat treatments, the couples are placed in an uncontaminated (new) holder, returned to the resistance furnace, and heated in vacuum for long-time periods at a selected temperature within the range 1700 to 2100°C.

Determination of Uranium Penetration. When the heat treatment is completed, the diffusion couple is removed from the furnace and a large portion of one coupon is removed by means of a small milling machine. Next, a wedge of the couple is removed in such a manner that the exposed surface may be represented by an inclined plane which passes through the uranium carbide layer and out through the adjacent coupon. It is possible to lay a photographic film on the inclined plane and obtain some autoradiographic information about the concentration profile. However, the current objective is to determine C_o as well as D; accordingly, this technique has been bypassed and the angle, ϕ, of the inclined plane with respect to the original interface is merely recorded.

The specimen is then sectioned by removing incremental volumes which are cut 90 deg to the original interface. The uranium content of each section is determined by wet chemical analysis. (Activation techniques have been utilized and are still under consideration.) Although the precision associated with the wet analyses is somewhat disappointing, it is felt that one of the two analytical procedures mentioned should yield the best absolute values of M and C_o. Based on the angle, ϕ, the

dimensions of the increments, and the analytical results, one can prepare plots of the experimental data in terms of M/A, the weight of uranium remaining[13] per unit area parallel to the original interface, versus the location, x, of the increment (or the surface of the cut) with respect to the interface.

Results

Status of Experimental Program. Ten couples have been subjected to various phases of the overall procedure; however, complete results are available for only five of the ten. Three of the five experiments completed represent "blank runs" (no diffusion heat treatment) to determine the effects of fabrication procedures on $C(x,0)$, that is, the initial concentration profile. The results of the "blank runs" indicated that the carbide/carbon interface is sharply defined. It was concluded, therefore, that the migration of uranium during fabrication is negligible. Results for the remaining couples, each heat treated, are shown in Fig. 17. Although the amount of data is limited, several interesting features pertinent to the experiments are demonstrated by the curves on this figure.

Residual Uranium Content. The first point of interest in regard to Fig. 17 involves the residual or background uranium content which is associated with the horizontal portions of the curves. Starting at zero penetration, the curves follow a relationship such as Eq. (2) up to penetrations around 5×10^{-3} cm. At this point the curve becomes a horizontal line which is not given by Eq. (2); in fact, this line indicates that the concentration is zero at all values of x greater than 5×10^{-3} cm since the slope is zero in this region. A tentative interpretation of the horizontal lines is that they represent either a background associated with the analytical technique or a contamination of the back side of the couple. Recent analyses of the specimen holders suggest that it would be difficult to attribute the background value to a surface or vapor migration mechanism. In any event, reasonable curves may be obtained by subtracting the average background value from all of the experimental points and replotting these versus x.

---

[13] From this point on, the increment (x_2-x_1) referred to in Eq. (2) shall be $[(x \rightarrow \infty) - (x_i)]$.

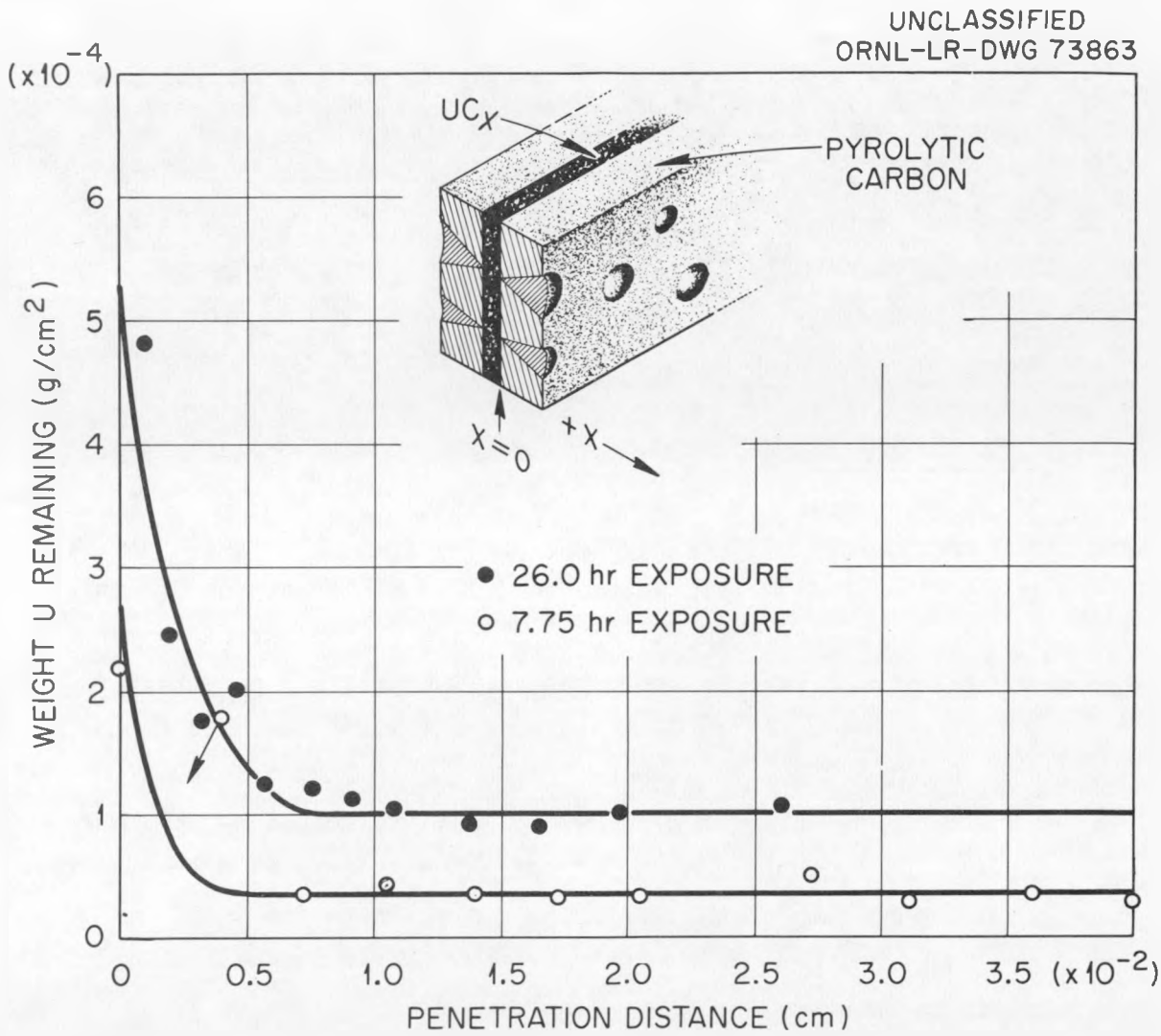

Fig. 17. Plot of Uranium Remaining, per Unit Area, as a Function of Distance from the Interface of Uranium Carbide – Pyrolytic-Carbon-Diffusion Couples Heated for 7.75 and 26.0 hr, Respectively, at 2100°C in Vacuum.

Computation of D and C_o. The first and most difficult step in the correlation of the data involves the estimation of x = 0 and $[M(0,t)]/A$. At present, the interface can be located only to within one increment or approximately ±15μ; this level of uncertainty, of course, leads to large errors in $[M(0,t)]/A$ values. Extrapolations of the data at $x > 0$ are the primary basis for these estimates. Once the values at x = 0 are selected and the background is subtracted out, the ratios $[M(x,t)]_{exp}/[M(0,t)]$ are computed and are plotted versus x. Comparisons of this plot with plots of the generalized function, $Y = (\pi)^{1/2}$ ierfc(u) versus u, where $u = (x)/2(Dt)^{1/2}$, yield an average value for D. One may calculate C_o from the relationship $[M(0,t)]/A = 2C_o(Dt)^{1/2}$ once D is established.

Based on the data in Fig. 17 and the procedure given above, one finds that $D = 6 \times 10^{-11}$ cm^2/sec and $C_o = 0.162$ g U/cm^3. The curves which appear in Fig. 17 are based on these values of D and C_o and the known background value.

Tentative Conclusions. The relatively high value obtained for C_o has been the most significant finding to date. This is clearly shown in Fig. 18 wherein plots of C(x,t) versus x, based on the experimentally determined C_o and D, are well within the range of direct measurement. The integral of the error function describes the total uranium transport; the error function describes the concentration profile; and the driving force for diffusion appears to remain constant with time. To obtain definitive results, heat-treatment periods should be increased from the range of 8 to 24 hr to periods of 200 to 1000 hr, depending on the temperature. Appreciable amounts of diffusion are observed because of the high C_o value even though diffusion coefficients are low.

To obtain fundamental information from experiments of this type, microscopic techniques should be considered since preferred-region (conical-surface) migration is involved. The nature of the classical diffusion equations is such that the effects associated with this type of migration will be hidden in the parameters, C_o and D. Regardless of the microscopic details, however, the experimental values of C_o and D coupled with the equations will yield reasonable estimates of the migration behavior.

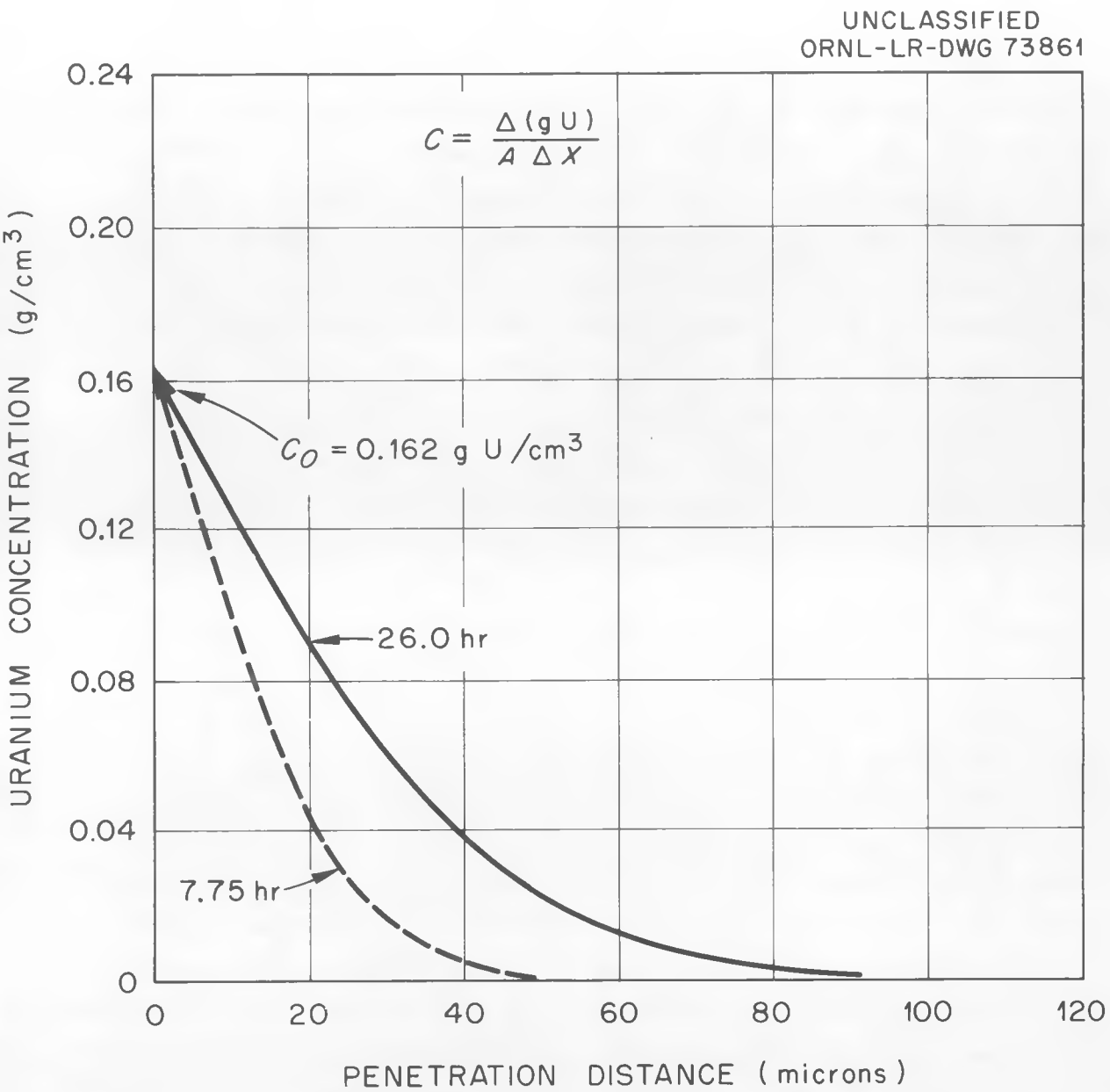

Fig. 18. Calculated Concentration Profiles.

Compatibility of Pyrolytic-Carbon-Coated Uranium Carbide Particles With Water Vapor

(L. G. Overholser, N. V. Smith, and J. P. Blakely,
Reactor Chemistry Division)

These studies were undertaken to establish the rate of reaction of pyrolytic-carbon coatings on various lots of coated-uranium carbide particles with water vapor at approx 1000°C. In addition, the incidence of coating failure under these conditions, as determined by a HNO_3 leach test, was to be established. Studies of this type are of interest in high-temperature, gas-cooled reactor programs, since accidental in-leakage of water and subsequent contact with the hot coated particles is a potential hazard. All materials studied were supplied by the 3M Co. and the coatings were of the laminar type.

Tests at 900°C, Low H_2O Content

In the initial experiments coated particles from lots 3M-D and 3M-F were exposed at 900°C to flowing helium containing H_2O at a partial pressure of 20 mm Hg (total pressure, 1 atm). The gas was passed downward through a bed of the coated particles at a flow rate of approx 100 cm^3/min and the resultant weight change was determined. The results are given in Table 3. The weight of coating in a given batch was determined by difference using the uranium content and assuming that the uranium was present as UC_2. Amounts and rates of coating removal were calculated accordingly. The reaction rates listed represent average values for the indicated exposure times. The quantities of uranium leached from the particles by 8 M HNO_3 at 90°C for 8 hr following the tests were established by chemical analyses of the leach solution.

The results show that the loss in weight of the coated particles was greater in all cases for lot 3M-D than for lot 3M-F. On the other hand, after the test exposures more uranium was leached from 3M-F particles than from 3M-D particles. These data indicate that the extent of the damage, which may be associated with a different mode of attack, actually was greater for lot 3M-F than for lot 3M-D. Irregularities in the coatings giving rise to thin coverage also could be responsible. Microscopic examination revealed only a shallow attack on the outer region of the coatings.

Table 3. Reactivity of Pyrolytic-Carbon-Coated Particles from Lot Nos. 3M-D and 3M-F With Helium Containing H_2O at a Partial Pressure of 20 mm Hg (Total Pressure, 1 atm) at 900°C

Sample No.	Weight of Sample (g)	Time (hr)	Weight Loss (g)	Calculated Amount of Coating Removed (%)	Calculated Rate of Coating Removal (g/g-hr)	Uranium Removed by HNO_3 Leach	
						(g)	(% of Total U)
3M-D-3	2.01	8	0.018	3.5	0.004	0.0005	0.04
-4	1.66	24	0.040	9.4	0.004	0.001	0.09
-2	1.85	50	0.070	14	0.003	0.008	0.6
-1	1.79	100	0.070	15	0.002	0.009	0.8
3M-F-3	1.61	8	0.002	0.8	0.001	0.001	0.08
-4	1.96	24	0.005	1.3	0.0006	0.004	0.3
-2	1.56	50	0.008	2.7	0.0005	0.030	2.5
-1	2.05	100	0.021	5.3	0.0005	0.027	1.8

Tests at 700 to 1000°C, Intermediate H_2O Contents

Samples from lots 3M-113 and 3M-114 were exposed at 1 atm to helium containing H_2O at partial pressures of 50 to 350 mm Hg at 700 to 1000°C, leached with 8 M HNO_3 (as described previously), and examined microscopically. The results listed in Table 4 show that, as anticipated, the reaction rates increased with increasing temperature and steam pressure. The apparent order of the reaction was less than one under the conditions of these experiments. The reaction rates observed at 800, 900, and 1000°C are in good agreement with extrapolated data of Pilcher, Walker, and Wright.[14] The one run at 700°C showed that the rate of attack is extremely slow at this temperature. This suggests that prolonged exposure would be required to cause serious damage to the coatings at temperatures of 700°C and below.

The data indicate that lot 3M-113 is more susceptible to damage than lot 3M-114. For example, in runs 3M-113-4 and 3M-114-6 the quantities of coating removed are comparable, but much more uranium was leached from 3M-113-4. The coatings on lot 3M-114 apparently are more protective after serious attack than are the coatings on lot 3M-113. Metallographic examination of a number of samples of these particles provides some explanation of this difference in behavior. In Fig. 19a the mode of attack on lot 3M-113 particles is shown to be quite localized. This same type of attack at a more advanced stage is shown in Fig. 19b, where pits are seen in many of the coatings. This type of attack would result in exposure of the uranium carbide core without extensive removal of the coating. It is to be noted that a number of the particles show signs of only a superficial attack.

Examination of lot 3M-114 coated particles revealed a different mode of attack, as illustrated in Fig. 20. This series of figures shows the results of exposing these particles to increasingly more severe conditions. Figure 20a shows the superficial attack on the outer layer of the coating after 6 hr at 800°C, during which 3.3% of the coating was removed. The particles shown in Fig. 20b suffered a 14% loss of the coating after 6 hr at 900°C and show significant attack of several particles, including separation of the outer layer. This effect was accentuated as the degree of attack increased, as seen in Fig. 21a after 4 hr at 1000°C, during which 21%

[14] J. M. Pilcher, P. L. Walker, Jr., and C. C. Wright, Ind. Eng. Chem. 47, 1742 (1955).

Table 4. Reactivity of Pyrolytic-Carbon-Coated Particles from Lot Nos. 3M-113 and 3M-114 With Helium Containing H_2O at Partial Pressures of 55–355 mm Hg (Total Pressure, 1 atm) in the Temperature Range 700 to 1000°C

Sample No.	Weight of Sample (g)	Time (hr)	Temp. (°C)	Partial Pressure of H_2O (mm Hg)	Weight Loss (g)	Calculated Amount of Coating Removed (%)	Calculated Rate of Coating Removal (g/g-hr)	Uranium Removed by HNO_3 Leach (g)	Uranium Removed by HNO_3 Leach (% of Total U)
3M-113-6	2.16	6	700	355	0.0025	0.2	0.0003	0.0001	0.02
-5	2.18	4	800	355	0.041	2.6	0.006	0.0232	4.0
-3	2.47	6	800	355	0.108	6	0.010	0.0021	0.3
-4	2.56	7	800	355	0.203	11	0.016	0.147	22
-2	2.51	6	1000	355	0.450	25	0.042	0.654	97
3M-114-4	2.50	6	800	233	0.036	3.2	0.005	0.0031	0.3
-1	2.45	6	800	355	0.036	3.3	0.006	0.0107	0.9
-9	1.99	6	900	233	0.127	14	0.024	0.001	0.1
-10	1.95	6	900	233	0.121	13	0.023	0.001	0.1
-3	2.41	4	900	355	0.159	15	0.037	0.002	0.2
-2	2.56	6	900	355	0.211	18	0.030	0.0177	1.4
-8	2.01	4	1000	55	0.099	11	0.027	0.001	0.1
-7	2.03	4	1000	92	0.149	16	0.041	0.002	0.2
-6	2.02	4	1000	149	0.193	21	0.053	0.001	0.1
-5	2.43	4	1000	355	0.424	39	0.097	0.016	1.3

a.

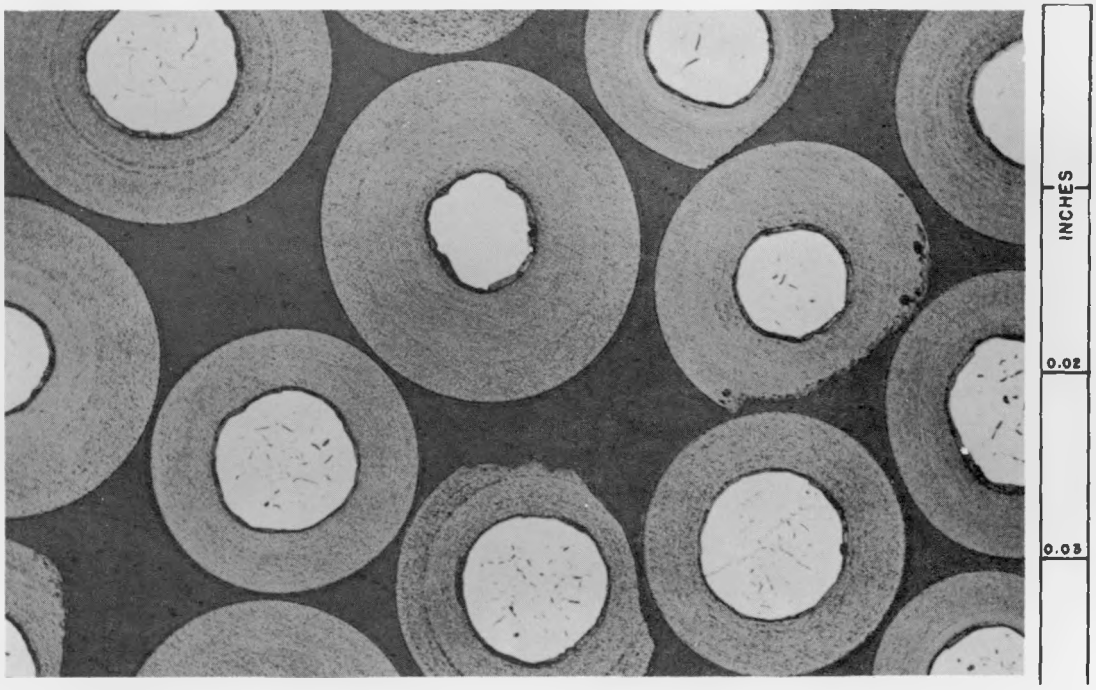

b.

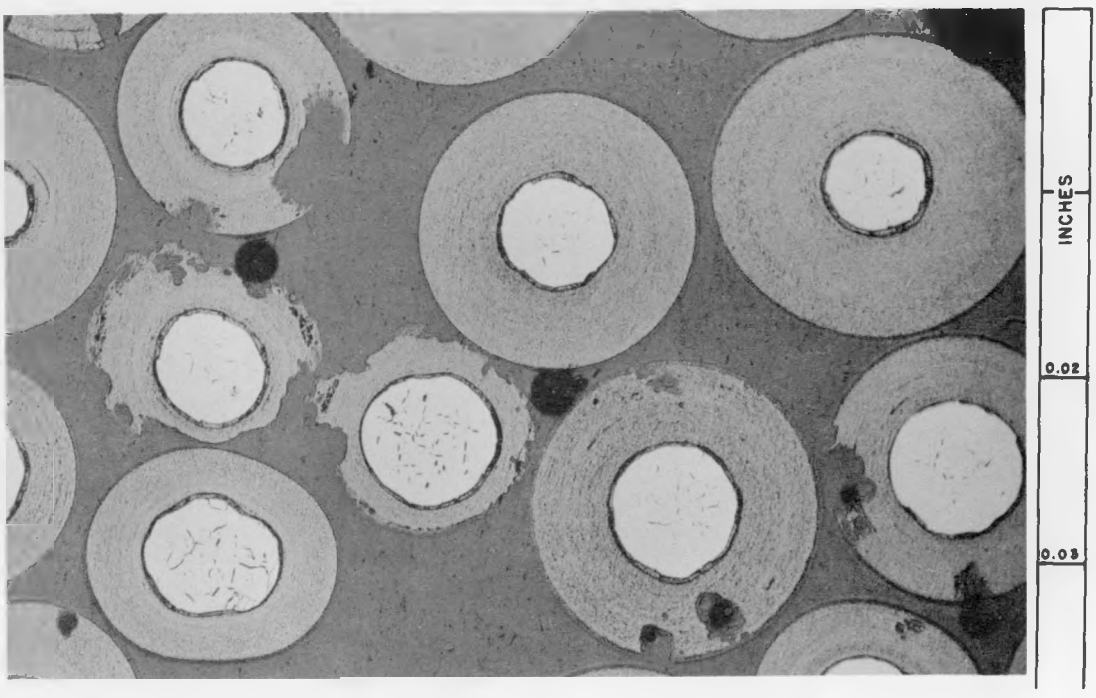

Fig. 19. Coated Particles from Lot No. 3M-113 Exposed at 800°C to Helium Containing H_2O at a Partial Pressure of 355 mm Hg (Total Pressure, 1 atm). a. Exposed for 6 hr; b. exposed for 7 hr. As-polished. 100X.

a.

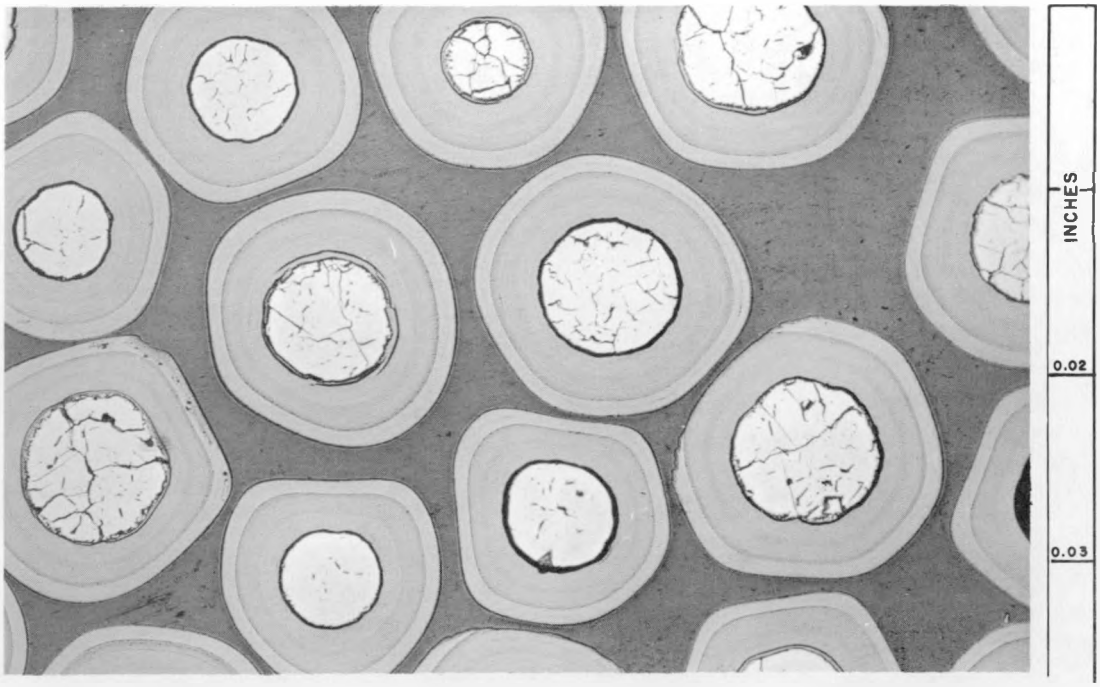

b.

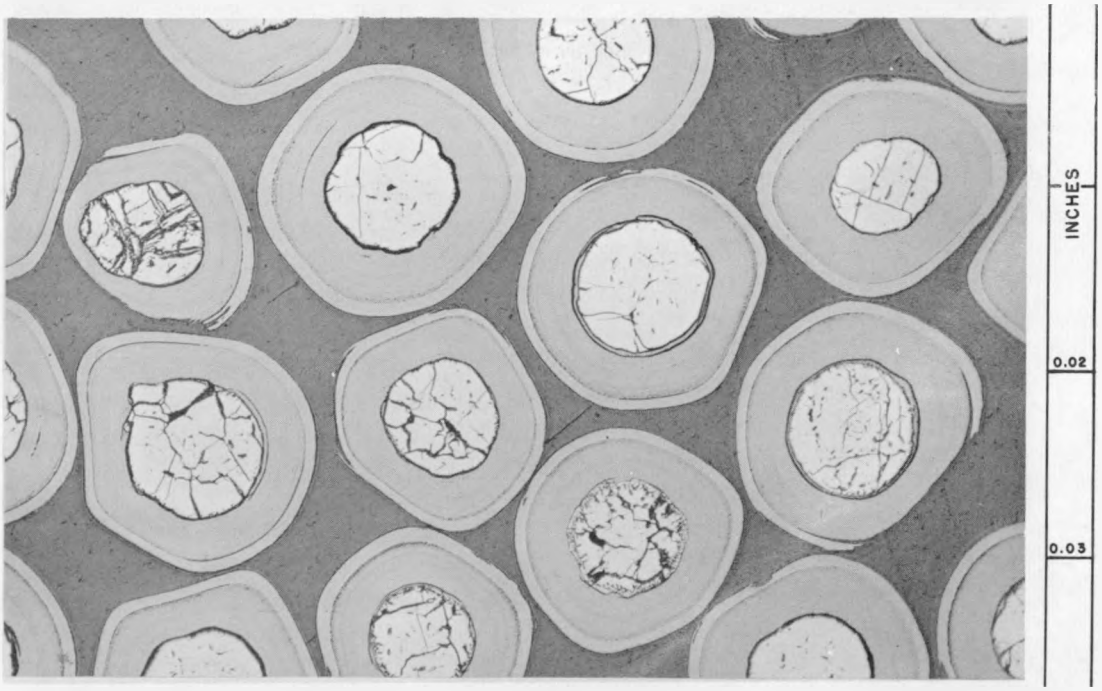

Fig. 20. Coated Particles from Lot No. 3M-114 After 6-hr Exposure to Helium Containing H_2O at a Partial Pressure of 233 mm Hg (Total Pressure, 1 atm). a. Exposed at 800°C; b. exposed at 900°C. As-polished. 100X.

a.

b.

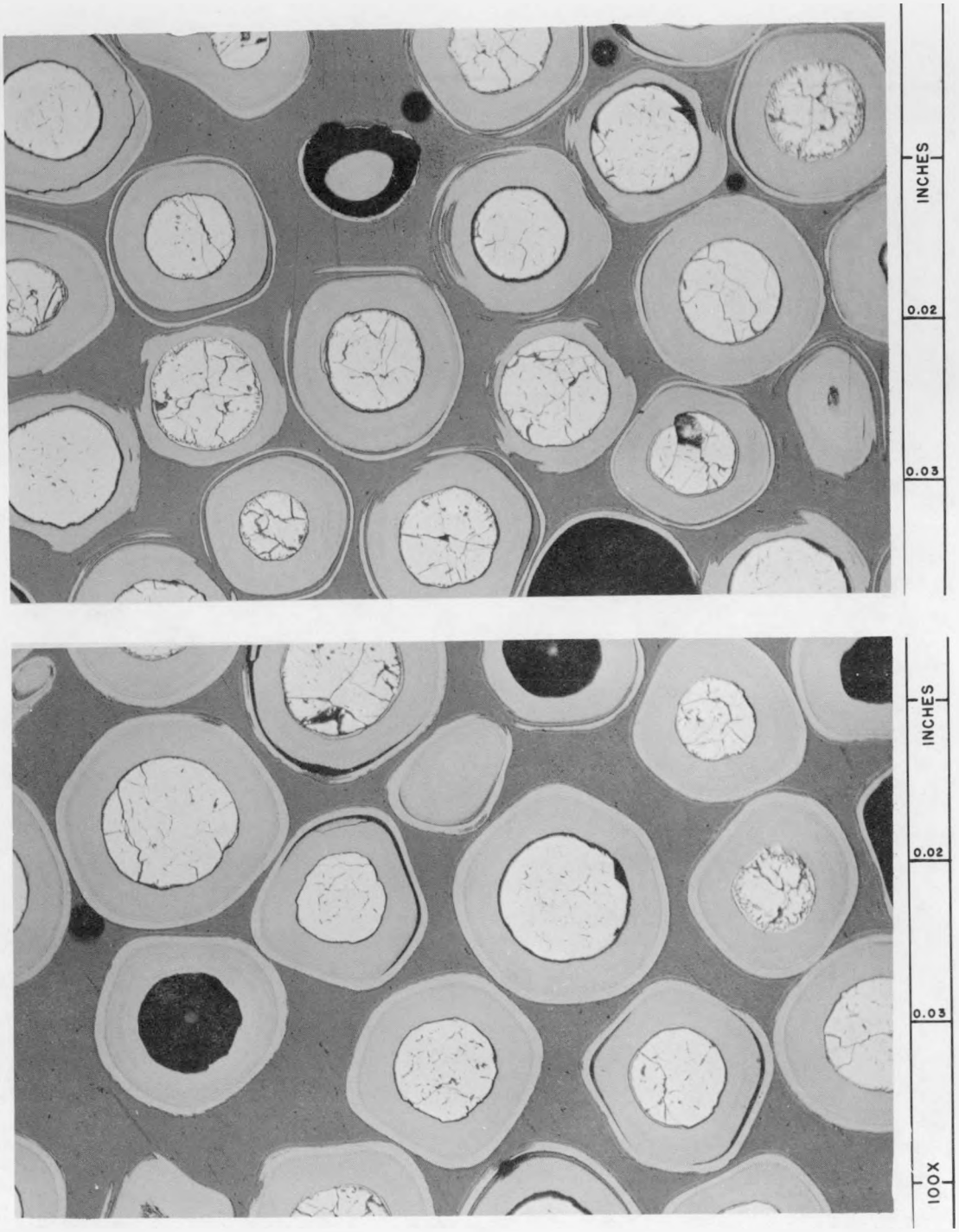

Fig. 21. Coated Particles from Lot No. 3M-114 After 4-hr Exposure at 1000°C to Helium Containing H_2O (Total Pressure, 1 atm). a. Partial pressure of H_2O of 149 mm Hg; b. partial pressure of H_2O of 355 mm Hg. Large dark areas are a result of fuel-particle removal during metallographic preparation. As-polished. 100X.

of the coating was removed. All particles were damaged and peeling of the outer layer was very evident, as illustrated in Fig. 21b, after an exposure of 4 hr at 1000°C at a higher partial pressure of H_2O. These latter conditions resulted in removal of 39% of the coating. In several cases most of the pyrolytic carbon was removed but no path was opened to the fuel particle. Generalized attack on coated particles from lot 3M-114 probably accounted for the protection afforded these particles even after substantial amounts of the coating were removed.

Tests at 800 to 1100°C, High H_2O Contents

More recently coated particles from lot 3M-117 were tested using, in some cases, higher partial pressures of H_2O and also higher temperatures. The results, presented in Table 5, indicate that the susceptibility of these particles to attack by steam is similar to that for lot 3M-114. The loss in weight of the two lots of particles at 900 and 1000°C are in fair agreement. The coatings in lot 3M-114 appear to be somewhat more protective than those in lot 3M-117, but both afford much better protection than was observed for lot 3M-113. Visual examinations of lot 3M-117 indicate that a pitting type of attack occurred.

Failure of a large number of the coatings occurred at 1100°C in the one run made at this temperature. It appears unlikely, therefore, that the coatings will remain intact at this temperature for as long as an hour when exposed to 1 atm of H_2O. At temperatures of 800°C and below, however, prolonged exposure may be permissible for some of the lots of coated particles.

Tentative Conclusions

The results of tests on five lots of pyrolytic-carbon-coated particles, all having the laminar type of coating, show marked differences in behavior that must be associated with different modes of attack by H_2O. Differences in reaction rates for different coatings have been observed at comparable exposure conditions. Furthermore, there is no clear-cut relationship between the amount of pyrolytic carbon removed from the coating and the incidence of failure of the coating as determined by the HNO_3 leach. This behavior suggests that it would be necessary to experimentally evaluate a particular lot of material before its compatibility with H_2O at 900 to 1000°C could be predicted with any degree of

Table 5. Reactivity of Pyrolytic-Carbon-Coated Particles from Lot 3M-117 with Helium Containing H_2O at Partial Pressures of 355–635 mm Hg (Total Pressure, 1 atm) in the Temperature Range 800–1100°C

Sample Number	Weight of Sample (g)	Time (hr)	Temperature (°C)	Partial Pressure of H_2O (mm Hg)	Weight Loss (g)	Calculated Amount of Coating Removed (%)	Calculated Rate of Coating Removal (g/g-hr)	U Removed by HNO_3 Leach	
								(g)	Percent of Total U
3M-117-20	2.072	4	800	355	0.069	6.4	0.016	0.004	0.4
-16	2.102	1	800	635	a	a	a	0.001	0.1
-23	1.980	4	800	635	0.163	15.9	0.04	0.011	1.3
-5	2.056	1	900	355	0.030	2.8	0.028	0.027	3.0
-6	2.101	2	900	355	0.075	6.9	0.035	0.057	6.3
-22	2.063	4	900	355	0.115	10.9	0.027	0.032	3.5
-13	1.832	4	900	355	0.074	7.9	0.020	a	a
-17	2.028	4	900	355	0.142	13.5	0.034	0.053	5.9
-21	2.008	4.5	900	355	0.117	11.3	0.025	0.024	2.7
-8	2.132	1	900	635	0.078	7.1	0.071	0.006	0.6
-24	1.615	1	900	635	0.052	6.2	0.062	0.030	4.1
-7	2.012	2	900	635	0.172	16.6	0.083	0.037	4.1
-3	2.556	1	1000	355	0.084	6.4	0.064	0.050	4.4
-2	1.979	2	1000	355	0.186	18.3	0.092	0.122	14
-14	2.069	2	1000	355	0.179	16.8	0.084	a	a
-19	2.048	2	1000	355	0.133	12.5	0.063	0.031	3.4
-12	2.012	4	1000	355	0.417	40	0.10	0.061	6.8
-1	2.337	4	1000	355	0.521	43	0.11	0.046	4.5
-10	1.924	1	1000	635	0.114	11.5	0.12	0.036	4.1
-25	1.778	1	1100	635	0.421	46	0.46	0.32	40

[a]Not determined.

certainty. It appears that prolonged exposure at 800°C and below may be permissible for some lots of coated particles; at 1100°C, however, it is unlikely that the coatings will remain intact for as long as 1 hr.

COMPATIBILITY STUDIES WITH LIQUID COOLANTS

(E. L. Compere, S. A. Reed, D. M. Richardson, and L. F. Woo
Reactor Chemistry Division)

The development of a variety of coated-particle fuel elements of promising quality for use in gas-cooled reactor systems suggested that a potential of high performance exists in liquid-cooled systems. The use of ceramic coated particles offers the possibility of good neutron economy and the capability of high temperatures and long burnup in liquid-cooled reactor fuels. The major questions concerning this application involve fission-product retention and compatibility.

The purpose of this phase of the program is to assess the compatibility problem, including the effects of gamma radiation, in a variety of liquid coolants. By general classification the liquids investigated are pressurized water, organic-moderator coolants, and molten fluoride salts.

PRESSURIZED WATER

In studies with pressurized water, the major emphasis has been on the effects of high rates of heat transfer on coated fuel particles and graphite matrices in flowing systems. Test materials have been special grades of unfueled matrix graphite and specimens fueled with alumina-coated UO_2 and pyrolytic-carbon-coated uranium carbide particles procured from National Carbon Company and Speer Carbon Company. Specimens of massive pyrolytic carbon and a high-purity, high-density spectrographic grade of graphite also have been tested for comparison with the matrix grades.

Heat fluxes of 300,000 to greater than 1,000,000 Btu/hr·ft^2 have been generated by electrically resistance heated, 1/4-in.-diam rod specimens immersed in flowing (2 to 6 fps) water at 225–300°C. The apparatus, shown schematically in Fig. 22, was specially designed for placement in a bypass line of a 100-gpm pump loop.

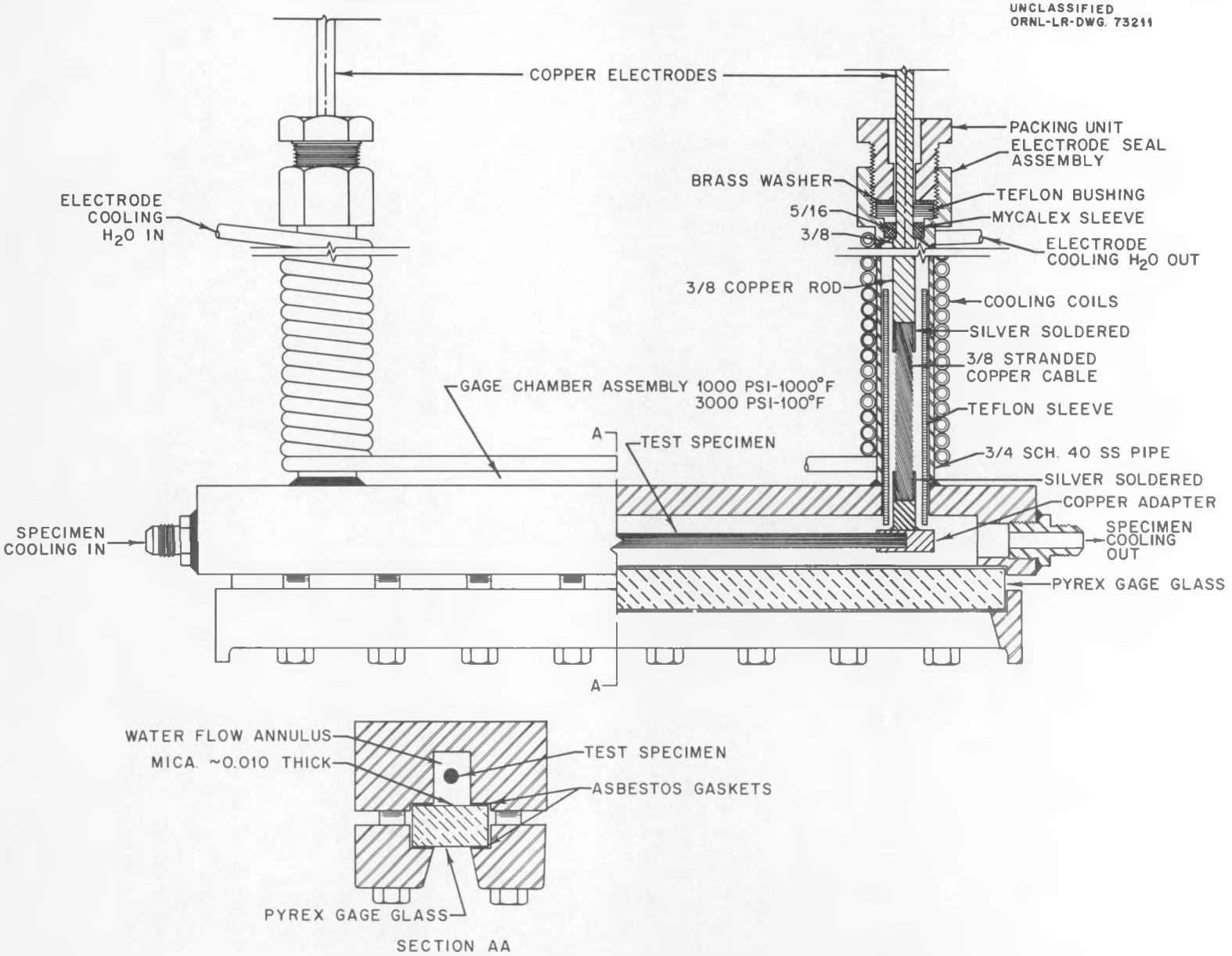

Fig. 22. Test Apparatus Used in By-Pass Line of Pump Loop for Testing Compatibility of Electrically Heated Graphite-Base Materials in Flowing, Pressurized Water.

The pyrolytic-carbon specimens were machined from massive plate material in such a manner that the large, columnar grains were essentially perpendicular to the longitudinal rod axis. Thus, a wide range of crystallographic directions in this highly anisotropic material was exposed to the flowing water. A specimen of this type was not detectably attacked after a 24-hr exposure to water at 250°C, a flow velocity of 2 fps, and a generated heat flux of 500,000 Btu/hr·ft^2. However, under similar conditions but at a flux of 600,000 Btu/hr·ft^2 for 250 hr, mild attack occurred at the edges of the layered structure of the pyrolytic carbon. A third specimen, tested under similar conditions, splintered longitudinally as shown in Fig. 23 after 50 min at a flux of 860,000 Btu/hr·ft^2. Again, there was evidence of preferential attack along the layers of the structure.

A photograph of the spectrographic grade graphite specimen is shown in Fig. 24 after a 45-min exposure at a flux of 900,000 Btu/hr·ft^2 in 300°C water flowing at 2 fps. The attack on this specimen can be described as generally uniform with a rather more pronounced attack at a region near the downstream end. Calculations indicated that the critical (burnout) heat flux for the material probably was exceeded under the conditions employed. It is inferred that under film-boiling conditions the rod became so hot as to permit the steam-carbon reaction to proceed at a substantial rate.

Two specimens of unfueled grades of matrix graphite supplied by Speer Carbon Company were exposed at generated heat fluxes of approximately 1,000,000 Btu/hr·ft^2 under conditions which were essentially similar to those used for the spectrographic graphite specimen. Visual examination indicated that these specimens were not attacked during 250-hr tests.

In initial screening tests in static autoclaves, coupon specimens of several lots of conventional graphitized grades of nuclear graphite and experimental grades of extruded or molded types of matrix graphites were exposed submerged in nitrogen-sparged water at 320°C (1500 to 1600 psig) for 200-hr periods. Tests were completed with National Carbon Company graphitized grades AGOT, ATJ, CEQ, and TSX, and with special grades TS-148, TS-160, and FE-3, each of the latter grades having been baked at 1400, 2000, and 2800°C. Massive pyrolytic carbon furnished by High Temperature Materials, Incorporated, also was tested. In all cases, weight and and dimensional measurements indicated that no attack occurred.

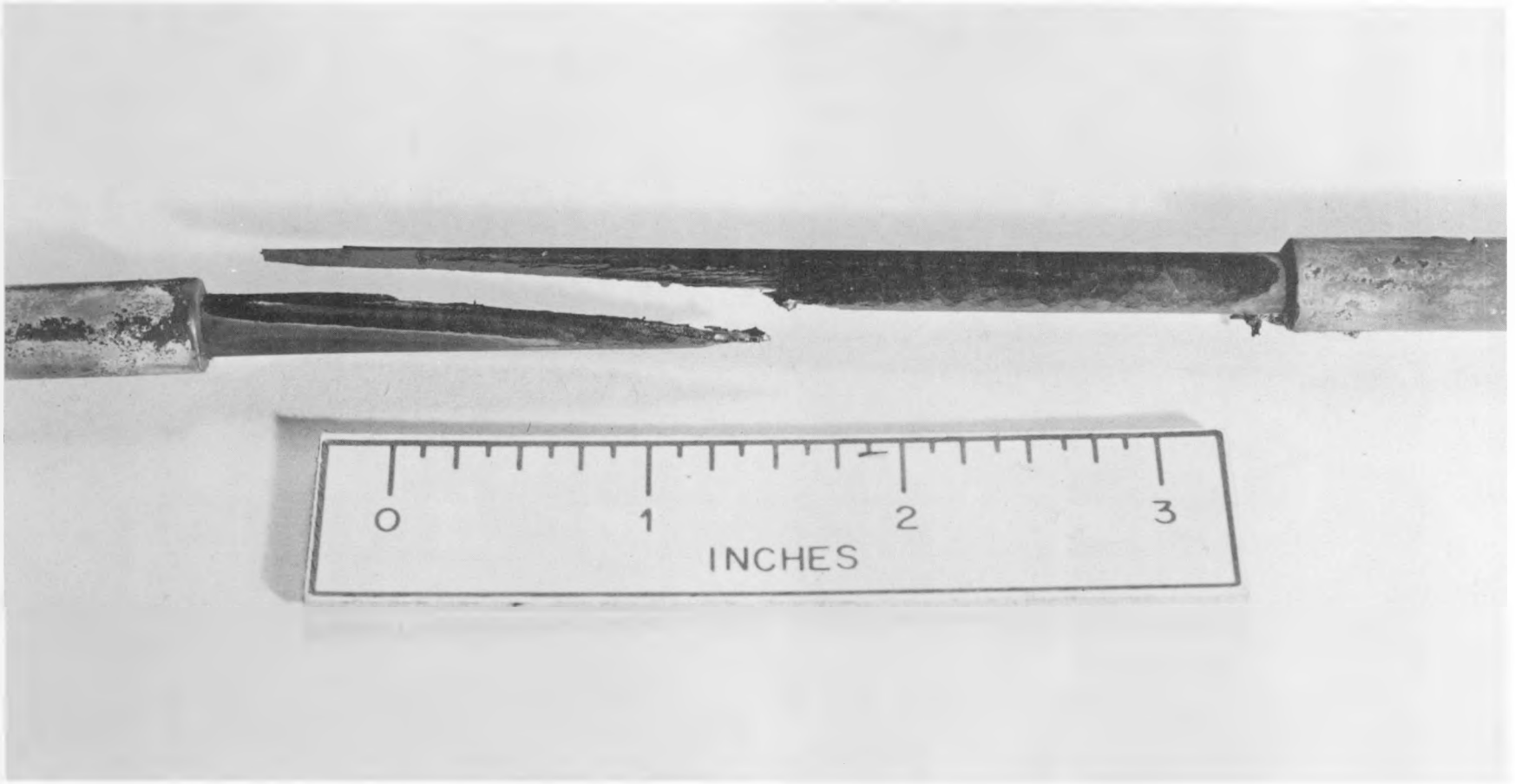

Fig. 23. Pyrolytic-Carbon Rod Which Failed After 50 min Exposure at a Heat Flux of 260,000 Btu/hr·ft^2 in 250°C Water at a Flow Rate of 2 fps.

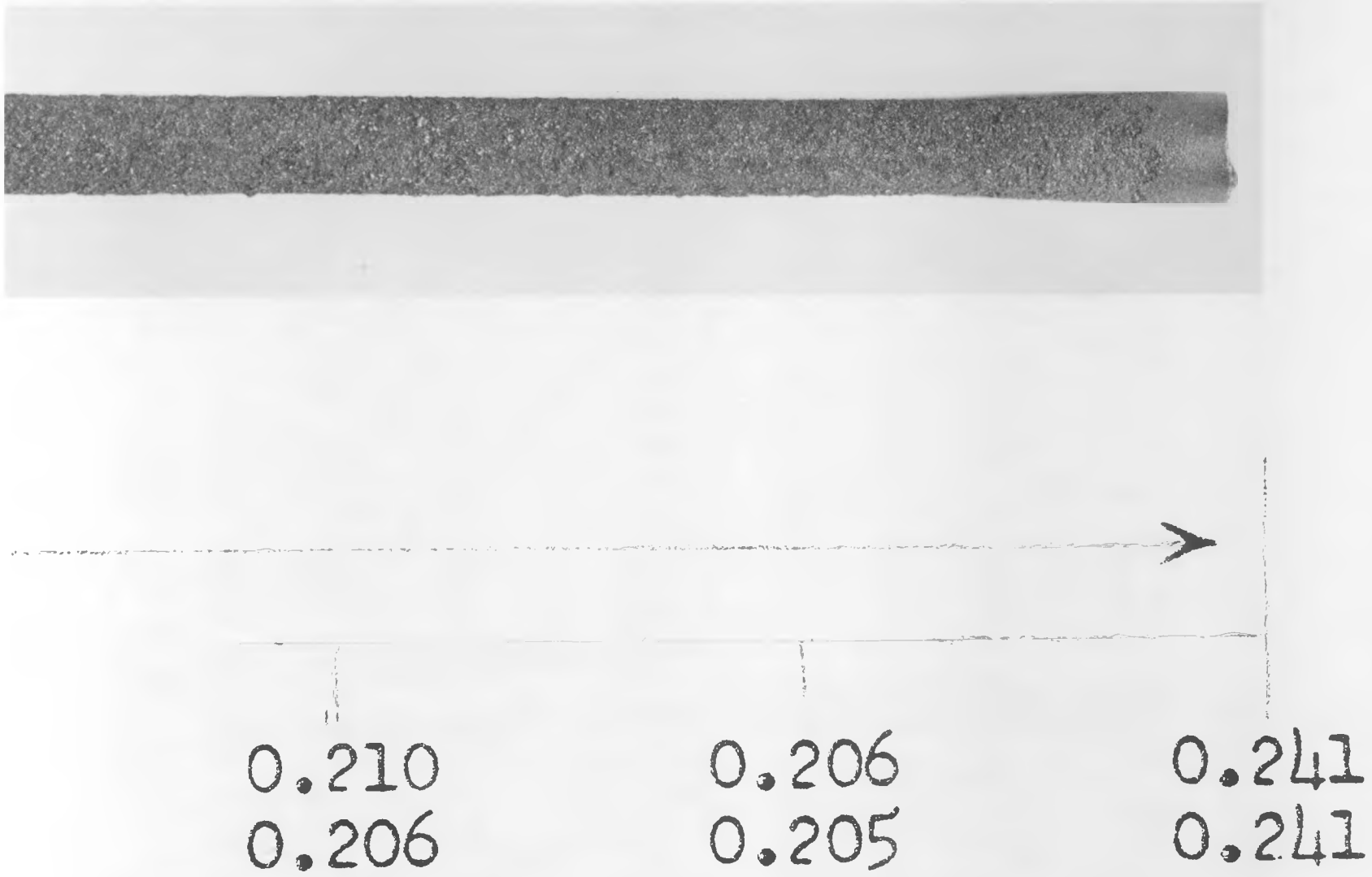

Fig. 24. Spectrographic Grade Graphite Specimen After 45-min Exposure at a Heat Flux of 900,000 Btu/hr.ft^2 in 300°C Water at a Flow Rate of 2 fps. Direction of flow is indicated by the arrow. The numbers denote mutually orthogonal diametral dimensions, in inches, measured after the test at the positions indicated.

ORGANIC-MODERATOR COOLANTS

A forced-flow test loop has been designed and constructed for studying the compatibility of organic-moderator coolants such as Santowax-R with graphite-base, coated-particle materials. With this apparatus, tests involving high rates of heat transfer can be carried out in a manner similar to that described for the pressurized-water tests.

MOLTEN FLUORIDE SALTS

The compatibility of coated-particle materials with molten fluorides has been studied in static crucible tests in vacuum and with helium and hydrogen as cover gases. Test temperatures in the range 800—1000°C were selected to produce accelerated effects as well as to investigate the region of hot-spot conditions of interest in nuclear reactors employing molten fluorides. The fluoride salt mixture used in almost all the tests was the LiF-NaF eutectic (mp 652°C) prepared by mixing pure, commercial materials.

Alumina-coated UO_2 particles (CP-2-NUMEC 915) were found to be incompatible with the molten fluorides. The coatings were either dissolved or severely corroded, and cracking was frequently observed. Alpha-alumina spheres, 1 mm in diameter and obtained from the Linde Company corroded more rapidly with increasing temperature and with increasing partial pressure of hydrogen as shown in Table 6.

Table 6. Average Attack by LiF-NaF Eutectic on 1-mm-diam Alpha Alumina Spheres (μ/100 hr)

Partial Pressure of H_2[a] (atm)	Temperature (°C)		
	800	900	1000
1	21	b	(spheres consumed)
1/20	0[c]	29	b
0	0[c]	13	b

[a] Total pressure, 1 atm.

[b] Not determined.

[c] Surfaces lightly etched; some cracks visible.

The alumina spheres were also tested in LiF-NaF-KF eutectic ("flinak") at 600°C with helium cover gas. The average attack was 38μ in 100 hr. Since the "flinak" used had been especially treated to remove water and oxidizing impurities, the aggressive attack might have been due to the KF component or to FeF_2 and CrF_2 impurities.

Early tests of pyrolytic-carbon-coated fuel particles were performed concurrently with those for alumina spheres. The particles were placed on top of the salt and remained there throughout the test. (This behavior was indicative of nonwetting since the average particle density was greater than the density of the molten salt.) Under these conditions there was never any evidence of damage to the coatings.

Recent tests of pyrolytic-carbon-coated particles were conducted with the particles submerged in the salt in nickel crucibles at 900 to 1000°C for 200 hr in hydrogen at a pressure of 3 atm. The coatings were damaged and in some batches a stain identified as UO_2 was found on the bottom of the crucibles. Many particles were flattened where they contacted the nickel crucible. The coating damage observed is believed to have been due to carbon diffusion into the nickel as well as to the nickel-catalyzed reaction of carbon and hydrogen to form methane.

EFFECTS OF GAMMA RADIATION

The compatibility of liquid coolants with coated-particle materials could be substantially affected by irradiation. If fission products are contained, the effects would for the most part be limited to those associated with neutrons and gamma rays. Initial studies have been concerned with the effects of gamma radiation.

Irradiation of autoclaves containing coated particles and graphite-base materials has been carried out in a (nominal) 10,000-curie Co^{60} source. The experimental apparatus, shown schematically in Fig. 25, is located in a corner of the source cavity. The dose rate is estimated to be 1.1×10^{-3} w/g of graphite (0.85×10^{18} ev/min·ml).

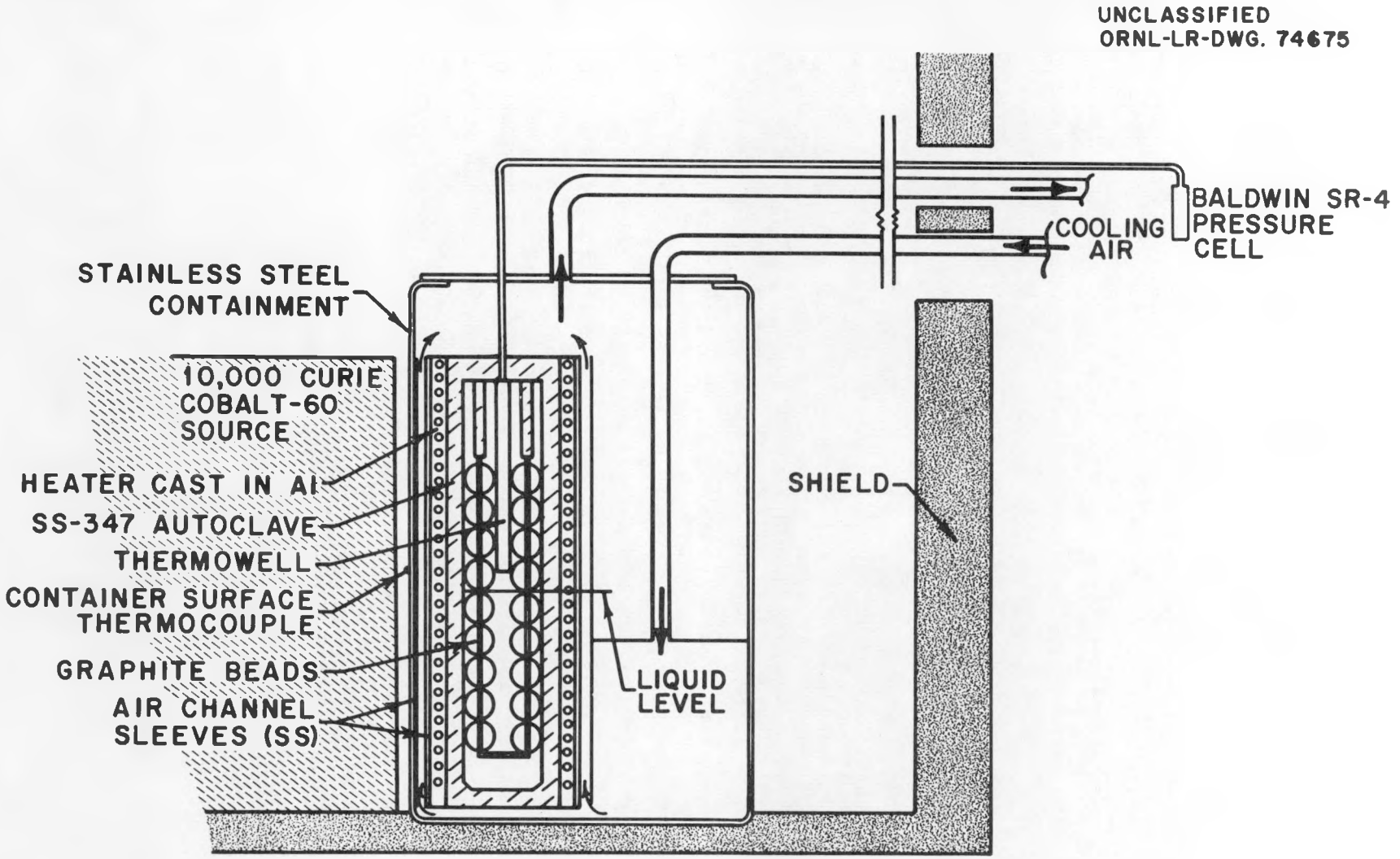

Fig. 25. Schematic Drawing of Gamma-Irradiation Experiment.

A 2155-hr test was completed on a type 347 stainless steel autoclave containing 1/4-in.-diam spheres of type AGOT graphite, pyrolytic carbon, and graphite mixes NCC grade TS-148 (baked at 2000°C) and NCC grade TS-160 (baked at 2000°C) in contact with D_2O pressurized with helium at 330°C. A small quantity of gas was generated during the test. This gas was collected and, based on the average of results of mass spectrometry and gas chromatography, was found to contain 132 μmole of CO_2 and 20 μmole of D_2; neither CO nor hydrocarbons were detected. These results are not consistent with those to be expected from the simple reaction of carbon with heavy water which would produce twice as much D_2 as CO_2. A selective sorption of D_2 in the graphite pores could account for this inconsistency. Microscopic examination of the surfaces of the spheres revealed that no significant attack had occurred. Diameter increases of 0 to 0.1% were observed.

An autoclave experiment is currently in operation to test the compatibility of coated particles and graphite-base materials with Santowax-R at 400°C in the presence of a gamma field. The autoclave contains spheres of the type described above for the D_2O tests pressurized with helium; in addition, there are two small, evacuated Pyrex capsules containing Santowax-R with alumina-coated UO_2 particles (CP-2-NUMEC 915) and pyrolytic-carbon-coated uranium carbide particles (CP-3-National Carbon 201). As of October 5, 1962, the test had been in operation for 1025 hr of which 1000 hr were at 400°C.

Another autoclave experiment is being fabricated for use in testing the compatibility of graphite-base materials with molten fluoride salts at 600°C in a gamma field. The INOR-8 autoclave is to be equipped with two helium-filled nickel capillary tubes for purging and sampling the gas phase during irradiation.

CHEMICAL PROCESSING OF COATED-PARTICLE FUELS

(L. M. Ferris, Chemical Technology Division)

Chemical processing of irradiated fuel elements is only one of the many steps in the overall fuel cycle and consists of dissolution of the fuel values, uranium and thorium, followed by a decontamination procedure to effect separation of these elements from the fission products.

Currently, extraction of the uranium and thorium from nitric acid solutions with tributyl phosphate is the best method for achieving the desired decontamination. Initial laboratory work has been concentrated on graphite-base fuels which contain either pyrolytic-carbon- or alumina-coated particles. At least five processing methods for these fuels are being evaluated. They are "grind-leach,"[15,16] combustion-dissolution,[16] the 90% HNO_3 process,[16,17] anodic disintegration, and chloride volatility.[18] A brief description of these techniques and a summation of the results obtained are presented below.

GRIND-LEACH PROCESS

This process involves mechanically grinding the fuel elements fine enough to ensure rupture of the particle coatings, and then leaching the resulting powder with nitric acid or HNO_3–HF to recover the uranium and thorium. This technique is applicable to all types of graphite-base fuel elements, the extent of grinding being dependent primarily on the size of the coated particles. In principle, the technique is applicable to other types of high-temperature reactor fuels, e.g., those having alumina or BeO matrices. When grinding is fine enough (–200 mesh for most coated-particle fuels), uranium and thorium are recovered almost quantitatively by leaching for 6 to 8 hr in a suitable boiling reagent. The results of a number of tests are given in Table 7.

---

[15]M. J. Bradley and L. M. Ferris, Nucl. Sci. Eng. 8, 432 (1960).

[16]L. M. Ferris, A. H. Kibbey, and M. J. Bradley, Processes for Recovery of Uranium and Thorium from Graphite-Base Fuel Elements, Part II, ORNL-3186 (Nov. 16, 1961).

[17]M. J. Bradley and L. M. Ferris, Ind. Eng. Chem. 53, 279 (1961).

[18]T. A. Gens, ORNL Chemical Technology Division, unpublished data.

Table 7. Uranium and Thorium Recovery from Fueled Graphite by the Grind-Leach Process

(Fuel ground to −200 mesh and leached for 6 to 8 hr with boiling reagent)

Fuel	Composition of Fuel Body (wt %) Uranium	Thorium	Leachant	Recoveries (wt %) Uranium	Thorium
Uncoated UO_2-ThO_2	1.2	8.0	13 M HNO_3–0.04 M HF–0.1 M $Al(NO_3)_3$	99.9	99.9
Uncoated UC_2-ThC_2	1.5	7.2	13 M HNO_3–0.04 M HF–0.1 M $Al(NO_3)_3$	90	88
Alumina-coated UO_2	8.0	--	15.8 M HNO_3	99	--
Pyrolytic-carbon-coated UC_2-ThC_2	9.7	33.8	15.8 M HNO_3	98.8	99.9
Pyrolytic-carbon-coated UC_2-ThC_2	9.6	33.5	13 M HNO_3–0.04 M HF–0.1 M $Al(NO_3)_3$	99.4	99.9

Several engineering problems must be solved before this method can be considered practicable. The feasibility of finely grinding fuels containing refractories and abrasives such as SiC and alumina must be demonstrated. Methods for filtering or centrifuging large volumes of graphite slurries and for adequately washing graphite beds must also be developed.

COMBUSTION-DISSOLUTION PROCESS

Combustion, in oxygen, of graphite-base fuels containing carbon-coated fuel particles followed by dissolution of the oxide ash leads to quantitative recovery of uranium and thorium, as shown in Table 8.

Table 8. Uranium and Thorium Recovery from Fueled Graphite by the Combustion-Dissolution Process

(Fuel burned in oxygen at 750 to 850°C; ash leached 6 to 10 hr in boiling reagent)

Fuel	Composition of Fuel Body (wt %)				Leachant	Recoveries (wt %)	
	U	Th	Si	Fe		U	Th
Uncoated UC_2-ThC_2	1.7	8.0	--	--	13 M HNO_3–0.04 M HF–0.1 M $Al(NO_3)_3$	100	100
Pyrolytic-carbon-coated UC_2-ThC_2	9.9	33.0	--	--	13 M HNO_3–0.04 M HF–0.1 M $Al(NO_3)_3$	100	100
Alumina-coated UO_2	8.0	--	--	--	10 M HNO_3	9.9	--
Uncoated UC_2	3.7	--	--	0.1	10 M HNO_3	99.8	--
Uncoated UC_2	0.7	--	--	0.4	10 M HNO_3	98.0	--
Uncoated UO_2	7.0	--	2.0	--	10 M HNO_3	99.6	--
Uncoated UO_2	6.8	--	20.3	--	10 M HNO_3	97.8	--

This technique may also be applicable to fuels containing BeO-coated particles using dissolution techniques developed for sintered BeO.[19] Fuel elements containing alumina-coated particles present a nearly impossible situation because of the inertness of sintered alumina. The graphite matrix burns readily, but the coated particles are virtually unaffected by the combustion. Fuels that are coated with materials such as SiC or that contain impurities such as iron yield combustion residues from which quantitative leaching of the uranium and thorium as difficult. For example, the ash from a graphite-base fuel sphere coated with siliconized SiC retained 2% of the uranium in insoluble form when leached with boiling 10 M HNO_3.

The combustion-dissolution process is not without its shortcomings, however. Because of the high temperatures involved the choice of materials for burner construction is limited, and CO, which can form explosive mixtures with oxygen, is formed in preference to CO_2 unless an excess of oxygen is present. Methods for safely disposing of the radioactive off-gas will have to be developed. In addition, the ash from thorium-bearing fuels can be dissolved only in nitric acid containing small amounts of fluoride ion, a somewhat corrosive solution. Because of the markedly different thermal and environmental conditions imposed in the two steps of the process, it is quite unlikely that a single vessel can be used for the combustion and dissolution.

Low-temperature combustion may alleviate many of these problems. Preliminary work in this area has indicated that the ignition temperature can be lowered several hundred Centigrade degrees by the use of catalysts such as manganese, copper, or lead. For example, United Carbon Products spectroscopic-grade graphite does not ignite below 720°C in a stream of pure oxygen; however, the ignition temperature can be reduced to about 345°C by presoaking the graphite in 0.07 M lead acetate solution, as shown in Table 9. Furthermore, combustion is catalyzed well below the ignition temperature. Untreated graphite showed at most a 0.4% weight loss when exposed for 3 hr to a stream of oxygen at 460°C, but a piece

---

[19] K. S. Warren, L. M. Ferris, and A. H. Kibbey, Dissolution of BeO- and Al_2O_3-Base Reactor Fuel Elements. Part I, ORNL-3220 (Jan. 30, 1962).

of graphite that had been soaked for 3 min in 0.25 M $KMnO_4$ solution lost 34% of its weight under the same conditions. Further work with such catalysts is in progress.

Table 9. Catalysis of the Combustion of United Carbon Products Graphite (Ultrapurity, spectroscopic grade from Lot 5387; density, 1.55 g/cm^3)

Catalyst[a]	Ignition Temperature (°C)	Combustion Temperature (°C)	Time (hr)	Weight Loss (%)
None	720			
		311	3	0.00
		334	3	0.00
		459	3	0.37
		459	3	0.05
		471	3	0.23
0.07 M Lead Acetate	345			
		311	3	3.2
		334	3	6.0
0.25 M $KMnO_4$	482			
		448	3	33.6
		459	3	34.4
3.15 M $Cu(NO_3)_2$	482			
		459	3	13.5
		471	3	11.9

[a]Each specimen soaked for 3 min in the indicated solution.

90% HNO_3 PROCESS

Graphite matrices are readily disintegrated in 90% HNO_3 (21.5 M) at temperatures from 25°C to the boiling point, about 93°C. Unfortunately, only the matrix is affected; both pyrolytic-carbon- and alumina-coated particles are unaffected. For example, the results presented in Table 10 show that when specimens containing coated particles were disintegrated

to powder (mean particle size about 700μ) in boiling 90% HNO_3, less than 7% of the uranium and thorium was solubilized. This technique, therefore, does not appear applicable to the processing of graphite-base fuels containing coated particles.

Table 10. Uranium and Thorium Recovery from Fueled Graphite by the 90% HNO_3 Process

(Fuel disintegrated and leached twice for 4 hr with boiling 21.5 M HNO_3)

Fuel	Fuel Composition (wt %)		Recoveries (wt %)	
	Uranium	Thorium	Uranium	Thorium
Uncoated UC_2	3.0	--	99.4	--
Uncoated UC_2	15.2	--	99.9	--
Uncoated UC_2-ThC_2	1.3	15.0	99.9	99.8
Pyrolytic-carbon-coated UC_2-ThC_2	9.7	33.5	6.5	4.6
Alumina-coated UO_2	8.0	--	0.8	--

The technique was studied briefly, however, as a destructive method for evaluating the integrity of coated fuel particles. A similar technique based on electrolytic disintegration has been used at Battelle Memorial Institute.[20] The amount of uranium (and/or thorium) dissolved during the acid treatment would be proportional to the number of particle coatings which were defective (or which were susceptible to oxidation). Commercial grades of graphite generally are oxidized very slowly in concentrated nitric acid. Studies with type GBF graphite showed that digestion of powdered samples for periods of up to 100 hr resulted in oxidation of less than 2% of the carbon. Amorphous carbons, however, are oxidized at a much higher rate. Therefore, pyrolytic-carbon coatings that are not highly graphitized may be oxidized.

[20]R. A. Ewing, T. S. Elleman, and R. B. Price, Trans. Am. Nuclear Soc. 4(1), 152 (1961).

Two batches of pyrolytic-carbon-coated uranium carbide particles were tested using the 90% HNO_3 technique, with results as shown in Table 11. In two 6-hr leaches with boiling acid less than 2% of the uranium was dissolved from batch 3M-D; on the other hand about 48% of the uranium was dissolved from batch NCC-J. Since the weight losses were about those expected from the amounts of uranium dissolved, it is concluded that these results reflect the degree to which the particle coatings were defective. The ultimate usefulness of this technique will be determined only after more intensive study.

Table 11. Evaluation of Pyrolytic-Carbon Coatings on Uranium Carbide Particles Using 90% HNO_3

(Each sample leached twice for 6 hr with boiling 21.5 M HNO_3)

Type of Particles	Uranium Content of Sample (wt %)	Uranium Solubilized (wt %)		Weight Loss (%)	
		First Leach	Second Leach	Calculated	Observed
3M-D	69.24	0.34	2.5	1.9	0
3M-D	68.58	0.33	1.0	0.9	0
NCC-J	44.00	11.8	35.8	21	16.9
NCC-J	43.86	11.5	36.4	21	17.2

ANODIC DISINTEGRATION

Electrolytic disintegration in hot (93°C) 15.8 M HNO_3 did not result in satisfactory recovery of uranium from fueled-graphite specimens containing pyrolytic-carbon-coated uranium carbide fuel particles. The graphite matrix was readily disintegrated, but the particle coatings were not markedly affected; as expected, less than 2% of the uranium was found in solution. Similar results were obtained on unsupported pyrolytic-carbon-coated particles[21] and at Battelle Memorial Institute with fuels containing alumina-coated UO_2 particles.[20]

[21] A. H. Kibbey and L. M. Ferris, U-Th Recovery from Pyrolytic-Carbon Coated Carbide Fuel Particles by Electrolysis in Nitric Acid, ORNL-TM-384 (Sept. 26, 1962).

CHLORIDE VOLATILITY PROCESS

Very little work has been done on chloride volatility processing of coated-particle fuels. Two variations are being studied. In the first, uranium would be converted to a volatile chloride using one of several reagents such as CCl_4, Cl_2, or $COCl_2$ and sublimed away from the graphite matrix (graphite reacts only very slowly with chlorinating agents even at relatively high temperatures). The recovered uranium chloride would either be fluorinated to UF_6 or dissolved in an aqueous solution preparatory to solvent extraction. Chlorination techniques are also applicable to the recovery of uranium from combustion ashes.

SUMMARY AND CONCLUSIONS

At this stage of development, combustion-dissolution must be considered the best method for processing graphite-base coated-particle fuels. The chief foreseeable problems with this technique are the treatment of large volumes of radioactive off-gas from the burning step and the probable need for transferring the solid combustion ash to a suitable metallic vessel for the acidic dissolution. In addition, it is doubtful that a single vessel can be utilized for both burning and HNO_3-HF dissolution because of the corrosiveness of the acidic reagents in the high-nickel-content alloys required to withstand the oxidation conditions.

The alternative method, that of grinding followed by acid leaching, is plagued with potential engineering problems. Grinding is a formidable operation, and even if it could be conducted efficiently the resulting powder would be so fine that its separation from the acidic leach liquor would be extremely difficult by either centrifugation or filtration. The "chemical grinding" methods, 90% HNO_3 and electrolytic disintegration, are inapplicable to the processing of coated-particle fuels, but have found application in the evaluation of as-received and irradiated coated particles.

ACKNOWLEDGMENT

The careful and critical review of this paper by J. H. Coobs of the Metals and Ceramics Division and M. W. Rosenthal of the Reactor Division is hereby gratefully acknowledged.

* * *

DISCUSSION

Question, P. Murray (UKAEA): "In view of the data reported for the high-burnup experiments on coated particles, it would appear that UC_2 changes less with radiation than does UO_2. Is this true?"

Reply, W. O. Harms (ORNL): "It is certainly indicated from the results that the changes in the carbide structure are less than those based on both calculated and observed changes in uranium dioxide specimens. The fact that the coatings did not fail in these experiments, however, may not be wholly inconsistent with the probability that significant changes did occur in the carbide structure. One of the several reasons may be associated with the free volume which exists between the particle and its coating."

Question, P. Murray (UKAEA): "What type of temperature cycling have you exposed the particles to?"

Reply, W. O. Harms and F. L. Carlsen (ORNL): "There was more thermal cycling of the matrix specimens than of the unsupported particles. The effect of a change in the operating temperature was more noticeable than that of temperature cycling."

Question, W. J. O'Leary (AC): "Why are you using particles with diameters of 300 microns?"

Reply, F. L. Carlsen (ORNL): "A fuel particle size of 150 to 200 microns was selected to minimize fission recoils into the coatings without producing excessive center temperatures. It is also said to be an optimum size for the coating process. The coating thickness of about 100 microns gives sufficient coating strength to permit incorporation of particles into a matrix without cracking the coatings. In addition, coatings thinner than 100 microns have not performed satisfactorily during irradiation."

PYROLYTIC-CARBON-COATED CARBIDE FUEL PARTICLES AND THEIR USE IN GRAPHITE-MATRIX FUEL COMPACTS*

Edited By W. V. Goeddel
John Jay Hopkins Laboratory for Pure and Applied Science
General Atomic Division of General Dynamics Corporation
San Diego 12, California

ABSTRACT

A summary of the development and evaluation of pyrolytic-carbon-coated carbide fuel particles and graphite-matrix fuel compacts is presented.

A process that has been developed for the preparation of particles of thorium-uranium dicarbide is described. Granulated particles composed of powdered UO_2, ThO_2, and carbon are suspended in a bed of graphite flour and heated to convert the oxides to dicarbides. The particles are then melted to densify and spheroidize them, while the graphite flour keeps them separated so they will not flow together.

Coating the $(Th, U)C_2$ particles with pyrolytic carbon is accomplished in a fluidized-bed apparatus using a methane-helium mixture at a temperature of ~1400°C. Data are presented on the properties of coatings deposited at temperatures to 2400°C.

Graphite-matrix fuel compacts of high density are prepared by a hot-pressing process. Graphite flour is used as the filler and pitch as the binder; the use of graphite flour, rather than coke, permits the attainment of good thermal properties in the compacts without the necessity for high processing temperatures. The hot-pressing process is described and the properties of the compacts are given.

The thermal stability of coated fuel particles has been evaluated at temperatures to 2000°C and for times up to one year. Some coated particles were found to fail in thermal gradient tests because of the movement of the particle through the coating on the high-temperature side; this has been named the "amoeba effect." Tests of coated particles prepared by the techniques described in this report show that there should be no thermal instability at temperatures up to 1500°C for periods of at least three years.

* This work was supported in part under U. S. Atomic Energy Commission Contract AT(04-3)-314, and in part under a joint program of General Atomic and Empire State Atomic Development Associates, Inc.

Results of extensive irradiation tests of graphite-matrix fuel compacts prepared by the hot-pressing process are presented. The compacts containing uncoated (Th, U)C_2 particles were dimensionally stable after burnups of 6.9×10^{19} fissions/cm^3 at 1100° to 1500°C. Compacts containing coated particles were tested to burnups of 1.2×10^{20} fissions/cm^3 at temperatures as high as 2000°C. A few per cent of the particle coatings were found to be broken after these tests. Possible explanations for these failures are presented.

The results of all of these studies show that hot-pressed graphite-matrix fuel compacts containing pyrolytic-carbon-coated (Th, U)C_2 fuel particles will perform satisfactorily at the conditions to be encountered in the Peach Bottom HTGR (maximum temperature less than 1500°C in a purged fuel element).

I. INTRODUCTION

This report is a review of research on pyrolytic-carbon-coated carbide fuel particles and graphite-matrix fuel compacts through the spring of 1962. In the main, this work was directed toward the development of fuel elements for the Peach Bottom High-temperature Gas-cooled Reactor (HTGR).

The subject matter covered in this report includes the following:

1. Preparation of (Th, U)C_2 fuel particles.
2. Pyrolytic-carbon coating of fuel particles.
3. Graphite-matrix fuel compacts.
4. Thermal stability testing.
5. Radiation testing.

A review of fission-product release studies is presented in a companion report by L. R. Zumwalt, E. E. Anderson, and P. E. Gethard.*

A bibliography of General Atomic reports dealing with coated-particle fuels and graphite-matrix fuel compacts is given in the Appendix.

*Fission-product Release from (Th, U)C_2–Graphite Fuels, General Atomic, Report GA-3599.

II. HTGR FUEL ELEMENT

The Peach Bottom High-temperature Gas-cooled Reactor (HTGR) is a helium-cooled, graphite-moderated reactor in which the fuel (U^{235}) and fertile material (Th^{232}) are in the form of carbides dispersed in a portion of the moderator. Outwardly, the proposed fuel element has the appearance of a solid graphite cylinder 3.5 in. in diameter by 144 in. long. There is an upper reflector section, a fuel-bearing middle section, and a bottom reflector section. A graphite sleeve made of low-permeability graphite extends from the upper reflector section to the bottom of the fuel element and contains fuel compacts. In this reactor the approach is not to attempt hermetic containment of fission products within the fuel elements, but rather to control the escape of these fission products and retain them in traps in such a way that the activity in the primary circuit is maintained at a satisfactorily low level.

Within the fuel element, annular fuel compacts are stacked on a cylindrical graphite spine. The compacts, which are 1.5 in. long, 2.75 in. in outside diameter, and 1.75 in. in inside diameter (Fig. 1), contain a mixture of graphite and fissile and fertile materials. Concentrating the fuel material in an annular ring helps to lower the maximum fuel temperature from that of a cylindrical compact with uniform fuel distribution. Grooves are molded into the outer surface of the compacts to provide flow area for the purge gas.

The uranium and thorium within the fuel compacts are in the form of carbides, which are uniformly dispersed as particles in a graphite matrix. The $(Th,U)C_2$ particles are from 100 to 400 μ in diameter. Each particle is pyrolitically coated with a 50- to 60-μ thickness of dense carbon. This coating is designed to protect the fuel material from oxidation reactions during fuel fabrication and to increase the retention time of fission products during reactor operation.

The performance requirements placed on the fuel compacts by the HTGR design may be summarized as follows:

1. Spatial fixation of fuel. The fissile-fertile phases must remain fixed within the graphite matrix; i.e., they must not migrate or evaporate at the elevated operating temperature of the HTGR.

2. Transfer of heat at desired temperatures. Good high-temperature thermal conductivity and thermal-stress resistance are

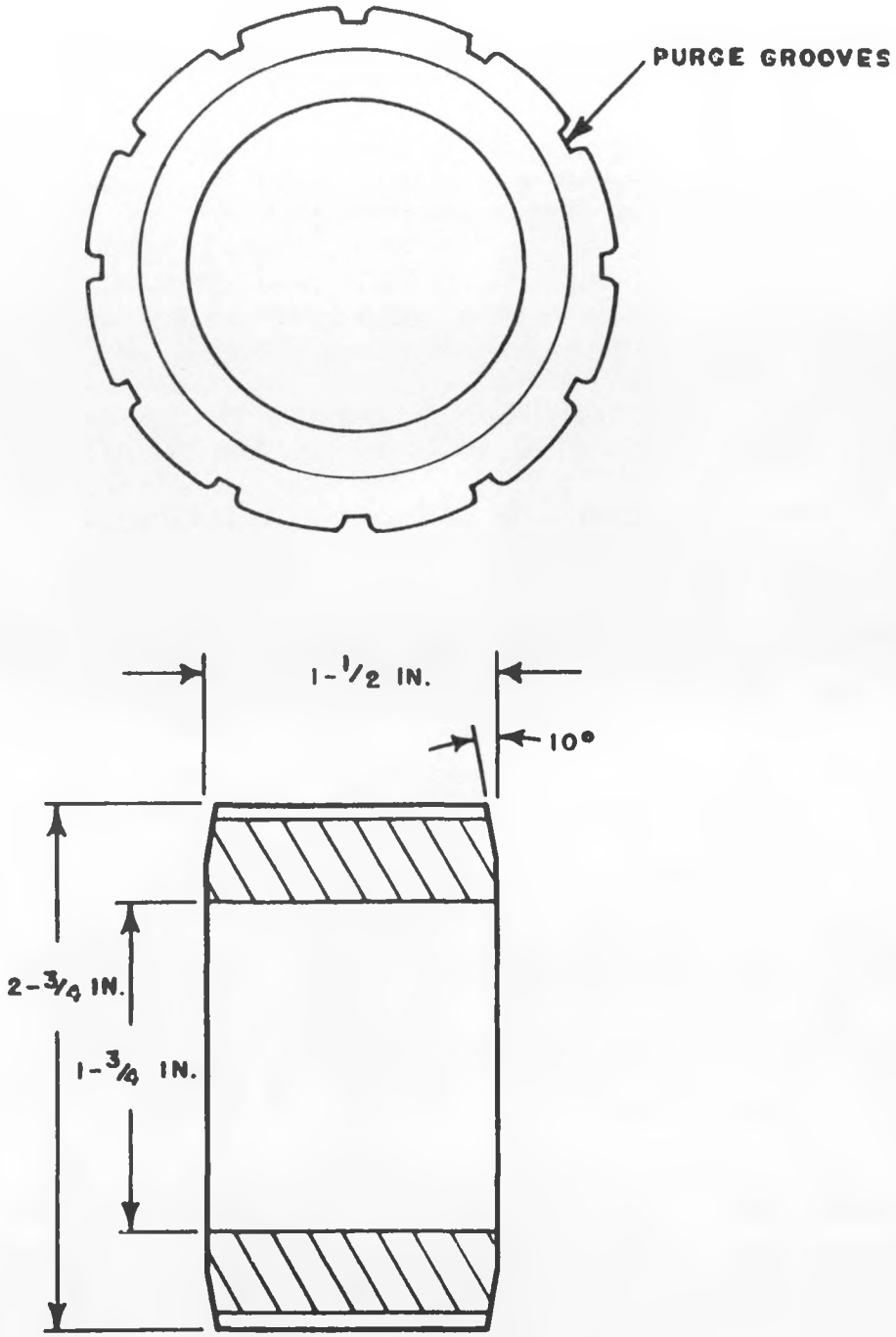

Fig. 1--HTGR fuel compact

required to accommodate the high HTGR power densities and permit the removal of heat without undue thermal gradients.

3. Mechanical and dimensional stability. The fuel compacts must retain their integrity and remain dimensionally stable under prolonged high-temperature irradiation.

4. Retantion of fission products. Fission products must be retained within the fuel compacts as long as possible to minimize the load on the fission-product trapping system.

5. Low cost. Low fuel costs, of course, constitute an important requirement for all commercial power-reactor programs.

More specific compositional and operational parameters are summarized in Table 1.

Table 1

HTGR FUEL-COMPACT PARAMETERS

Composition:	
Uranium (93% enriched), wt-%	2.8
Thorium, wt-%	16.1
Total metal, wt-%	18.9
Graphite, wt-%	81.1
C:Th:U atom ratio	562:5.8:1
C:Metal atom ratio	82:1
Dimensions:	
Outside diameter, in.	2.750
Inside diameter, in.	1.750
Length, in.	1.50
Temperature:	
Maximum fuel-compact temperature, ^{o}C	1340
Average fuel-compact temperature, ^{o}C	980
Burnup (3-yr core life at 80% load factor):	
Fissions per original fissile atom	0.6
Mw-days(t) per metric ton of $U^{235} + Th^{232}$	60,000
Fissions/cm^3	0.67×10^{20}
Kw-hr/cm^3	600

It should be pointed out that the major portion of the General Atomic effort to date on coated fuel particles has been directed toward fuel for the Peach Bottom reactor. These studies have shown that coated particles in a graphite matrix are chemically stable and will perform satisfactorily at Peach Bottom conditions (maximum temperature of less than 1500°C in a purged fuel element). In this application the carbon coatings present two distinct advantages. First, because they protect the carbide from hydrolysis during exposure to air, they simplify handling of the fuel and fabrication of the compacts and the fuel elements. Second, because they retain a major portion of the fission products within the particle, they greatly reduce the load on the fission-product trapping system.

III. PREPARATION OF (Th, U)C_2 PARTICLES

Several techniques were investigated for producing rounded (Th,U)C_2 particles of 200- to 400-μ diameter from the metal oxides and carbon. These techniques fell into two general classifications: (1) the materials were reacted and then formed into particles, and (2) the materials were formed into particles and then reacted. Several examples of each type of process received experimental evaluation.

ThO_2 and UO_2 powders were chosen for starting materials to minimize costs. For each type of process the metal oxide powders were agglomerated with carbon powder, and the aim was to produce the carbide particles in molten form to encourage high density and sphericity.

One process in particular appeared quite promising. The agglomerated pellets of mixed ThO_2, UO_2, and carbon powders were suspended in fine graphite powder in a graphite container and heated in vacuo to 2100° to 2300°C to convert the oxides to dicarbides. The temperature was then raised above the melting point of the carbides (~2450°C) to densify and spheroidize the particles. The powdered-graphite bed prevented the particles from flowing or sintering together, and in fact a partial graphite coating adhered to the surface of the particles. The excess graphite powder was readily separated from the carbide particles by screening.

Particles prepared by this "graphite-bed sintering and melting" process were found to be of high density, and X-ray diffraction showed them to be (Th, U)C_2. Starting with granulated particles 300 to 420 μ in diameter, carbide particle yields of 80% 175 to 250 μ and 95% 175 to 300 μ were obtained. Since this appeared to be the most promising process for early fruition, it was selected for Peach Bottom HTGR particle fabrication. Particles prepared by this technique are shown in Figs. 2 through 7.

A brief description of the graphite-bed sintering and melting process for the preparation of (Th, U)C_2 particles is presented below.

GRAPHITE-BED SINTERING AND MELTING PROCESS FOR (Th, U)C_2 PARTICLES

Powdered ThO_2, UO_2, and carbon are mixed and formed into particles about 75 μ larger than the carbide particles desired. These particles are

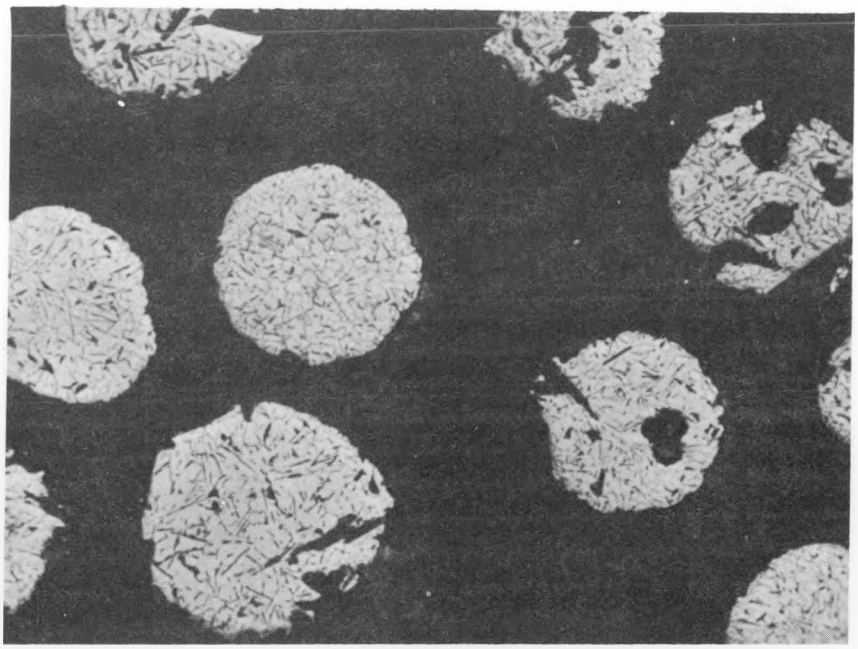

(75×)

Fig. 2--Photomicrograph of $(Th, U)C_2$ particles produced by sintering and melting in a powdered graphite bed

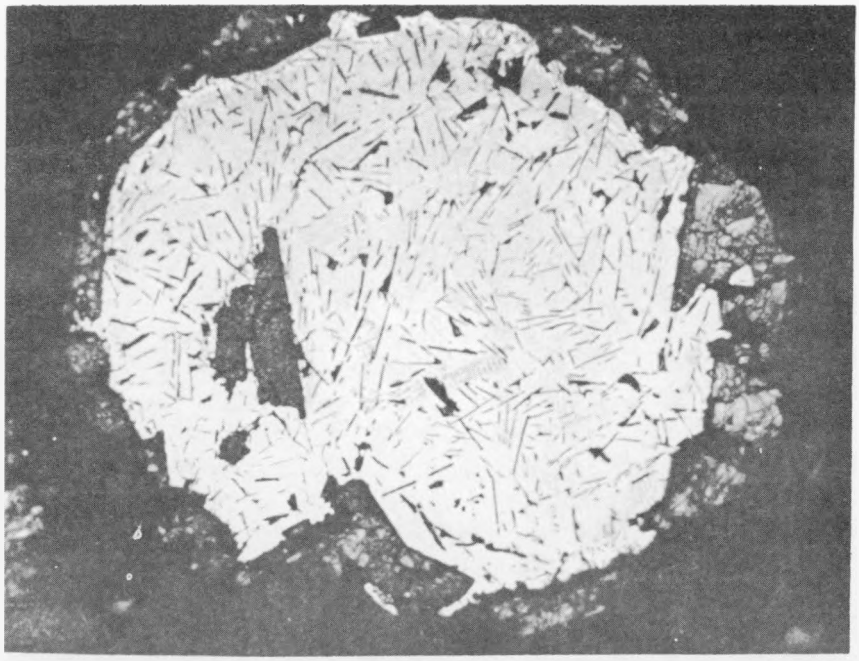

(210×)

Fig. 3--Photomicrograph of $(Th, U)C_2$ particle produced by sintering and melting in a powdered graphite bed

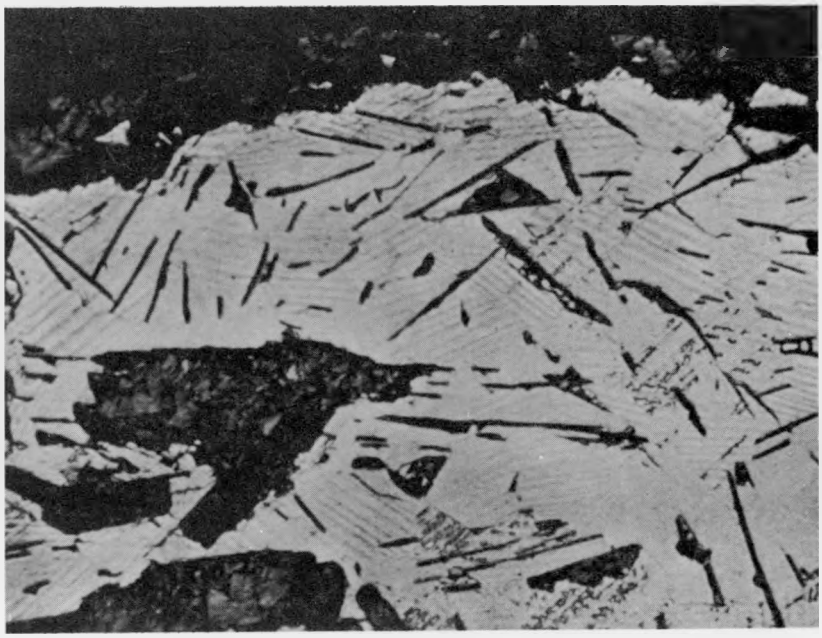

(575×)

Fig. 4--Photomicrograph of portion of $(Th, U)C_2$ particle produced by sintering and melting in a powdered graphite bed; note graphite inclusions and coating

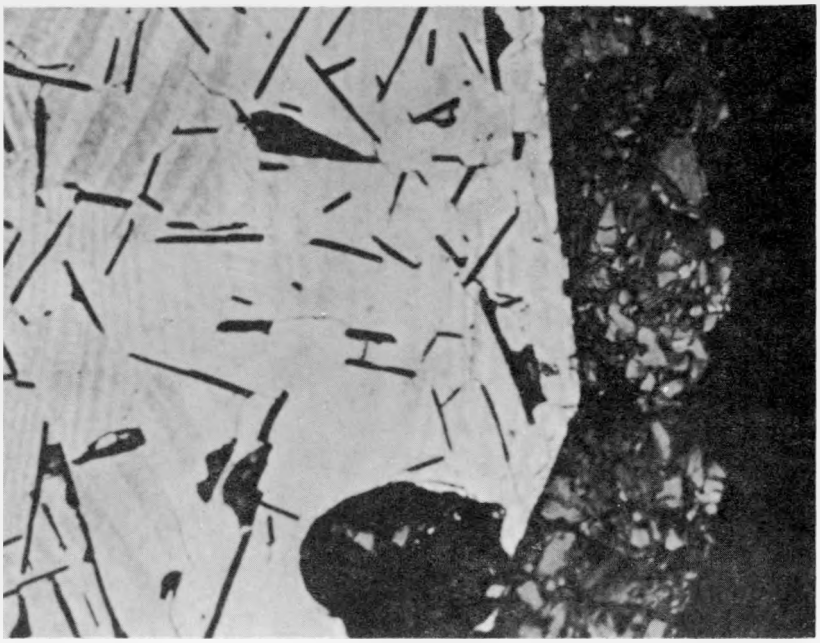

(1000×)

Fig. 5--Photomicrograph of portion of $(Th, U)C_2$ particle produced by sintering and melting in a powdered graphite bed; note adhering coating of graphite

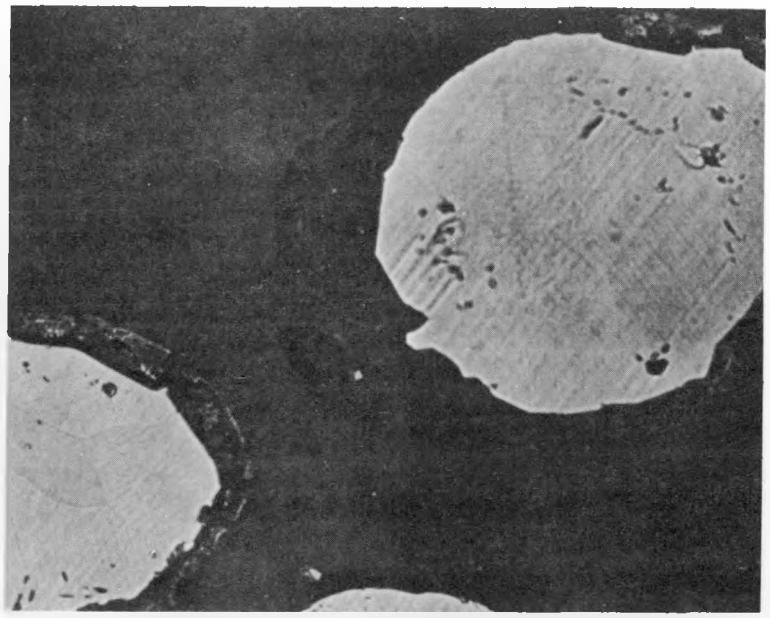

(250×)

Fig. 6--Photomicrograph of UC_2 particle produced by sintering and melting in a powdered graphite bed

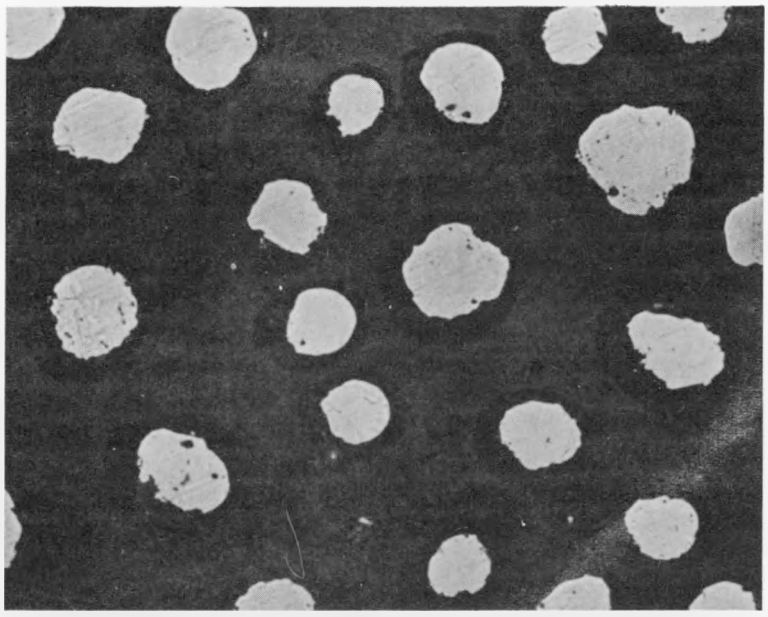

(75×)

Fig. 7--Photomicrograph of UC_2 particles produced by sintering and melting in a powdered graphite bed

are dispersed in graphite powder and heated to over 2000°C in vacuo to cause reduction of the oxides to the mixed dicarbide. The temperature is then raised above the melting point of the ThC_2–UC_2 to cause densification. The graphite powder prevents the molten particles from sticking together.

Since excess carbon is present in the bed during sintering (reaction) and melting, it has been found desirable to prepared the eutectic mixture, (Th, U)C_2–C, rather than the stoichiometric dicarbide. This also makes melting the particle easier.

MATERIALS

The optimum materials for particle preparation by this process were found to be as follows:

ThO_2	nuclear grade, fine particle size
UO_2	nuclear grade, fine particle size
Carbon	Pettinos 6353, fine particle size
Binder	ethyl cellulose
Vehicle	trichloroethylene

Other carbons (GP-38, Speer 170), binders (methyl cellulose, pitchs, resins, polyvinyl alcohol, shellac, Lucite, bakelite, furfuryl alcohol resin, paraffin, etc.), and vehicles (water, benzene) may also be used.

Composition

Sufficient carbon is required to reduce the oxides to dicarbides and, in most cases, form the eutectic mixture. Two per cent binder is optimum. Compositions to produce some various carbide particles are given below:

1.	UC_2	85.0 g UO_2 15.1 g carbon powder
2.	ThC_2	85.0 g ThO_2 15.5 g carbon powder
3.	ThC_2–UC_2 (Th:U = 10:1)	80.0 g ThO_2 8.0 g UO_2 16.0 g carbon powder
4.	ThC_2–UC_2–C eutectic (Th:U = 10:1)	70.0 g ThO_2 7.0 g UO_2 16.7 g carbon powder

Number 4 is the Peach Bottom composition.

Particle Agglomeration

The powdered ThO_2, UO_2, carbon, and ethyl cellulose are mixed together dry; then the trichloroethylene is added to dissolve the binder and form a slurry. Continued mixing produces agglomerated particles (granulating process). Large batches are most readily prepared in a P-K Twin-Shell Blender with intensifier bar; small batches and reworking of off-size particles are done in a Hobart mixer. Particles from mixers are oven-dried at 140°F and then sieved to obtain 295- to 495-μ (+48 -32 mesh) particles. Off-sized particles are recycled through the mixing operations with the addition of more tricloroethylene.

Sintering (Reacting) and Melting

The presized, agglomerated particles are mixed with graphite flour in an 8-to-1 particle-to-graphite ratio by weight, and loaded into a graphite crucible. The loaded crucible is placed in the heating apparatus (Fig. 8), evacuated, and heated to 2000° to 2200°C to reduce the oxides to dicarbides. A marked decrease in outgassing signals the completion of the reaction process, and the temperature is then raised to about 2500°C to melt and densify the particles.

Particle Separation and Sizing

After cooling, the crucible is transferred to an inert-atmosphere glove box and the contents (graphite powder and (Th, U)C_2 particles) are sieved using 35- and 100-mesh screens. The material in the pan is graphite powder insulation and a very small percentage of undersized particles. This mixture is reused directly as insulation in subsequent runs. Yields of 150- to 420-μ particles should be about 99%. Particles are stored in sealed containers until coated with pyrolytic carbon.

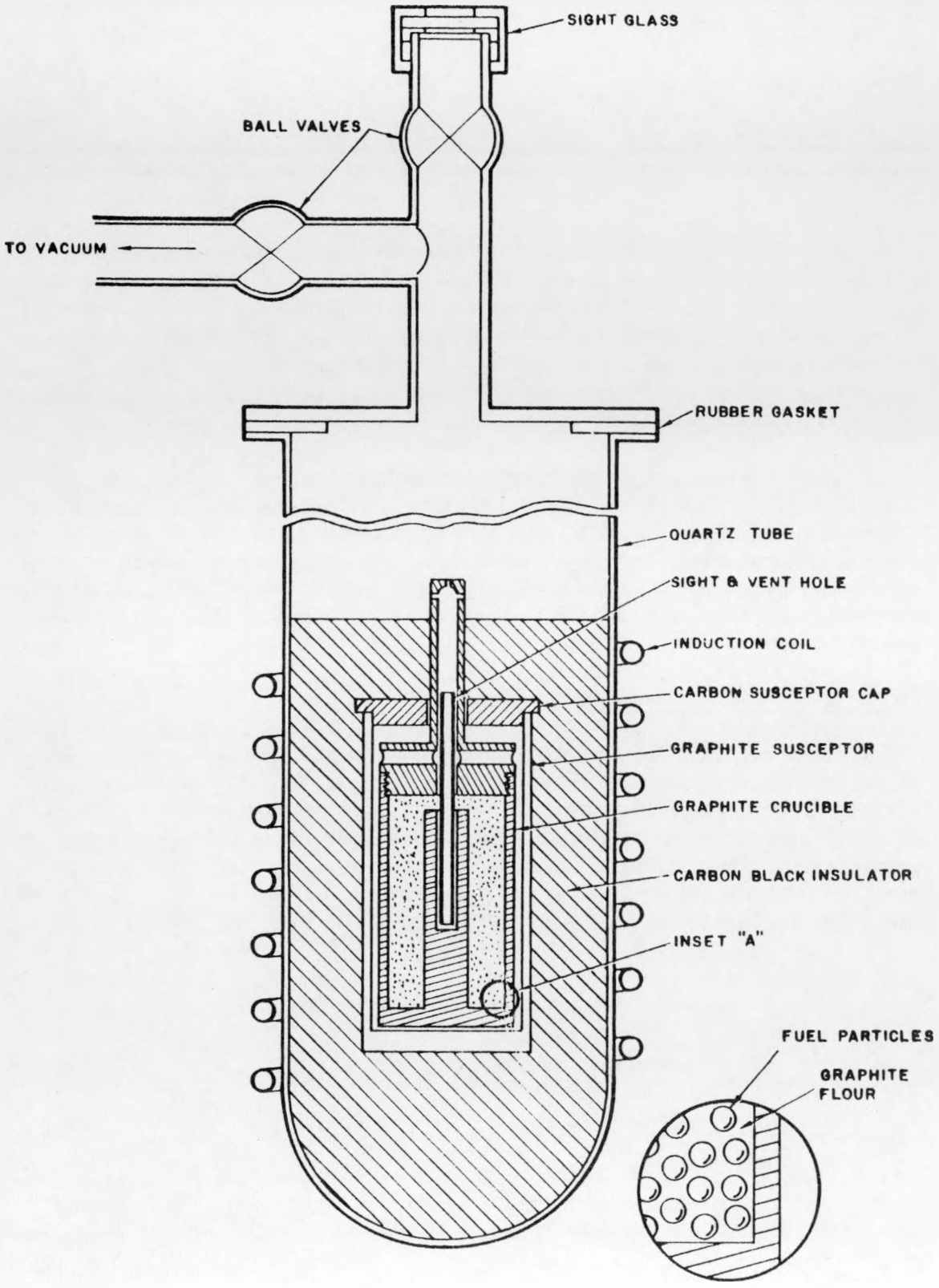

Fig. 8--Graphite-bed sintering and melting apparatus for the preparation of (Th, U)C_2 particles

IV. PYROLYTIC-CARBON COATING OF PARTICLES*

$(Th, U)C_2$ is extremely reactive with moisture, and fuel compacts containing unprotected $(Th, U)C_2$ disintegrate by hydrolysis after a few hours' exposure to air. In order to overcome this problem, the use of carbon coatings on the $(Th, U)C_2$ particles was investigated.

Battelle Memorial Institute developed a process for coating fuel particles with pyrolytic carbon, and this work was extended at General Atomic. Testing of these coated carbides showed that not only did the coatings render the fuel compacts inert to moisture, but they also substantially improved fission-product retention. In addition, since no carbon is consumed from the matrix by a conversion reaction, the integrity of the fuel particle–graphite matrix interface was improved (see Figs. 15 and 16).

Coating of the particles is performed in a fluid-bed reactor. Helium is the fluidizing gas and acetylene or methane furnishes the carbon. Basically, the process consists of jettisoning the carbide particles from a semifluid bed into the hot zone of a vertical combustion tube by means of a high-speed stream of inert gas containing the hydrocarbon. The actual coating temperature is between 1000° and 1400°C with 0.10 to 0.25 atm partial pressure of CH_4. These conditions give a coating rate of 8 to 12 μ/hr.

Two types of fluidized-bed coating units have been used. One has a mullite tube and is heated by a silicon carbide resistance furnace (Fig. 9), and the other has a graphite tube and is induction heated (Fig. 10). Data on these coating apparatus are given in Table 2, and the low-temperature unit is described in detail below.

COATING APPARATUS

The low-temperature apparatus (Fig. 9) consists of a mullite combustion tube 1 in. in inside diameter at the top and 33 in. long, with a Pyrex joint sealed at the top to the disentrainment bulb. The inside diameter of the bottom 3 in. of the tube is reduced to 1/4 in. and is sealed to a Pyrex ball joint.

*Details of the development of the pyrolytic-carbon-coating process may be found in reports 13 and 30 of the Appendix.

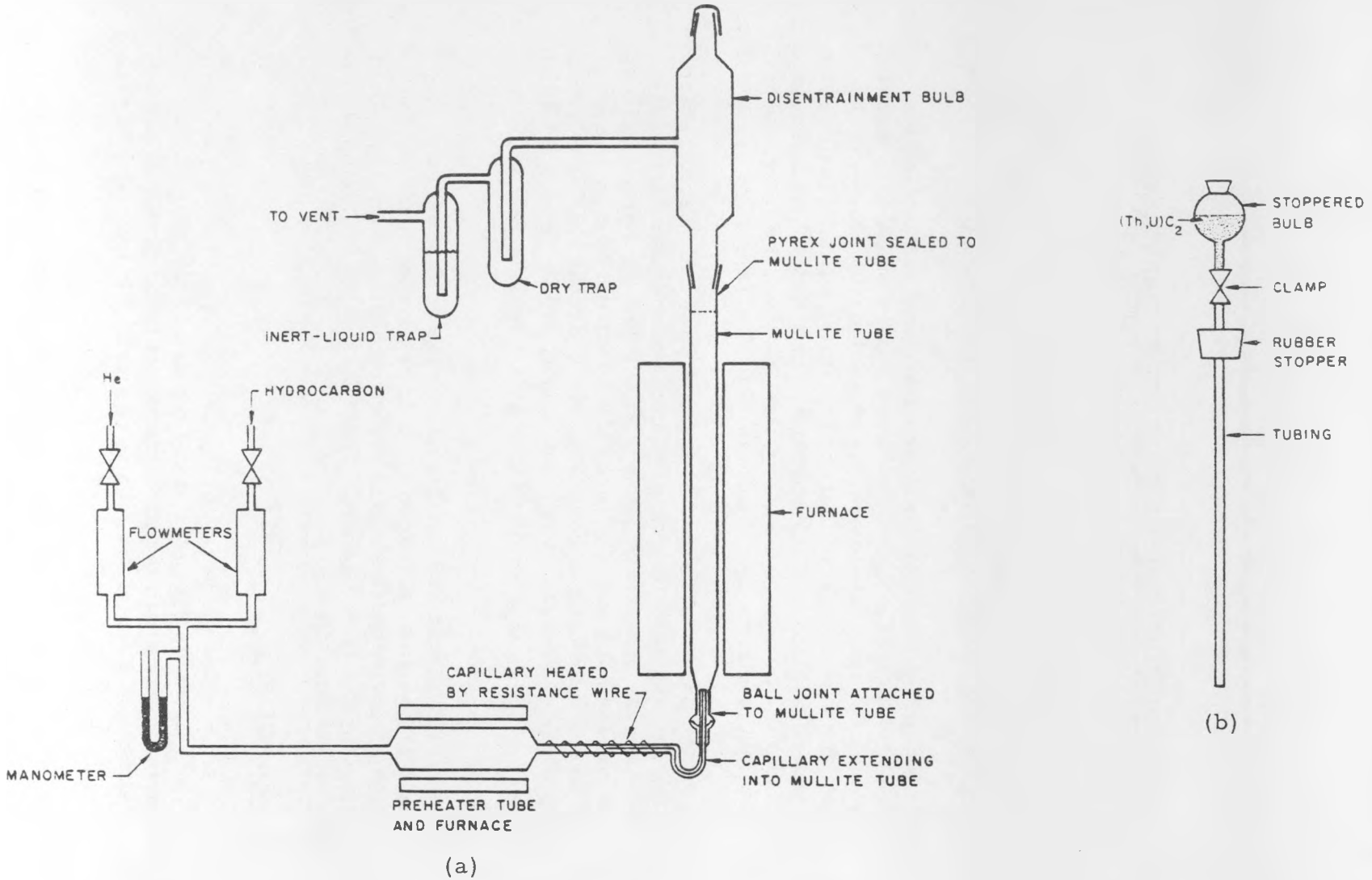

Fig. 9--Diagram showing (a) mullite tube fluid-bed coating apparatus and (b) apparatus for transferring (Th, U)C_2 particles from dry box to coating apparatus

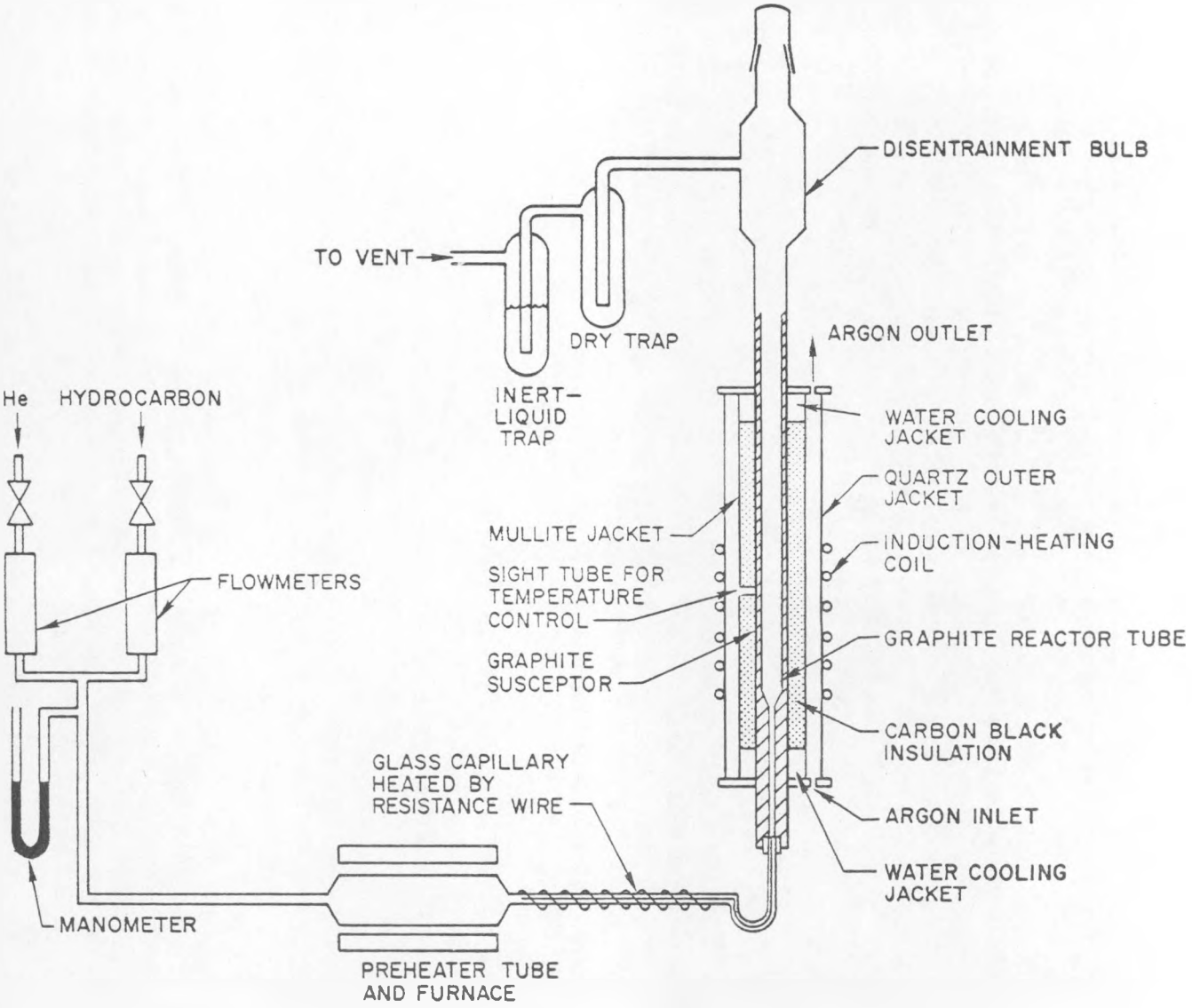

Fig. 10--Diagram of graphite tube fluid-bed coating apparatus

Table 2

DATA ON COATING APPARATUS

	Mullite Tube (Low Temp.)	Graphite Tube (High Temp.)
Heat source	SiC resistance furnace	Induction furnace
Temperature range, °C	700-1500	1000-2500
Reaction-tube dimensions, in.		
Entrance tube:		
Diameter	0.04	0.125
Length	2.5	8.0
Reaction-tube hot zone*:		
Diameter	1.00	4.00
Satisfactory total flow-rate range, $cm^3/min/g$	20-25	40-80
Capacity, g (100-500 μ powder):		
Minimum	75	25
Maximum	150	50

*Particles cascade in hot zone.

One end of a quartz capillary extends into the small end of the mullite tube; the other end is connected to a preheater tube filled with quartz packing. The capillary is provided with insulated resistance wire, thus making it part of the preheater. The preheater is a standard wire-wound resistance furnace.

The reactor tube is heated by a standard silicon carbide resistance furnace provided with an alumina muffle to diffuse the heat. A Pt–Pt-10% Rh thermocouple placed between the muffle and the reactor tube is connected to a standard controller to measure and regulate the temperature.

A disentrainment bulb is connected to the top of the reactor tube to reduce the velocity of the gas stream leaving the tube. This arrangement reduces the loss of carbides by entrainment in the exit gas stream. The exit gases are passed through a dry trap and an inert-liquid (dibutyl phthalate) trap before entering the laboratory venting system.

Standard flowmeters and mercury manometers are used to measure flow rates and gas pressures, respectively. The entire apparatus is enclosed in a dust-tight hood, which is vented through a filter.

The loading apparatus consists of a stoppered transfer flask, which is fitted with a clamped exit line. This is used for transferring (Th, U)C_2 from a dry box to the coater. The transfer flask is connected to a rubber stopper containing a quartz tube that directs the powder into the reactor tube (see Fig. 9).

COATING PROCEDURE

After the apparatus is assembled, the system is purged with helium, the temperature raised to 1200°C, and the preheater temperature brought to 400°C. With the reactor tube at 1200°C, the helium flow is adjusted to 3200 cm^3/min and the capillary heater is then turned on. A sample of (Th, U)C_2 (150 g) (weighed in an argon-filled glove box) is placed in the transfer flask. The loading apparatus is seated at the top of the fluid-bed apparatus and the carbide powder is dropped slowly into the reactor tube by manipulating the clamp. After the loading is completed, the temperature is increased to 1400°C, the hydrocarbon gas is introduced at the rate of 800 cm^3/min, and the helium flow is reduced to 2400 cm^3/min. The coating reaction then proceeds for a predetermined time. At the end of the coating period, the hydrocarbon flow is discontinued and the helium flow is increased to 3200 cm^3/min during the cooling cycle. After the reactor has reached room temperature, the capillary is removed and the coated carbide particles are collected at the bottom of the tube.

The following are typical coating conditions:

Hydrocarbon	CH_4
Temperature	1400°C
Helium flow rate	2400 cm^3/min
Methane flow rate	800 cm^3/min
Total flow rate	3200 cm^3/min
Methane partial pressure	0.25 atm
Approximate coating deposition rate	10 μ/hr

Pyrolytic-carbon-coated (Th, U)C_2 particles are shown in Figs. 11 and 12.

STUDIES ON PYROLYTIC CARBON COATING*

X-ray diffraction measurements were obtained on samples of pyrolytic carbon coatings. Coated particles were crushed in a mortar and the (Th, U)C_2 was removed by leaching in hot HNO_3. The carbon powder was placed in glass capillaries and Debye-Scherrer powder patterns were obtained. Patterns from a commercial moderator graphite (AGOT) and a commercial pyrolytic carbon were used for comparison.

Carbon coatings deposited at 1400°C at a pressure of about 250 mm Hg produced diffuse bands in the region of the (00ℓ) and (hk) Bragg reflections and no general (hkl) reflections. The structure of the commercial pyrolytic carbon was quite similar to that of the carbon deposited at 1400°C, except that the bands were much sharper and were shifted to higher Bragg angles. In contrast, in the pattern obtained from AGOT graphite, the (hk) bands were replaced by the (101) and (100) lines, the three-dimensional (112) peak was present, and the (00ℓ) lines were much sharper and were shifted to higher Bragg angles. The higher angle reflection (006) was sufficiently intense to be recorded on the film.

These data indicated that the structure of the deposited carbons was two-dimensional, consisting of layers stacked in parallel groups but not otherwise mutually oriented (i. e., the layers showed a complete random orientation with respect to rotation about the layer norm). The three-dimensional patterns obtained from AGOT graphite were not observed.

Increasing the temperature of deposition above 1400°C and decreasing the CH_4 pressure to about 100 mm Hg changed the appearance of the deposited carbon. The macrostructure of the coatings appeared to change abruptly from a gross layered structure when deposited at 1400°C to a

*Data presented in this section were taken from reports 14 and 17 in the Appendix.

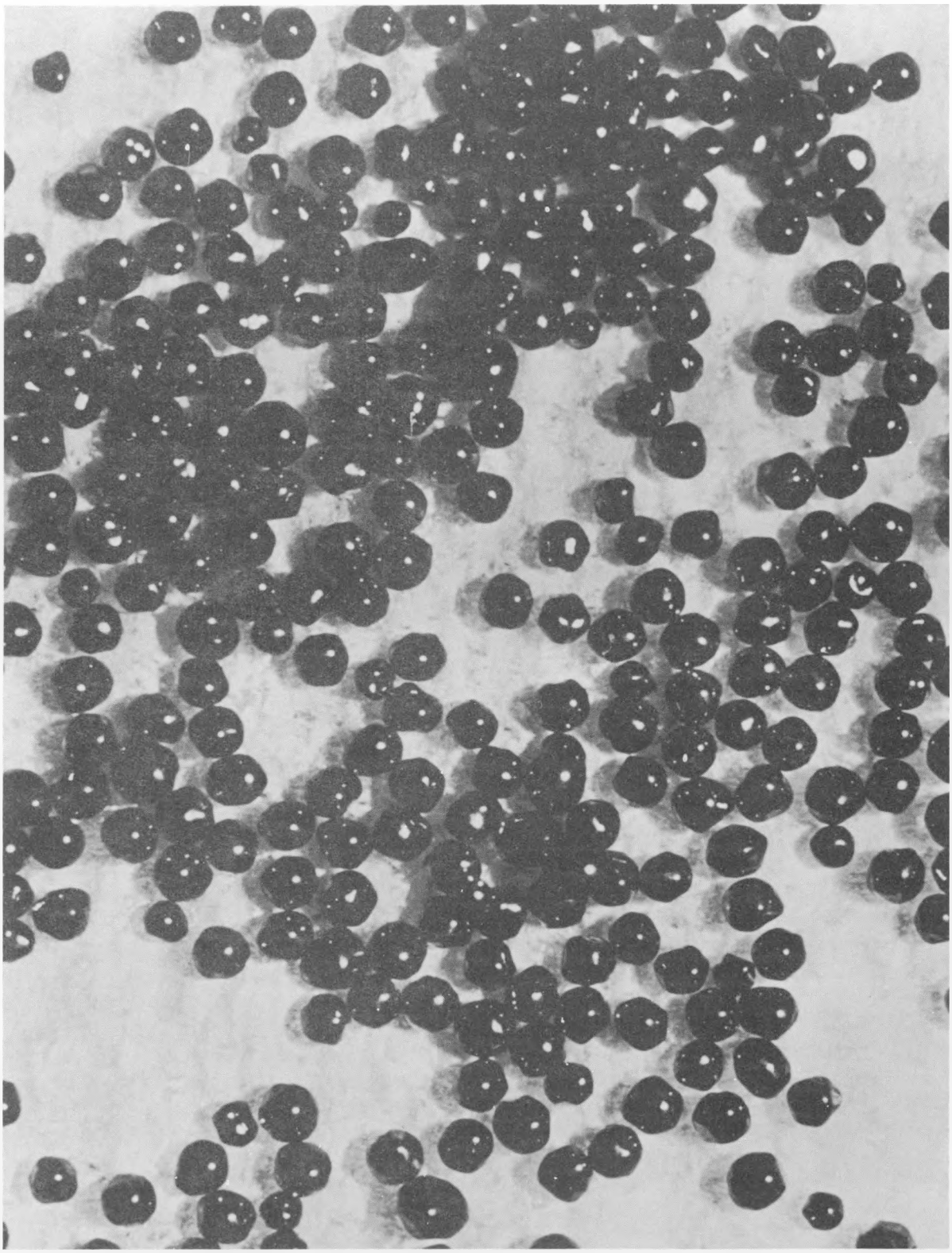

(~40×)

Fig. 11--Pyrolytic-carbon-coated (Th, U)C_2 particles

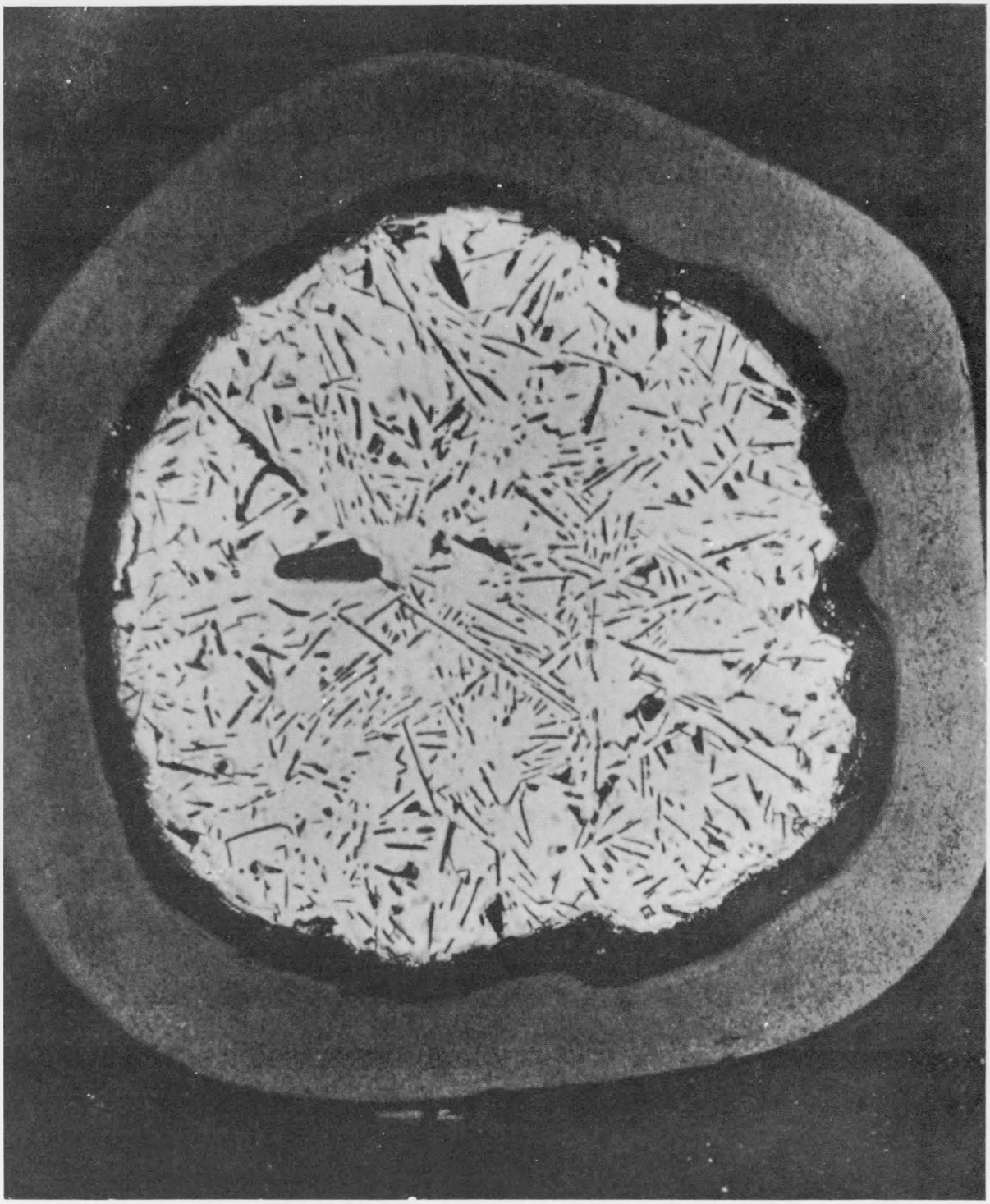

(500×)

Fig. 12--Pyrolytic-carbon-coated $(Th, U)C_2$ particle

mottled, or grainy, structure when deposited at 1800° and 2000°C. Increasing the temperature of deposition to 2200° and 2400°C gave the layered structure again, though the grains were not completely obliterated (photomicrographs of carbon deposited at various temperatures are shown in Fig. 13). The significance of the change of structure was not clear. Examination of the X-ray traces indicated only that the two-dimensional structure became better developed as the temperature of deposition was increased. Because of the diffuse character of the (00ℓ) bands, the position of their maxima and thus the inter-layer spacing (C_o) could not be calculated with any degree of certainty. However, the layer spacing (C_o) for all carbon structures, including the commercial pyrolytic carbon, was greater than 6.80 Å. A considerable amount of incoherent scattering and scattering by noncrystalline carbon was present.

The annealing of these coatings at 2400°C had a marked effect on their structures. The effects observed directly on the X-ray diffraction patterns were:

1. The (10) two-dimensional band split into two, three-dimensional peaks, the (101) and the (100);
2. The three-dimensional (112) peak appeared; and
3. The (00ℓ) lines sharpened and moved toward higher Bragg angles.

The degree to which these changes occurred depended on the temperature at which the carbon coatings were originally deposited.

The modulation of the (10) band and the appearance of the (112) reflection were apparent for the coatings deposited at 1400°, 1800°, 2200°, and 2400°C, whereas the coating deposited at 2000°C retained, to a large extent, its two-dimensional character. This indicates that annealing the coatings deposited at 1400°, 1800°, 2200°, and 2400°C transformed at least a portion of the carbon structure to three-dimensional graphite structure. The transformation was much less complete for graphite deposited at 2000°C. Further, the pattern for the carbon coatings deposited at 1400°C and subsequently annealed at 2400°C indicated a slightly better graphitic structure than that formed from material deposited at 2200° and 2400°C.

Lattice parameters A_o and C_o were calculated directly from line spacings on the films using the (004) and (110) reflections, respectively. The layer spacings approached those of a highly graphitic body for the annealed coatings deposited at 1400°, 2200°, and 2400°C, whereas the layer spacing for annealed coatings deposited at 1800° and 2000°C were considerably larger. Although the X-ray trace of the 1800°C sample was quite similar in appearance to that of the 2200°C sample, the (002) and (004) lines occurred at lower Bragg angles.

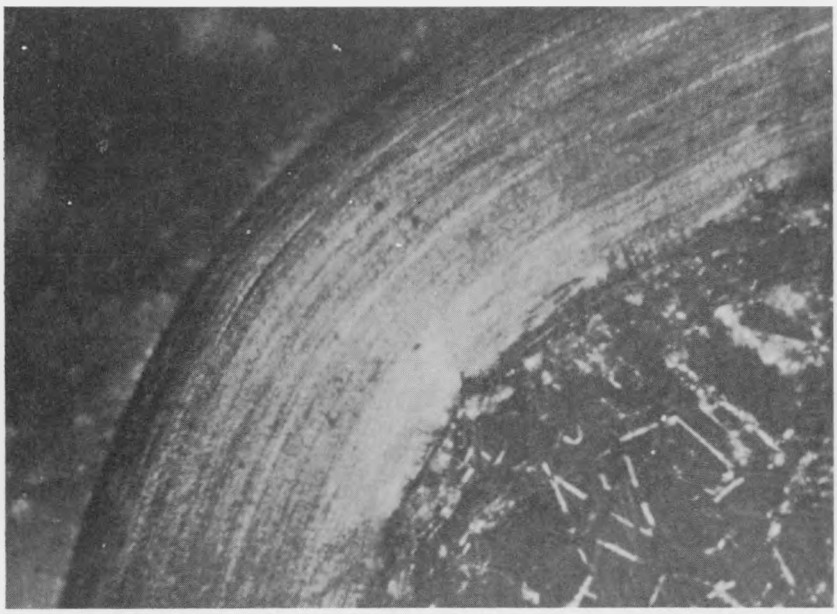

(615×)

(a)

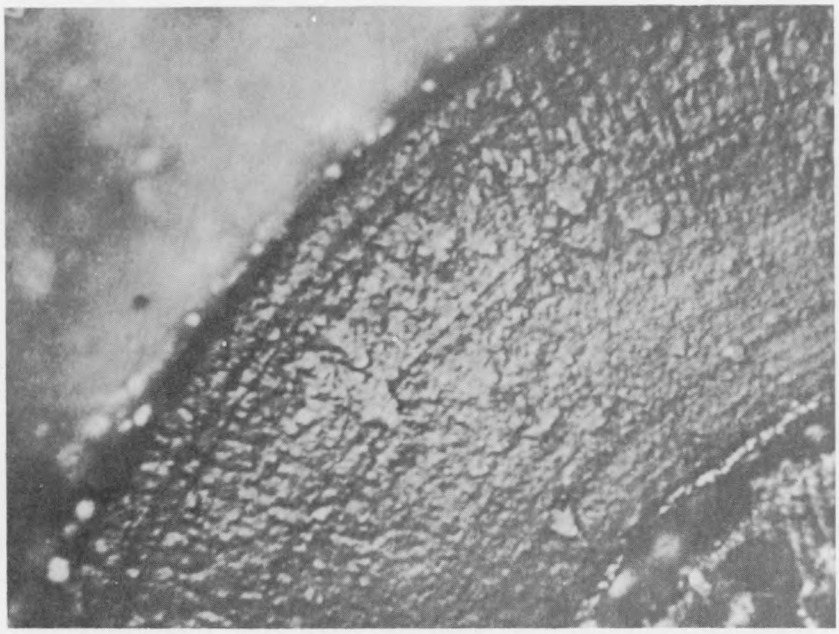

(1000×)

(b)

Fig. 13--Macrostructure of carbon deposited at various temperatures from methane: (a) at 1400°C (b) at 1800°C

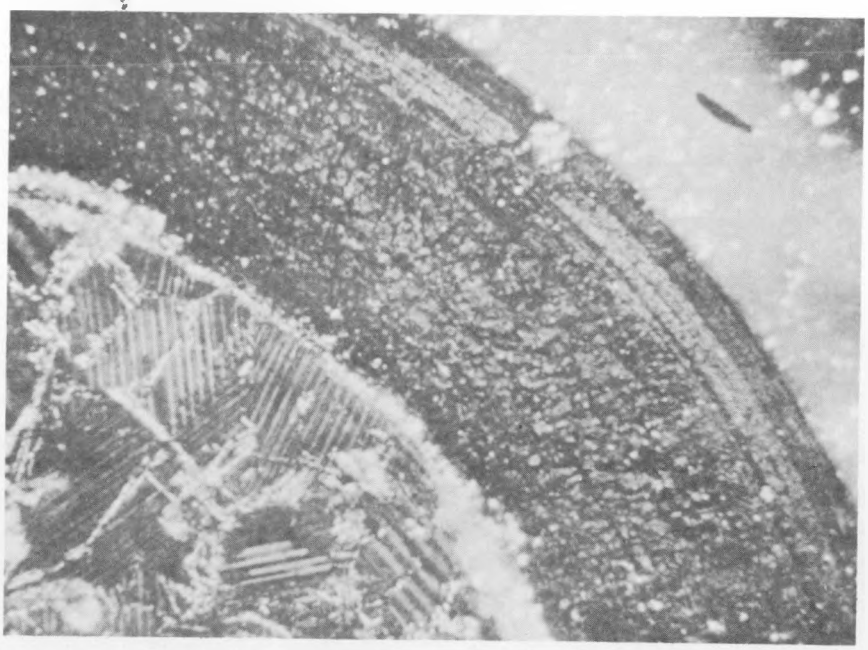

(470×)

(c)

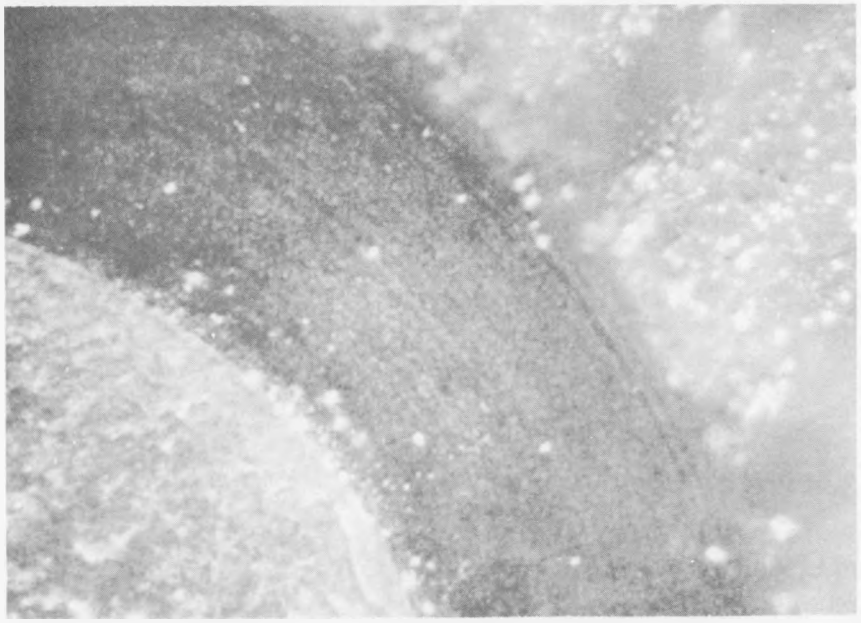

(640×)

(d)

Fig. 13 (continued)--Macrostructure of carbon deposited at various temperatures from methane: (c) at 2000°C, (d) at 2200°C

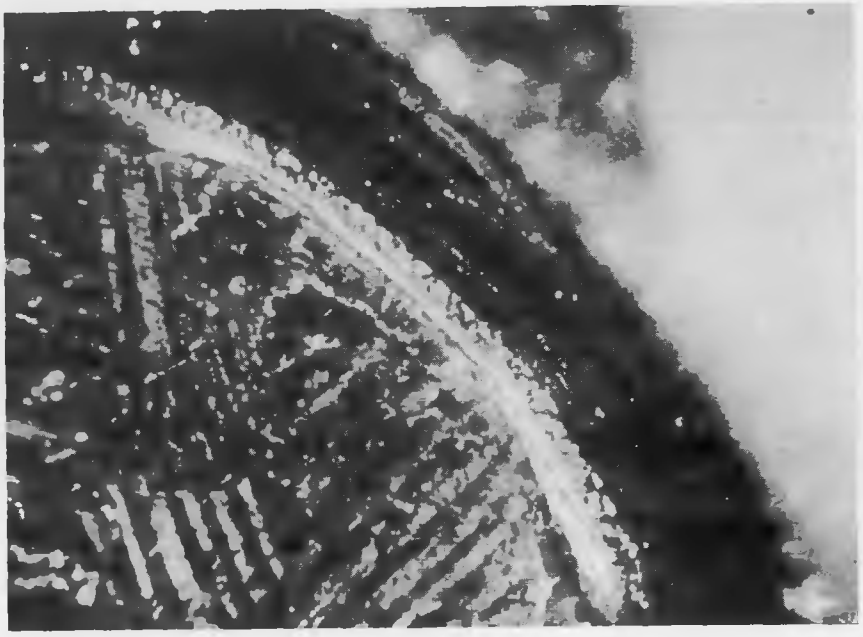

(e) (530×)

Fig. 13 (continued)--Macrostructure of carbon deposited at various temperatures from methane: (e) at 2400°C

It was also noted that the macrostructure of the 1800°C coating did not undergo a major change, i. e., the mottled, or grainy, appearance persisted. In the annealed samples the grains appeared larger and contained so called growth cones; the apexes of the cones were oriented toward the substrate.

These results indicate that material deposited at 1400°C is essentially a graphitizable carbon, while carbon deposited in the intermediate range 1700° to 2100°C is essentially nongraphitizable.

To supplement the X-ray data, additional samples deposited at 1400° and 1800°C were annealed at 2000°, 2200°, and 2400°C and examined optically. The surface appearance of the specimen deposited at 1400°C apparently did not undergo a major change. The layered or shell-like structure still persisted, although for the annealed specimens, these layers appeared to be thicker.

Initial work was done on obtaining reflection electron-diffraction patterns from a single, individual coated particle. Diffuse electron-diffraction patterns were obtained which showed the (002) reflection at a d-spacing of approximately 3. 5 Å, representing a C_o approaching 7. 0 Å.

Also shown in the patterns were the unresolved (100) and (101) lines and the unresolved (110) and (112) lines. This pattern is not a room-temperature pattern, but one representing a much higher temperature, as the particle is heated by the beam to an orange glow. There is general agreement between these electron diffraction patterns the X-ray diffraction patterns from ground coatings.

Two special aspects of electron-diffraction analysis of coated particles that may be used to advantage are that one particle at a time can be studied, having been selected by optical or X-ray microscopy, and that the particle can be heated up in the beam, yielding a high-temperature pattern.

V. GRAPHITE-MATRIX FUEL COMPACTS*

Incorporation of uranium in graphite by impregnation with aqueous solutions results in uranium carbide of such extremely small particle size that fission-recoil damage to the surrounding graphite and fission-product release are unnecessarily high. The arrangement of fissile-fertile particles is most desirable when the mean distance between particles is larger than the range of fission-fragment recoil. Most of the graphite matrix of the fuel compact is thus free from fission-fragment damage, and there is a continuous web of undamaged matrix material, so that the fuel compact will retain many of its desirable preirradiation properties. Calculations show that matrix damage increases rapidly as the fuel particle size drops below 100 μ (see Fig. 14).

Since discrete fuel particles of 100 μ or larger are desirable for the HTGR fuel compacts, and since they have to be uniformly dispersed in the graphite matrix, the admixture approach was chosen for this work. Also, the size, dimensional, and property requirements imposed on the fuel compacts by the HTGR design indicated that molding processes would offer several advantages over extrusion (higher density and hence--it was hoped--lower permeability, higher thermal conductivity, and better adaptability to short lengths).

The fuel compacts are prepared by mixing the fissile-fertile phase particles with graphite and pitch and then hot-pressing this material to form a dense, strong compact. By using graphite flour bonded with a minimum of binder for the fuel-matrix material, high (graphitizing) temperatures are not required to produce good graphite properties in the compacts. Only 10 wt-% pitch binder is required, and after hot pressing only 5% of it remains, leaving a high-density matrix of 95 vol-% graphite and 5 vol-% carbon.

The compact fabrication process was originally intended to make use of thorium-uranium dioxide solid-solution fuel particles, converted in situ to dicarbides during a final heating operation. With the development of the carbon-coated thorium-uranium dicarbide fuel particles, the compact fabrication process was altered so that the coated carbide particles could be incorporated into the hot-pressed graphite matrix. The two processes are compared in Fig. 15.

*Development and evaluation of graphite-matrix fuel compacts are described in detail in reports 15 and 18 of the Appendix.

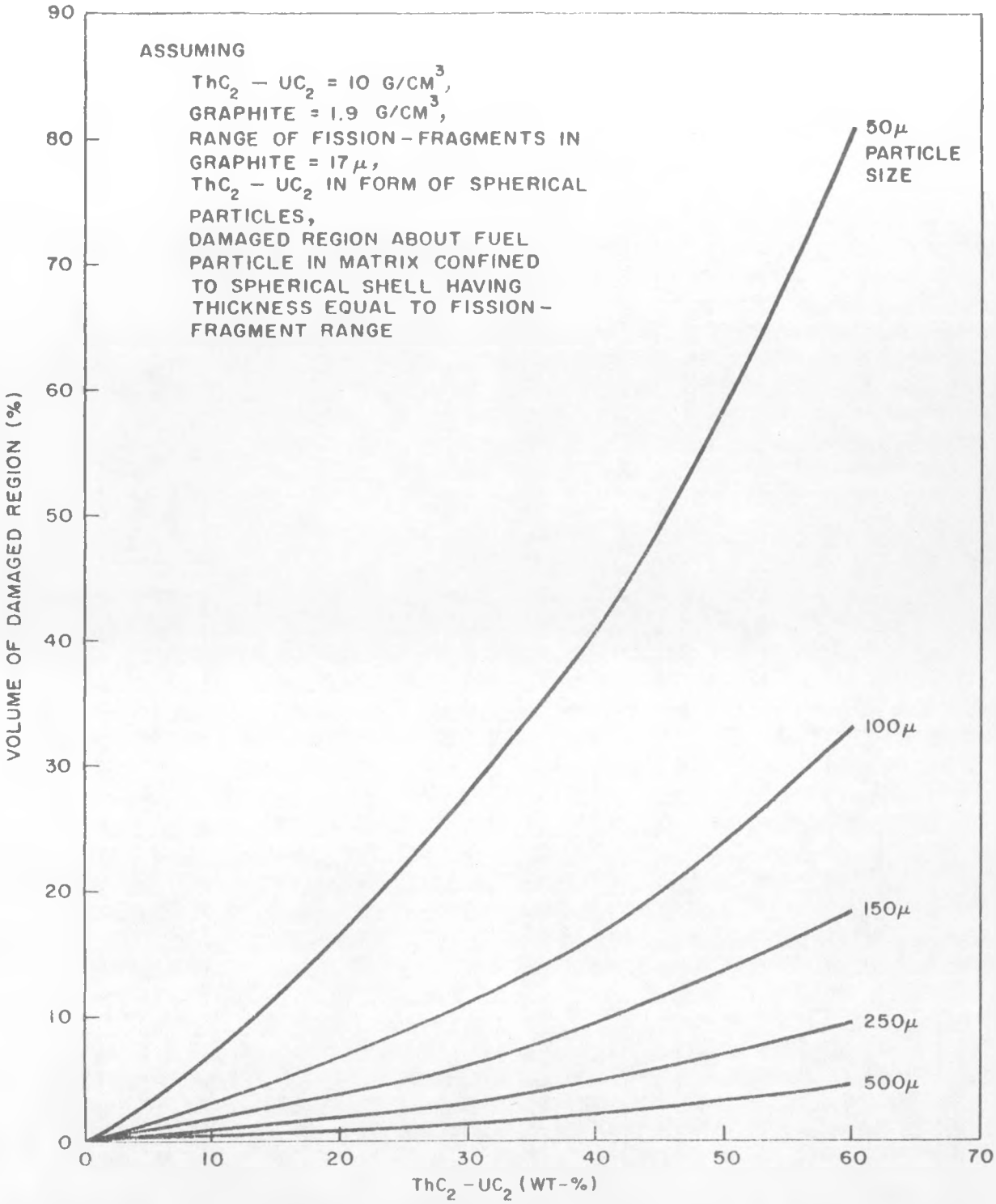

Fig. 14--Variation of matrix volume subject to fission-fragment damage with ThC_2—UC_2 concentration for various fuel-particle sizes

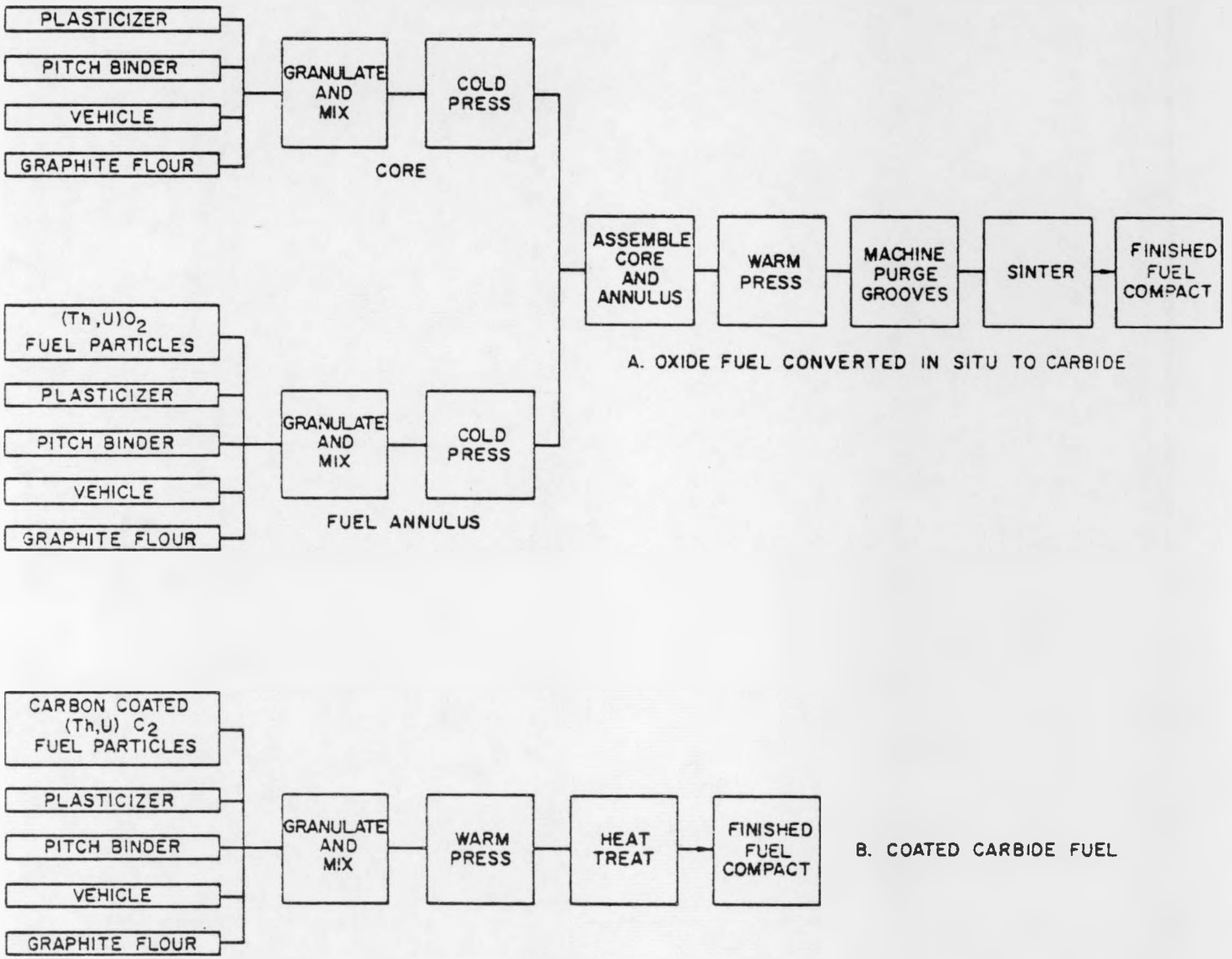

Fig. 15--Fuel-compact fabrication processes

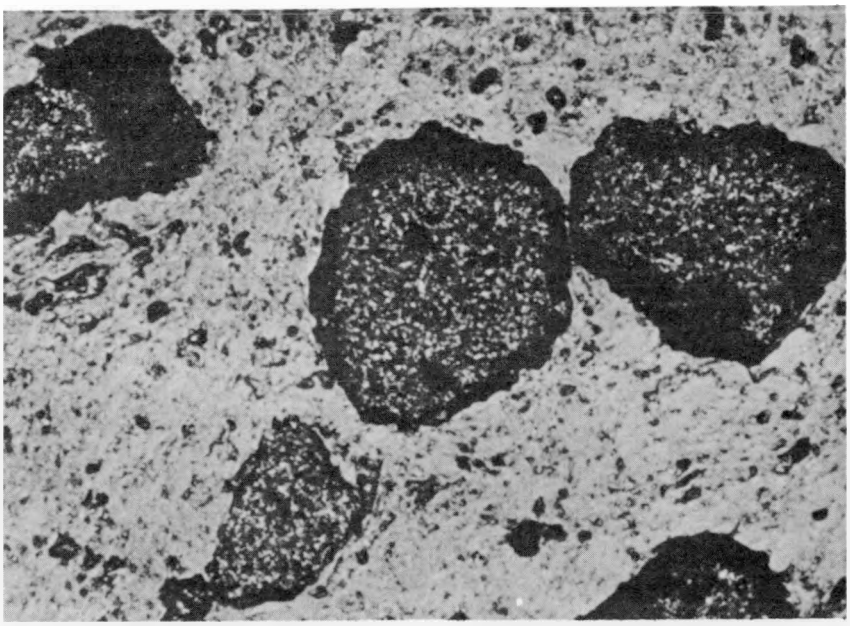

(250×)

Fig. 16--Photomicrograph of (Th, U)C_2 fuel particles formed by in situ conversion of (Th, U)O_2 particles during fuel-compact fabrication; note voids between particles and graphite matrix

The coated-carbide process involves fewer operations and has the added advantage of producing stable compacts which can be exposed to air without damage due to hydrolysis of the carbide fuel by atmospheric moisture. By omitting cold-pressing (which may break the coatings on the fuel particles), a penalty of about 7% in compact density is paid. Metallographic examination of pyrolytic-carbon-coated (Th, U)C_2 fuel particles in a compact shows greatly improved contact between particle and matrix as compared to compacts prepared with oxide fuel particles (see Figs. 16 and 17).

Close dimensional control of complex shapes is achieved by this hot-pressing process. Purge grooves are readily molded into the fuel compacts (refer to Fig. 1) during hot-pressing, and no machining of the compacts is required. Materials and process details are discussed below.

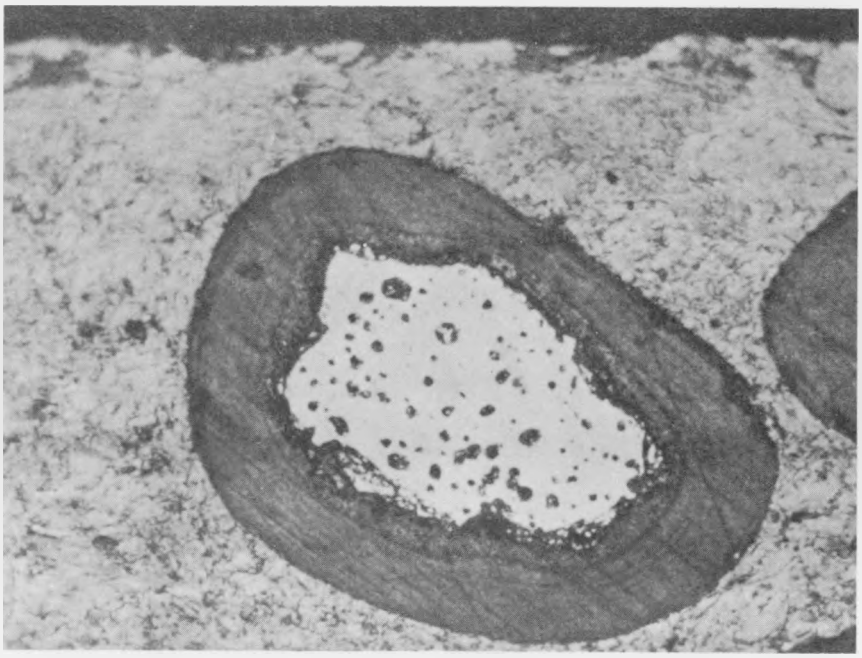

(250×)

Fig. 17--Pyrolytic-carbon-coated (Th, U)C_2 particle in graphite matrix; note good bond between particle and matrix

COMPACT MATERIALS

Graphite Flour

In order to obtain the desirable properties of a graphite matrix without having to heat-treat the fuel compacts to graphitizing temperatures, graphite flour was selected instead of carbon or coke as the starting material. National Carbon Company grade GP-38 graphite powder was selected because of its low ash and boron content, fine particle size, low cost, and availability. It is a manufactured rather than a natural graphite. Natural graphites were tried in early work, but they produced compacts which were weaker in compression tests than those made from synthetic graphite.

The GP-38 used is 98% minus-200-mesh material with an average particle size of less than 20 μ (estimated).

Binder

Pitch, the traditional binder in the carbon and graphite industries, has proven equally satisfactory in making fuel compacts. The initial work

was performed using Gasco No. 2387 pitch. This pitch was very satisfactory but the supply was not, so a program was undertaken to evaluate other commercial pitches. (Other binders such as furfuryl alcohol, polyethylene, and phenol-formaldehyde resins were also tried, but these did not produce compacts with as high a strength.) Barrett No. 30 medium pitch was selected as the binder.

Plasticizer

To aid in granulating the fuel mixture, a plasticizer was incorporated in the mix. The plasticizer is ethyl cellulose, grade N-200, manufactured by the Hercules Powder Company.

Vehicle

A liquid-phase vehicle is used to facilitate mixing and to aid in distributing the pitch. The two most promising vehicles were benzene and trichloroethylene because of solvency for the pitch and fast evaporation rate. Trichloroethylene (Triclene D manufactured by the Du Pont Chemical Company) was selected because of its lower toxicity and flammability.

MIXING

Granulation of the mixed fuel materials is necessary to prevent segregation of the dense carbide particles from the light graphite flour.

Graphite flour and pitch binder are used in a ratio of 9 to 1, i. e., 10% pitch. One per cent ethyl cellulose is added to aid in granulation, and about 7 cm^3 of trichloroethylene per gram of pitch is used as the fluid medium for mixing. The required amounts of graphite flour, pitch, ethyl cellulose, and coated carbide particles are weighed, mixed, and granulated into pellets approximately 1/8 to 3/8 in. in diameter. The granulated fuel pellets are dried to remove all of the trichloroethylene, and are then ready for hot-pressing.

HOT-PRESSING

Graphite dies and punches have been employed for hot-pressing. (ATJ, manufactured by National Carbon Company, and HLM, manufactured by Great Lakes Carbon Company, are both satisfactory die-and-punch materials.) Two means of heating have been employed: (1) external, by a resistance furnace or induction coil, and (2) internal, by passing heavy currents through the punches and compact. A typical hot-press unit for producing annular fuel compacts is shown in Fig. 18. The graphite die is reinforced by an external, water-cooled steel jacket.

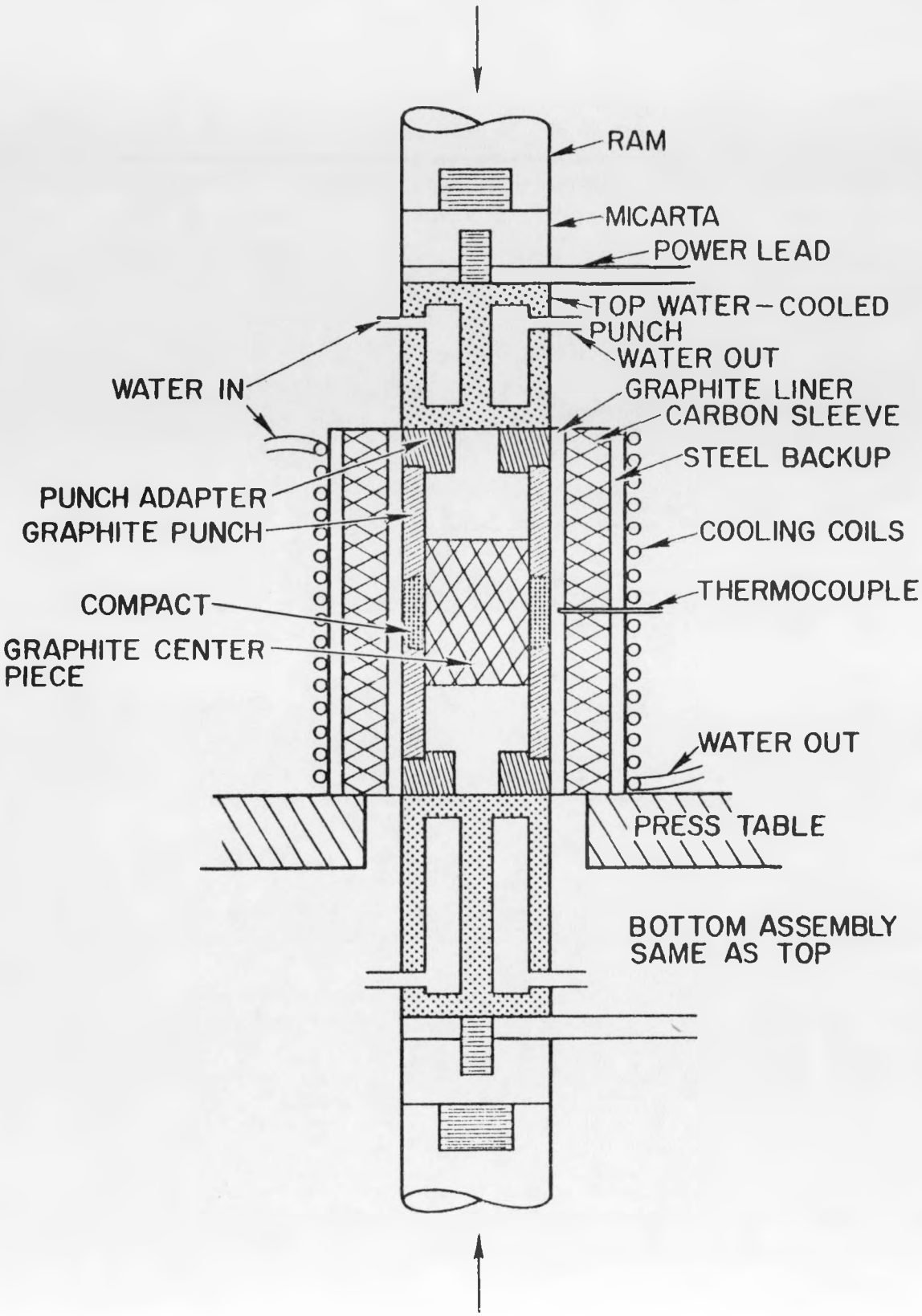

Fig. 18--Hot press used in making annular fuel compacts

Hot-pressing may also be done in metal dies with top and bottom floating punches and an internally heated and instrumented metal core rod. The entire die may be resistance-heated by means of an external, graphite, solid-tube resistance heater.

The granulated fuel mixture is placed in the die, a pressure of about 1000 psi applied, and heating begun. After the temperature reaches 250°C, the pressure is increased to 4500 psi. The maximum temperature reached is about 750°C. The total time to make one compact, including cooling time, is approximately 20 min.

Following hot-pressing, the compacts are given a stabilizing heat treatment at 1800°C in vacuum to complete the removal of volatiles and to minimize dimensional changes due to subsequent thermal treatments.

Pilot-scale facilities for producting HTGR fuel compacts have been in operation for several months, and a great many compacts have been fabricated. These compacts, in addition to furnishing production experience, have been used for physical-property and irradiation testing and for quality-control studies. Several sets of compacts containing pyrolytic-carbon-coated (enriched) $(Th, U)C_2$ have been produced for the in-pile loop experiment. Typical full-sized compacts are shown in Figs. 19 and 20.

This experience indicates that graphite-matrix fuel compacts containing pyrolytic-carbon-coated $(Th, U)C_2$ fuel particles can be successfully produced for the HTGR.

Figure 21 is a macrophotograph of a sectioned fuel compact showing the adherence of the coated particles to the matrix graphite and uniform distribution of the particles in the matrix.

PARTICLE-COATING BREAKAGE DURING COMPACT FABRICATION*

A method has been developed for determining the number of coatings which are broken during fabrication. This operation consists of electrolytic disintegration of the compacts in a nitric acid solution. After the compact is disintegrated, the particles are exposed to the nitric acid, and particles with damaged coatings are dissolved. By determining the amount of uranium dissolved in the nitric acid, it is possible to arrive at the amount of breakage which occurred during fabrication. Table 3 summarizes some typical results. From these and similar data, it has been concluded that breakage of coatings during fabrication will be well under 1% and normally should be about 0.5%.

*Data courtesy of W. L. Wyman, General Atomic.

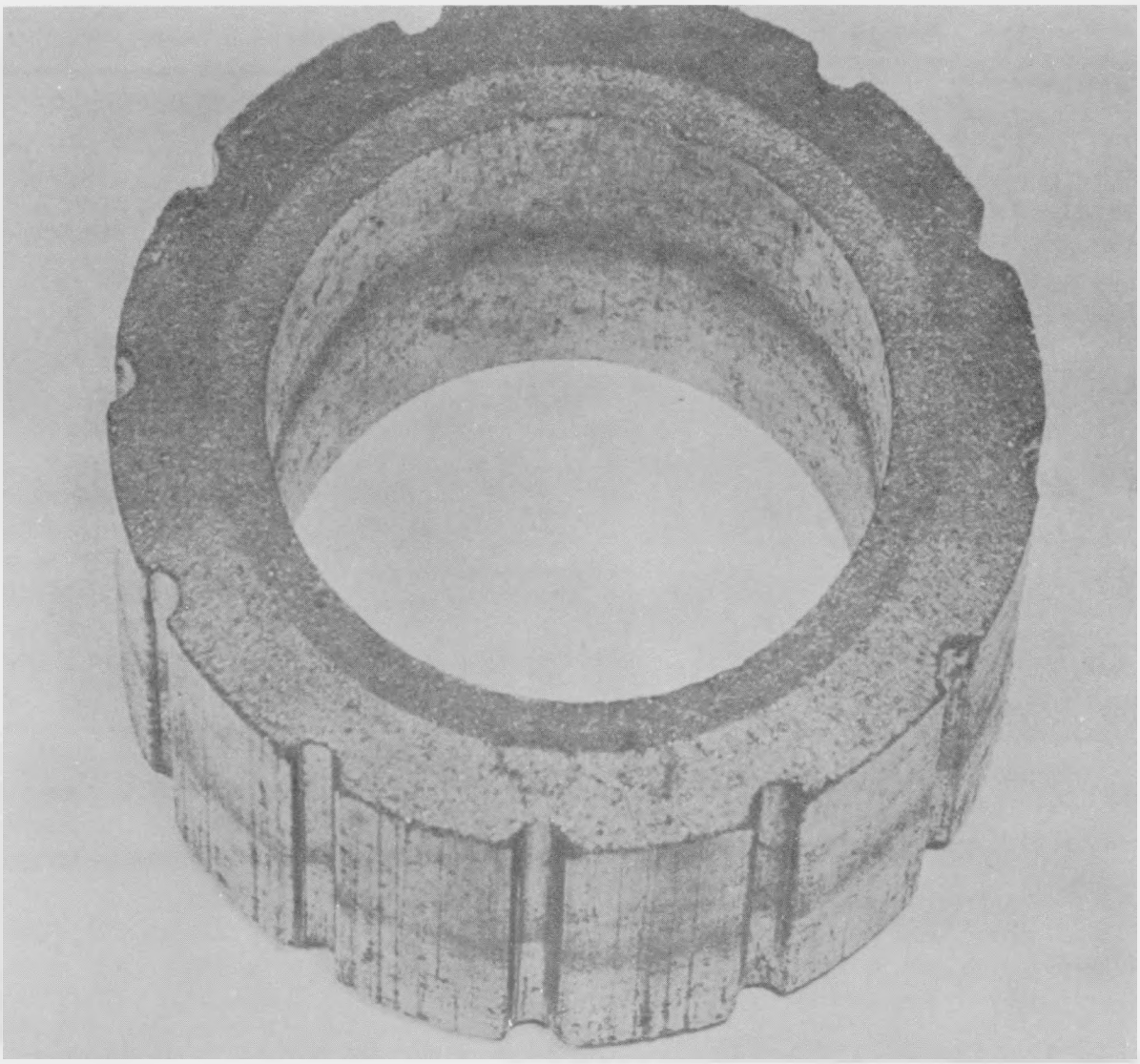

Fig. 19--Annular fuel compact containing carbon-coated (Th, U)C_2 particles; compact is 2.25 in. in outside diameter

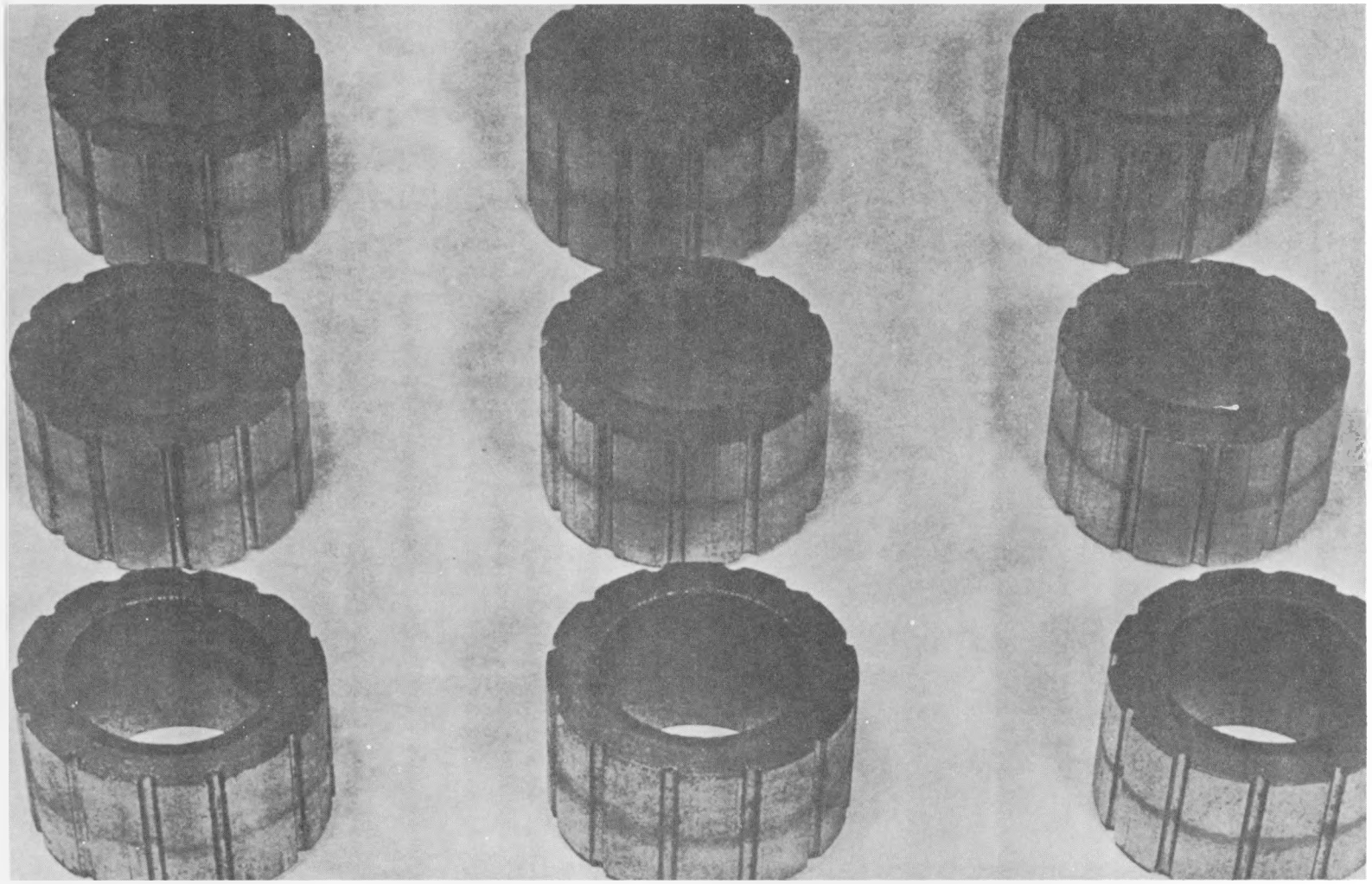

Fig. 20--Annular fuel compacts containing carbon-coated (Th, U)C_2 fuel particles; compacts are 2.25 in. in outside diameter

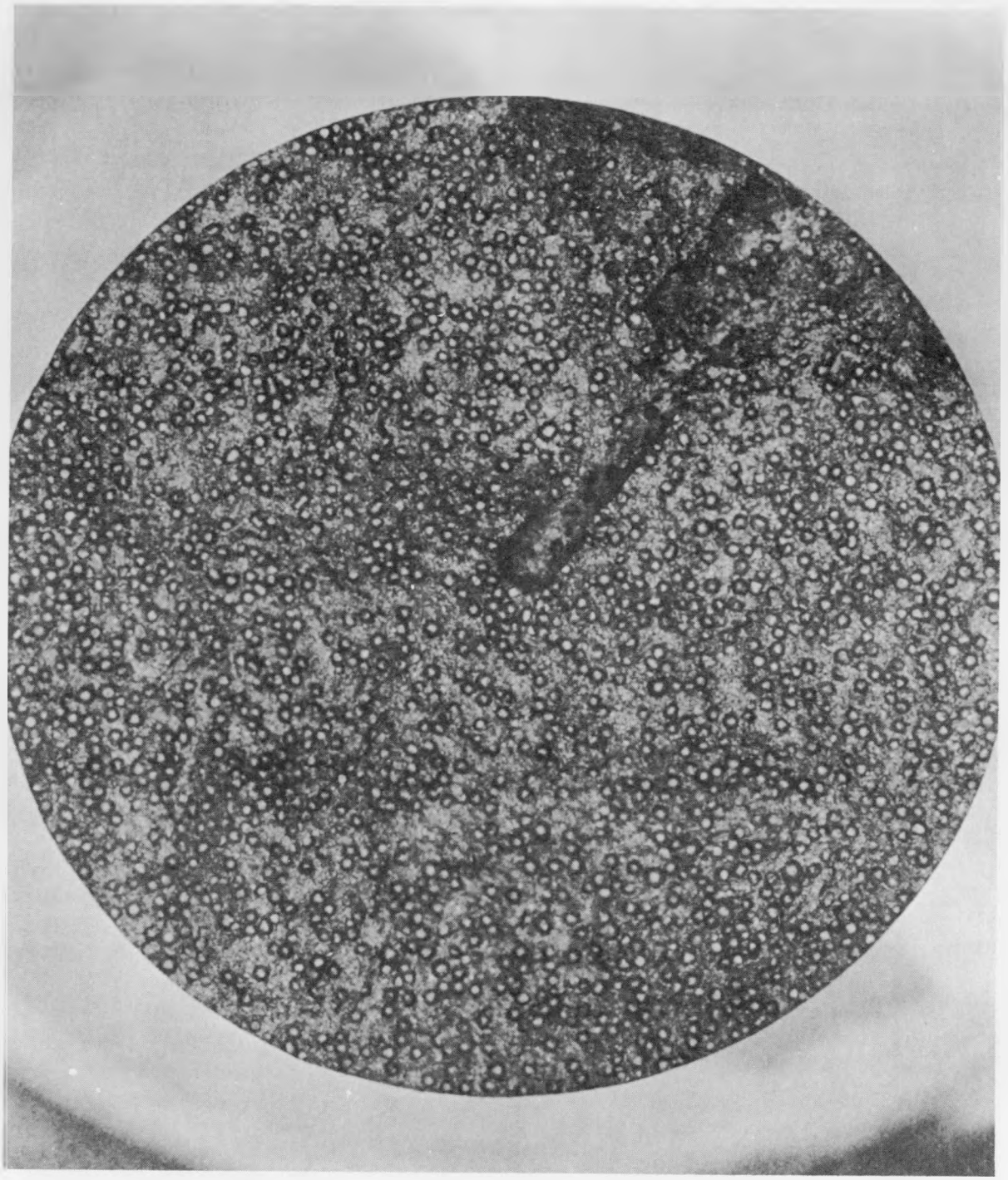

Fig. 21--Sectioned fuel compact containing carbon-coated (Th, U)C_2 fuel particles; 1 in. diameter compact was split by chisel (upper right-hand edge); particles adhered to broken surfaces and did not pull out or break

Table 3

SUMMARY OF PARTICLE-COATING BREAKAGE DURING FABRICATION

Compact No.	Compact Weight (g)	Weight of Coated Carbide in Compacts (g)	Weight of Uranium (g)	Uranium Dissolved (g)	Uranium Dissolved (%)
S1-189	185.738	61.3	13.5	0.004*	0.03
S1-200	183.985	64.1	13.4	0.018	0.13
S1-201	182.258	64.8	13.6	0.059	0.44
B1-96	168.095	38.1	8.3	0.044	0.53

*Limit of the sensitivity of the chemical analysis.

FUEL-PARTICLE DISTRIBUTION IN COMPACT FABRICATION*

For the proper operation of the fuel elements, the fuel particles must be uniformly distributed in the compact. Radiographic inspection is satisfactory for determining if the finished compact is acceptable; however, it is desirable to inspect the fuel mixture to assure proper distribution of the fuel particles in the graphite prior to hot-pressing the fuel compacts. The testing method must be fast, accurate, and simple, and further, the sample should be small. After completion of the test, the sample should be suitable for reusing in the compact line. This means that the test must not break the particle coatings or delay processing of the batch mix.

A test which fulfills these requirements consists of removing small controlled samples of the blended mix and spreading the specimens out in a thin layer on a paper surface. The thin smear is X-rayed and the number and distribution of the coated particles are observed. After completion of the X-ray exposure, the test batch can be reloaded into the blender and processed into compacts. Interpretation of the X-ray film is based on the fact that for a known volume of mix a certain number of coated particles should be observed. Random sampling of each batch will then show the distribution throughout the batch.

PROPERTIES OF HOT-PRESSED FUEL COMPACTS

A number of physical and thermal properties have been determined for the graphite-matrix fuel compacts prepared by the hot-press process described in the previous sections. Also, fairly extensive irradiation and fission-product-retention testing has been conducted with this material.

*Data courtesy of W. L. Wyman, General Atomic.

Some typical properties are summarized in Table 4. Discussions of the test programs and results are presented in the following sections.

Table 4

TYPICAL PROPERTIES OF GRAPHITE-MATRIX FUEL COMPACTS

Graphite density	1.90-1.95 g/cm^3
Crushing strength*:	
Transverse	8500 psi
Longitudinal	7500 psi
Thermal expansion* (to 1000°C):	
Transverse	7.5×10^{-6}/°C
Longitudinal	2.25×10^{-6}/°C
Thermal conductivity at 2000°C, radial	0.3 w/(cm^2)(°C/cm)
	0.07 cal/(cm^2)(sec)(°C/cm)
Electrical resistivity	3.5×10^{-3} ohm-cm
Permeability (He at 1 atm)	2×10^{-3} cm^2/sec
Pore structure	<1% of porosity due to pores >1 μ in diameter
Radiation stability	<0.1% contraction after 6×10^{19} fissions/cm^3 at 1100°-1500°C

*Direction with reference to grain orientation.

Thermal Stress and Shock Resistance

Of the many severe thermal-cycle, stress, and shock tests these compacts have been subjected to, none has caused failure (cracking, spalling, etc.). In this respect, the compacts behave like a high-density, petroleum-coke-base pitch-bonded graphite. Compacts have been heated both directly (by resistance) and indirectly (in a furnace) to temperatures as high as 2600°C. In serveral instances compacts were repeatedly heated from room temperature to 2600°C in less than 1 min without failure.

Permeability

The log of the helium permeability of the fuel compacts was found to decrease linearly with increasing compact density (Fig. 22). Since low permeability is a desirable attribute (to increase fission-product retention), high compact densities were desirable.

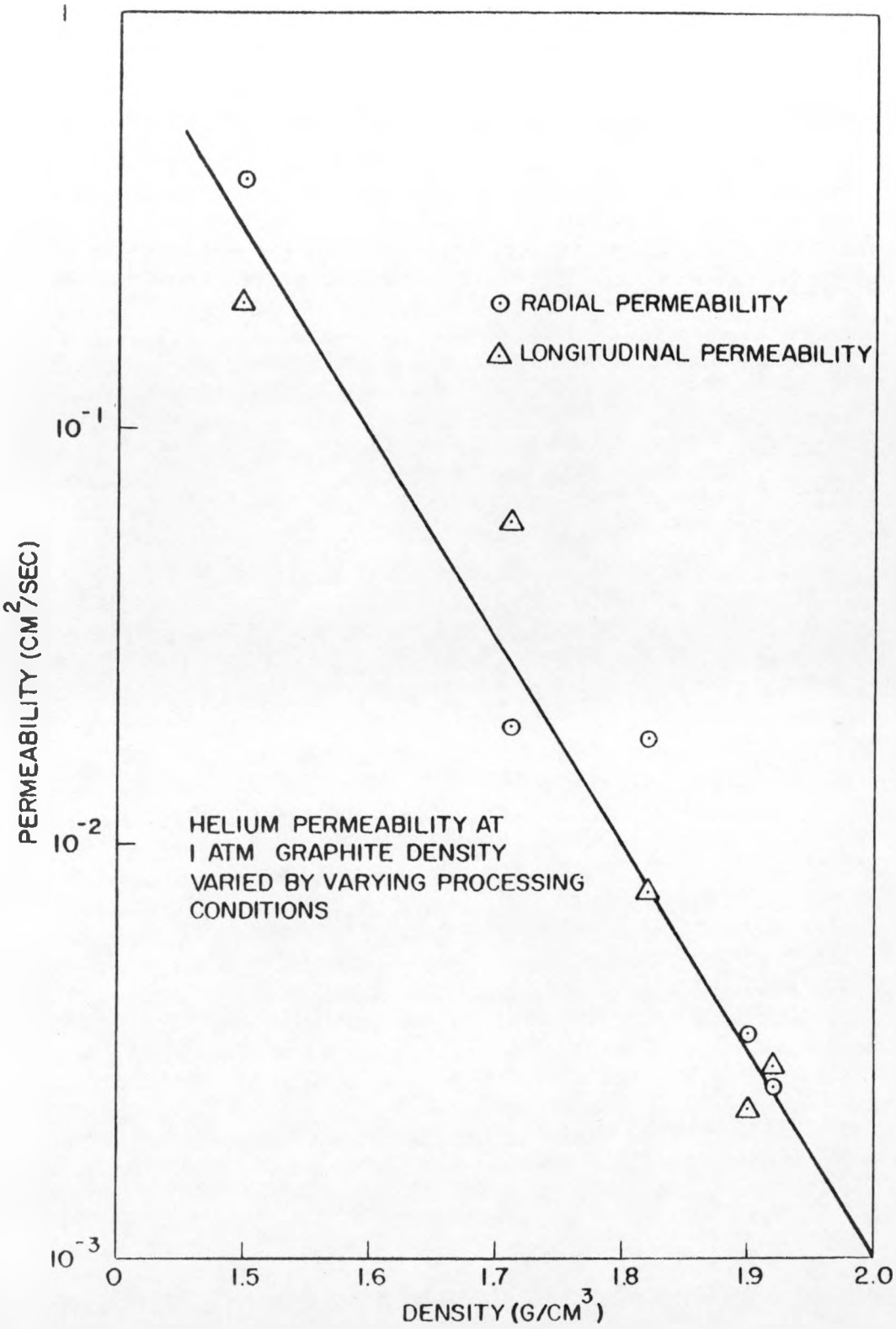

Fig. 22--Permeability versus density of graphite-matrix material for the HTGR fuel compacts

Porosimetry

Pore spectra (Fig. 23) were determined with a hydraulic, mercury-intrusion porosimeter. The long tail at high pore radii found with most commercial graphites is noticeably lacking with the hot-pressed graphite fuel matrix. The uniform structure revealed by the porosimetry data is visually confirmed in Fig. 24, which shows the graphite fuel matrix.

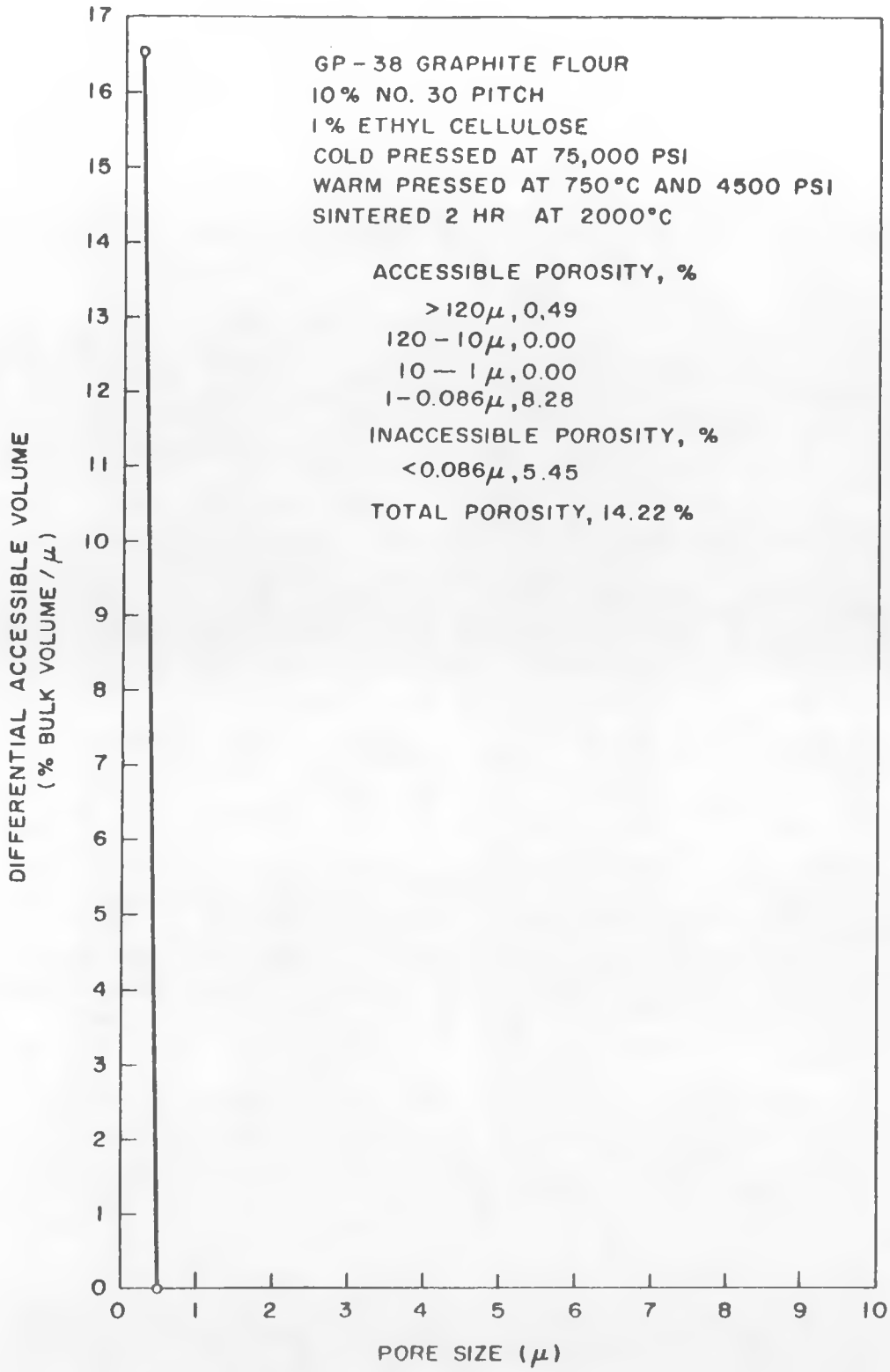

Fig. 23--Pore spectrum of hot-pressed graphite fuel matrix

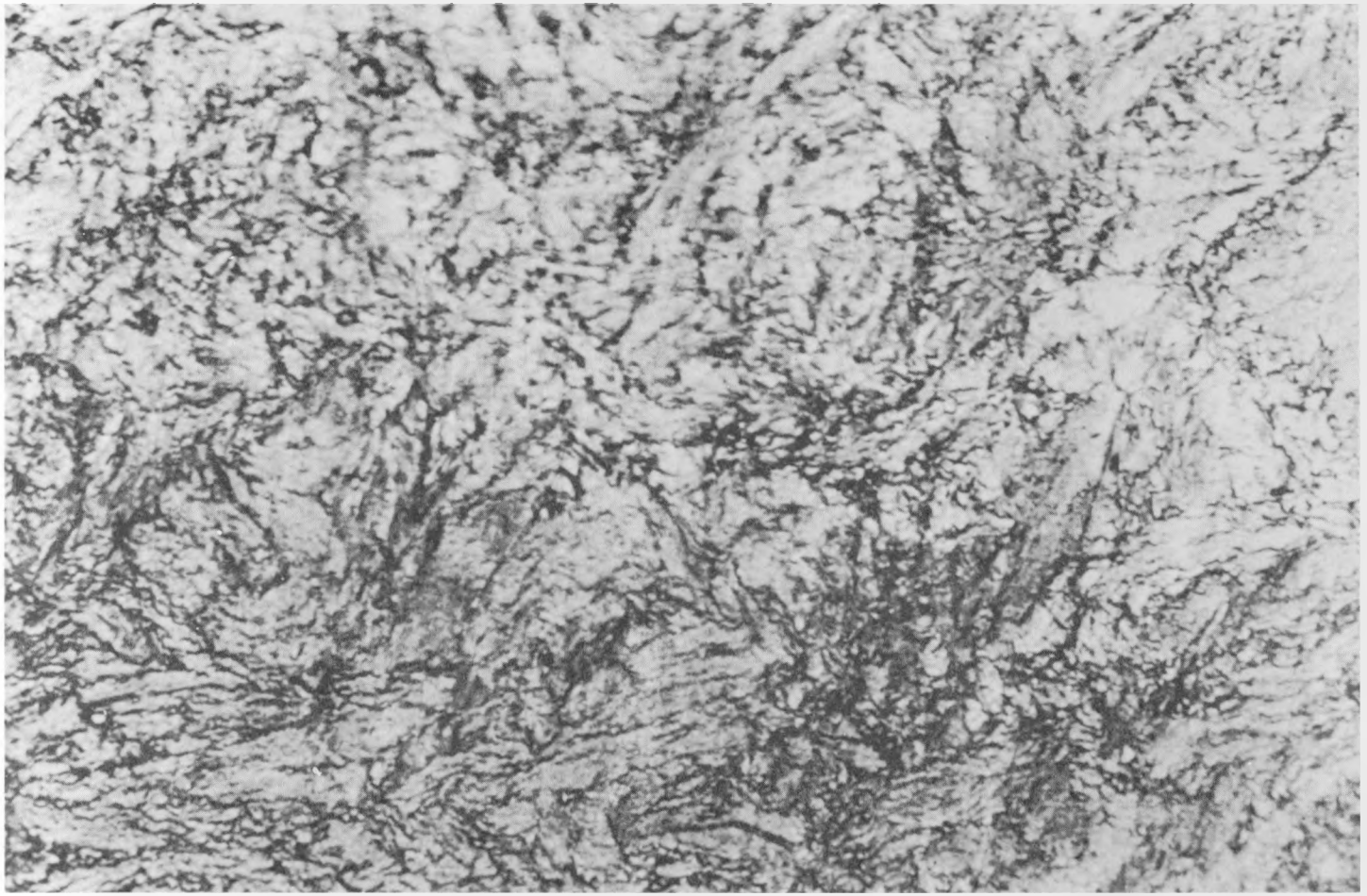

Fig. 24--Photomicrograph of hot-pressed graphite fuel matrix

VI. THERMAL COMPATIBILITY STUDIES*

The mobility of the fuel and fertile phases constitutes an important factor in the stability of a graphite-dispersion-type fuel element. The migration of uranium and thorium in such a fuel element may well determine the upper temperature limit of operation. The accumulation or depletion of uranium and thorium in certain regions of a reactor core could have the following deleterious effects:

1. Fission-product birth in undesirable locations,
2. "Hot-spots" and enhanced fuel evaporation and fission-product release,
3. Poor utilization of fertile material, and
4. Deterioration of fuel particles resulting in enhanced fission-product release and fission-recoil damage to the graphite.

The thermal stability of pyrolytic-carbon-coated carbide fuel particles and graphite-matrix fuel compacts containing these particles has been studied to assist in determining the upper operating temperatures of such fuel systems and to aid in the development of more stable systems. Emphasis has been given to the effects on thermal stability of various particle types and compositions and of various types of coating. Testing conditions have included, in addition to time and temperature variations, thermal-gradient conditions and thermal cycling at elevated temperatures (to study possible solution and precipitation of carbon). This thermal-test program has been integrated with the radiation-test program so that these effects may be studied separately and together.

The fuel-migration test equipment is shown in Fig. 25. Fuel compacts (1 in. in diameter by 2 in. long) are clamped between graphite electrodes and resistance heated in a vacuum chamber. Radial temperature gradients equivalent to those calculated for the HTGR are produced, and the compacts are maintained at elevated temperatures for prolonged periods. A tubular graphite heater surrounding the fuel compact is used for isothermal tests. Coated particles may be tested free of a graphite

*Thermal compatibility studies may be found in reports 6, 17, and 19 of the Appendix

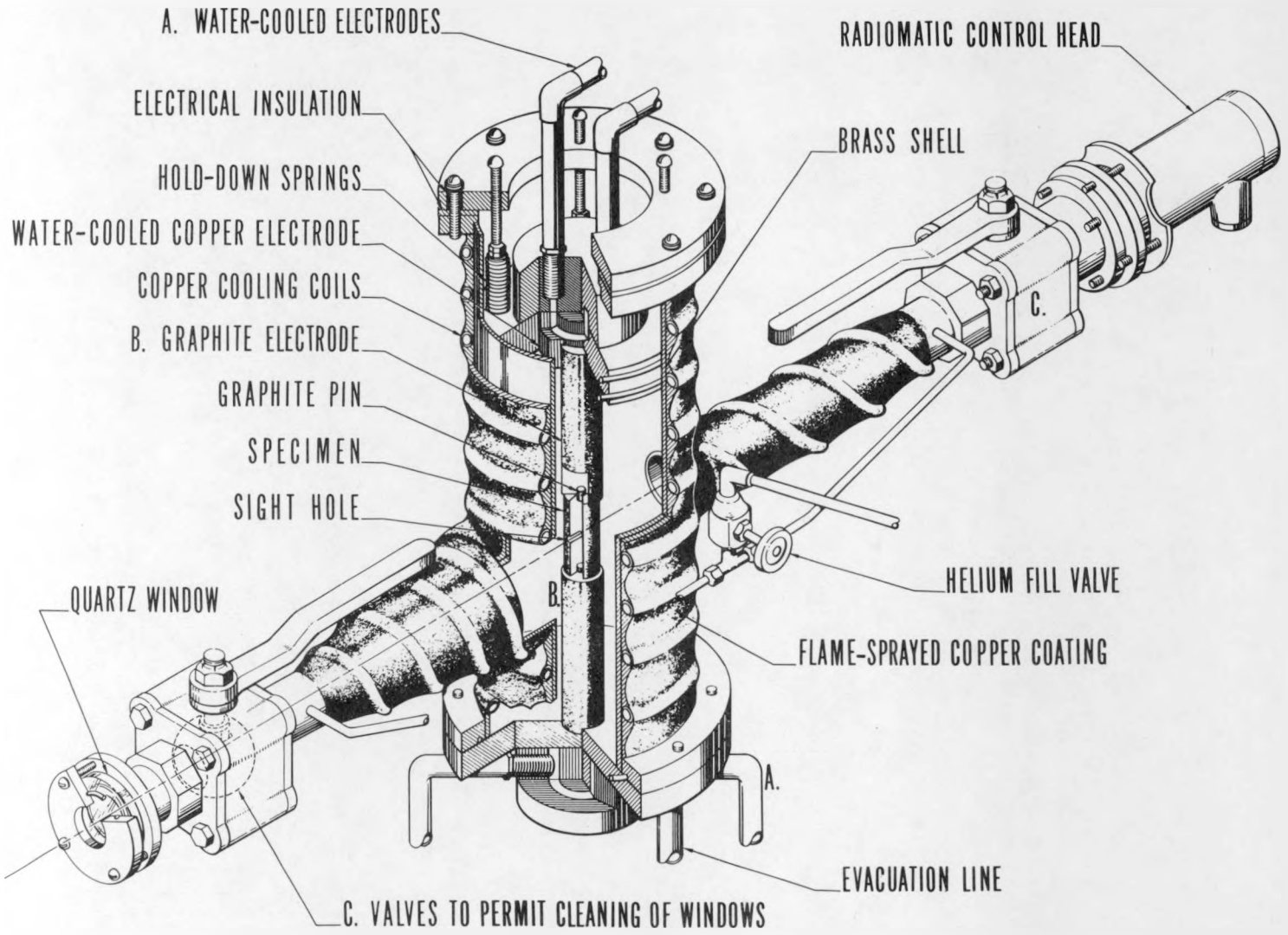

Fig. 25--Thermal compatibility test apparatus

matrix by placing them in graphite crucibles located within the tubular heater. Close temperature control is maintained, and the tests may be run in vacuum or in a controlled atmosphere. Heated samples are evaluated by metallography and microradiography and by measurement of fission-product release.

THE "AMOEBA EFFECT"

In early tests, coatings on (Th, U)C_2 fuel particles in graphite compacts failed in 150 to 250 hr at centerline temperatures of 1900°C and above. (Surface temperatures were about 150°C lower.) Metallographic examination indicated that coating failure was due to carbide attack on the coating on the high-temperature side of the particle (Fig. 26). In all cases, the particles appeared to be moving toward the center (hottest region) of the compact, as may be seen in Figs. 27 through 30, which are photomicrographs of pyrolytic-carbon-coated (Th, U)C_2 particles in a graphite matrix after heating in the range 1850° to 2000°C for 140 hr.

This movement of the carbide particle toward the region of higher temperature has been termed the "amoeba effect". It is apparently caused by solution ("eating") of the pyrolytic carbon coating on the high-temperature side and precipitation ("excretion") behind the particle on the low-temperature side. This amoeba effect has been observed under temperature gradient conditions at temperatures above 1800°C. At 1700°C and below, it has not been observed, nor has it been observed at higher temperatures when the compact is heated isothermally. Tests must be made for several hundred hours at 1700°C before the reaction between carbide and coating becomes detectable. However, at 1800° to 2000°C the attack is quite rapid and is readily observable after 150 hr of testing.

The temperature gradient across a particle (assuming a uniform gradient from the center to the edge of a compact) is about 3°C. This is a small gradient for the large effects observed. However, the effect appears to be closely related to the thermal gradient. Isothermal tests (duplicating previous temperature gradient tests) showed no amoeba effect; i.e., the attack on the coating was uniform rather than concentrated on the high-temperature side of the particles. Carbon-coated UC_2 particles were found to fail in the same manner as the (Th, U)C_2 particles.

LONG-TERM TESTS

Compacts containing coated (Th, U)C_2 particles prepared at General Atomic were examined after tests of 500 hr at 1700°C and 150 hr at 1900°C. Two 1-in.-diameter compacts were tested at each temperature: one contained particles coated with carbon deposited from acetylene; the second

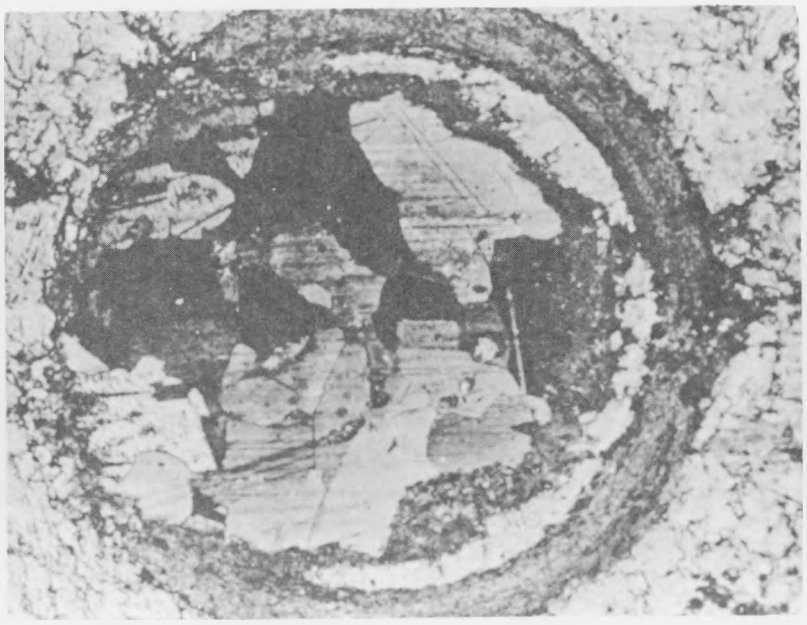

(250×)

Fig. 26--Carbon coated UC_2 particle in graphite matrix after testing for 150 hr in the temperature range from 1780° to 1920°C; the carbide particle has migrated in the direction of increasing temperature; this has been termed the "amoeba effect"

was prepared with particles that had been coated in methane. Each test was made under a radial temperature gradient: the 1700°C test had a compact centerline temperature of 1700°C and a surface temperature of 1600°C; corresponding temperatures for the 1900°C test were 1900° and 1770°C. No evidence of reaction between particle and coating was observed on metallographic examination (see Figs. 31 through 33). Previous tests of the same duration with vendor-supplied particles resulted in coating failure at 1900°C due to selective attack on the high-temperature side ("amoeba effect"), and at 1700°C the reaction between coating and particle had consumed about 40% of the coating (Figs. 34 and 35). Results of fission-gas-release testing showed no increased release of xenon from these four compacts as a result of the prolonged heating.

Two compacts similar to those described above were tested for 3100 hr at a centerline temperature of 1700°C (surface temperature was 1600°C). Particles prepared at General Atomic and coated from methane were in one compact, and the other compact contained particles of the same batch coated from acetylene. Some reaction between the particles and coatings was noted in each case, but the extent of the reaction was greater in the fuel coated from acetylene. Particles near the center of

(50×)

Fig. 27--Random particles; thin side of coating is toward center (hottest region) of compact

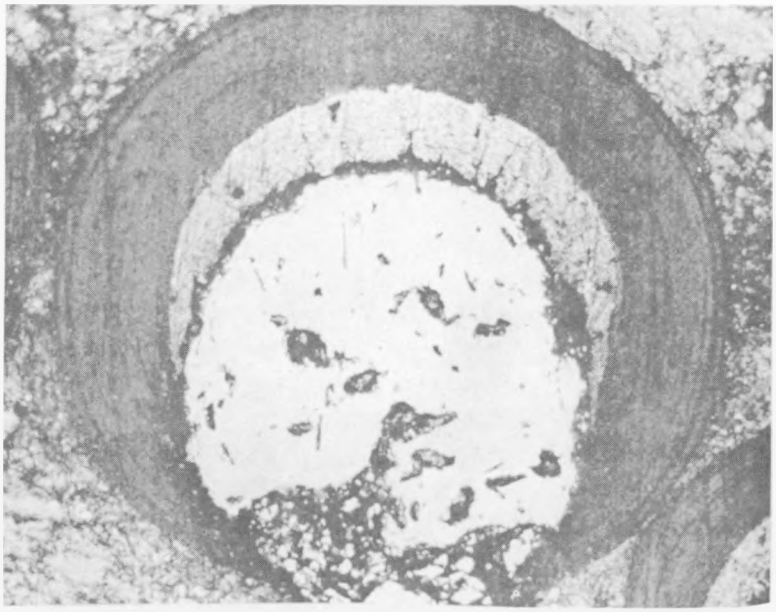

(220×)

Fig. 28--Particles near edge of compact; lowest temperature (~1850°C) and highest thermal gradient

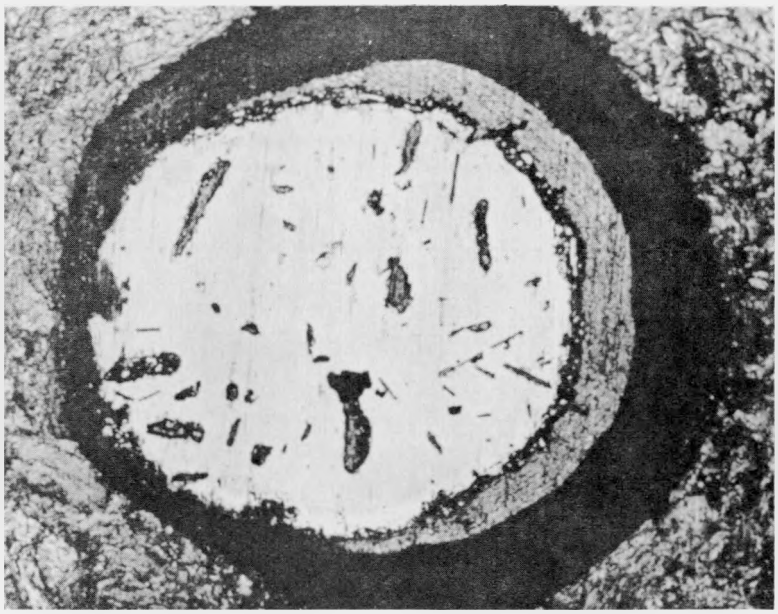

(220×)

Fig. 29--Particle midway between edge and center of compact; temperature ~1950°C

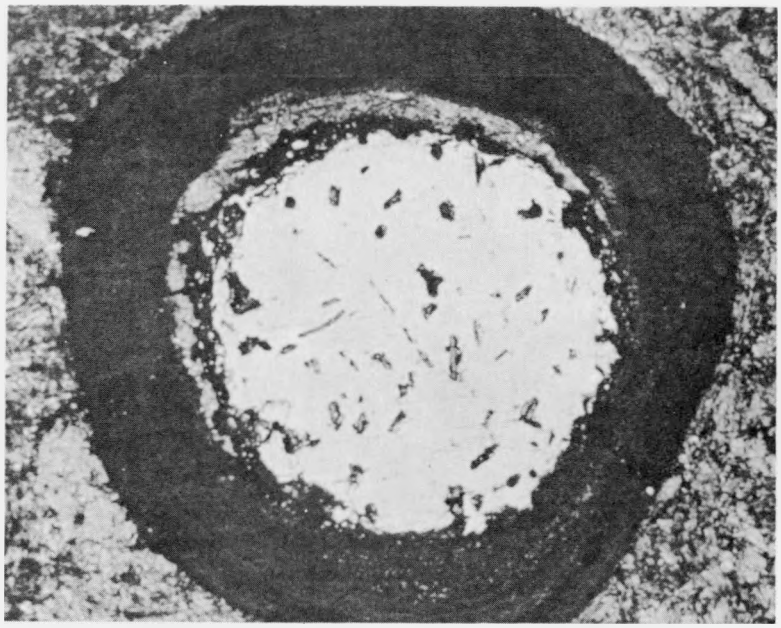

(220×)

Fig. 30--Particle at center of compact; highest temperature (~2000°C) and least thermal gradient

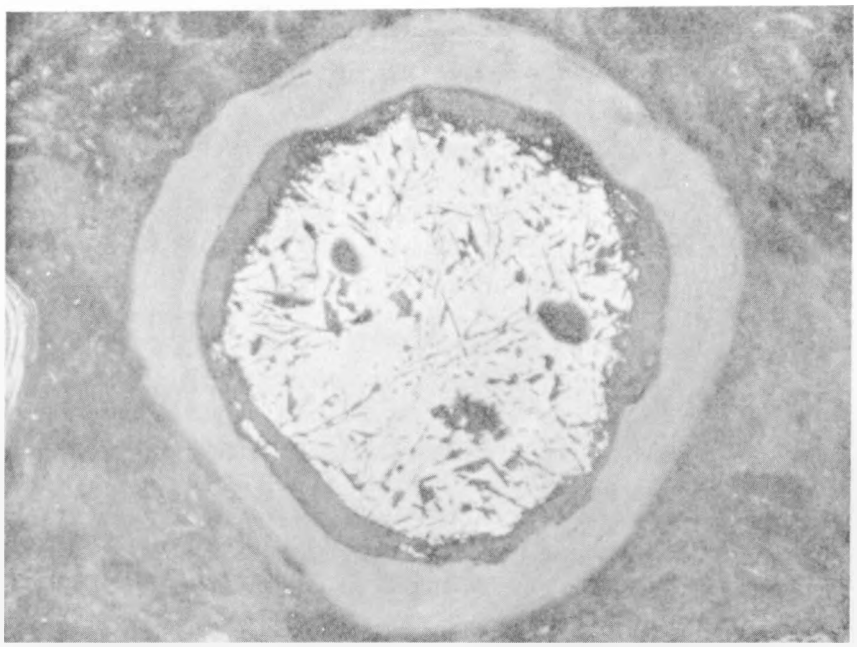

(200×)

Fig. 31--Pyrolytic-carbon-coated General Atomic (Th, U)C_2 particle in a graphite-matrix fuel compact prior to thermal testing

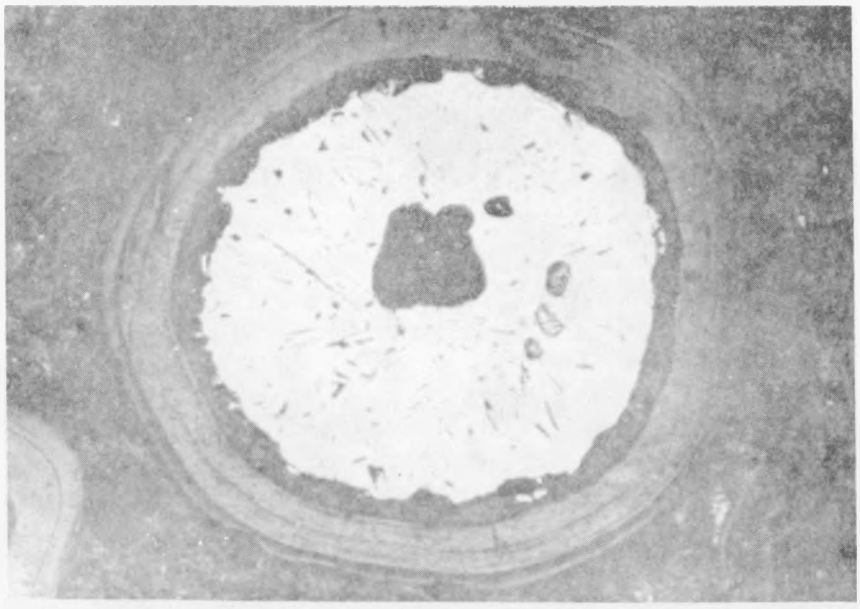

(160×)

Fig. 32--Pyrolytic-carbon-coated General Atomic (Th, U)C_2 particle in a graphite-matrix fuel compact after heating at 1900°C for 150 hr

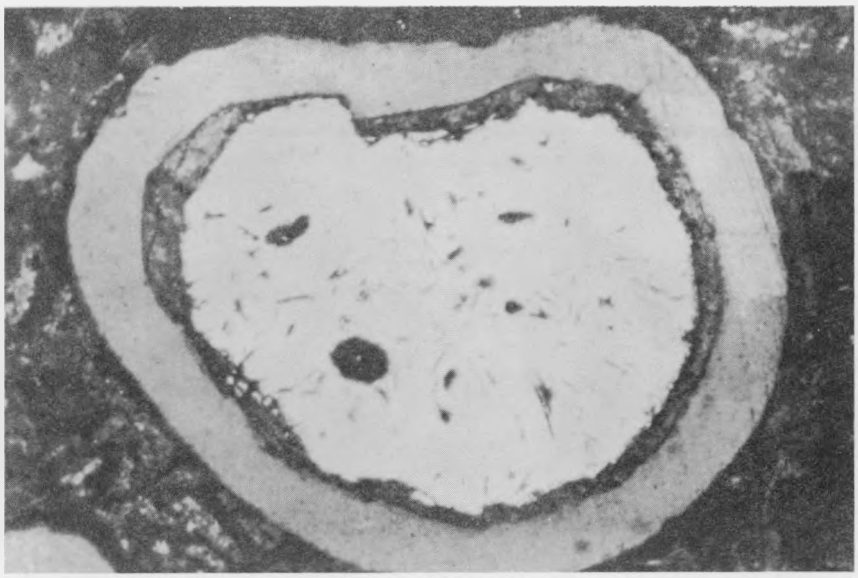

(200×)

Fig. 33--Pyrolytic-carbon coated General Atomic $(Th, U)C_2$ particle in a graphite-matrix fuel compact after heating at 1700°C for 500 hr

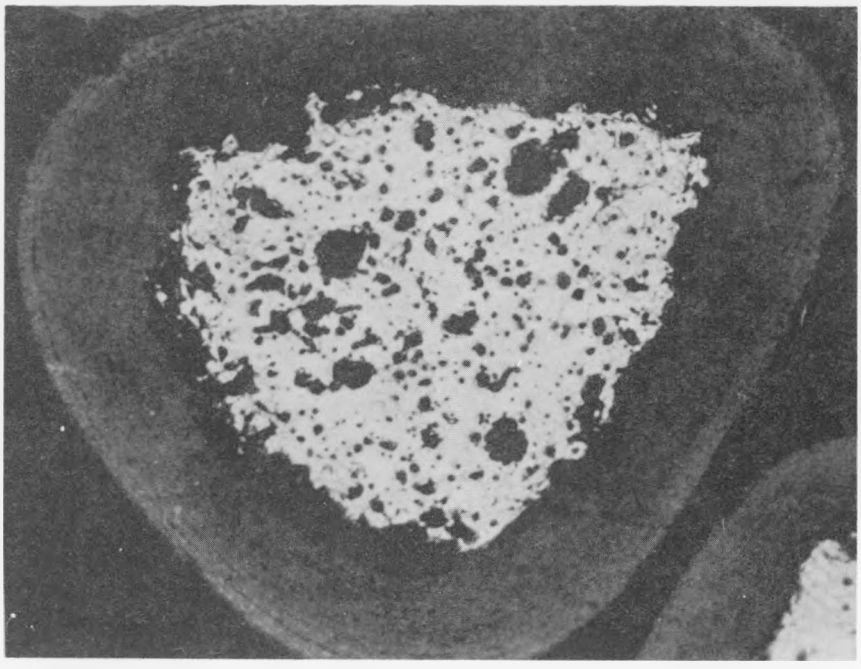

(250×)

Fig. 34--Pyrolytic-carbon coated vendor-supplied $(Th,U)C_2$ particle in a graphite-matrix fuel compact prior to thermal testing

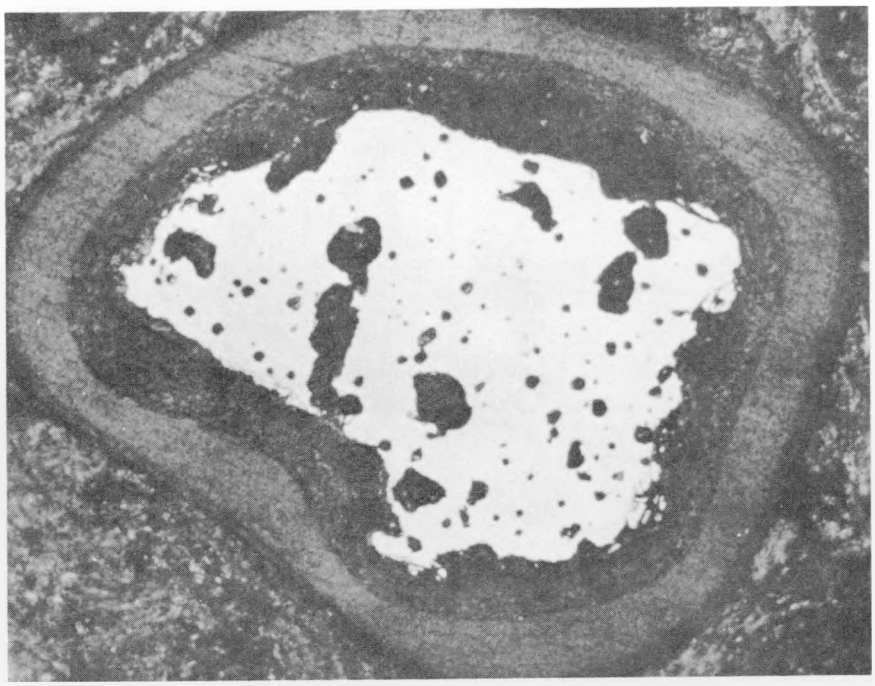

(250×)

Fig. 35--Pyrolytic-carbon-coated vendor-supplied (Th, U)C_2 particle in a graphite-matrix fuel compact after heating at 1700°C for 500 hr

this compact had reacted as much as half-way through the coatings, but less attack was noted on particles located near the edge of the compact. This difference is attributable to the temperature difference between the center (1700°C) and edge (1600°C) of the compact. Such a difference in reaction was not observed in the other compact in which the particles had been coated from methane. These latter particles showed less reaction, with maximum penetration of less than one-third the coating thickness. In all cases, the attacks were uniform; i. e., no amoeba effect was observed. Tests of two duplicate compacts at a centerline temperature of 1550°C have logged over 7000 hr. These compacts will be examined at 10, 000 hr.

The results of these tests show that compacts prepared with the General Atomic coated-carbide fuel particles are more stable at elevated operating temperatures than were the previously available particles. The higher carbon content of the particles prepared at General Atomic and/or the surface layer of adherent graphite may account for this improved behavior. No thermal instability is anticipated with these fuel systems during the 3-year core life of the HTGR at the maximum predicted fuel temperature of 1400°C.

One test is being made in which carbon-coated (Th, U)C_2 fuel particles are suspended in graphite powder and heated at 1400°C. Samples have been removed and examined after 3700, 5000, and 8700 hr at temperature. There has been no discernible reaction between the particles and their coatings. This test is continuing.

VII. IRRADIATION STUDIES*

The physical characteristics of representative graphite-matrix fuel compacts in a radiation field have been studied by means of two types of irradiation capsule: (1) the GA-308 series capsules (see Fig. 36), in which as many as six compacts in tandem are simultaneously irradiated, and (2) the GA-309 series capsules (see Fig. 37), which are used for the study of the release of gaseous fission products from the fuel compacts during irradiation. The high-temperatures produced in the compacts by fission heating are controlled by the variation in thermal conductivity of a binary gas mixture in a control annulus located between the test specimen and the capsule coolant.

GA-308 SERIES CAPSULE TESTS

The test conditions are listed in Tables 5 and 6 and the results of several irradiation tests discussed below are summarized in Tables 7 to 9. All of the graphite-matrix fuel compacts were prepared by the hot-press process previously described.

Table 5

FUEL-COMPACT COMPOSITIONS AND DIMENSIONS FOR GA-308 CAPSULE IRRADIATIONS

	GA-308-2	GA-308-3	GA-308-4
Composition:			
Uranium (93% enriched), wt-%	3.1	6.5	6.0
Thorium, wt-%	7.25	15.5	14.4
Silicon, wt-%	---	---	6.6
Total metal, wt-%	10.3	22.0	22.0
C:Th:U, atom ratio	570:2.4:1	240:2.4:1	255:2.4:1
Dimensions:			
Outside diameter, in.	1.00	1.0	1.00
Inside diameter, in.	---	0.50	0.50
Length, in.	1.10	1.78	1.78

*Capsule irradiation tests have been described in reports 15, 17, and 20 of the Appendix.

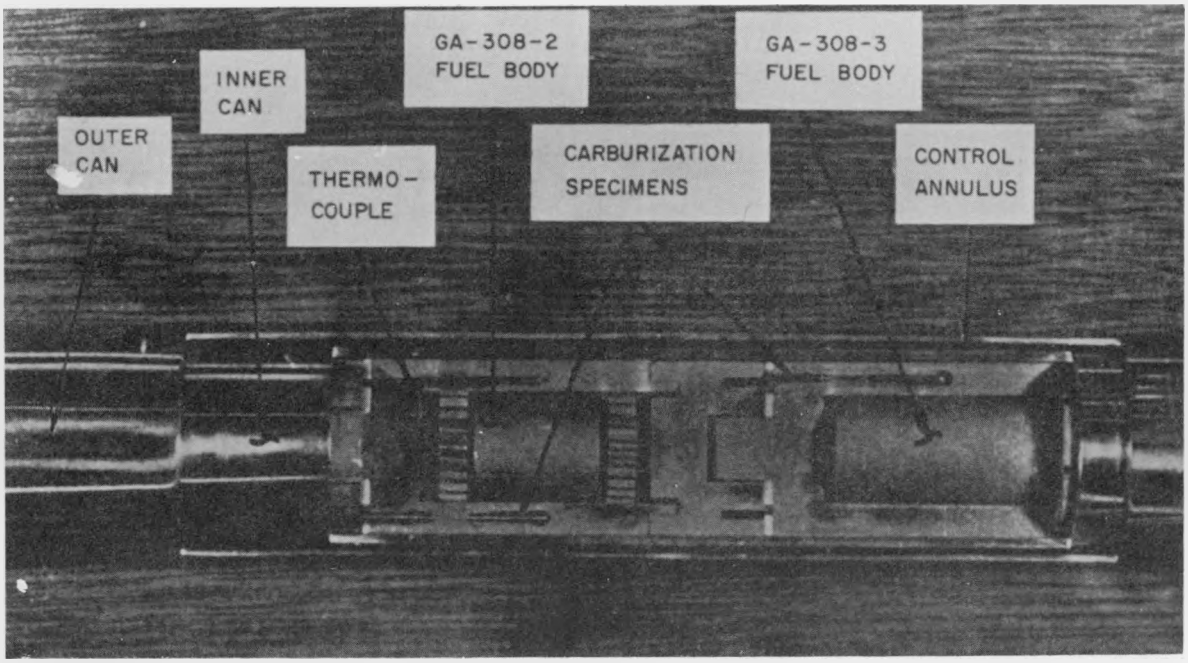

Fig. 36--GA-308 series irradiation capsule

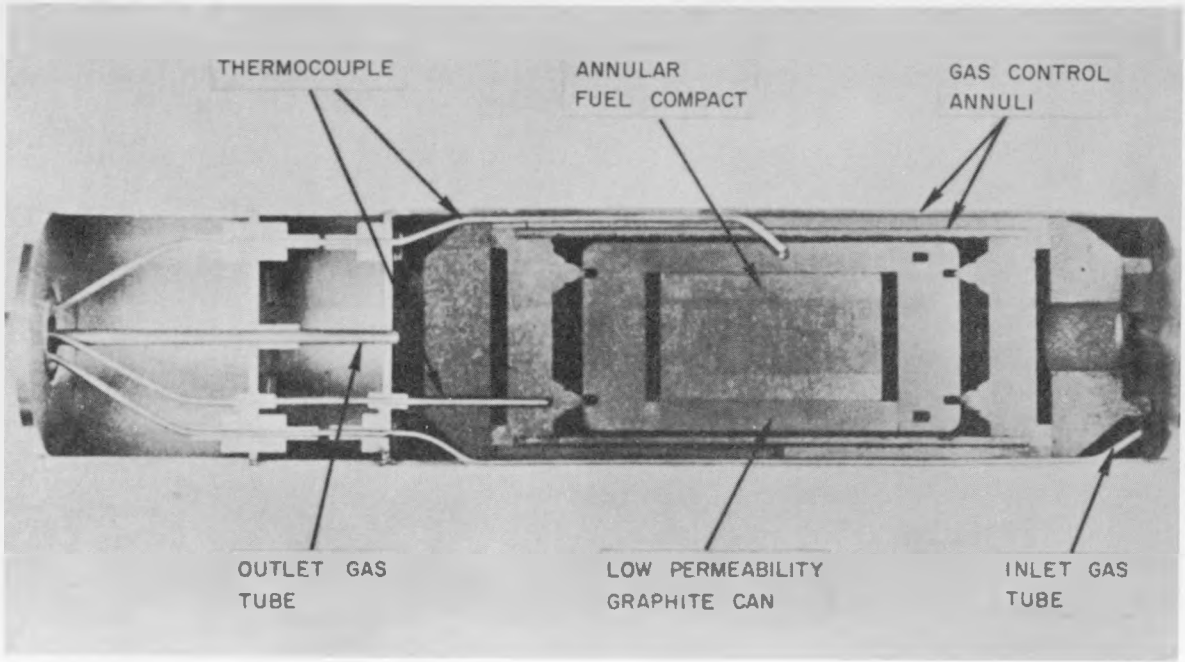

Fig. 37--GA-309 series irradiation capsule

Table 6

TEMPERATURES OF IRRADIATION AND BURNUPS FOR GA-308 CAPSULE IRRADIATIONS

	GA-308-2	GA-308-3	GA-308-4
Temp. at compact centerline, °C	1050-1200	1150-1480	1090-1480
Burnup*			
U^{235}, %	16.7	18	18
Fissions/cm^3	4.25×10^{19}	6.9×10^{19}	6.0×10^{19}
MwD/T	48,000	51,000	51,000
Kw-hr/cm^3	210	600	600

*Design burnup for HTGR is 0.67×10^{20} fissions/cm^3.

Irradiation Test of Capsule GA-308-2

The fuel compacts for the irradiation of capsule GA-308-2 were right circular cylinders 1.00 in. in diameter by 1.10 in. long. Solid-solution (Th, U)C_2 fuel particles 110 to 250 μ in diameter were formed by the in situ conversion of (Th, U)O_2. The fuel content was 3 wt-% U^{235}; the thorium content was 7 wt-%.

During irradiation the temperature of the graphite cans containing the fuel compacts varied from 775° to 830°C in the region of highest flux. The fuel-compact temperatures were calculated to be 275°C higher than the temperature of the cans. The maximum calculated burnup was 16.7% of U^{235}, or 48,000 Mw-days/ton, which is equivalent to 4.25×10^{19} fissions/cm^3.

When this capsule was disassembled, it was noted that the appearance and integrity of all the fuel compacts were excellent (see Fig. 38). The dimensional measurements of the fuel compacts, which were checked against the preirradiation values, are given in Table 7.

Irradiation Test of Capsule GA-308-3

The fuel compacts in the irradiation test of capsule GA-308-3 differed in three major respects from those tested in the previous irradiation. First, these compacts were of an annular design (in order to correspond more closely to the configuration of the HTGR compact); second, the metal (Th + U) loading was increased from 10 wt-% to 22 wt-% (6.5% U, 15.5% Th); third, three different particle sizes of fuel material were used to permit

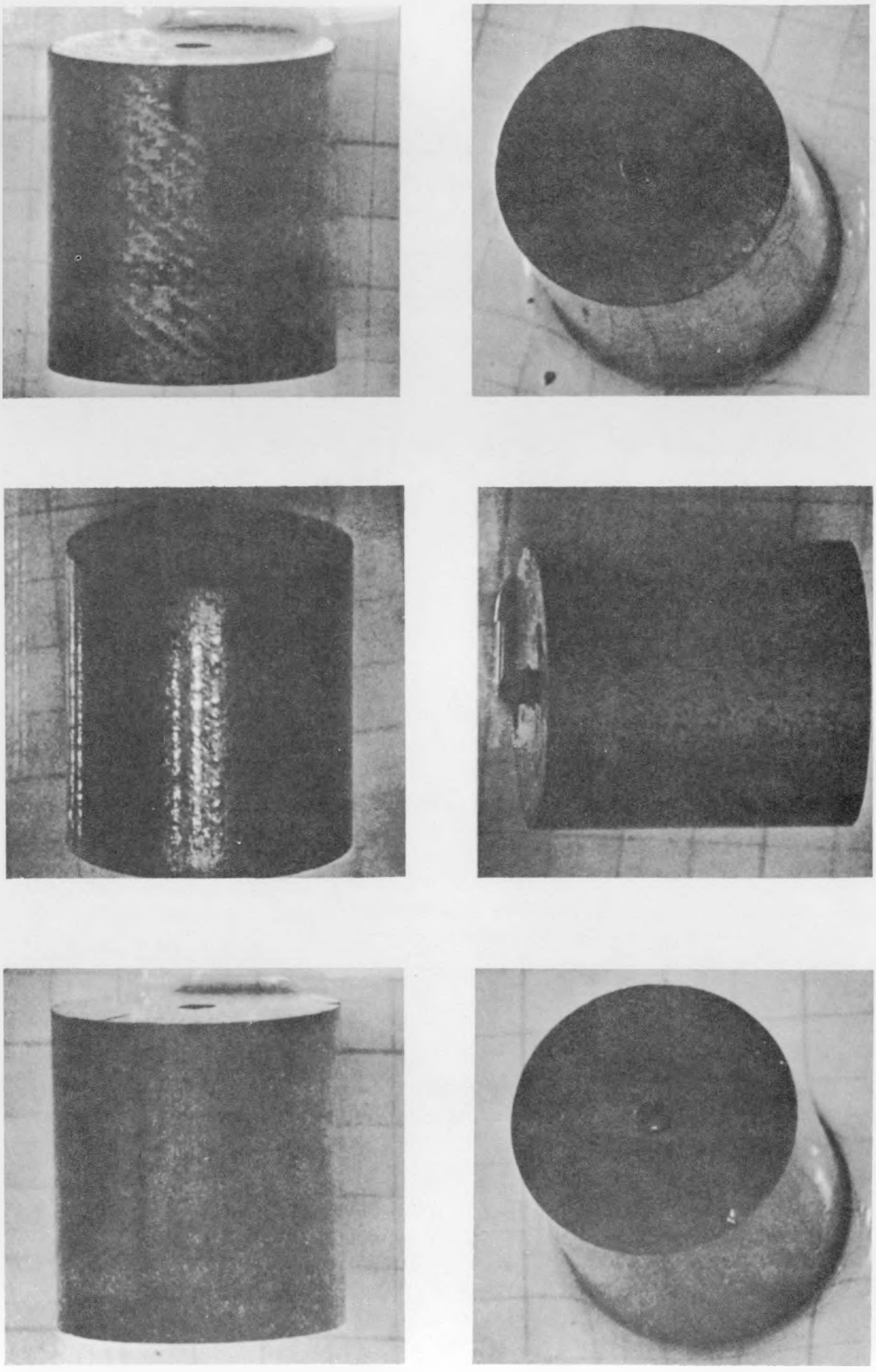

Fig. 38--Compacts from capsule GA-308-2 after irradiation to 4.25×10^{19} fissions/cm^3 at 1050° to 1200°C

Table 7

DIMENSIONAL CHANGES OF FUEL COMPACTS
FROM GA-308-2 IRRADIATION

Compact	Avg. Temp. of Graphite Can (°C)	Fuel-compact Centerline Temp., Calc. (°C)	Dimensional Changes (%)	
			ΔD	ΔL
4	820	1200	-0.2	0
5	830	1200	-0.1	-0.1
6	775	1050	0	0

comparison of radiation effects as a function of fuel-particle size. The sizes of the particles were <50 μ, 110 to 250 μ, and 250 to 500 μ. Six compacts were tested, two with each size of fuel particle. The compacts were made from solid-solution (Th, U)O_2 particles that were converted in situ to (Th, U)C_2 during compact fabrication. Each compact was 1.00 in. in outside diameter, 0.50 in. in inside diameter, and 1.75 in. long; and a graphite rod was inserted in the center of each compact to simulate the unfueled region in the HTGR fuel compact.

During irradiation, the temperature of the compacts ranged from 650° to 925°C; the burnup reached was 18% of the U^{235}, 6.9×10^{19} fissions/cm^3, or 600 kw-hr/cm^3. The dimensional changes and other pertinent data are recorded in Table 8.

Table 8

DIMENSIONAL CHANGES OF FUEL COMPACTS
FROM IRRADIATION OF CAPSULE GA-308-3

Compact	Fuel-particle Size (μ)	Avg. Temp. of Graphite Can, Calc. (°C)	Fuel-compact Centerline Temp., Calc. (°C)	Dimensional Change (%)	
				ΔD	ΔL
1	250-500	650-760	1200	0	+0.2
2	110-250	730-840	1300	-0.2	+0.2
3	<50	840-900	1400	-1.7	+2.2
4	<50	900-925	1480	-2.2	+3.0
5	110-250	760-840	1200	-0.3	<-0.1
6	250-500	700-790	1150	0	<+0.1

The postirradiation appearance of the six fuel compacts was as good as those from the previous capsule. A typical fuel compact prior to irradiation is shown in Fig. 39, and Fig. 40 shows photographs of the irradiated compacts. (The speckled surface is a result of partial hydrolysis of particles near the surface of the compact that were exposed to air during hot-cell examination.)

It will be noted that while the diametral change in these compacts was one of contraction, the longitudinal dimension of the bodies increased. Furthermore, the largest variations occurred in compacts with fuel particles smaller than 50 μ. These changes are characteristic of neutron radiation effects on unfueled graphite, which contracts at temperatures greater than 300° to 400°C. However, the effect of small fuel particles is much larger than would be expected for pile-grade graphite under equivalent neutron exposure. This indicates a contribution from fission recoils, as one would expect. The smallest particle size that will produce dimensional stability apparently lies somewhere between 50 and 100 μ.

The expansion of these compacts along the fuel axis cannot be conclusively explained at this time. The compressive force was in this direction when the compacts were molded, however, and this expansion may be a relaxation of residual stresses. Or, as the preferred orientation of the basal planes of the crystallites is perpendicular to the longitudinal direction, the expansion may be a manifestation of the spreading of these planes in the c-direction or parallel to the length of the compact. This latter explanation seems more probable, since the smaller fuel particles have a greater influence on the dimensional changes in the compact.

Irradiation Test of Capsule GA-308-4

The fuel compacts for capsule GA-308-4 differed in only one respect from the GA-308-3 compacts: they were prepared from thorium-uranium silicide (7.4 wt-% Si) fuel rather than thorium-uranium oxide. The thorium and uranium were converted to dicarbides and the silicon to SiC in situ during fuel-compact fabrication. Dimensions, fuel loadings, and fuel-particle size were the same as for the GA-308-3 test.

The centerline temperatures of these compacts during irradiation ranged up to 1480°C, as determined by melt wires placed in the graphite core of each compact. Burnup was 6.0×10^{19} fissions/cm^3, 18% of the U^{235}, or 51,000 kw-hr/cm^3. Dimensional changes are summarized in Table 9.

The appearance of these compacts was good, although surface roughening was noted on one fuel compact. The exact cause of this condition is not known. The general appearance of the fuel compacts before irradiation

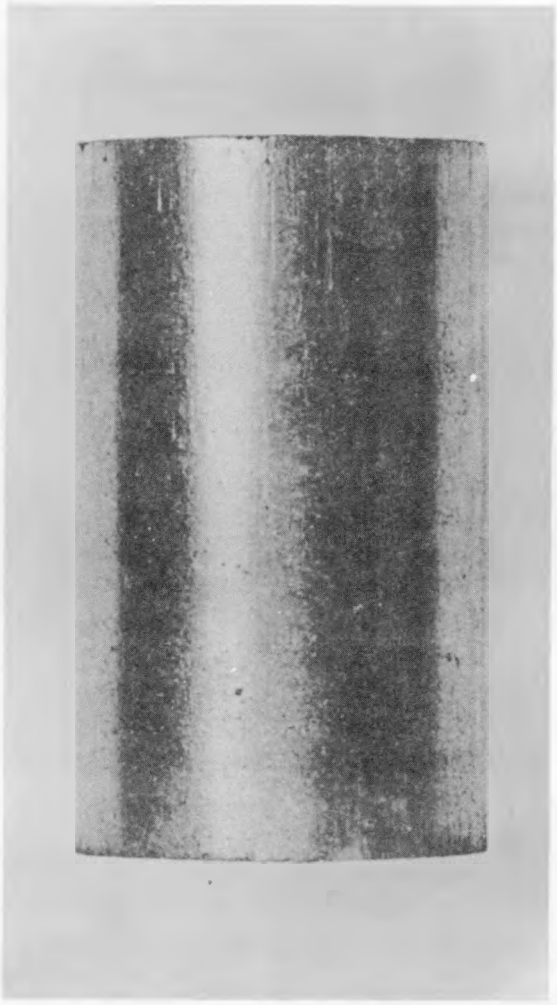

Fig. 39--Fuel compact of the type prepared for the irradiation of capsule GA-308-3

Compact No. 3; fuel particles <50 μ

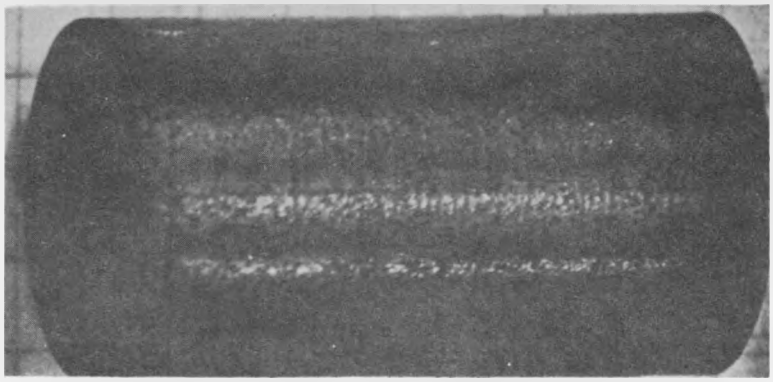

Compact No. 2; fuel particles 110-250 μ

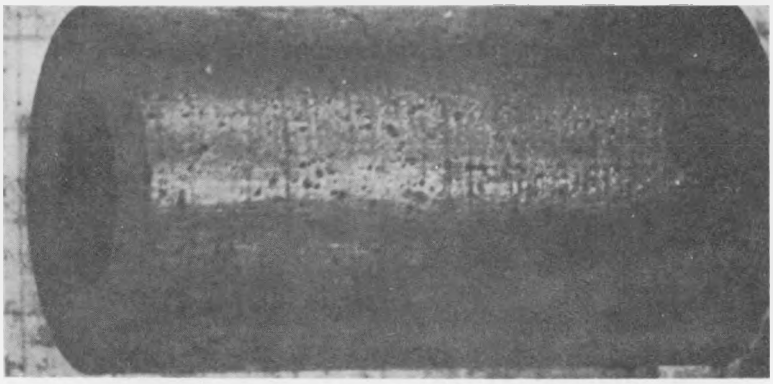

Compact No. 6; fuel particles 250-500 μ

Fig. 40--Fuel compacts from capsule GA-308-3 after irradiation to 6.9×10^{19} fissions/cm^3 at 1150° to 1480°C; surface pips are due to partial hydrolysis of carbide fuel during hot-cell examination

Table 9

DIMENSIONAL CHANGES OF FUEL COMPACTS
FROM IRRADIATION OF CAPSULE GA-308-4

Compact	Fuel-particle Size (μ)	Avg. Temp. of Graphite Can (°C)	Fuel-compact Centerline Temp., Calc. (°C)	Dimensional Changes (%)	
				ΔD	ΔL
1	<50	650-760	1090*	-0.9	+3.0
2	250-500	700-790	1290	0	+0.3
3	<50	790-870	1370	-0.8	+0.8
4	110-250	870-925	1480†	-0.1	<+0.1
5	250-500	790-840	1230	0	+0.1
6	110-250	730-815	1175	0	+0.1

*Measured.
†Determined by melt-wire analysis.

was similar to that shown in Fig. 39. Except for the surface roughening of compact 3 and a crack in compact 5, the condition of the remaining compacts (see Fig. 41) in this capsule is comparable to that before irradiation.

The dimensional changes, again, indicate the importance of particle size. In this capsule one of the fuel compacts containing small particles was placed in a cold region and another in the hot region. In both cases there was a maximum contraction, indicating that the fission-recoil effect is rather insensitive to temperature in this range.

The data obtained from these capsule irradiations indicate that, in general, these graphite-matrix compacts are acceptable from the point of view of dimensional and physical integrity at metal loadings up to 22 wt-%. The dimensional stability can be affected by fuel-particle size, although it seems to be somewhat insensitive to temperature. The burnups for these capsules are 60% of that expected for the HTGR fuel. The starting material, whether oxide or silicide, performed satisfactorily.

GA-309 SERIES CAPSULE TESTS

The GA-309 series irradiation capsules were designed to study the release of gaseous fission products from graphite-matrix fuel compacts during irradiation at elevated temperatures. In these experiments, three capsules of the type shown in Fig. 37 are irradiated in the same test hole in the reactor. From time to time the capsules are purged with helium;

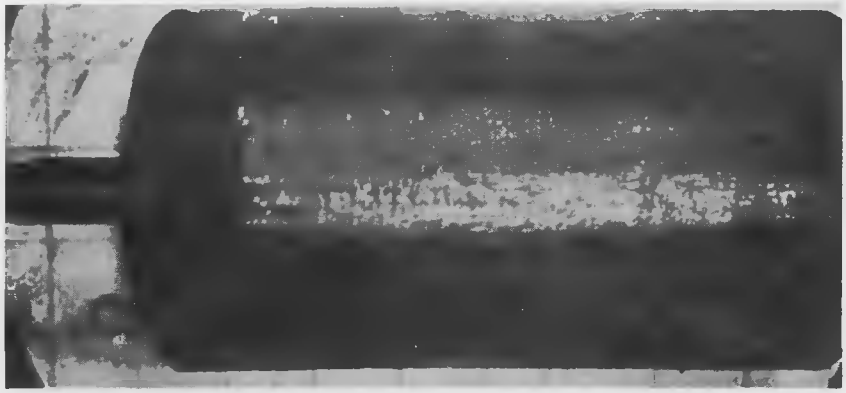

Compact No. 1; fuel particles <50 μ

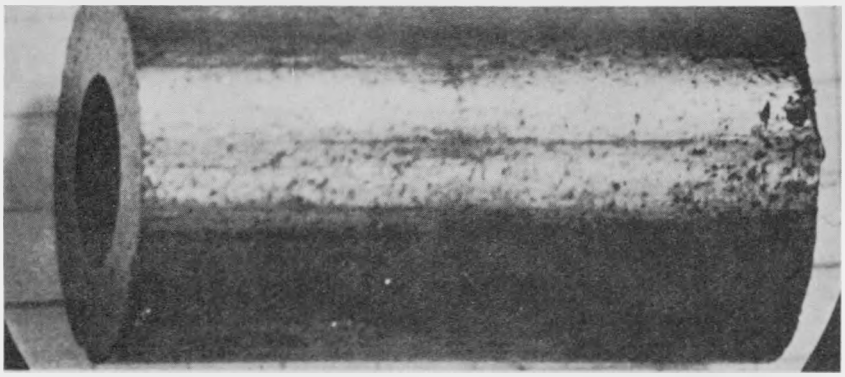

Compact No. 6; fuel particles 110-250 μ

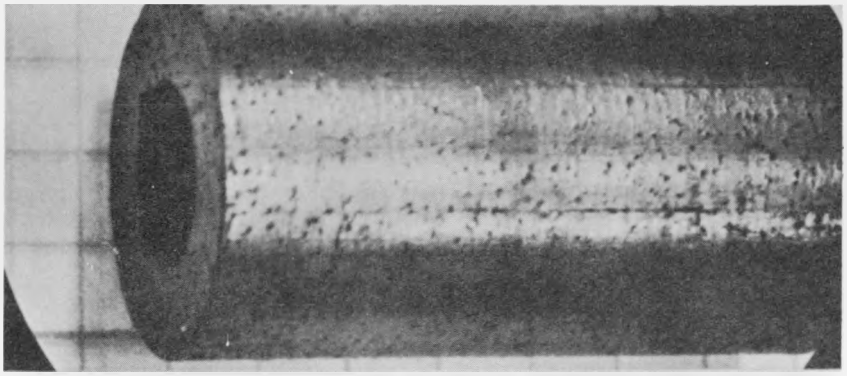

Compact No. 2; fuel particles 250-500 μ

Fig. 41--Fuel compacts from capsule GA-308-4 after irradiation to 6×10^{19} fissions/cm^3 at 1090° to 1480°C; surface pips are due to partial hydrolysis of carbide fuel during hot-cell examination

the released fission-product gases are then allowed to accumulate for the order of 24 hr and the capsule purged again with helium. This latter purge is sampled, aliquoted, and analyzed.

Graphite compacts containing pyrolytic-carbon-coated (Th, U)C_2 particles were used for the two groups of GA-309 capsule irradiations. Each capsule was designed for the same power generation (4500 w); therefore the fuel loadings were different for each compact to compensate for the axial flux distribution in the reactor.

All of the compacts were annular, were 1 in. in outside diameter by 1/2 in. in inside diameter by 1.75 in. long, and contained 18% to 24% fuel (Th + U). The fuel used in capsules GA-309-4, -5, and -6 was some of the first coated-carbide fuel produced. Particle densities were low and coatings were thin (25 μ) (Fig. 42). The compacts in the other three capsules were prepared with improved coated particles. Two of these compacts contained fuel with thick (50 to 60 μ) pyrolytic-coatings (Figs. 43 and 44), and the third contained thin (10 to 15 μ) coatings (Fig. 45) to simulate possible end-of-life conditions. All six capsules were exposed to a perturbed thermal neutron flux of 4.0 to 4.8 $\times 10^{13}$ neutrons/cm^2-sec. Additional data on the irradiations are presented in Table 10. The burnups experienced by these compacts are compared to Peach Bottom design requirements in Table 11. Descriptive summaries of the fuel materials and irradiation histories are given in Tables 12 and 13.

Table 10

IRRADIATION DATA FOR CAPSULES
GA-309-4, -5, -6, -7, -8, AND -9

Capsule	No. of GETR Cycles	Fuel Temp. (°C)	Time Above 1400°C (hr)	Exposure (nvt)	
				Thermal	Fast
GA-309-4	6	850-1700	1760	5.7 to 6.9×10^{20}	3.8 to 4.6×10^{19}
GA-309-5	6	1000-1950	2430	5.7 to 6.9×10^{20}	3.8 to 4.6×10^{19}
GA-309-6	6	950-1950	2180	5.7 to 6.9×10^{20}	3.8 to 4.6×10^{19}
GA-309-7	4	1000-1700	820	3.9 to 4.7×10^{20}	2.6 to 3.1×10^{19}
GA-309-8	4	1200-2050	1460	3.9 to 4.7×10^{20}	2.6 to 3.1×10^{19}
GA-309-9	4	1250-1600	1210	3.9 to 4.7×10^{20}	2.6 to 3.1×10^{19}

Pictures of the fuel compacts and photomicrographs of the fuel particles are shown in Figs. 46 through 55.

Table 11

BURNUP DATA FOR CAPSULES GA-309-4, -5, -6, -7, -8, AND -9

	U^{235} (%)	Metal (Th+U) (%)	Fissions/cm^3	Portion of 3-year Life (%)
Peach Bottom design	63	6	0.67×10^{20}	100
Capsules GA-309-4, -5, -6	29-33	8-10	1.2×10^{20}	180
Capsules GA-309-7, -8, -9	20-24	6-7	0.8×10^{20}	120

On postirradiation examination, many of the coated particles in capsules GA-309-4, -5, and -6 were found to have broken coatings. (All these capsules contained water, which may account for the poor appearance of the fuel compacts. The compacts were generally weak and crumbly, typical of the effects caused by moisture reacting with (Th, U)C_2 particles with broken coatings.) The broken pieces of coating still looked good (i.e., the coatings appeared much as they did prior to irradiation).

Metallographic examination of the compacts from capsules GA-309-8 and -9 indicated that the majority of the coated particles in the central regions of the compacts were intact and in good condition; only 4% broken particle coatings were counted on a polished cross section of GA-309-8 and only 15% on GA-309-9. The coatings that did fail appeared to have done so as a result of tensile stresses (see Figs. 53, 54, and 55). Several contributing factors would lead to tensile stresses in the carbon coatings during high-temperature irradiation, namely: (1) neutron and fission recoil exposure leading to shrinkage; (2) annealing or graphitizing of the coating from purely thermal effects, which would also lead to shrinkage; (3) differential thermal expansion between coating and particle; (4) fission gas pressure; and (5) possible expansion of the carbide particle during irradiation. No coating breakage due to thermal effects alone has been experienced with these materials. Further tests will be required to assess the role of radiation in these failures.

The fission-product-release data for capsules GA-309-8 and -9 were indicative of 15% and 75% to 100% coating failures, but metallographic examination indicated only about one-fifth this amount of breakage. To check the possibility of increased permeability of the coatings due to microcracks generated during irradiation, ten coated particles were separated from compact GA-309-8 and tested for fission-product release at temperatures up to 1900°C. A total of 28% of the Xe^{133} was released.

Examination of these separated particles after they had been heated to 1900°C for fission-product-release testing revealed a delamination of

Table 12

GA-309-4, -5, AND -6 PURGE-CAPSULE IRRADIATION TEST OF COATED-CARBIDE FUEL PARTICLES

Fuel compacts	Annular; 1 in. OD, 1/2 in. ID, 1.75 in. long; 18%-24% fuel (Th + U)
Coated fuel	25-μ-thick carbon coating on Malinckrodt (Th, U)C_2
Fuel can:	
Capsule GA-309-4	AGOT graphite
Capsule GA-309-5	Hawker-Siddeley low-permeability graphite
Capsule GA-309-6	National Carbon low-permeability graphite
Irradiation history	Inserted 11/13/60, discharged 8/15/61; six cycles in GETR
Fuel temperature:	
Capsule GA-309-4	850°-1700°C, above 1400°C for 1760 hr
Capsule GA-309-5	1000°-1950°C, above 1400°C for 2430 hr
Capsule GA-309-6	950°-1950°C, above 1400°C for 2180 hr
Flux	Thermal perturbed, 4.0 to 4.8×10^{13} neutrons/cm^2-sec
Exposure:	
Thermal	5.7 to 6.9×10^{20} nvt
Fast	3.8 to 4.6×10^{19} nvt
Burnup:	
U^{235}	29%-33%
Metal (Th + U)	8%-10%
Fissions/cm^3	1.2×10^{20}

Table 13

GA-309-7, -8, AND -9 PURGE-CAPSULE IRRADIATION TEST OF COATED-CARBIDE FUEL PARTICLES

Fuel compacts	Annular; 1 in. OD, 1/2 in. ID, 1.75 in. long; 18%-24% fuel (Th + U)
Coated fuel, General Atomic carbon coating on Minnesota Mining $(Th, U)C_2$:	
Capsule GA-309-7	10-15 μ coating from acetylene
Capsule GA-309-8	50-60 μ coating from methane
Capsule GA-309-9	50-60 μ coating from acetylene
Fuel can	General Atomic impregnated HLM-85 graphite
Irradiation history	Inserted 5/1/61, discharged 9/17/61; 4 cycles in GETR
Fuel temperature:	
Capsule GA-309-7	1000°-1700°C, above 1400°C for 820 hr
Capsule GA-309-8	1200°-2050°C, above 1400°C for 1460 hr
Capsule GA-309-9	1250°-1600°C, above 1400°C for 1210 hr
Flux	Thermal perturbed, 4.0 to 4.8×10^{13} neutrons/cm^3-sec
Exposure:	
Thermal	3.9 to 4.7×10^{20} nvt
Fast	2.6 to 3.1×10^{19} nvt
Burnup:	
U^{235}	20%-24%
Metal (Th + U)	6%-7%
Fissions/cm^3	8.2×10^{19}

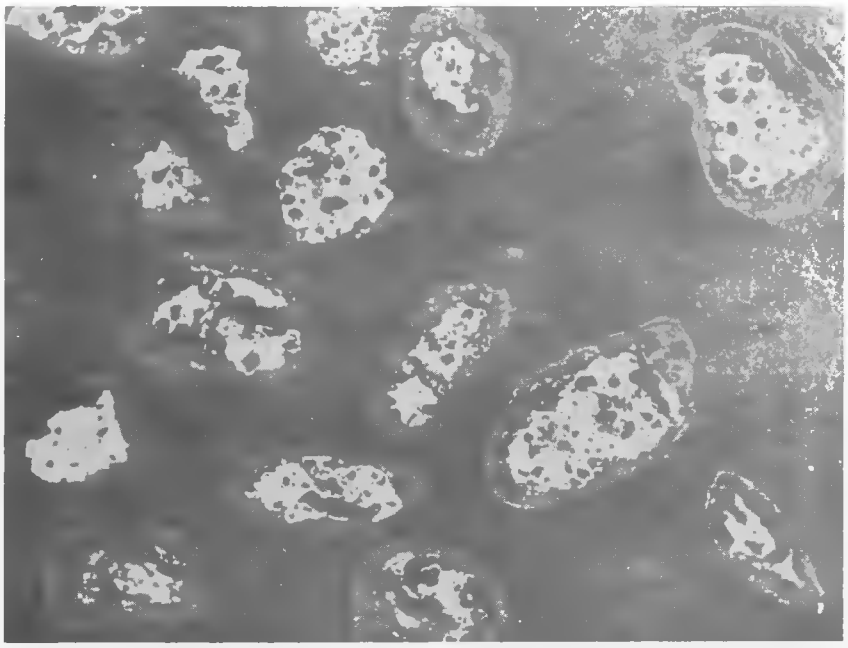

(75×)

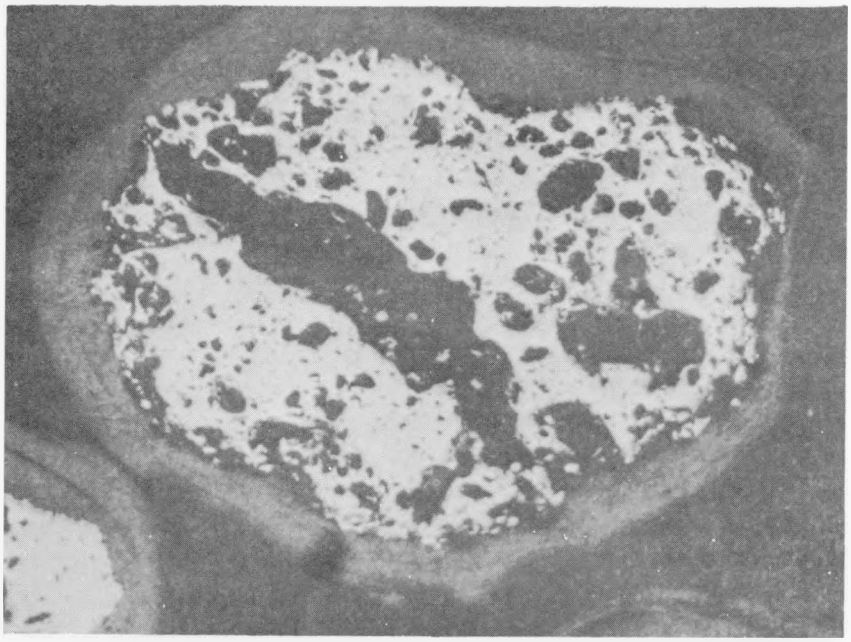

(250×)

Fig. 42--Pyrolytic-carbon coated (Th, U)C_2 fuel particles prepared for GA-309-4, -5, and -6 capsule irradiations; coatings deposited from acetylene at 1400°C

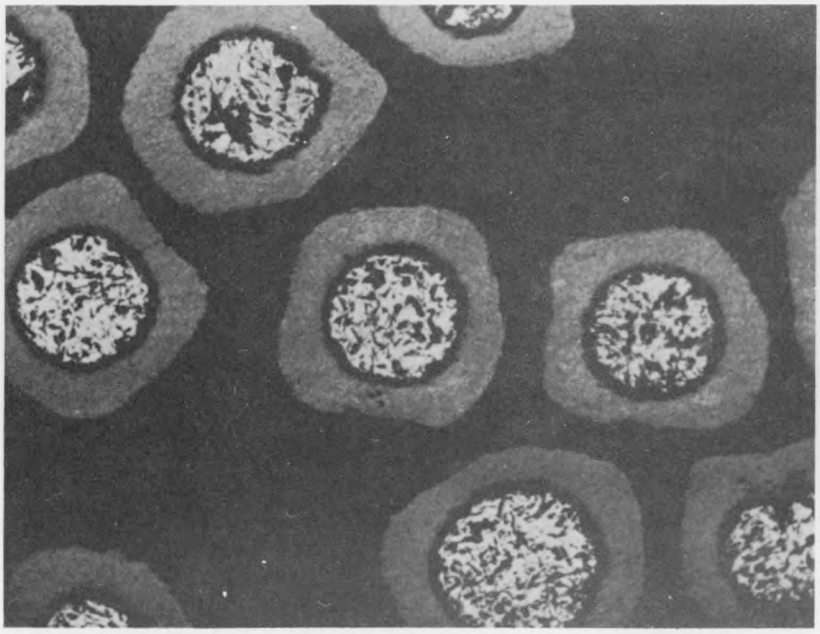

(75×)

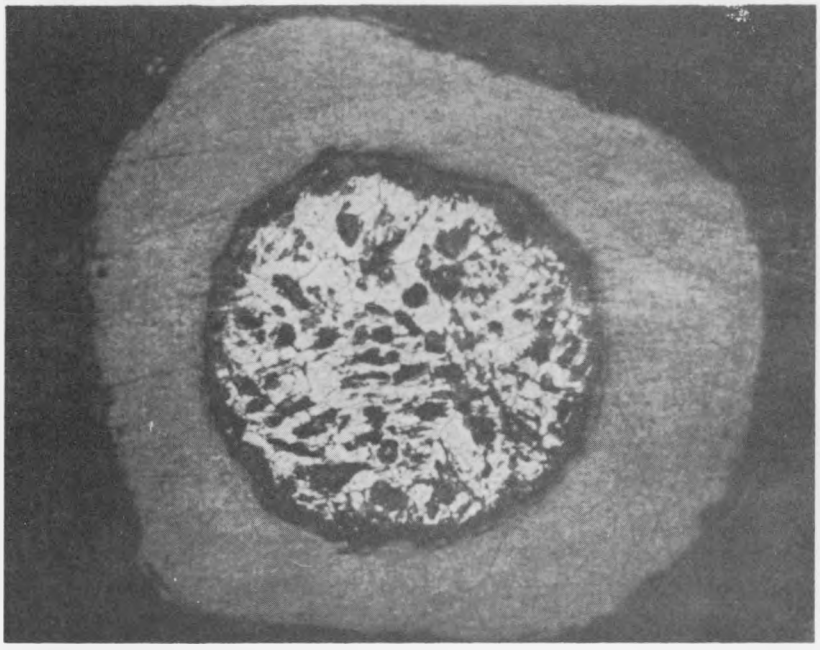

(200×)

Fig. 43--Pyrolytic-carbon-coated (Th, U)C_2 fuel particles prepared for irradiation of capsule GA-309-9; coating was deposited from acetylene at 1400°C

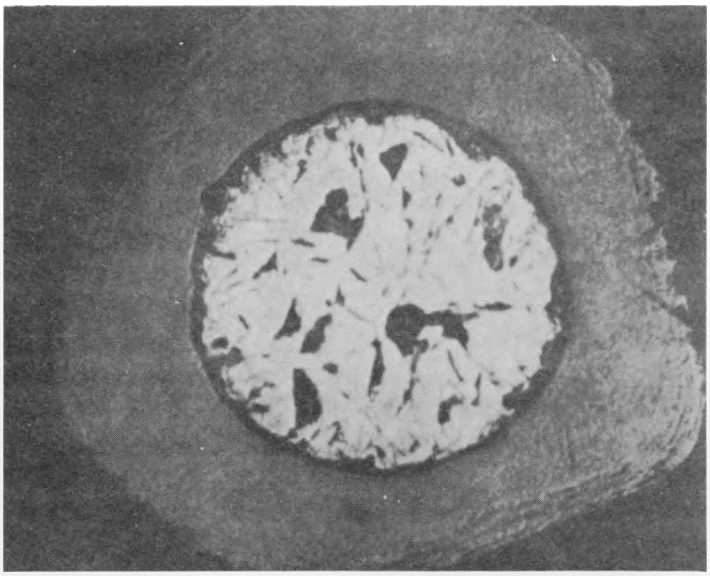

(210×)

Fig. 44--Pyrolytic-carbon-coated (Th, U)C_2 fuel particle typical of those prepared for irradiation of capsule GA-309-8; coating was deposited from methane at 1400°C

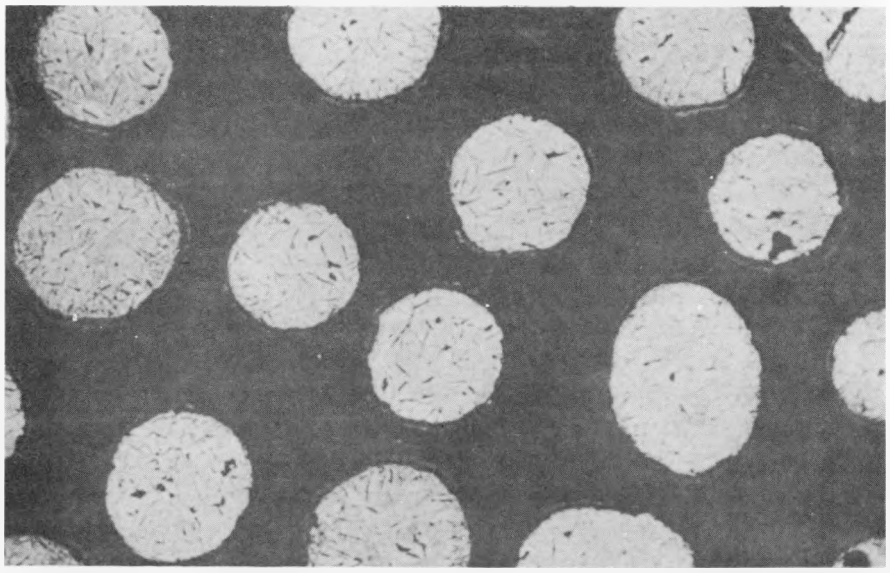

(75×)

Fig. 45--Thinly coated (Th, U)C_2 fuel particles prepared for irradiation of capsule GA-309-7; 10-μ coating deposited from acetylene at 1400°C

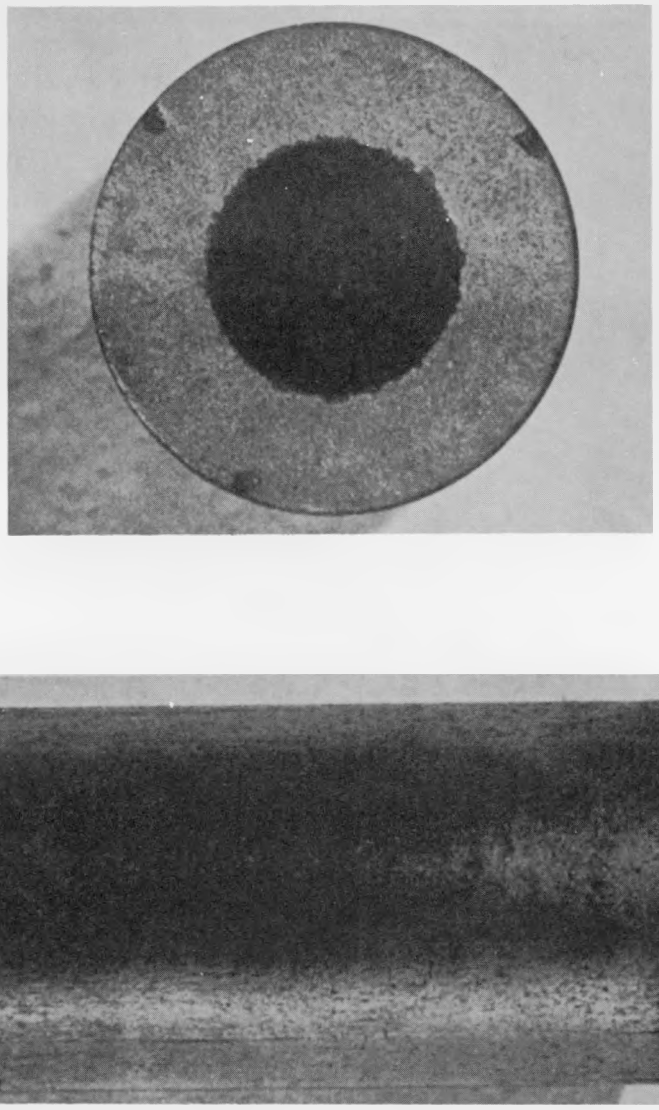

Fig. 46--Fuel compacts containing pyrolytic-carbon-coated $(Th,U)C_2$ fuel particles typical of those prepared for the GA-309-4, -5, and -6 and GA-309-7, -8, and -9 capsule irradiations

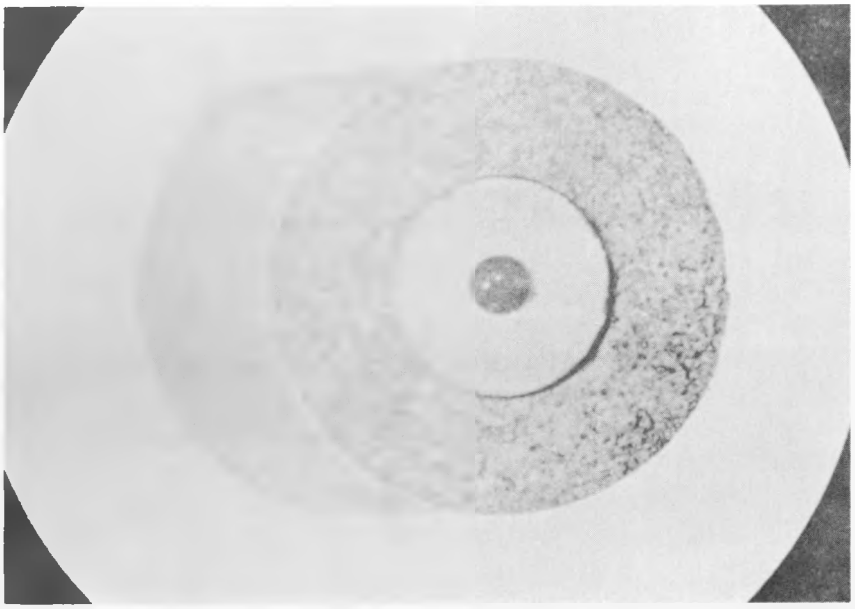

(2.25×)

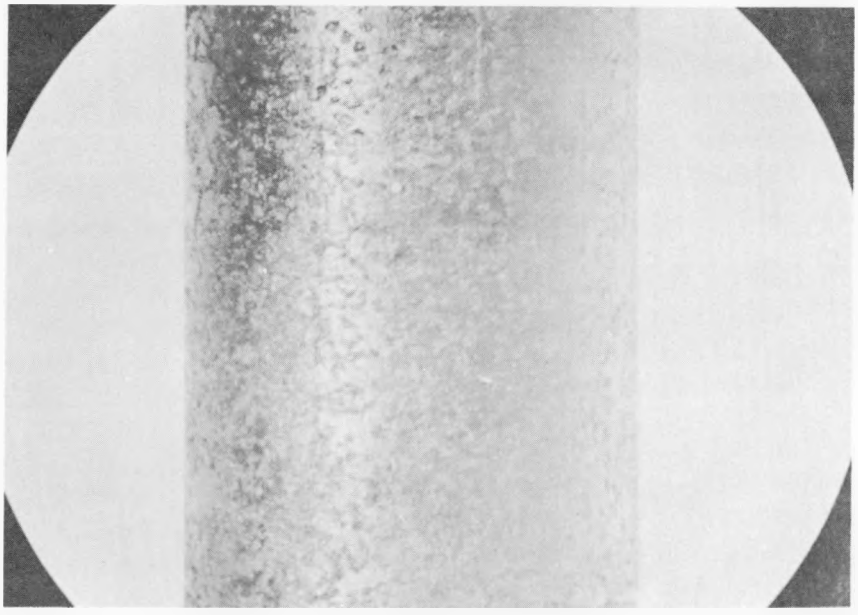

(2.25×)

Fig. 47--End and side views of fuel compact from capsule GA-309-5

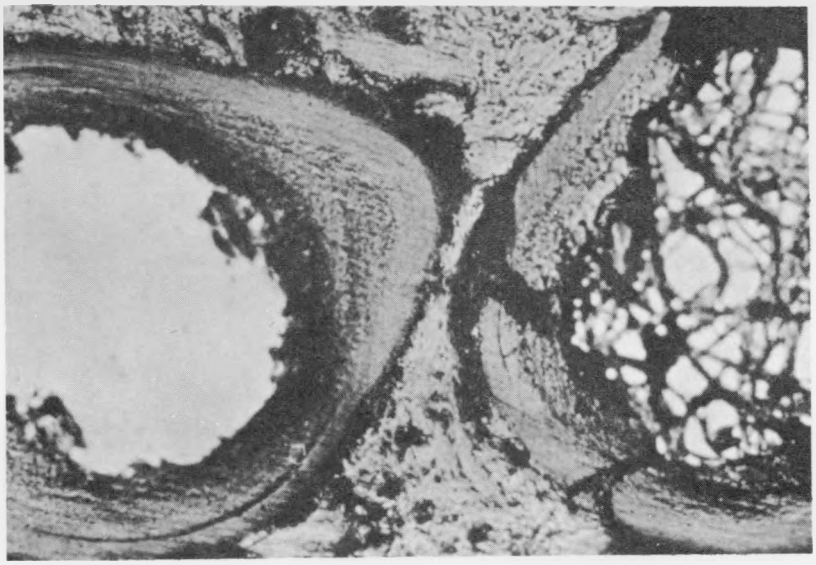

Fig. 48--Broken and intact fuel-particle coatings from capsule GA-309-4

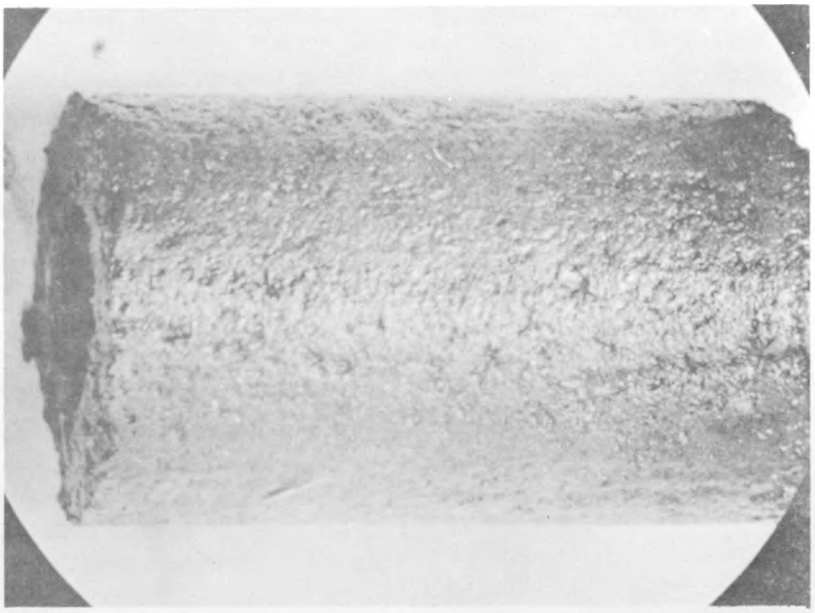

(2.25×)

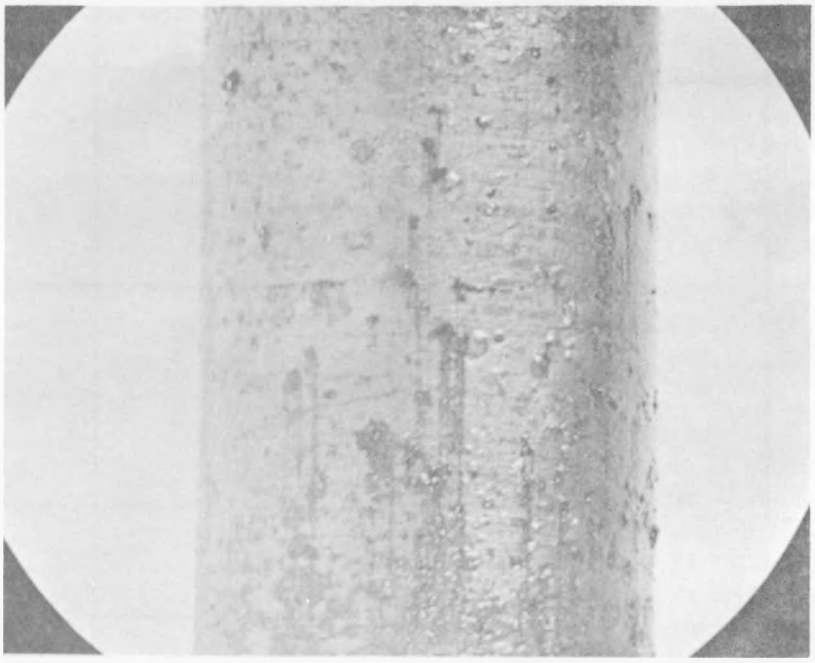

(2.25×)

Fig. 49--Fuel compacts from capsules GA-309-8 (top) and GA-309-9 (bottom); surface roughness is primarily due to hydrolysis of (Th, U)C_2 particles with broken coatings during hot-cell examination

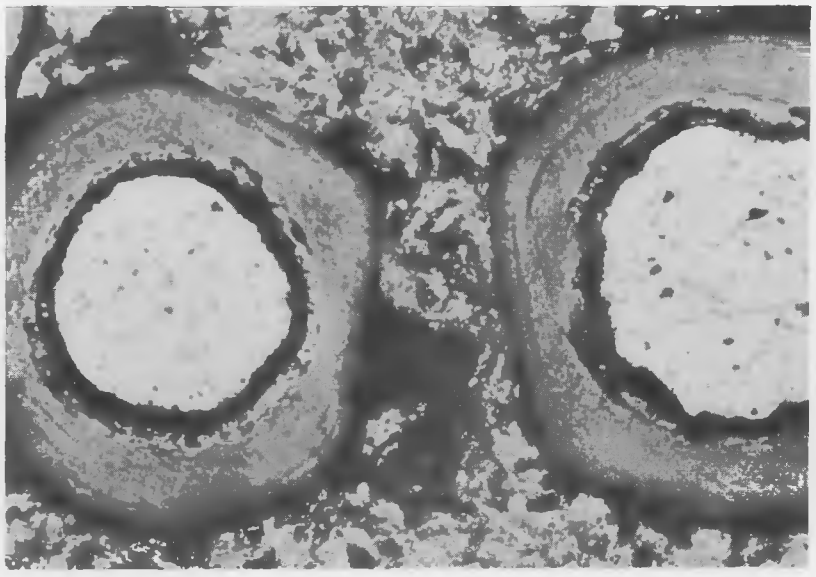

(100×)

Fig. 50--Fuel particles in capsule GA-309-8

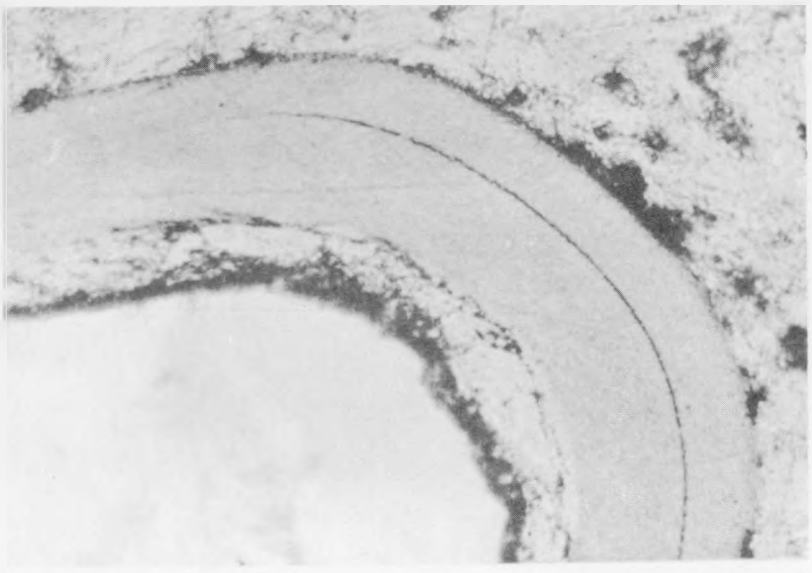

(500×)

Fig. 51--Portion of coated particles from capsule GA-309-8 showing matrix-coating and coating-particle interfaces

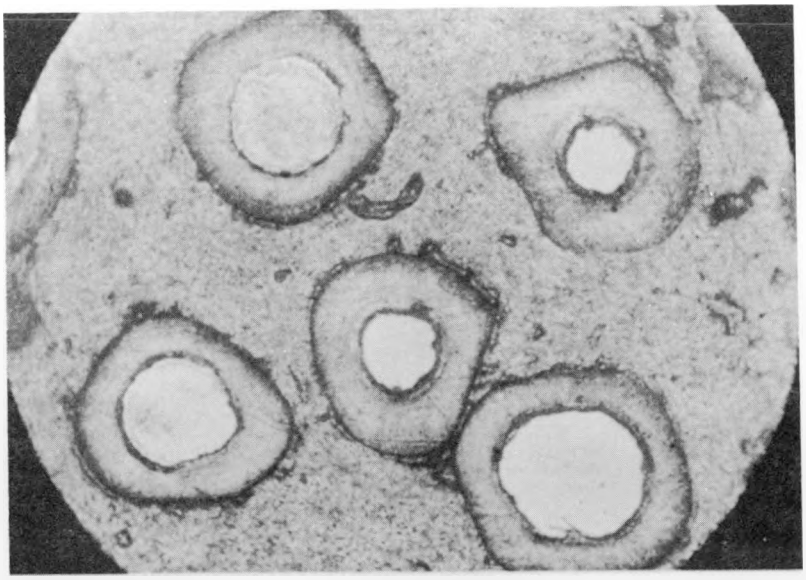

(100×)

Fig. 52--Fuel particles in capsule GA-309-9

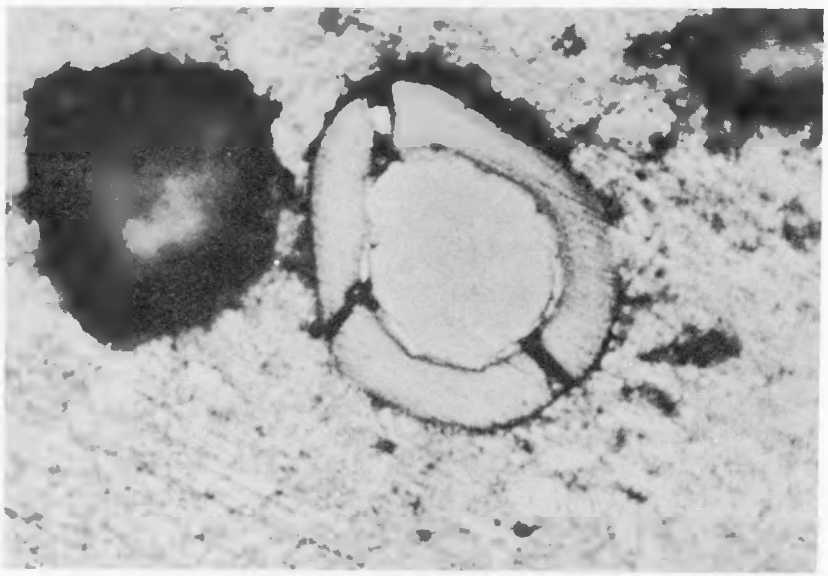

(200×)

Fig. 53--Fuel particle with broken coating from capsule GA-309-9

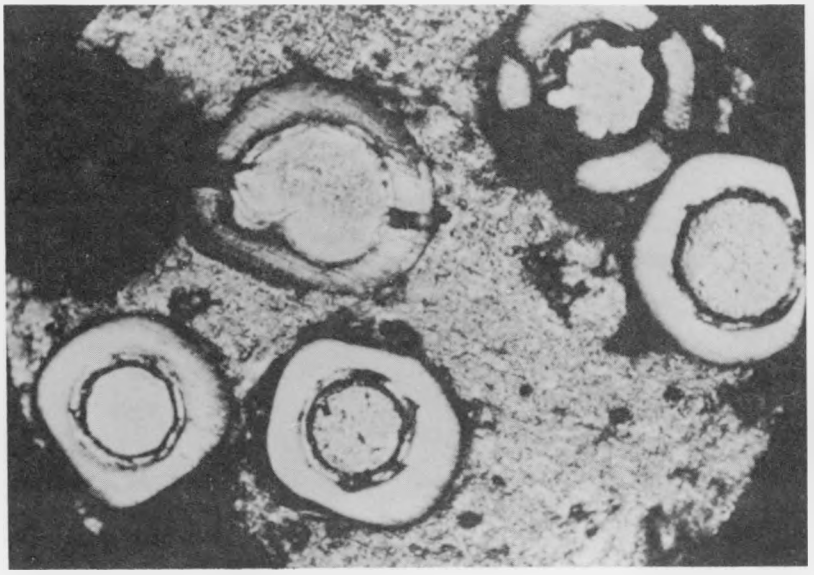

(100×)

Fig. 54--Group of fuel particles with intact and broken coatings from capsule GA-309-9

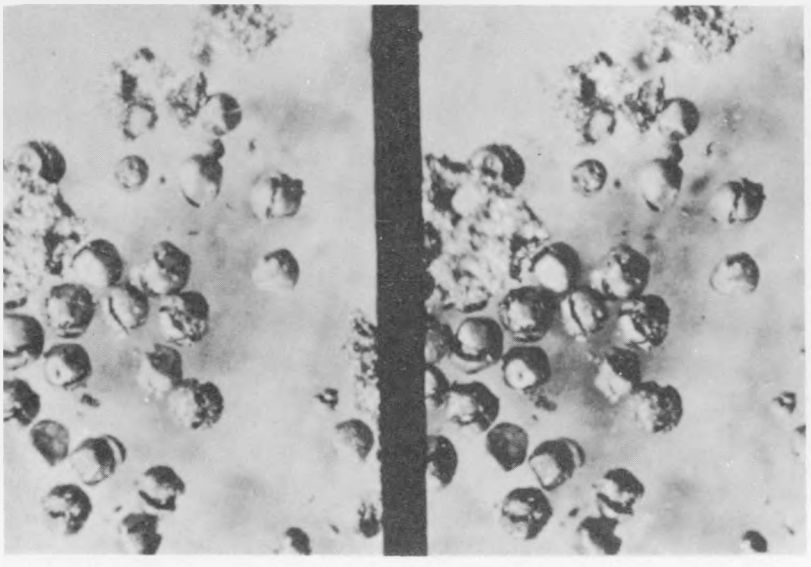

(21×)

Fig. 55--Stereo-photograph of fuel particles with broken coatings, removed from end of capsule

the "onion-ring," or layered, structure of the pyrolytic-carbon coating. Tests were conducted to see if this could have been caused by the nitric acid electrolysis used to separate the particles from the compact.

One of the spare compacts that had been prepared for the capsule irradiations was electrolyzed to recover the coated fuel particles. These particles, along with a control group of coated particles from the same lot that had not been incorporated into a fuel compact, were subjected to thermal treatments. Metallography and acid leaching were performed on the particles before and after (1) thermal cycling ten times to 2000°C and (2) thermal annealing for 24 hr at 1900°C.

No significant differences were observed between the two samples, and no exfoliation or other coating damage was noticed. This indicates that acid electrolysis alone is not detrimental to the thermal stability of the coated particles. One question remains unanswered: Are irradiated particles more susceptible to damage by acid electrolysis? Additional tests will have to be made to answer this question.

Metallographic examination of the compact from capsule GA-309-7 (10 μ original coating) revealed very few intact particles. However, the ones that were intact looked quite good. The carbide particles were still dense and appeared to be spherical.

No "amoeba effect" was observed on the irradiated samples from the GA-309 series capsules.

ACKNOWLEDGMENTS

A great many people at General Atomic have taken part in these fuel-development studies. In particular, I would like to acknowledge the contributions of the following individuals: H. E. Shoemaker and J. H. Thompson (carbide fuel particles); G. B. Engle and C. S. Luby (pyrolytic-carbon coating of particles); R. J. Pyle, J. Pontelandolfo, E. Shoffner, and J. Bowden (graphite-matrix fuel compacts); H. K. Lonsdale and P. R. Macy (thermal stability testing); W. W. Godsin, R. A. Meyer, J. H. Sleigh, and F. Brown (radiation testing); A. Mosen (analytical chemistry); and D. Menken and J. Furth (metallography). I would also like to express my appreciation to W. P. Wallace, under whose direction many of the materials studies for the Peach Bottom HTGR were conducted, and to R. A. Meyer for helpful discussions during these programs.

Appendix

GENERAL ATOMIC REPORTS DEALING WITH COATED-PARTICLE FUELS AND GRAPHITE-MATRIX FUEL COMPACTS

1. GA-1235, 40-Mw(e) Prototype High-temperature Gas-cooled Reactor Research and Development Program, Quarterly Progress Report for the Period Ending December 31, 1959.
2. GA-1378, ibid., Quarterly Progress Report for the Period Ending March 31, 1960.
3. GA-1640, ibid., Quarterly Progress Report for the Period Ending June 30, 1960.
4. GA-1774, ibid., Quarterly Progress Report for the Period Ending September 30, 1960.
5. GA-1982, ibid., Quarterly Progress Report for the Period Ending December 31, 1960.
6. GA-2204, ibid., Quarterly Progress Report for the Period Ending March 31, 1961.
7. GA-2493, ibid., Quarterly Progress Report for the Period Ending June 30, 1961.
8. GA-2747, ibid., Quarterly Progress Report for the Period Ending September 30, 1961.
9. GA-2861, ibid., Quarterly Progress Report for the Period Ending December 31, 1961.
10. Anderson, E. E., P. E. Gethard, and L. R. Zumwalt, Recent Data Obtained on Fission Products Released from (Th, U)C_2-Particle-Graphite Fuels, GA-3119, May, 1962.
11. Anderson, E. E., P. E. Gethard, and L. R. Zumwalt, Steady-state Release Fraction of Krypton and Xenon Fission Products at High Temperatures from (U, Th)C_2-Graphite Fuel Matrix in Out-of-Pile Experiments, GA-3211, June, 1962.
12. Engle, G. B., Metallography of Carbide Fuel Compounds, GA-2067, March, 1961.
13. Engle, G. B., Development of Carbon-coating Process for (Th, U)C_2 Fuel Particles, GA-2301, October, 1961.

14. Engle, G. B., C. S. Luby, and J. C. Bokros, Evaluation of (Th, U)C_2, Carbon-coated (Th, U)C_2 Particles, and Carbon Coatings, GA-3067, April, 1962.

15. Goeddel, W. V., The Development and Evaluation of Graphite-matrix Fuel Compacts for the HTGR, GA-2289, August, 1961.

16. Goeddel, W. V., G. R. Tully, Jr., and R. A. Meyer, The Use of Graphite in High-temperature Nuclear Fuel Elements, GA-2304, September, 1961.

17. Goeddel, W. V., Summary of Coated-particle-fuels Development at General Atomic for the Period October, 1961, to April, 1962, GA-3109, April, 1962.

18. Goeddel, W. V., Procedures for the Preparation of Graphite-matrix Fuel Compacts Containing Pyrolytic Carbon Coated (Th, U)C_2 Fuel Particles, GAMD-2221, April, 1961.

19. Goeddel, W. V., Thermal Stability Testing of Graphite-matrix Fuel Compacts Containing Pyrolytic-carbon Coated Carbide Particles with Comments on the Amoeba Effect, GAMD-2675, September, 1961.

20. Goeddel, W. V., Coated Fuels Irradiation Tests, A Materials Summary, GAMD-2729, October, 1961.

21. Goeddel, W. V. (ed.), Coated Fuel Particle Newsletter, Part 1, GAMD-2646, April-June, 1961

22. Ibid., Part 2, July, 1961.

23. Ibid., Part 3, August-September, 1961.

24. Ibid., Part 4, October, 1961.

25. Ibid., Part 5, November, 1961.

26. Ibid., Part 6, October-December, 1961.

27, Ibid., Part 7, January, 1962.

28. Ibid., Part 8, February, 1962.

29. Ibid., Part 9, May-July, 1962.

30. Luby, C. S., Apparatus and Procedure for Coating Thorium-Uranium Carbides with Carbon at 1000° to 1400°C, GA-2241, May, 1961.

31. A Review of Fuel Element Research and Development for the High-temperature Helium Gas-cooled Reactors, GA-2283, June, 1961.

DISCUSSION

Question, C. W. Kuhlman (UNC): "What are the densities of the uranium carbide and the thorium-uranium carbide particles?"

Reply, W. V. Goeddel (GA): "The densities are about 95 per cent of theoretical when corrections are made for excess carbon."

Question, M. Lepie (Ray): "What is the temperature required to produce the eutectic uranium-thorium carbide particles?"

Reply, W. V. Goeddel (GA): "About 2500 C. The actual temperature depends on the proportions of ThC_2 plus UC_2."

Question, M. Lepie (Ray): "On melting of the UC_2, don't you get sticking of graphite to the particles? If you do, can you estimate the volume per cent of the graphite which adheres to the UC_2?"

Reply, W. V. Goeddel (GA): "Yes, but I don't know the percentage. It is a thin and adherent coating, and it doesn't come off in the coating reactor."

Question, J. R. Gough (DrgP): "What were the fuel processing losses, the amount of recycling, and the moisture content of the atmosphere?"

Reply, W. V. Goeddel (GA): "This is a laboratory process and we have not been primarily concerned with the yield. Some uranium did end up in the graphite flour used in the spheroidizing. No recycling was done. We have tried to maintain the moisture content of the atmosphere at about 50 ppm."

FISSION-PRODUCT RELEASE FROM $(Th,U)C_2$-GRAPHITE FUELS*

By L. R. Zumwalt, E. E. Anderson, and P. E. Gethard
John Jay Hopkins Laboratory for Pure and Applied Science
General Atomic Division of General Dynamics Corporation
San Diego 12, California

ABSTRACT

$(Th, U)C_2$ fuel particles coated with pyrolytic carbon had good xenon retention at first, but degradation occurred as high fuel burnup was achieved. Barium was found to permeate pyrolytic-carbon coatings which were impermeable to xenon, particularly at temperatures above 1400°C. Retention of iodine and tellurium by carbon coatings, although not quite as good as xenon retention, was much better than iodine and tellurium retention by uncoated $(Th, U)C_2$ particles.

In postirradiation annealing runs, the rate of release of Xe^{133} from coated and uncoated $(Th, U)C_2$ fuels was measured at 1000° to 1700°C. The release of Ba^{140}, Te^{132}, and I^{131} was also determined for lightly irradiated samples.

Xenon-133 release was interpreted in terms of the "equivalent spheres" approach. Release rates for short-half-life xenon predicted by this treatment are in approximate agreement with steady-state Xe^{138} and Xe^{139} release rates obtained out-of-pile for uncoated $(Th, U)C_2$ particles by using an electron linear accelerator to produce a steady rate of photofissions. Data for Kr^{85m}, Kr^{87}, Kr^{88}, and Kr^{89} were also obtained in these out-of-pile experiments.

In-pile experiments on samples of coated particles were performed to determine the effects of high fuel burnup and temperature on the retention of krypton and xenon fission-product nuclides.

Activation energies for release were found to be about 29 kcal/mole for krypton and 39 kcal/mole for xenon.

* This work was supported by the U. S. Atomic Energy Commission under Contract AT(04-3)-314.

INTRODUCTION

This paper is a review of studies made at General Atomic over a two-year period (1960-1962) of the fission-product-release characteristics of both pyrolytic-carbon-coated and uncoated (Th, U)C_2* particles. These nuclear-reactor fuel particles were in some cases dispersed in a graphite matrix and in other cases in the form of loose particles held in a porous graphite container. The size of the homogeneous (Th, U)C_2 particles (of irregular or spheroidal shape) was, in general, of the order of 200 μ, and the thickness of the pyrolytic-carbon (PyC) coatings was of the order of 50 μ.

A detailed account of the preparation of carbide–graphite-matrix fuel bodies, the coating of particles, and the testing of these fuel materials is presented in a companion paper, "Pyrolytic-carbon-coated Carbide Fuel Particles and Their Use in Graphite-matrix Fuel Compacts," (GA-3588) edited by Walter V. Goeddel.

It is to be noted that in General Atomic's initial studies of dispersion-type (Th, U)C_2–graphite fuel bodies for the Peach Bottom High-temperature Gas-cooled Reactor (HTGR),[1] the fission-product-release behavior of uncoated particles was investigated. Subsequently, PyC coatings were found, in general, to substantially decrease fission-product release as determined by laboratory and in-pile experiments.[2]

Much of the data presented in this paper has been given previously in HTGR progress reports.[2] However, this is the first time that studies of the fission-product release of fuels, tested in the course of the development of the Peach Bottom HTGR, have been reviewed. Results obtained on uncoated-(Th, U)C_2-particle fuel materials in the course of this work are considered pertinent to coated-particle fuels, because of the likelihood that the fission-product-release behavior of the uncoated materials approximates that of related coated-particle fuels where radiation or thermal effects have caused coatings to be severely damaged. Accordingly, considerable data from out-of-pile studies of uncoated (Th, U)C_2 particles is presented.

*The formula (Th, U)C_2 is used to signify a solid-solution (Th, U), single-phase carbide with approximately two carbon atoms per metal atom.

OUT-OF-PILE EXPERIMENTS

EXPERIMENTAL PROCEDURES

In out-of-pile studies of the fission-product-release behavior of various (Th, U)C_2 fuel materials, helium-purged, graphite-tube resistance furnaces were used. These furnaces are adaptations[3] of the type of electric furnace first developed by King[4] for spectroscopic investigations. They are particularly suitable for the study of carbide-graphite fuel bodies such as those designed for the HTGR, owing to the fact that the graphite-tube heater element in which samples are placed and the helium atmosphere employed closely simulate the physical and chemical environment of the actual reactor. These furnaces require little insulation (only graphite and tantalum radiation shields are used), so outgassing is minimized and the furnaces may be brought to a given temperature very quickly. Thus, with preliminary outgassing under vacuum (about 30 min at 1000°C), the furnaces can be brought to operating temperatures of 2000°C in 1 min and 3000°C in 3 min. Furthermore, the King furnace can be readily adapted so the graphite tube serves as a conduit to permit helium gas (about 1 liter/min) to sweep past the sample and carry volatile fission products to a cold finger within the furnace and xenon and krypton to activated-charcoal cold traps and associated radiation-detection equipment located at a considerable distance from the furnace. Figures 1 and 2 show the graphite heater tube, water-cooled copper electrodes, and graphite radiation shields of King furnace I. Figure 3 is a view of King furnace III with the water-cooled gas-containment (or vacuum-containment) dome raised. This furnace was designed for heating samples in runs of many hours' duration at temperatures up to 3000°C. Accordingly, it was constructed with a water-cooled copper heat sink supported over the base-plate, a double-walled water-cooled dome, and well-cooled copper electrodes (so epoxy-resin insulators passing through the base-plate would not overheat).

Many of the annealing experiments involved the determination of the fraction, ϕ_{Xe}, of Xe^{133} retained as a function of time from fuel materials lightly irradiated in General Atomic's TRIGA research reactor (10^{13} to 10^{14} fissions per sample). To let short-lived activities decay out, the experiment was usually carried out around five days after the irradiation. More recently, the release of Ba^{140}, I^{131}, and Te^{132} has been determined by measuring collected activities with the aid of a multichannel gamma-ray spectrometer. The barium activity is collected on a nest of four 1/16-in.-thick, concentric graphite sleeves placed around the sample, while the iodine and tellurium activities are collected on the copper-plated end of a

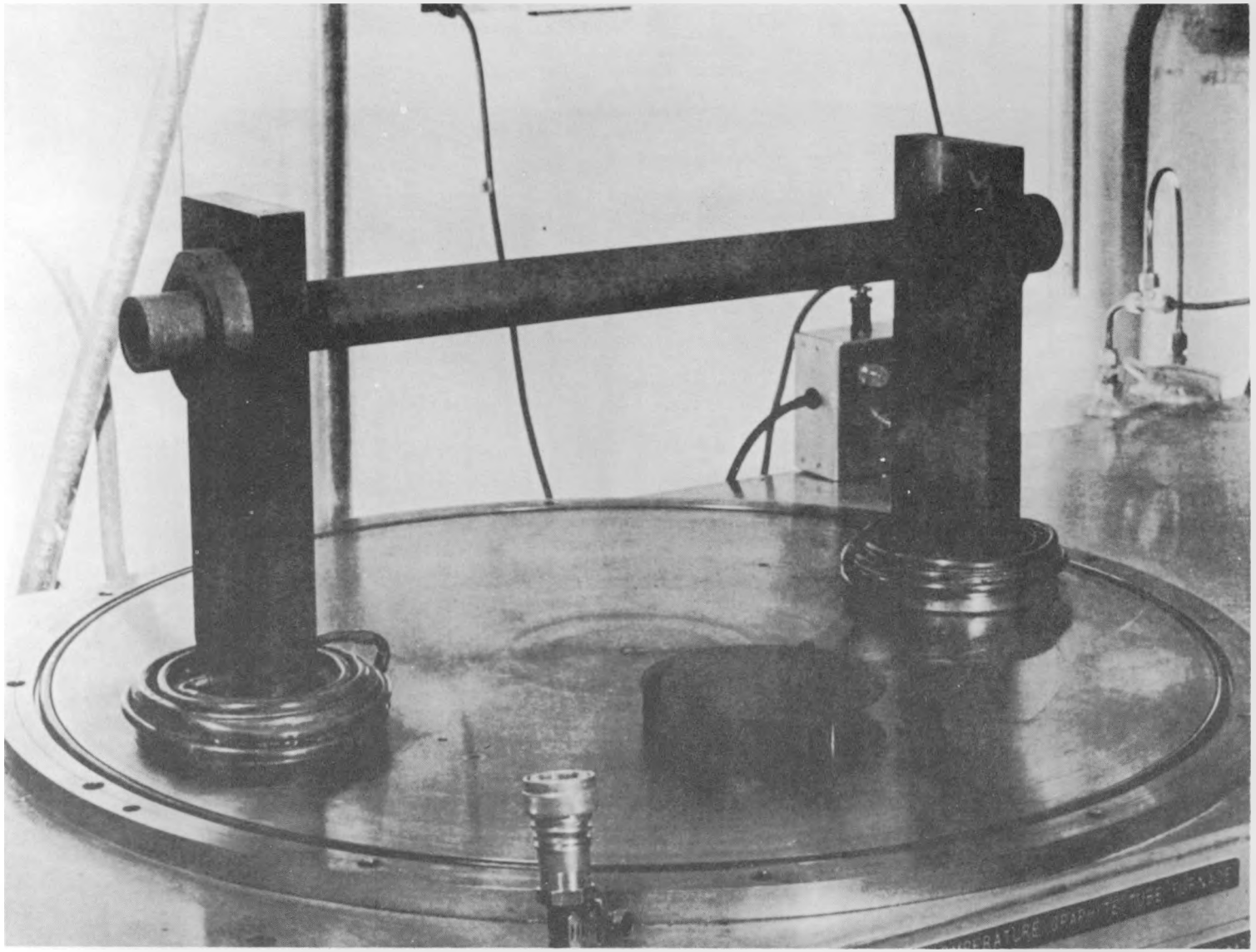

Fig. 1--King furnace I with dome raised, showing graphite heating element (radiation shielding removed)

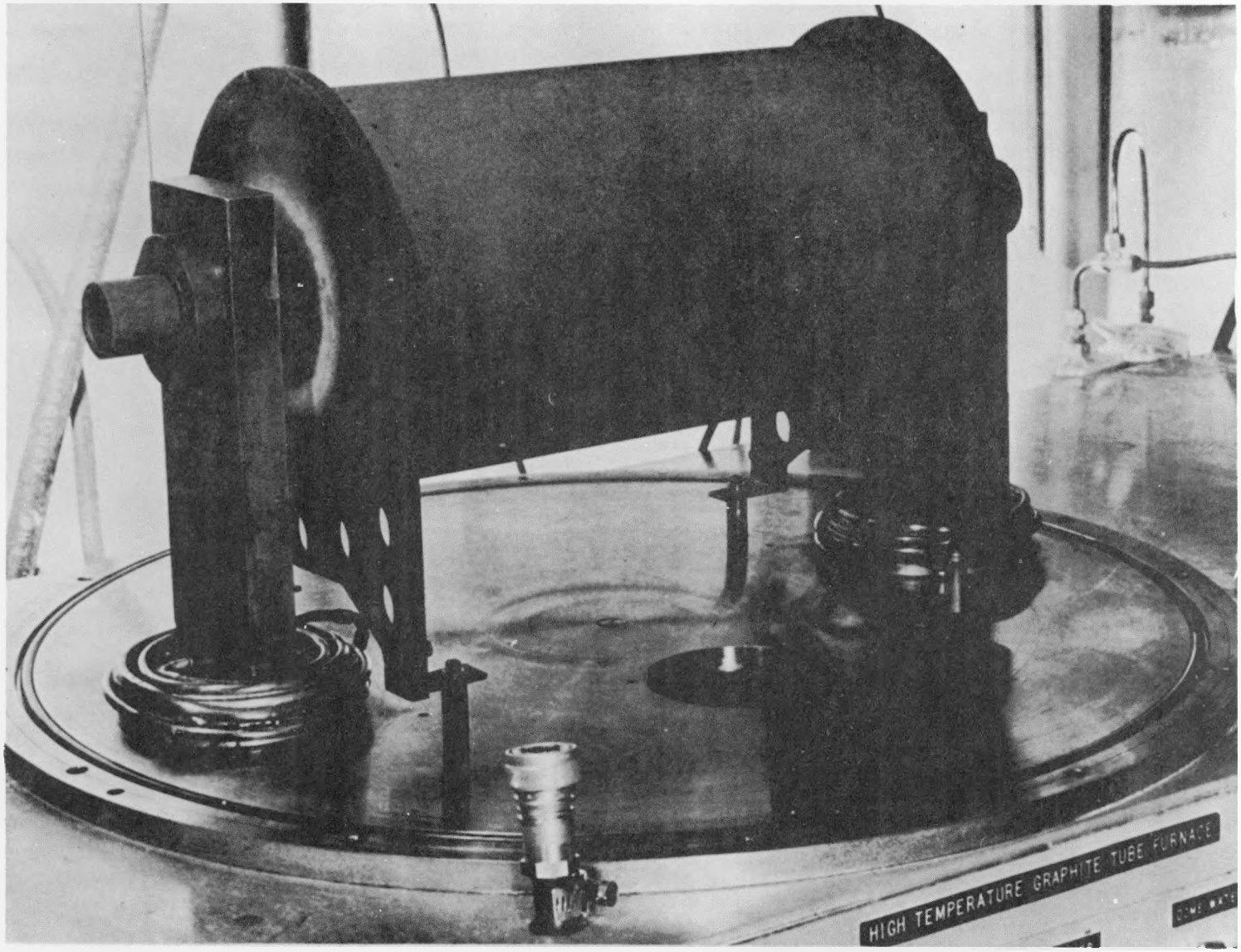

Fig. 2--King furnace I with radiation shielding in place

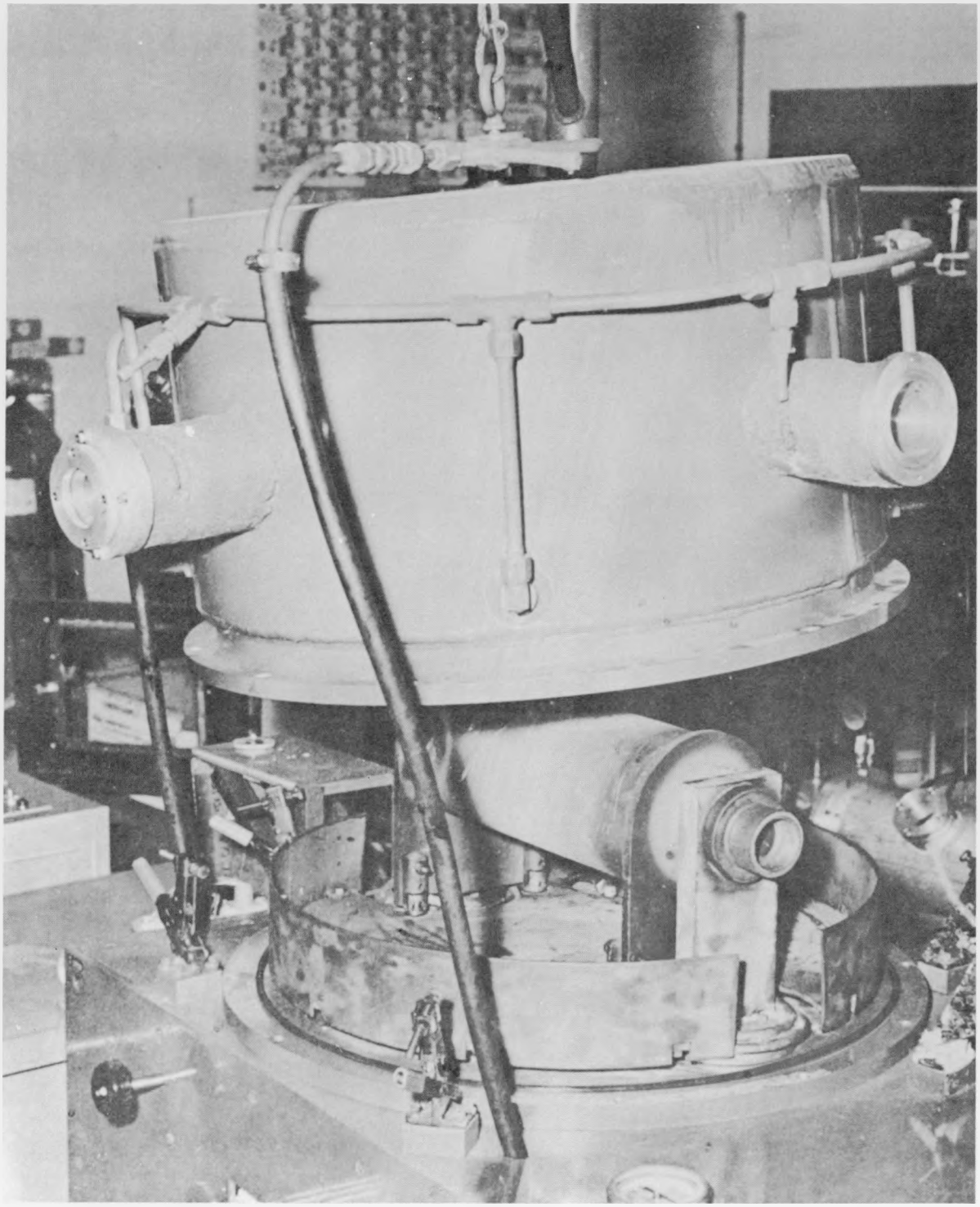

Fig. 3--King furnace III with dome raised to show water-cooled copper heat sink supported over base-plate

stainless steel, water-cooled cold finger located centrally in the graphite heater tube about 2 in. downstream of the sample. In addition, high-burnup experiments have been carried out on a small quantity of pyrolytic-carbon-coated (Th, U)C_2 (Th:U^{235} = 2.25:1) particles, centrally disposed in a graphite-matrix fuel compact 1 in. in diameter by 1 in. long. These particles were irradiated to a fission-to-metal ratio approximately equivalent to full burnup in the HTGR. In this case, the fraction of activity released, ϕ, was determined for both Xe^{133} and Kr^{85} as a function of time.

In these annealing experiments, the activity of Xe^{133} (and Kr^{85}, when present) collected on a liquid-nitrogen-cooled charcoal trap is continuously monitored with a single-channel gamma-ray spectrometer. The fractional release of Xe^{133} can be determined by driving off all the Xe^{133} at the end of a run by heating the sample to 2400°C or higher for a sufficiently long period (several hours may be required). Also, the number of fissions occurring in the sample can be estimated from a flux monitor and the U^{235} content, or by determining the La^{140} activity in the sample prior to annealing. The latter method is preferred. Other activities, such as Ba^{140}, I^{131}, and Te^{132}, are determined by counting activities collected on the cold finger or the graphite sleeves, using a multichannel gamma-ray spectrometer. Only one point or a very few points are obtained per experiment for the ϕ versus time curves of these activities. Radiochemical analysis of residual activities in the fuel bodies, such as Ba^{140}, may also be carried out at the end of a run to obtain ϕ values.

In the experiments on the steady-state release of shorter-lived krypton and xenon activities from uncoated-particle fuel bodies, the General Atomic electron linear accelerator (Linac) was used to generate photofission at a constant rate in samples heated in a King furnace. The furnace used, King II (see Fig. 4), was especially designed for remote operation and was provided with a tungsten target mounted in a re-entrant tube that fit into the front viewing port. With this arrangement, the electron beam could be brought with little scattering loss to the target located only 4 in. from the graphite heater tube. A cone of gamma rays (energy $\leq$ 20 Mev) passed through the tube and the fuel sample contained therein, causing photofission of the thorium and uranium in the sample. The details of this experiment have been reported elsewhere.[5] However, in brief, the release of Xe^{139}, Xe^{138}, Kr^{89}, Kr^{87}, Kr^{88}, and Kr^{85m} was determined by a direct-comparison technique wherein a (Th, U) stearate target (having thorium and uranium in the same ratio as in the fuel material) was used as a standard. This target was made about the same size as the fuel bodies and was placed in the furnace tube at the same position as the fuel samples, but was maintained at room temperature. It thereby served as a fission-product-release standard where F was known to be unity. This was possible owing to the high emanation power which the (Th, U) stearate diaplays for noble-gas fission products. Wahl[6] estimates a >99% escape

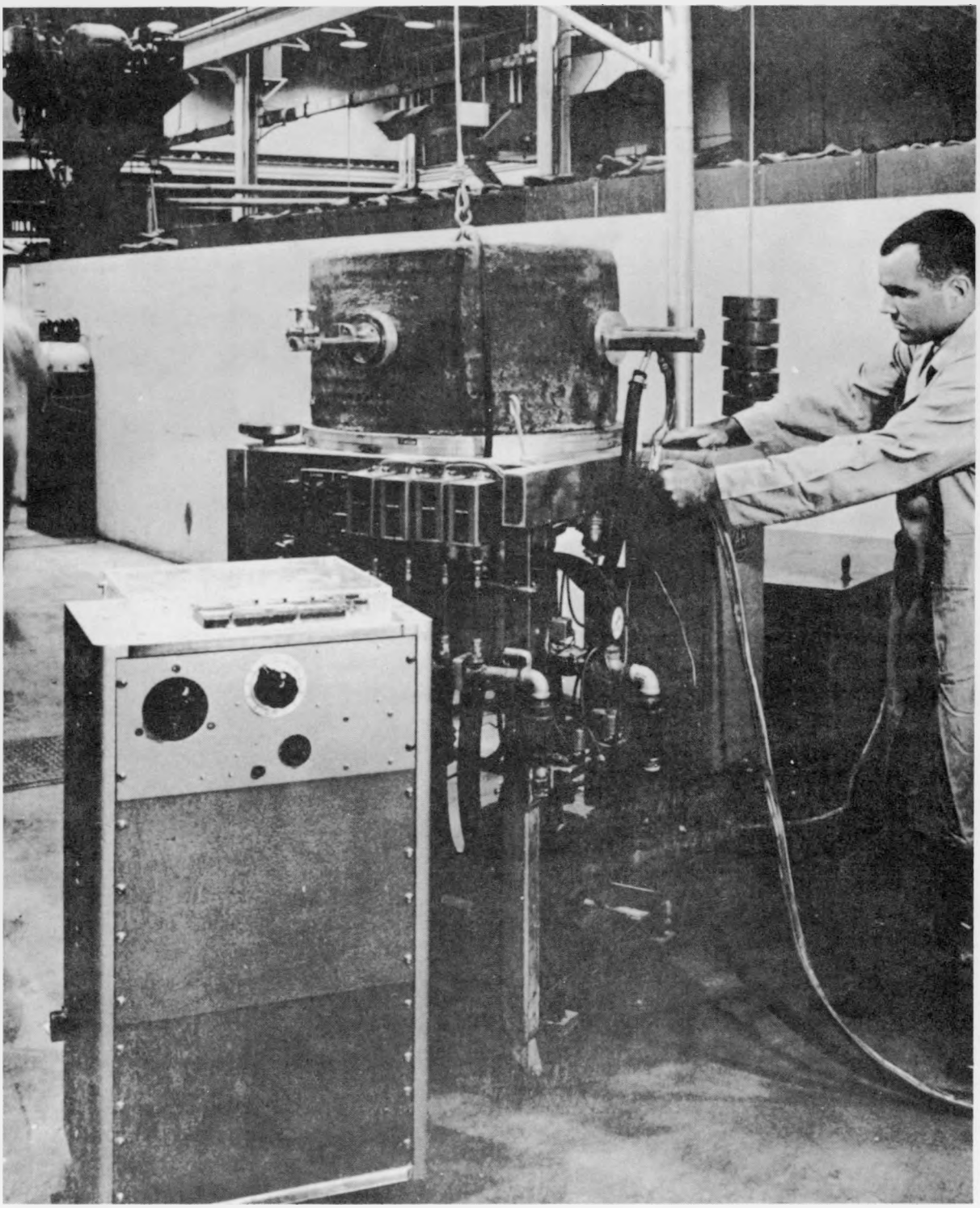

Fig. 4--King furnace II, for fission-product-release studies with the linear accelerator; the beam tube protrudes from the dome above the operator's hands

from barium stearate (uranium and other stearates behave similarly) in the case of krypton and xenon isotopes with half lives $\geq$ 4 sec.

For a given set of experiments, the fuel bodies were brought to temperature and irradiated for 1 hr in a steady beam of gamma rays. The (Th, U)-stearate reference target was irradiated in exactly the same manner. The delays between counting various nuclides, the counting times, and the counting efficiencies were the same for all runs.

RESULTS FOR UNCOATED-PARTICLE FUEL MATERIALS

Xenon-133 Release in Annealing Experiments

Several series of annealing experiments have been carried out on lightly irradiated (10^{13} to 10^{14} total fissions) experimental fuel bodies consisting of uncoated (Th, U)C_2 particles in a graphite matrix. These fuel bodies were usually 1 in. in diameter by 1 in. long. A photomicrograph of this type of fuel material is shown in Fig. 5. Isotherms for Xe^{133} release (plots of fraction retained versus time at a given temperature) showed quite a variation. It was found that care was necessary to avoid oxidation and hydrolysis of the very reactive (Th, U)C_2. Figure 6 shows isotherms from two series (A and B) which indicate the difference in data obtained in annealing experiments where care had been taken to obtain reproducibility. However, the effects of differences in material and difficulties in experimental technique cannot be entirely excluded.

Experiments were carried out to determine if the size of the (Th, U)C_2-particle–graphite-matrix fuel body had a significant effect on Xe^{133} release. In a number of cases, the release from a fractured or crushed fuel body was compared with that from an intact body. No significant effect was found. This tends to indicate that in-pore diffusion in the graphite matrix was not rate-controlling in determining Xe^{133} release.

In general, a "burst" effect was shown by Xe^{133}. Thus, the release of xenon appeared to consist of a "fast"-diffusion followed by a slow-diffusion process. Some of the fast diffusion may be due to the release of Xe^{133} atoms which are descendants of the 133 chain precursors that have recoiled from the (Th, U)C_2 particles into surrounding grains of the graphite matrix. In this case, diffusion of Xe^{133} out of these graphite grains to the pores of the fuel material would be the rate-controlling step for release. However, with 200-μ particles, only a few per cent of the fission products recoil out of the particles. The rest of the fission products are deposited in carbide crystallites or grains and have to diffuse through the grains to grain boundaries and then outside of the carbide particles before they reach the relatively porous structure of the graphite matrix.

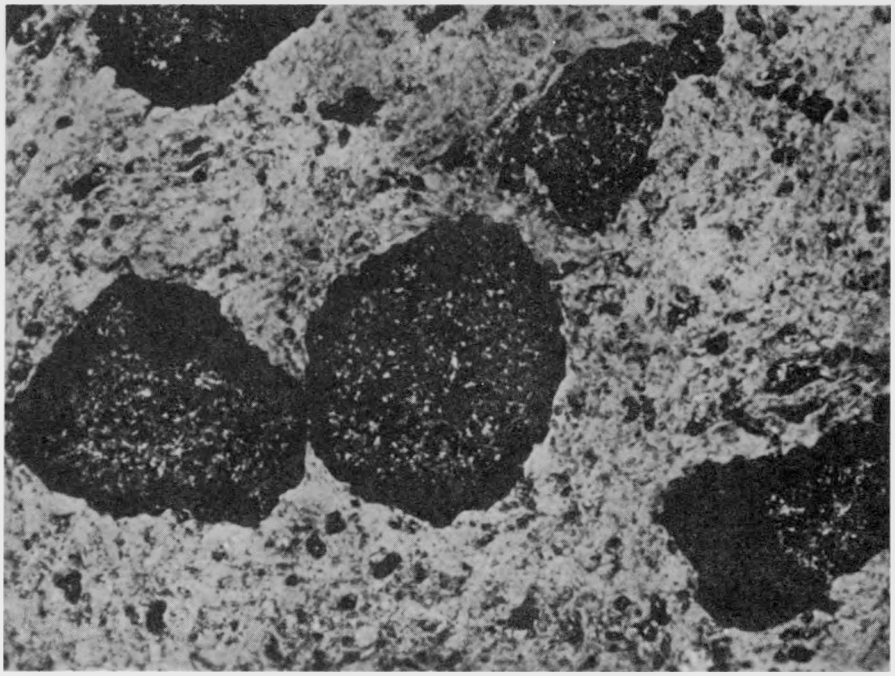

(150×)

Fig. 5--Photomicrograph of a fuel compact comprised of uncoated (Th, U)C_2 particles in a graphite matrix

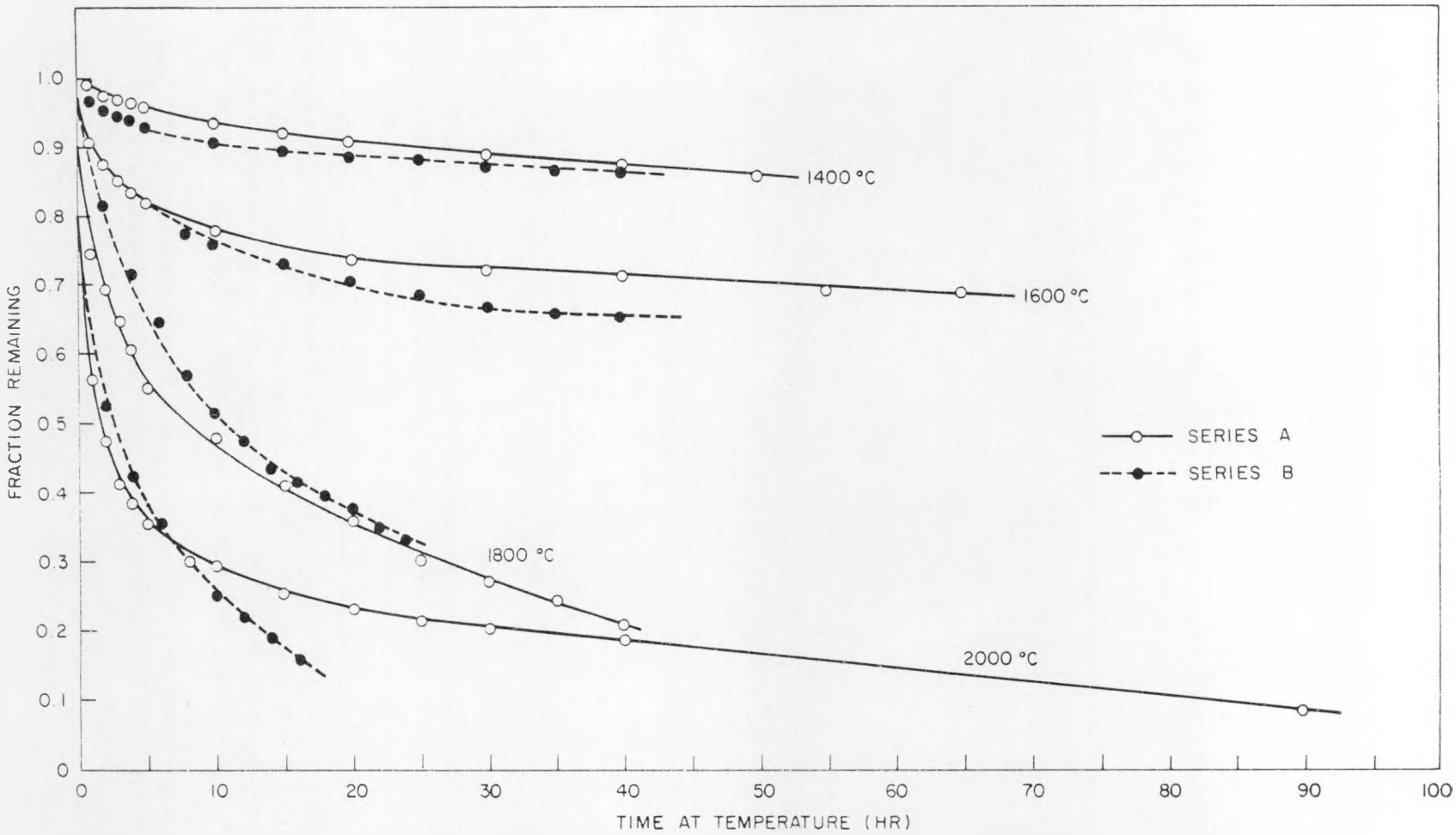

Fig. 6--Release from uncoated-particle compacts (series A and B)

It was initially postulated that for volatile species, and particularly krypton and xenon, the diffusion of fission products out of the carbide crystallites or grains plus diffusion of a small per cent of the recoiled fission products from graphite grains are the rate-limiting processes for release. In accordance with this, it has been assumed that release can be approximately represented as diffusion from a number of kinds of spherical grains (differing in size and/or material). Then the fractions, $\phi(t)$, of a volatile fission product retained at time t can be represented by

$$\phi(t) = \sum_{i=1}^{n} c_1 \mathcal{F} \frac{t}{\tau_i} \quad , \tag{1}$$

where

$$\sum c_i = 1 \tag{1a}$$

and

$$\mathcal{F} \frac{t}{\tau_i} = \frac{6}{\pi^2} \sum_{m=1} \frac{1}{m^2} \exp\left(\frac{-m^2 \pi^2 t}{\tau_i}\right) \quad . \tag{1b}$$

Approximations (1c) and (1d) which follow are useful when $t/\tau \leq 1/\pi^2$ (as given by Booth and Rymer[7]) and when $t/\tau \geq 1/\pi^2$, respectively:

$$\mathcal{F} \frac{t}{\tau} = 1 - \frac{6}{\sqrt{\pi}} \sqrt{\frac{t}{\tau}} + 3\frac{t}{\tau} \quad , \tag{1c}$$

$$\mathcal{F} \frac{t}{\tau} = \frac{6}{\pi^2} \exp\left(\frac{-\pi^2 t}{\tau}\right) \quad . \tag{1d}$$

In the case of annealing experiments of 2 or 3 days' duration, an Xe^{133} release isotherm can be fairly well approximated by two components. Thus, for two series of experiments values for the fraction released, c_i, and the characteristic diffusion time, τ_i, were obtained (see Table 1) which reasonably fit the Xe^{133} release curves shown in Fig. 6.

It may be seen that the curves (and the parameters c_i and τ_i) for these two series agree only very roughly. This kind of agreement (or lack of it) has frequently been our experience in fission-product-release studies. One reason is that carbide-particle–graphite reactor fuel materials are not well defined or highly reproducible. Also, in the case of uncoated (Th, U)C_2 fuel material, oxidation and hydrolysis take place

Table 1

XENON-133 RELEASE DATA FROM UNCOATED-PARTICLE COMPACTS

Temp. (°C)	c_i		τ_i (hr)	
	Fast	Slow	Fast	Slow
Series A				
2000	0.30	0.70	1.15	160
1800	0.13	0.87	9.1	470
1600	0.24	0.76	8.8	24,000
1400	0.05	0.95	7.1	58,000
Series B				
2000	0.48	0.52	6.8	640
1800	0.14	0.14	1.5	410
1600	0.20	0.80	62	36,000
1400	0	1.00	---	25,000

readily in a slightly moist atmosphere. Thus, unless great care is taken, the fuel material will change upon standing or while being handled.

The fraction of the fast-diffusion component appears, in general, to increase with temperature. Also, an additional burst (fast-release component) of Xe^{133} appears upon increasing the temperature of samples which have been annealed long enough to show a slow-release component.

Such behavior has been observed in the study of the diffusion of Xe^{133} from uranium-impregnated graphite at high temperatures.[8] In this case, most of the xenon was escaping from graphite grains which had been penetrated by fission-recoil particles. Japanese workers[9] have recently studied this phenomenon and interpret the data as indicating that the xenon is captured at imperfections or sites with a considerable range of binding energies and the activation energy of diffusion shows a corresponding range of energies. Burst phenomena leading to anomalous intercepts for release factor versus square root of time (of annealing) curves have also been reported in studies of the diffusion of Xe^{133} from UO_2.[10]

Kelley has developed a theory for the diffusion of "attached" inert (noble) gas activity from oxide powders.[11] This theory, which gives, in agreement with experiment, a linear increase of fractional release with temperature, assumes a spectrum of activation energies lower than the activation energy for volume (bulk) diffusion. The "attached" atoms according to the theory do not undergo a random walk motion but a single

rate-controlling jump. It is of interest to speculate on whether the "burst" effect in the release of xenon, etc., from carbide fuel particles is of this nature (and thus not a true Fick's law diffusion phenomenon). More experiments must be performed to resolve this matter. In the meanwhile, we have tentatively treated fission-product-release data as though Fick's law applies to all diffusion components.

Accordingly, when Eqs. (1) through (1d) represent release in an isothermal annealing experiment on a fuel body, then at a constant fission rate, the steady-state-activity release fraction (R/B value) of nuclide j from the fuel body is given by

$$\left(\frac{R}{B}\right)_j = \frac{\text{activity outside of fuel body}}{\text{total activity}}$$

$$= \sum_{i=1}^{n} c_i \frac{3}{A_{ij}} \left(\coth A_{ij} - \frac{1}{A_{ij}}\right), \qquad (2)$$

where $A_{ij} = \sqrt{\tau_i \lambda_j}$ and λ_j is the radioactive decay constant of j.

The above formulae, (1) through (1d) and (2), correspond to considering the fuel-particle–graphite-matrix system as comprising an assemblage of n types of "equivalent spheres"[7] (each with a weighting factor, c_i) in which fission products are uniformly deposited and from which the fission products diffuse. Then,

$$\tau_i = \frac{a_i^2}{D_i}, \qquad (3)$$

where a_i is the radius of the equivalent sphere of type i and D_i is the diffusion coefficient for a sphere of type i.

This formulation is useful, although only an approximation, in that the characteristic diffusion times, τ_i, and the coefficients, c_i, may be extracted from annealing-data (ϕ versus t) curves by graphical analysis and values of $(R/B)_j$ calculated. The curves shown in Fig. 7 were calculated in this manner from the c_i and τ_i values of series-A Xe^{133} release data (given in Table 1). The observed values, which roughly fall on the curves, are release fractions (in per cent) determined for Xe^{139} and Xe^{138} in Linac experiments with King furnace II. The Linac experiments were carried out in such a way that only fast components (τ_i of the order of 1 hr) would have reached a steady state. Thus, the $(R/B)_j$ calculated from Eq. (2) should be greater than the observed values.

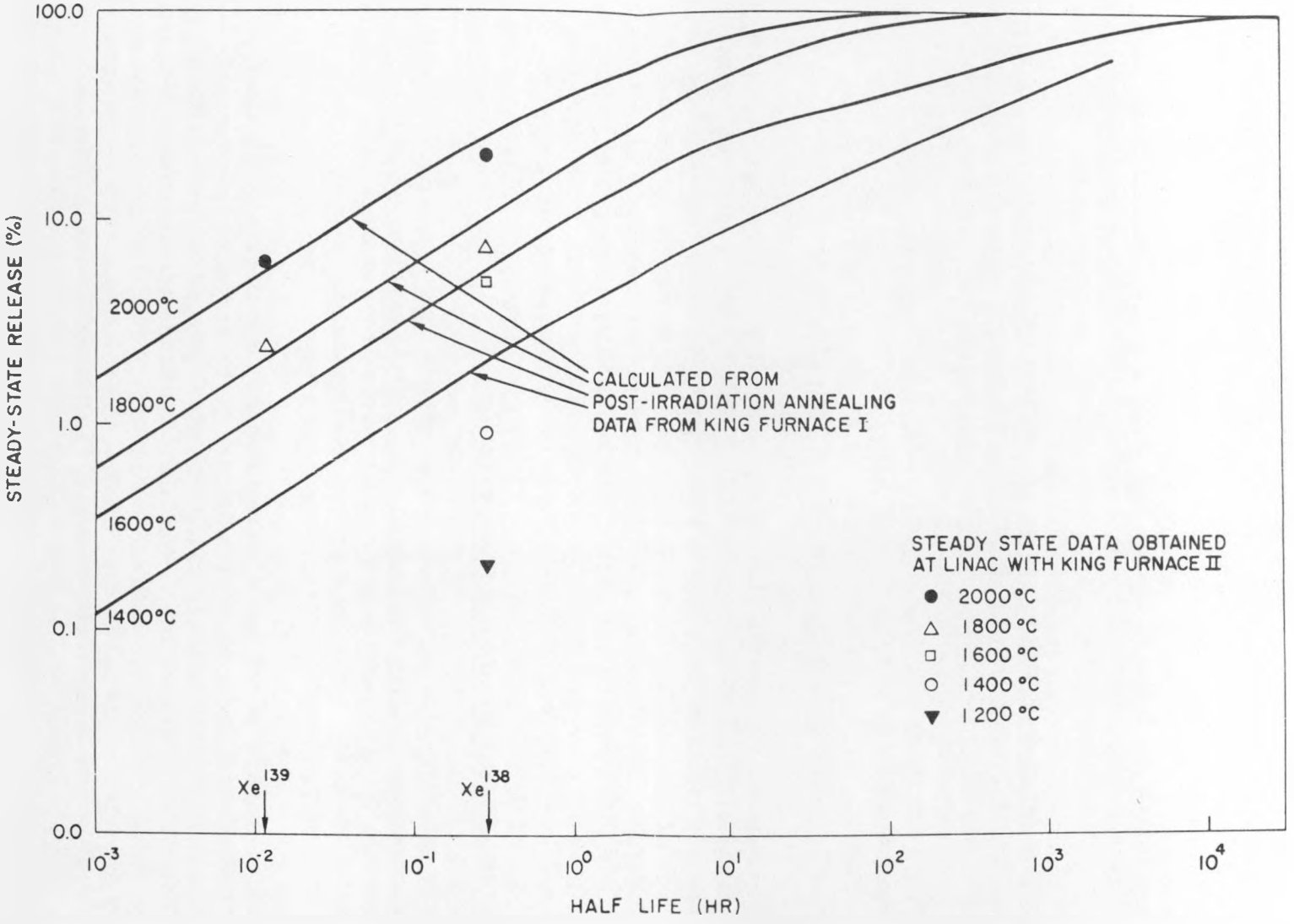

Fig. 7--Xenon release from uncoated (Th, U)C_2 particles in graphite-matrix fuel bodies

The slow component of release is most likely the one characteristic of diffusion out of the larger (Th, U)C_2 grains in which the fission products are lodged after recoil. From the various results for the slow component at 1400°C, we find that

$$D'_{Xe} = \frac{1}{\tau_{Xe}} \cong (1 \text{ to } 2) \times 10^{-8} \quad (\text{sec}^{-1})$$

If the radius (a) of the carbide grains are of the order of 10 μ,

$$D_{Xe} \cong (1 \text{ to } 2) \times 10^{-14} \quad (\text{cm}^2/\text{sec}) \ ,$$

and if the radius (a) is of the order of 30 μ,

$$D_{Xe} \cong (1 \text{ to } 2) \times 10^{-13} \quad (\text{cm}^2/\text{sec}) \ .$$

These grain sizes are guesses but seem reasonable on the basis of photomicrographs of polished sections of fuels. Thus, very roughly we estimate the diffusion coefficient of xenon in (Th, U)C_2 crystals at 1400°C to be 1×10^{-14} to 2×10^{-13} cm^2/sec. It is interesting to note that from the work of Cubicciotti,[8] one may estimate a diffusion coefficient of approximately 1×10^{-11} cm^2/sec at 1400°C for xenon in graphite grains. For the diffusion of xenon in fused UO_2, Booth and Rymer[7] found a diffusion coefficient of about 3×10^{-14} cm^2/sec at the above temperature.

Krypton and Xenon "Steady-state" Release

The determination of steady-state release fractions (R/B values) of the shorter-lived (a few minutes to a few hours) krypton and xenon fission products gives an indication of the effect of the more rapid diffusion components. Furthermore, data are obtained which may be directly applied to reactor engineering calculations.

Values of R/B which were obtained under conditions of a constant rate of photofission induced by gamma rays (1-hr period of irradiation) are given in Figs. 8 through 12, where they are plotted as the logarithm of per cent release versus the reciprocal of absolute temperature (°K). It is seen that at temperatures above 1000° to 1100°C, the curves show a straight-line Arrhenius behavior, and thus the fractional release appears to have a well-defined activation energy. At 1000°C or less, fractional release becomes less temperature-dependent. This may be due to fission recoil becoming an important release process. To investigate this, a Linac experiment was performed with a fuel sample at room temperature (25°C). The fractional steady-state release values obtained are given in

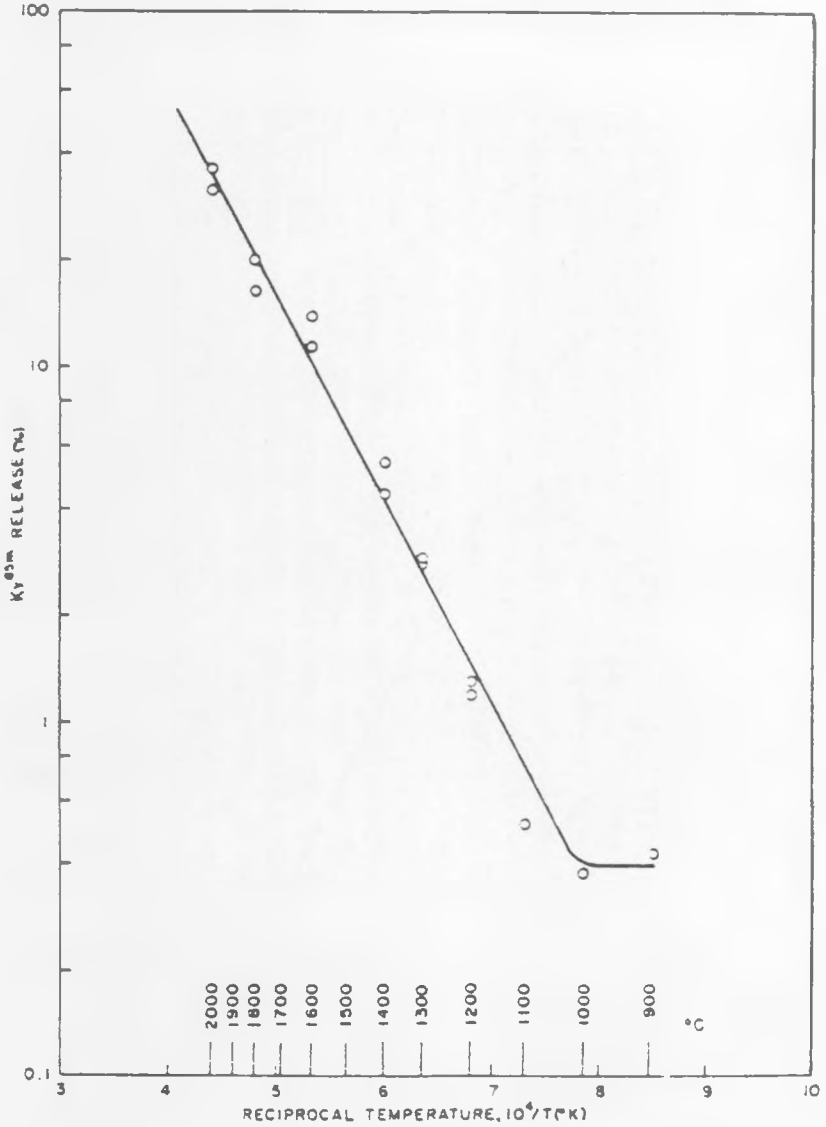

Fig. 8--Steady-state release fraction of Kr^{85m}

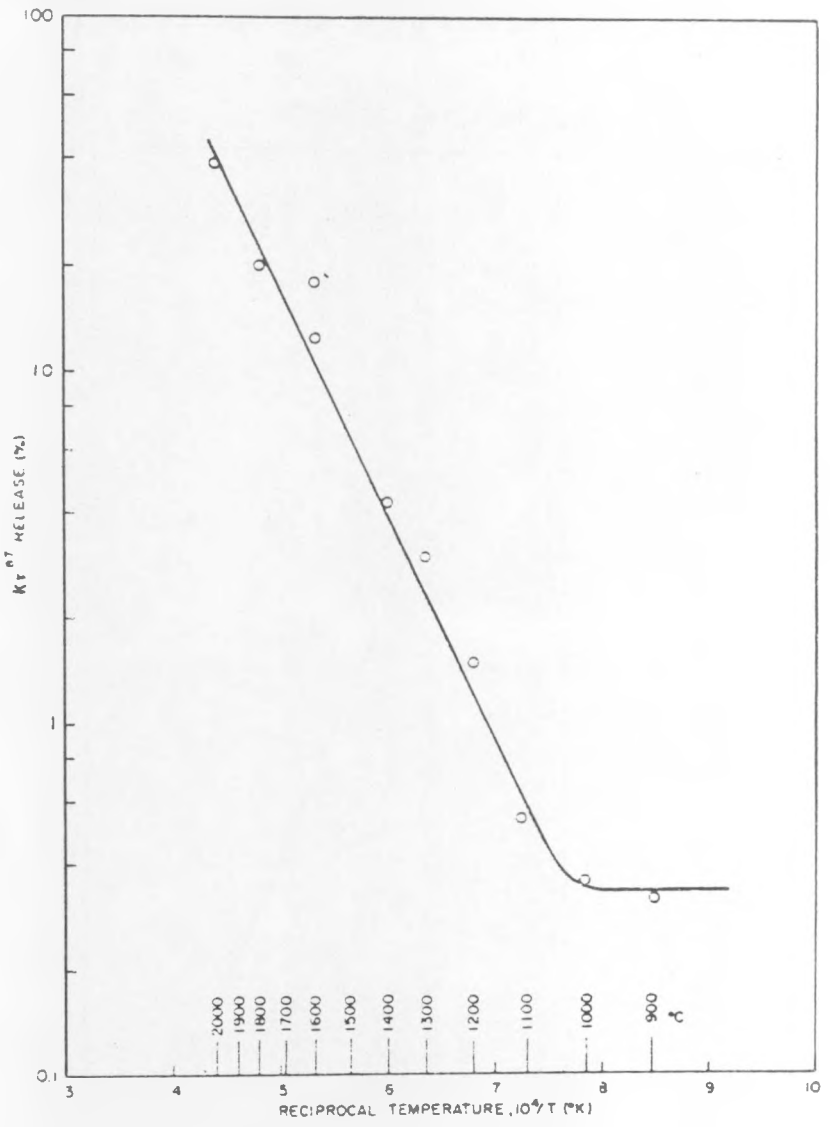

Fig. 9--Steady-state release fraction of Kr^{87}

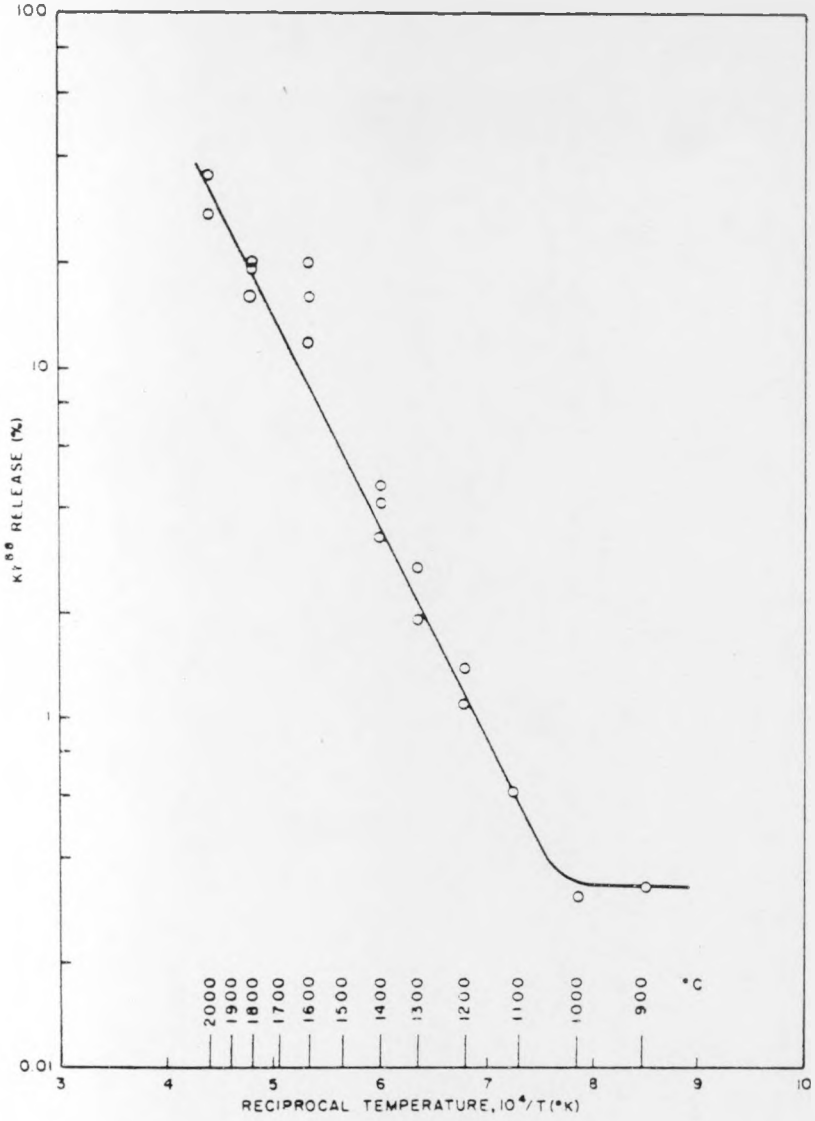

Fig. 10--Steady-state release fraction of Kr^{88}

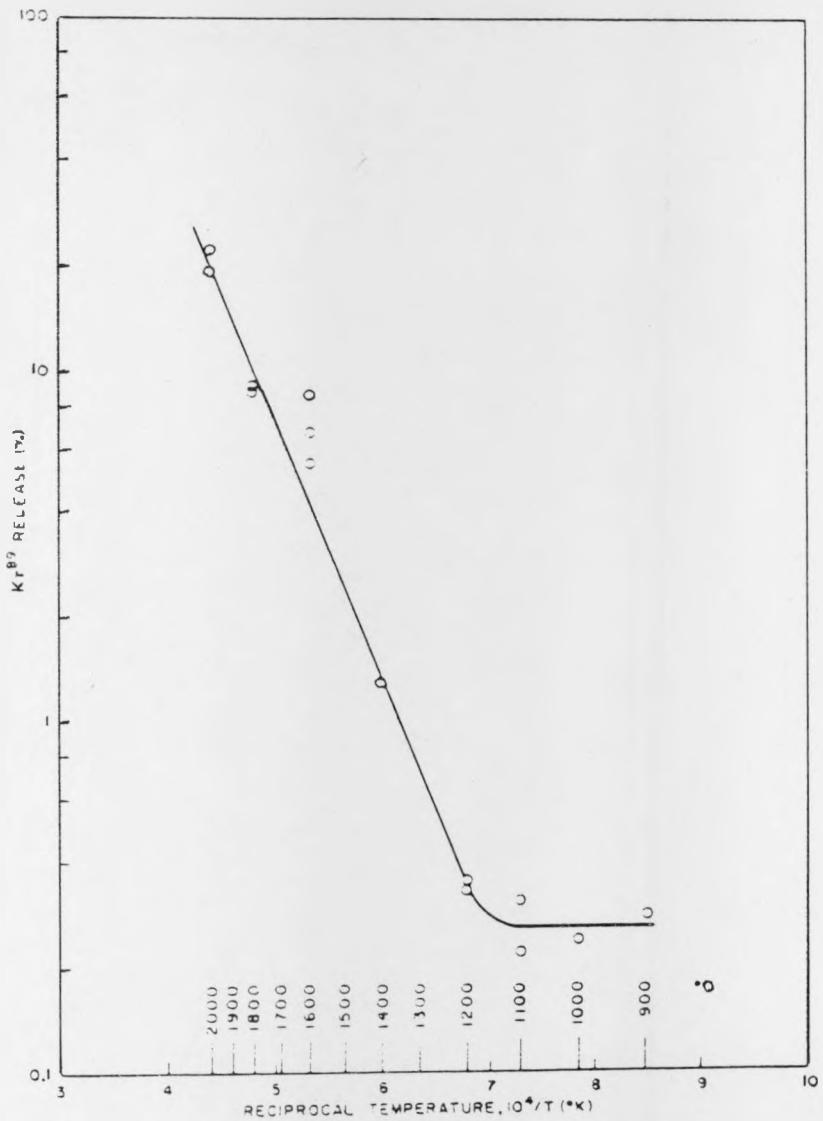

Fig. 11--Steady-state release fraction of Kr^{89}

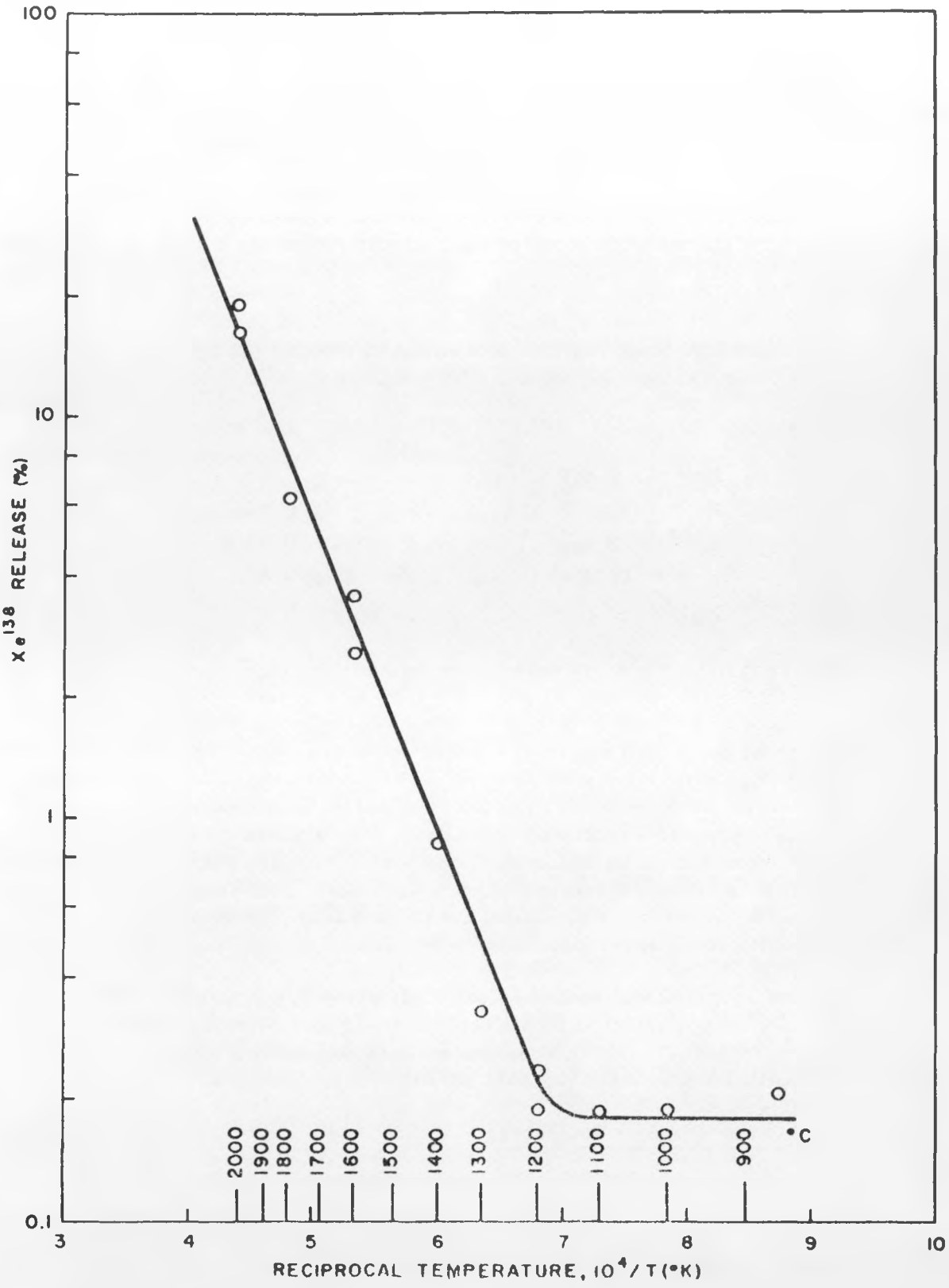

Fig. 12--Steady-state release fraction of Xe^{138}

Table 2. If this release were independent of diffusion, a constant steady-state release for all the rare-gas isotopes would be obtained. The half-life dependence of krypton release at room temperature shows that even release by fission recoil is controlled to some extent by a diffusion process.

Table 2

KRYPTON AND XENON RELEASE FROM HTGR PROTOTYPE FUEL ELEMENT AT 25°C

(In per cent)

Kr^{89} (3.2 m)	0.051
Kr^{87} (78 m)	0.075
Kr^{88} (2.8 h)	0.11
Kr^{85m} (4.4 h)	0.13
Xe^{138} (17 m)	0.053

Apparent activation energies corresponding to the constant slope of the curves in Fig. 8 through 12 at the higher temperature were calculated, and the results are given in Table 3. The average apparent activation energies for krypton and xenon are different. The close adherence of R/B at higher temperatures to Arrhenius behavior indicates that however complex the diffusion process may be, the various components must have approximately the same activation energy. The activation energy for diffusion is expected to be twice the apparent activation energy obtained from the R/B versus 1/T curve. This is because the components of R/B are expected to be proportional to the square roots of the respective diffusion coefficients involved.

Figure 13 gives the steady-state R/B value for krypton release from uncoated (Th, U)C_2 particles in a graphite matrix at various temperatures plotted versus half life. It is to be noted that the curves do not correspond to a simple $(R/B) \propto \sqrt{\text{half-life}}$ relationship.

Release of Other Fission Products

The release of Te^{132}, I^{131}, and Ba^{140} from uncoated-(Th, U)C_2-particle fuel materials has been determined (along with the Xe^{133} release) in a number of annealing experiments. An example of data obtained early in our studies is given in Table 4. It is to be noted that xenon and iodine are released most readily; barium and tellurium are substantially released in 2 or 3 days' time at higher temperatures (>1400°C). A comparison of the release from coated and uncoated particles is given below.

Table 3

APPARENT ACTIVATION ENERGIES FOR KRYPTON AND XENON RELEASE
(In kcal/mole)

Kr^{89}	34.0
Kr^{87}	29.3
Kr^{88}	27.6
Kr^{85m}	26.3
Average for krypton release	29
Xe^{139}	42
Xe^{138}	35.7
Average for xenon release	39

Table 4

UNCOATED-$(Th, U)C_2$-PARTICLE–GRAPHITE FUEL COMPACTS

Temp. (°C)	Time (hr)	Fission-product Release (%)			
		Xe^{133}	Ba^{140}	I^{131}	Te^{132}
2000	90	92.3	22.7[a]	9.2[b]	84.0
1800	48	80.0	20.2	27.7[b]	30.0
1600	64	31.5	7.6	34.8	12.0
1400	96	14.4	0.94	16.4	<2
1100	60	4.97	0.062	0.642	0.363

[a]The collection efficiency of Ba^{140} at 2000°C is less than 100%.

[b]The collection efficiency of I^{131} by the cold finger at 1800°C and 2000°C is less than 100%.

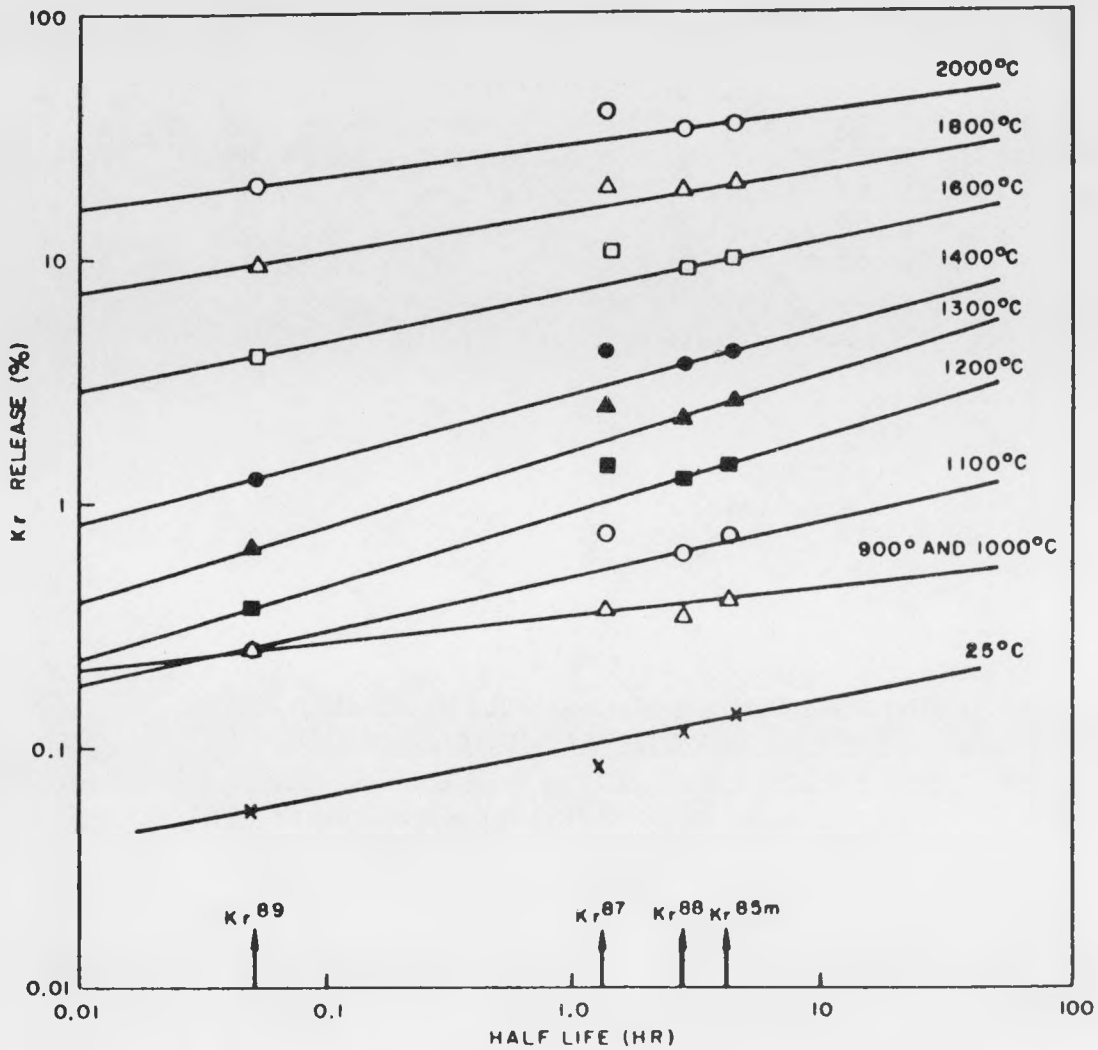

Fig. 13--Steady-state krypton release from uncoated carbide particles in graphite-matrix fuel bodies

RESULTS FOR PYROCARBON-COATED-PARTICLE FUELS

It has been our experience that, in general, lightly irradiated, virgin pyrolytic-carbon-coated (Th, U)C_2 particles 30 to 60 μ thick show negligible Xe^{133} release upon being heated to temperatures up to 1700° to 2000°C for 2 or 3 days. However, they deteriorate in a short time (a matter of minutes) if heated to temperatures $\geq$ 2400°C.

An example of the xenon release behavior of a coated-particle fuel material under extreme conditions is shown in Fig. 14. In simulating a reactor excursion, a lightly irradiated fuel body was held at 3000°C for 38 min after being heated at 1400°C for over an hour without showing a measurable Xe^{133} release. Loss of Xe^{133} began immediately at 3000°C, but was not really spectacular until the furnace current was turned off and the sample rapidly cooled. It is believed that cooling opens up cracks in the pyrolytic-carbon coating that are initiated upon severe heating.

Table 5 gives an example of Xe^{133}, Ba^{140}, I^{131}, and Te^{132} release from fuel compacts consisting of pyrolytic-carbon-coated (Th, U)C_2 particles in a graphite matrix. The small fractional Xe^{133} release is believed to be due to cracked particles (most of which were probably produced during the compact manufacturing, or hot-pressing, process). It is to be noted that the Xe^{133} release appears to be temperature-independent and that I^{131} and Te^{132} release are of the same order of magnitude. Ba^{140} release, on the other hand, is much larger at temperatures $\geq$1600°C. This and many other experiments have indicated that barium can dissolve in and diffuse through pyrolytic-carbon coatings that are impermeable to xenon. It is suspected that this is also true for other electropositive fission products, such as strontium and the rare earths. Experiments are under way to see whether or not this idea is correct.

COMPARISON OF RELEASE FROM COATED AND UNCOATED PARTICLES

Studies of fission-product release as a function of temperature have been recently completed for samples of coated and uncoated fuel particles prepared as fuel materials for use in an in-pile test (GAIL*-IIIC). The fuel is (Th, U)C_2 with a Th:U ratio = 2.5:1. Four runs were made with each of the coated (pyrolytic carbon) and uncoated particles: at 1700°, 1400°, 1200° and 1000°C. The fission-product-release data are given in Tables 6 and 7.

All the samples of the uncoated particles were irradiated in purge cans, which were flushed with helium prior to annealing in the King furnace in an attempt to measure the Xe^{133} lost by recoil. The release was higher

*General Atomic in-pile loop.

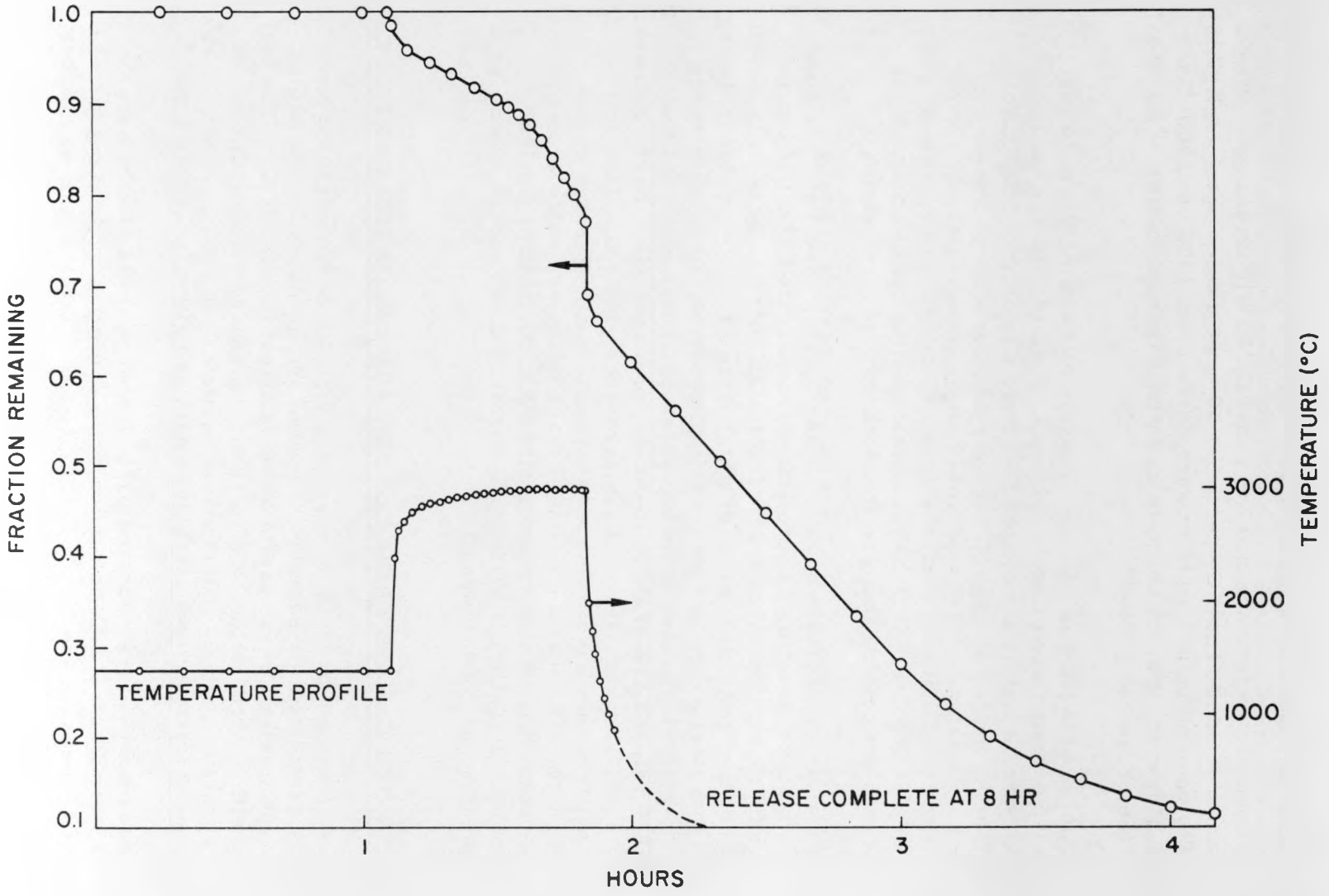

Fig. 14--Effect of an excursion to 3000°C on a fuel compact prepared from coated particles (King furnace III)

Table 5

FISSION-PRODUCT RELEASE IN FUEL COMPACTS CONSISTING OF PYROLYTIC-CARBON-COATED (Th, U)C_2 PARTICLES IN GRAPHITE

Temp. (°C)	Time (hr)	Fission-product Release (%)			
		Xe^{133}	Ba^{140}	I^{131}	Te^{132}
2000	48	0.69	15.6[a]	(b)	0.84
1800	48	0.45	26.3	0.19[b]	1.54
1700	50	0.075	2.17	0.15	0.083
1600	48	0.25	2.32	0.23	0.18
1400	48	0.45	0.024	0.018	0.10

[a]The collection efficiency for Ba^{140} at 2000°C was low owing to incomplete retention of barium by the nest of graphite cylinders placed around the sample.

[b]The collection efficiency for I^{131} by the cold finger at 2000° and 1800°C is less than 100%.

Table 6

FISSION-PRODUCT RELEASE FROM GAIL-IIIC UNCOATED PARTICLES

Temp. (°C)	Time (hr)	Fission-product Release (%)			
		Xe^{133}	Ba^{140}	Te^{132}	I^{131}
1700	70	68.5	95.4	39.6	39.6
	In purge	28.7	---	---	---
		97.2 total			
1400	75	15.0	32.6	4.24	4.17
	In purge	3.56	---	---	---
		18.56 total			
1200	21	7.40	---	0.052	0.86
	44	8.45	---	0.074	0.96
	66	8.85	8.44	0.089	0.99
	In purge	6.42	---	---	---
		15.27 total			
1000	21	4.02	---	0.024	0.22
	44	4.85	---	0.027	0.32
	67	5.36	0.78	0.046	0.35
	In purge	1.13	---	---	---
		6.49 total			

Table 7

FISSION-PRODUCT RELEASE FROM GAIL-IIIC COATED (PyC) PARTICLES[a]

Temp. (°C)	Time (hr)	Fission-product Release (%)			
		Xe^{133}	Ba^{140}	Te^{132}	I^{131}
1700	65	$<1.7\times10^{-5}$	36.9	6.1×10^{-3}	3.5×10^{-2}
1400	65	$<2.7\times10^{-5}$	0.69	3.14×10^{-3}	1.8×10^{-2}
1200	20	$<2.2\times10^{-5}$	2.6×10^{-3}	6.7×10^{-4}	3.0×10^{-3}
1200	48	$<2.2\times10^{-5}$	8.04×10^{-2}	1.2×10^{-3}	6.5×10^{-3}
1200	69	$<2.2\times10^{-5}$	1.15×10^{-1}	1.5×10^{-3}	7.8×10^{-3}
1000	15	$<1.8\times10^{-5}$	1.19×10^{-3}	3.6×10^{-4}	8.5×10^{-4}
1000	64	$<1.8\times10^{-5}$	1.22×10^{-3}	6.2×10^{-4}	1.9×10^{-4}

[a]Two samples were irradiated in purge cans and yielded 3.4×10^{-3} % and 3.7×10^{-3} % release at room temperature. However, the counts measured in each case (90 cpm) were not far above blank corrections (60 cpm) for the containers used. The high blank values were most likely a result of contamination of the cans by traces of uranium, since new purge cans give a zero blank value.

than expected in most cases, and serves as an indication of the extent to which the carbide particles reacted with air that had probably leaked into the containers after they had been placed into "gas-tight" cans. In the worst case, 28.7% Xe^{133} was already free at room temperature, and when the container was opened the characteristic odor of the metal-carbide–moist-air reaction was detected. Most of the remaining Xe^{133} (68.5% out of 71.3%) was released at 1700°C, and it may be assumed that the xenon release at this temperature was actually about 96% within the time of the run (70 hr).

The outstanding feature of these uncoated particles is their tellurium retention at 1200° and 1000°C. It is ten times as good as their iodine retention, which is comparable to that shown by other uncoated particles.

In an attempt to account for all the Ba^{140} released in the experiment, a graphite sleeve was inserted in the furnace heater tube. This sleeve was almost as long as the heater tube itself and was electrically insulated by a ceramic ring on each end. The inside of the sleeve was lined with tantalum foil, which served as a diffusion barrier. A sample of particles in a closed, 1 in. by 1 in., cylindrical, relatively porous, graphite (AGOT) container was centered in this sleeve, the container lying directly on the tantalum liner.

On each side of the container was placed a row of three short (each 3 in. long) graphite sleeves in contact with each other, the inner two being in contact with the container. The outer two extended into the cold zones of the heater tube. This arrangement ensured that all the released barium would be collected by the container and the six sleeves. The sleeves and container were removed at the end of the run for analysis. At the end of the run (uncoated particles at 1700°C), no La^{140} was detected on any of the sleeves (it was all in the graphite container). What was surprising, however, was the fact that I^{131} and Te^{132} were found on the three sleeves on the helium-outlet side of the sample. These isotopes were also found in loose carbon dust that had accumulated inside the tube. This indicates that to some extent, iodine and tellurium may be escaping in a form.such as aerosols or dust particles, that cannot be collected efficiently by a cold finger. It has been observed that in the first few hours of heating a sample, a sooty deposit is picked up on the cold finger. Transfer of tellurium and iodine to the sleeves may have occurred during the cooling-down period at the end of the run, since these elements would not be expected to remain on graphite at 1700°C. Table 8 shows the distribution of the Te^{132} and I^{131}.

Table 8

DISTRIBUTION OF Te^{132} AND I^{131} RELEASED FROM UNCOATED GAIL-IIIC PARTICLES AT 1700°C

Location	Te^{132} (%)	I^{131} (%)
1st sleeve (outermost)	0.42	0.50
2nd sleeve	1.87	1.99
3rd sleeve (in contact with sample)	2.57	2.96
Dust	2.05	1.22
Cold finger	32.7	32.9
	39.61	39.57

ACTIVATION ENERGIES

Arrhenius plots (logarithm of fraction released versus 1/T (°K)) were made for the release data obtained for the GAIL-IIIC uncoated and coated particles. Activation energies for release of fission products were estimated and are shown in Table 9.

In the case of the uncoated particles, the Arrhenius plots (straight lines) obtained were not very good, with the exception of the plot for Te^{132}

release, which appeared to have an activation energy of 76 kcal/mole over the entire temperature range.

It is to be noted that the energy of activation for the permeation of Ba^{140} through the pyrolytic-carbon coating is also about 76 kcal/mole and is substantially higher than the activation energy for release of barium from uncoated (Th, U)C_2 particles. A permeation coefficient of the order of 10^{-13} cm^2/sec at 1400°C is estimated for the barium penetration of the carbon coating.

Table 9

ACTIVATION ENERGIES FOR RELEASE OF FISSION PRODUCTS

Isotope	Activation Energy (kcal/mole)		
	1000°-1400°C	1400°-1700°C	1000°-1700°C
GAIL-IIIC Uncoated Fuel Particles			
Xe^{133}	8	47	
Ba^{140}	39	--	
Te^{132}	76	76	
I^{131}	27	49	
GAIL-IIIC Coated Fuel Particles			
Xe^{133}			----
Ba^{140}			76.4
Te^{132}			16.2
I^{131}			22.0

IN-PILE EXPERIMENTS

EXPERIMENTS ON GA-309 CAPSULES

In the GA-309 series of experiments, fuel compacts made of pyrocarbon-coated (Th, U)C_2 particles were irradiated in purge capsules placed in the water reflector adjacent to the core of the General Electric Test Reactor (GETR). The temperature of the capsules was determined by fission heating plus the composition of the purge gas, a helium-neon mixture, that was employed.

The fuel compacts were annular, 1 in. in outside diameter, 0.5 in. in inside diameter, and 1.75 in. long. They contained 18 to 24 wt-% fuel (Th:U = 2.2:1) in a graphite matrix.

The fuel particles were of (Th, U)C_2, ~200 μ in diameter, and coated as shown in Table 10. Photomicrographs of polished sections of these fuel particles are included as Figs. 42, 43, 44, and 45 in GA-3588.

Table 10

FUEL PARTICLES FOR IN-PILE PURGE-CAPSULE RUNS

Capsule	Coating	Mass U^{235} (g)
GA-309-4	25-μ pyrocarbon (BMI) from C_2H_2	2.64
GA-309-5	25-μ pyrocarbon (BMI) from C_2H_2	1.81
GA-309-6	25-μ pyrocarbon (BMI) from C_2H_2	2.29
GA-309-7	10 to 15-μ carbon from C_2H_2	2.62
GA-309-8	50 to 60-μ carbon from CH_4	1.80
GA-309-9	50 to 60-μ carbon from C_2H_2	2.27

Capsules GA-309-4, -5, -6 (inserted 11/13/60 and discharged 8/15/61) underwent six GETR cycles, or approximately 4,935 Mw-days of reactor time (nominal reactor power 30 Mw). Capsules GA-309-7, -8, -9 (inserted 5/1/61 and discharged 9/17/61) underwent four GETR cycles, or approximately 3,323 Mw-days of reactor time.

The range of fission rates in the fuel compacts was 4.5 to 8.6×10^{13} fissions/sec. The estimated burnup of U^{235} based on the

original U^{235} content of fuel compacts and the average fission rates calculated from estimated fission rates is given in Table 11.

Table 11

ESTIMATED U^{235} BURNUP

Capsule	Average Fission Rate (sec^{-1}) ($\times 10^{-13}$)	U^{235} Burnup[a] (%)
GA-309-4	6.7	14.1
GA-309-5	7.3	22.2
GA-309-6	6.3	15.3
GA-309-7	6.1	8.7
GA-309-8	7.4	15.4
GA-309-9	6.4	10.6

[a]These values are at variance with about two-thirds of the values estimated from burnup data obtained on earlier capsules (GA-308-1, -2).

The temperature history of the capsules was very complex, and somewhat uncertain because of thermocouple failures. The range of capsule temperatures during irradiation was as follows:

GA-309-4 . . . . . 900° to 1700°C
GA-309-5 . . . . . 1090° to 1900°C
GA-309-6 . . . . . 1010° to 1870°C
GA-309-7 . . . . . 1100° to 1820°C
GA-309-8 . . . . . 1070° to 1990°C
GA-309-9 . . . . . 1290° to 2160°C

To determine fission-product krypton and xenon release, the capsules were first purged with helium, the released fission-product gases were then allowed to accumulate (usually for about 24 hr), and the capsules were purged again with helium. The latter purge was sampled, aliquoted, and analyzed using a multichannel gamma spectrometer. The disintegration rates of the fission-product nuclides Xe^{138}, Kr^{87}, Kr^{88}, Kr^{85m}, Xe^{135}, Xe^{133}, and Kr^{85} at sampling time were determined on the basis of their decay schemes and half lives and the known gamma-counting efficiency of the scintillation detector of the spectrometer. Fission rates for the fuel specimens were calculated from their U^{235} content and the neutron flux, which was known as a function of reactor power and capsule position. The fractional steady-state release of nuclide i (F_i) was calculated from

$$F_i = \frac{R_i / y_i \left(1 - e^{-\lambda_i t}\right)}{R_f} ,$$

where R_f = corrected fission rate,

R_i = disintegration rates of nuclide i at sampling time (t) in the purged gas,

λ_i = decay constant for i,

y_i = fractional fission yield of i,

t = accumulation time.

KRYPTON-85 AND XENON-133 RELEASE FROM A HIGH-BURNUP COMPACT

Compact GA-313, a 1-in.-diameter by 1-in.-long simulated fuel compact containing 1 mg of U^{235} in the form of coated fuel particles, was placed in the General Electric Test Reactor (GETR) for one reactor cycle in the region of highest thermal-neutron flux. The particles used in this experiment consisted of solid-solution UC_2-ThC_2, in the ratio of 2:4.5, coated with pyrolytically deposited carbon. The coatings, averaging 25 μ in thickness, were deposited at 1400°C at Battelle Memorial Institute (BMI) on fuel particles supplied by the Mallinckrodt Chemical Company.

After irradiation at a flux of 2×10^{14} neutrons/cm^2-sec (equivalent to about 3 yr in the Peach Bottom HTGR), the sample was stored for 2 months for decay, and then the release of Xe^{133} and Kr^{85} was determined at 1700°C using King furnace I (see Fig. 15 for the release curves). This sample was initially heated to 1000°C for 1.5 hr, during which time a release of 0.42% was observed for Xe^{133}. The temperature was then raised to 1700°C and maintained there for 2.79 days. In order to be certain of the true relative release rate, the sample was finally thermal-shocked ten times from room temperature to as high as 2600°C to completely drive out the remaining xenon and krypton. Figure 16 gives the rate of release observed in the course of the thermal-shock treatment. A thermal shock consisted in rapidly heating a compact from room temperature to a predetermined maximum temperature (2400° or 2600°C), holding it there for a minute or two, and then cooling it to room temperature.

In order to compare the release of the high-burnup compact with that of the unirradiated material, an identical control compact containing 10 mg of U^{235} was irradiated in the TRIGA reactor to 10^{13} fissions. This compact was then heated to 1700°C in the furnace for 40 hr; the Xe^{133} release was determined to be about 0.5% (see Fig. 15).

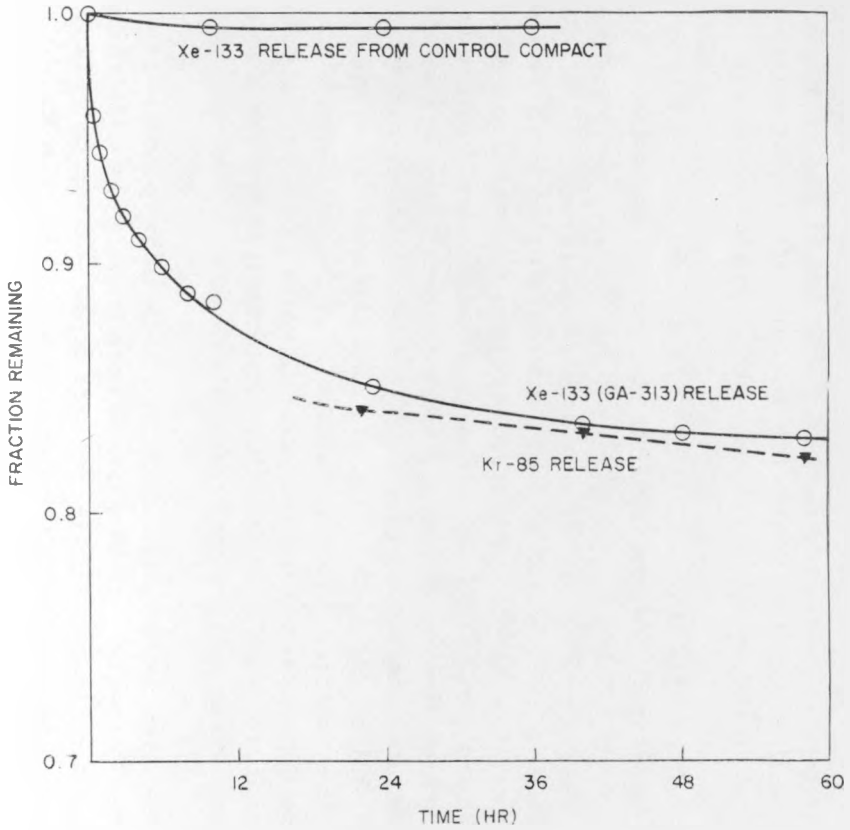

Fig. 15--Fission-product release at 1700°C from compact GA-313 (high burnup)

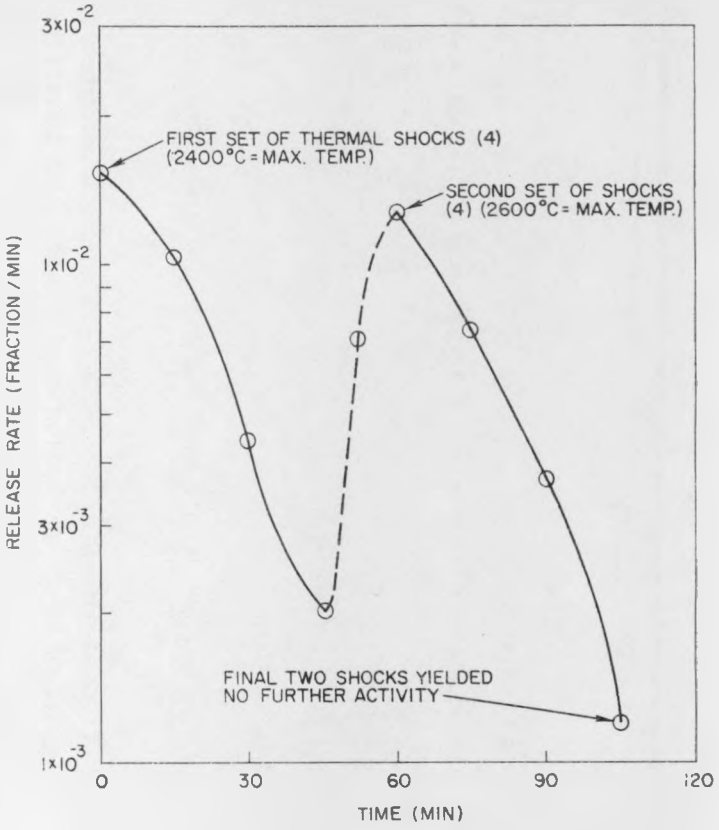

Fig. 16--Rate of Xe^{133} release from compact GA-313

The integrity of the particles was most certainly affected by the 3-yr equivalent burnup. However, the degradation was not nearly so severe as it might have been, since all particles could have burst because of the pressure of volatile fission-product gas built up inside the particles. The release characteristics of the irradiated compact showed evidence that a majority of the particles were still intact and that only a few had ruptured. The observed release (Xe^{133}) was similar to that observed for an uncoated-particle compact, which apparently is the behavior to be expected for particles that have been broken open.

At the end of the run, the inside of the King furnace was highly contaminated. This activity was concentrated on the parts of the furnace downstream from the sample and had to have diffused through the heating tube to get there. The principal contaminants observed from gamma-spectrum analysis were Cs^{137} and I^{131}, although relatively little of these isotopes was found on a plug of copper shreddings that was placed inside the heater tube downstream from the sample to act as an iodine collector.

The heating tube itself was also highly contaminated. The distribution of activity was determined by passing the tube past a 1/2-in. slit in 4 in. of lead shielding and integrally counting the gamma energies above 0.5 Mev. The contaminants were found to be concentrated in three locations in the tube (see Fig. 17). Gamma spectrometry revealed that Cs^{137} had concentrated in a relatively cold zone downstream from the sample (a trace had also collected upstream in the cold zone). Ba^{140}-La^{140} was concentrated in a region downstream from the sample. Activity located at the approximate position of the sample in the tube is believed to be Zr^{95}-Nb^{95}.

GAIL-IIIA TEST

An irradiation test of a full-diameter, quarter-length, prototype HTGR fuel element was begun in October, 1961. This experiment, GAIL-IIIA, provided its own nuclear heat of 70 kw at full power. The experiment was conducted in the GETR.

The in-pile loop was comprised of a fuel element, a main helium-coolant loop, and an internal helium purge system separated from the main-loop coolant. In the fuel element, a low-permeability graphite sleeve was used to separate the main coolant gas from the internal purge gas. The graphite sleeve had a room-temperature helium permeability of approximately 10^{-5} cm^2/sec at 1 atm.

Steady-state fission-product release was measured throughout the experiment by removing gas samples from the fission-product purge stream and from the main coolant loop. The following isotopes were measured

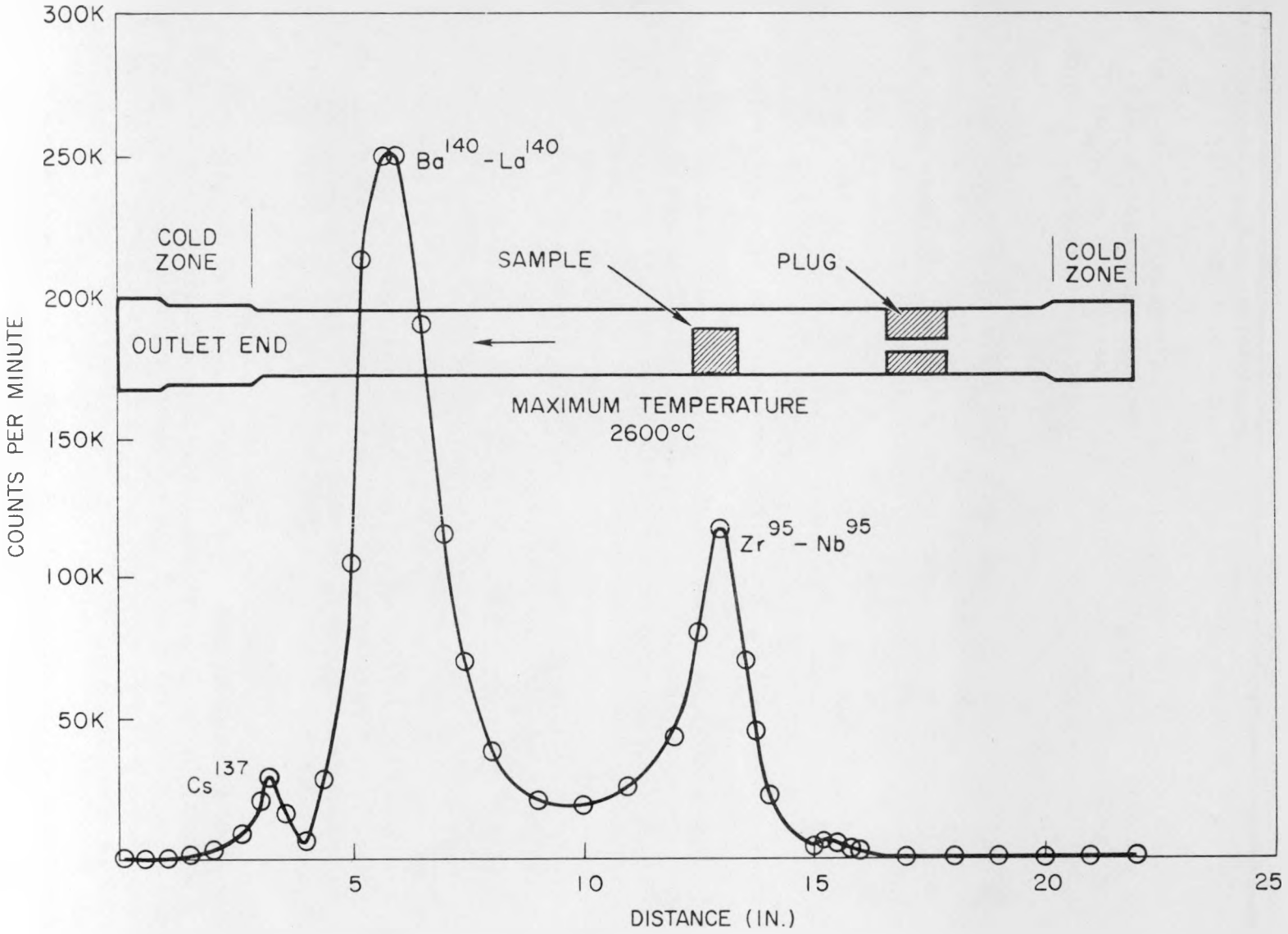

Fig. 17--Distribution and identity of the principal contaminants along the King-furnace heating tube after running compact GA-313

using conventional multichannel gamma-ray spectrometry: Kr^{85m}, Kr^{87}, Kr^{88}, Kr^{89} (as Rb^{89}), Xe^{133}, Xe^{135}, and Xe^{138} (as Cs^{138}).

Measurements of the gross noble-gas fission products in gas samples from both the purge stream and the main coolant loop showed roughly a factor of 10^{-3} less activity per cubic centimeter in the main loop than in the purge stream. An evaluation of the permeability of the sleeve to xenon and krypton at ambient temperature and pressure agreed reasonably well with the permeability determined by the conventional room-temperature helium measurement.

When this experiment was concluded in February, 1962, the element had received a total of 133 Mw-hr burnup, which is equivalent to 8, 850 Mw-day/ton. The fuel element was subsequently examined and dismantled in the General Atomic Hot Cell. Samples were taken for determination of fission-product distribution of the less-volatile elements in the graphite fuel-element sleeve and in adjacent materials.

The fuel-body temperatures in the GA-309 capsule were held at different levels (by controlling capsule cooling with helium-neon gas mixtures) for each run (sample series) in order to determine the effect of temperature on the steady-state release fraction. Assuming that radiation dosage (megawatt-days exposure) has a secondary effect, one might expect the steady-state release fraction, F_i (R/B value), to follow an Arrhenius behavior, with

$$(R/B)_i = F_i = F_i^o \, e^{-E_a/RT} ,$$

where E_a is the apparent activation energy. Figures 18 through 23 show curves giving the per cent release ($F_i \times 100$) for the krypton and xenon nuclide versus the reciprocal of the absolute temperature for purge capsules GA-309-4, -5, and -6. Although the data points show quite a bit of scatter, they appear to follow the Arrhenius equation. Table 12 gives the apparent activation energies, E_a, corresponding to slopes of the lines shown, which roughly fit the data.

The average apparent activation energies for krypton and xenon release for the GA-309 capsules (28 and 39 kcal/mole, respectively) are just about the same as those obtained in the Linac experiments with uncoated-carbide-particle fuel compacts (29 and 39 kcal/mole, respectively). An interpretation of the GA-309-4, -5, and -6 release behavior, consistent with these measurements, is that krypton and xenon (or their precursors, such as bromine or iodine) are significantly released only from particles with broken or defective coatings and that such release is similar in character to release from uncoated carbide particles. In the latter case,

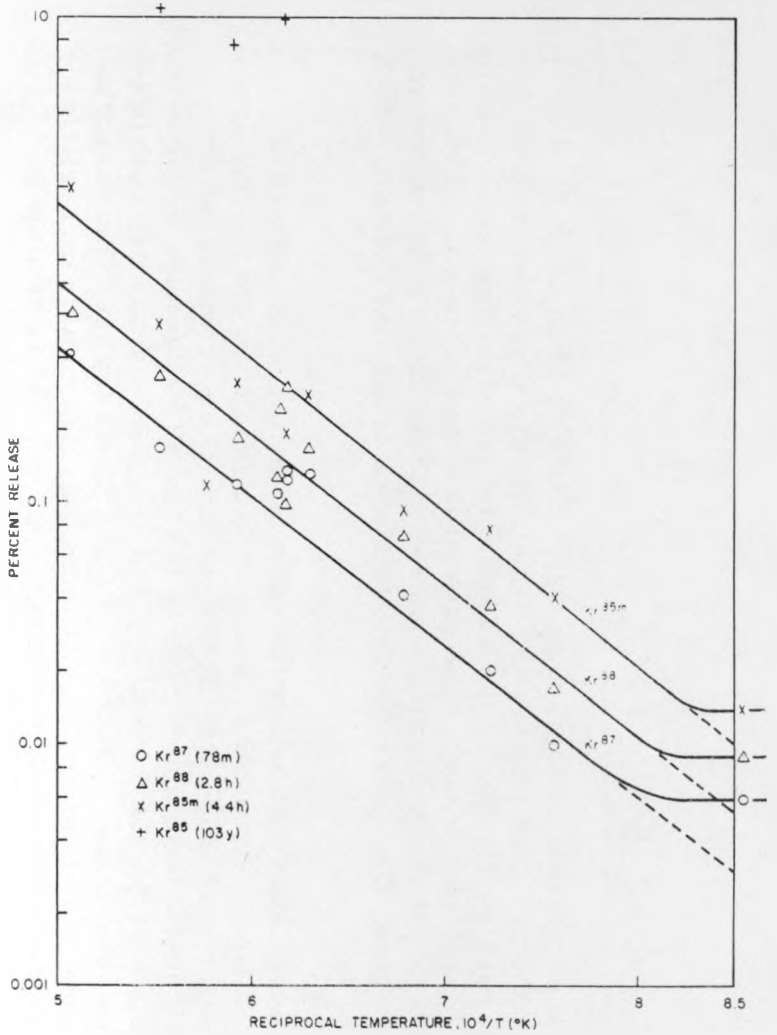

Fig. 18--Capsule GA-309-4, krypton release versus reciprocal temperature

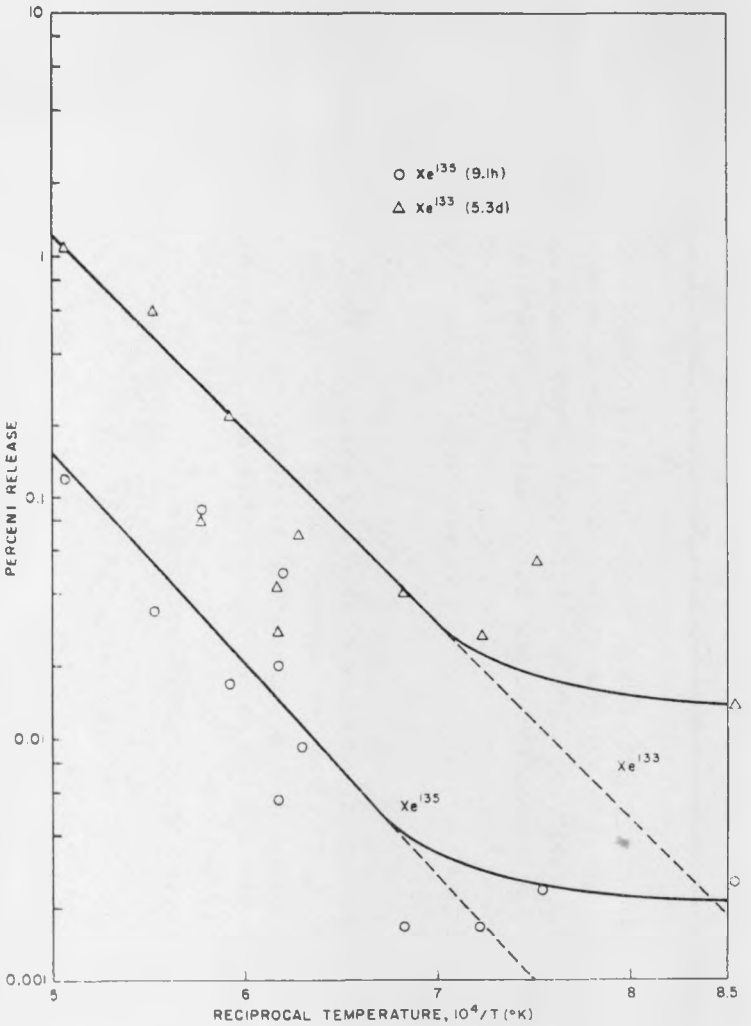

Fig. 19--Capsule GA-309-4, xenon release versus reciprocal temperature

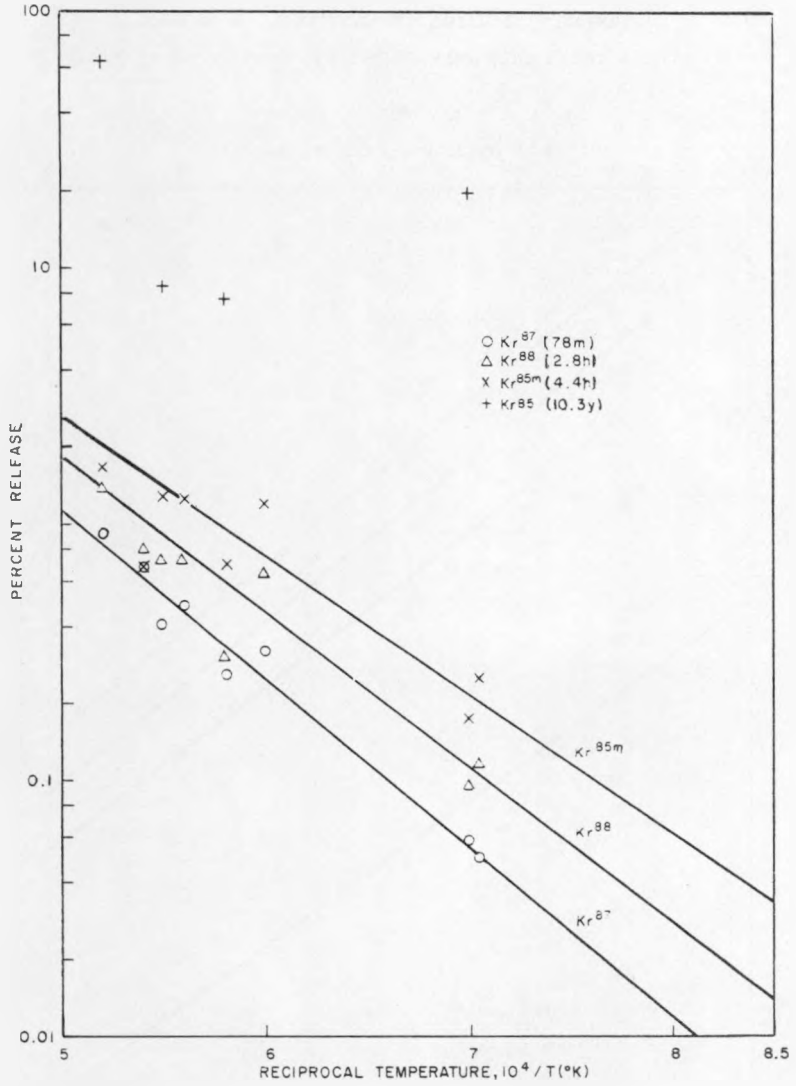

Fig. 20--Capsule GA-309-5, krypton release versus reciprocal temperature

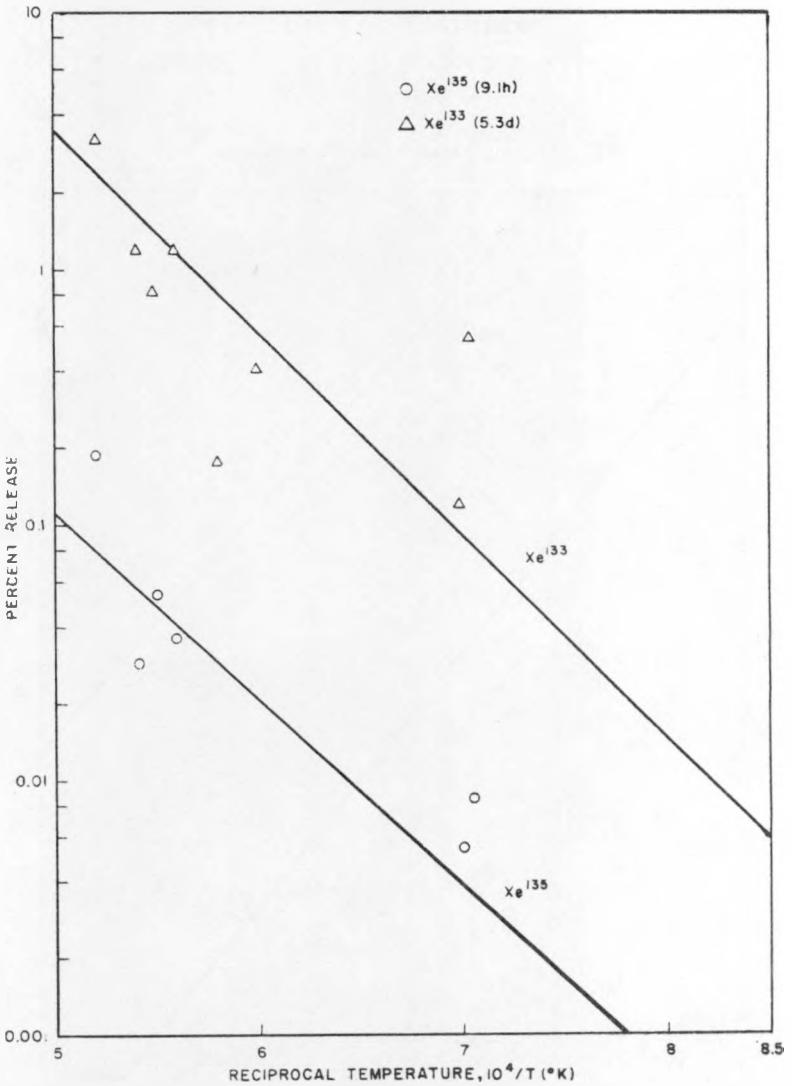

Fig. 21--Capsule GA-309-5, xenon release versus reciprocal temperature

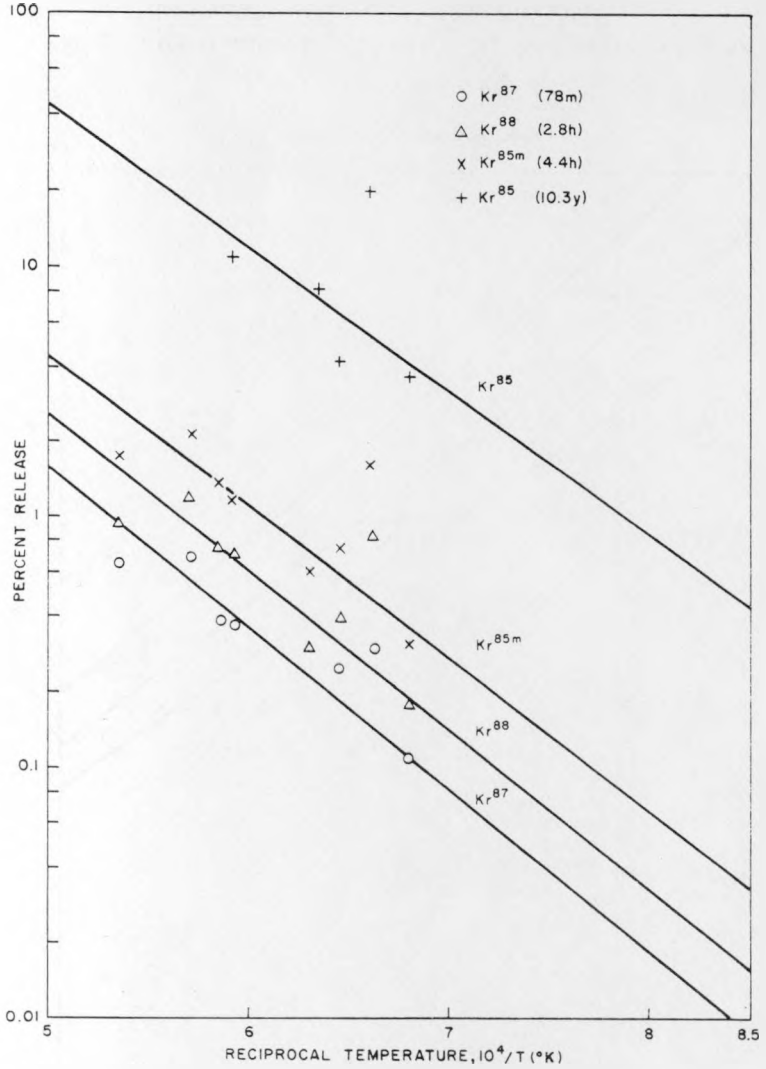

Fig. 22--Capsule GA-309-6, krypton release versus reciprocal temperature

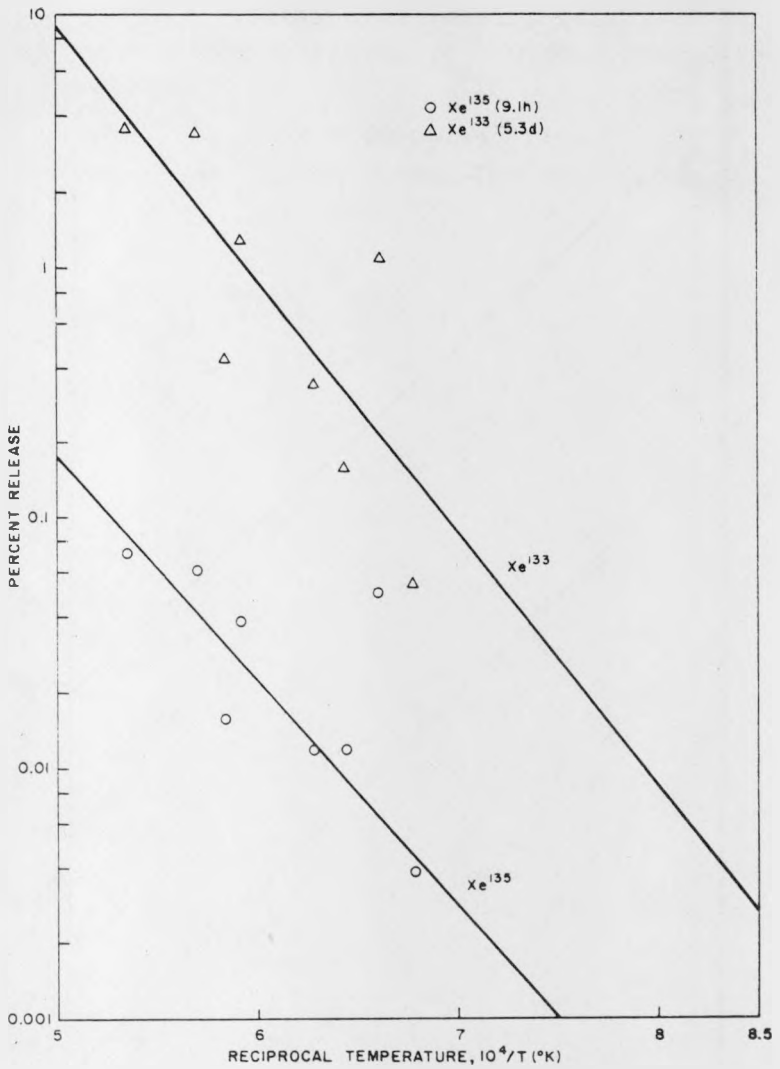

Fig. 23--Capsule GA-309-6, xenon release versus reciprocal temperature

it is likely that diffusion of fission products out of carbide grains, in which they are deposited by the fission-recoil process, is the rate-controlling process for release.

Table 12

APPARENT ACTIVATION ENERGY FOR KRYPTON AND XENON RELEASE

Capsule	Apparent Activation Energy, E_a[a] (kcal/mole)					
	Kr^{87}	Kr^{88}	Kr^{85m}	Kr^{85}	Xe^{135}	Xe^{133}
GA-309-4	28.1	28.4	29.1	---	40.2	36.8
GA-309-5	30.1	27.5	24.8	---	33.4	36.2
GA-309-6	24.1	29.0	27.6	26.6	41.1	45.8

[a]Average for krypton, E_a = 28 kcal/mole; average for xenon, E_a = 39 kcal/mole.

The Xe^{135} release-fraction data in the preceding and following figures were calculated neglecting the effect of neutron burnup, $\sigma\phi$. If these values are multiplied by $5[\cong(\sigma\phi + \lambda)/\lambda]$, one obtains the approximate F value which would be observed if neutron burnup of Xe^{135} did not occur.

In order to separate the effect of temperature from the effects of time and radiation exposure, all available krypton and xenon release data (F_i values) were corrected to a common temperature (1667°K) with the assumption that $F_i = F_i^o \exp(-E_a/RT)$, with E_a = 29 kcal/mole for krypton and E_a = 39 kcal/mole for xenon. This was done on the basis that the krypton and xenon release appeared to follow an Arrhenius behavior quite closely and, indeed, with about the same activation energy as shown by krypton and xenon release from uncoated (Th, U)C_2-particle fuel bodies in the Linac experiments. Figures 24 through 35 give the per cent release versus megawatt-days of reactor time for krypton (Kr^{87}, Kr^{88}, Kr^{85m}, and Kr^{85}) and for xenon (Xe^{133} and Xe^{135}).

There is quite a bit of scatter in the data, but it is seen that with the exception of the capsule GA-309-7 data, the release fractions show a pronounced increase with time in the reactor. A completely satisfactory theory for this behavior is still to be developed. However, it is believed that the activation energies of 29 kcal/mole for krypton release and 39 kcal/mole for xenon release are connected with an initial step involving diffusion of recoil-deposited krypton and xenon nuclides or their precursors from the (Th, U)C_2 particles. A second step involving further delay may

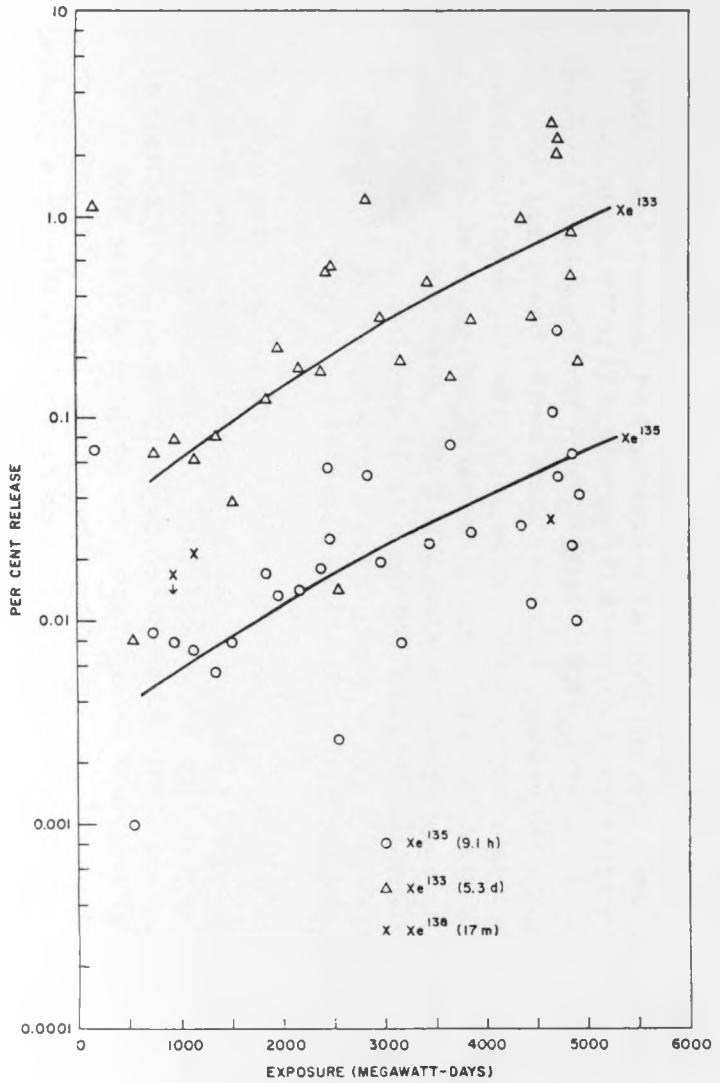

Fig. 24--Steady-state xenon release for capsule GA-309-4 (all points normalized to 1667°K)

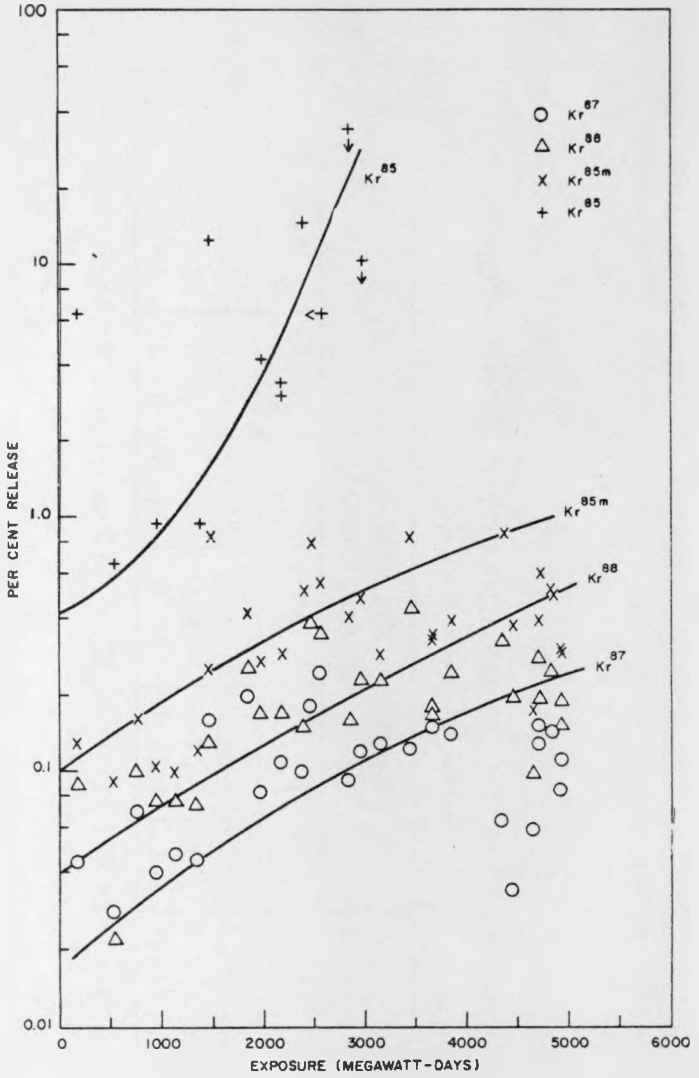

Fig. 25--Steady-state krypton release for capsule GA-309-4 (all points normalized to 1667°K)

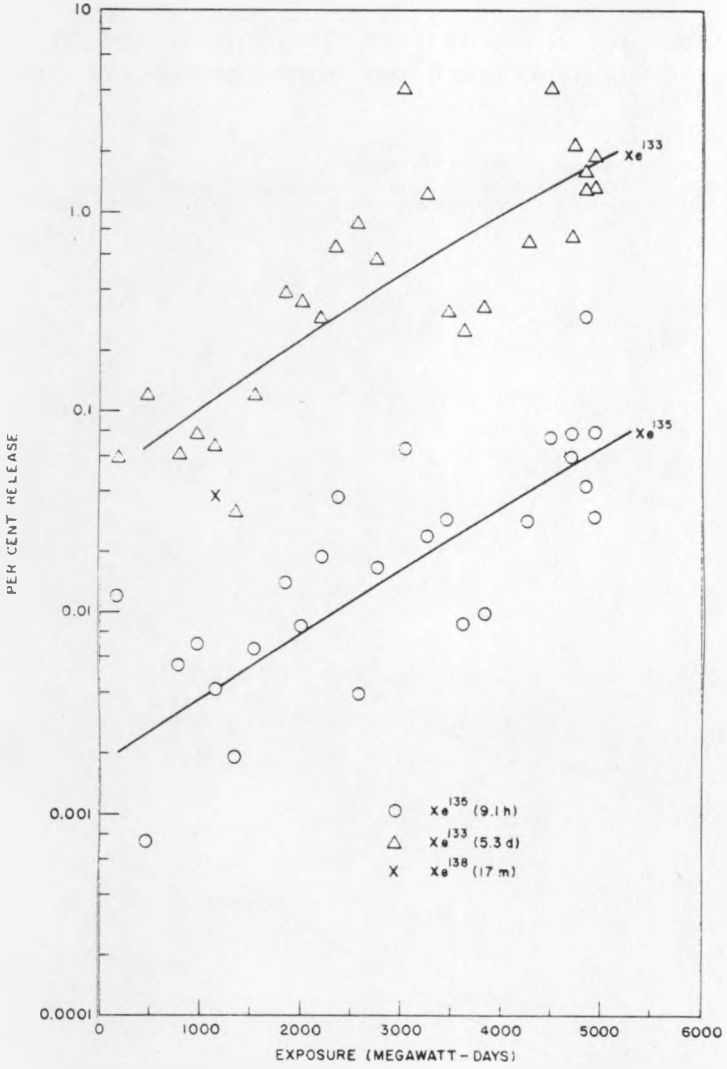

Fig. 26--Steady-state xenon release for capsule GA-309-5 (all points normalized to 1667°K)

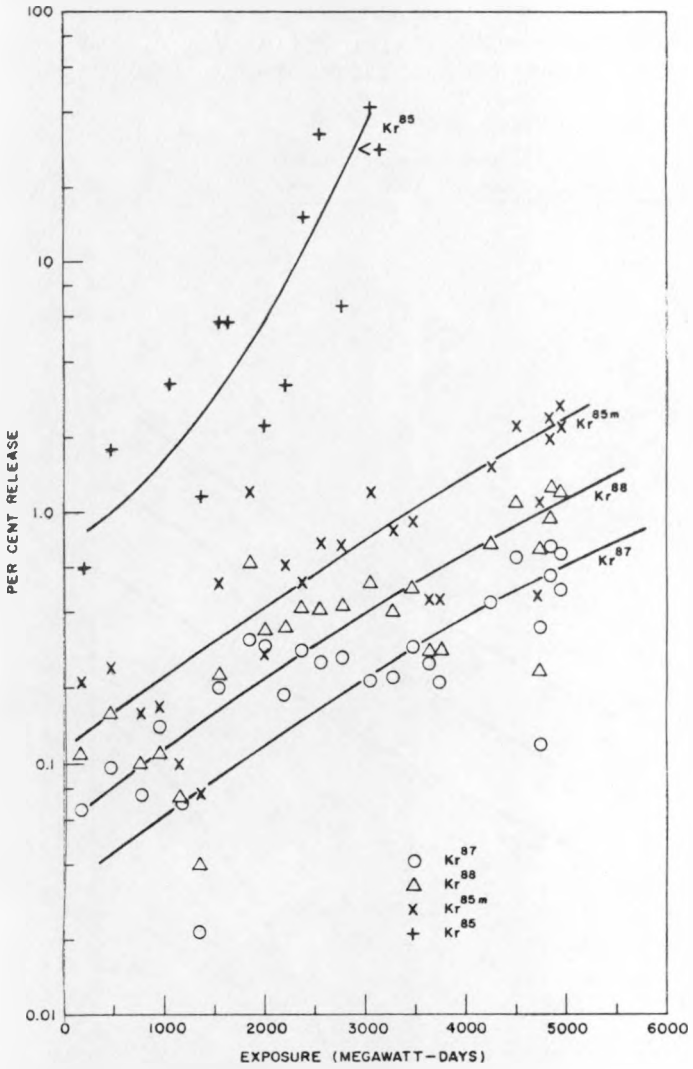

Fig. 27--Steady-state krypton release for capsule GA-309-5 (all points normalized to 1667°K)

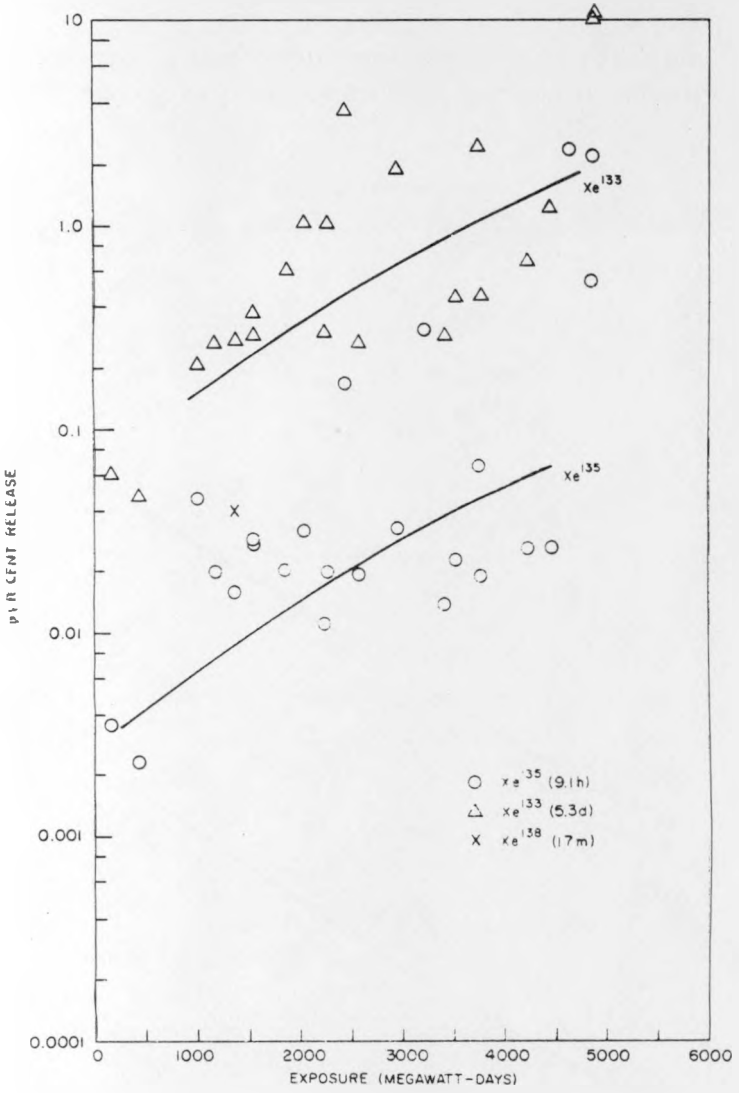

Fig. 28--Steady-state xenon release for capsule GA-309-6 (all points normalized to 1667°K)

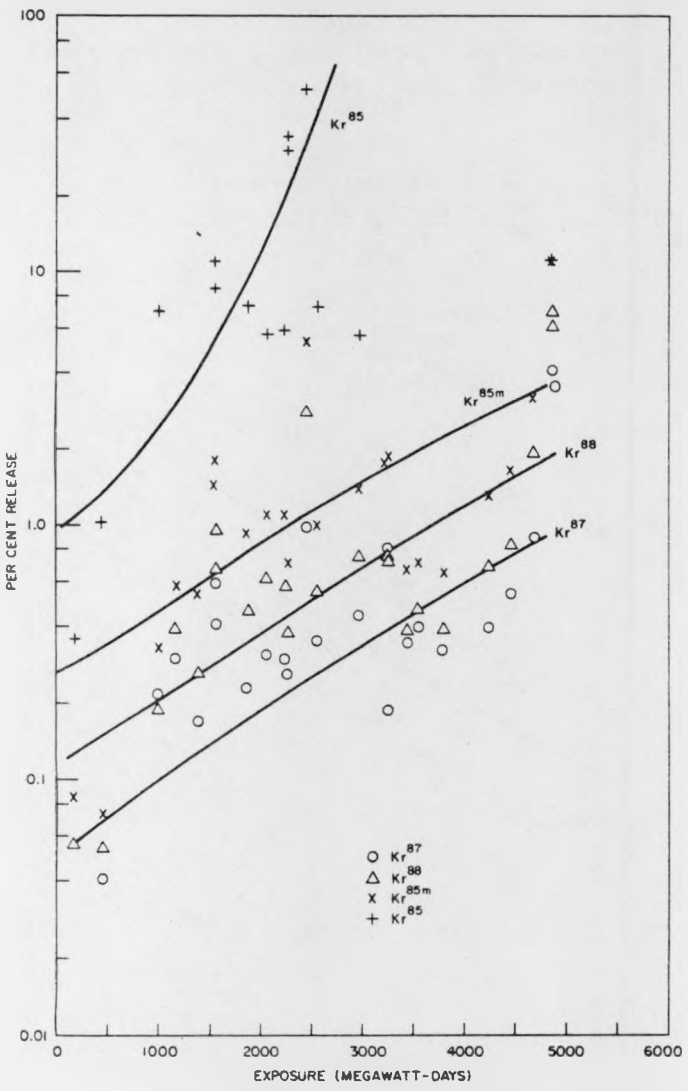

Fig. 29--Steady-state krypton release for capsule GA-309-6 (all points normalized to 1667°K)

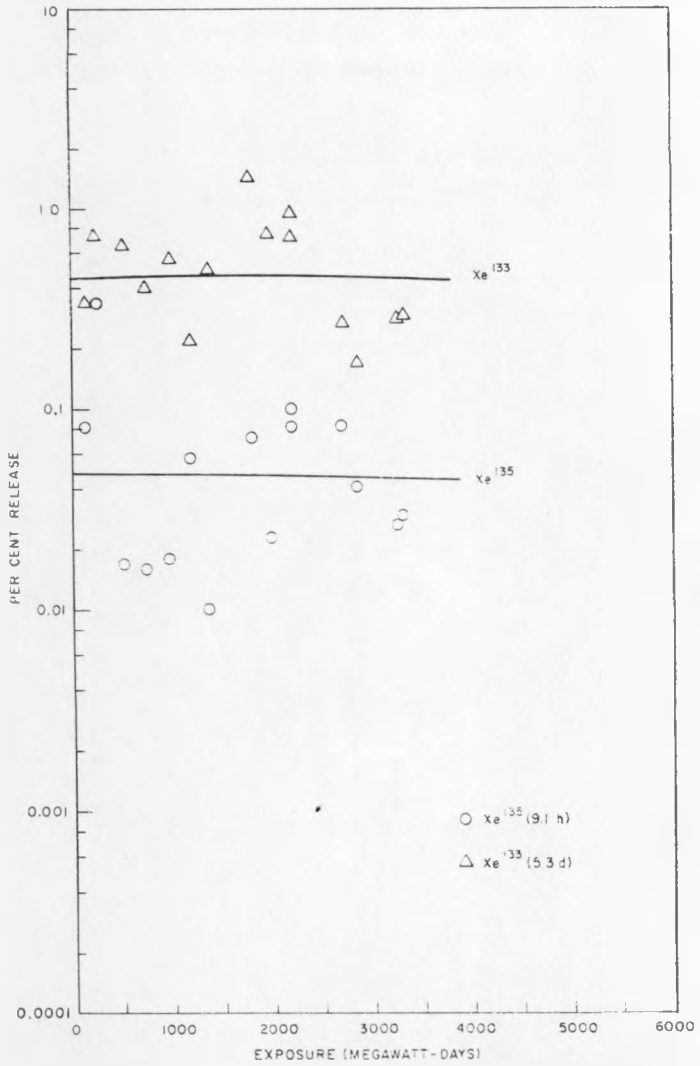

Fig. 30--Steady-state xenon release for capsule GA-309-7 (all points normalized to 1667°K)

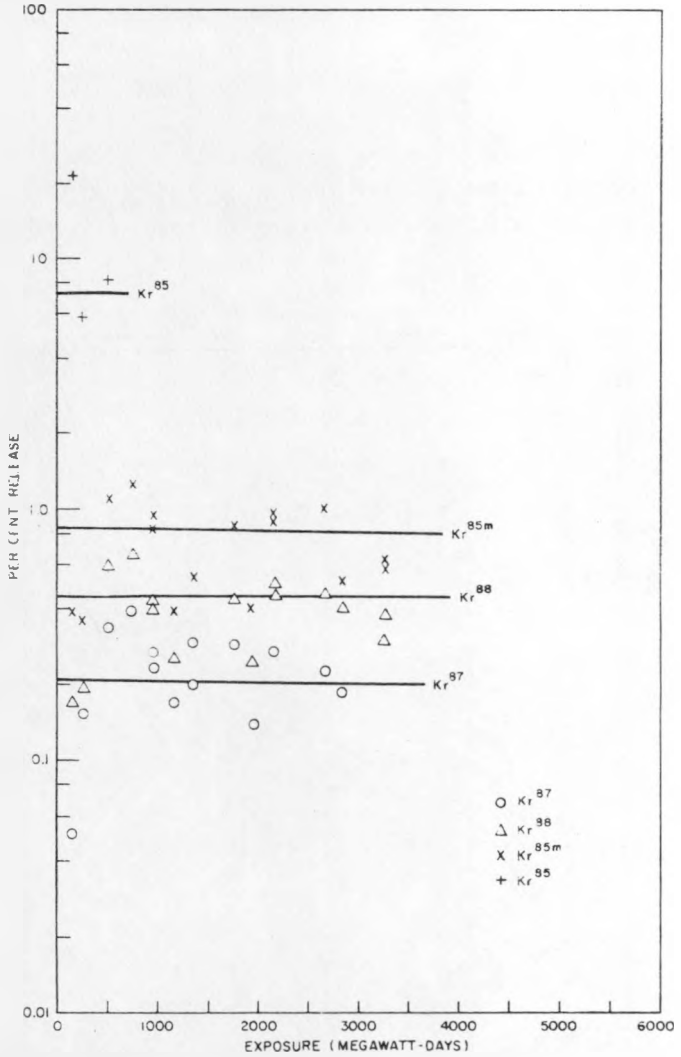

Fig. 31--Steady-state krypton release for capsule GA-309-7 (all points normalized to 1667°K)

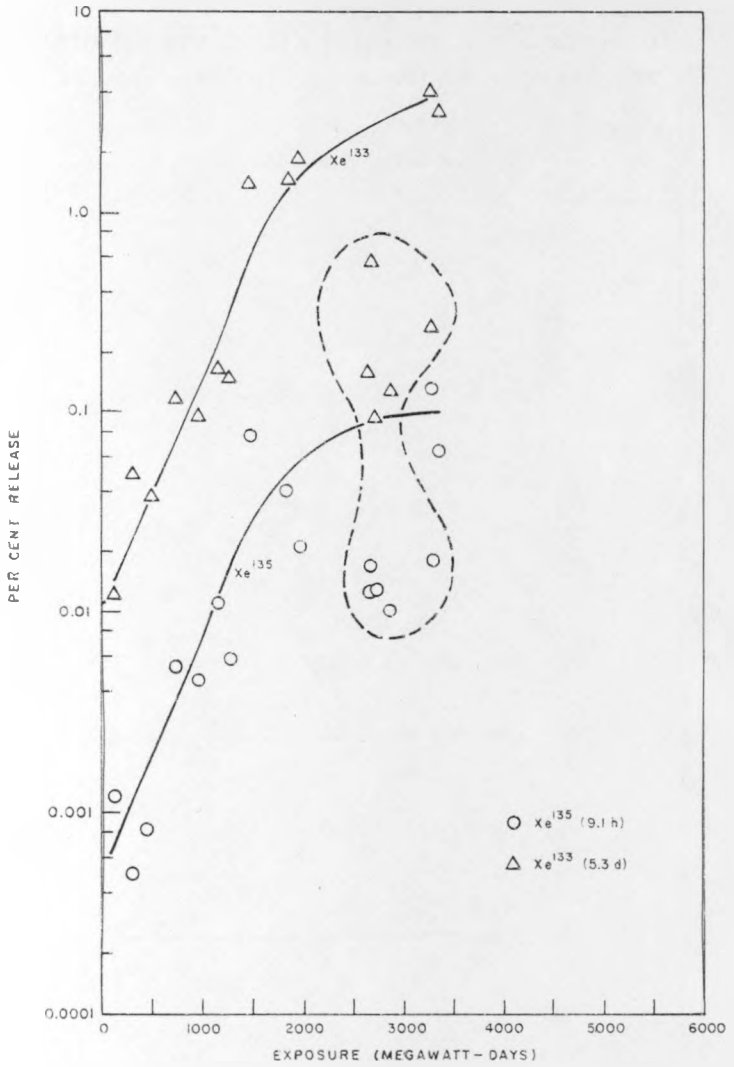

Fig. 32--Steady-state xenon release for capsule GA-309-8 (all points normalized to 1667°K)

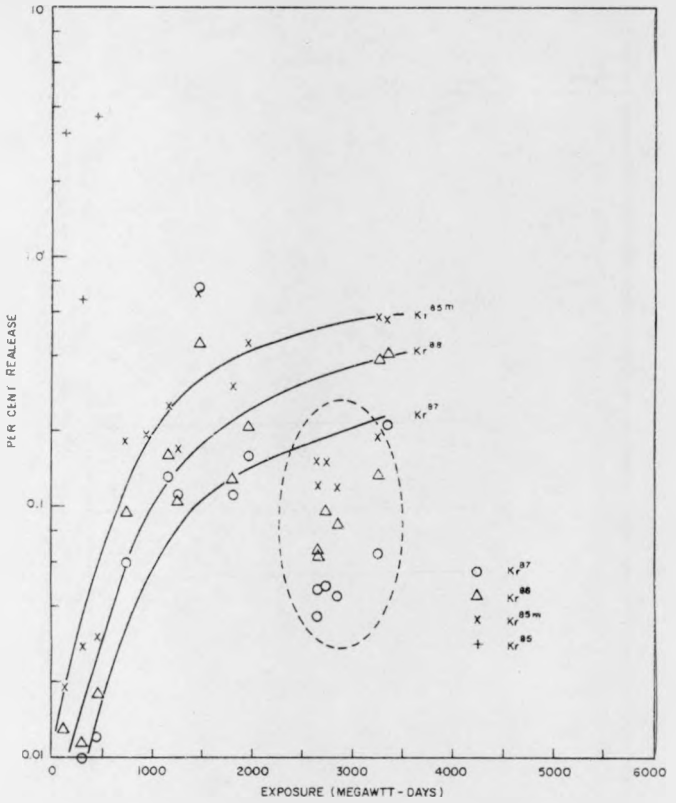

Fig. 33--Steady-state krypton release for capsule GA-309-8 (all points normalized to 1667°K)

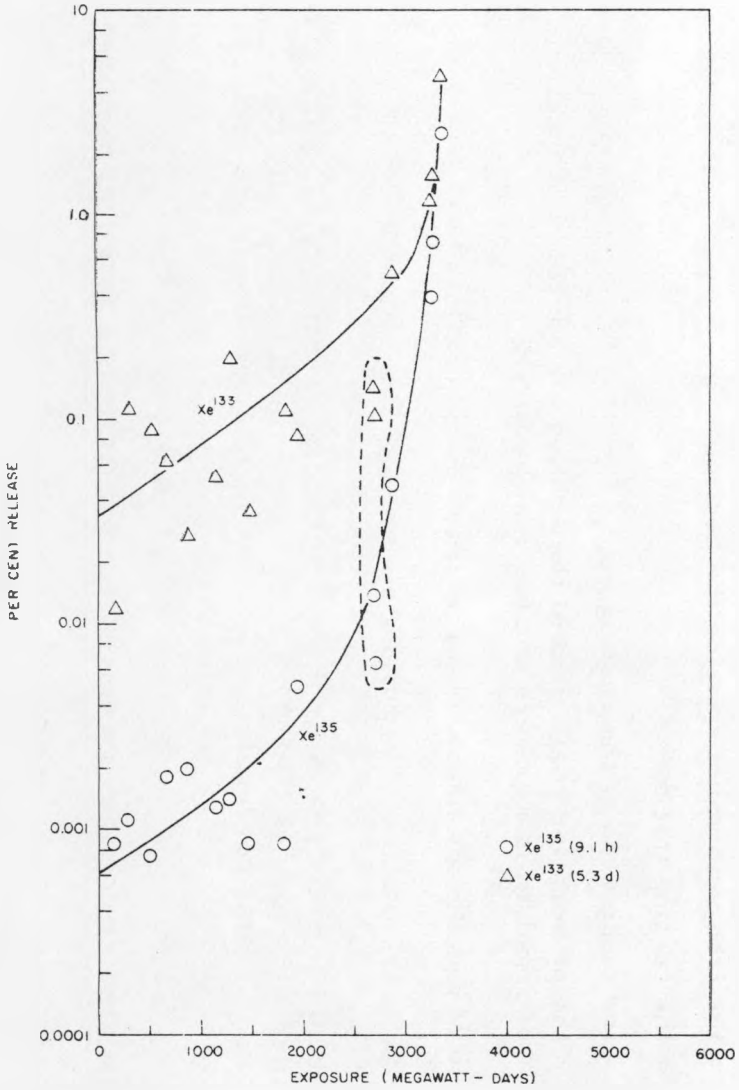

Fig. 34--Steady-state xenon release for capsule GA-309-9 (all points normalized to 1667°K)

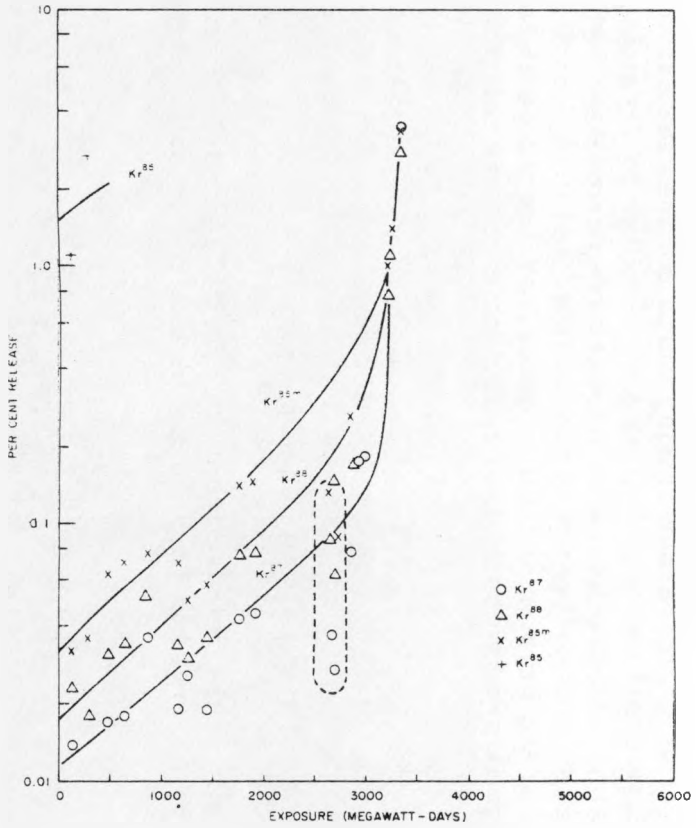

Fig. 35--Steady-state krypton release for capsule GA-309-9 (all points normalized to 1667°K)

involve the permeation of the carbon coating which encases the particles. The effect of radiation and thermal cycling may be either to develop microcracks in the coating, and thus increase its effective permeation coefficient, or to develop large cracks or breaks in the coating, and thus completely effect the release of the krypton and xenon diffusing from the particles. If the first process is predominant, the steady-state release fraction will be given by

$$F_i = F_i' \cdot F_i'',$$

where

$$F_i'(\lambda) = F_i^o(\lambda) \exp(-E_a/RT)$$

and is characteristic of the release from the $(Th, U)C_2$ particles (similar to release behavior observed in Linac experiments on uncoated particles), and where

$$F_i''(\lambda) = \frac{1/\lambda_i}{1/\lambda_i + \tau_p^i}.$$

Here, λ_i = the radioactive decay constant for the nuclide of element i,

$\tau_p^i = V'L/K_iA$ = the characteristic permeation time,

V' = the free void volume inside the coating,

L = the coating thickness,

A = the mean area of the coating,

K_i = the permeation coefficient of the coating for species i (a function of irradiation exposure and thermal history).

In the case of a complete break or large crack in the coatings,

$$F_i''(\lambda) = 1 .$$

It should be noted that near the end of the final reactor cycle, a thermocouple failed and capsules GA-309-8 and -9 were run at an unusually high temperature. Points corresponding to these high temperatures are enclosed by the dashed lines in Figs. 32 through 35.

KRYPTON AND XENON RELEASE FROM THE GAIL-IIIA FUEL ELEMENT

Results of the GAIL-IIIA test described above can be simply given by comparing the steady-state release fraction (R/B values) obtained as a

function of burnup (expressed as fissions per gram of thorium plus uranium) of the fuel particles with similar data for the GA-309 capsules (normalized to 1400°C). This is done for two representative fission products, Kr^{85m} and Xe^{133}, in Figs. 36 and 37, respectively. It is seen that while the steady-state release fractions are low in the case of GAIL-IIIA, they are not inconsistent with the early values shown by some of the GA-309 capsules and show a tendency to increase with burnup.

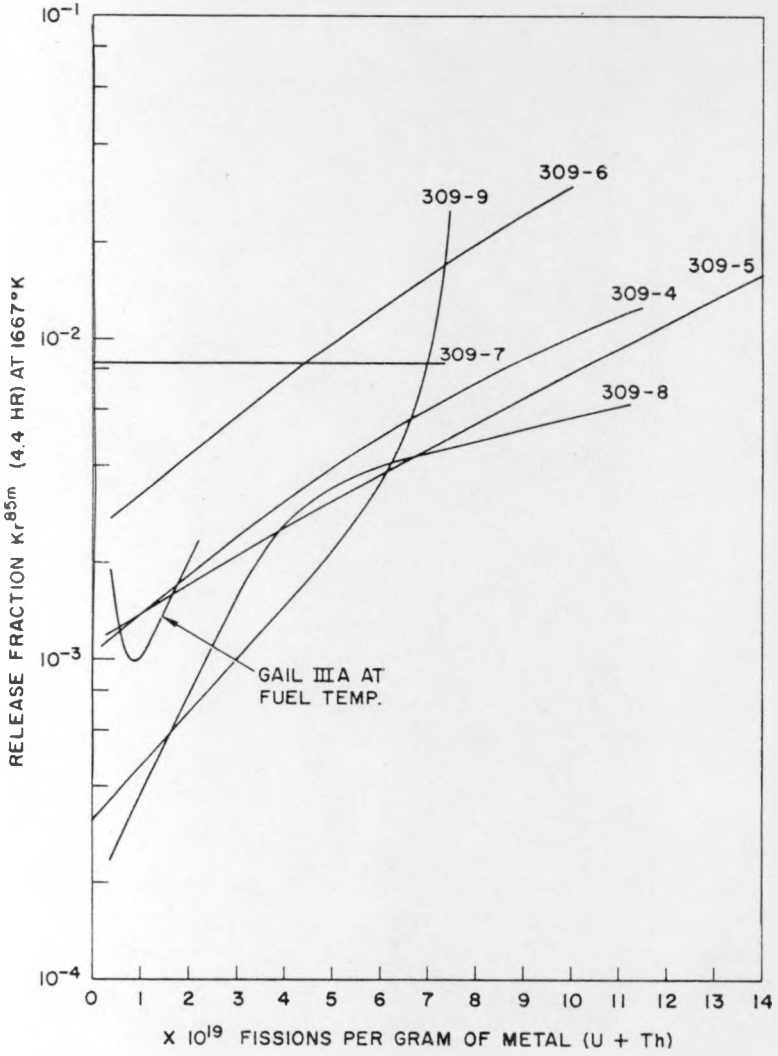

Fig. 36--In-pile steady-state release of Kr^{85m}

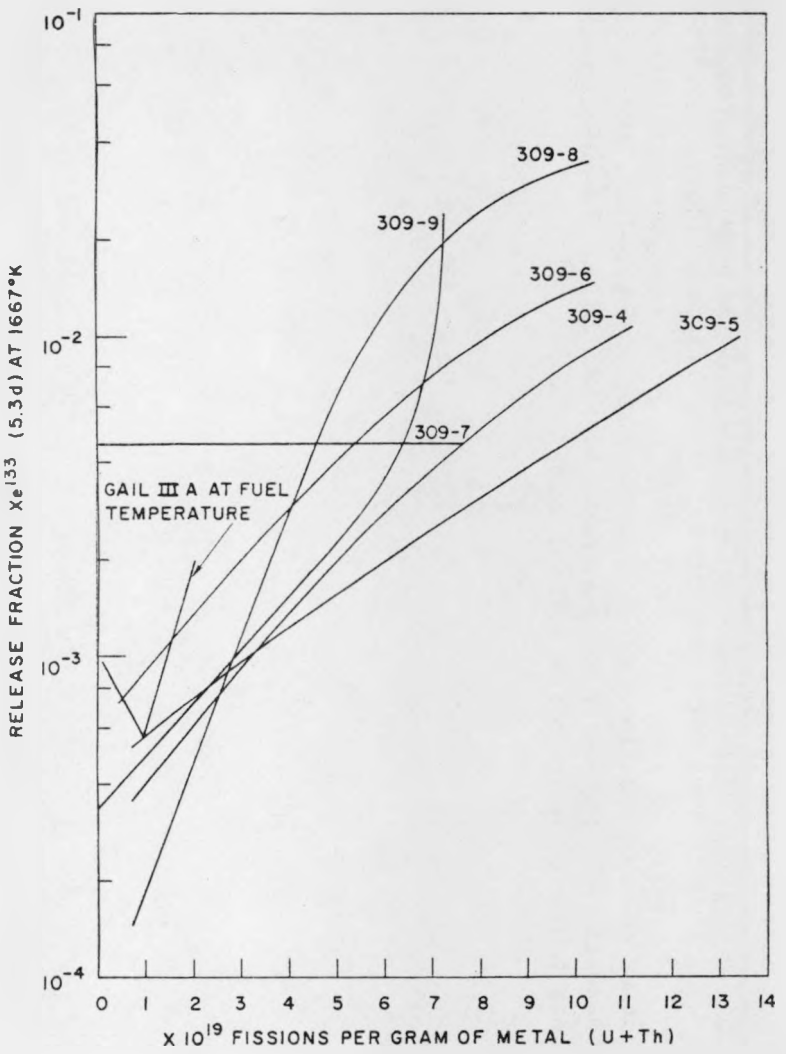

Fig. 37--In-pile steady-state release of Xe^{133}

SUMMARY

FURTHER INVESTIGATIONS

Our experience indicates that additional or new studies should be carried out on coated carbide fuel materials (which might include composite SiC or ZrC pyrolytic-carbon coatings as well as improved pyrolytic-carbon single or multiple coatings) to determine the following:

1. Krypton and xenon fission-product release as a function of burnup and type of neutron (fast or slow) flux.
2. Barium solubility and diffusion in various pyrolytic-carbon materials as functions of structure and density.
3. Cesium, strontium, barium, samarium, and europium retention by various types of pyrolytic-carbon and composite-carbide, pyrolytic-carbon coatings.
4. Diffusion of uranium and thorium in pyrolytic-carbon and carbide coatings.

CONCLUSIONS RELATIVE TO COATED-PARTICLE FUELS INVESTIGATED

The following conclusions have been reached from the studies reported here on Peach Bottom HTGR fuel materials consisting of pyrolytic-carbon-coated particles:

1. Barium and possibly other electropositive fission products penetrate pyrolytic-carbon-coated $(Th, U)C_2$ fuel particles (especially at temperatures $\geq 1400^{\circ}C$) and thus must be expected in the graphite fuel matrix and in fuel-element spine and sleeve graphite material.
2. Irradiation effects and high temperatures may lead to fuel-coating deterioration so that fission-product release becomes similar to that of uncoated fuel-particle material. Accordingly, to be conservative, the Peach Bottom HTGR fission-product trapping system was designed to handle steady-state release fractions (R/B) of the magnitude found for uncoated-particle fuel materials.
3. Present indications and further investigations of promising coated-particle fuel materials will very likely make conservative designs of HTGR fission-product trapping systems unnecessary.

REFERENCES

1. Fortescue, P., D. Nicoll, C. Rickard, and D. Rose, "HTGR-Underlying Principles and Design," Nucleonics, Vol. 18, No. 1, 1960, p. 86.

2. HTGR Quarterly Progress Reports: 40-Mw(e) Prototype High-temperature Gas-cooled Reactor Research and Development Program, General Atomic Reports GA-1235 (December 31, 1959); GA-1378 (March 31, 1960); GA-1640 (June 30, 1960); GA-1774 (September 30, 1960); GA-1982 (December 31, 1960); GA-2204 (March 31, 1961); GA-2493 (June 30, 1961); GA-2747 (September 30, 1961); GA-2861 (December 31, 1961); GA-3132 (March 31, 1962); GA-3396 (June 30, 1962).

3. Anderson, E. E., P. E. Gethard, and L. R. Zumwalt, Use of the King Furnace in Fission Product Retention Studies of Graphite Reactor Fuels, General Atomic Report GA-2394, October, 1961.

4. King, A. S., "An Electric Furnace for Spectroscopic Investigations with Results for the Spectra of Titanium and Vanadium," Astrophys. J., Vol. 28, 1908, p. 335.

5. Anderson, E. E., P. E. Gethard, and L. R. Zumwalt, Steady-state Release Fraction of Krypton and Xenon Fission Products at High Temperatures from (U, Th)C_2-Graphite Fuel Matrix in Out-of-pile Experiments, General Atomic Report GA-3211, June, 1962.

6. Wahl, A. C., "Nuclear Charge Distribution in Fission: Cumulative Yields of Short-Lived Krypton and Xenon Isotopes from Thermal-Neutron Fission of U^{235}," J. Inorg. & Nuclear Chem., Vol. 6, 1958, p. 263.

7. Booth, A. H., and G. T. Rymer, Determination of the Diffusion Constant of Fission Xenon in UO_2 Crystals and Sintered Compacts, Atomic Energy of Canada Limited Report CRDC-720, August, 1958.

8. Cubicciotti, D., The Diffusion of Xenon from Uranium Carbide-Impregnated Graphite at High Temperatures, North American Aviation Report NAA-SR-194, October 13, 1952.

9. Yajima, S., S. Ichiba, Y. Kamemoto, K. Shiba, and M. Kori, "The Behavior of Fission Products Captured in Graphite Powder by Nuclear Recoil: IV. Further Studies on the Diffusion of Xenon-133 in Graphite," Bull. Chem. Soc. Japan, Vol. 34, May, 1961, p. 694.

10. Belle, Jack (ed.), Uranium Dioxide: Properties and Nuclear Applications, Naval Reactors, Division of Reactor Development, U.S. Atomic Energy Commission, Washington D.C., 1961.

11. Kelley, Rodger, "The Diffusion of 'Attached' Inert-Gas Activity," Can. J. Chem., Vol. 39, 1961, p. 2411.

RADIATION BEHAVIOR OF GRAPHITE MATERIALS*

By H. H. Yoshikawa

Hanford Atomic Products Operation
General Electric Company, Richland, Washington

INTRODUCTION

The graphite work at Hanford has been concerned primarily with the radiation effects and chemical behavior of polycrystalline moderator graphite in a radiation environment. In recent years, with the discovery of radiation-induced contraction in graphite, the primary concern has been the dimensional stability of graphite at high temperatures. As part of the effort to understand the mechanism of dimensional changes in graphite, studies were begun on graphites having unusual structures. Our hypotheses on the mechanism of radiation-induced contraction are being tested by measuring the dimensional stability of these nonconventional graphite materials, such as pyrolytic graphite and low-permeability graphites. By reviewing the radiation effects in moderator graphite and by presenting some recent data on nonconventional graphite we hope to stimulate useful ideas and discussion in connection with the radiation effects observed in coated fuel particles.

The effects of irradiation at high temperature on the dimensional stability of moderator graphite and on polycrystalline graphites containing carbon blacks will be reviewed briefly. We will then describe some of our recent results on pyrolytic graphite. Finally, we will present some preliminary data on the effects of radiation on ceramics and on coated graphites. The irradiation effects in all cases are due to displacements created by fast neutrons. In the case of coated fuel particles, one must also consider the effects of fission fragments. However, in all probability the qualitative effects of the two types of irradiations are similar.

*Work performed under Contract No. AT(45-1)-1350 between the Atomic Energy Commission and General Electric Company.

SUMMARY AND CONCLUSIONS

Radiation-induced dimensional changes are emphasized. As a result of reactor radiation at high temperature, conventional graphites contract in both orientations. Pyrolytic carbon contracts in the direction parallel to the planes and expands perpendicular to the planes, while ceramic materials expand. In addition, an oxidation-resistant coating on graphite was shown to be resistant to radiation.

IRRADIATION EFFECTS ON POLYCRYSTALLINE GRAPHITES

Irradiations below approximately 300 C cause moderator graphites to expand transverse to the extrusion axis and contract parallel to the extrusion axis (Figure 1).[1] These effects can be traced to an expansion of the layer planes caused by interstitial atoms and groups of atoms and to a buckling of the planes. Expansion of the crystallographic c spacing and contraction of the a spacing are consistent with this idea. The expansion of the c axis is reflected in a bulk expansion transverse to the extrusion axis. Contraction parallel to the extrusion axis is not as well understood, but has been ascribed to buckling of the planes along the a axis. The different rates of contraction of several grades of graphite shown on Figure 1 can be explained by the different anisotropies and different graphitization temperatures.

As the irradiation temperature is increased above 30 C, the dimensional changes are greatly reduced. The effect of irradiation temperature on dimensional changes transverse to the extrusion axis is shown in Figure 2.[2] At approximately 300 C, contraction transverse to the extrusion axis is observed. This is shown in more detail in Figure 3.[3] A slight expansion occurs initially in most graphites followed by a fairly linear contraction. Again, the contraction rates can be explained fairly well by differences in the anisotropy and crystallinity of the graphites.

Although the contraction rates shown in Figure 3 are relatively small, relatively large displacements can occur in a large graphite structure after a 20-yr exposure. For example, in the case of CSGBF graphite the contraction rate is approximately 0.015 per cent per 1000 MWD/AT. When extrapolated to 150,000 MWD/AT, the total depression at the top of a 30-ft horizontal graphite

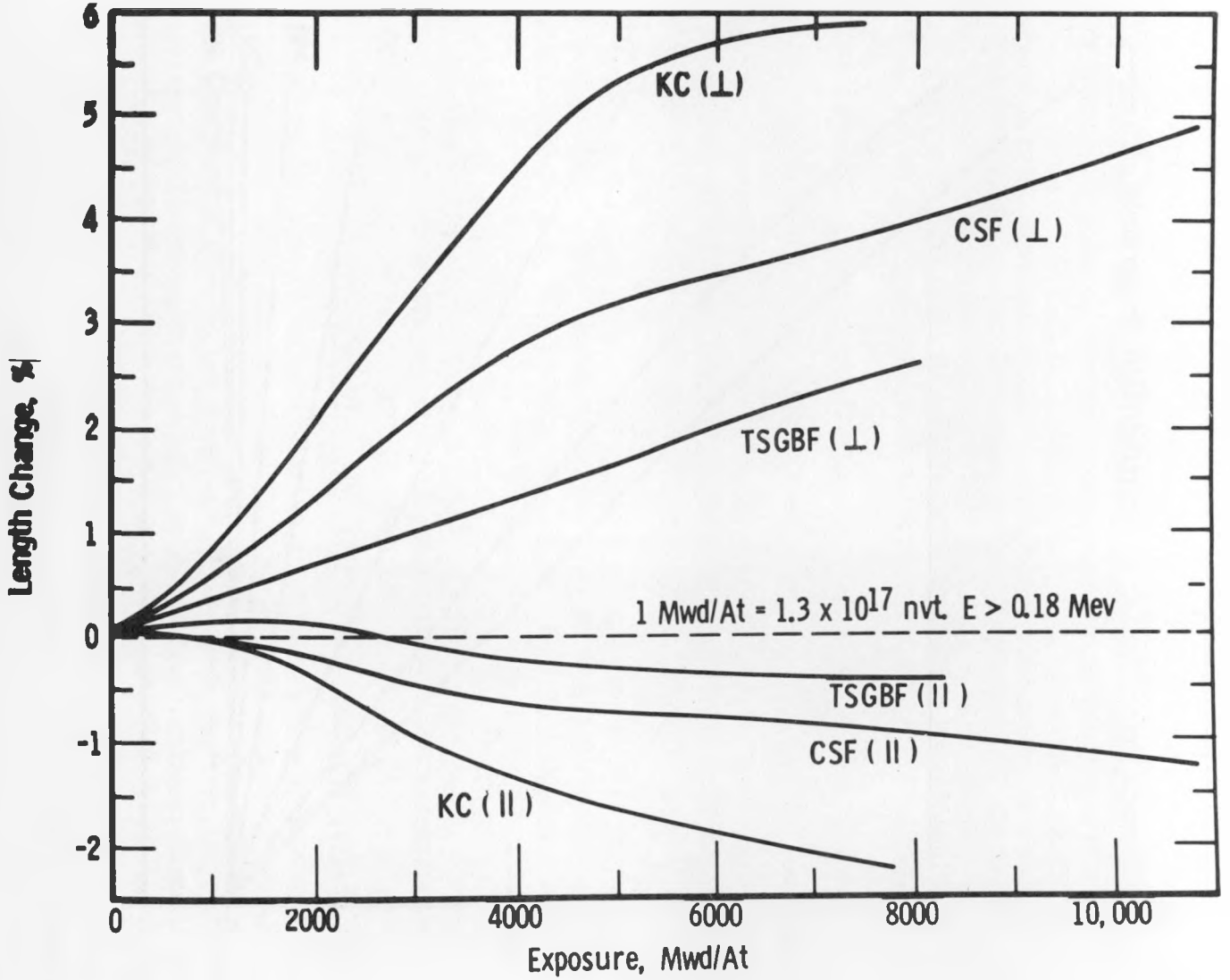
KC (⊥)
CSF (⊥)
TSGBF (⊥)
1 Mwd/At = 1.3 x 10^17 nvt. E > 0.18 Mev
TSGBF (II)
CSF (II)
KC (II)
Length Change, %
Exposure, Mwd/At
6
5
4
3
2
1
0
-1
-2
0
2000
4000
6000
8000
10,000

FIGURE 1

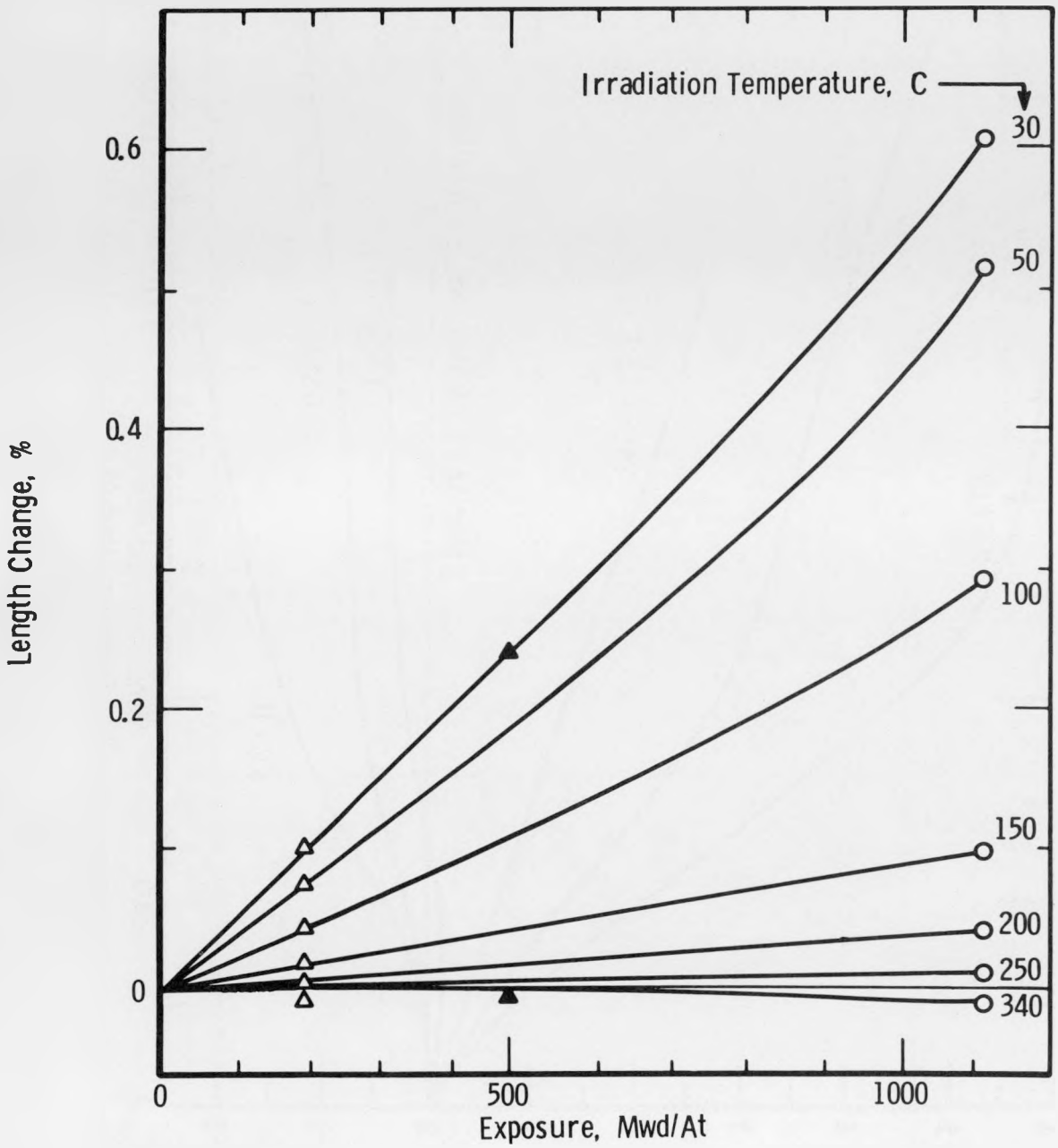
Irradiation Temperature, C
30
50
100
150
200
250
340
0.6
0.4
0.2
0
0
500
1000
Length Change, %
Exposure, Mwd/At

FIGURE 2

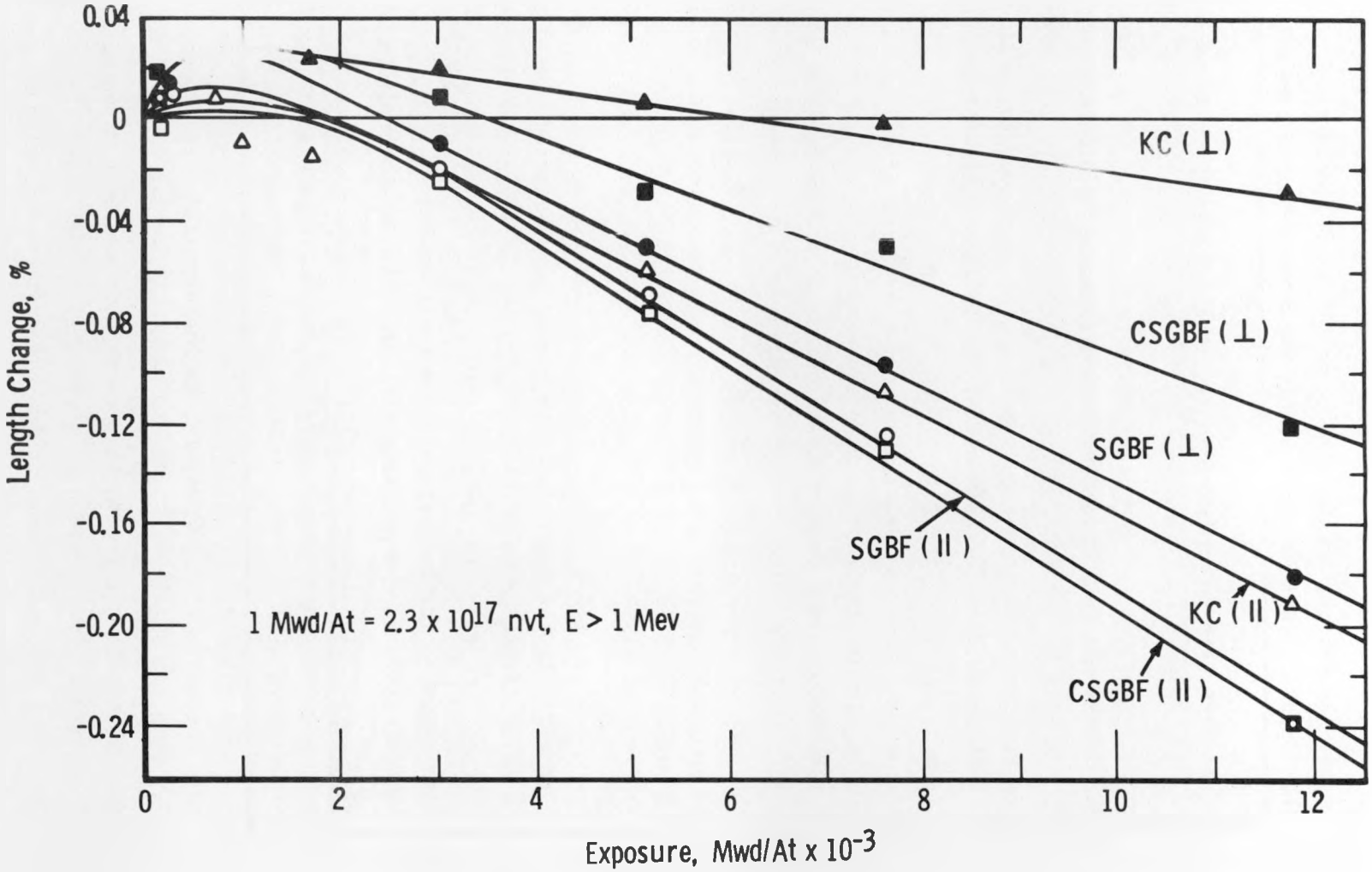
0.04
0
-0.04
-0.08
-0.12
-0.16
-0.20
-0.24
Length Change, %
0
2
4
6
8
10
12
Exposure, Mwd/At x 10^{-3}
1 Mwd/At = 2.3 x 10^{17} nvt, E > 1 Mev
KC (⊥)
CSGBF (⊥)
SGBF (⊥)
SGBF (II)
KC (II)
CSGBF (II)

FIGURE 3

stack would be 8 in. This is a very large dimensional change to accommodate in the reactor design. Hence there has been a concerted effort in recent years to ascertain whether the contraction continues at a linear rate and also to develop graphites that are more stable under high-temperature irradiation.

Irradiations have been conducted recently in the temperature range 475 to 800 C to much higher neutron exposures.[4] The results for CSF graphite transverse to the extrusion axis are illustrated in Figure 4. The maximum exposure of 8.6×10^{21} nvt ($E > 0.18$ Mev) is approximately equivalent to 60,000 MWD/AT. It will be noted that even after this relatively long exposure the contraction transverse to the extrusion direction continues to be linear with exposure with no evidence of saturation. It is also interesting to note that in this temperature range the rate of contraction decreases with irradiation temperature. Davidson and Helm[5] have conducted a few irradiations as high as 1200 C. A minimum contraction rate was observed at about 800 C, and at higher temperatures the rate of contraction again increases.

The general behavior parallel to the extrusion axis is somewhat similar[4] except that the rate of contraction is higher (Figure 5). Similar observations have been made on graphites that will be used in the Experimental Gas Cooled Reactor at Oak Ridge.[4]

In addition to the technological interest in dimensional stability of graphite, the contraction effect itself is of considerable scientific interest. Contraction transverse to the extrusion axis cannot be attributed simply to changes in the crystallites because they actually expand, even at high irradiation temperatures. The following general observations need to be explained by any mechanism proposed for radiation-induced contraction.

1. Graphite shrinks in the predominant c direction when irradiated above 300 C, while at the same time the c spacing expands.
2. Factors that increase the ultimate crystallinity reduce the contraction rate.
3. Most of the shrinkage transverse to the extrusion axis does not anneal, whereas shrinkage parallel to the extrusion axis does anneal when the sample is heated to high temperatures.

A mechanism that accounts for these observations has been proposed by de Halas and Yoshikawa.[6] Contraction is attributed to two separable processes. The first process is akin to low-temperature radiation damage and involves a slight expansion of the crystallites parallel to the c axis

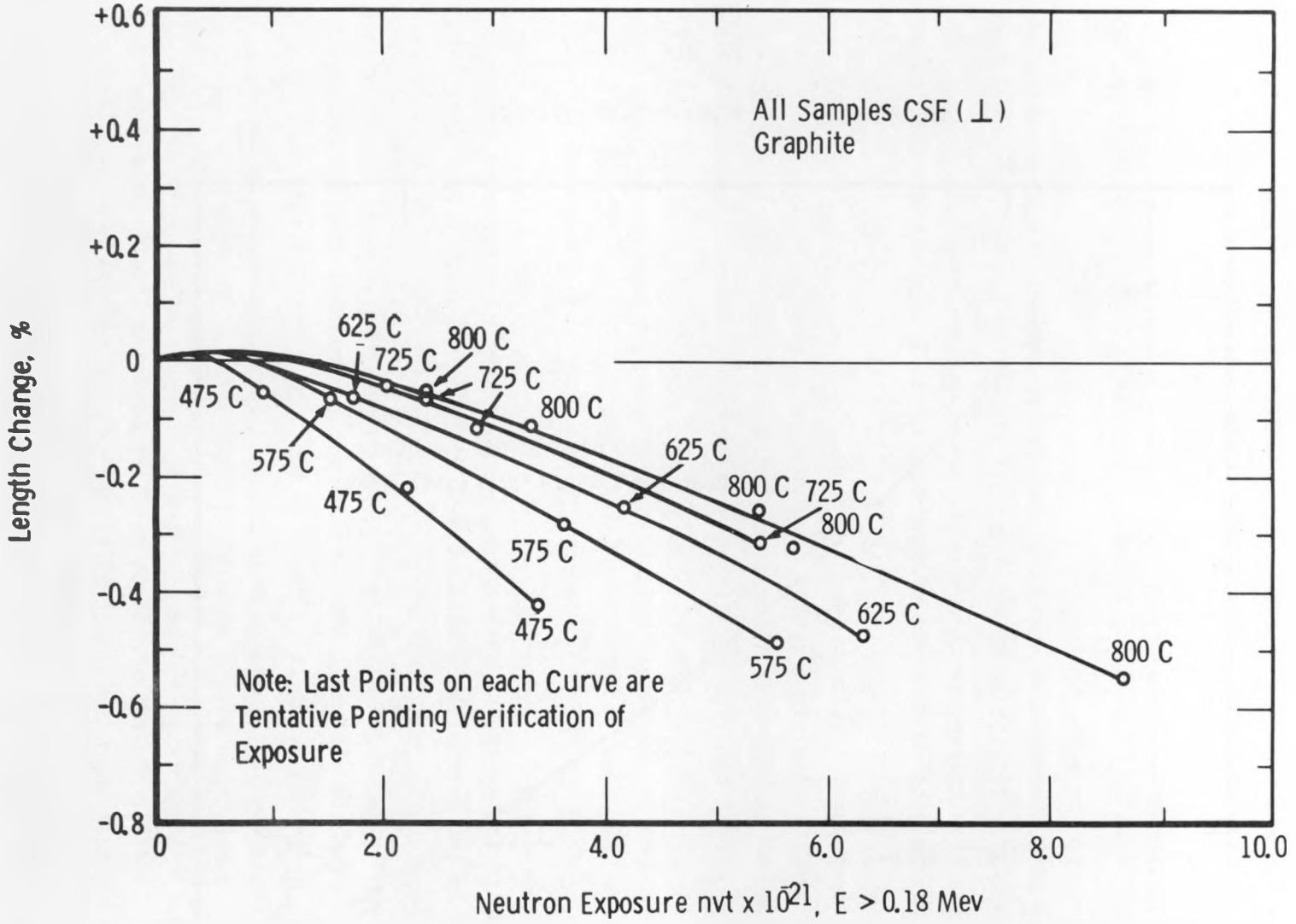
All Samples CSF (⊥)
Graphite
Length Change, %
+0.6
+0.4
+0.2
0
-0.2
-0.4
-0.6
-0.8
0
2.0
4.0
6.0
8.0
10.0
Neutron Exposure nvt x 10^21, E > 0.18 Mev
625 C
725 C
800 C
725 C
800 C
475 C
575 C
625 C
800 C
725 C
800 C
475 C
575 C
625 C
800 C
475 C
575 C
Note: Last Points on each Curve are
Tentative Pending Verification of
Exposure

FIGURE 4

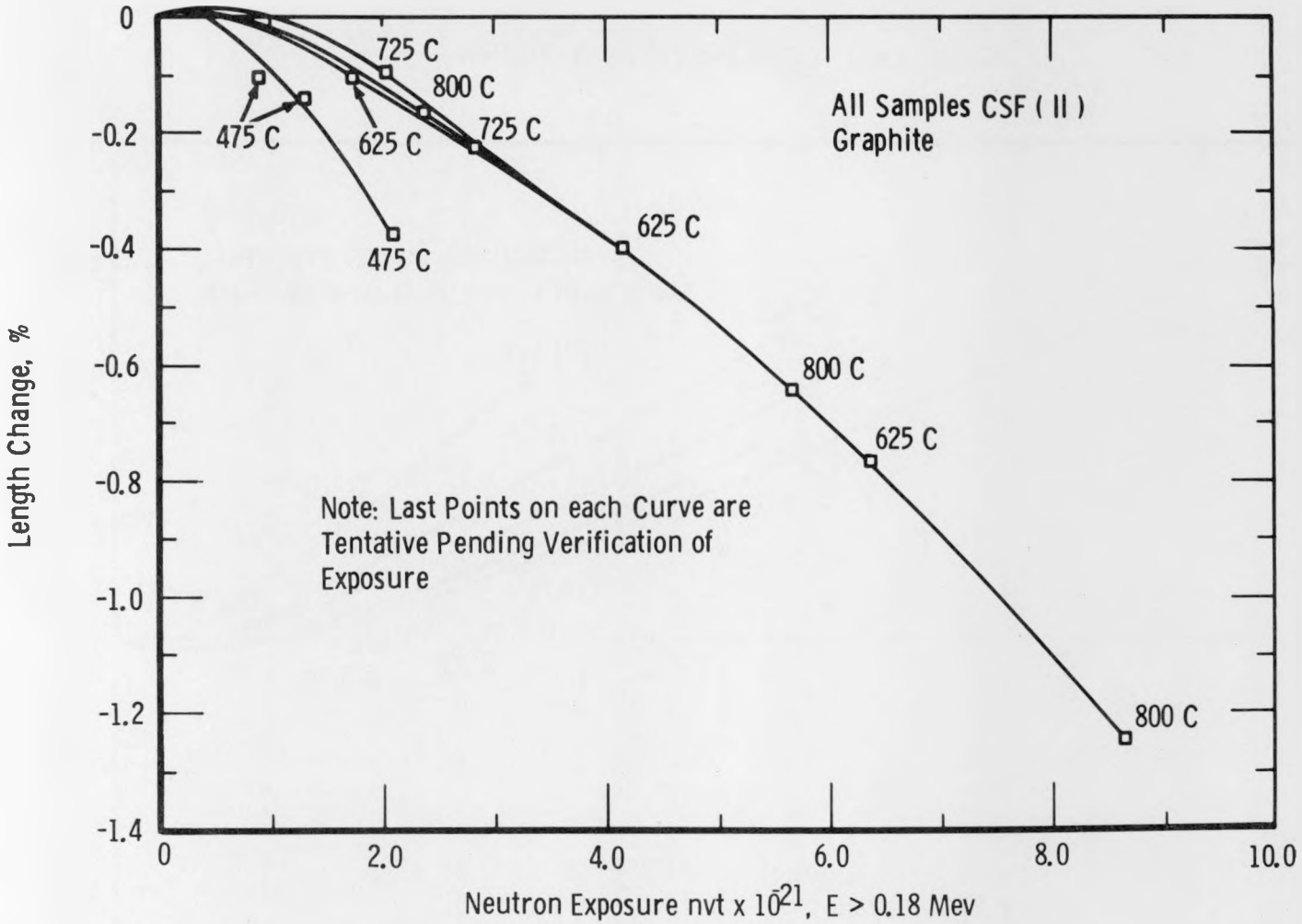
0
-0.2
-0.4
-0.6
-0.8
-1.0
-1.2
-1.4
Length Change, %
0
2.0
4.0
6.0
8.0
10.0
Neutron Exposure nvt x 10^21, E > 0.18 Mev
All Samples CSF (II)
Graphite
725 C
800 C
475 C
625 C
725 C
625 C
475 C
800 C
625 C
800 C
Note: Last Points on each Curve are
Tentative Pending Verification of
Exposure

FIGURE 5

and a corresponding contraction parallel to the a axis. Because this type of damage is annealable, the amount of crystallite expansion and contraction is a function of the irradiation temperature, and this largely accounts for the temperature dependence in the radiation stability of graphite. The second process is nonannealable and seems to result from a graphitization-like phenomenon in poorly graphitized regions of polycrystalline graphite. The poorly graphitized regions appear to originate primarily in crystallite boundaries and particle boundaries, i.e., the binder in the graphite. The degree of anisotropy of the graphite largely determines the interaction of the annealable and nonannealable dimensional changes and hence controls the over-all behavior of graphite under high-temperature irradiation. The use of low graphitizing temperatures or poorly graphitizing filler or binder increases the amount of nonannealable contraction and decreases the stability of the graphite.

IRRADIATION EFFECTS ON MIXED GRAPHITE-LAMPBLACK MATERIALS

The effect of a nongraphitic component on the dimensional stability of a body is of interest because the graphite matrix for fuel particles usually contains lampblack or binder that has not been fully graphitized. Data are presented in Table 1 for graphites with several concentrations of lampblack added to a pregraphitized filler and graphitized to 3000 C. It is apparent that the addition of lampblack reduces the dimensional stability of the material. The dimensional change observed in the material with 50 per cent lampblack was approximately five times as great as for the material with no lampblack addition. Thus graphite fuel matrices which contain sizable lampblack additions must be expected to contract as a result of continued irradiation at elevated temperatures.

A sample of 100 per cent lampblack-based graphite heat treated to 1400 C is being irradiated in an attempt to attain saturation in contraction. Thus far a total linear contraction of 3 per cent has been observed, which is one-fourth the linear contraction necessary for theoretical density.[8] It appears, however, that the rate of contraction is decreasing with increasing exposure.

TABLE 1. IRRADIATION[a] OF GRAPHITE-THERMAX SERIES[7]

Mix Composition, per cent of filler by weight			Length Change, per cent	
Artificial Graphite Powder	Thermax Carbon Black	Pitch Binder	Transverse	Parallel
100	0	440	-0.014 ± 0.008	-0.035 ± 0.015
80	20	285	-0.044 ± 0.008	-0.039 ± 0.006
75	25	285	-0.047 ± 0.005	-0.046 ± 0.000
67	33	265	-0.043 ± 0.005	-0.060 ± 0.004
50	50	310	-0.068 ± 0.008	-0.061 ± 0.004
CSF (for comparison)			0.000	-0.015

(a) Exposure: 6.2×10^{20} nvt, E > 0.18 Mev.

IRRADIATION EFFECTS ON PYROLYTIC GRAPHITE

Radiation effects on the dimensions of samples and on the coefficient of thermal expansion have been obtained. These irradiation studies were initiated since pyrolytic graphite was thought to be analogous to the small, fairly perfect crystallites which occur in reactor-grade graphites. On the basis of data assembled on reactor graphite, it was anticipated that during irradiation at approximately 600 C pyrolytic specimens would expand in the direction transverse to the layer planes and contract in the parallel direction. Previous preliminary data had indicated an expansion in both directions; however, those results were obtained on cleaved sections from laboratory-produced material. Both the deposition conditions and the cleavage undoubtedly yielded samples in highly stressed condition. Later data were obtained on samples cut from the full thickness of material obtained from a production facility. Deposition temperature was 2200 C at a few millimeters gas pressure. The original slab was about 1/3 in. thick and 2 sq ft in area. All samples were machined from this one plate. Hence the data reported here are believed more reliable.

The dimensional changes in pyrolytic graphite which occurred as a result of irradiation are presented in Figure 6. A small contraction occurred in the parallel direction and an expansion in the transverse direction. Thus these dimensional changes conformed to expectations based on earlier studies. Data points for CSF, a typical reactor-grade graphite, are included to illustrate the different behavior of pyrolytic graphite. The total maximum irradiation exposure to the samples was on the order of 6×10^{20} nvt ($E > 0.18$ Mev), and the temperature of irradiation was about 650 C.

The effect of radiation on the coefficient of thermal expansion was most pronounced in the transverse direction with a change from 23×10^{-6} in./in./C to 20×10^{-6} in./in./C over the range 25 to 425 C after 6×10^{20} nvt. In the parallel directions, changes were quite small and were variable; the average change for four samples was zero. Changes were on the order of $\pm 0.05 \times 10^{-6}$ in./in./C.

It may be inferred from these data that irradiations would cause a decrease in circumference of pyrolytic carbon shells but a slight increase in thickness. An exact analysis would be quite difficult since both temperature and exposure gradients exist radially. In addition the relation

FIGURE 6

RADIATION INDUCED DIMENSIONAL CHANGES IN PYROLYTIC GRAPHITE

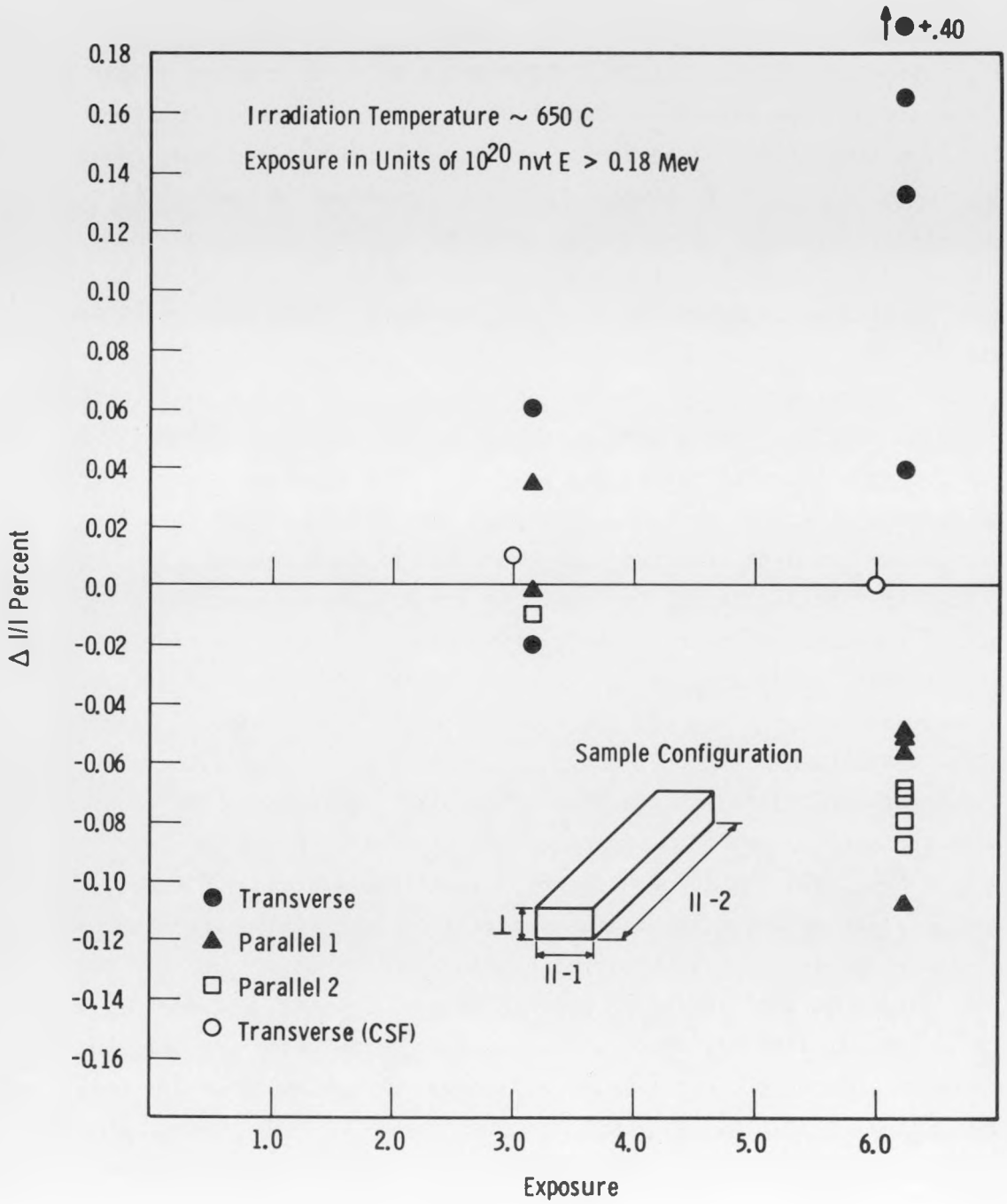

between fission-fragment damage and fast-neutron damage must be known. However, if the enclosed fuel material did not contract, thus inhibiting contraction in the coating, tensile tangential stresses tending to cause splitting may develop in the coating.

IRRADIATION EFFECTS ON CERAMICS AND COATINGS

Some information on dimensional changes as a result of irradiation on ceramic materials has been obtained. Samples 1/2 in. in diameter by 4 in. long of polycrystalline aluminum oxide, magnesium oxide, and translucent high-density aluminum oxide were irradiated and the results are presented in the next figure. Each point represents a separate sample, thus the data at the two exposures were obtained on different sets of samples. Measurement accuracy is ± 0.003 per cent or ± 0.0001 in. As one can see, expansions on the order of 0.15 per cent were observed in aluminum oxide samples whereas the expansion in magnesium oxide was on the order of 0.10 per cent. The exposures are on the order of 3×10^{20} and 6×10^{20} nvt at approximately 650 C. These results are pertinent to the fission-fragment-induced strain studies on ceramic disks being conducted here at Battelle. Both studies are in agreement that irradiation produces an expansion of the material.

The last item involves the testing of siliconized-silicon carbide coatings on graphite samples.[9] The objective of this work is to determine the feasibility of using such coatings to protect graphite from oxidation. These graphite-coated samples were first tested in air at 1000 C for approximately 150 hr prior to irradiation to test the integrity of the coatings. Weight losses were less than 0.05 per cent; therefore, the graphite was adequately protected. After irradiation to approximately 2×10^{21} nvt at 500 C, samples were again tested at 1000 C in air. Samples made from fairly isotropic graphites with a coefficient of thermal expansion of 3.9 and 5.0×10^{-6}/C (closely matching the value of 4.0×10^{-6}/C for SiC) were superior in performance. During tests up to 500 hr only one out of ten such samples failed. Of the four samples tested to 500 hr, the maximum weight loss was 0.004 per cent. Thus it is apparent that under these test conditions siliconized SiC coatings afford excellent protection against oxidation even after reactor radiation.

FIGURE 7

RADIATION INDUCED DIMENSIONAL CHANGES IN CERAMICS

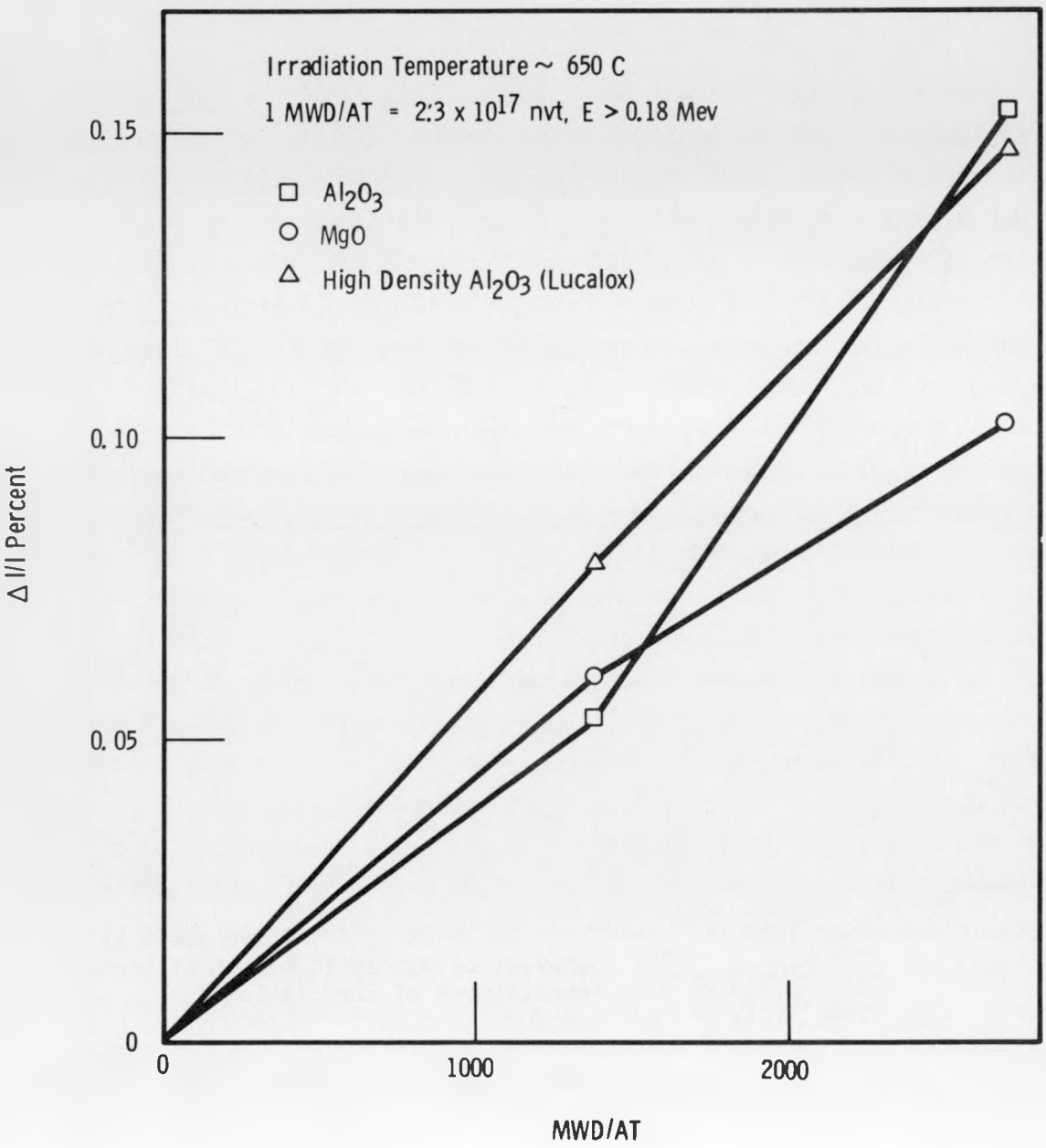

REFERENCES

1. J. M. Davidson, et al., High Temperature Radiation-Induced Contraction in Graphite, in Proceedings of the Fourth Conference on Carbon Held at the University of Buffalo, pp. 599-605, Pergamon Press, New York, 1960.
2. J. F. Fletcher, Hanford Atomic Products Operation, Hanford Laboratories, unpublished data, 1956.
3. R. E. Nightingale, H. H. Yoshikawa, and E. M. Woodruff, Chapter 9, Radiation-Induced Structural and Dimensional Changes, in Nuclear Graphite, pp. 259-293, Academic Press, 1962.
4. H. H. Yoshikawa, et al., IAEA Symposium on Radiation Damage in Solids and Reactor Materials, Venice, May 7-11, 1962.
5. J. M. Davidson and J. W. Helm, Effect of Temperature on Radiation-Induced Contraction of Reactor Graphite, in Proceedings of the Fifth Conference on Carbon Held at Pennsylvania State University, June 19-23, 1961, Pergamon Press, 1962.
6. D. R. de Halas and H. H. Yoshikawa, Mechanism of Radiation Damage to Graphite at High Temperatures, in Proceedings of the Fifth Conference on Carbon Held at Pennsylvania State University, June 19-23, 1961, Pergamon Press, 1962.
7. E. M. Woodruff, Hanford Laboratories, unpublished data, 1962.
8. H. H. Yoshikawa, Hanford Laboratories, unpublished data, 1962.
9. J. L. Jackson, The Effect of Irradiation on Siliconized-Silicon Carbide Coatings for Graphite, USAEC Report HW-68494, Hanford Atomic Products Operation, February 1961.

* * *

DISCUSSION

Question, L. L. Lyon (LASL): "Would you make an intuitive guess as to the behavior of pyrolytic carbon at higher temperatures of irradiation?"

Reply, H. H. Yoshikawa (HAPO): "I expect similar behavior but perhaps smaller expansion in the transverse direction."

COATED FUEL PARTICLE DEVELOPMENT AND EVALUATION

By C. C. Browne and R. E. Latta

Nuclear Materials and Propulsion Operation
General Electric Company, Cincinnati 15, Ohio

INTRODUCTION

The objective of the work on coated fuel particles at the Nuclear Materials and Propulsion Operation of the General Electric Company is to prepare coated fuel particles less than 50 microns in diameter and to evaluate them in ceramic matrices for possible fuel-element application. Work areas include preparation of spherical particles, coating of the spheres with oxidation-resistant ceramic materials, and incorporation of the particles in a ceramic matrix for tests of strength, thermal stability, oxidation stability, and performance under irradiation. Accomplishments have included spheroidization of powders with melting points up to approximately 3300 C, vapor-process deposition of alumina coatings on spheres down to 44 microns in diameter, preparation of sols, and incorporation of sol materials in ceramic matrices to yield sintered bodies with good high-temperature stability.

PREPARATION OF SPHERICAL PARTICLES

Powders of high-melting-point oxides have been spheroidized in plasma flames. Initially, particles were spheroidized in the flame of a Thermal Dynamics plasma gun of the type shown in Figure 1. The plasma was formed by electrical discharge between two electrodes. Particles, transported by a carrier gas, entered the plasma near the exit end of the gun; and the hot spheres were cooled and collected in the collecting chamber shown in Figure 2.

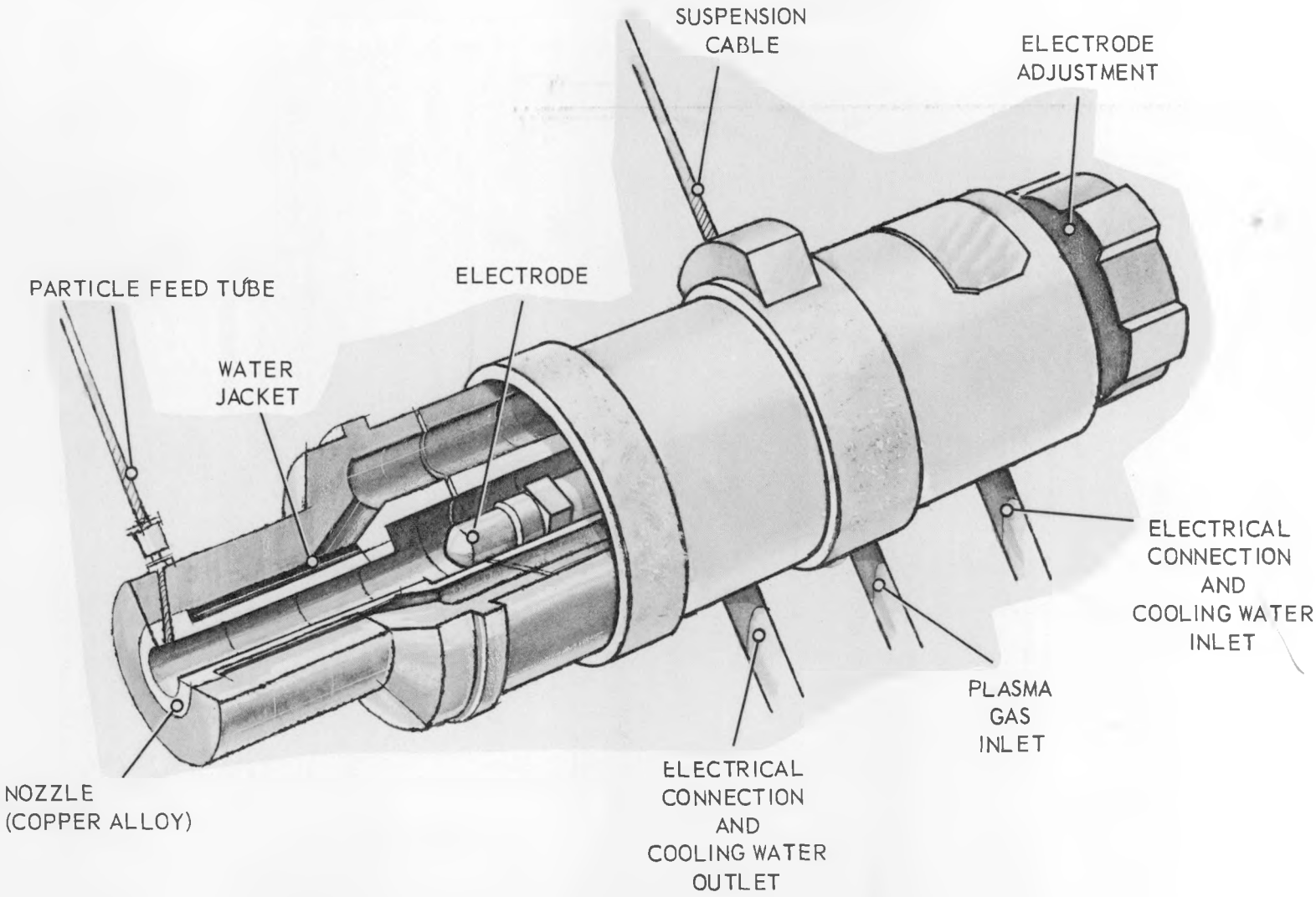

Figure 1 - Thermal dynamics gun modified for power spheroidization.
AS-153

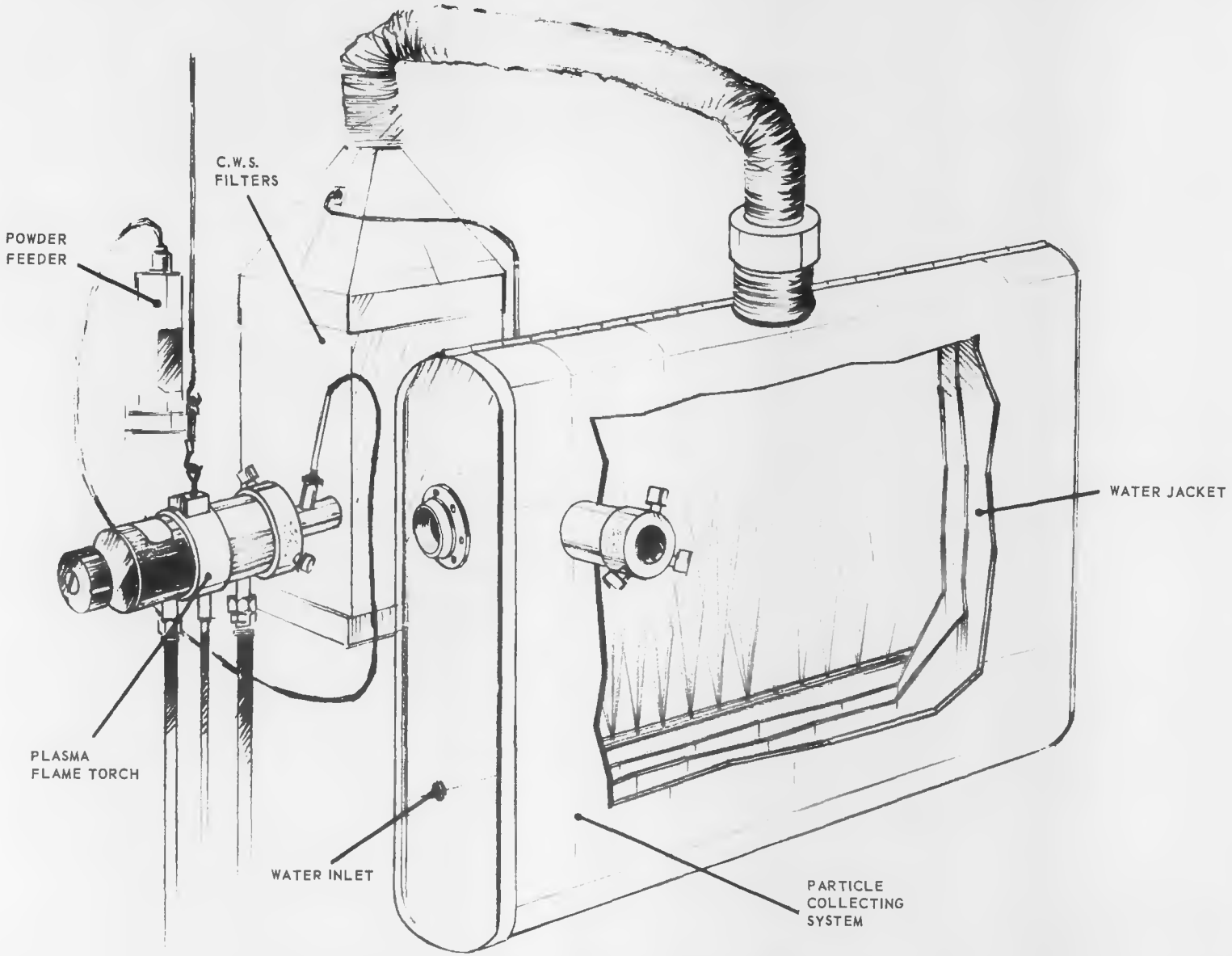

Figure 2 - Schematic diagram of fuel particle collecting system.
AS-160

A mixture of argon and helium was usually used to form the plasma, and a flow of nitrogen gas through a modified DeVilbiss powder blower assembly carried the feed particles to the plasma region. Spheroidizing of powder particles in the -270 +325 U.S.B.S. sieve-number size range was carried out at settings of 600 amp and 32 v with gas flows of 30 scfh argon and 10 scfh helium to the plasma gun and 3 scfh of nitrogen through the particle feed system.

Uranium dioxide particles in the -270 +325-mesh size range have been spheroidized in the Thermal Dynamics plasma gun. Good spheroidization of over half of the particles was attained. However, a small fraction of the spheres was contaminated with copper from the electrodes, and a few particles contained large voids caused by gas entrapment during spheroidization. Some progress was made in reducing the voids, but work with the Thermal Dynamics equipment was recessed eventually in favor of work with an electrodeless system.

A plasma can be formed by coupling rf power of sufficiently high frequency from an induction coil to a gas flowing spirally through a tube placed in the coil. The plasma is initiated by heating graphite or a refractory metal momentarily in the field and continues to propagate against the gas flow. A 7.5-kw Lepel Induction Generator at GE-NMPO* has been modified to generate power at approximately 5 mc and is being used to spheroidize refractory powders with the assembly shown in Figure 3. The particles are dropped through a quartz tube and are spheroidized while passing through the plasma zone. Important features of the apparatus are (1) the water jacket for cooling the quartz tube, (2) the system for aligning the concentric tubes to provide a symmetrical flow pattern, and (3) the aspirator system (not shown) for controlling rate and uniformity of particle feed. To obtain a smooth flow of particles it is necessary that the range in particle size be narrow. In Figures 4, 5, and 6 are shown photomicrographs of ThO_2, UO_2, and ZrO_2 particles, respectively, before and after spheroidization. As may be noted, spheroidization is essentially complete with each material, but some porosity remains. With the exception of the visible porosity, the density of the spherodizied particles is quite high. Whether or not the porosity is desirable may depend upon the reactor application of the particles and should be a subject of future investigation.

---

*Nuclear Materials and Propulsion Operation of the General Electric Company, Cincinnati 15, Ohio

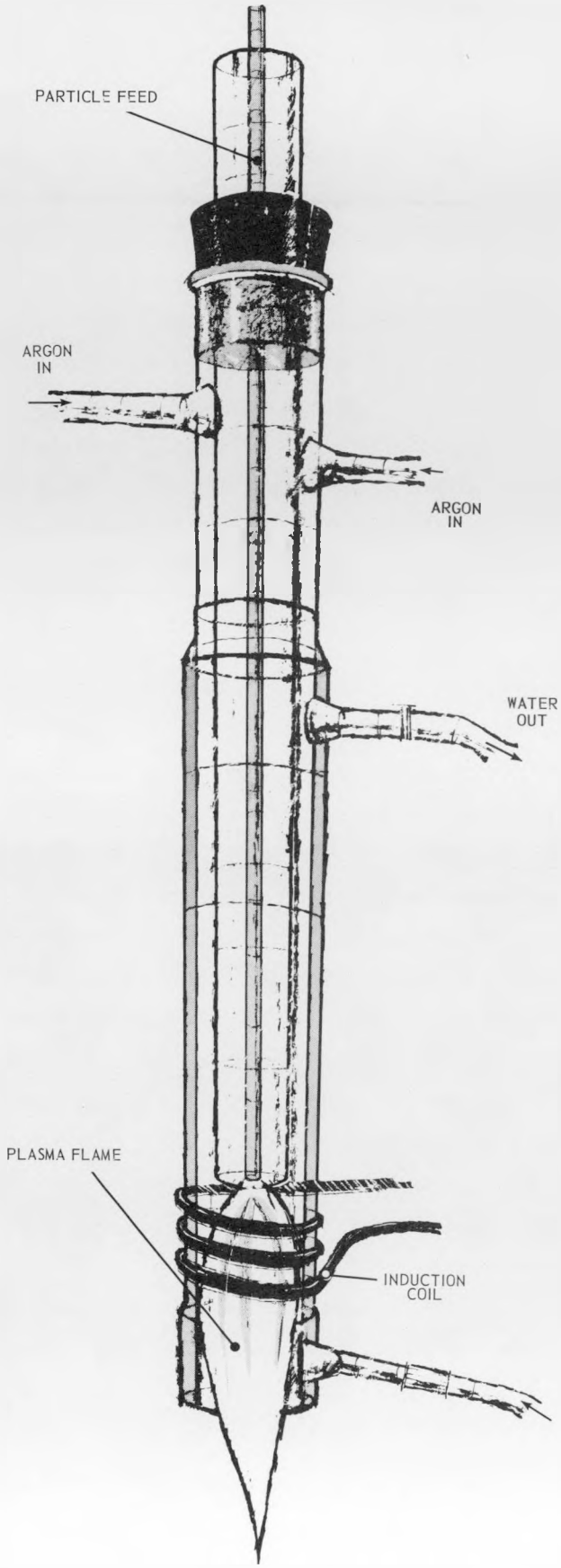

Figure 3 - Assembly for spheroidizing particles in the inductively coupled plasms apparatus. AS-116

Neg. No. 1582 Unetched 500X

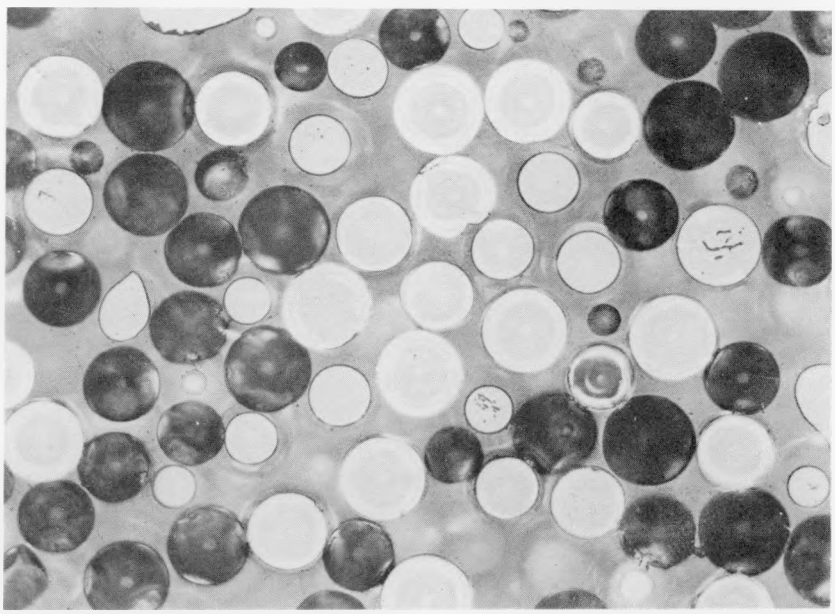

Neg. No. 1583 Unetched 500X

FIGURE 4. Thoria particles before and after spheroidization in inductively coupled plasma apparatus.

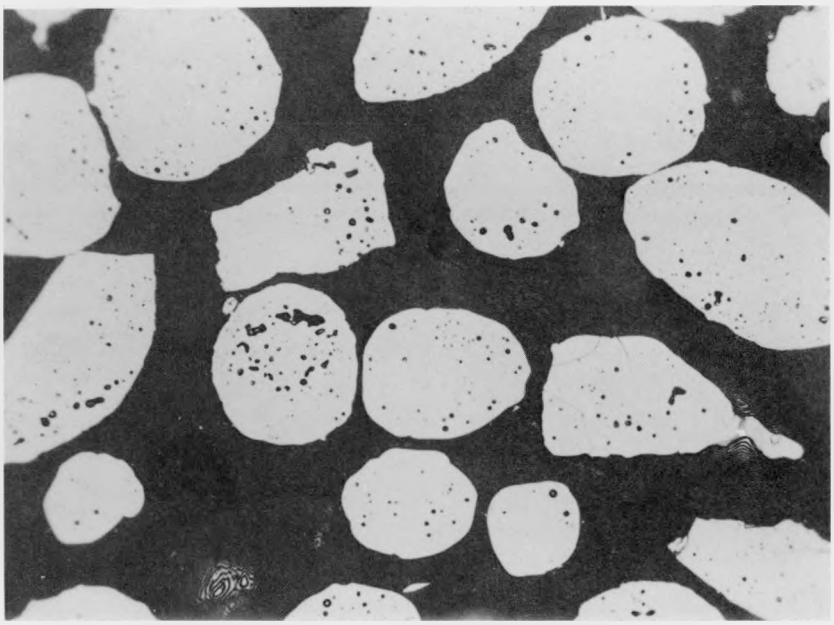

Neg. No. 1304 Unetched 500X

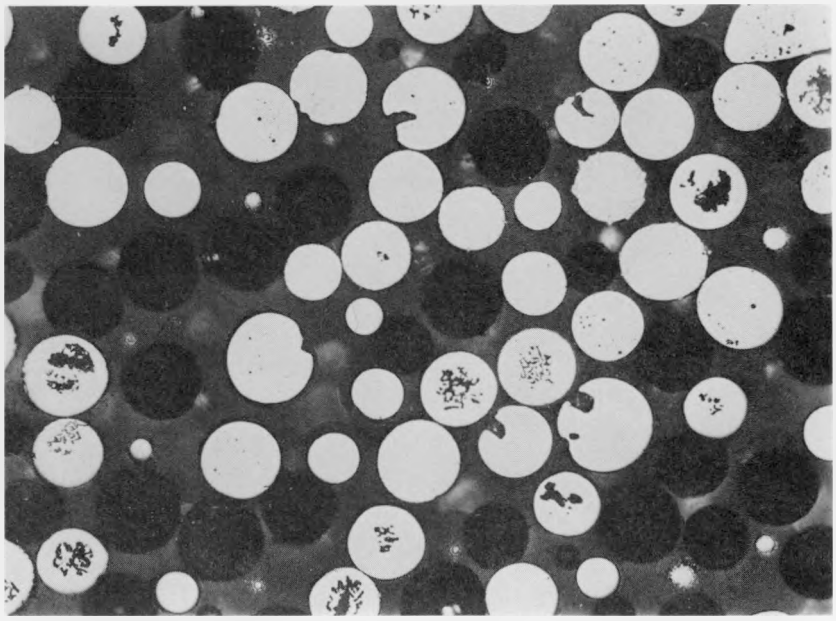

Neg. No. 1584 Unetched 500X

FIGURE 5. Urania particles before and after spheroidization in inductively coupled plasma.

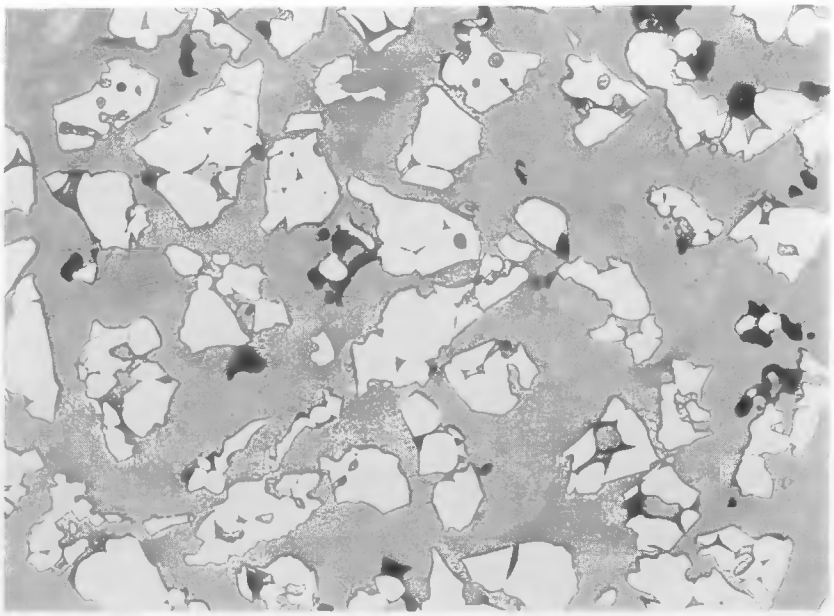

Neg. No. 1585 Unetched 500X

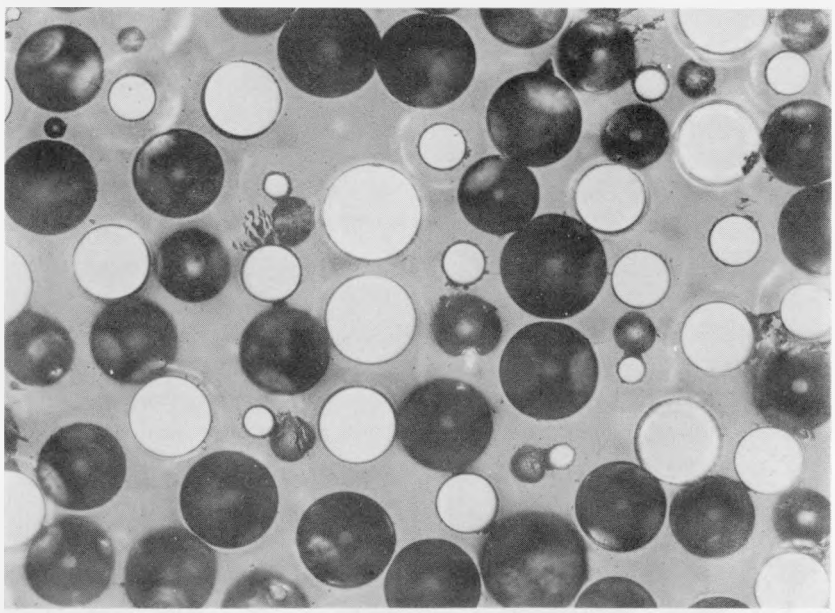

Neg. No. 1586 Unetched 500X

FIGURE 6. Zirconia particles before and after spheroidization in inductively coupled plasma apparatus.

Wet Chemistry

The objective of the wet-chemistry method is to coat spherical fuel particles with a hydrous oxide which can be thermally converted to the desired oxide. Such a coating might be attained by homogeneous hydrolysis of a salt of the desired oxide in a solution in which the fuel particles are kept in suspension by stirring. As shown in Figure 7 a coating has been applied to NUMEC UO_2 particles by the urea hydrolysis of aluminum chloride in the presence of succinate anion. As has been shown earlier*, the physical character of the p ate in homogeneous precipitation is considerably affected by the p: of certain anions, and essentially no coating was deposited when the ysis of aluminum chloride with urea was carried out in the absence cinate anion.

Vapor Reaction Processes

A spiral-bed coating apparatus, shown in Figure 8, has been used to deposit alumina coatings on fuel spheres by a vapor-reaction coating process. The coating oxide is produced in the coating chamber by the reaction of a metallic chloride with water vapor as shown in the following chemical equation:

$$MCl_x + \frac{x}{2} H_2O \longrightarrow MO_{x/2} + xHCl.$$

The required water vapor can be produced in the reaction chamber by the reaction:

$$H_2 + CO_2 \longrightarrow H_2O + CO.$$

In the spiral-bed apparatus the reacting gases are brought to the reaction chamber along two separate paths as shown in Figure 8. Along one path the gases enter tangentially through the wall of the reaction chamber, and the fuel particles are thus caused to spiral upward. The increase in hydraulic diameter with height causes a gradual decrease in velocity of the spiraling gases and thus permits the particles to drop from the gas stream alongside the tube projecting from the floor of the chamber. Therefore, the particles pass repeatedly through the coating zone near the bottom of the chamber. The fluidizing efficiency of the bed appears to be quite high, and fuel

*L. Gordon, M. L. Salutsky, and H. H. Willard, Precipitation from Homogeneous Solution, John Wiley and Sons, Inc., New York (1959).

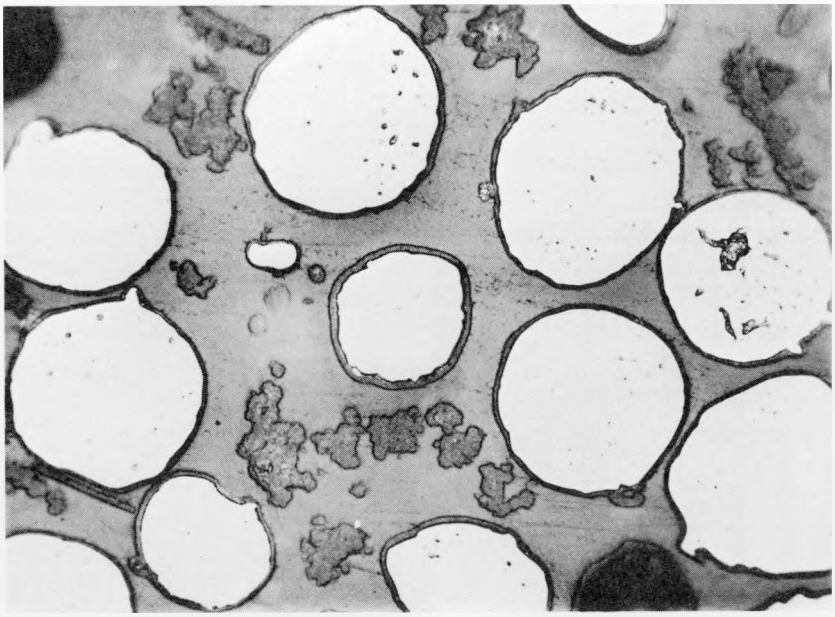

Neg. No. 1376 Unetched 500X

FIGURE 7. NUMEC urania particles coated by the urea hydrolysis of $AlCl_3$.

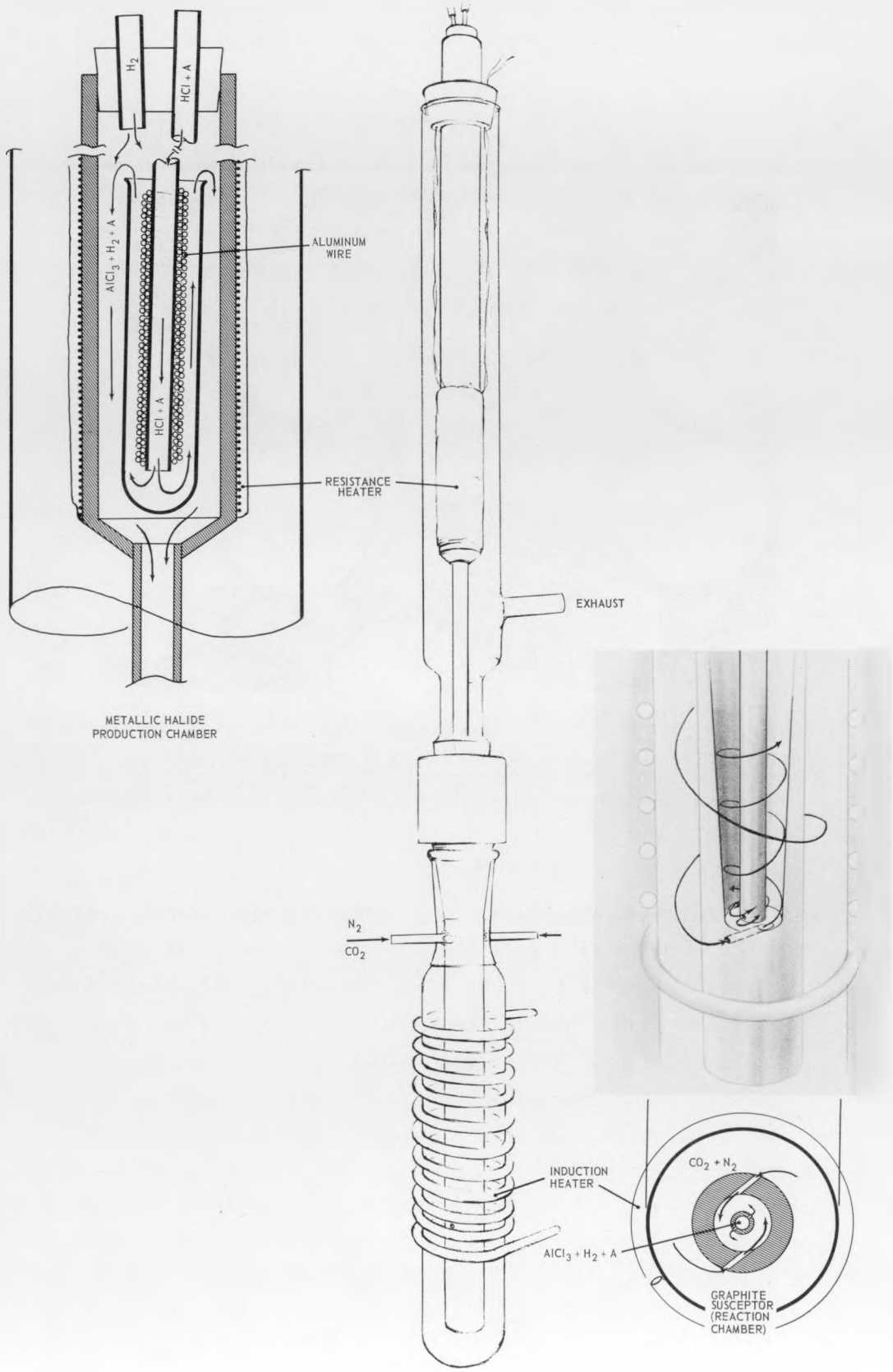

Figure 8 - Spiral bed vapor reaction coating apparatus. AS-104

particles down to 37 microns in diameter have been fluidized up to 8 hr at 1000 C without any evidence of agglomeration of particles or freezing of the bed.

Using this apparatus, UO_2-containing spheres in the -270 +325 mesh size range have been coated with about 7 microns of Al_2O_3 in 4 hr at approximately 1000 C. The coated particles were tested in 8 molar HNO_3 for 8 hr at 70 C. At the end of 8 hr about one-fourth of the fuel cores had been attacked by the HNO_3. It is expected that with further coating experience the fraction of particles attacked can be considerably reduced. The coated particles before and after testing are shown in Figure 9.

SOLS

Preparation of Sols

Water sols of ZrO_2 and UO_2 have been prepared at GE-NMPO by use of the electrodialysis system shown schematically in Figure 10. When the system is in operation, the solution that is to undergo electrodialysis flows from the cathode compartment of the electrodialysis cell to the hydrolysis kettle. There it is heated to a temperature in excess of that for the remainder of the system, and most of the hydrolysis of the metal ion and formation of sol particles occurs. The solution then flows through the cooling coil to the pH and conductivity cells, which are both immersed in a water bath maintained at 25 C. From the conductivity cell the solution is pumped through a flowmeter back to the cathode compartment of the electrodialysis cell, where some of the hydrogen ions are discharged at the cathode. A UO_2 sol was prepared by the electrodialysis of a uranyl chloride solution, and contained small spherical particles of UO_2 averaging 50 millimicrons in diameter, as shown in Figure 11. As may be noted some of the particle substructure was resolvable at a magnification of 150,000.

Processing of Sols

Zirconia sols with sol particles averaging 3 to 7 millimicrons were received from the Washington Research Center of W. R. Grace and Company under the ANP program and incorporated in a beryllia matrix to prepare sintered beryllia bodies. The small ZrO_2 particles in additions of less

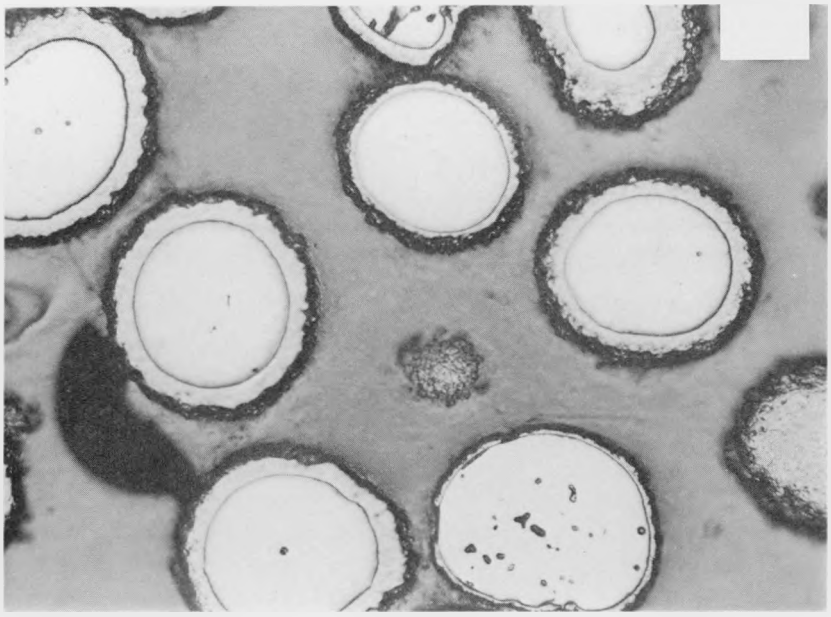

Neg. No. 1105 Unetched 500X

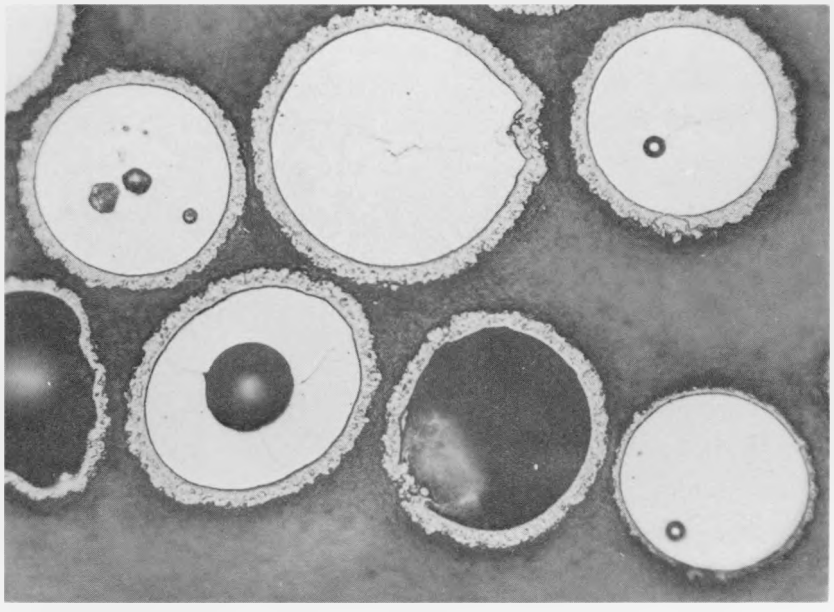

Neg. No. 1107 Unetched 500X

FIGURE 9. Urania-containing spheres coated with Al_2O_3 in the spiral bed apparatus. (Before and after leach test in HNO_3).

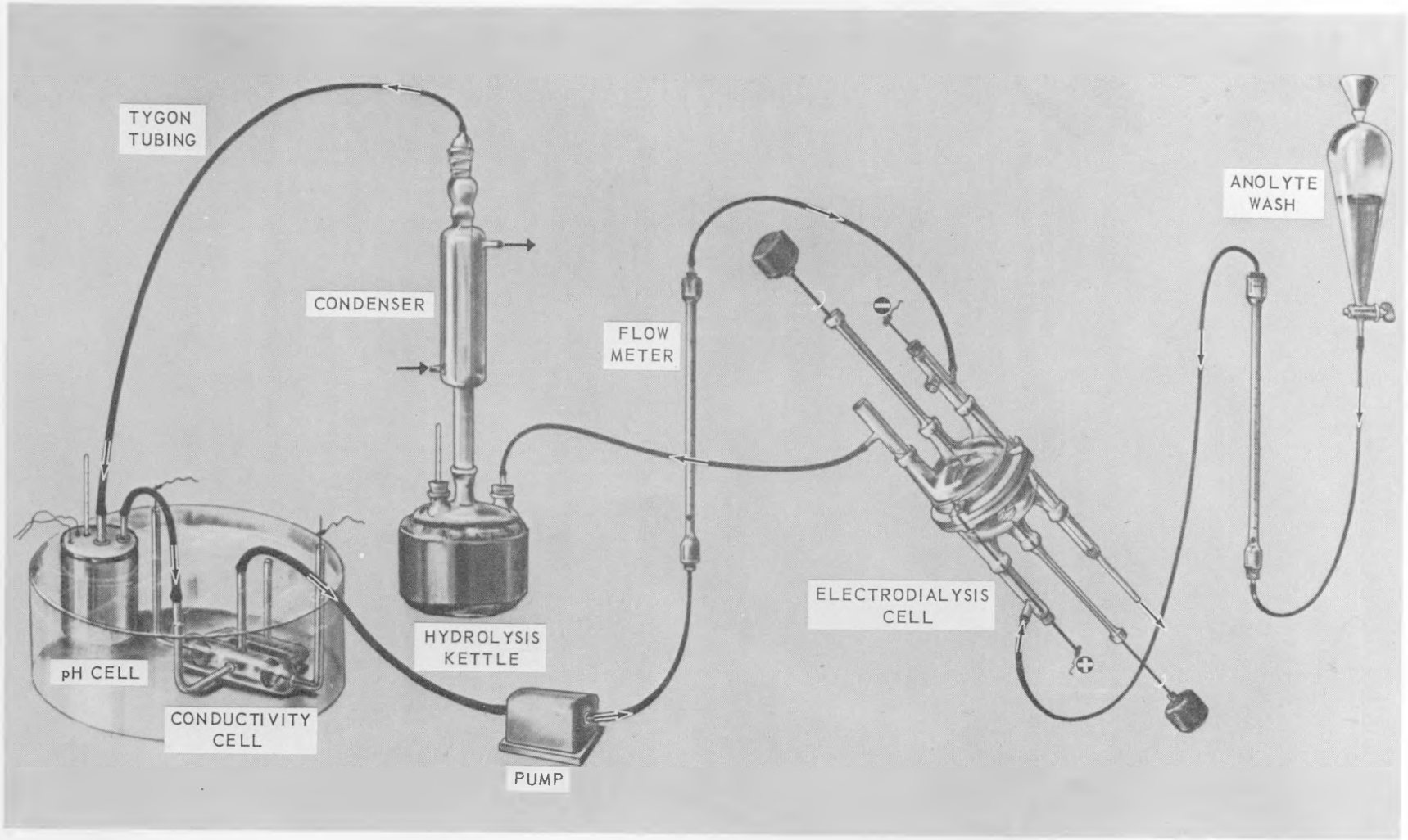

Figure 10 - Flow sketch of the electrodialysis system. AS-70

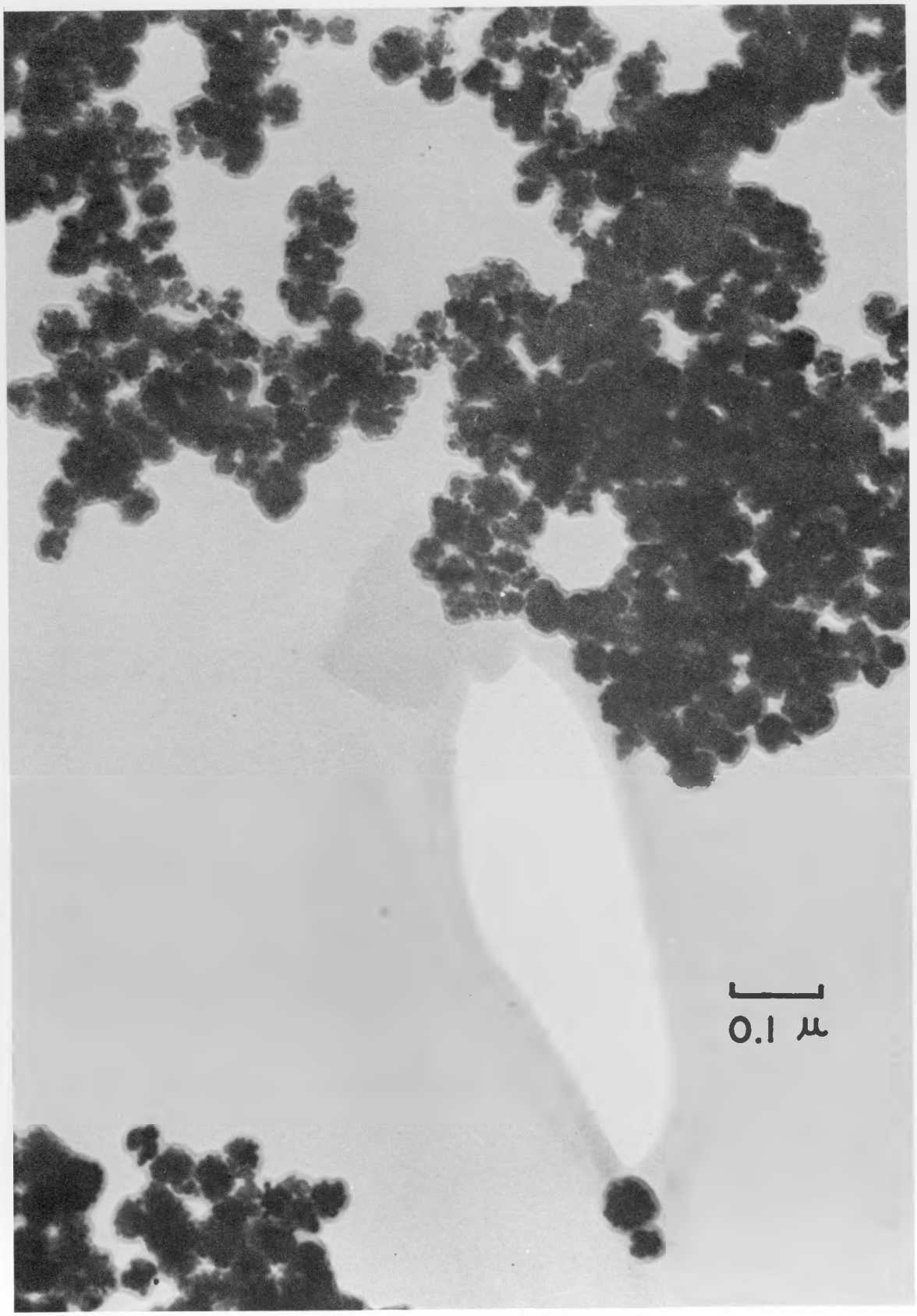

(Neg. 487C) **Figure 11 - Urania sol particles** 150,000 X

than 5 weight per cent were effective in inhibiting beryllia grain growth at temperatures up to 1500 C and imparted to the sintered bodies a high modulus of rupture. Data for sintered bodies containing sol size ZrO_2 particles are presented in Table 1. Data for sintered beryllia bodies containing MgO as additive are included for comparison.

TABLE 1. MODULUS-OF-RUPTURE DATA FOR SINTERED BODIES CONTAINING ZIRCONIA, ADDED AS SOL, OR MAGNESIA

Composition, weight per cent			Sintered Density, per cent of theoretical	Modulus of Rupture, 10^3 psi
BeO	ZrO_2	MgO		
99.5	0.5	--	91.4	28.8
99.0	1.0	--	97.0	32.3
98.0	2.0	--	97.6	33.9
97.0	3.0	--	97.1	37.3
96.0	4.0	--	97.9	37.9
99.5	--	0.5	--	21.9

PLANS

Coated fuel particles will be prepared and subjected to bench tests to determine completeness of coverage and resistance to thermal shock. Particles from batches which pass the bench tests will be incorporated in beryllia matrix to yield extruded and sintered beryllia bodies. Sintered bodies will be evaluated for matrix grain growth and physical strength, and bodies from batches passing these tests will be subjected to irradiation testing.

DISCUSSION

Question, H. A. Taylor (UKAEA) "Why have you limited your studies to particle sizes of 50 microns or less?"

Reply, C. C. Browne (NMPO): "Some concepts under consideration require this particle size. This is backup work for the program at BMI."

Question, L. P. Pepkowitz (NUMEC): "Do you have information on the temperature distribution in your plasma?"

Reply, R. E. Latta (NMPO): "According to Reed's data from MIT, the temperature is 12,000 to 20,000 K at the center and 9000 K at the outside. The distribution will be a function of the power and of the flow rate of the gas."

Question, L. P. Pepkowitz (NUMEC): "Have you measured this distribution?"

Reply, R. E. Latta (NMPO): "No, it's rather expensive to set up the equipment to measure it, and at present we have nothing available for the measurements."

Question, W. Duckworth (BMI): "What plasma guns were used?"

Reply, C. C. Browne (NMPO): "The spherical particles were made by the RF process. Other techniques will require more work."

Question, P. A. Tucker (ML): "Have you characterized your UO_2 particles to see if you still have UO_2?"

Reply, R. E. Latta (NMPO): "We have not done oxygen analyses, but we do know that we are losing some uranium by this method. We do intend to check oxygen content."

Comment, P. A. Tucker (ML): "It has been our experience using similar techniques that the particles are oxidized to U_3O_8. ZrO_2 appears to remain stable in argon since the diffusion of oxygen in ZrO_2 is less than in UO_2."

Question, G. B. Greenough (UKAEA): "Why is the emphasis on high-density fuel particles? Shouldn't less dense particles be considered to allow room for expansion?"

Reply, C. C. Browne (NMPO): "We have been wondering about this also, but have experienced differences of opinion on the desirability of porosity. We would appreciate hearing about any additional experimental studies in this area."

Comment, W. O. Harms (ORNL): "With pyrolytic-carbon-coated, high-density uranium carbide particles, we have had acceptable performance up to 300,000 MWD/T. We plan to test the effects of void volume on UO_2 particles."

NUCLEAR CAPABILITIES OF THE RESEARCH DIVISION OF AMERICAN METAL PRODUCTS COMPANY

By T. A. Jameson

American Metal Products Company
Ann Arbor, Michigan

The Research Division of the American Metal Products Company has been involved in nuclear work since its inception, as the Engineering Science Division, in 1958. Our earliest work was with the carbides and nitrides of uranium, and by late 1959 our Division was producing many other compounds of uranium and refractory metals as well.

Our experience with fluidized-bed coating of particles with niobium and other elements dates from early 1960. From that time, until the middle of this year, we have been supplying developmental quantities of a variety of coated particles to a number of customers. Since this is an unclassified discussion, I am unable to describe in detail the products with which we were most concerned; however, I may state that we have successfully applied coatings of niobium, chromium, zirconium, tungsten, niobium carbide, zirconium carbide, pyrolytic graphite, and combinations of these coatings by fluidized-bed techniques to base materials such as uranium dioxide, uranium monocarbide and dicarbide, magnesium oxide, aluminum oxide, and zirconium oxide. These base materials have been in the form of spheres and cylinders of various sizes. Our products may be characterized by the extreme purity of both coating and substrate and by the uniformity and completeness of the coatings. We have also devoted a large portion of our nuclear efforts to the development and adaptation of analytical techniques for the quality control of nuclear fuel material products and processes.

Since our Company does not possess facilities for the conversion of UF_6 or for the recovery of scrap materials, both of which are necessary in conjunction with sintering and plating facilities for a fully integrated fuel-particle manufacturing capability, we have decided to forego any expansion into full-scale production. In fact, in order to emphasize certain

other lines of endeavor, we are curtailing all our activities in regard to nuclear materials.

During the past four years, however, we have amassed a considerable amount of know-how and equipment, and have demonstrated and proved our technical capability. We therefore offer, on a mutually agreeable consulting basis, and within the bounds of classification requirements, to make our knowledgeable personnel and our facilities available to anyone interested in investigating or establishing a position in this field.

DIAMOND ALKALI EXPERIENCE WITH COATING NUCLEAR FUEL PARTICLES

By T. S. Perrin

Diamond Alkali Company
T. R. Evans Research Center, Painesville, Ohio

Several years ago, Diamond Alkali Company sponsored fuel particle coating work at Battelle Memorial Institute. Later the investigations were continued at the Diamond Alkali Company Research Center near Painesville, Ohio. The work there was at first limited to metal type coatings but later extended to the preparation of fuel particles themselves. More recently, ceramic-type coatings have been studied. During the past three years, coated particles have been successfully made on a production basis. New and larger production facilities are under construction and should be ready for use by the year's end.

GENERAL ATOMIC COATED PARTICLE CAPABILITY

By A. R. Matheson

Fuel Operations Division
General Atomic Division of General Dynamics Corporation
San Diego 12, California

General Atomic has an established capability in its Fuel Fabrication Facility to produce coated uranium carbide and uranium-thorium carbide particles in large quantities. Particles ranging from 50 to 1000 microns can be made with varying carbon contents. Coatings of pyrolytic carbon from 10 microns upwards can be provided. Figure 1 is a microradiograph of 50 to 150 micron uranium dicarbide particles coated with 21 microns average thickness of pyrocarbon. Figure 2 is a photomicrograph of similar particles.

General Atomic, in addition, is prepared to fabricate graphite matrix fuel elements containing coated uranium-thorium dicarbide particles for use in the Peach Bottom Reactor. Graphite spheres containing coated particles have been fabricated with and without an external unfueled graphite shell.

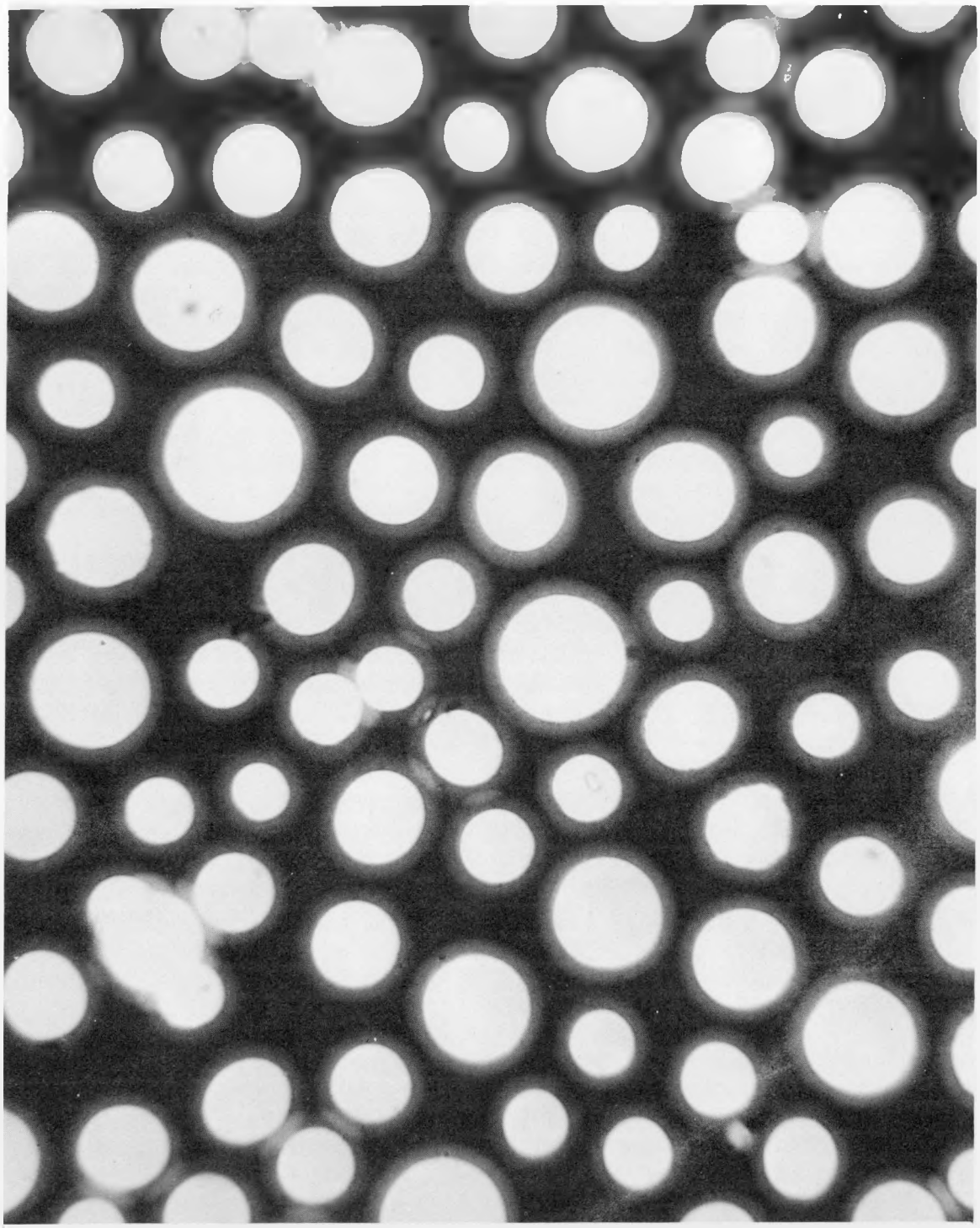

FIGURE 1

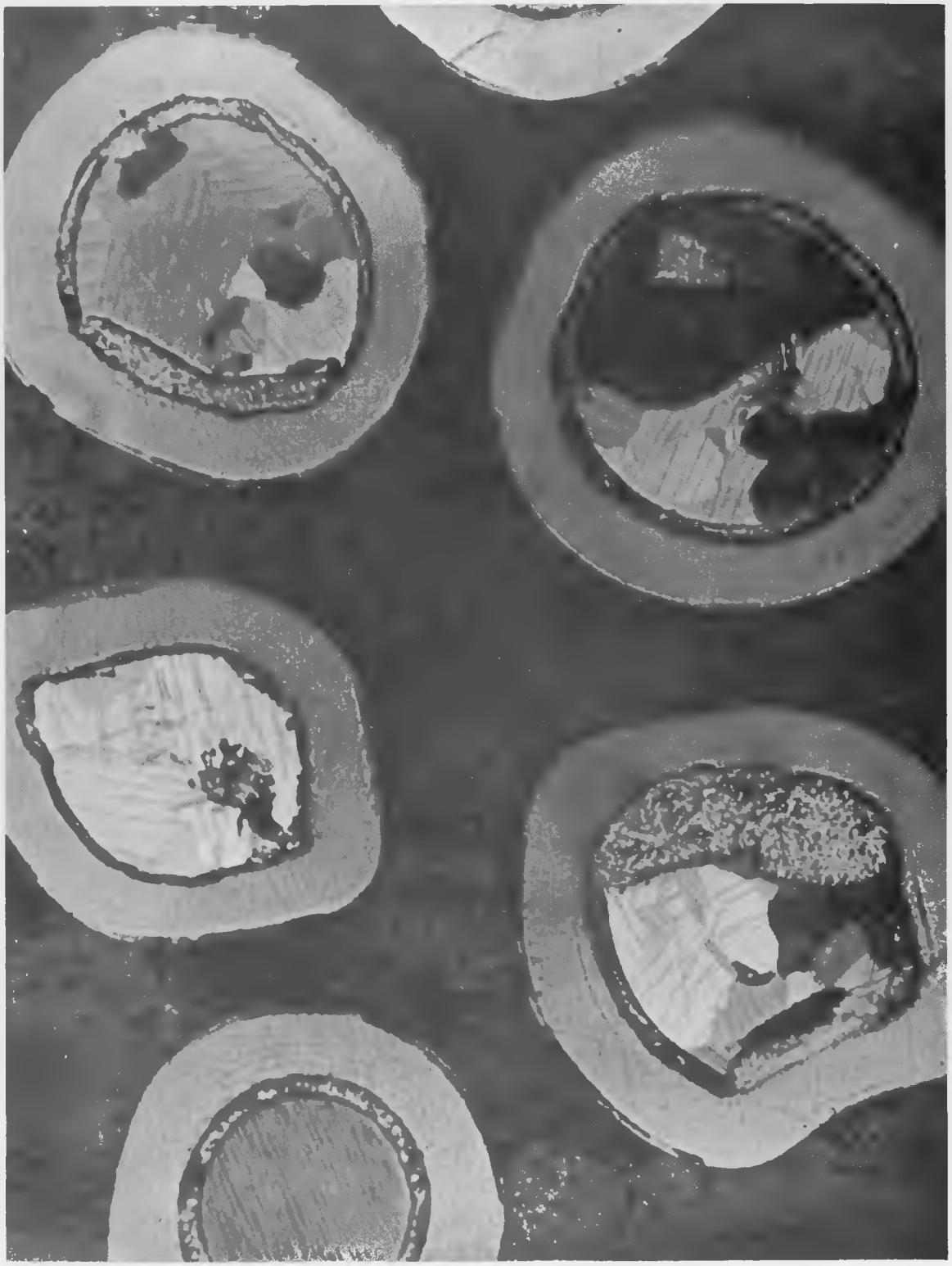

FIGURE 2

CERAMIC COATED PARTICLES AND GRAPHITE MATRIX FUELS

By H. G. Sowman

Minnesota Mining and Manufacturing Co.
St. Paul, Minnesota

The emphasis in reactor materials at the 3M Company has been placed on high-temperature reactor components for a number of years. All of its development activities have been privately financed. Its efforts which are of interest to this meeting can be categorized as follows:

I. Spherical Reactor Particles
   A. Control Materials
   B. Fuel Particles
II. Graphite-Matrix Fuels

I. Spherical Reactor Particles

The advantages of spherical particles include their greater fracturing resistance and minimum surface area. In coated particles the spherical shape eliminates stress points which are present with angular particles. Fracturing resistance is important in preventing breakup during fabrication and minimum surface area reduces reaction with matrix and atmospheres.

A. Absorber Materials. Although various carbides in spherical-particle form have been produced in small quantities, B_4C has been fabricated and sold in larger quantities. Particle sizes range from 30 to 500 μ or larger. The exterior appearance of these particles is similar to that of UC_2 particles shown in Figure 1. Pyrolytic-carbon

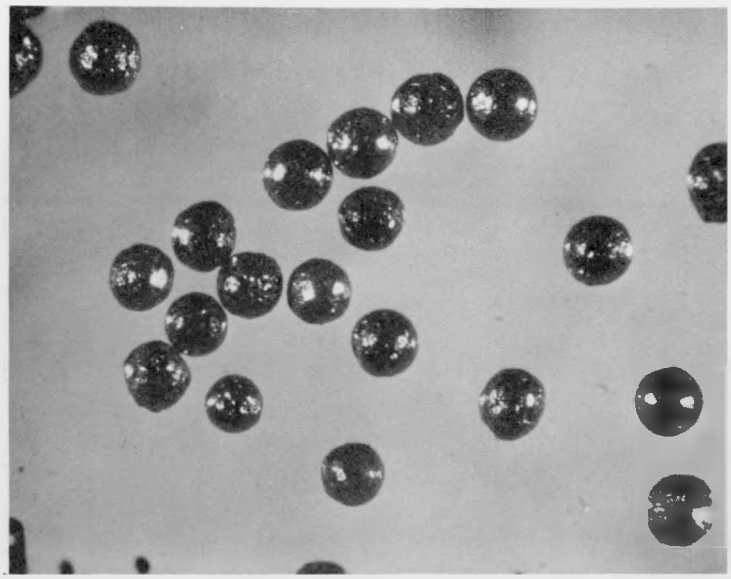

Figure 1. Exterior view of 200 μ particles

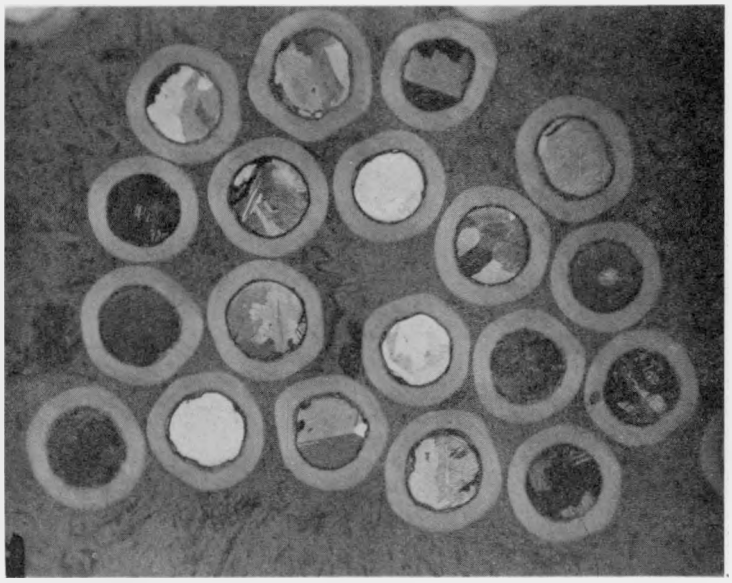

Figure 2. Sectioned UC_2 particles, 200 μ diameter with 50 μ PyC

coating of B_4C particles has been done in sufficient quantities to establish feasibility of mass production.

B. Fuel Particles. 3M Fueled Microspheres are spherical particles of fuel compositions such as uranium carbide, UC_2, and thorium-uranium carbide combinations, $(ThU)C_2$. These particles are essentially spherical as shown in Figure 1. They can be supplied commercially in multikilogram quantities in sizes ranging from 20 to 500 μ or larger.

Uranium dicarbide particles which have been coated with pyrolytic carbon are shown in Figure 2. The microstructure of these particles is typically polycrystalline. The uniformity of coating thickness can be controlled so that the maximum deviation is in the order of ±10%. Even more precise control is expected in the future.

Although the microstructure of the ordinary UC_2 particles is polycrystalline and somewhat striated, it is possible to prepare particles which are relatively free of striae with either polycrystalline or monocrystalline structure. The particles of Figure 3 are monocrystalline. Although these are not as readily available in large quantities as the ordinary polycrystalline particles, they have been supplied to a number of laboratories for study. With the absence of grain boundaries, the apparent purity and freedom from voids, one might speculate on the comparison of this material with the polycrystalline material with regard to fission-product retention. A monocrystalline particle coated with pyrocarbon is shown in Figure 4.

Although the greater commercial readiness at the 3M Company lies in the area of pyrocarbon-coated particles of UC_2, $(UTh)C_2$, UO_2, UO_2-ThO_2, etc., other types of coated particles have been prepared, and the capability of scaling up production exists if demanded. These include particles of various compositions coated with pyrographite, niobium carbide, and niobium, as well as multiple coatings of various combinations.

II. Graphite-Matrix Fuels

3M has supplied materials for a number of years for various graphite-matrix fuel programs. Its program in the past has involved the development of fabrication techniques for preparing graphite fuels with dispersed coated fuel particles. It has pioneered in the development of the concept of a fueled-

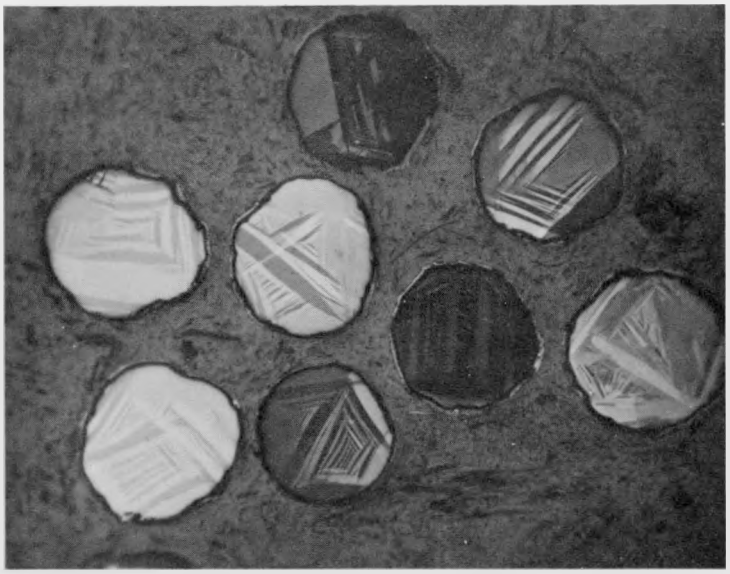

Figure 3. Monocrystalline UC_2 particles, 150 μ in diameter

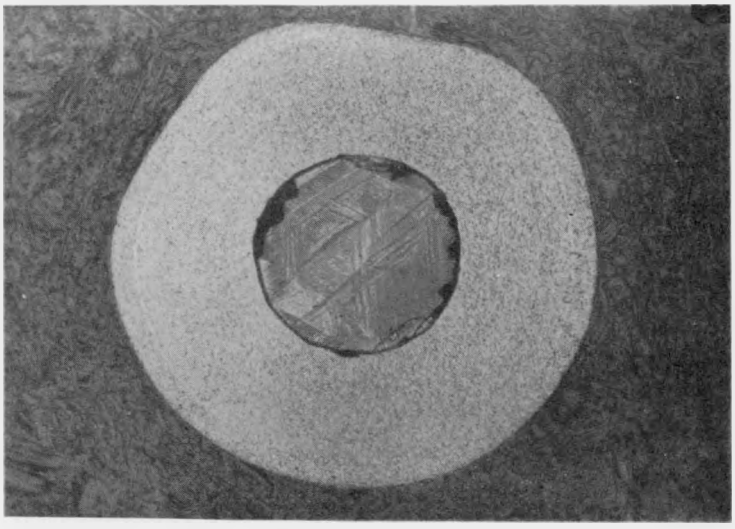

Figure 4. Pyrocarbon-coated monocrystalline UC_2 particle

graphite core surrounded by an integrally bonded unfueled graphite cladding. Its present capabilities lie in the area of fueled-graphite balls, pellets, sleeves, or other small-sized fuel elements.

Conclusion

Considerable technology exists within industrial concerns which can be applied to future requirements for ceramic-matrix fuels. In most cases, basic technology needed to satisfy requirements is known. It is important that these requirements and product specifications be known to industrial concerns, especially those such as 3M not involved in AEC R&D contracts, but still active in the field. This will provide the necessary prospectus for guiding suppliers, especially with reference to scale-up requirements.

PRODUCTS AVAILABLE FROM NATIONAL CARBON COMPANY

By L. D. Stoughton

National Carbon Company, Union Carbide Corporation
New York, New York

A. Graphite-Matrix Fuel Elements
   (1) Molded or extruded shapes with or without an integral unfueled shell
   (2) Fuel loadings such as UO_2, UC_2, or pyrolytic-carbon coated UC_2 or $(Th,U)C_2$.

B. Fuel Particles
   (1) UC_2 and $(Th,U)C_2$ spherical shot in sizes ranging from 50 to 500 microns
   (2) Pyrolytic-carbon coated UC_2 or $(Th,U)C_2$ shot with coating thicknesses ranging from 20 to 150 microns and either laminar, columnar, or duplex coating structure.

DESCRIPTION OF NUMEC'S FACILITIES AND CAPABILITIES

By L. P. Pepkowitz

Nuclear Materials and equipment Corporation
Apollo, Pennsylvania

NUMEC's development of processes for coating particulate materials has opened up the possibility of obtaining very uniform cermet, ceramic-in-ceramic, ceramic-in-metal, metal-in-ceramic, and metal-in-metal fabricated parts and pieces for a variety of applications where high-temperature, corrosion-resistant, thermal-shock-resistant materials are mandatory. In nuclear research and reactor applications, coated fuel particles hold promise of offering major improvements in fuel-element design. Among these improvements are better retention of fission products in fuel materials and elements; improved thermal conductivities; higher fuel densities; increased resistance to corrosion, erosion, abrasion, and irradiation damage; and greater dimensional stability.

The original concept of coating individual fuel particles with a protective coating was submitted by NUMEC to the U.S. AEC in the proposal entitled, "The Preparation of Corrosion Resistant and Radiation Damage Resistant Uranium Metal", dated August, 1957. Subsequently, NUMEC was awarded AEC contracts for the development of a number of coatings for nuclear fuel materials. The first publicly presented paper on coated particles was presented by NUMEC at the Symposium on "Fuel Element Fabrication with Special Emphasis on Cladding Materials" in Vienna, Austria, in 1960.

NUMEC's coating experience includes metallic coating of niobium, molybdenum, vanadium, chromium, beryllium, silicon, nickel, and tungsten on uranium substrates; oxide coatings of Al_2O_3 and BeO on UO_2 and ceramic and metallic substrates; carbide coatings on pyrolytic graphite and on UO_2; and duplex coatings of chromium-nickel, nickel-copper, chromium-niobium,

and molybdenum-niobium on ceramic substrates; gold, platinum, and other precious-metal coatings on a variety of substrates including stainless steel, uranium metal, etc.

Techniques employed at NUMEC include a wide variety of methods including vapor-phase reactions, electrophoresis, electroplating methods, chemical displacement, chemical reduction, evaporation methods, and plasma-arc procedures. NUMEC can provide all the above either on a laboratory developmental scale or on a production basis.

PYROGRAPHITE COATING OF NUCLEAR FUEL PARTICLES

By M. P. Lepie
Research Division, Raytheon Company
Waltham, Massachusetts

ASBTRACT

Gas cooled nuclear reactors are designed to use fuel elements of UC_2 and/or ThC_2 spherical powders. The stability of these powders is enhanced by coating them with a refractory, impervious film. Two methods are discussed for the deposition of pyrolytic graphite or carbide coatings. Also treated are methods for spheroidization of these fine powders.

I. INTRODUCTION

The High Temperature Materials Department of the Research Division, Raytheon Company, has been engaged in the research, development and production of pyrolytic graphite and carbides since 1959. Massive pieces in special shapes are being produced as well as coatings on graphite and the refractory metals. The High Temperature Materials Department has become interested in the pyrolytic coating of powders because of a need for them in the gas cooled nuclear reactor. The following is a description of the preliminary phase of this program.

II. METHODS FOR COATING POWDERS

Two methods have been investigated for the coating of fine powders by the pyrolytic technique.

The first method involved the use of a rotating drum or cage made of graphite (Fig. 1). This apparatus was used to apply coatings in the range of 1600° to 2000°C. The cage was rotated in a graphite resistance furnace. Vacuum was maintained by the use of rotating seal on the shaft connected to a variable speed motor. Methane entered the cage at the front and left the coating chamber through a rear section designed to trap any powder that was carried out of the coating area by the gas stream. The forward section had four equally spaced vanes so shaped that they picked up the powder and allowed it to fall free just short of the top of the drum. Process conditions were worked out by the use of a plexiglas model with air as the gas and molybdenum powder replacing UC_2. Optimum agitation without blow-by was observed to occur in our geometry at a rotation of 4 rpm and a gas flow rate of 1 lpm.

Another method for coating powder utilized the fluid bed technique. (Fig. 2). Our apparatus consisted of a quartz tube with an enlarged section at the top and a necked down section at the lower portion. The latter had a loose packing of graphite felt held in place by a stainless steel screen. A Kanthal tube furnace was used to heat the quartz reaction chamber. Dry helium flowed through a benzene vaporizer and then through a heated line into the quartz tube.

To assist in the design of the fluid bed apparatus, reference was made to standard formulae used in this technique. Figures 3 and 4 show the amount of flowing argon required to maintain a stable fluid bed with a given static bed and tube diameter. Figure 5 is the pressure drop through the fluid bed for a given static bed height. Figures 6 and 7 illustrate the weight of UC_2 required to give a static bed height for various size tubes. Figure 8 shows the quantity of heat necessary to raise the fluidizing gas to the process temperature. Assumptions made were that the particles were perfect spheres and that normal packing results in 40% bed voids. Reynold's factor and friction-factor values were taken from "Unit Operations" by G. G. Brown, John Wiley and Sons, Inc., 1950.

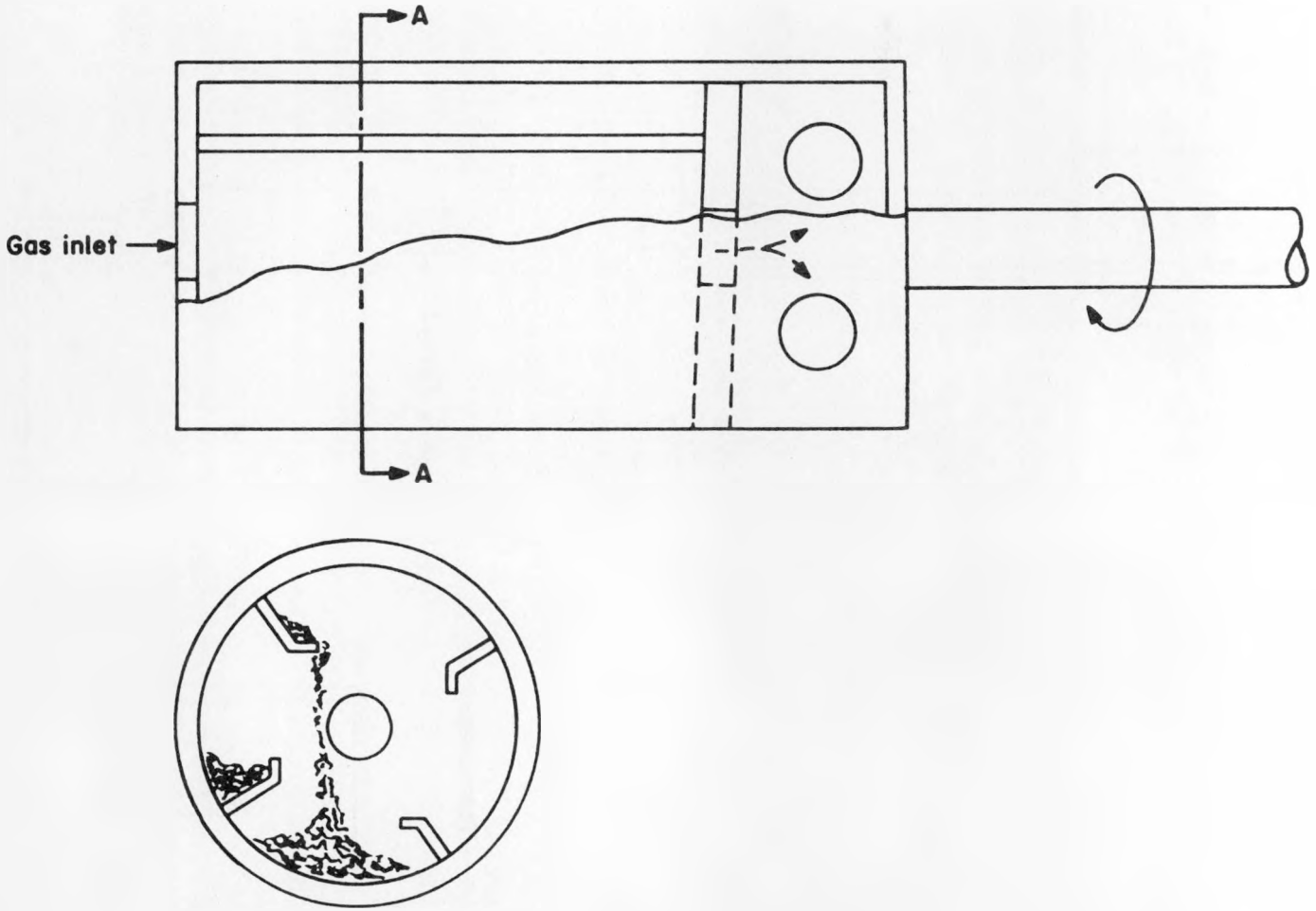

ROTARY CAGE FOR COATING POWDERS

FIGURE 1

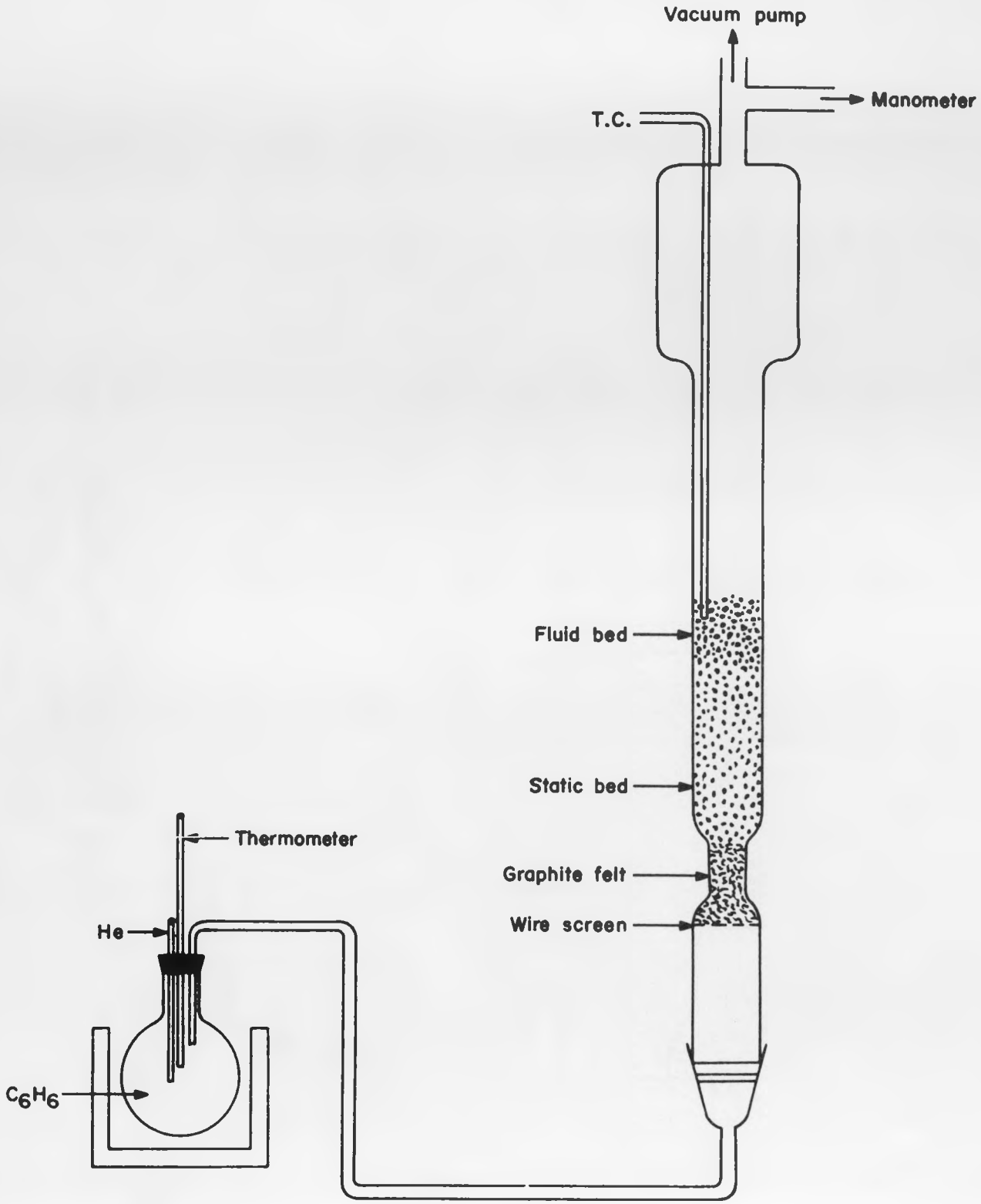

COATING POWDERS BY FLUIDIZED BED METHOD

FIGURE 2

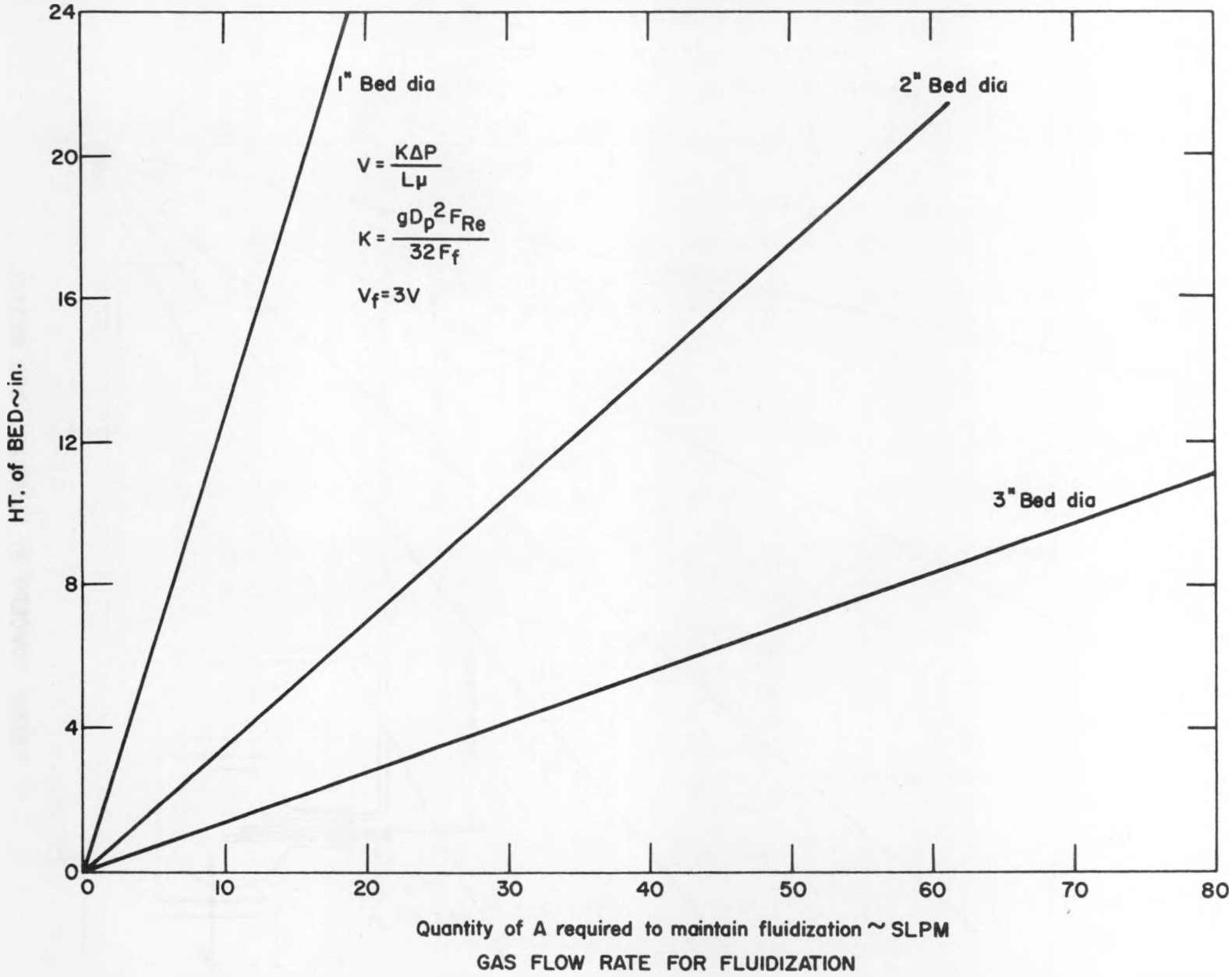

GAS FLOW RATE FOR FLUIDIZATION

FIGURE 3

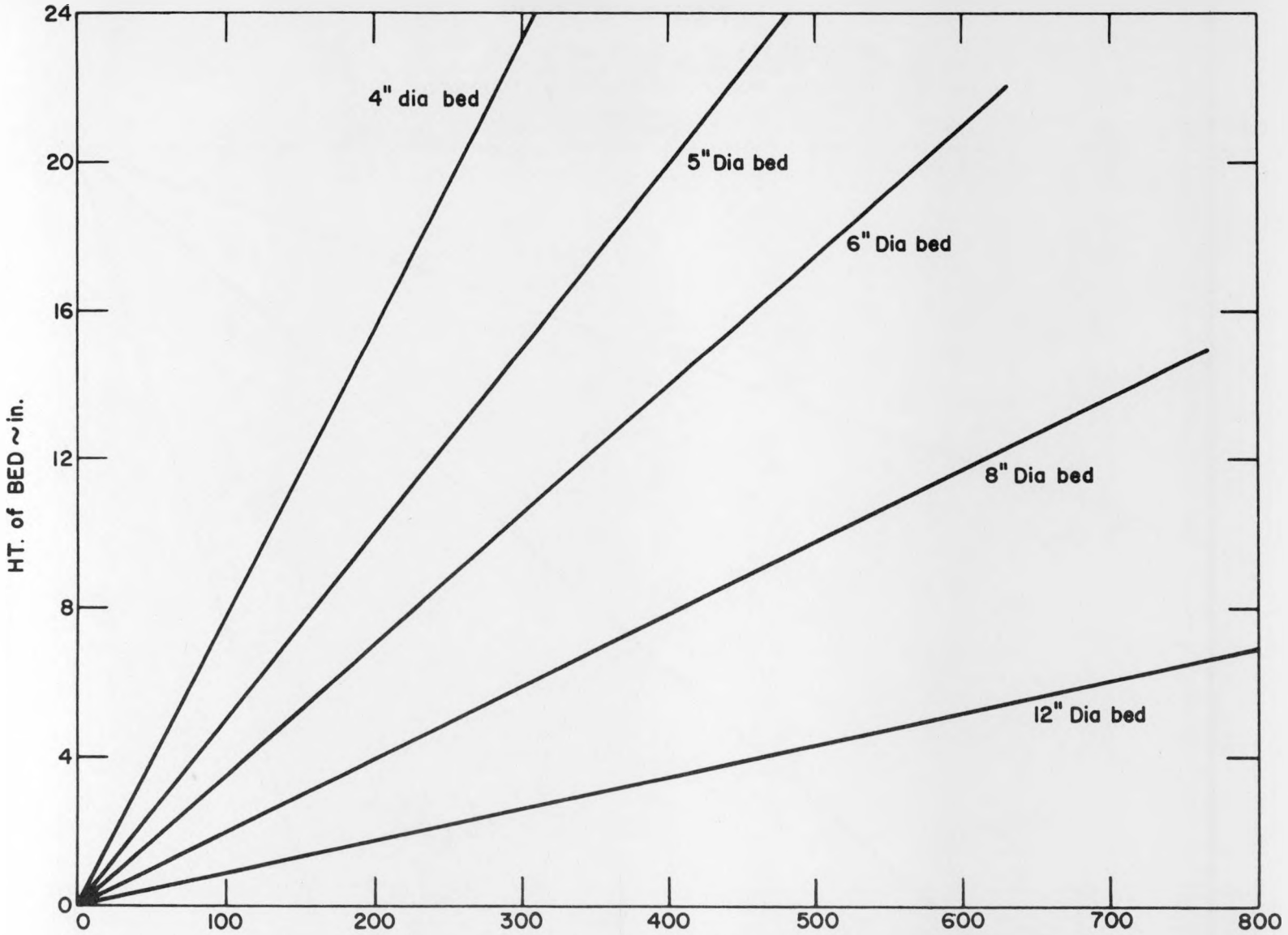

GAS FLOW RATE FOR FLUIDIZATION

FIGURE 4

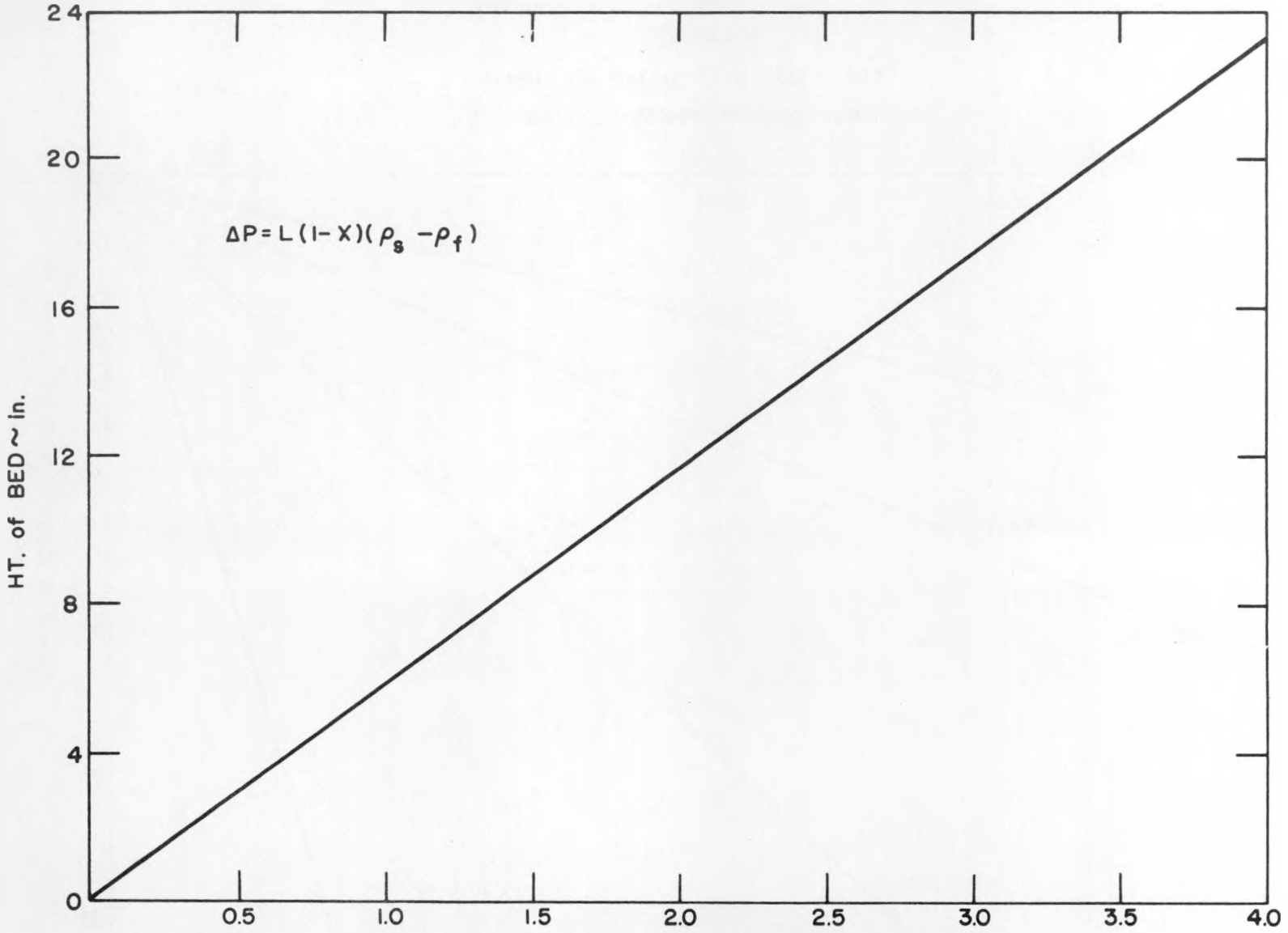

PRESSURE DROP THROUGH FLUID BED

FIGURE 5

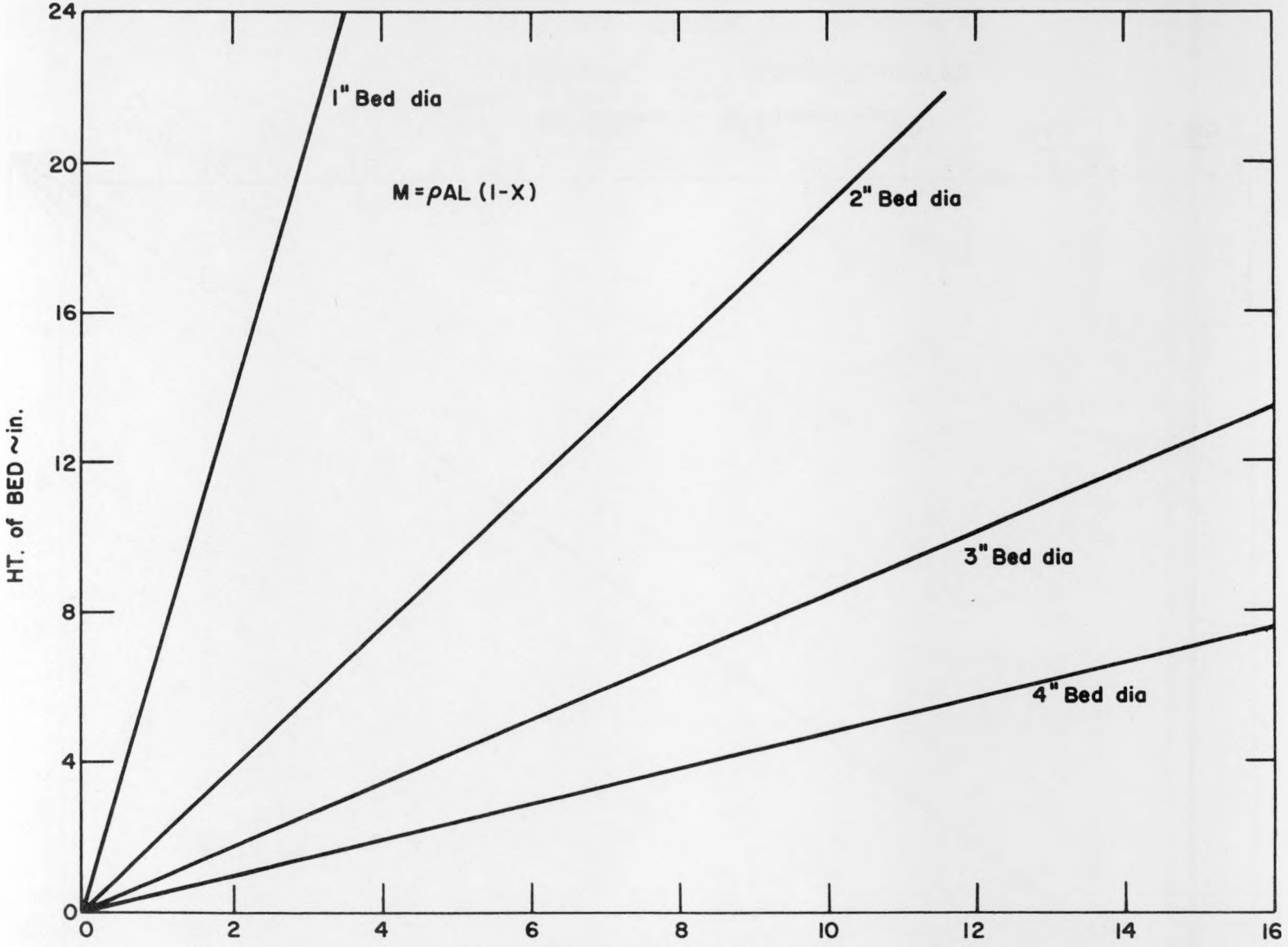

WEIGHT OF MATERIAL IN STATIC BED

FIGURE 6

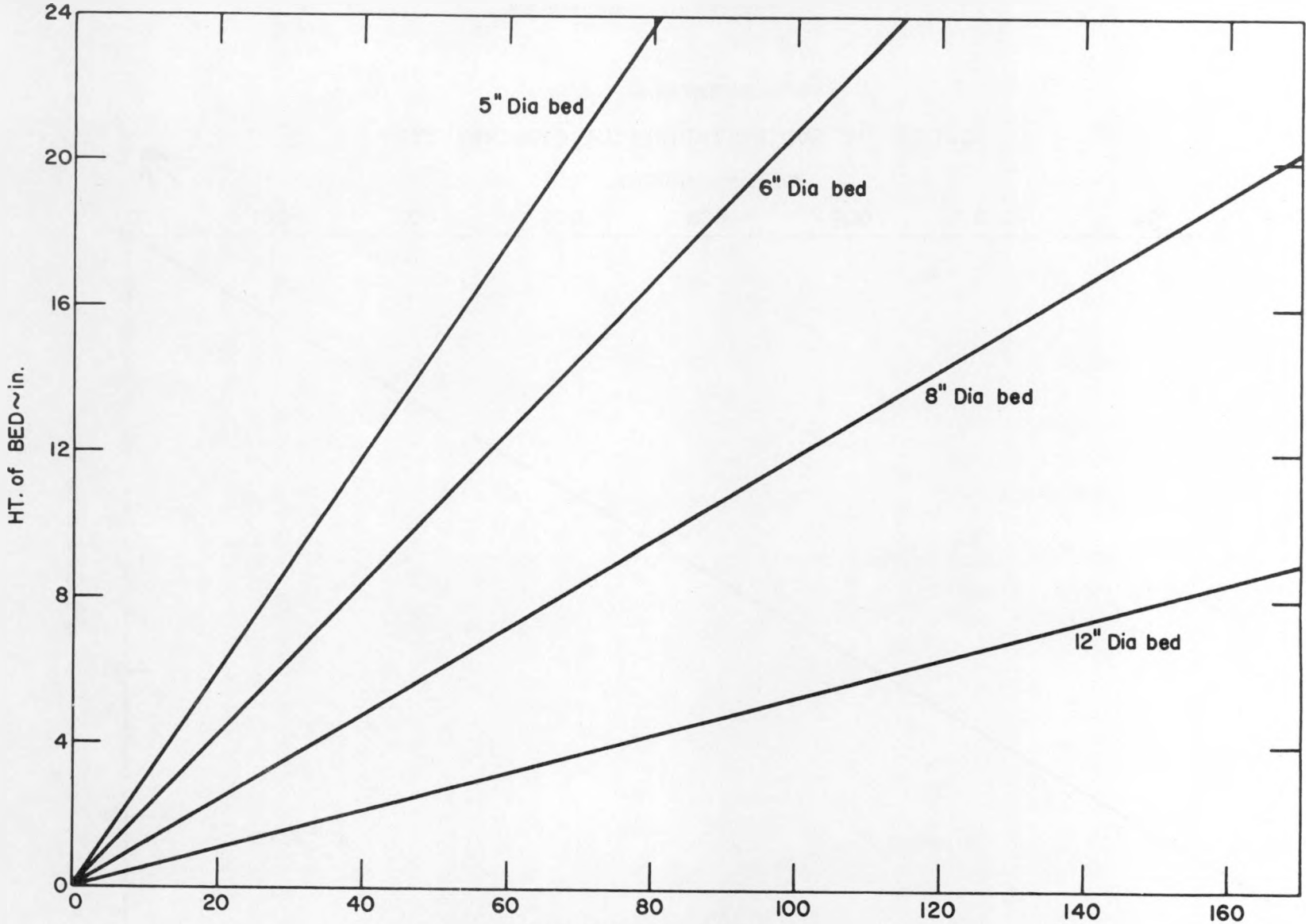

WEIGHT OF MATERIAL IN STATIC BED

FIGURE 7

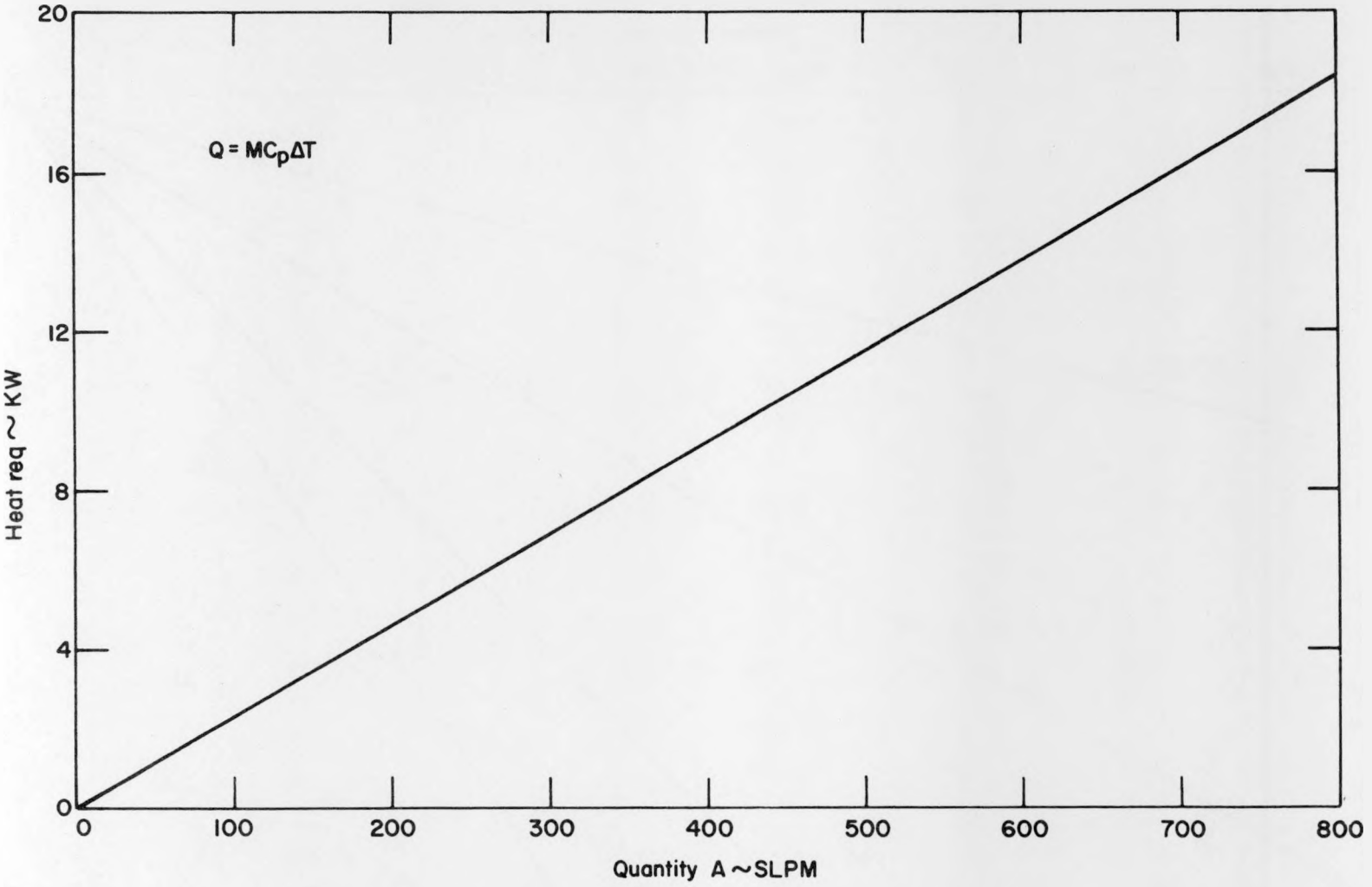

HEAT ABSORBED BY FLUIDIZING GAS AT 1000°C

FIGURE 8

Figure 9 shows UC_2 spheres - average particle size 100 microns - coated with pyrolytic carbon made by this method. Figure 10 is an enlargement of spheres that have been polished and etched in a solution of nitric and acetic acids. The coatings run about 25μ in thickness and show the typical Maltese cross in polarized light.

III. COATING MATERIALS

As mentioned previously two different carbon sources have been used in the coating of UC_2 spheres. Benzene vapor at lower temperatures gives an onion skin layer type while methane at higher temperatures produces a cone shaped growth.

While the graphite coatings on uranium and/or thorium dicarbide are desirable for the retention of fission products and the prevention of decomposition due to moisture in the air, these coatings pose a problem in that the graphite reacts with the carbide at elevated temperatures and any free metal diffuses out. A possible solution to this is the use of multiple coatings. For example, a coating of zirconium Pyrocarbide followed by one of pyrolytic graphite can be produced (Fig. 11). The solubility of carbon in ZrC is low with the eutectic melting temperature for C-ZrC above 2850°C. This exceeds the C-UC_2 melting point. Experiments in our laboratory have shown that C-ZrC is exceptionally strong yet somewhat ductile at temperatures above 2000°C. As for the zirconium carbide-uranium dicarbide interface, there is not the tendency to form mixed crystals as is true with uranium monocarbide. Finally, the steep transition from the high coefficient of thermal expansion of uranium carbide to the low expansion for graphite could be eased by the intermediate layer of zirconium carbide whose value is between the two extremes.

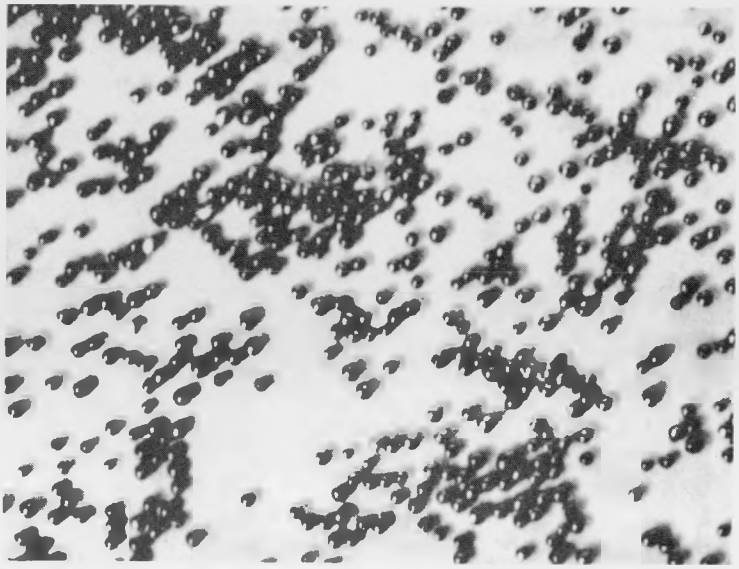

PG COATED UC_2 SPHERES (avg dia 100 μ)

FIGURE 9

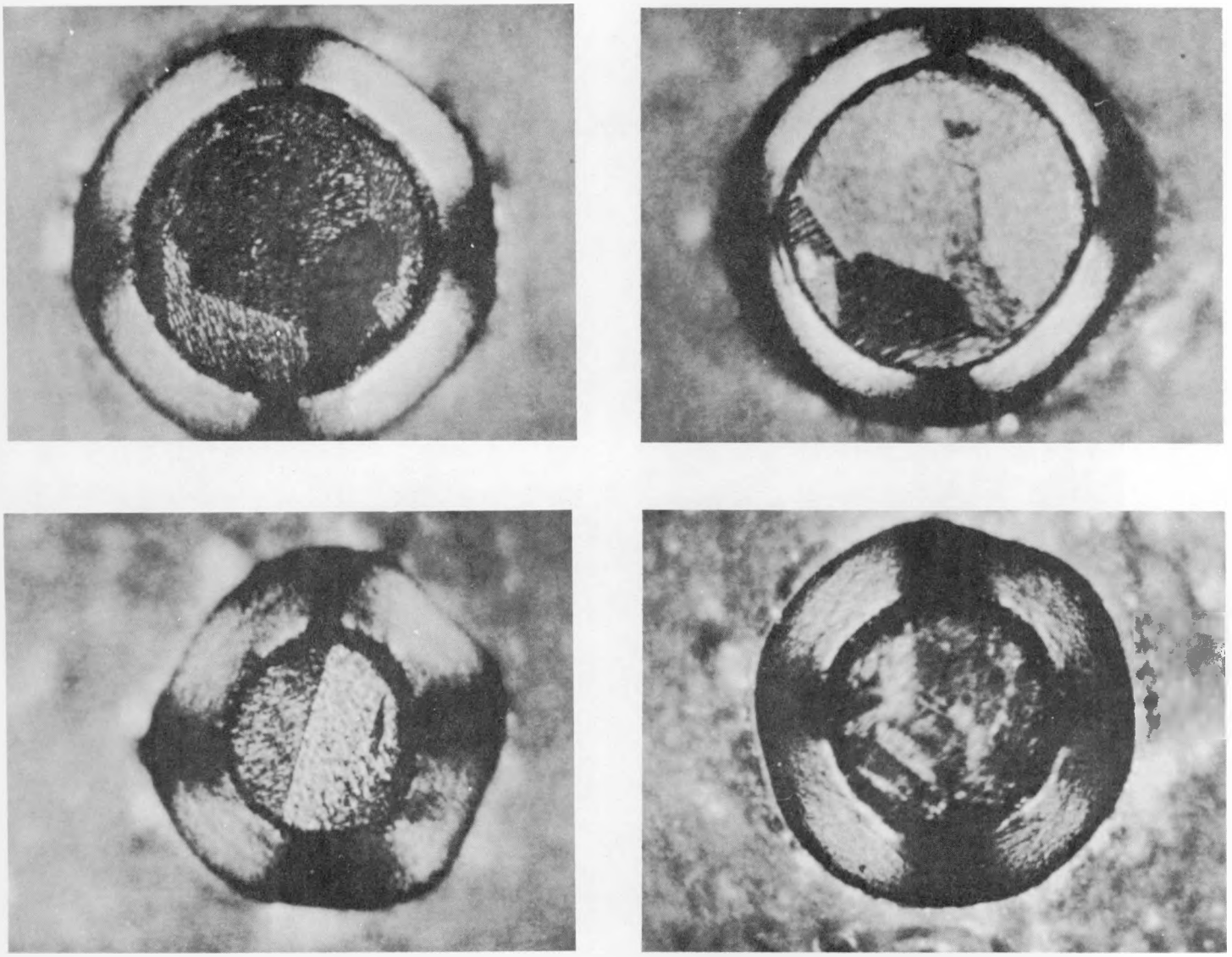

FIGURE 10

CROSS-SECTION OF PG COATED UC_2 SPHERES ETCHED, 500X, POLARIZED LIGHT

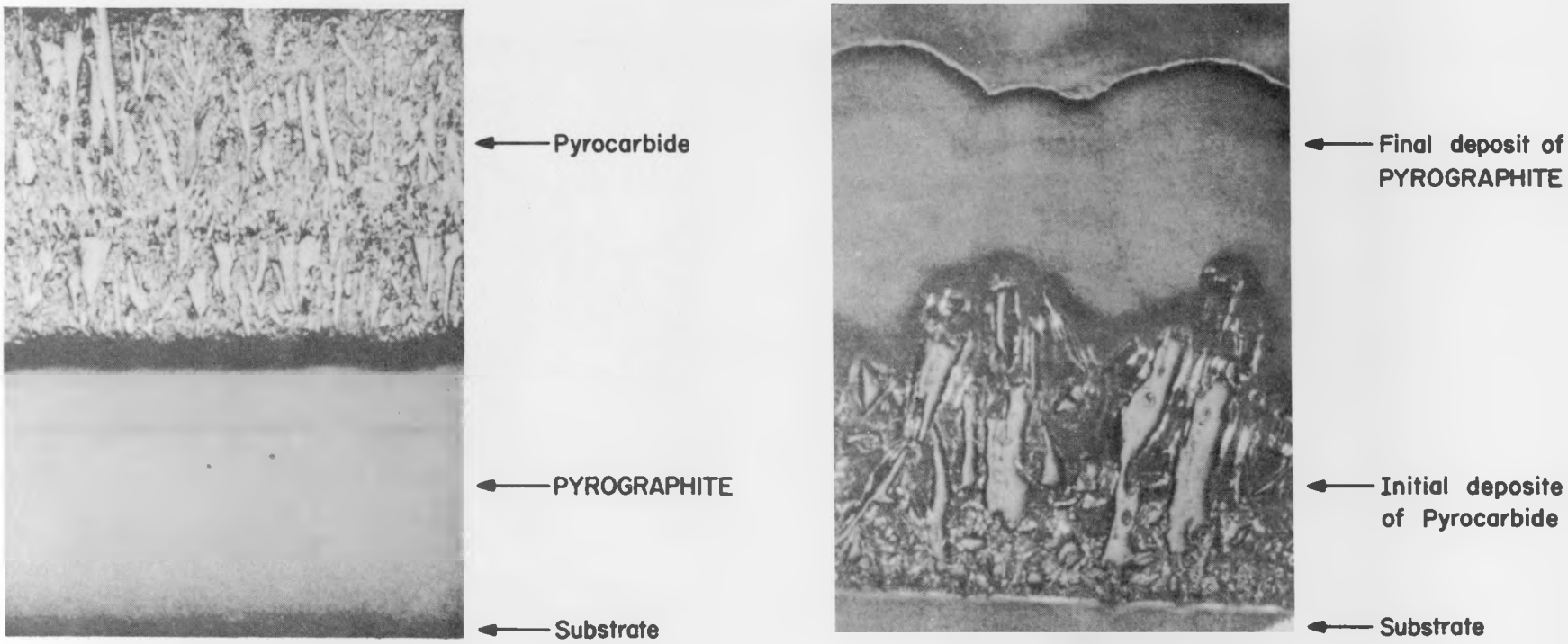

(a) (b)

a) 65 X unetched

b) 30 X unetched

POLISHED SECTIONS OF GRADED STRUCTURES

FIGURE 11

IV. SPHEROIDIZATION OF UC_2 PARTICLES

Packing considerations make it desirable that the particles that make up the fuel element be in the shape of spheres. Also, stresses that develop in the coatings can be controlled in the case of small, spherical particles. For this reason we have been conducting experiments on the production of spherical powders from random shaped powders.

There are a number of different ways to produce spherical powders of UC_2. One method, used in England, involves the reduction of UO_2 with Ca. The U is distributed in the form of spheres with a matrix of CaO which is soluble in acetic acid. The metal can then be carburized. Since the metal spheres average only 20μ in diameter and are pyrophoric, this technique is not too desirable. Battelle Memorial Institute has reported on the spheriodizing of powder by dropping it through a graphite tube furnace. Results with WC were poor, except when the size was -325 M. We at Raytheon have run preliminary studies on spheroidizing by dropping powders through a three electrode carbon arc. A better than 90% yield of Ni and Cr spheres was obtained but with Al_2O_3 and ZrO_2 only 30% of the particles were converted. Apparently, the temperatures obtained are not elevated enough to overcome the poor thermal diffusivity and short residence time of the ceramic materials. Another method we plan to investigate is the use of a plasma torch to make carbide spheres.

USE OF COATED PARTICLES IN GRAPHITE MATRIX FUEL ELEMENTS

By W. E. Parker
Research Laboratory, Speer Carbon Co.
Niagara Falls, New York

Speer Carbon Company has been quite active in research and development on the use of coated fuel particles in graphite matrix elements since shortly after the Battelle group made available limited quantities of alumina coated UO_2 particles. Having furnished machined spheres of Speer 901S for the Sanderson and Porter program of fuel element development for the Pebble Bed Reactor concept and having just completed a subcontract from Sanderson and Porter on the infiltration process for producing loaded spheres (1), it followed that Sanderson and Porter should ask Speer to fabricate graphite spheres containing coated fuel particles. Unfortunately, our first attempts with alumina coated UO_2 particles provided by Battelle and with pyrocarbon coated UC_2 particles prepared by High Temperature Materials resulted in something less than unqualified success.

Realizing that many phases of conventional graphite processing procedure could lead to particle coating rupture by mechanical abrasion, Speer conducted a research program to establish fabrication techniques suitable for producing graphite matrix fuel elements in complex shapes in which even the most fragile coated particles could be utilized. Also realizing that graphite matrix fuel elements could be subjected to surface abrasion such that particles coatings could easily be broken, Speer developed the concept of the continuous matrix unfueled graphite shell. To date the unfueled shell concept has been applied to spherical and annular fuel elements and, we believe, can be applied to virtually any shape. This work was described in a previous paper (2).

More recently, Speer has contracted with the Chemistry Division at ORNL to produce a series of graphite matrix fuel elements containing alumina coated UO_2 particles* and pyrocarbon coated UC_2 particles**. The Al_2O_3 - UO_2 particles are 300 μ in diameter and are loaded to provide

*Furnished by ORNL

**Obtained from Minnesota Mining and Manufacturing Co.

a uranium concentration of 0.08 g/cc. in the elements. The UC_2 particles are -60 + 80 mesh with a PC coating of 80 $\pm$ 20 μ in thickness and are loaded to a concentration of 0.09 g/cc. of uranium. These elements are in two sizes, 1" x 1/2" x 1/8", molded coupons and 1/4" diameter extruded rods. In samples of this size, obtaining uniform distribution can be a problem. Figures 1 and 2 are photographic reproductions of x-radiographs of the Al_2O_3 - UO_2 and PC - UC_2 particle containing coupons. Although the photographic reproduction is not of high quality, it is easy to discern that fuel distribution is generally good, except at the edges. Figures 3 and 4 are similar reproductions showing the excellent fuel distribution in the rods. Figure 5 is a polished section of a rod sample taken at random. Coating integrity is to be noted.

Unfueled shell spherical fuel elements have also been improved as a result of further research. The molding flash around the equator of the 1 1/2" diameter spheres has been minimized through improved die design as shown in Figure 6. Another major deficiency in earlier specimens, non-sphericity in the loaded inner core, has been the subject of an intensified research effort. The degree of success attained can be seen from a close examination of the polar and equatorial sections shown in Figures 7 and 8. These spheres were prepared using copper powder as the loading medium in order to optically enhance the demarcation line between the loaded and unloaded portions of the continuous matrix. When viewed under the microscope this technique produced the desired result. Although much of the contrast was lost in the photographic reproduction, a close examination reveals that the inner and outer spheres are indeed concentric within narrow tolerances.

While there has been no opportunity to produce a significant quantity of any form of these graphite matrix fuel elements on which to base physical property measurement values with any degree of statistical significance, Figure 9 shows some results which we believe can be considered as typical. The carbon density values presented are, in general, those specified by the purchaser and are not to be considered as the maximum attainable. Strength levels appear to be adequate for any fuel elements application proposed to date. Although no data is shown, chemical analyses have been made which demonstrate the nuclear purity of Speer graphite matrix fuel elements. The coupon and rod samples provided for ORNL have been reported (3) to be free from uranium contamination to levels below 5×10^{-3} % .

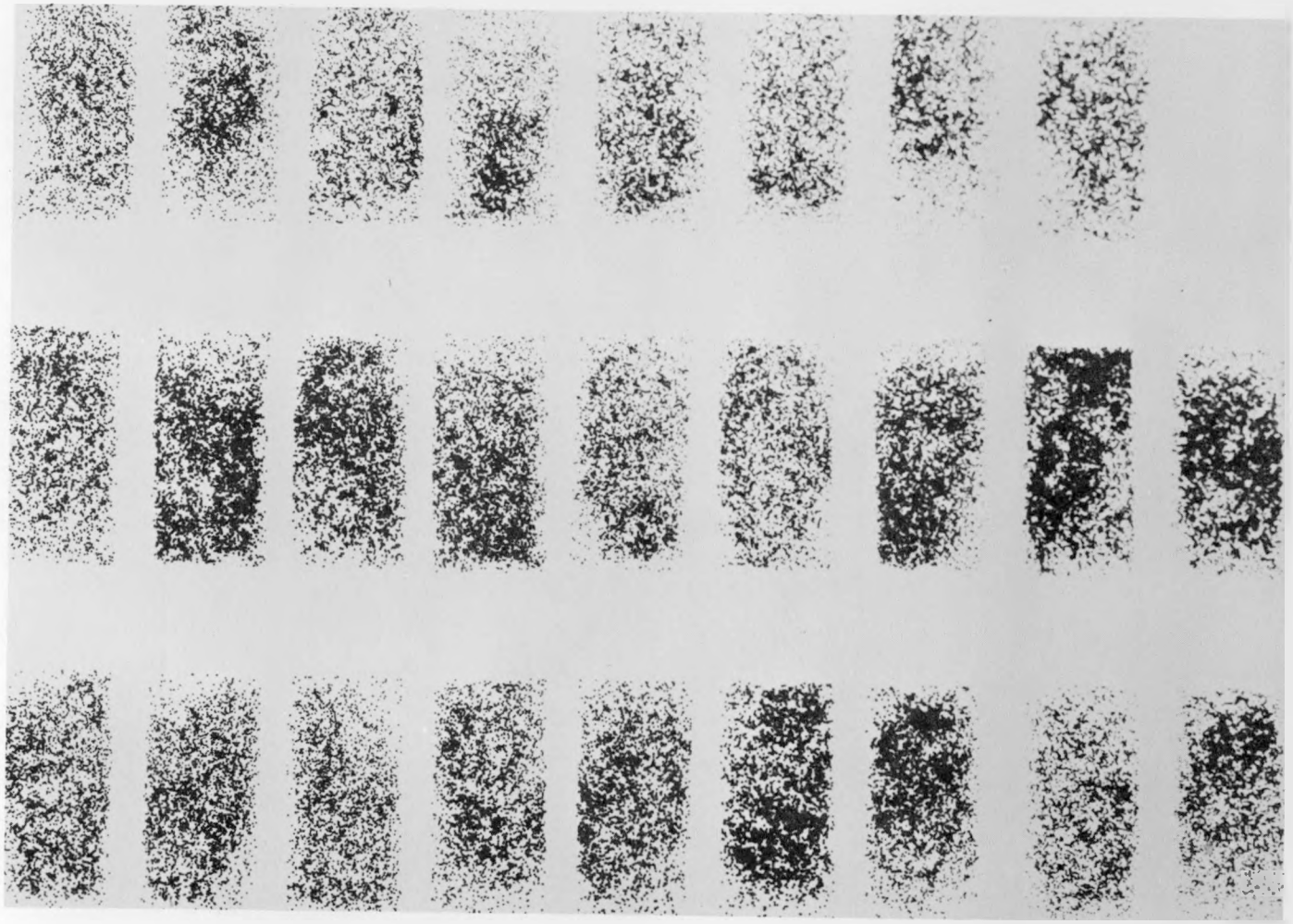

FIGURE 1. FUEL DISTRIBUTION IN 1/8-IN.-THICK COUPONS - Al_2O_3-COATED UO_2, GRAPHITE MATRIX

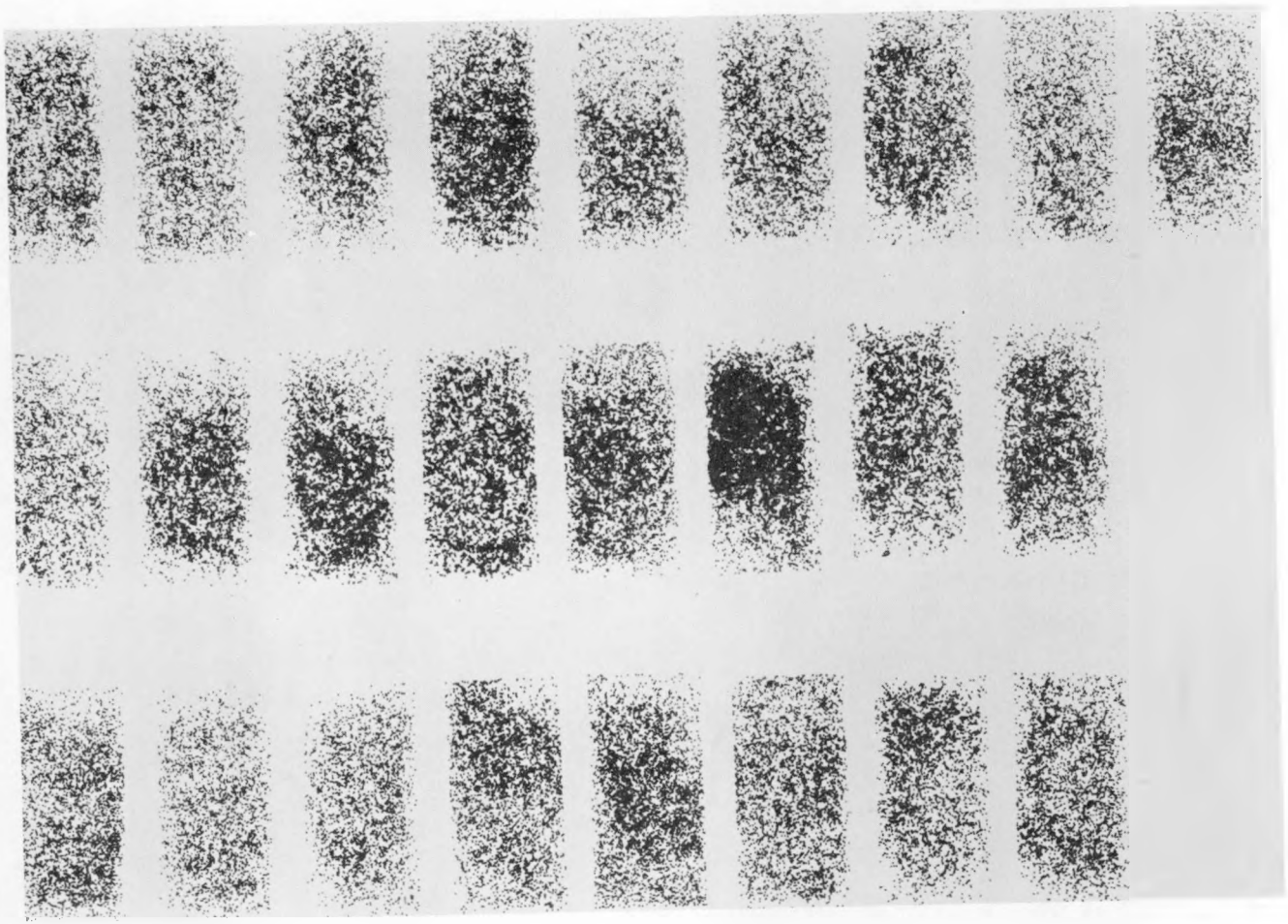

FIGURE 2. FUEL DISTRIBUTION IN 1/8-IN.-THICK COUPONS - PC-COATED UC_2, GRAPHITE MATRIX

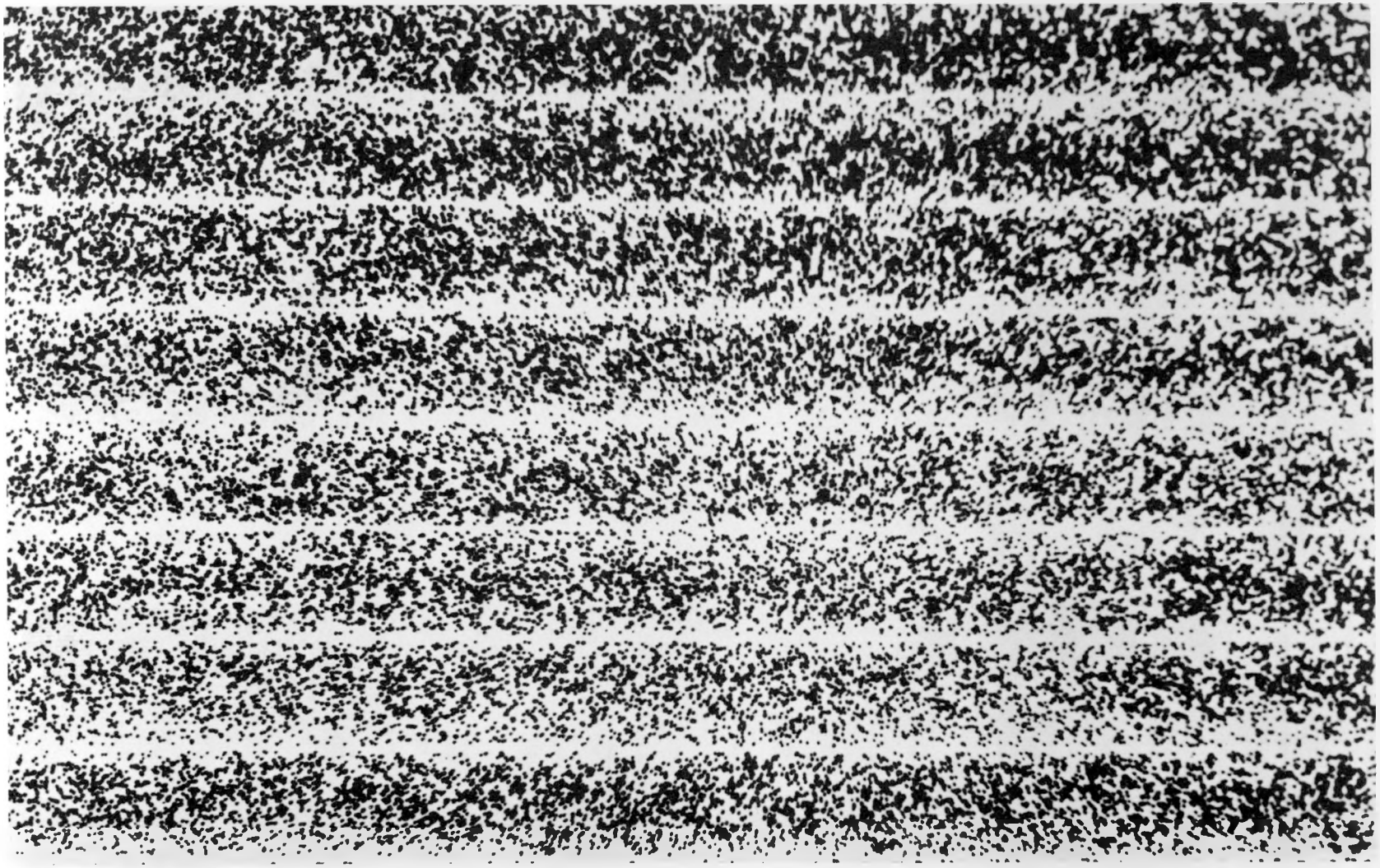

FIGURE 3. FUEL DISTRIBUTION IN 1/4-IN. RODS - Al_2O_3 COATED UO_2 IN GRAPHITE MATRIX

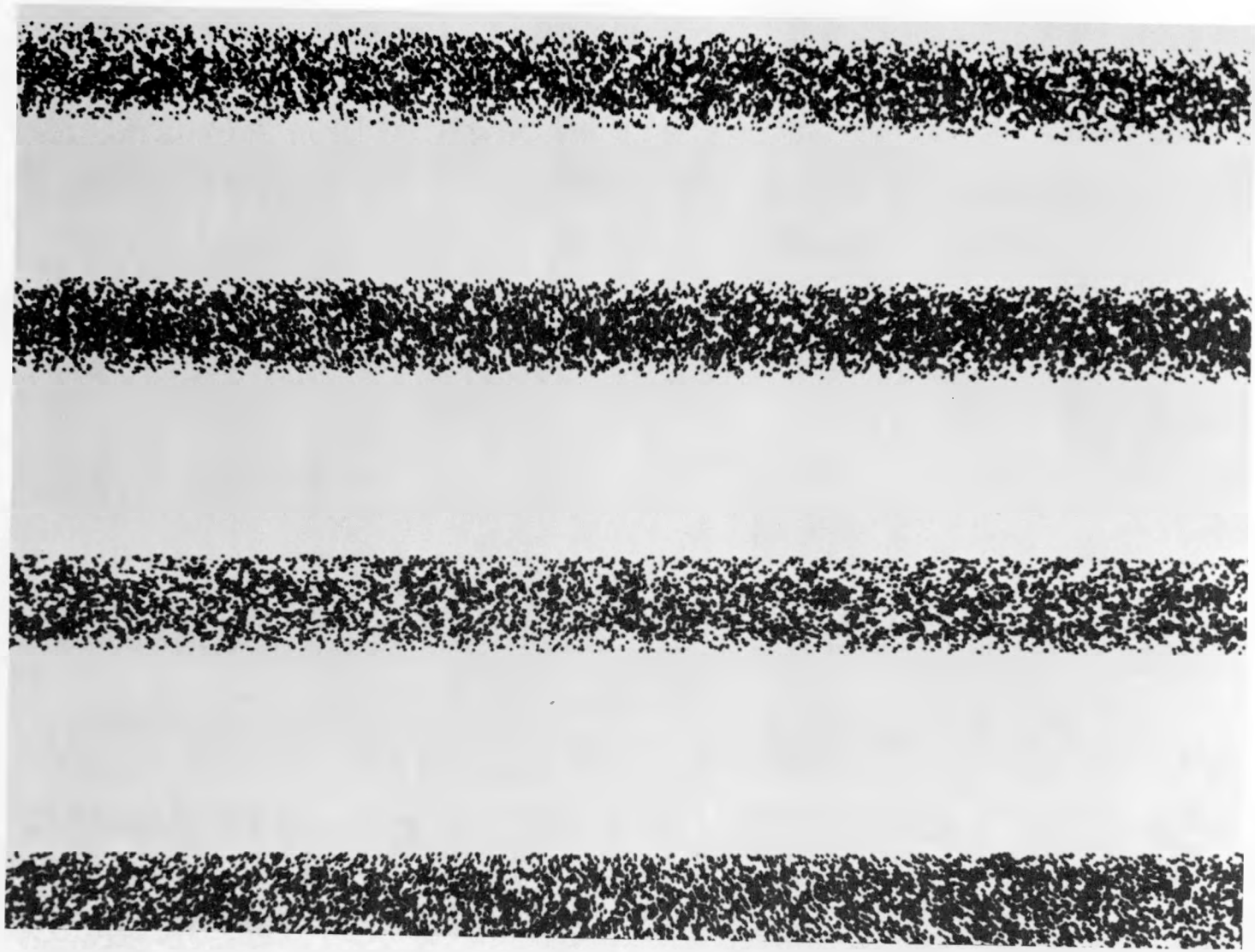

FIGURE 4. FUEL DISTRIBUTION IN 1/4-IN. RODS - PC-COATED UC_2, GRAPHITE MATRIX

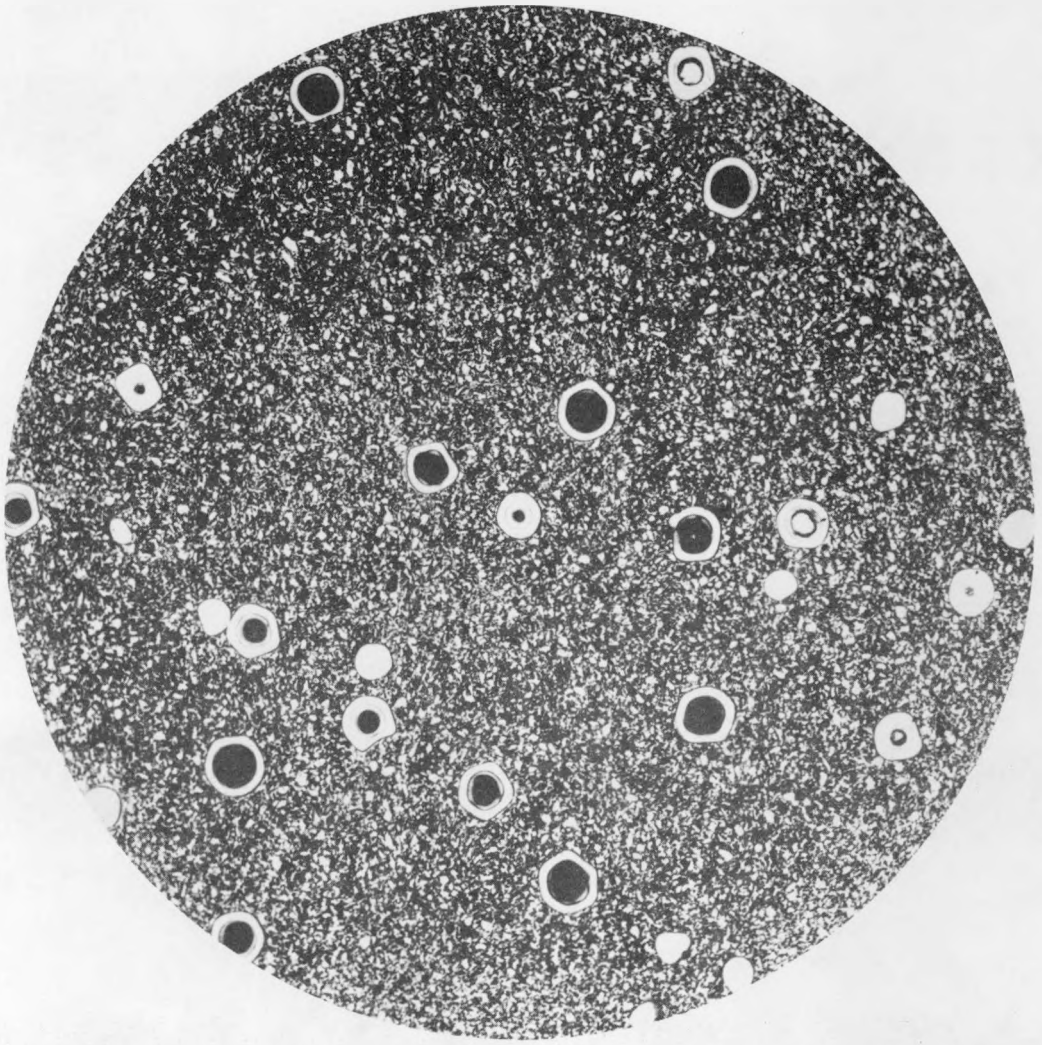

FIGURE 5. FUEL DISTRIBUTION IN CROSS SECTION OF 1/4-IN. ROD AT 10X - PC-COATED UC_2, GRAPHITE MATRIX

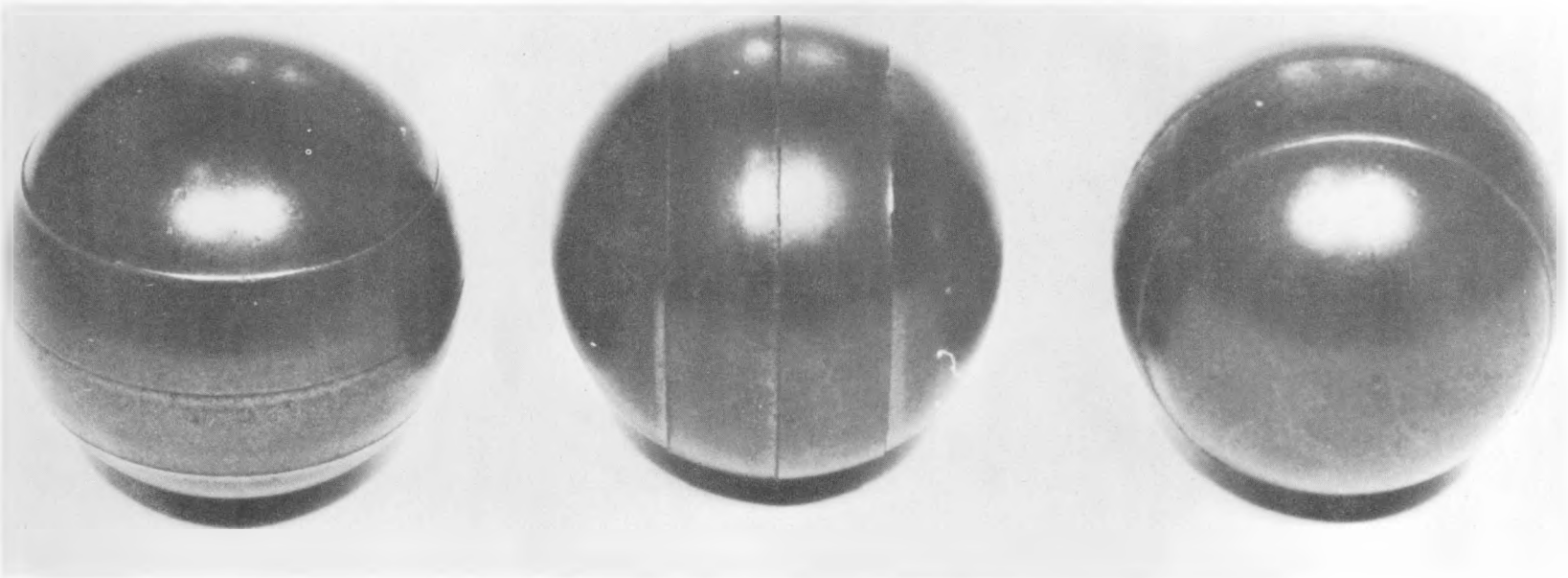

FIGURE 6. AS-MOLDED GRAPHITE-MATRIX SPHERICAL FUEL ELEMENTS

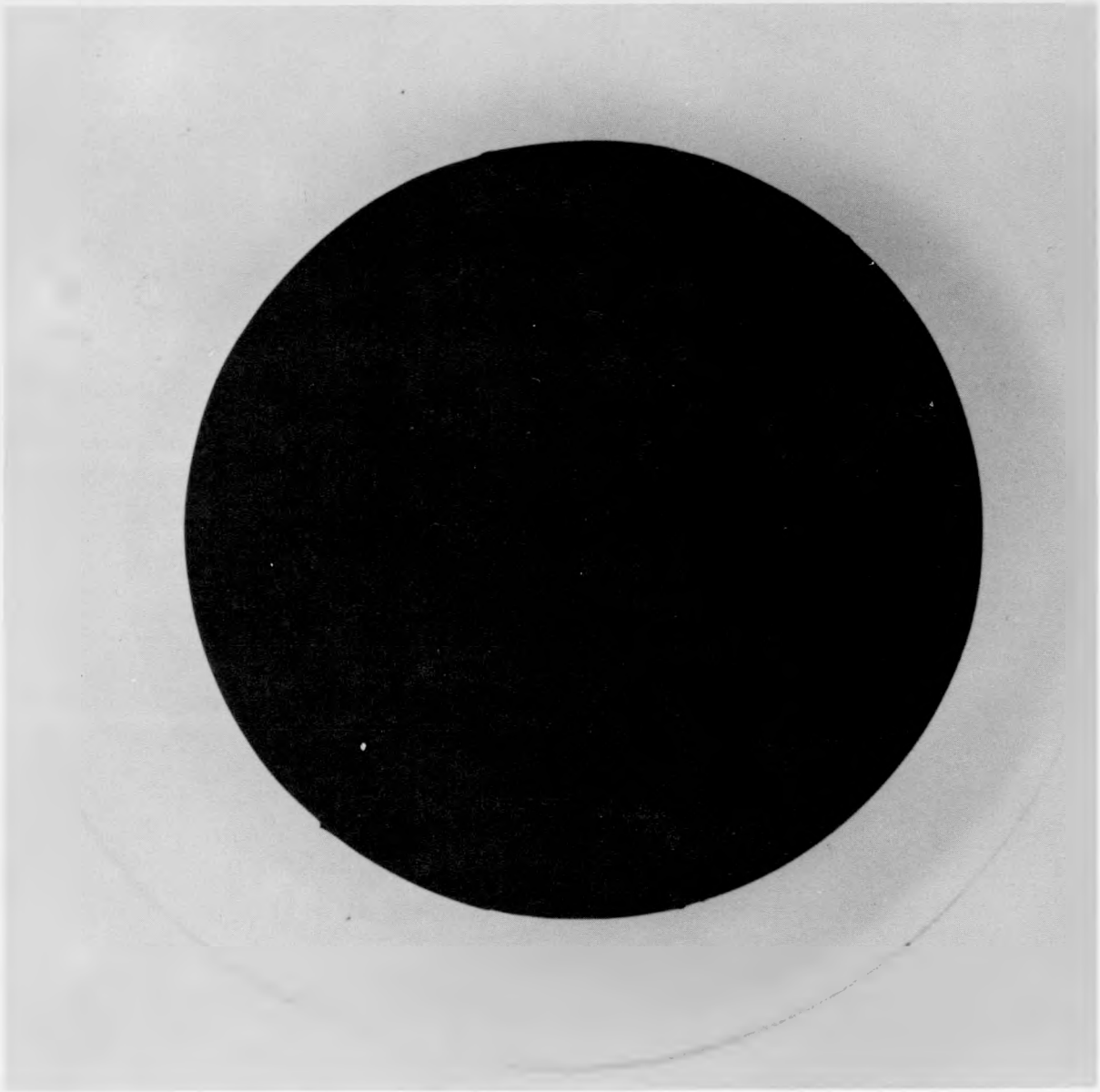

FIGURE 7. SPHERE WITH UNFUELED SHELL, POLAR SECTION

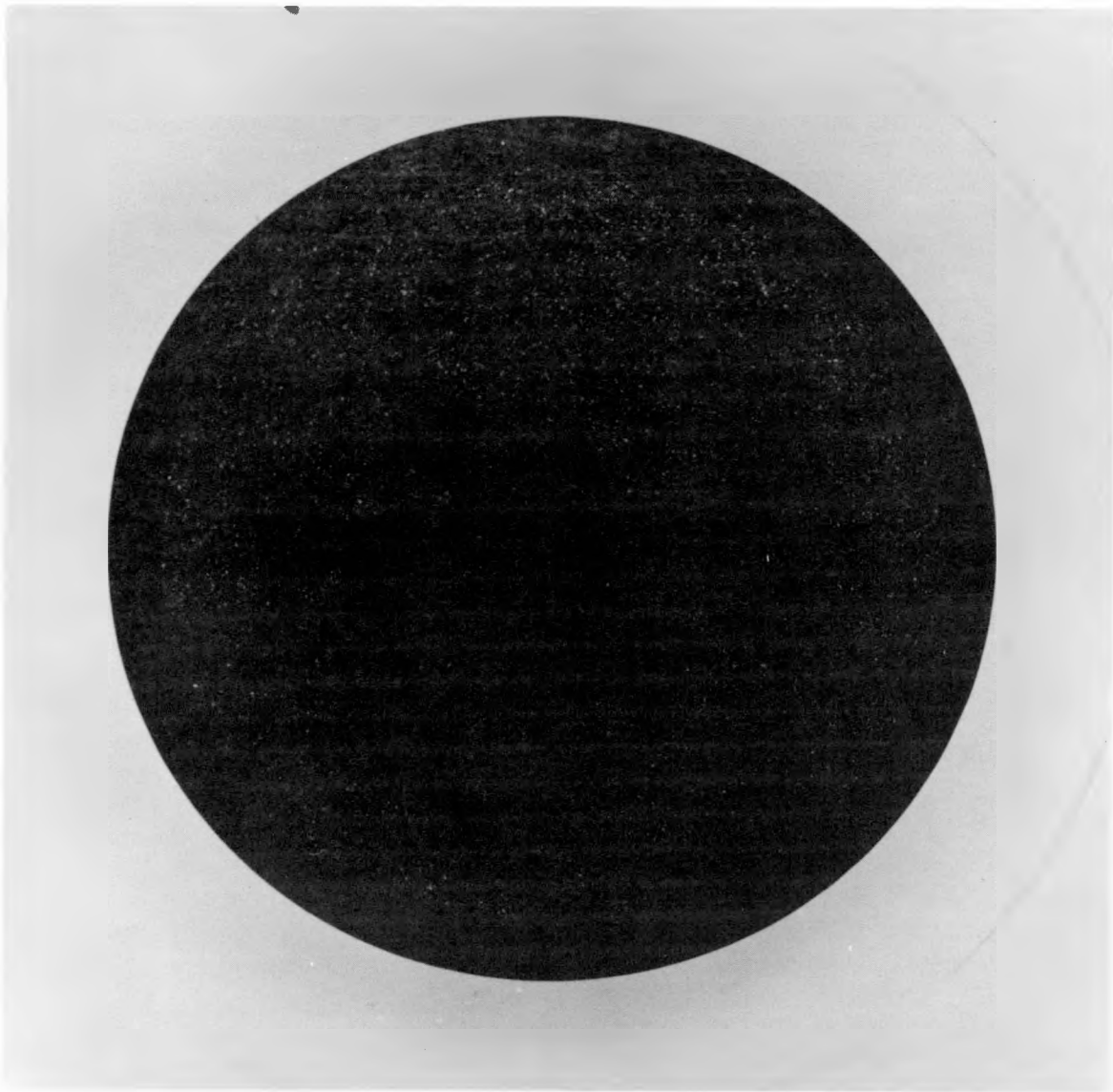

FIGURE 8. SPHERE WITH UNFUELED SHELL, EQUATORIAL SECTION

FUEL ELEMENT TYPE *	FUEL TYPE	CARBON DENSITY (gm/cc)	STRENGTH (psi)		C.T.E. (/°C)	
			COMPRESSIVE	FLEXURAL	∥	⊥
SPHERICAL (1½" d)	PC-UC_2	1.65-1.75	1500 – 2500	——	3.5	6.5
RODS (¼" d)	PC-UC_2	1.69	——	6135	——	——
	Al_2O_3-UO_2	1.50	——	3800	——	——
COUPONS (1" x 0.5" x 0.125")	PC-UC_2	1.70	——	5736	——	——
	Al_2O_3-UO_2	1.50	——	2180	——	——
ANNULAR ⅝" od. x ⅜" id.	PC-UC_2	1.40 – 1.50	3000 – 4000**	——	——	——

* CHEMICAL IMPURITIES WERE MINIMIZED IN ALL CASES.

** A.R.F. BRITTLE RING TEST.

FIGURE 9. TYPICAL PROPERTIES OF SPEER GRAPHITE-MATRIX FUEL ELEMENTS

As a result of the work reported above, the Speer Carbon Company is prepared to consider fabrication of graphite matrix fuel elements containing coated particles in complex shapes, with or without unfueled shells, to meet any set of reasonable specifications.

References Cited

1) NYO 9059, W. E. Parker and F. Rusinko, Jr. Thorium Oxide Infiltration of Graphite Spheres, June 15, 1960

2) W. E. Parker and M. J. Smith Development of Graphite Matrix Fuel Elements, Trans. Amer. Nuclear Soc., 4, No. 2, November 1961, p 343

3) Private communication from Dr. S. Reed, Chemistry Division, Union Carbide Nuclear Corp., ORNL

PRODUCTION CAPABILITIES OF UNITED NUCLEAR CORPORATION-CHEMICALS DIVISION FOR PRODUCTION OF COATED CERAMIC PARTICLES

By C. W. Kuhlman

Chemicals Division, United Nuclear Corporation
St. Louis 7, Missouri

The United Nuclear Corporation-Chemicals Division, formerly the Mallinckrodt Nuclear Corporation, has continued the general policy of providing a source of fuel materials required by the nuclear industry.

United Nuclear Corporation is prepared to supply UO_2, UO_2-ThO_2, and other solid solutions with UO_2, UC_2, UC_2-ThC_2, and ThO_2, all in the form of spherical particles. The particle size of these substrates is in the range 50 to 500 microns in diameter, although product outside that particle-size range might be delivered by special development efforts. As an example of the magnitude of this production capability, the United Nuclear plant has the capability of producing in excess of 250 lb per week of fully enriched uranium dioxide shot of a particular common specification.

United Nuclear Corporation has an established plant with capabilities for coating the above substrates with tungsten, molybdenum, nickel, niobium, tantalum, vanadium, and chromium.

A pilot-plant facility exists for pyrolytic-carbon coating with prospects of production-scale facilities shortly after January 1, 1963. It is further anticipated that hardware capabilities for beryllium oxide, aluminum oxide, and magnesium oxide coating will be established by spring of 1963.

PYROLYTIC CARBON COATED FUEL PARTICLES

By L. E. Short

Davison Chemical Company Division of
W. R. Grace and Company
Erwin, Tennessee

Davison's Nuclear Reactor Materials Plant, located at Erwin, Tennessee, is operated by Davison Chemical Company, a Division of W. R. Grace and Company. Though small in size in comparison to most AEC-operated plants, Davison has fully integrated production facilities and analytical services required for producing reactor fuels.

In the field of uranium carbides and pyrolytic-carbon-coated fuel particles, Davison became actively engaged in supplying quantities of uranium monocarbide and dicarbide to Atomics International about two years ago, under the sodium graphite reactor program. Using the technical know-how gained under the program, concerted development efforts were made during the past year to produce spherical uranium dicarbide. The first phase of this development program was directed at producing spherical uranium dicarbide meeting the following requirements:

(1) Density greater than 95 per cent of theoretical (11.3 g/cm^3)
(2) Low oxygen content
(3) Stoichiometric U/C ratio
(4) Spherical population greater than 98 per cent.

Full-size production equipment was used to produce 1 and 2-kg quantities during test runs. Product evaluation for this program was somewhat simplified, since the materials testing laboratory was fully equipped for evaluating NR-8 fuel.

After exploiting what was thought to be potential production processes for making spherical uranium-dicarbide, the field narrowed down to essentially three basic process routes by which essentially the same end product could be attained. These process routes are summarized briefly as follows:

Route I — Production of spherical UC_2 by fluidizing low-density, highly porous UO_2 spheres in a reactive carbon gas atmosphere generated by the thermal decomposition of hydrocarbon gas at 1850 C

Route II — Fixed-bed sintering of UO_2 plus carbon in a vacuum induction furnace to produce irregularly shaped UC_2 grains, followed by subsequent fluidization and coating with pyrolytic carbon as outlined above

Route III — Reduction of a uranium oxide and carbon mixture to a dense metallic UC_2 cake, followed by size reduction and spheroidization in an inert-gas atmosphere at a temperature in excess of 2000 C.

The second phase of the development program involved coating spherical UC_2 with either columnar- or laminar-type pyrolytic-carbon coatings. It was discovered that each type of coating was related directly to the deposition temperature and deposition rate. As a result of more than 60 pyrolytic-carbon coating runs, deposition rates were established in order to control coating thickness.

COATED-PARTICLE FUEL FOR THE DRAGON REACTOR EXPERIMENT

By R. A. U. Huddle, J. R. Gough, and H. Beutler

O.E.C.D. High-Temperature Reactor Project
Dragon Project Office, A.E.E., Winfrith

Abstract

A brief description of the core of the Dragon Reactor is presented with emphasis on the major objectives concerning fuel-element development.

Reference is made to the proposed specification for the initial charge in describing the methods chosen for production of the coated-particle fuel assemblies. An experimental fluidized bed employed for all coating studies is described, and the development of the prototype production apparatus is traced through its various stages.

Methods used for making composite coatings of pyrolytic carbon/graphite and silicon carbide are discussed, and initial results of the evaluation studies presented.

1. INTRODUCTION

Early in 1956 a small team was formed at the Atomic Energy Research Establishment, Harwell, to investigate the possibilities of the high-temperature gas-cooled reactor system. As part of this work, a design study of a relatively small [10-20 MW(t)] reactor experiment was carried out: in addition a considerable amount of research and development work associated with such a reactor was initiated. In April 1959 the responsibility for this work was taken over by the O.E.C.D. High Temperature Gas-Cooled Reactor Project (the DRAGON Project) at the Atomic Energy Establishment, Winfrith, the major objective being to build and operate a reactor experiment.

The main purpose of this reactor experiment is to demonstrate the principles on which any high-temperature gas-cooled reactor must be based.

Its principal features are the use of helium as coolant, with fuel elements of low-permeability graphite, containing fuel cartridges in which the dispersed fissile and fertile material is in the carbide, oxide, or other ceramic form. Provision is made for the removal of fission products which escape from the fuel cartridge by passing a fraction of the total coolant (the purge flow) directly over the cartridges and into a fission-product clean-up system. Even with such a fission-product clean-up system, it has been accepted from the outset that the primary coolant circuit would be active.

A diagrammatic arrangement of the reactor is shown in Figure 1. The development of the design has been described in a previous paper[1] whilst details of progress are given in the Project Annual Reports[2]. In this paper the major steps in the development of the fuel cartridge are described with particular reference to coated-particle fuel.

2. THE FUEL ELEMENTS

In the design of the core, efforts have been made to avoid those problems which were considered to restrict the development of conventional gas-cooled reactors. To this end, all parasitic material has, where possible, been avoided, and the fuel elements have been designed so that the whole core, including the graphite moderator is replaceable on each fuel change. The core (Figures 2 and 3) consists of 37 fuel elements each of which comprises 7 fuel tubes of low-permeability graphite, joined at the top by a metal-reinforced graphite block and at the bottom by a stainless steel assembly which serves to route the fission-product purge flow to the fission-product clean-up system (Figure 4). Each tube has a bore 1-3/4 in. in diameter by 5 ft in length into which the fuel cartridges are inserted. This design, which will be used for the initial charge, is appropriate for fuel which is expected to release a significant proportion of its fission products. With the satisfactory accomplishment of the development of fission-product retaining fuel, such a fuel element would be inappropriate, and it is inevitable that major changes will be incorporated when such fuels have been proven.

From the outset, it was appreciated that the problem of retaining fission products within the fuel element required major technical developments, and the whole philosophy of the design of the reactor experiment has been based on a fission-product emitting system involving an active primary circuit coupled with a fission-product clean-up system.

Although this principle has been adhered to, the advantages of having a retaining fuel element were self-evident, and soon after the initiation of the

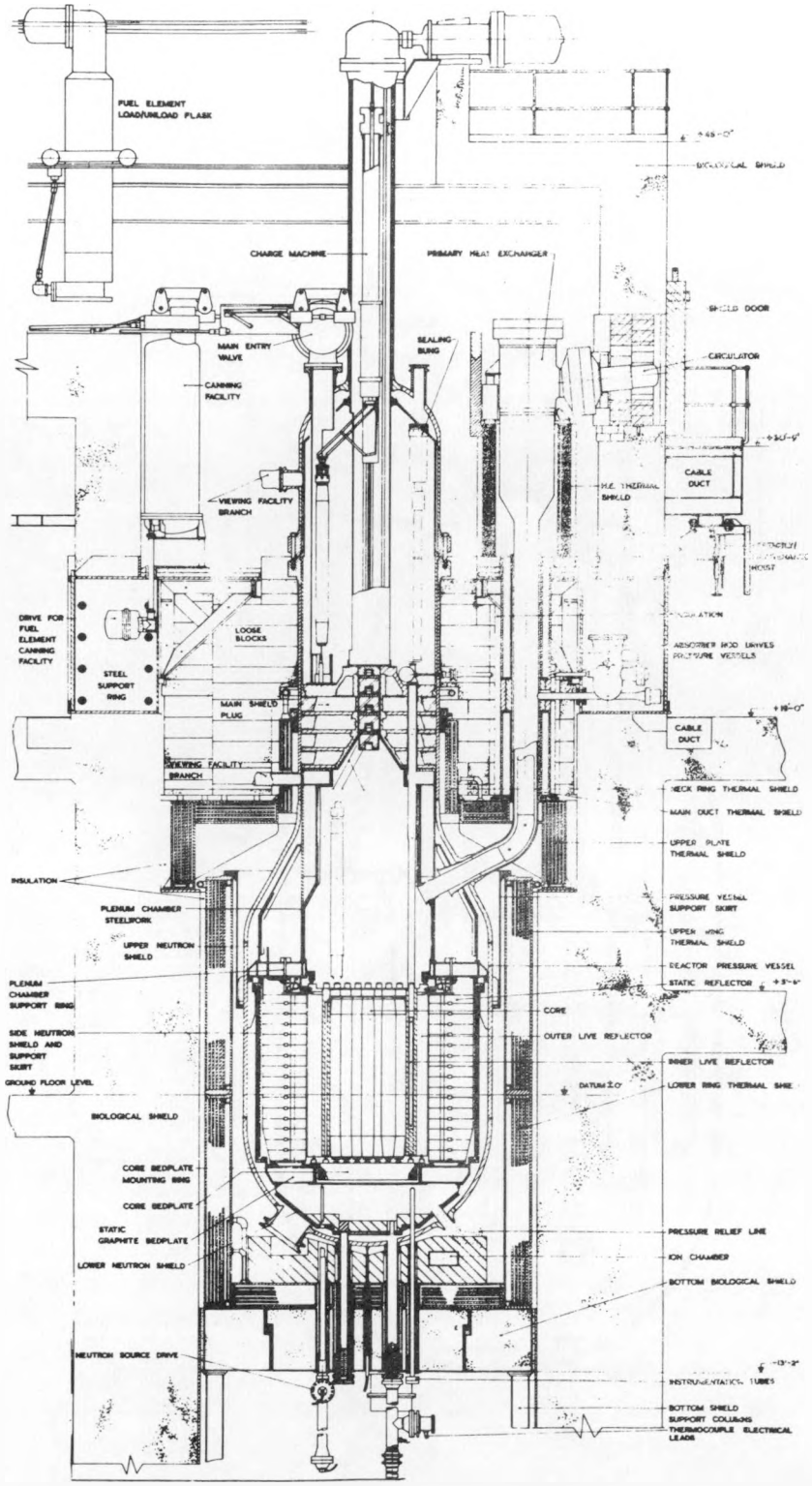

Fig. 1. DRAGON REACTOR EXPERIMENT DIAGRAMMATIC ARRANGEMENT OF REACTOR

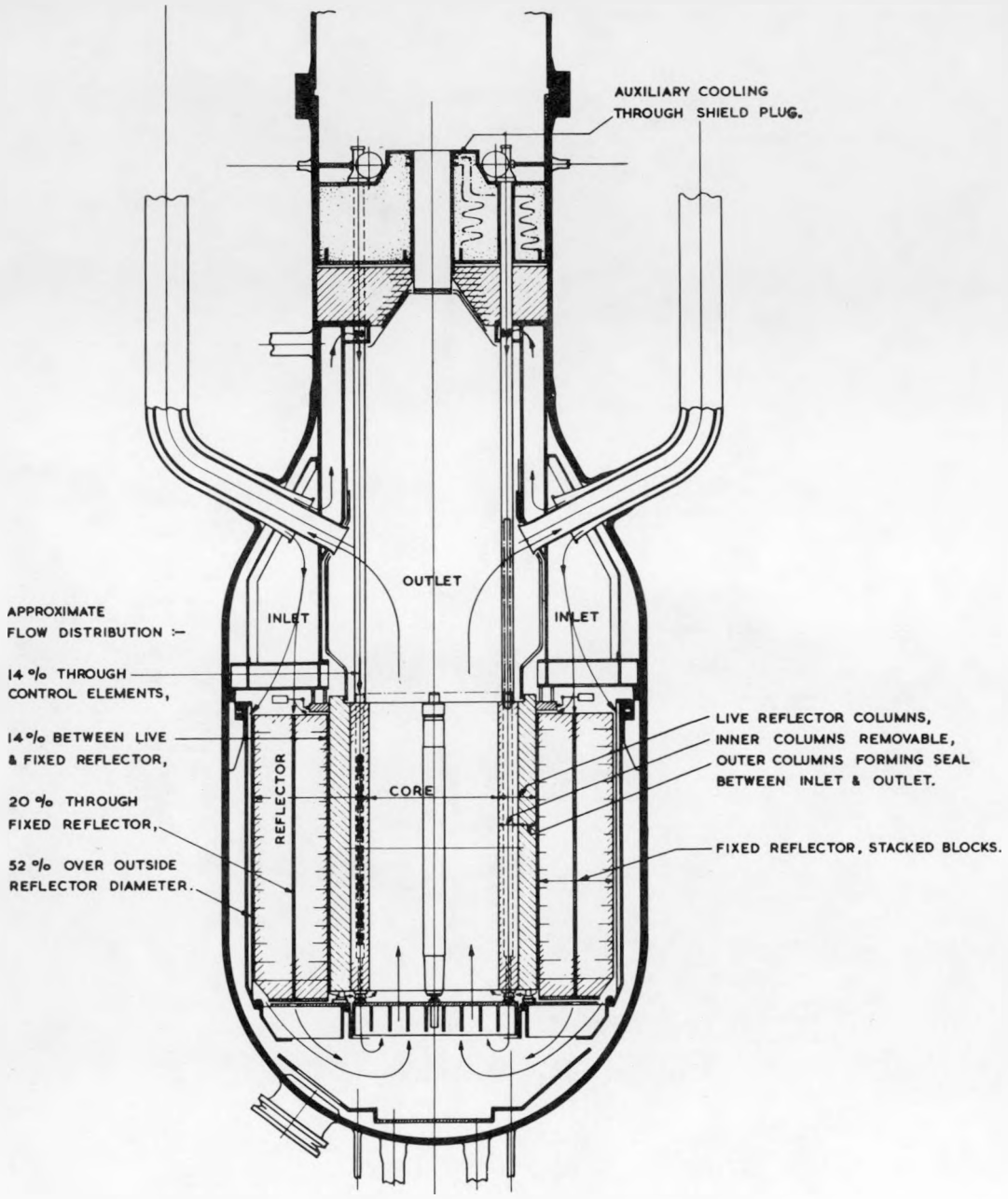

FIG. 2 SECTIONAL DIAGRAM OF REACTOR

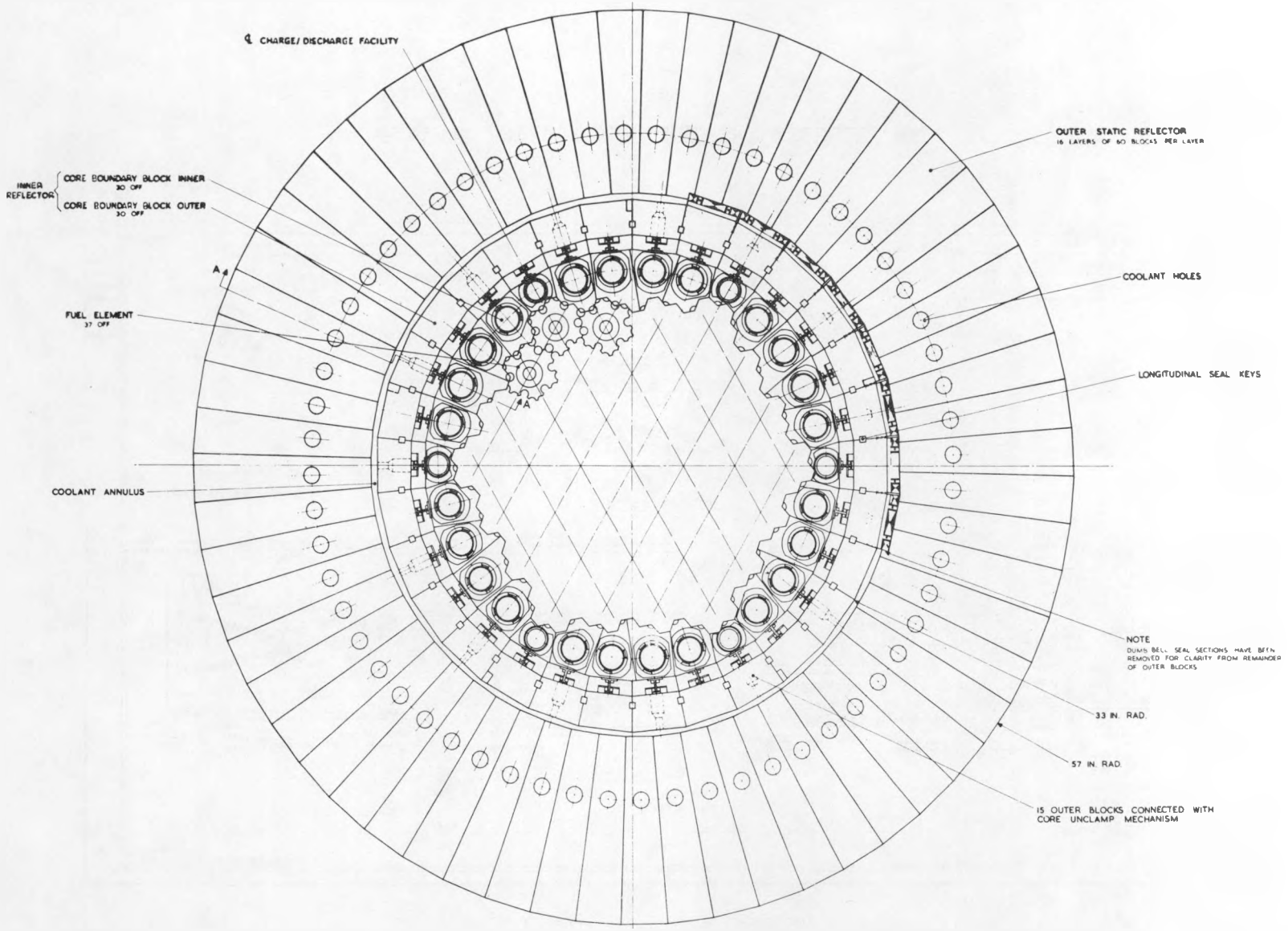

Fig. 3. PLAN VIEW OF CORE AND REFLECTOR

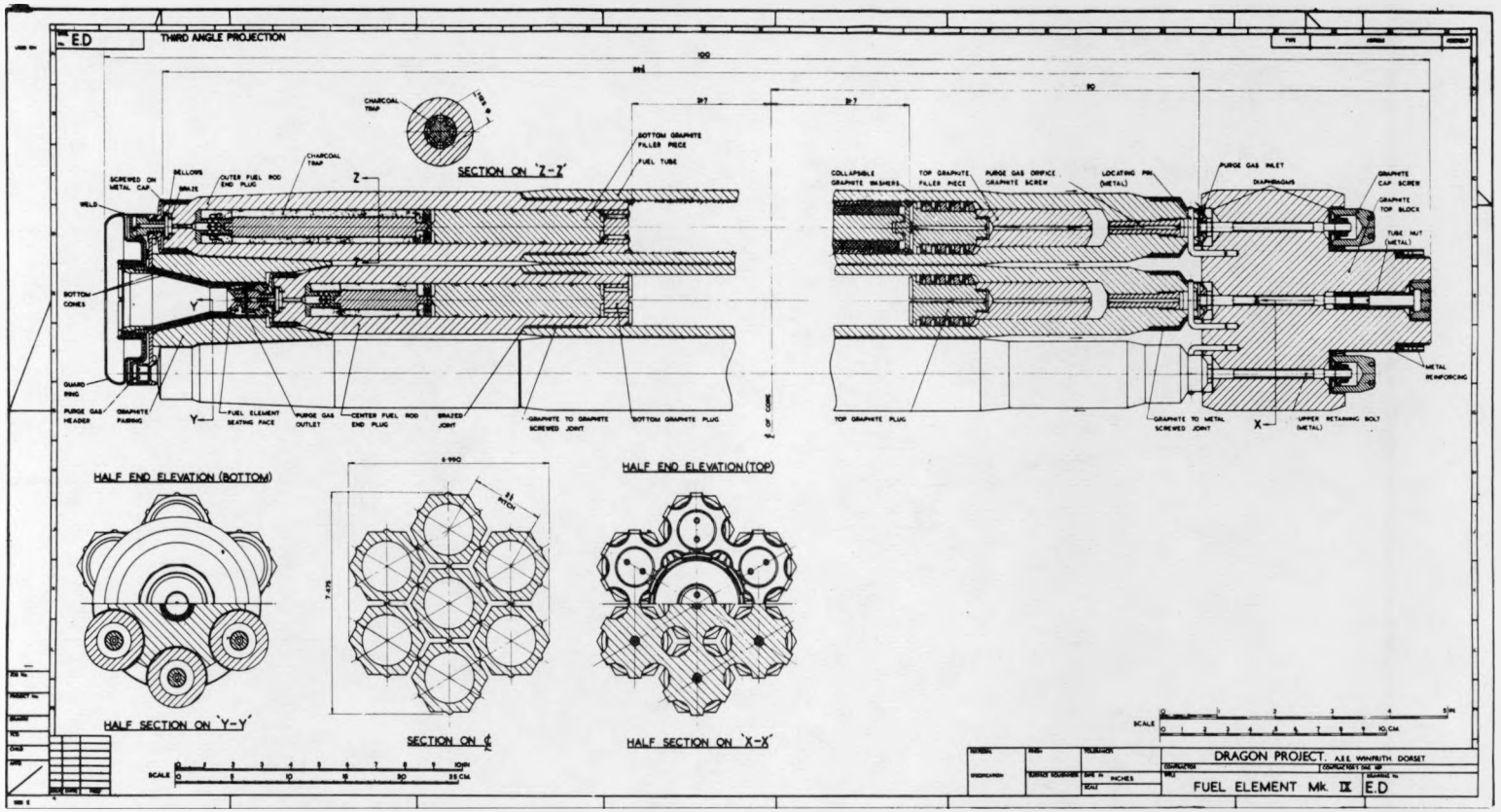

Fig. 4. DRAGON FUEL ELEMENT ASSEMBLY MARK IX

Design Study thoughts were directed towards the methods which seemed likely to produce satisfactory fission-product retention. Of the various methods considered the coated particle seemed the most appropriate, and some experimental work was carried out on pyrolytic-carbon coatings at A.E.R.E., Harwell.

As the detailed design proceeded the necessity for effecting some fission-product control within the fuel element itself became apparent, and a cartridge comprising annular fuel inserts of uranium and thorium dicarbides dispersed in graphite, and sealed in a fuel box of ultra-low-permeability graphite, was developed and recommended for the initial charge of the reactor; in addition, a delay trap of active charcoal was incorporated into the bottom of each fuel rod. This system has been developed to the production stage.

Recent physics calculations concerning the possibility of experimental elements remaining in the core for periods comparable to that required for the fuel elements of a large power reactor have demonstrated the necessity for departing from homogeneous loading; at present a two-zone core is recommended in which the thorium is concentrated in the center zone. In the case of coated-particle fuel it seems unlikely that an unalloyed fully enriched fissile particle could withstand a burnup (fissions per initial fissile atom - F.I.F.A.) of the order of 30 to 50 per cent, and it is therefore necessary to employ a diluent for the fuel in the outer zone; for this, zirconium has been chosen. At the present time an atomic ratio of Th/U^{235} of 15/1 is recommended for the inner zone, while for the outer zone the Zr/U^{235} ratio is 8/1.

3. COATED-PARTICLE FUEL

During 1960 experimental information concerning the fission-product control circuit emphasized the desirability of providing fuel with the maximum degree of retention possible for the first charge. In any case, in such a novel system it seemed the right philosophy to start off with the primary circuit having as low an activity as possible, so as to reduce the load on the fission-product plant, and to minimize maintenance problems of the primary circuit which will inevitably arise during the initial stages of operation of the reactor experiment. It was therefore decided to mount a major research and development program to ascertain the possibility of employing coated-particle fuel for the initial charges. The objectives of this work were:

(a) To develop the optimum process for producing a fission-product retaining insert.

(b) To develop a "Pilot Plant" production apparatus.

(c) To test the resultant products for their fission-product retention characteristics.

At that time facilities available within the Project were fully occupied with the development of the "Fuel Box" cartridge and all work associated with this program was carried out in signatory countries under research and development contracts. The work on particles has been concentrated in Austria at Metallwerk-Plansee (Reutte, Tyrol) and S.G.A.E., (Seibersdorf, Vienna) and also at the C.E.N., Mol, in Belgium; work on coating has been carried out at the Royal Aircraft Establishment, Farnborough, England. Since the commissioning early this year of the Dragon Fuel Element Laboratories development work has been carried out by Project staff at Winfrith.

3.1 The Fuel Particle

In Austria the work was directed initially to solving the problems associated with the fabrication of uranium dicarbide and thorium/uranium dicarbide. However, during 1961, it became apparent that the method under development (involving fabrication of the massive dicarbide followed by comminution and sizing) was running into serious difficulties in that it was not possible to obtain adequate yields bearing in mind the nature of the materials involved. It was decided therefore, following an over-all assessment of the situation, that the powder-metallurgy agglomeration process as developed at C.E.N., Mol, for oxide fuels[3] should be studied as an alternative.

Initially, experiments were carried out with uranium dicarbide to see what general modifications were required to the methods previously employed for oxide fuel. Experiments showed that some modifications were in fact necessary and the appropriate techniques to fabricate spherical particles in the "green" state were defined; these particles can be sintered to provide a range of porosity. Because of the encouraging results obtained, this process has been chosen for the development of production equipment. It is capable of giving very high efficiencies without complicated recycling; furthermore, its inherent flexibility to produce any composition of fuel is a most important factor in its favor. Preliminary experiments employing this method for the fabrication of the Zr/UC fuel have been successful.

Early work on the fission-product retention of carbon-coated fuel particles had shown that one of the essentials for good retention was that the fuel particles should be spherical. It was not known, however, if this

improved retention was due to the better geometry of a sphere (from the point of view of the coating as a pressure vessel) or if it was associated with the fact that the spherical particles tested had been melted. It is still not clear whether the "high burnup" retention characteristics will favor the porous or the high-density particle. The powder-metallurgy agglomeration process enables both types to be fabricated side by side.

Work on the equilibrium of the thorium-uranium-carbon system has shown that the dicarbide is not stable at temperatures below about 1550 C; it does, in fact, break down into the monocarbide (or possibly the sesquicarbide) and carbon, even though the rate is very slow. Now this reaction is accompanied by an increase in volume, and it is therefore possible that the coating of fuel particles made by melting (and therefore in the dicarbide form) could be ruptured, as sufficient decomposition takes place at the operating temperature - accelerated by the irradiation - to provide the necessary expansion. Although this mechanism is not necessarily responsible for the poor retention characteristics of certain batches of fuel, it is certainly a possible explanation of the observed effects, and suggests experiments on fuel made from the truly stable components. Such experiments are in hand.

Two methods of melting such agglomerates have been studied:

(a) A three-phase arc system employing hydrogen in the feed to give an extended plasma.

(b) A specially developed plasma torch.

The work on the three-phase arc system has been carried out at S.G.A.E., Seibersdorf, whilst the plasma-arc method has been developed within the Project at Winfrith.

Work within the Project has been directed towards evaluating the various processes as well as producing specimens for irradiation tests. Having considered the alternatives, the following steps are proposed for the development of a prototype production process:

(a) Thorium/uranium fuel

(i) A mixture of uranium metal powder and carbon is reacted at 1500 C to form the dicarbide.

(ii) After grinding to -37 microns the uranium dicarbide powder, together with the appropriate quantities of thorium metal powder and carbon powder is mixed with a binder (e.g., camphor) and a solvent (e.g., isopropyl alcohol) to form a cake.

(iii) Agglomerates of the required size are prepared from this cake by granulation through a sieve.

(iv) If porous particles are required, these green agglomerates can be spheroidized by tumbling in a rotating cylinder, the inside of which is covered with a fine abrasive.

(v) The resultant spheroids are sintered to form the equilibrium phase having the desired porosity.

(vi) If melted spheres are required, the particles are melted either by passing through a plasma jet or through a three-phase arc.

(b) Zirconium/uranium fuel

(i) Zirconium metal powder, uranium metal powder, and carbon powder (to form the monocarbide) are mixed in the atomic ratio, Zr/U:3/1. After compacting, the mixture is reacted at 1200 C to form a solid-solution monocarbide master alloy.

(ii) After grinding, the zirconium/uranium monocarbide is mixed with additional zirconium metal powder and carbon powder to give the desired composition.

(iii) This mixture is treated in the same way as the thorium/uranium dicarbide agglomerates to produce spherical particles. Precise details of the sintering procedure are presently being evaluated.

While the precise particle size is still to be determined, present work is based on a diameter of 300 ± 50 microns.

3.2 Coating

The work on coating has been divided as follows:

(a) Laboratory-scale work, for investigating the major parameters involved in the coating process and for the preparation of irradiation specimens.

(b) Production equipment for working on the kilogram scale.

Laboratory Scale Work. Considerable experience existed at the R.A.E., Farnborough, on the deposition of pyrolytic carbon and other refractory coatings, and following the successful application of fluidizing techniques for coating fuel particles by J. H. Oxley and his co-workers at Battelle Memorial Institute, Columbus, Ohio, a fluidizing system capable of operating continuously at temperatures up to 2250 C was developed at the R.A.E. by R. L. Bickerdike and H. C. Ranson.

Exploratory work was carried out using Perspex models to determine the optimum conditions for fluidization. Particular attention was paid to the design of the nozzle assembly to enable satisfactory coatings to be laid down at the higher temperatures without carbon deposition at the orifice. For working with thorium dicarbide as well as with fully enriched uranium, it was considered desirable to build the whole equipment to normal laboratory vacuum standards since this greatly facilitated problems associated with the handling of thorium dicarbide. Furthermore, such a system offers significant advantages in relation to the problems of "accounting and safety."

The graphite resistance furnace is water-cooled and can be evacuated to a pressure of 10^{-4} torr. A design has been standardized and is shown in Figures 5, 6, and 7. A number of such units have been constructed and are operating satisfactorily at Winfrith and at other contractors' laboratories The important characteristics of this equipment are given below:

Fluidizing vessel	1 in. in diameter by 15 in. long
Total gas throughput	2 l/min
Capacity	20 cm^3 particles
Pressure drop through nozzle and bed	1 psi
Furnace	Graphite resistance, single-phase 30 kva
Maximum temperature	2250 C
Length of hot zone	18 in.

The coating furnace is evacuated and flushed with purified argon before each run to ensure freedom from atmospheric contamination. Particles are charged into the hot furnace after the flow of carrier gas and hydrocarbon has been established. When the fluidizing operation is complete, discharge is effected through the nozzle system, it being unnecessary to dismantle the bed in any way. In the case of silicon carbide coatings (see below) the hydrocarbon is replaced by hydrogen, saturated (at room temperature) with methyltrichlorosilane.

A program of research and development has been carried out at the R.A.E., Farnborough, and within the Project laboratories on the deposition of pyrolytic-carbon coatings from propane, methane, and hexane at different concentrations and at different temperatures. This work, by R. L. Bickerdike, H. C. Ranson, and C. Vivante, has shown that it is possible to obtain particles with coatings of different density and having different structures. At high

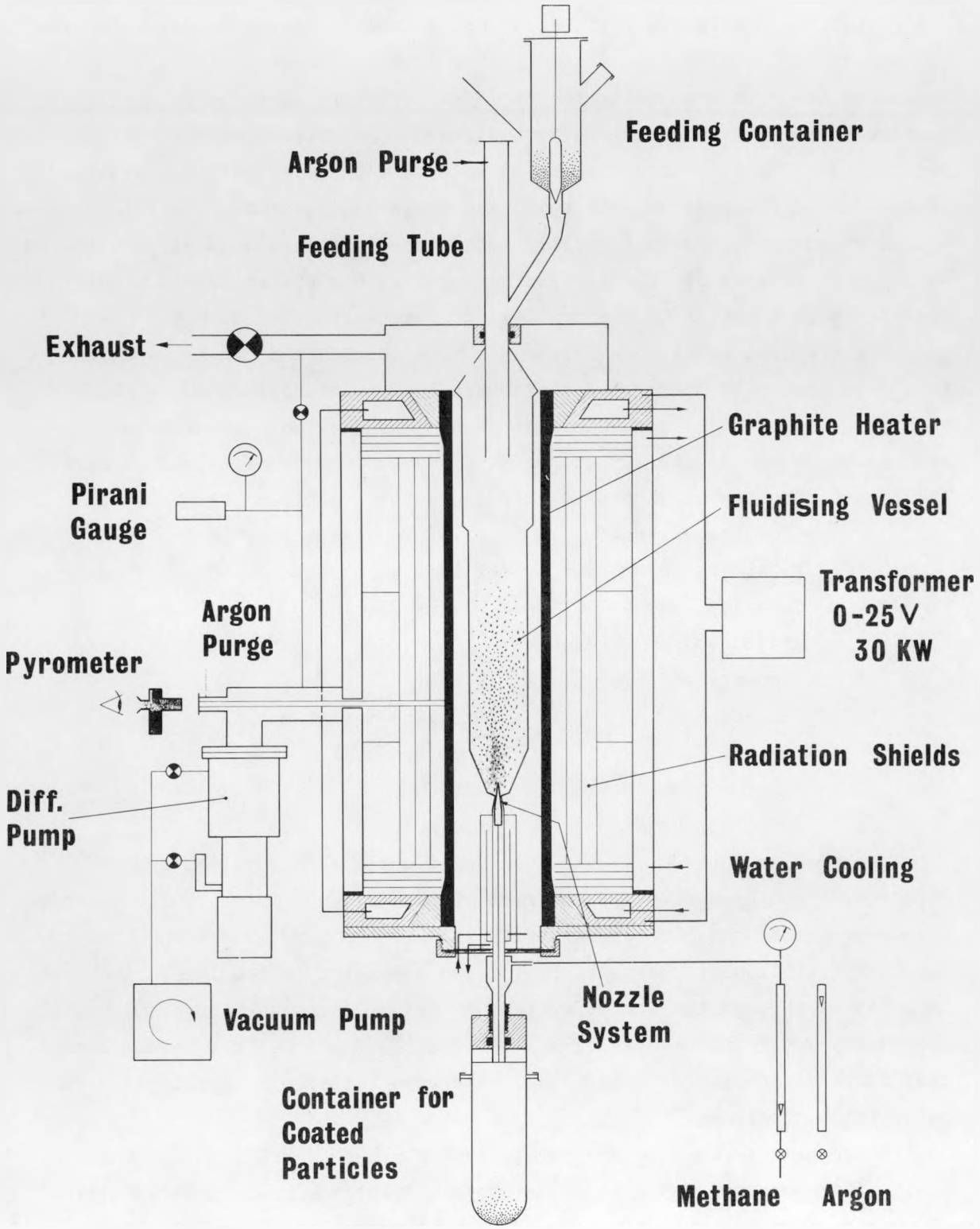

FIG. 5 SCHEMATIC DIAGRAM OF LABORATORY SCALE FLUIDISING FURNACE.

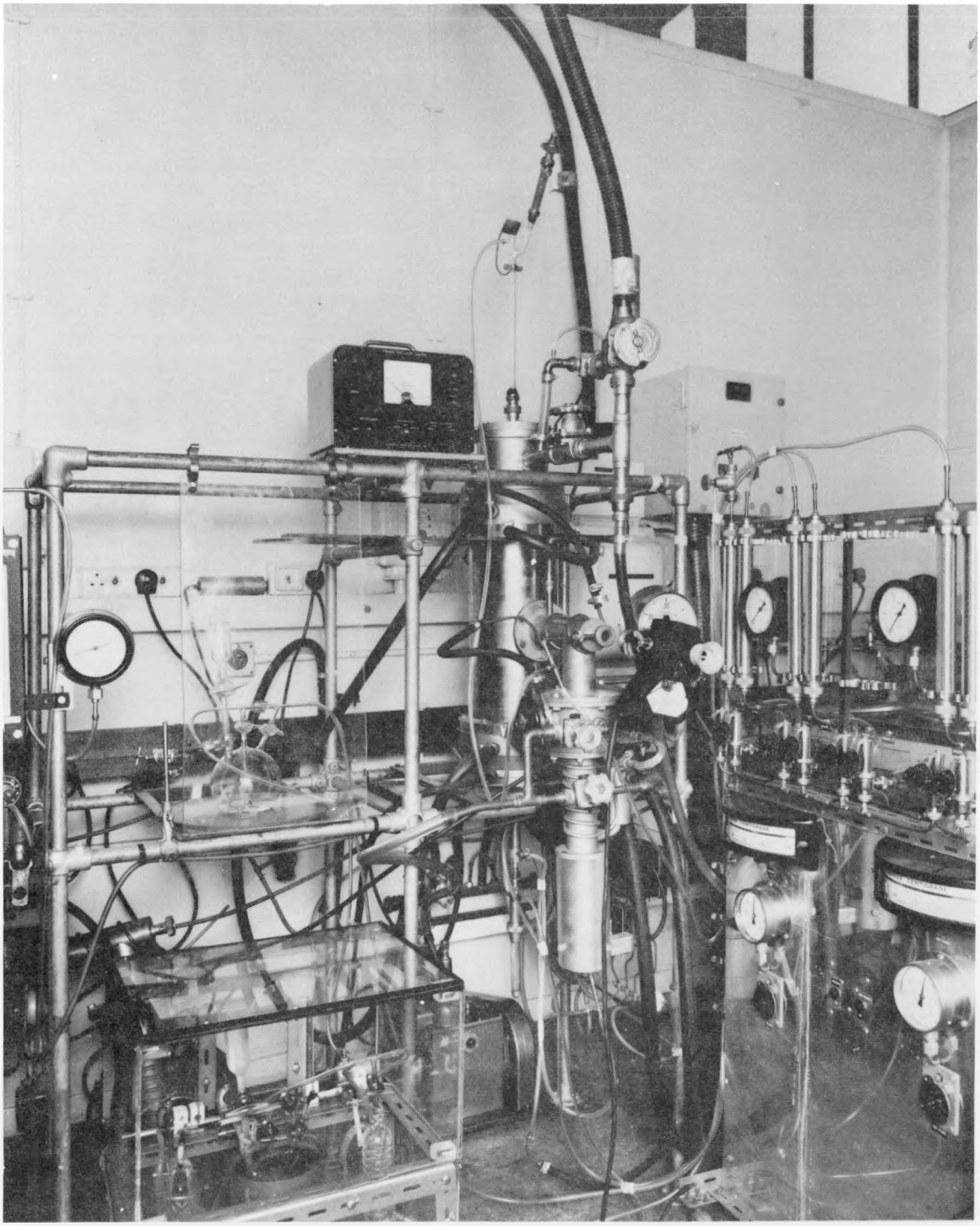

Fig. 6. LABORATORY SCALE FLUIDISING EQUIPMENT SHOWING FURNACE ASSEMBLY AND GAS PURIFICATION AND CONTROL PANEL

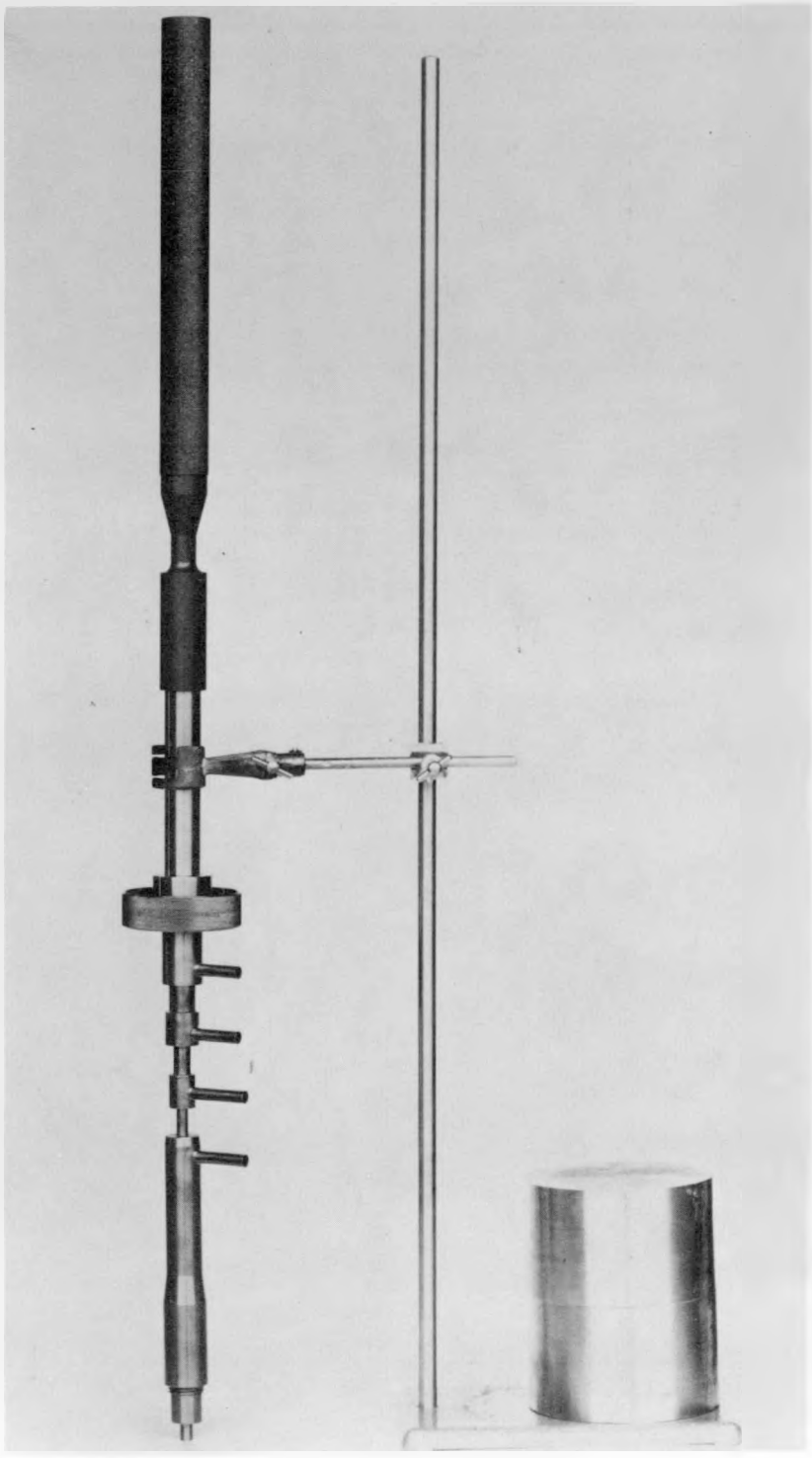

Fig. 7. WATER COOLED NOZZLE AND 1 INCH FLUIDISING REACTOR

concentrations (i.e., high rates of deposition) the coatings have an onion-skin appearance, while at low concentrations (i.e., low rates of deposition) a columnar structure is observed. With intermediate conditions the coatings are generally referred to as "structureless" since no obvious structure can be seen on metallographic examination of the unetched section. The relationship between the density, temperature of deposition, flow rate, and deposition rate, using methane as a source of carbon, is shown in Table I.

TABLE I. DENSITIES OF CARBON DEPOSITS ON URANIUM DICARBIDE PARTICLES

Bed Temperature, C	Methane Flow Rate, cm^3/min	Deposition Rate, cm/sec	Density, g/cm^3
1450	375	5.5×10^{-7}	1.83
1600	100	5.5×10^{-7}	1.46
	200	1.2×10^{-6}	1.37
	375	2.2×10^{-6}	1.36
1800	375	2.2×10^{-6}	1.61
2000	100	5.9×10^{-7}	2.14
	200	1.1×10^{-6}	2.07
	400	2.9×10^{-6}	1.90

Preliminary results on the evaluation of these particles, involving neutron activation followed by out-of-pile heating to determine the release of fission products, by J. S. Stubbs at A.E.R.E., Harwell, showed that some factor not directly associated with a diffusion phenomenon, was influencing the results. This was shown, by an alpha-counting technique to be due to

uranium contamination at the surface of the coating. It was observed that such contamination was always present when the coating temperature was in excess of 1500 C; and it was concluded that a complex mechanism resulting in uranium migration was operative above this temperature.

Since the fuel will operate at temperatures in excess of 1500 C, it is essential that the coating should be produced at a higher temperature in order to avoid failure due to the difference of expansion between fuel and coating. The above fact, together with the experimental results on diffusion of barium through carbon coatings, directed attention towards alternative diffusion barriers such as silicon carbide, and work on composite coatings of pyrocarbon/silicon carbide/pyrocarbon is now in progress. Exploratory results on the evaluation of these composite coatings are now becoming available and it appears that such coatings offer significant resistance to fuel migration and fission-product diffusion. However, it will not be until the results of "purged capsule" irradiation experiments are available that the effectiveness of this type of coating will be proven.

According to our present knowledge, the following procedure is recommended:

Stage	Thickness, microns	Deposition Temperature, C	Coating Agent
1	10-15	1350	Hexane
2	30	1800	Methyltrichlorosilane in hydrogen
3	30	1800	Hexane
Total	70-75		

Representative micrographs of such duplex coatings are shown in Figure 8, 9, and 10.

Prototype Production Apparatus. Following work at Metallwerk-Plansee, a prototype fluidizing apparatus has been developed in the Project laboratories employing the general principles of the laboratory model. Safety considerations in particular criticality, restrict the capacity of each unit to 1 kg of fuel particles. With such a system, three units, each capable of independent operation, would be required to maintain the rate of production necessary for fabricating two fuel elements per week.

A perspective view of the prototype, which has recently been commissioned is shown in Figure 11. The fluidizing reactor, having a capacity of about

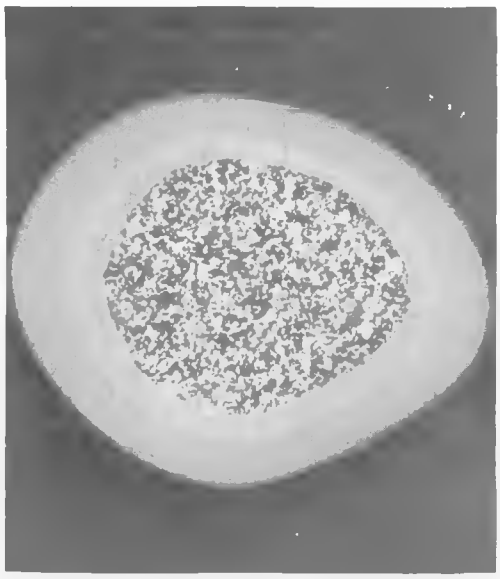

Fig. 8. SECTION OF 93% ENRICHED URANIUM DICARBIDE SINTERED PARTICLE 200 x 175μ DIAMETER COATED WITH TWO LAYERS OF PYROLYTIC CARBON

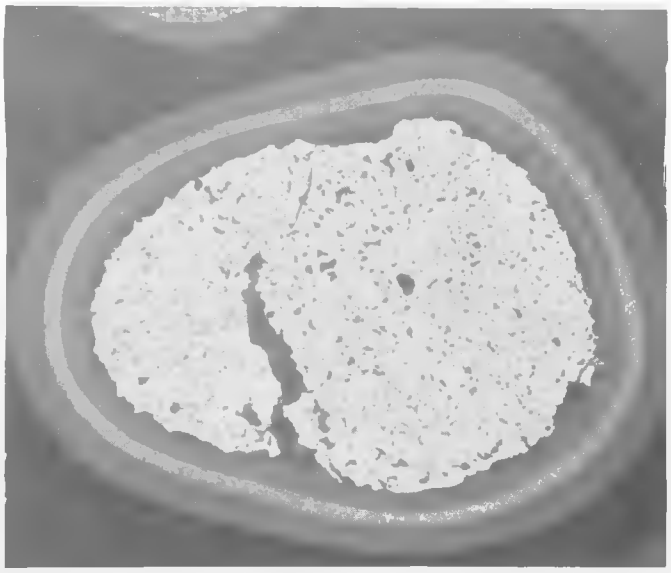

Fig. 9. SECTION OF URANIUM - THORIUM DICARBIDE SINTERED PARTICLE, COATED WITH PYROLYTIC CARBON, SILICON CARBIDE AND PYROLYTIC CARBON

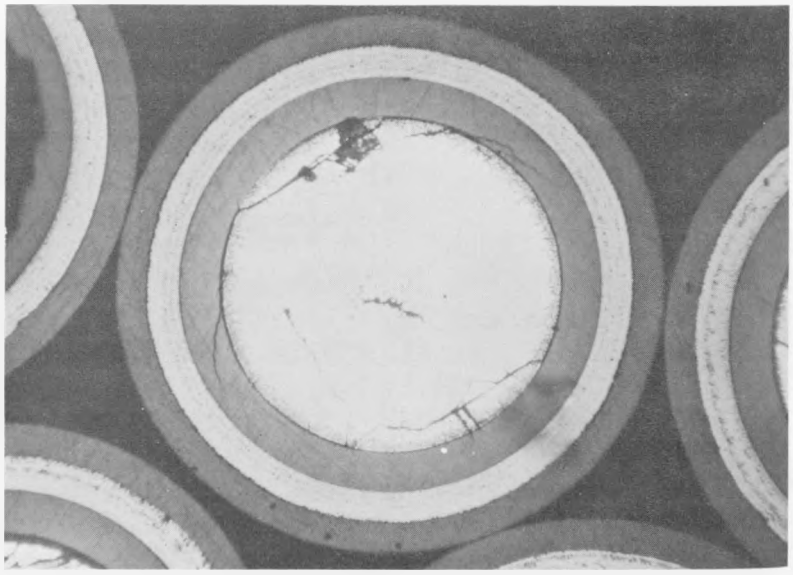

Fig. 10. SECTION OF URANIUM - THORIUM DICARBIDE MELTED PARTICLE, COATED WITH PYROLYTIC CARBON, SILICON CARBIDE AND PYROLYTIC CARBON. SHOWING CRACKS AFTER SEVERE THERMAL CYCLING

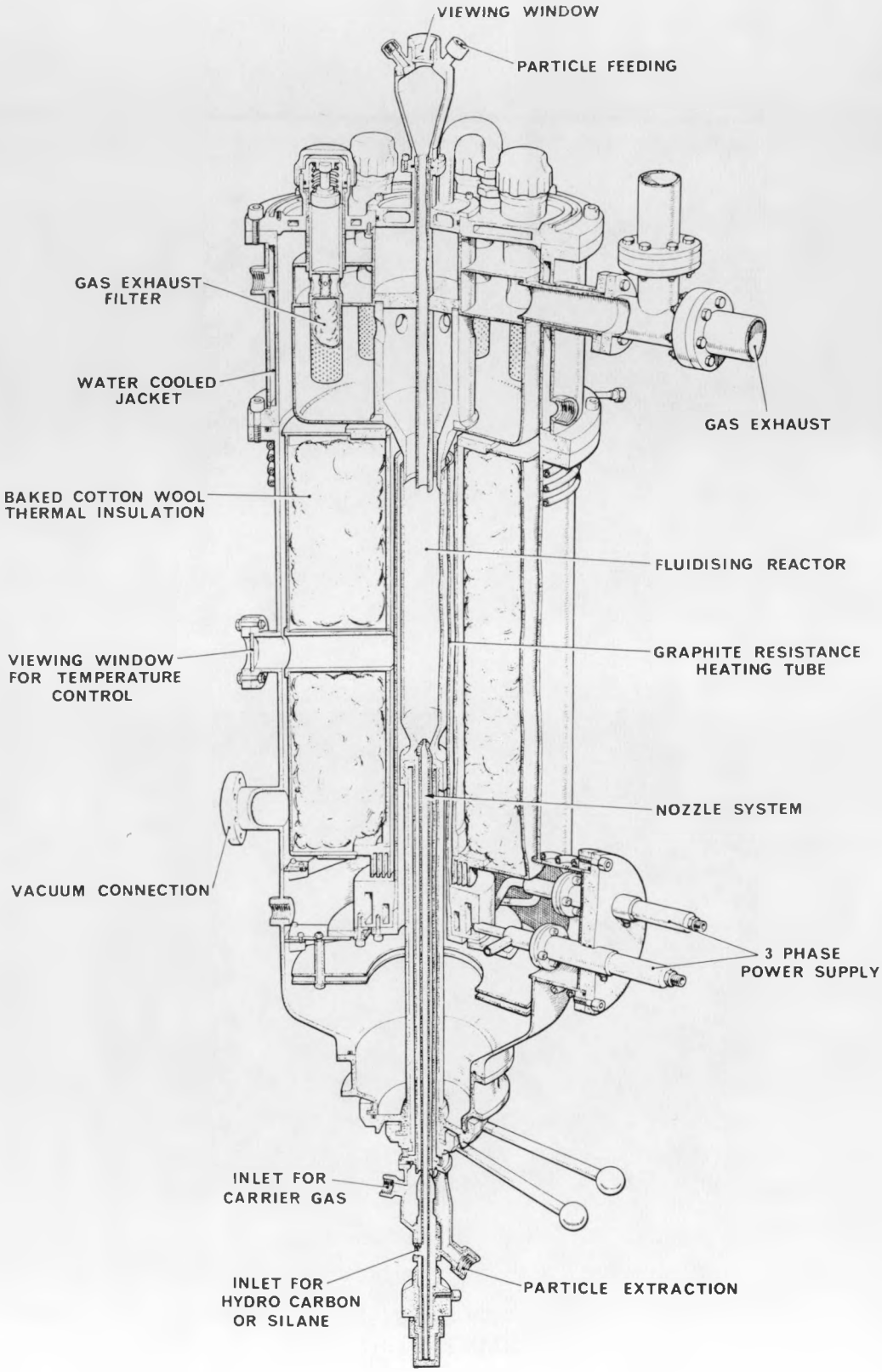

FIGURE 11 PROTOTYPE PRODUCTION SCALE FLUIDISED BED

750 cm^3, is constructed of graphite, with an internal diameter of 2 in. and an angle of the conical base of 60 degrees. This fluidizing reactor is fitted directly to a water-cooled nozzle system as shown in Figure 12. The center nozzle, made of molybdenum, reaches into the cone base of the fluidizing tube. It carries the hydrocarbon or silicon containing gas; the carrier gas enters through an annular gap surrounding the center nozzle. Such a design has made it possible to prevent carbon deposition (in the case of carbon coatings) at the entry zone of the fluidizing reactor, which would lead to serious blockage resulting in loss of fluidization. The entry velocity of the carrier gas can be varied by moving the center nozzle axially, relative to the fluidizing reactor, by means of a micrometer adjustment. Heating is accomplished by a specially developed 3-phase resistance furnace, the heater tube being split from the bottom into three segments. The current is fed into the bottom of each segment by means of a water-cooled clamping device, the top end of the heater acting as the neutral starpoint. The effective hot zone of the furnace is 20 in; it has an almost uniform temperature distribution within ±50 C. Carbonized cotton wool is used for thermal insulation. This prototype furnace, which consumes about 25 kw, has been operated up to 2250 C.

The particle-charging apparatus and the gas-exhaust system are situated on top of the furnace. The particles are fed through a molybdenum tube into the preheated furnace and can be discharged at an elevated temperature through the water-cooled nozzle assembly. The exhaust gases are passed through a filter system consisting of eight exchangeable filter units packed with silica fiber. By this means it is possible to retain active dust and excess carbon within the furnace; furthermore, the filters can be easily checked for uranium contamination after each run.

The whole apparatus is made to vacuum standards, and the top and bottom assemblies will be enclosed in glove boxes, purged with nitrogen. This is not only a safety requirement necessary for fissile-material accounting, but it avoids exposing the furnace to atmospheric contamination during charge and discharge.

The particle movement of this system was investigated (at room temperature) using transparent Perspex models. By appropriate adjustment of the entry velocity of the carrier gas, either a boiling bed or a spouting bed can be produced when using 300-micron-diameter particles. The adjustment for boiling conditions is somewhat critical since a slight change of gas throughout induces a tendency to slugging when the bed is charged to its full capacity.

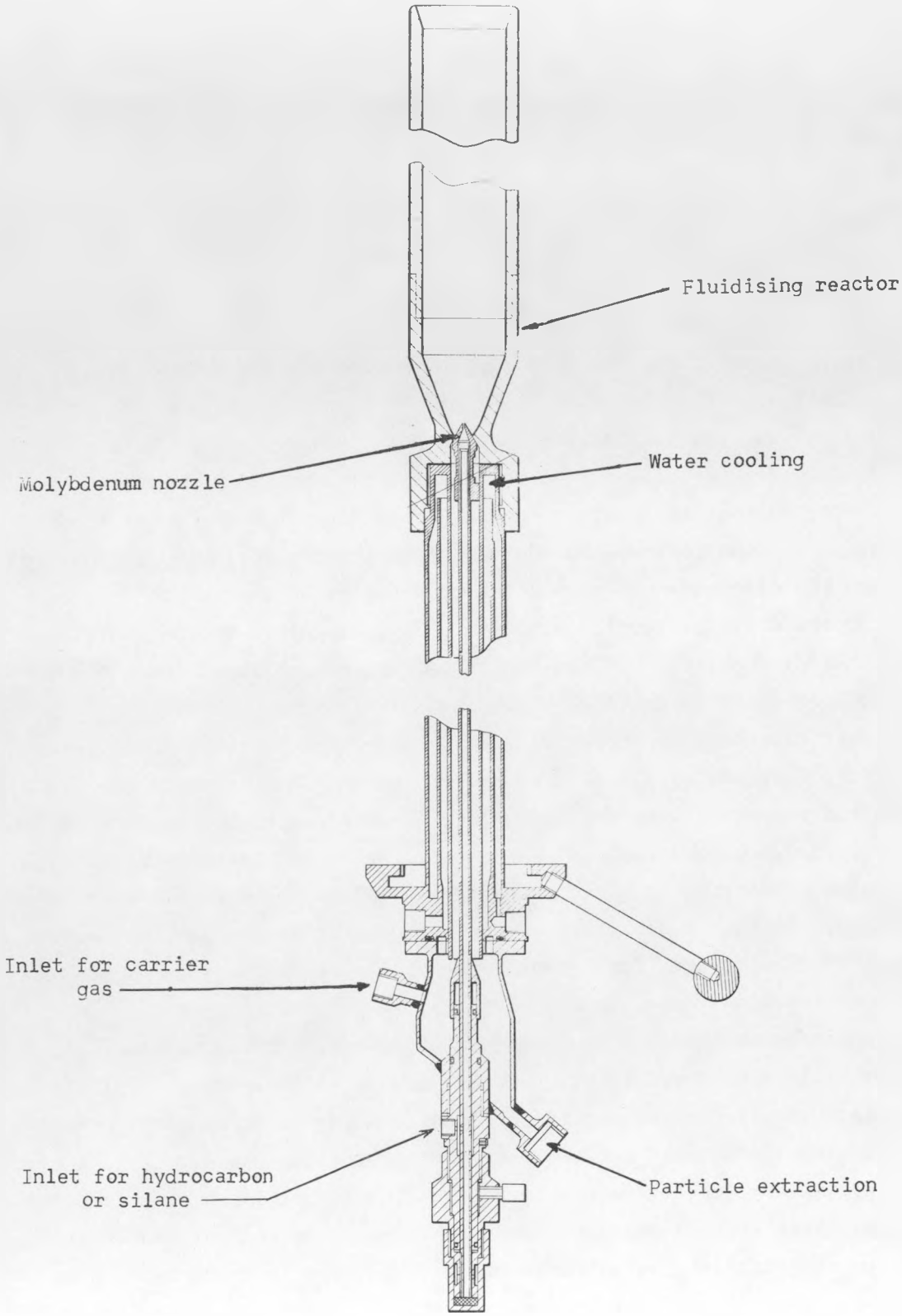

FIGURE 12 SECTION OF NOZZLE SYSTEM AND FLUIDISING REACTOR FOR PROTOTYPE PRODUCTION SCALE FLUIDISED BED

However, spouting conditions can be achieved easily with a charge of 1 kg together with good vertical mixing of the particles. It is important to appreciate that it is difficult to predict the operating conditions of such a system since the precise temperature conditions within the fluidizing vessel cannot be assessed accurately. Final operating conditions must therefore await operational experience with the prototype. The total gas throughput is expected to be of the order of 10 to 20 liters per min.

The operation of this apparatus involves, apart from charge and discharge, a complex procedure of flow and temperature control, particularly when working on composite coatings. To this end, development of such an automatic system has proceeded at Metallwerk-Plansee, and it is intended to employ such automatic control on the production apparatus.

4. CONSOLIDATION

Because of the desirability of avoiding excessive fuel temperatures attention has been given to reducing the maximum temperature of the coated-particle fuel under operational conditions in the reactor experiment. To this end, the fuel cartridge has been designed to give maximum heat flow to the inner wall of the fuel tube, and the fuel has been concentrated in as narrow an annulus as possible to reduce the center temperature. A photograph of the current conception of fuel cartridge is shown in Figure 13. Each cartridge of nominal length (2 in.) and diameter (1-3/4 in.) has a central hole of approximately 1 in. in diameter. The six longitudinal channels at the outer circumference carry the fission-product purge flow between the cartridge and the inner surface of the fuel tube; the chamber at one end obviates the need to align the grooves during assembly. Because of the required high concentration of fuel particles, a consolidation process developed at the R.A.E., Farnborough, has been adopted for the initial production fuel elements.

In this process, reactor-grade petroleum coke, previously micronized to less than 50 microns and graphitized, is coated with 12 to 14 per cent by weight of phenolic resin; it is then crushed and sized. Micronized and graphitized coke was found to have a higher bulk density than a range of other graphite powders; furthermore, graphitized material is desirable from the point of view of stability under irradiation. The prepared powder is mixed with coated particles in the required proportion, with a small addition of paraffin. The mixture is pressed at low pressure (up to 250 psi) to avoid

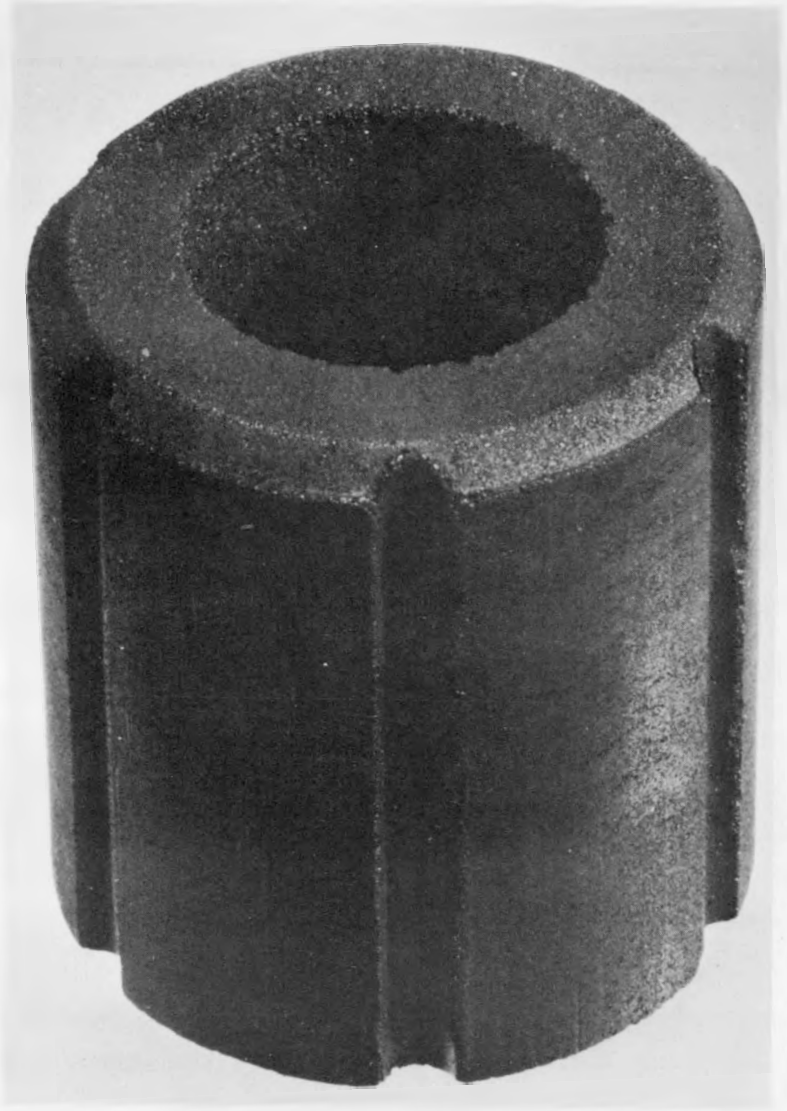

Fig. 13. CURRENT CONCEPTION OF FUEL CARTRIDGE

possible damage to the particle, the resin being polymerized at a low temperature (180 C) while the pressure is maintained. A typical die for this application is shown in Figure 14.

After removing the compact from the die, it is heated to 900 C in a stream of nitrogen carrier gas, saturated with benzene vapor at 45 C, or with hexane at room temperature. In this operation the resin is carbonized and pyrocarbon deposited into the pores of the matrix. As the pores become smaller, the temperature, and hence the rate of deposition, are successively reduced. Finally, the fuel cartridge is heat treated to remove occluded hydrogen.

Carbonization of the resin has been found to cause a uniform and consistent shrinkage of 0.5 per cent; this must be allowed for in the dimensions of the die. The gas cracking operation using benzene vapor in a nitrogen carrier gas increases the matrix density from 1.4 g/cm^3 "as pressed", to between 1.6 and 1.8 g/cm^3, depending on the time and temperature of treatment. The surface finish of the cartridge is good, and no machining operation is necessary. Final heat treatment results in a very small contraction of about 0.005 per cent.

Figure 15 shows radiographs of a fuel cartridge containing 93 per cent enriched uranium dicarbide fuel particles coated with pyrolytic carbon. The coated particles can be seen to be uniformly dispersed.

No results are yet available on the integrity, under operational conditions, of the full-size cartridges; however, specimens consolidated by this process and irradiated at temperatures between 1000 and 1750 C have remained intact and have shown only the contractions expected of such a material.

5. ACKNOWLEDGEMENTS

Acknowledgement is made to the Chief Executive, Dragon Project (Mr. C. A. Rennie) for permission to publish this paper. In addition, the authors wish to thank all those people associated with the Dragon Project, who have contributed towards this program.

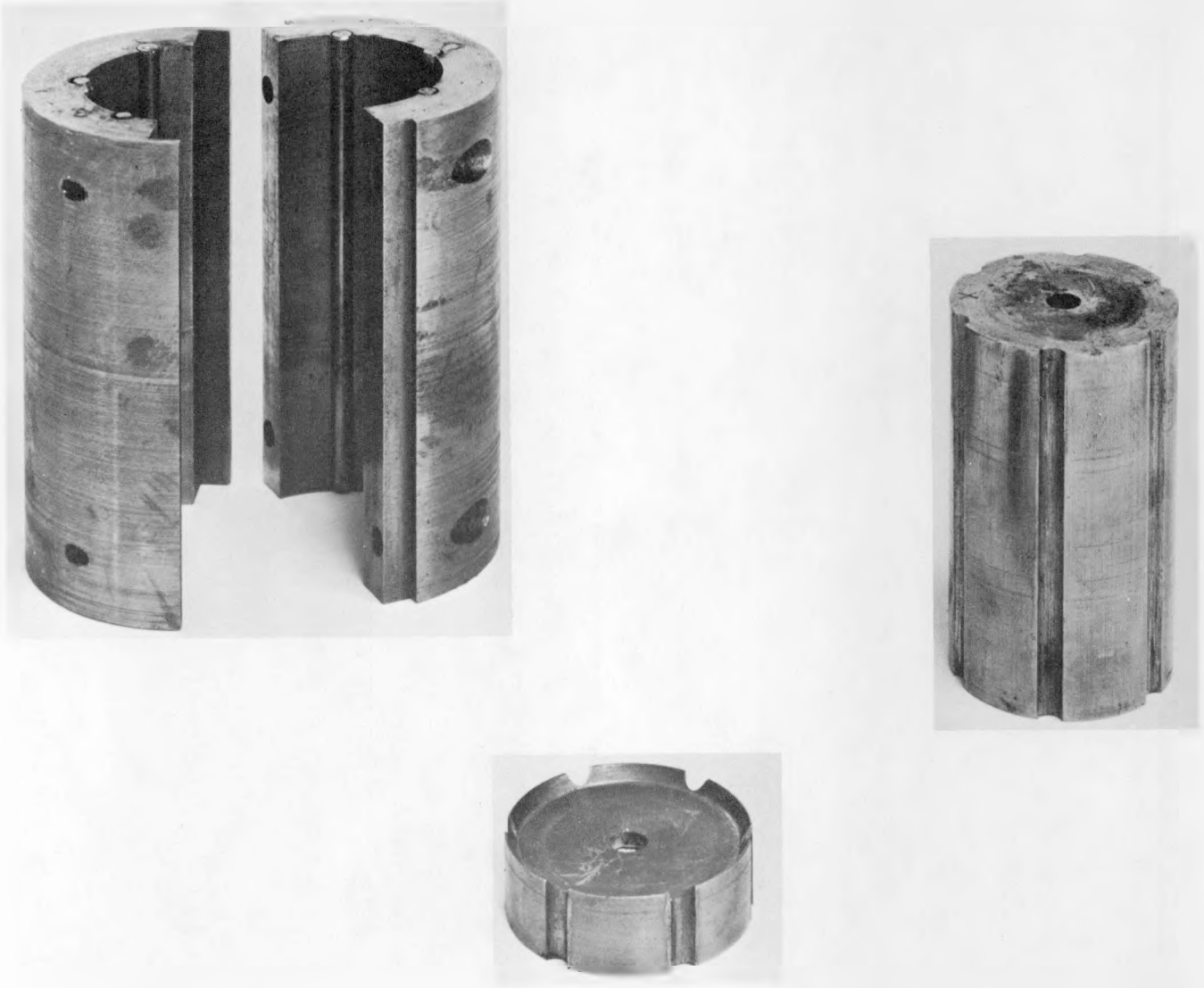

Fig. 14. TYPICAL DIE FOR WARM PRESSING OF FUEL CARTRIDGES

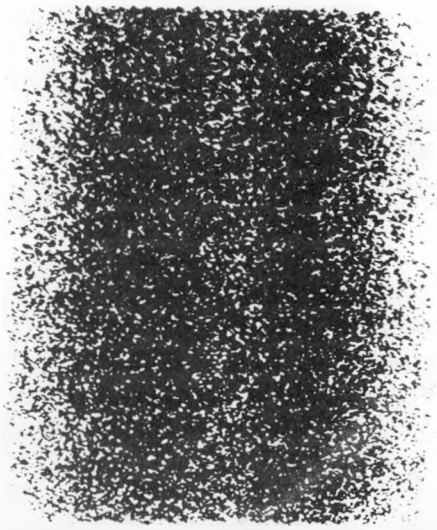

Fig. 15. RADIOGRAPHS OF FUEL CARTRIDGE SHOWING UNIFORM DISPERSION OF FUEL PARTICLES

6. REFERENCES

(1) G. E. Lockett and R. A. U. Huddle, The Dragon Reactor-"Development and Design of the H.T.G.C.", Nuclear Power, February, 1960.

(2) O.E.C.D. Dragon High Temperature Reactor Project, Annual Reports 1959-1960, 1960-1961, 1961-1962.

(3) F. Gorlé, J. Vangeel and E. Jonckheere, "Fabrication de Particules Spheriques." Plansee Seminar: Pulvermetallurgie in der Atomkerntechnik, 20th-24th June, 1961.

* * *

DISCUSSION

Question, A. K. Smalley (BMI): "In your studies with silicon carbide coatings, how fast are they applied, and how dense are they?"

Reply, H. Beutler (DrgP): "The deposition rate is 15 to 20 microns per hr. For temperatures above 1600 C, the coatings are porous, but at 1550 C and below, they are dense (3.2 g/cm^3) and dark gray in colour. The coatings are alpha silicon carbide."

Question, F. L. Carlsen (ORNL): "What burnup do you expect?"

Reply, L. R. Shepherd (DrgP): "In the Dragon reactor experiment, with the uranium-zirconium carbide we expect a burnup of 30 per cent of the U^{235}. With uranium-thorium carbide, we expect a burnup of 10 per cent of the heavy metal."

Question, F. L. Carlsen (ORNL): "What was the strength of the graphite body?"

Reply, R. A. Saunders (DrgP): "No strength data have been obtained, but a 1-3/4-in.-diameter solid cylinder withstood 10 tons under axial compressive loading, and the modulus of elasticity was about 6 x 10^5 psi."

Question, F. L. Carlsen (ORNL): "What are the conditions of your irradiation test?"

Reply, R. A. Saunders (DrgP): "The specimens are 10 mm in diameter by 1 in. long and were irradiated at 'high power density', about 400 watts per cm^3, at 1100 to 1750 C."

PREPARATION OF GRANULAR POLYMER-CARBON-COATED NUCLEAR FUEL

By Toshikatsu Ishikawa and Tohru Nagaoki

Research Laboratory, Nippon Carbon Co., Ltd.
Tokyo

ABSTRACT

Processes for coating uranium dioxide and uranium dicarbide particles with pyrolytic carbon are currently of wide interest. In the United States research organizations like the Oak Ridge National Laboratory, Battelle Memorial Institute, and General Atomic are among those active in work on carbon coatings of this type. In Japan the Nippon Carbon Co. has been developing a new concept of carbon-coated granular nuclear fuel.

When uranium dioxide was suspended by means of a suitable dispersion agent in a monomer of divinylbenzene which was then polymerized, spherical grains of divinylbenzene polymer about 1 mm diameter containing uranium dioxide particles were obtained. Uranium dioxide particles of two sizes, the smaller one several microns in diameter and the larger about 200 microns in diameter, were employed; good results were obtained in both cases. The spherical coated grains obtained were then heat treated to 800 C under controlled conditions to carbonize the divinylbenzene without disrupting the coating. The resulting product was a spherical granular carbon-coated nuclear fuel.

Examination under both optical and electron microscopy proved the coating surface to be extremely smooth and good. The alpha radioactivity was found by gas-flow counting to have been reduced by the carbon coating to 1/20 to 1/100 of the initial value. It was ascertained radiographically that the smaller urania particles were distributed dispersedly in the grains, while when the larger particles were used a ratio of about one urania particle to one grain of polymer was found.

When the grains were further heated to over 2000 C in vacuum or in an inert gas, the UO_2 was completely transformed into UC_2, with the carbon coating still remaining intact. Tests showed that the product is stable in humid air and to heat shock. Irradiation tests of the fuel particles now are under way in the Japan Atomic Energy Research Institute.

The following advantages may be anticipated from use of the carbon-coated granular nuclear fuel prepared by the foregoing method:

(1) The carbon constituting the coating is in polymer carbon form and is resistant to radiation as well as being very pure.

(2) The grain surface is smooth and grain size suitable, both contributing to facility of flow.

(3) Improved chemical stability is possible, thus overcoming one of the shortcomings of carbide fuel.

(4) Mixture with grains of a different size composed purely of carbon would permit simple mechanical separation by screening, thus simplifying reprocessing in a great measure.

(5) Fission-gas retention of the coated particle will be good.

PREPARATION OF POLYMER CARBON COATED FUEL PARTICLES

The procedure for preparing granular polymer-carbon-coated nuclear fuels can be summarized as follows:

(1) Pearl polymerization of divinylbenzene monomer, in which uranium dioxide is suspended, is carried out. Spherical grains of polymer about 1 mm in diameter containing UO_2 particles are produced.

(2) Carbonization of the polymer particles is accomplished by heat treating to 800 C under controlled conditions. Spherical carbon-coated fuel particles are obtained.

(3) Transformation of UO_2 to UC_2 is achieved by further heat treating of the carbon-coated fuel particles to over 2000 C.

(A) Raw Materials

The principal raw materials used in this experiment are UO_2 and divinylbenzene. Spherical UO_2 particles about 200 microns in diameter prepared by NUMEC and a powdery UO_2 about 2 microns in diameter prepared by the Yokozawa Chemical Company are employed. The divinylbenzene used is a Dow product having a purity of 55 per cent.

(B) Polymerization

Process variables in pearl polymerization have been examined. Following is a procedure that has been found to provide suitable conditions for polymerization: A mixture of divinylbenzene monomer and benzoyl peroxide (0.5 to 1.0 weight per cent) as a catalyst is thoroughly mixed with a 1 to 3 per cent aqueous solution of poval or starch. Then UO_2 wetted by oleophilic surface-active agent, is added to the solution and stirred for 2 to 3 hr at 70 to 75 C and for 0.5 to 1 hr at 85 to 90 C. One example of this procedure is shown in Table 1. By this procedure good polymer grains containing UO_2 were obtained. The yields were over 95 per cent by weight. The coated particles were 0.6 mm in diameter in the case of the spherical UO_2 and 1 to 2 mm in diameter in the case of the powdery UO_2. Typical coated particles are shown in Figure 1.

TABLE 1. TYPICAL PROCEDURE FOR PEARL POLYMERIZATION GIVING POLYMER-COATED PARTICLES CONTAINING ABOUT 10 PER CENT UO_2

Batch Composition	
Divinylbenzene	600 g
Benzoyl peroxide	3 g
Poval or starch (1 to 3 per cent aqueous solution)	1.8 liters
UO_2 (powder or spherical)	60 g
Oleophilic surface-active agent	6 g
Mixing Procedure	
Time at temperature	
70 to 75 C	2 to 3 hr
85 to 90 C	0.5 to 1 hr
Stirring speed	
Powdery UO_2	400 to 500 rpm
Spherical UO_2	1200 to 1500 rpm

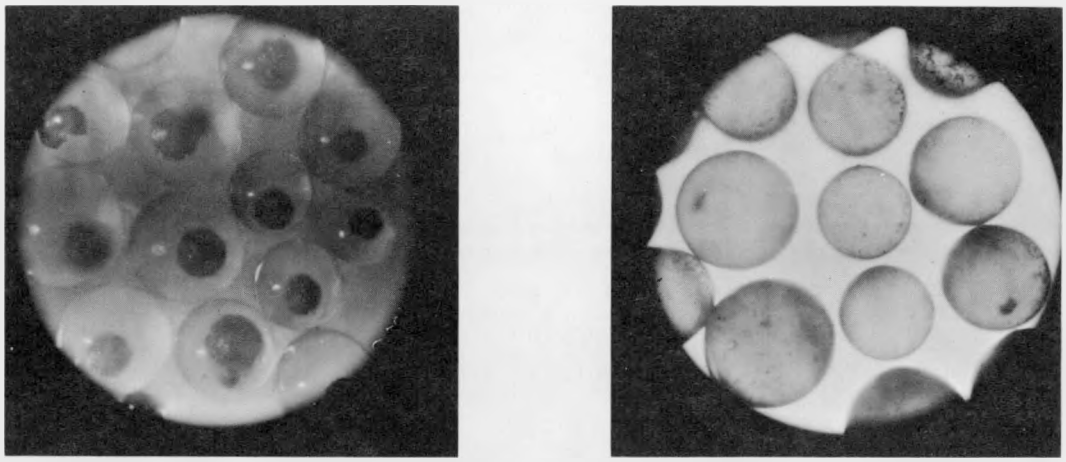

Spherical UO_2 Powder UO_2

FIGURE 1. POLYMER GRAINS CONTAINING FUEL (20X)

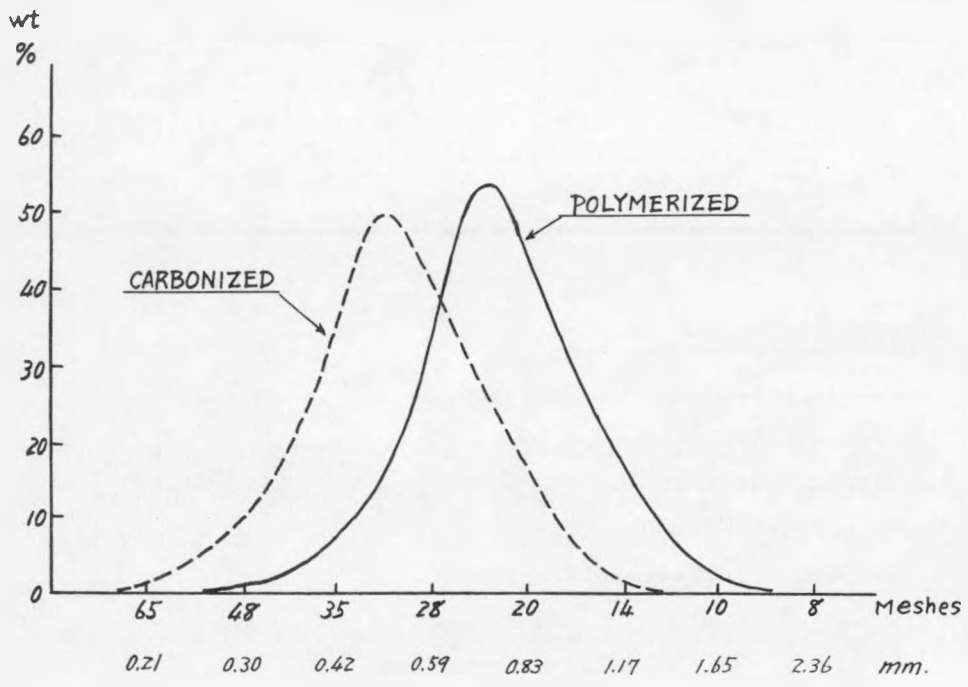

FIGURE 2. EFFECT OF HEAT TREATMENT ON SIZE DISTRIBUTION OF POLYMER-CARBON-COATED FUEL PARTICLES

(C) Carbonization of Polymers

The polymer grains containing powdery or spherical UO_2 are fired to 800 C under controlled conditions to produce spherical polymer-carbon-coated grains. At the first stage of this process, it is desirable to heat treat the polymer grains in sealed tube at 250 C for 15 hr, then continue the heating at the same temperature for 50 hr in air. In this stage, addition of oxygen to some radicals is accomplished. This reaction facilitates dehydration of the polymers without destruction of cross-linking during thermal decomposition in further heating.

The second stage is carbonization of the heat-treated polymers. The firing is carried out in nitrogen atmosphere. A slow rate of temperature rise is employed. The following firing schedule is preferred: 5 C/hr from 250 C to 500 C and 250 C/hr from 500 C to 800 C.

The grains thus obtained have a good carbon coating, resulting in a spherical granular carbon-coated nuclear fuel. During carbonization, the particle diameter decreases to about 75 per cent of the polymer's and 40 to 45 per cent of the weight is lost. Therefore, the weight ratio of UO_2 to carbon in the grains increases about twice. The effect of heat treatment on the particle size of a typical batch is shown in Figure 2.

(D) Transformation of UO_2 to UC_2

When the carbonized grains are further heated to over 2000 C in vacuum or in an inert atmosphere, UO_2 is completely transformed into carbide with the carbon coating still remaining intact. To transform the UO_2 completely into UC_2, a heat-treatment temperature over 2000 C is required and a comparatively slow heating rate is desirable in order to preserve a good carbon coating. Heat-treated particles are shown in Figure 3.

RESULTS OF EXAMINATIONS OF THE PARTICLES

(A) Observation of the Grain Surfaces

Under electron microscopic observation, the surfaces of the polymer-carbon-coated particles appeared extremely smooth compared with that of ordinary artificial graphite. Some smooth waves having about a 1-micron pitch were observed, but no visible voids or pores existed (Figure 4). This was further ascertained by means of mercury porosimetry, which showed that the pore radii on the grain surfaces were less than 0.5 micron.

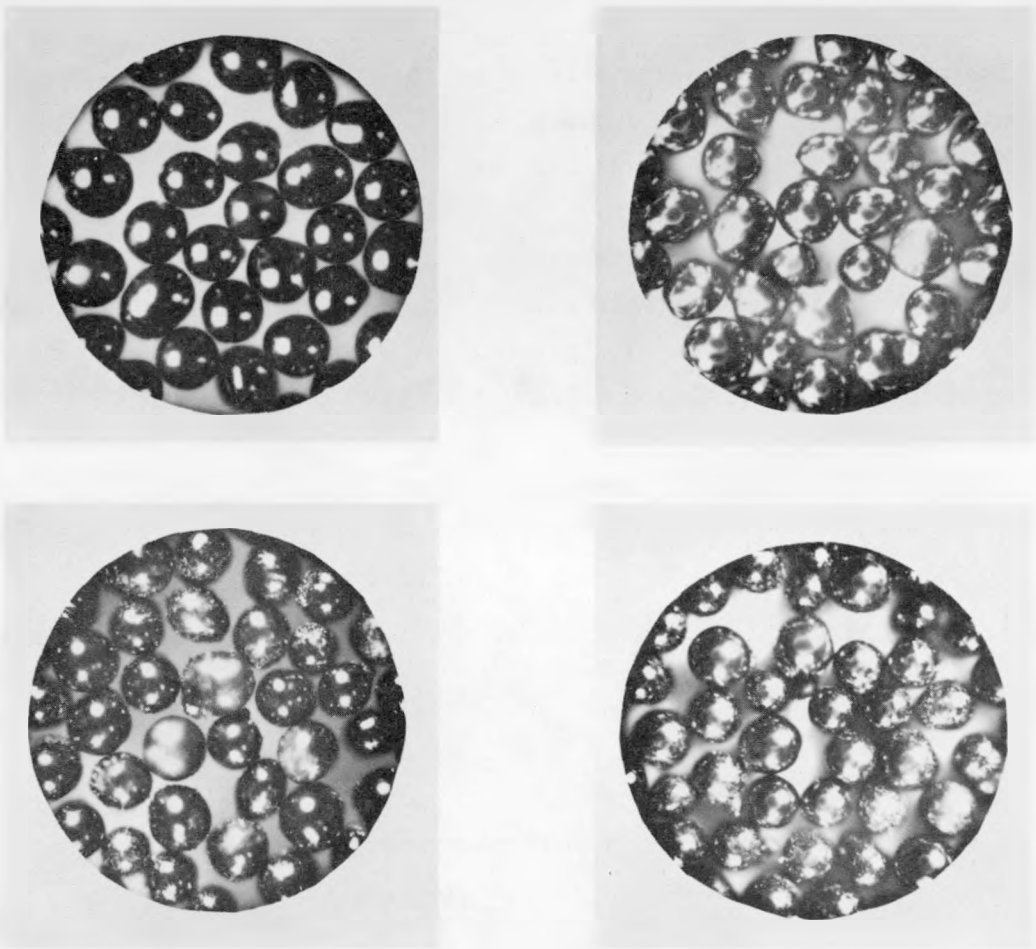

Heat Treated to 1000 C

Heat Treated to 2400 C

FIGURE 3. POLYMER-CARBON-COATED FUEL PARTICLES

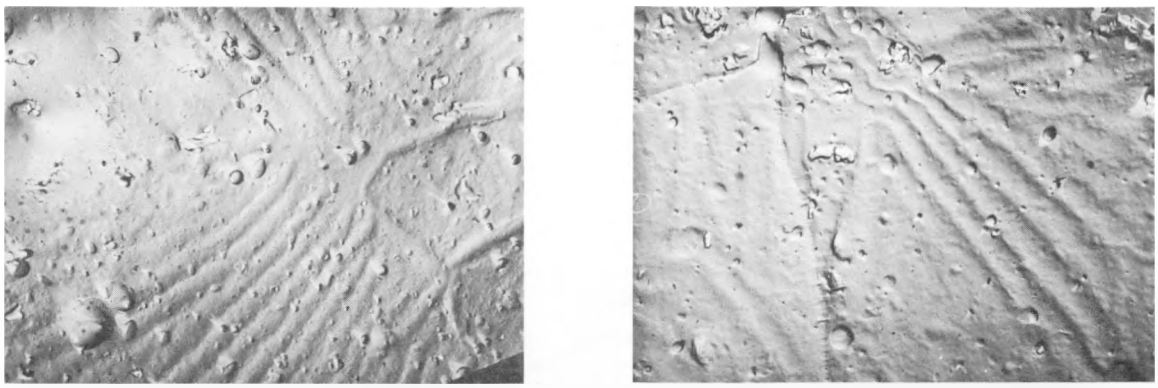

FIGURE 4. ELECTRON MICROGRAPHS OF THE SURFACES OF POLYMER-CARBON-COATED FUEL PARTICLES (3000X)

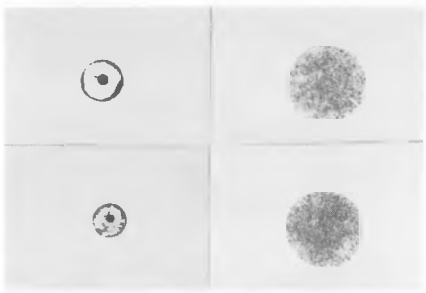

Left: Particles Containing Spherical UC_2
Right: Particles Containing Powder UC_2

FIGURE 5. RADIOGRAPHS OF POLYMER-CARBON-COATED UC_2 PARTICLES ILLUSTRATING LOCATION OF FUEL (5X)

(B) Location of the Nuclear Fuel Particles in Coated Grains

The location of the UO_2 and UC_2 particles in the polymer grains was examined radiographically, and it was ascertained that there was no change in fuel location during heat treating. Radiographs of typical particles are shown in Figure 5.

(C) Chemical Stability

In general, uranium carbide reacts readily with water or moisture and evolves hydrocarbon gases. We have examined the chemical stability of the coated grains by gas analysis and have not found appreciable reaction with water when the carbon coatings were good (Figure 6).

In 12 days of treating with water, UC_2 grains with satisfactory coatings evolved no gases, but poorly coated ones evolved hydrocarbon gases such as methane, ethane, etc. Coated grains containing UC_2 derived from the 2-micron UO_2 powder evolved very small amounts of gases. This evaluation has been attributed to attack of a small amount of UC_2 dispersed on surface of the grains.

(D) Reduction of Radioactivity by Carbon Coating

The alpha radioactivity was found by gas-flow counting to have been reduced by the carbon coating. But, owing to the relatively long range of beta radioactivity, the rate of the reduction was very small. These results are shown in Table 2. The data are expressed as the counting ratio of coated to uncoated samples containing the same weight of uranium.

TABLE 2. REDUCTION OF RADIOACTIVITY BY POLYMER-CARBON-COATING

Samples	Coated/Uncoated Particle Radioactivity Ratio	
	Alpha	Beta
Polymer-coated UO_2	1/30 - 1/50	2/3 - 2/5
Polymer-carbon-coated UO_2	1/20 - 1/40	1/2 - 1/3
Polymer-carbon-coated UC_2	1/30 - 1/40	1/2 - 2/5

(E) Thermal Stability

The coated grains are also stable to heat shock. Samples were heated to 1000 C for 10 min and then suddenly cooled to room temperature for 10 min in

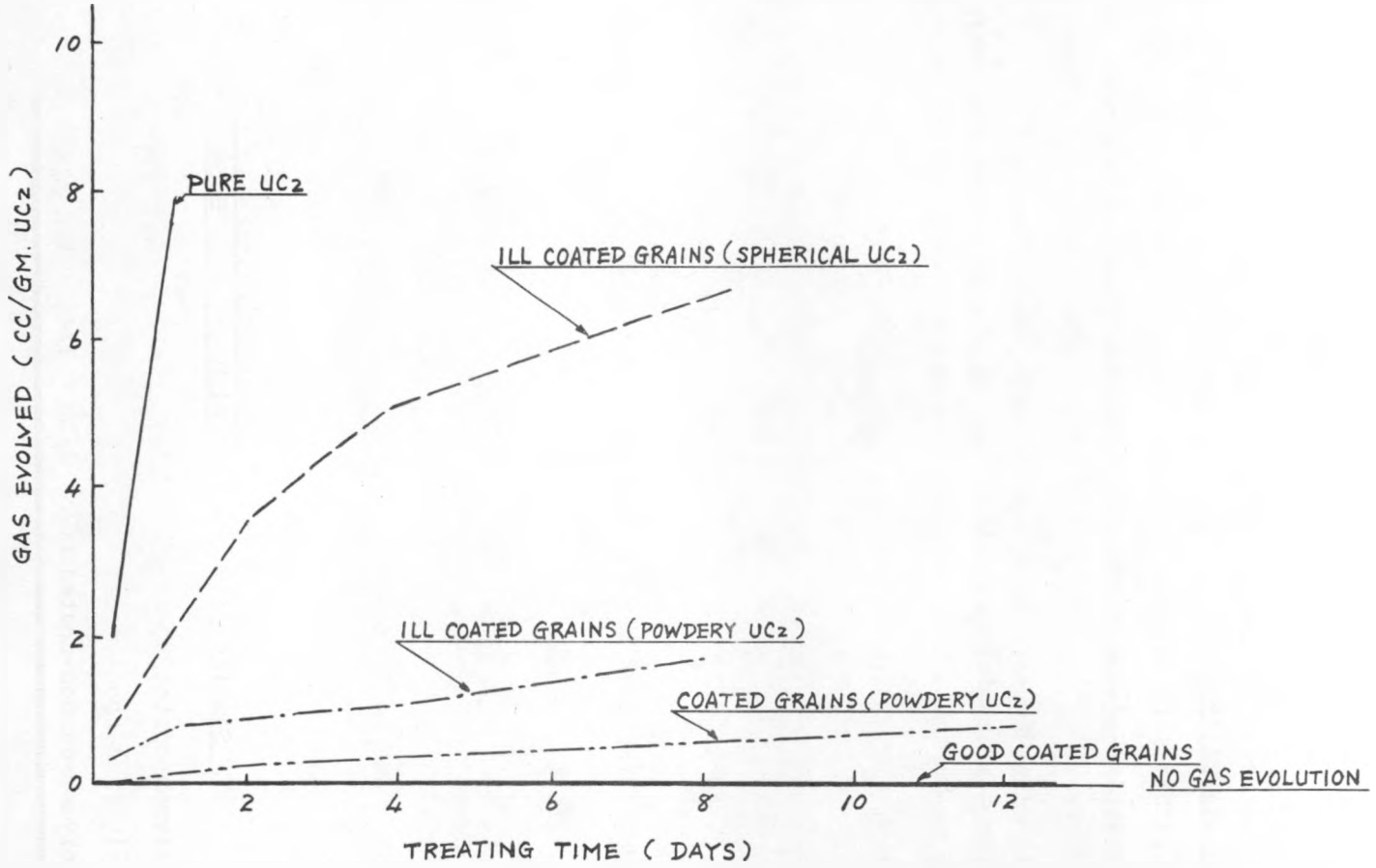

FIGURE 6. GAS EVOLUTION FROM POLYMER-CARBON-COATED UC_2 PARTICLES EXPOSED TO WATER

nitrogen atmosphere. This thermal cycle was repeated eight times. After these tests, except for merely slight increases (maximum of 10 per cent) of activity no appreciable changes were observed in the particles.

CONCLUSION

We have outlined principally the procedure we use for manufacturing polymer-carbon-coated UC_2 nuclear fuel particles stable to humidity. We have also explained some advantageous properties of the coating. Application studies of these particles, especially with respect to fission-gas retention, now are under way.

This work was supported by the government of Japan. We wish to thank Dr. S. Iwai for his helpful suggestions and Mr. T. Yoneshige, T. Masuyama, H. Teranishi, M. Morishita, H. Yamazoe, and their co-workers for their cooperation.

* * *

DISCUSSION

Question, C. W. Funk (AGN): "Can this process be extended to smaller particle size ranges?"

Reply, T. Nagaoki (NpnC): "In our case, 200 mesh was the smallest size."

PRODUCTION OF SPHERICAL URANIUM DIOXIDE PARTICLES AND METALLIC COATING THEREON

By Y. Akimoto, T. Suzuki, and C. Ito
Nuclear Material Division, Research Laboratory
Mitsubishi Metal Mining Co., Ltd.
Omiya, Saitama, Japan

The work described in the present paper is concerned with the production of spherical UO_2 particles starting from UO_3 powder dispersed in an oil medium and with the metallic coating experiments on the particles produced thus. The research is still in development; therefore, all data appearing in this paper should be considered as tentative results.

LAYOUT OF THE PROCESS

The distinctive features of this process can be summarized into the following two points:

(1) Adoption of UO_3 powder, an intermediate product of the UO_2 production process, as a feed material and the utilization of the hydration reaction for its granulation, and

(2) Application of surface-chemical technique to granulate and to sphere the particles.

Unlike UO_2 or U_3O_8, UO_3 easily forms various kinds of hydrates, UO_3-$2H_2O$ being the most common hydrate obtained by the reaction with liquid state water at room temperature. (2,5) When a stoichiometric amount of water is added to the UO_3 powder, the water initially acts as a binding agent, causing the particles to cohere, and then it is absorbed into the crystal lattice forming the hydrate. As the evolution of this hydrated water can only be attained with the accompanying lattice rearrangement,

no macroscopic pores may develop in the successive dehydration step as is usually observed on expelling an inert binding agent.

The most critical problem in applying the hydration to the granulation, however, is posed by the nature of the feed powder. In spite of the microscopic lattice rearrangement accompanying the hydration, only little change of the macroscopic powder skeleton is usually observed. Accordingly, the feed powder should, at most, consist of very loosely aggregated crystallites, especially when the aim is good compaction by granulation without external pressure. Further discussion of this matter will be given later.

To facilitate the good compaction, adequate pretreatment is necessary in promoting the deaggregation of the feed powder. In our case, wet milling is found to be satisfactory when an inert oil which does not prevent the subsequent UO_3 hydration is used. UO_3, unlike UO_2, generally forms a very viscous slurry that requires further dilution for the effective milling. The surface-chemical technique was developed with the object of facilitating the direct utilization of the slurry formed thus without separating the oil before the granulation.

Suppose that the necessary amount of water is dispersed as droplets in the powder-oil slurry. UO_3 is strongly hydrophilic. When it comes in contact with the water, its surface film of oil is replaced by water, and it is drawn into the water phase. By this means the particles of UO_3 are collected into the droplets of water where they are hydrated into solid spherules of UO_3-$2H_2O$. These spherules are screened from the ungranulated powder that remains in the oil dispersant. Washed and then dehydrated, the UO_3 spherules are sent to the hydrogen reduction stage where dense, spherical UO_2 particles are obtained by the promoted free sintering.

Following is a detailed explanation of major variables of this process.

UO_3 AS FEED MATERIAL

As stated above, this process asks for no external force to cause granulation, the cohesive force between the particles within the water droplets and the interfacial tension between the granules and the oil dispersant being all that is needed. On such granulation procedure, the most satisfactory results were obtained by using the UO_3 powder taken from an intermediate step of the swageable UO_2 production pilot plant. This powder, which is produced by calcining ADU (ammonium diuranate) from a specially controlled hydrolysis step, has the nature to be free sintered rapidly to dense nonadhesive UO_2 particles with the least amount of closed pores. Detailed discussion on this matter was given at the fourth Plansee Seminar in 1961 by H. Doi, et al. (1)

Fig. 1 shows the electron micrographs of ADU and UO_3 powders taken from the "ceramic" and "swageable" processes respectively. ADU from the "swageable" process consists of small, uniform primary crystallites which tend to form small, loose aggregates. Calcination to UO_3 does not change such structure. On the other hand, ADU and UO_3 obtained from ordinary "ceramic" UO_2 production steps consist of inhomogeneous and strongly bonded aggregates of coarse unit crystallites. Such powder cannot be disintegrated easily, and it was found to be unsatisfactory because the granulated particles were porous with a considerable amount of void space.

Fig. 2 shows the size distribution curves of the swageable UO_3 powder dispersed and disintegrated by a colloid mill in some oil media. A single peak is observed in every case. Transference of the powder to water phase causes the flattening of the peak. This leveling, probably caused by the deflocculation, shows that the disintegration is affected

Swageable Process

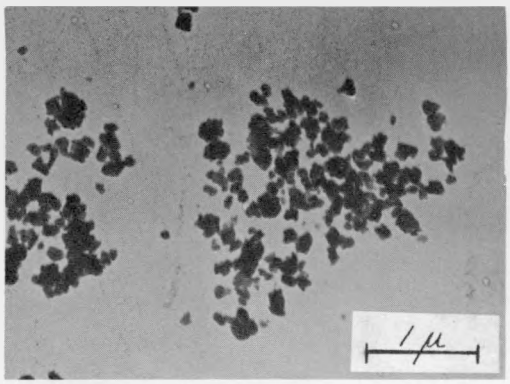

ADU

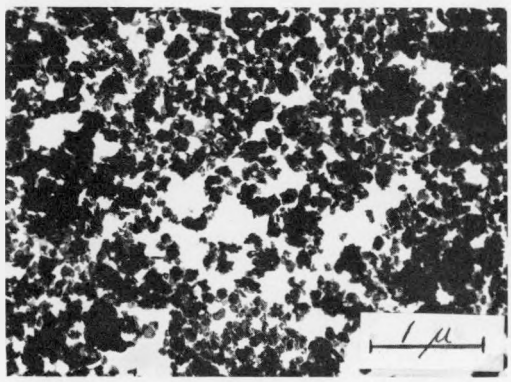

UO_3

Ceramic Process

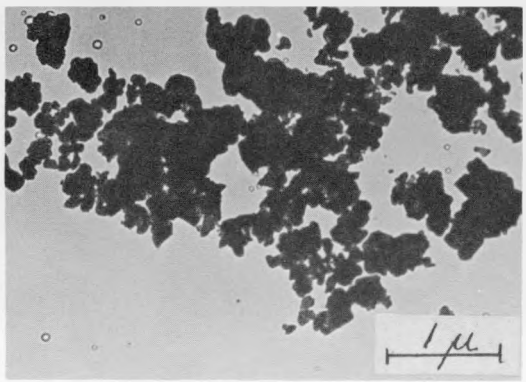

ADU

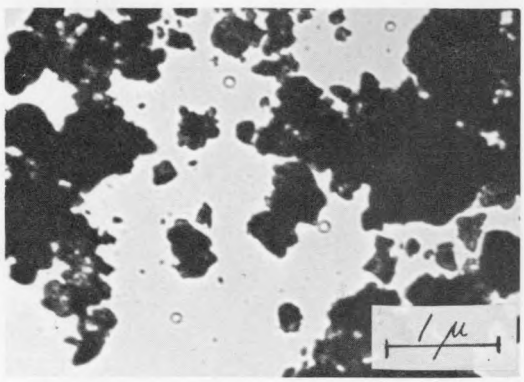

UO_3

Fig. 1. ELECTRON MICROGRAPH OF FEED POWDERS

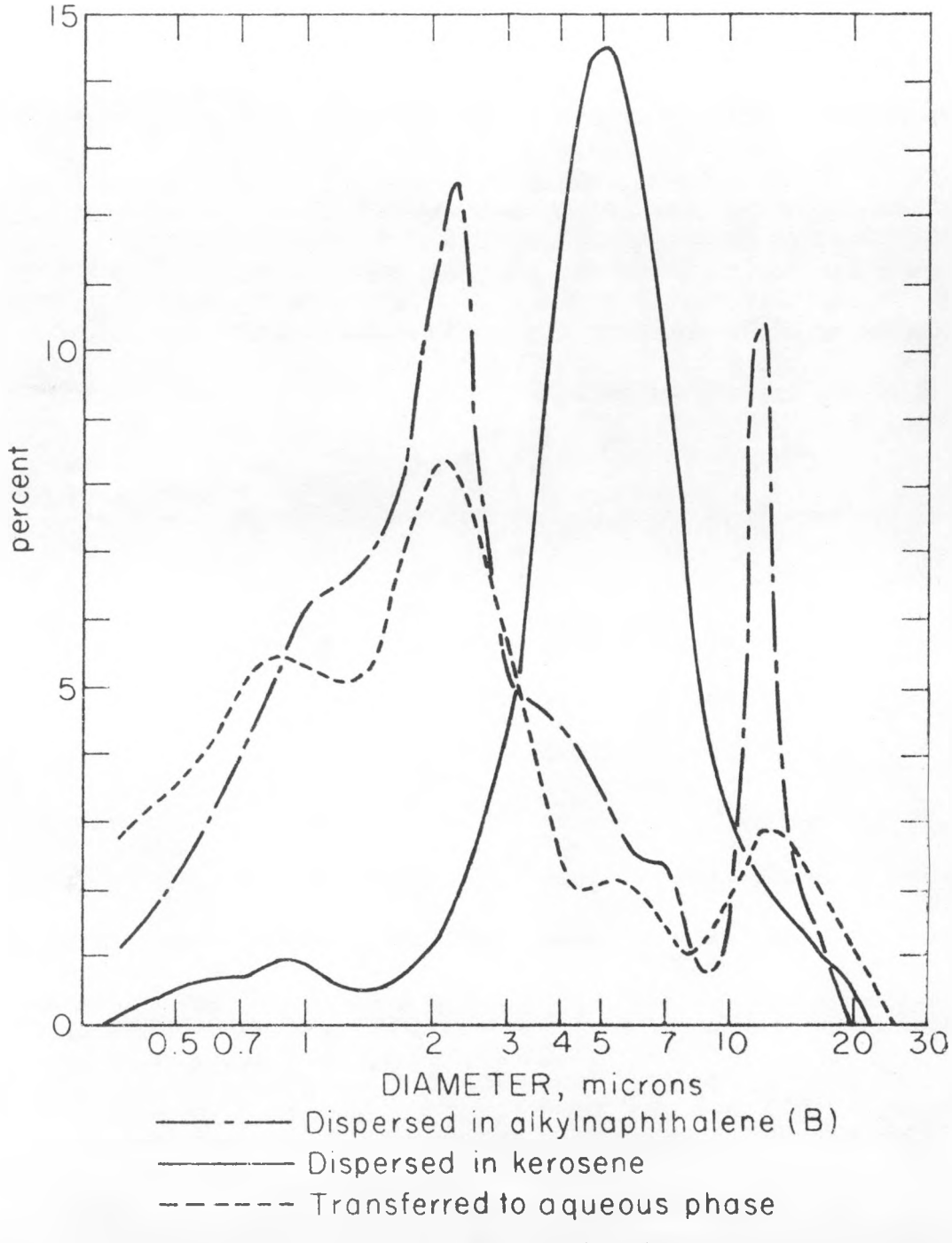

Size Distribution of Colloid-Milled UO_3 Powder.

FIGURE 2

to considerable extent by the colloid-milling of the "swageable" UO_3.

Fig. 3 shows the density of the spherical particles at every step of the production. It is clearly shown that high density UO_2 particles can only be obtained from highly compacted UO_3 hydrate particles.

OIL AS DISPERSANT

In order to prevent the flocculation of the UO_3 powder in an oil medium and to promote the appropriate transference of the powder into the aqueous phase, wetting behavior of the dispersant as well as the binding agent is one of the most critical controlling factors affecting the granulation.

Table 1 shows the experimental result on the wetting behavior of some oils. A uniformly packed powder column which contained 50 to 100 mesh fresh UO_3 was contacted at the bottom to the oil to be investigated. After the capillary rise was nearly equilibriated, water was substituted for oil. It pushed up the initially absorbed oil, forming the UO_3 hydrate. As the hydration reaction is involved in this case, so-called adhesion tension can not hold its strict physical meaning. However, the value calculated by assuming the ordinary surface-chemical formula seems to have some relationship with the actual granulation result. Good results are always attained when adhesion tension of the oil to UO_3 exceeds 30 dyne/cm and when that of the water to the oil-adsorbing UO_3 remains between 10 and 15 dyne/cm. Viscosity and density of the oil seem to be other factors affecting the granulation.

WATER AS BINDING AGENT

Some UO_3 dissolving agents were found to promote the close compaction at the granulation stage. The effect of these additives can be ascribed to the promotion of

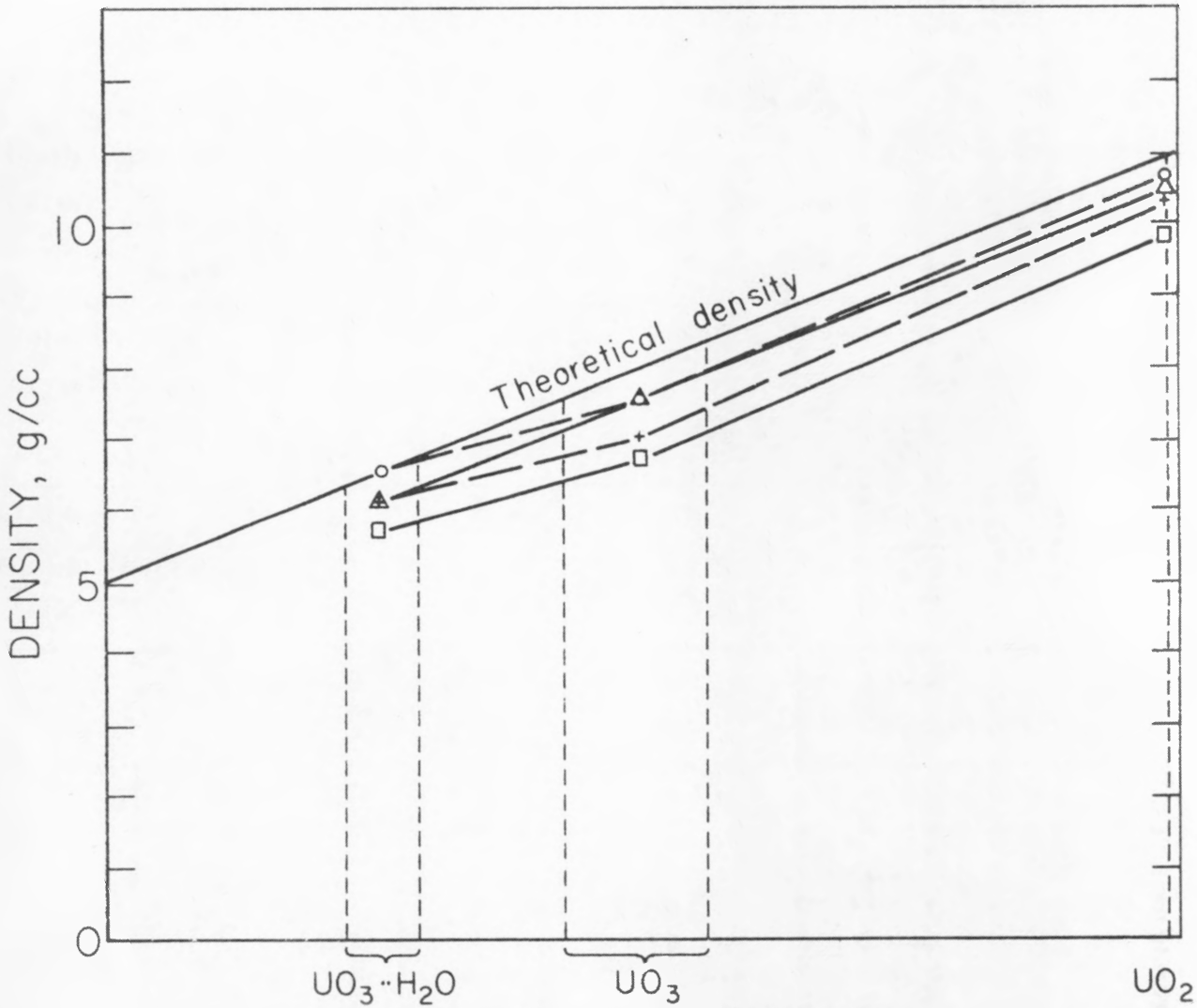

Densification of the Spherical Particles.

FIGURE 3

62-204

Table 1 Wetting behavior of some oils to UO_3

Oil			A		B	
	Density (d) g/cc	Viscosity (ρ) c. poise	Capillary ✡ rise (H) cm	Adhesion ✡✡ tension ($\gamma \cos\theta$) dyne/cm	Capillary ✡ rise (H) cm	Adhesion ✡✡ tension ($\gamma \cos\theta$) dyne/cm
Kerosene	0.775		29.6	25.1		
Benzene	0.879	0.636	29.2	28.2	24.2	26.7
Toluene	0.872	0.620	29.6	28.4	20.8	22.5
Alkylnaphthalene (A)	1.025		28.0	31.6	11.0	12.0
Alkylnaphthalene (B)	1.013	2.843	27.2	30.3	10.0	11.0
Alkylnaphthalene (C)	0.857	0.854	29.4	27.6	11.0	12.0
CCl_4	1.575	1.053	20.8	36.2	24.0	26.2
Aromatic chloride (A)	1.293	1.195	27.0	38.4	12.0	13.2
Aromatic chloride (B)	1.386	46.150	16.0	24.4		
None					30.5	33.4

A = Oil to fresh UO_3

B = Water to oil-absorbing UO_3

✡ 50 100 mesh UO_3 powder column

✡✡ $r = 2.24\ 10^{-3}$ cm assumed

$$H = \frac{2\gamma \cos\theta}{grd}$$

62-213

deagglomeration and stripping of initially adsorbed oil. The addition of some surface-activating agents is effective especially for the size-controlling purpose. Careful selection should be made to prevent emulsion formation. Neither metallic impurities nor nonvolatile material should be allowed. Polyoxyethylene alkyl alcohol is one of the most promising agents from this point of view.

The optimum amount of water changes slightly according to the powder pretreatment. As shown in Fig. 4, optimum amount of water for the colloid-milled powder granulation is slightly higher than the stoichiometric amount while the ball-milled powder requires the right amount to yield UO_3-$2H_2O$.

AGEING, SCREENING, AND WASHING

At the granulation stage, the dispersion of UO_3 powder and the water particles and the nature of the produced UO_3 hydrate granules are effected by the agitation. The duration of agitation required to complete solidification varies by the sort of oil and aqueous solution to be used. One to four hours, however, is sufficient to give the particle enough strength for the screening. Besides the sphered particles, the slurry contains ungranulated powder and particles which collapsed during the agitation. In most of our experimental conditions, UO_3 is granulated as spheres over 200 mesh. The particles are separated from the slurry by a 200-mesh screen, and then are washed by toluene or benzene for the overnight drying at the room temperature. Ungranulated UO_3 can be recovered by subsequent filtration of the slurry. Washing with water is effective to remove the adsorbed oil which can be recycled with the oil filtrate.

DEHYDRATION AND SINTERING

In order to prevent any rapid reactions which may lead to pore formation, dehydration

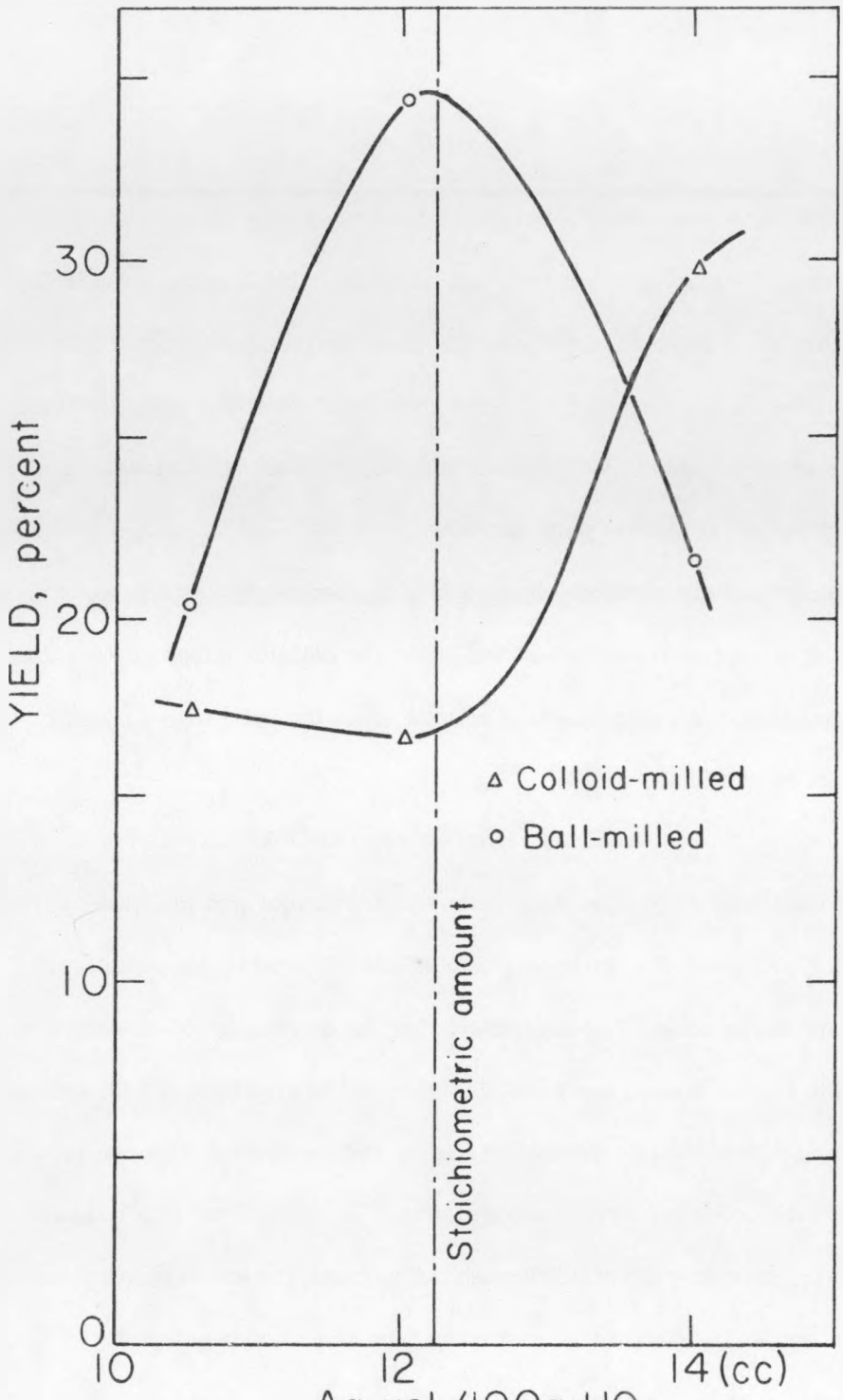

Granulation Yield of the Spherical UO_3 Hydrate. (Oil Dispersant: Kerosene)

62-206

FIGURE 4

of the sphered UO_3 hydrate should be carefully performed. Fig. 5 shows the dehydration behavior of the UO_3 hydrate obtained by the granulation method stated above. Thermal balance curve shows the very smooth changes in weight whereas the differential thermal analysis curve consists of several maxima and minima. Results of X-ray analysis on the specimen taken from each dehydration step is shown on Fig. 6. In spite of size effect which makes the diffraction patterns very broad, there is rough agreement with the X-ray data published previously. Adsorbed water, toluene, and kerosene dispersant are easily evolved up to 120° C. Transformation of the dihydrate to the monohydrate seems to occur at the same temperature range. The best assignment was made with UO_3-H_2O II reported by J. K. Dawson, et al. (2) At 190° C decomposition to further low hydrate seems to occur. No previously reported data were found to fit the present diffractograph, however. At 280° C weak diffraction patterns of hexagonal UO_3 are observed. Decomposition of UO_3 to U_3O_8 seems to begin as low as 425° C to some extent, whereas the main reaction is promoted near 600° C.

Gradual weight loss on the dehydration makes the dehydration controlling easy. At present, actual practice is done in a vacuum furnace to promote the desorption and dehydration. After an overnight drying at ambient atmosphere, the particles are given another 24 hours' drying in the vacuum furnace at less than 10^{-1} torr. Subsequent gradual heating is effected with 30 minutes' holding at every 50° C rise until 2 hours' heating at 300° C is reached. Spherical UO_3 produced thus is returned to the swageable UO_2 production plant where hydrogen reduction to spherical UO_2 is practiced at 1,500° C.

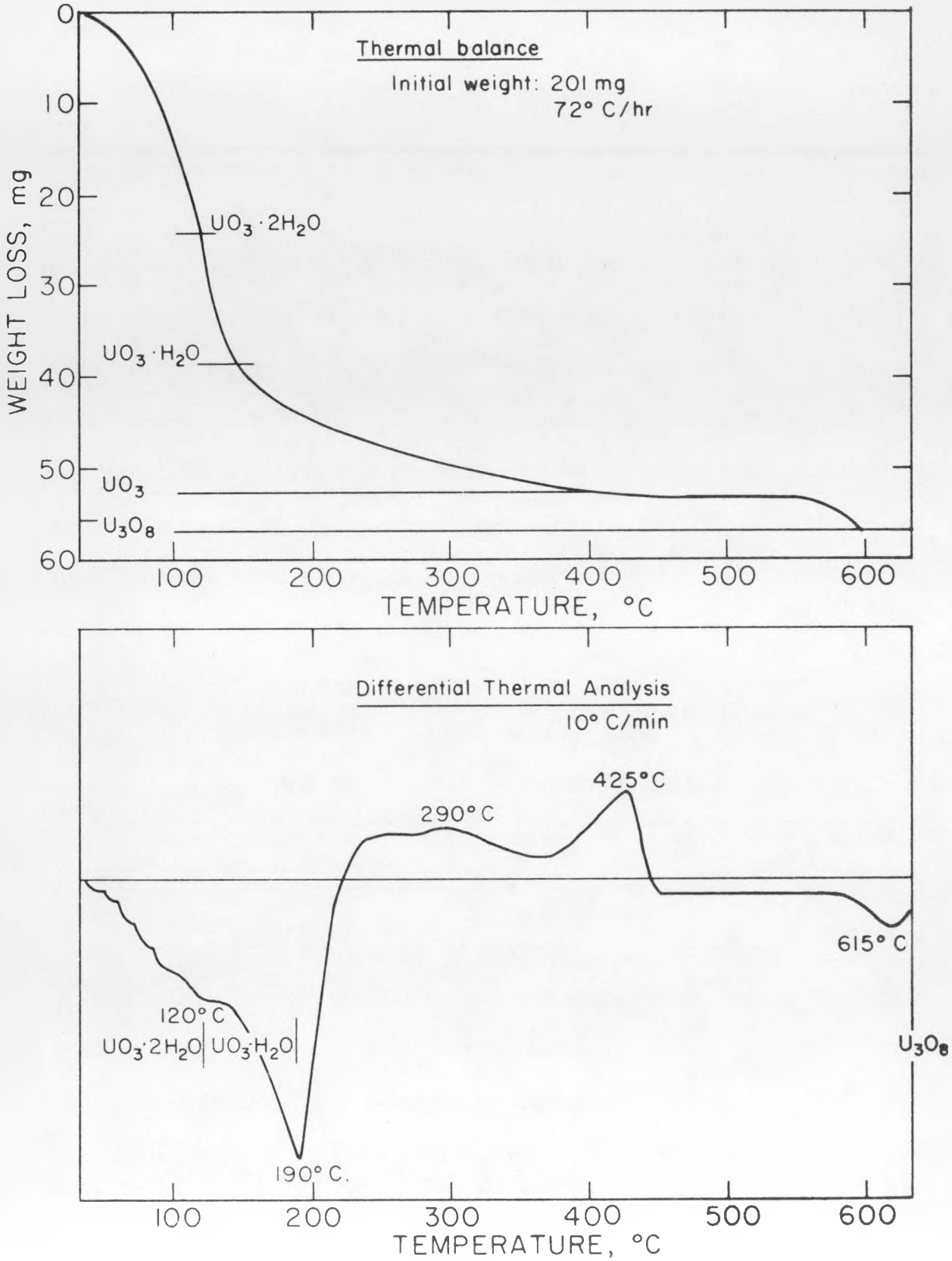

Dehydration Behavior of Hydrated UO_3.

FIGURE 5

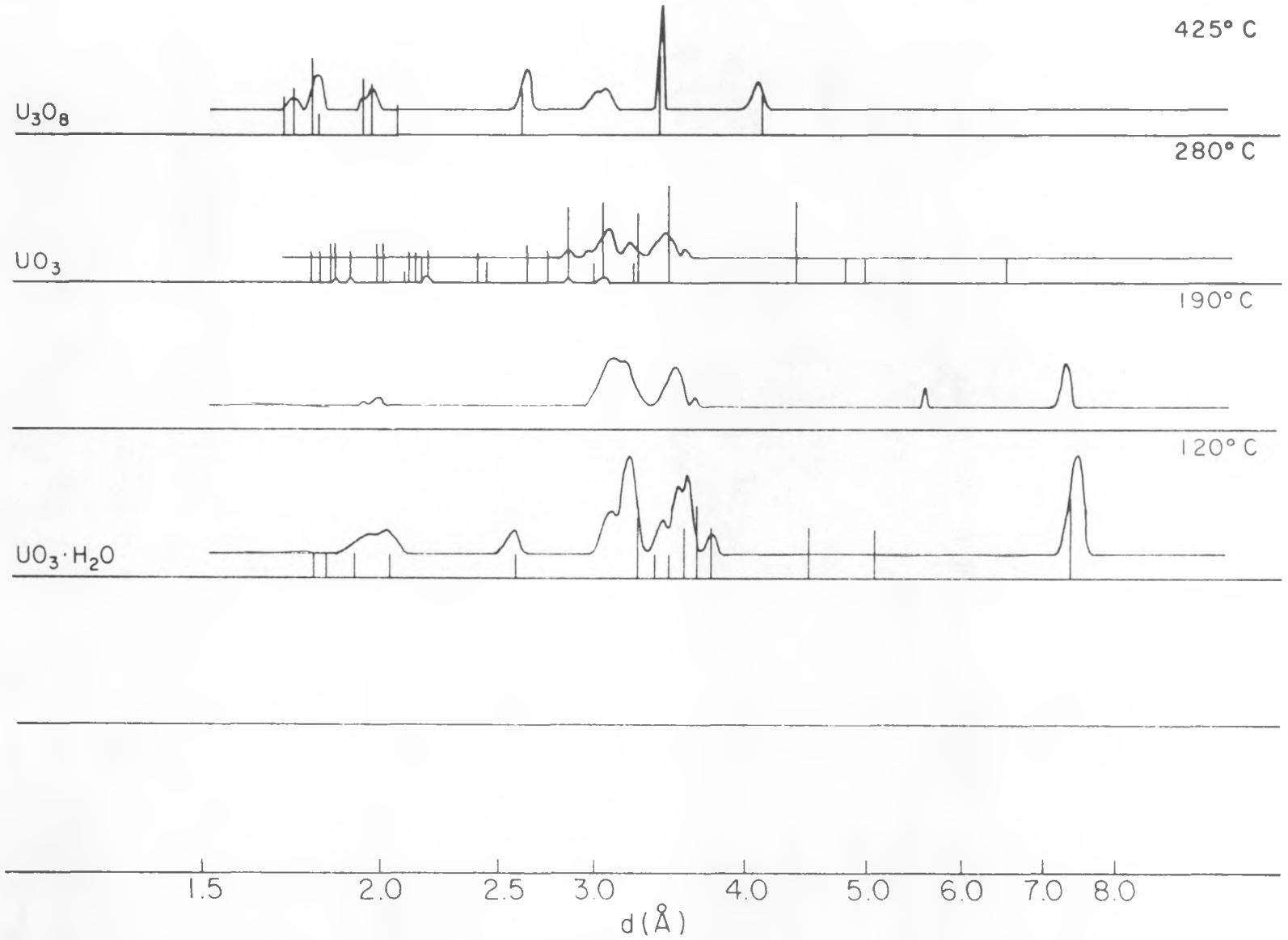

FIGURE 6 X-ray Analysis of $UO_3 \cdot 2H_2O$ Calcination Products.

SPHERICAL PRODUCTS

(a) Purity of the product

The chemical analysis of the UO_2 shown in table 2 shows that the use of organic materials in the granulation step does not result in carbon contamination in excess of acceptable limits in the final product. Silicon contamination comes from the ordinary vitrified corundum disk used for the colloid mill. Sheared corundum particles themselves, however, do not seem to be included in the particles. Application of a sintered UO_2 disk is now planned to reduce such troubles.

(b) Granulation yield

Granulation yield is mainly affected by the composition of the oil dispersant. Table 3 shows the dependence of the yield on the various oils and aqueous binding agents. At present, some aromatic chlorides give the highest yield.

(c) Size distribution

Various factors affect the size distribution. Several examples are shown on Fig. 7.

(d) Density

Density of the UO_2 particles mainly depends on the composition of oil dispersant. As shown in Fig. 8, some oils constantly give high density whereas others result in considerable fluctuation according to the granulation conditions.

(e) Shape

Fig. 9 shows the cross section and surface micrographs of UO_2 particles successfully produced by the present method. High densification was attained with the fewest closed pores. Fractured surfaces of the same particles are electron-micrographed in Fig. 10. Some unfavorable results are summarized in Figs. 11 and 12. Poorly granulated feed powder and/or improper oil dispersant result in excessive pores inside the

Table 2 Typical chemical analysis of the product

	ADU Feed powder	Spherical UO_3 hydrate	Spherical UO_2
Na	< 8 ppm	< 8 ppm	< 16 ppm
Ca	~25 ppm	~25 ppm	~25 ppm
Al	< 10 ppm	10 ppm	11 ppm
Si	50 ppm	100 ppm	120 ppm
Fe	50 ppm	45 ppm	< 22 ppm
C		1.02 %	< 48 ppm

62-214

Table 3 Granulation yield of UO_3, percent

Binding agent	UNH (A)		HNO_3 (B)	(A)+(B) 1:1
Oil dispersant	14cc/100g UO_3	12cc/100g UO_3	12cc/100g UO_3	14cc/100g UO_3
Kerosene	27.3	18.0	14.0	36.9
Toluene	9.6		4.0	13.8
Alkylnaphthalene (A)	24.9		41.6	33.2
Alkylnaphthalene (B)	33.2	24.0	19.8	
Alkylnaphthalene (C)	8.7			9.8
Aromatic chloride (A)	35.6	31.0	12.2	
Aromatic chloride (B)	13.4	13.0	17.0	
Aromatic chloride (C)	14.3	8.7	5.3	

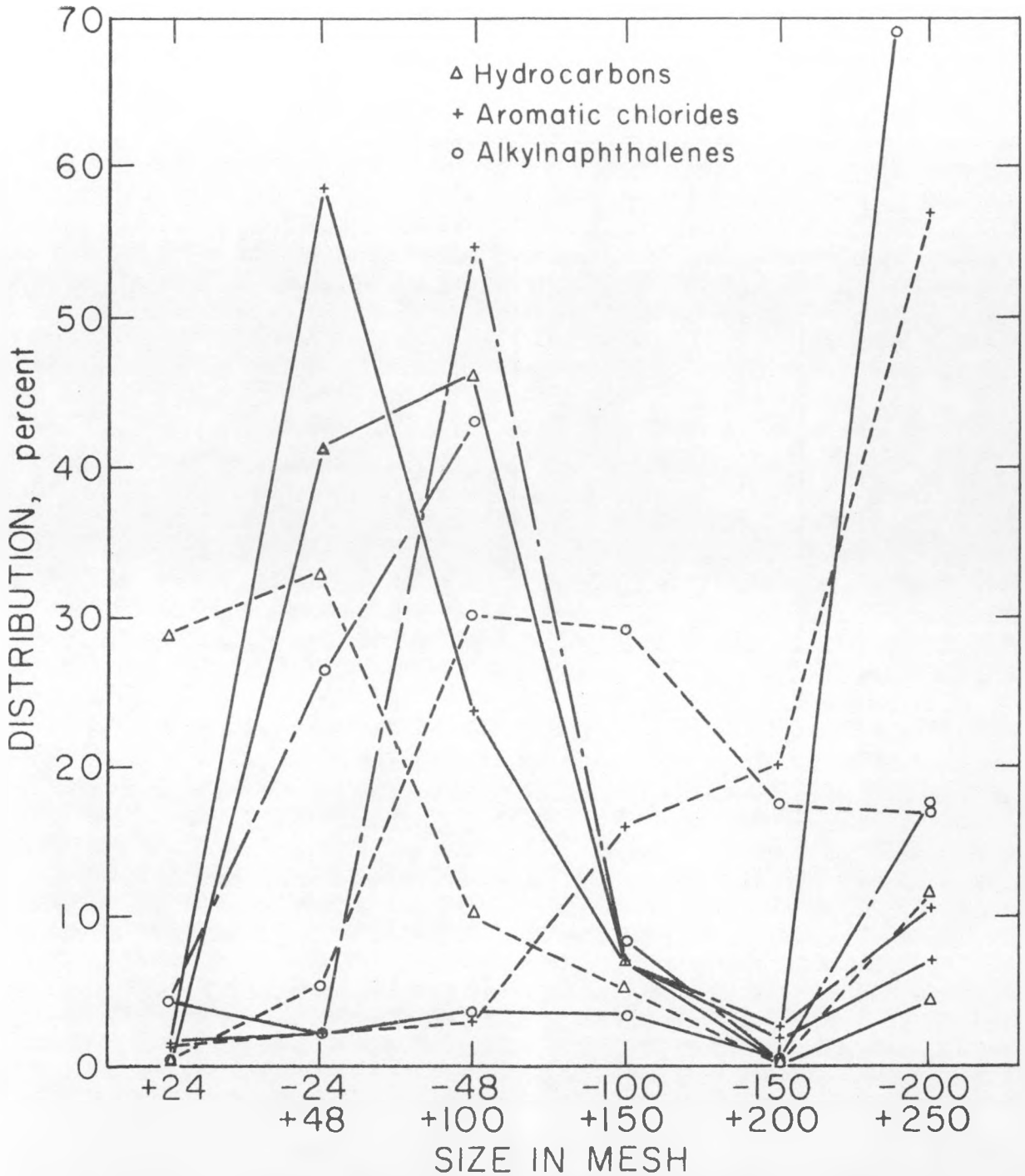

Typical Size Distribution of the Spherical UO_2.

FIGURE 7

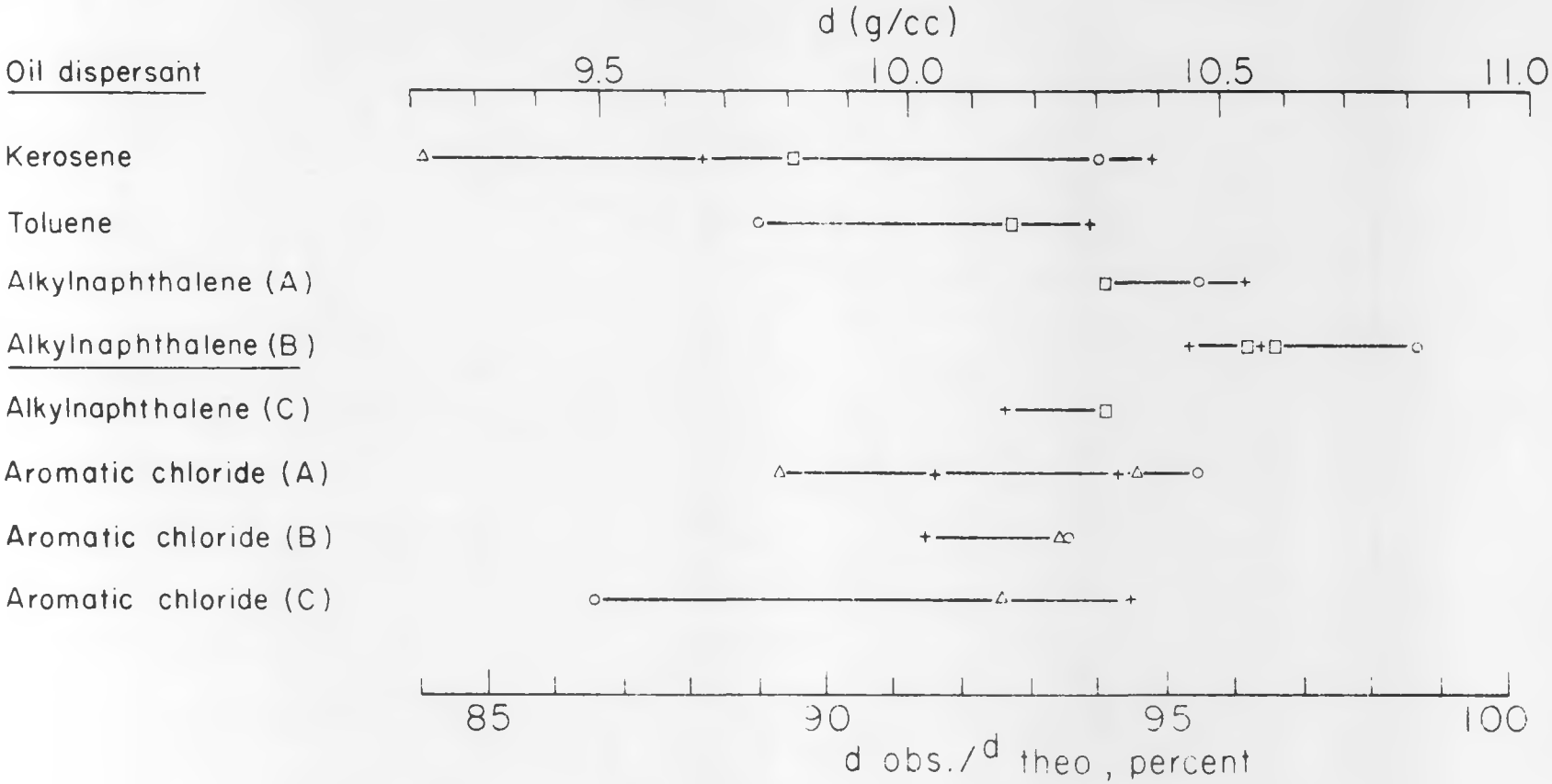

Density of the Spherical UO_2 Particles.

62-210

FIGURE 8

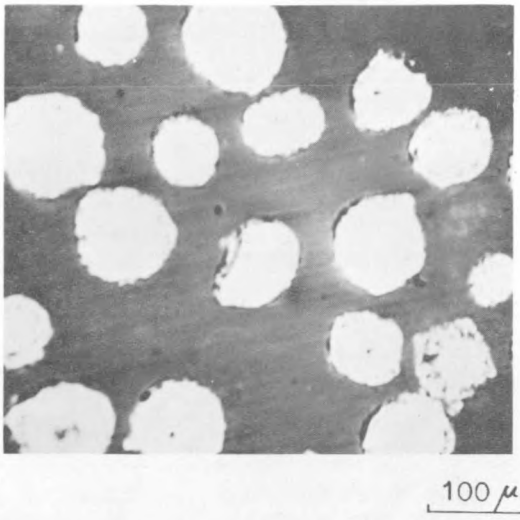

Photo 1 (Cross Section)

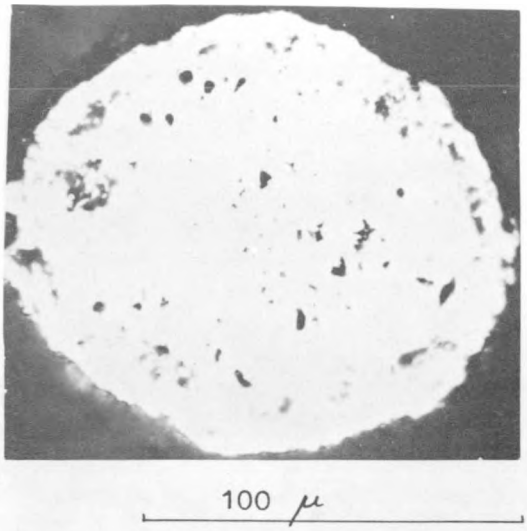

Photo 3 (Cross Section)

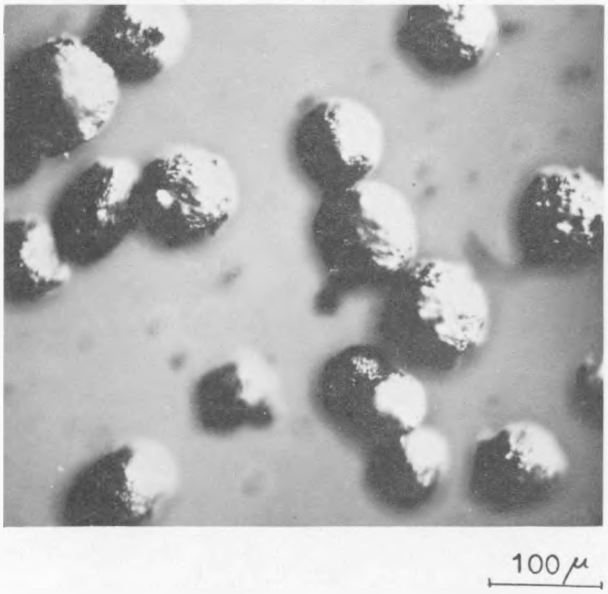

Photo 2 (Surface)

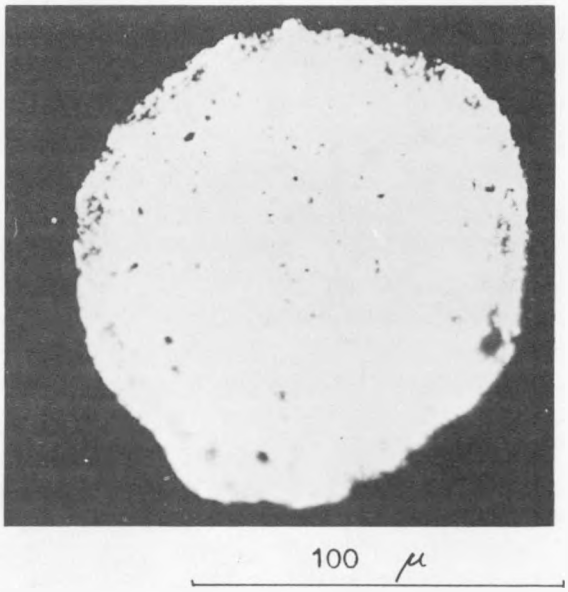

Photo 4 (Cross Section)

Fig. 9. Micrographs of Spherical UO_2 Particals

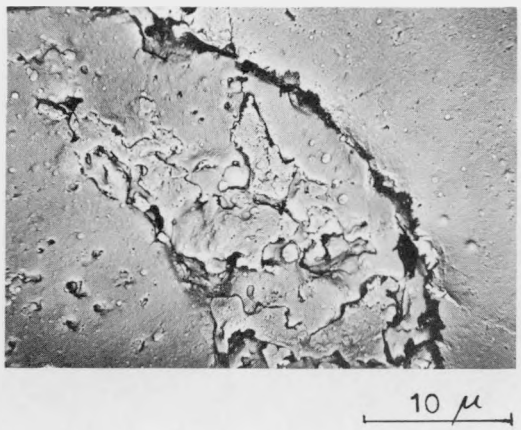

Photo. 1

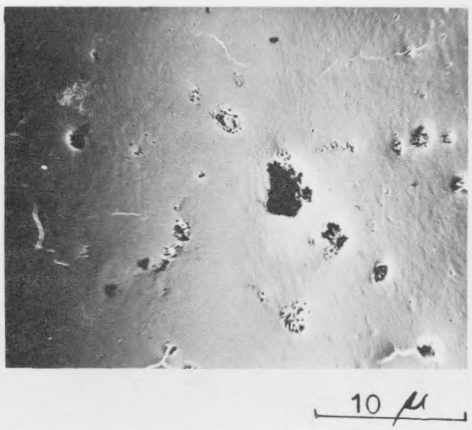

Photo. 3

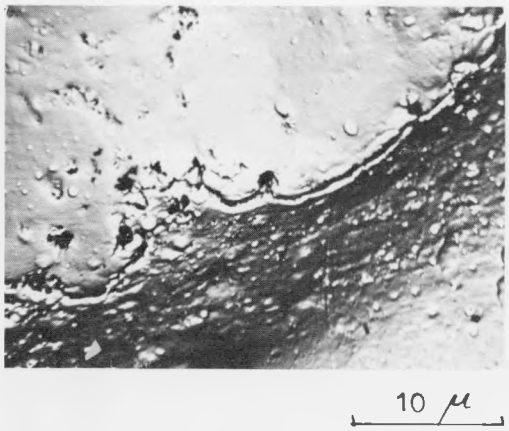

Photo. 2

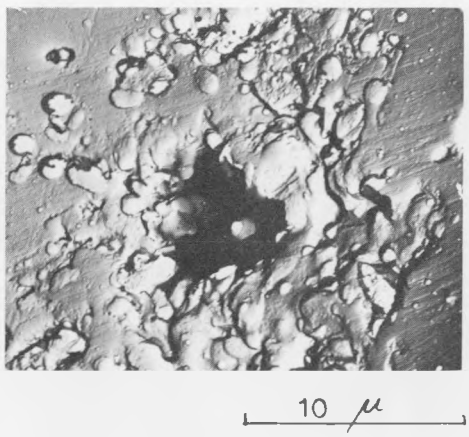

Photo. 4

Fig. 10. Electron Micrograph of Fractured Spherical UO_2

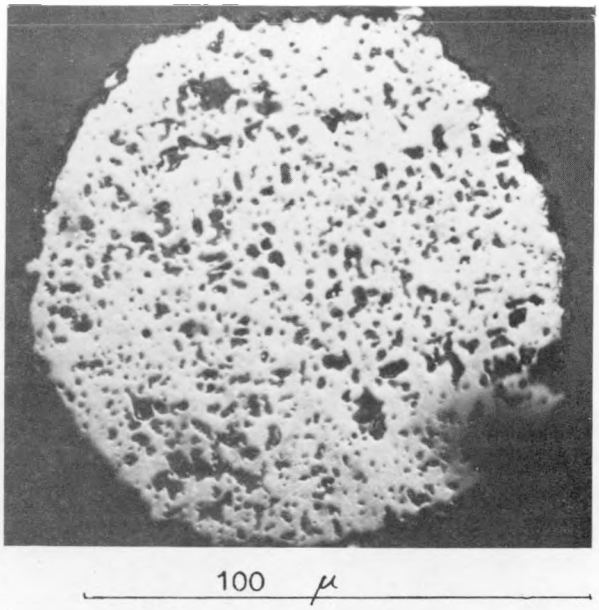

Photo 1 (Cross Section) Swageable Powder

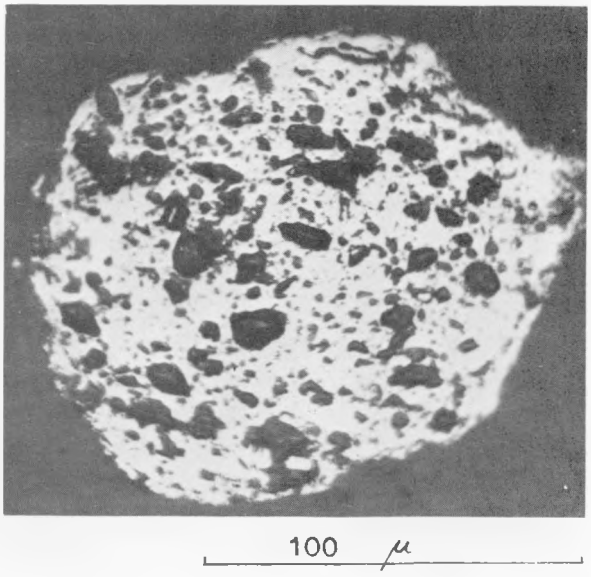

Photo 2 (Cross Section) Ceramic Powder

Fig. 11. Micrographs of unsuccessfully produced UO_2 Particals (I)

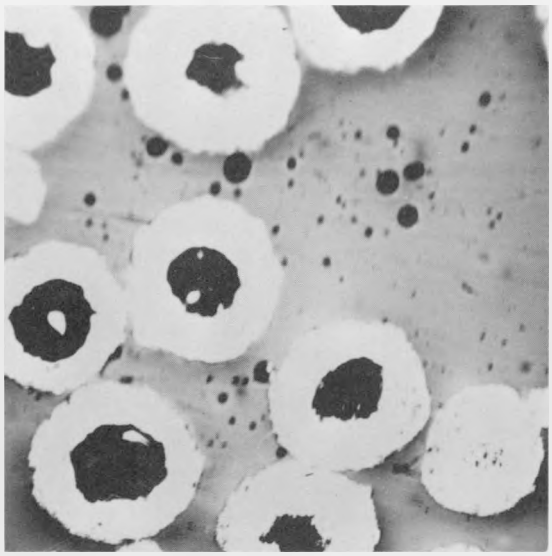

Photo 3 (Cross Section)
Center Pore

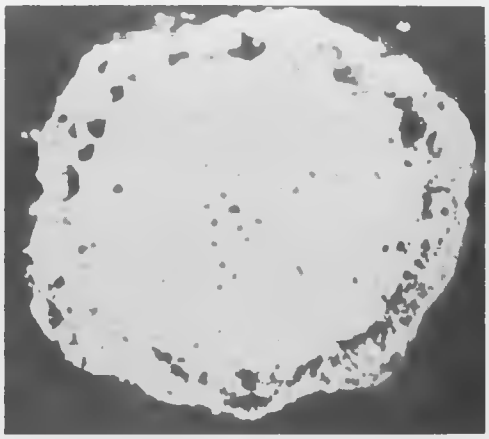

Photo 5 (Cross Section)
Double Structure

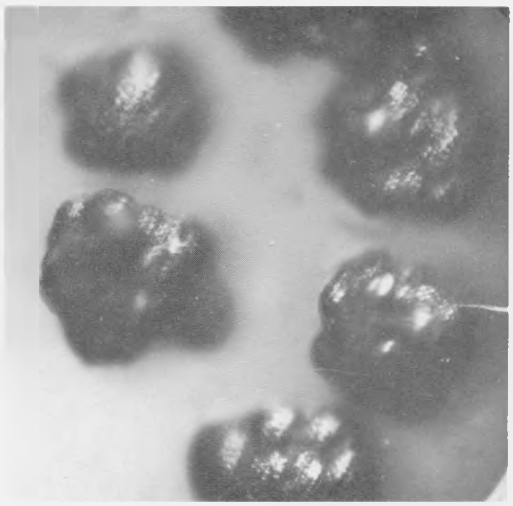

Photo 4 (Surface)
Mutual Adhesion

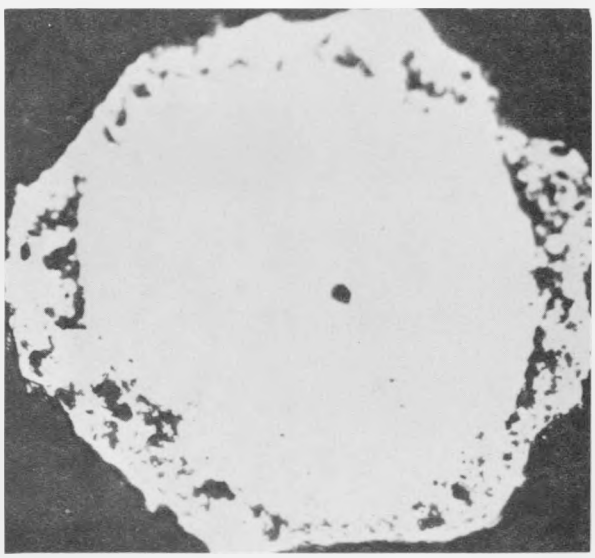

Photo 6 (Cross Section)
Double Structure

Fig. 12. Micrographs of unsuccessfully produced UO_2 Particals (II)

granules (Photo. 1). Photo. 2 shows that when ceramic UO_3 powder is used as a starting material, the sintered UO_2 particles produced are porous. Large pores at the center of the particles are attributed to the air bubbles which get mixed with the slurry during the granulation (Photo. 3). Viscous and polar oils are apt to lead to this kind of trouble. Double layer structure of Photos. 5 and 6 mainly results from excessively slow speed in adding the aqueous binding agent. When hydrated particles crush together before their sufficient solidification is effected, the ragged particles appearing on Photo. 4 are generally produced. At present, the complete elimination of this unfavorable phenomenon is found to be difficult. Further improvement of the agitation practice is now continuing.

METALLIC COATING

Several metallic coating experiments were carried out in a quartz reactor which was made closely after the design published by J. M. Blocher, et al. (6) Up to now, niobium and tungsten coatings have been proved to be successful by using $NbCl_5$ and WCl_6 as a starting material respectively. Fig. 13 shows the typical cross section of niobium-coated UO_2 particles. Photo. 1 shows a coated particle of UO_2 produced by the present method, and Photo. 2 shows a coated spherical UO_2 particle obtained from the Nuclear Materials and Equipment Corp., Apollo, Pa., U. S. A. and coated in our laboratory.

CONCLUSION

The present work has shown that the high density spherical UO_2 particles are successfully produced, starting from oil-dispersed UO_3 fine powder. The size of the particles can be varied between 50 and 250 mesh. Ninety-five percent of the theoretical density is easily attained. No difference from commercial, spherical UO_2 is observed as far as metallic coating practice is concerned.

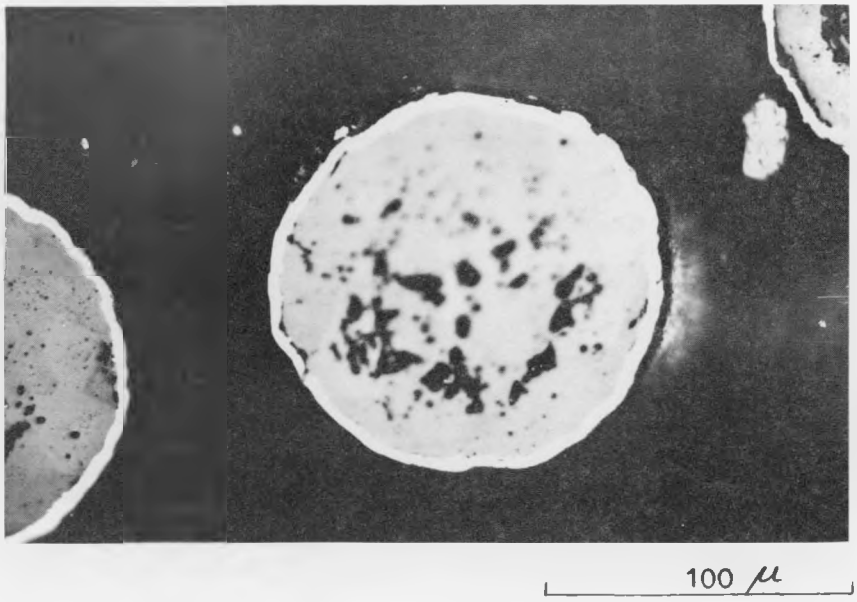

Photo 1. Present Method

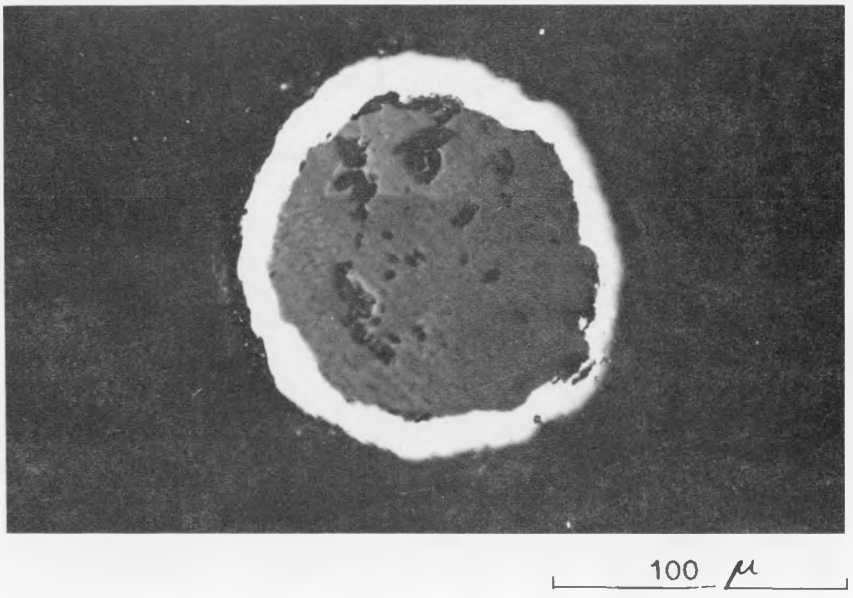

Photo 2. NUMEC Spherical UO_2

Fig. 13. Cross Section of Nb Coated Spherical UO_2

Although there still remain several points for further investigations, the present process promises to be one of the most economical methods for spherical UO_2 production. Fig. 14 shows the proposed flowsheet in producing spherical UO_2 particles, utilizing swageable UO_2 pilot plant facilities.

ACKNOWLEDGMENTS

The authors are indebted to Dr. S. Takahashi and Mr. S. Nagata for the electron micrographs. Thanks are due the late Dr. Y. Suehiro for his continued interest and stimulating discussions on this research. Our thanks are also due the members of our research team for their devoted help.

Finally, we are grateful to Mr. S. Yamagata, President of our Company, Mr. T. Oishi, Managing Director, Mr. M. Kamada, Director of our Laboratory, for their support and permission to publish this work.

Part of this work is carried out under the auspices of the Japanese Government. U.S. patent is being applied for.

REFERENCES

1. H. Doi, et al., On Ceramic and Swageable UO_2, the 4th Plansee Seminar, "Powder Metallurgy in the Nuclear Age" June, 1961.
2. J. K. Dawson, et al., J. Chem. Soc., (1956) 3531.
3. Bergstrom and Lundgren, Acta Chem. Scand., 10, 673 (1956).
4. Wamser, et al., J. Am. Chem. Soc., 74, 1022 (1952).
5. D. T. Vier, A-1277 (1944).
6. J. M. Blocher, Jr., N. D. Veigel, J. H. Oxley, et al., Fluidized-bed Coating of UO_2 Powder with Niobium and other Elements. BMI-1440, May 1960.

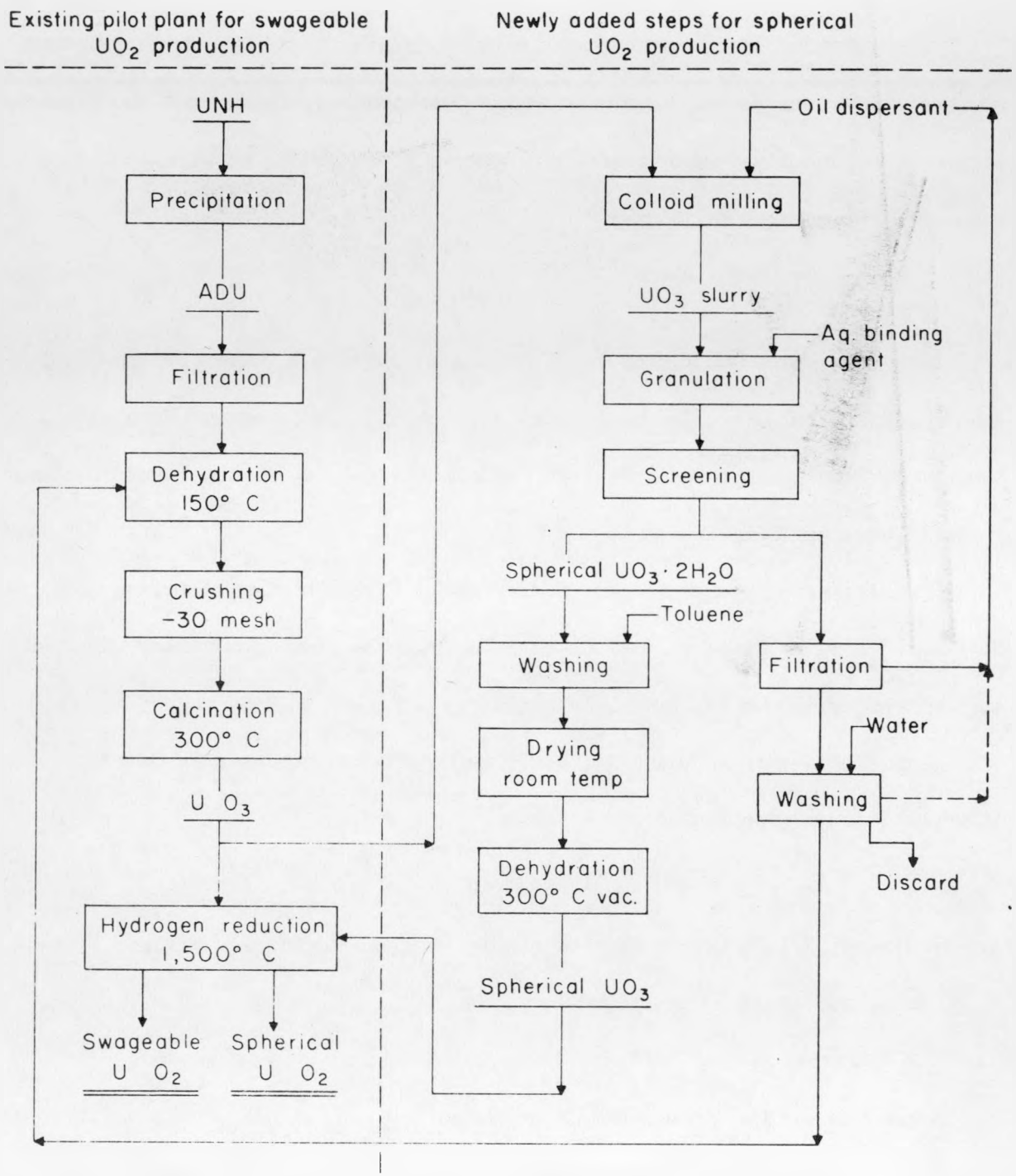

Proposed Flowsheet for the Spherical UO_2 Production.

62-216X

FIGURE 14

COATED-PARTICLE STUDIES FOR BERYLLIUM OXIDE DISPERSION-TYPE FUELS

By P. G. Alfredson and R. C. Cairns

Australian Atomic Energy Commission Research Establishment, Lucas Heights

ABSTRACT

A summary is given of progress on coated-particle studies at the Australian Atomic Energy Commission Research Establishment, Lucas Heights. Some preliminary results are given.

Conventional equipment is used for making near-spherical particles of UO_2 and $(U,Th)O_2$ as feed material for the coating studies. An alternative process based on melting the particles in a plasma jet, is also described. Anhydrous beryllium chloride is being produced by the chlorination of beryllium metal turnings.

Alumina coatings have been deposited on UO_2 and $(U,Th)O_2$ particles using vapor-phase hydrolysis of aluminium chloride in a fluidized bed. Runs at temperatures up to 1050 C and coating rates of 1 to 20 microns per hr have produced coatings 3 to 65 microns thick. Alumina-coated $(U,Th)O_2$ particles have been incorporated into a beryllium oxide matrix by hot pressing.

Beryllia coatings have been deposited on $(U,Th)O_2$ and UO_2 particles by the hydrolysis of beryllium chloride.

INTRODUCTION

The Australian Atomic Energy Commission is making a study of a high-temperature gas-cooled reactor system moderated by beryllia, in which the fuel material is dispersed as small particles throughout some or all of the moderator. For the dispersion fuel systems being studied the optimum particle size is considered to be in the range 100 to 200 microns.[1] To obtain a high outlet gas temperature, the core is to be completely ceramic, without metallic canning to contain fission products. It is desirable

for the coolant circuit to be free from fission products to eliminate the need for expensive fission-product clean-up equipment. The several possibilities for reducing fission-product release to the circuit include cladding the fuel elements with an impervious coating of beryllia, and coating the individual fuel particles with an impervious layer of beryllia before dispersion in the beryllia matrix. Coating of particles allows better fuel dispersion since particles are then separated by a distance at least equal to two coating thicknesses. Because of their physical and nuclear properties, alumina-coated particles could also be used in beryllia dispersion fuels.

The work described here is a summary of progress on feed material preparation and coated-particles research at Lucas Heights. So far no fission-product retention data have been obtained to evaluate coatings. The aim of the main effort to date has been to establish the variables that affect good coating deposition, using the technique of vapor-phase hydrolysis in a fluidized bed developed by Battelle Memorial Institute.[2]

FEED-MATERIAL PREPARATION

Dense near-spherical fuel particles of UO_2 and $(U,Th)O_2$ are produced using a conventional ceramic process to provide starting material for the coated-particle work. The process is essentially similar to that developed by Jones and Reeve.[3] For UO_2 particles, natural uranium oxide powder, nominally -300 B.S.S. Mallinckrodt Ceramic Grade, is compacted by mechanical pressing at 8 to 10 tsi into pellets 3/4 in. in diameter and 3/8 in. high. The pellets are crushed and sieved to a size about 20 per cent greater than finally required. Rounding by vibratory shaking for 4 hr gives yields of approximately 70 per cent of near-spherical particles. The rounded UO_2 particles are then sintered for 2 hr in a hydrogen atmosphere at 1450 C. The sintered particles are sieved, giving yields of particles in the required size range of approximately 80 per cent with densities of 97 per cent of the theoretical 10.95 g/cm^3. Figure 1 shows the particles produced.

Fuel particles of $(U,Th)O_2$ with an atomic ratio of U:Th of 1:50 are fabricated by a similar process. Thoria powder calcined at 900 C for 12 hr is wet ball milled with urania for 12 hr. Following pressing, crushing, rounding, and sieving, material of the required size range is sintered in hydrogen for 2 hr at 1700 C to give densities of 95-98 per cent of the theoretical 10.17 g/cm^3. Examination of polished sintered $(U,Th)O_2$

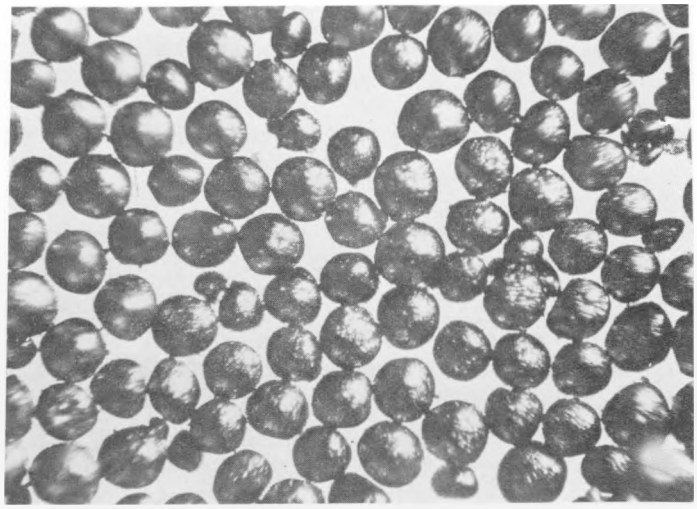

50X

FIGURE 1. SINTERED UO_2 GRANULES -100+150 B.S.S. (conventional process).

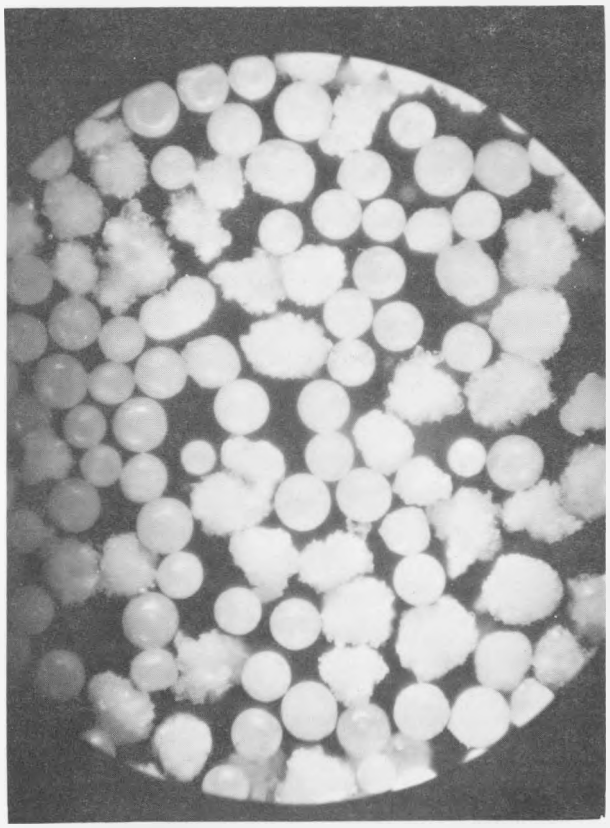

50X

FIGURE 2. ALUMINA PARTICLES FROM PLASMA JET

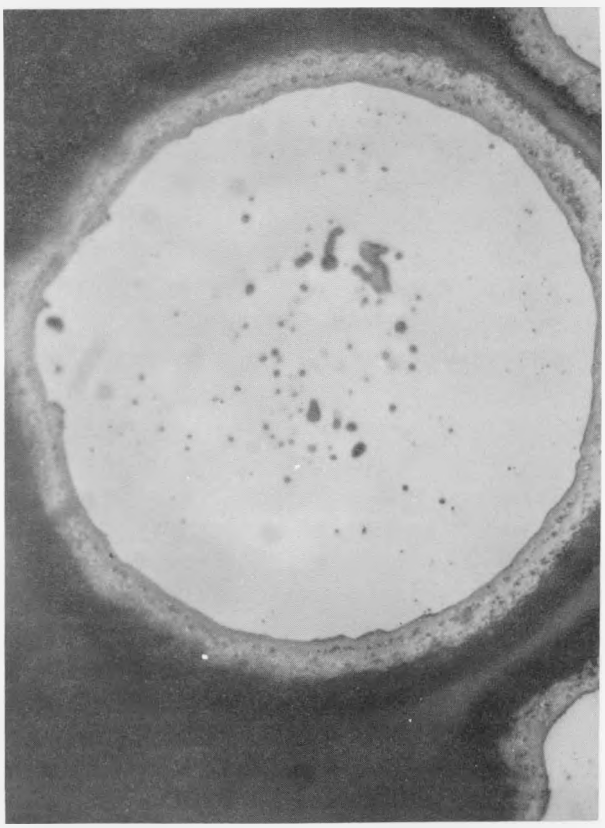

500X

FIGURE 3. ALUMINA COATING ON $(U,Th)O_2$ DEPOSITED AT 1000 C
Coating thickness is 10 microns.

particles by an electron-probe microanalyzer has shown that the U:Th ratio is uniform from particle to particle and, on the 5-micron scale in any one particle, the variation in atomic ratio of U:Th is from 0.8:50 to 1.3:50. Since the grain size of the particles is about 25 microns, this means the urania and thoria are present as a near homogeneous solid solution. This was confirmed by X-ray diffraction analysis of the particles which gave a pattern similar to that obtained for the thoria used and failed to show any urania peaks.

The plasma-jet technique[4] for producing dense spherical particles of refractory oxides has considerable potential. To investigate this method a 15-kw Radyne high-frequency induction-heating set was modified to 2.25 megacycles per sec.[5] To maintain a stable plasma, argon gas was fed tangentially,[6] at a rate of 20 litres per min, through a 25-mm-ID silica tube. Runs were made with -120+150 B.S.S.A.R. alumina powder as an analogue for $(U,Th)O_2$. Stable plasmas were achieved for spheroidization with feed rates of up to 20 g of alumina powder per min to give spherical particle yields greater than 40 per cent. At a feed of 4 g per min, the yield was 80 per cent. Figure 2 shows the nature of the particles produced. X-ray diffraction showed that the particles consisted of alpha alumina. Densities obtained were 90 per cent of the theoretical 3.98 g/cm^3. Considerable porosity was evident in polished specimens. Preliminary work using -72+100 B.S.S. uranium dioxide powder gave a yield of approximately 40 per cent of spherical particles, but considerable improvement on this conversion can be expected.

Plasma-jet feed material has not been used so far for the coated-particle work.

The anhydrous beryllium chloride required for beryllium oxide coating work has been produced conveniently by the direct chlorination of beryllium turnings in a static bed. Reaction temperature was held below 900 C by controlling the flow rate of the chlorine, and the beryllium chloride was condensed directly into the beryllium chloride vaporizer used for the coating experiments. This avoided moisture pickup during transfer of the hygroscopic material. Yields of approximately 90 per cent were achieved.

ALUMINA-COATED PARTICLES

The BMI technique of vapor-phase hydrolysis in a fluidized bed was used to produce alumina as well as beryllia coatings. The equipment used was essentially the same as that reported by Browning et al.[7] The bed temperature was measured with a stainless steel-sheathed Chromel-Alumel thermocouple exposed to the reaction conditions and inserted into the fluid bed through the water-vapor tube. Argon was used as the carrier gas, and progress of the hydrolysis reaction was followed by titration of the off-gas scrub liquor in the normal way.

Fuel particles of UO_2 and $(U,Th)O_2$ have been coated with alumina at fluid-bed temperatures in the range 700 to 1050 C to give coatings 3 to 65 microns thick. Runs of up to 5 hr in duration have been made, usually with particles in the size range -72+100 B.S.S. With a 50-g bed of particles, 20 to 40 per cent of the alumina, charged as aluminum chloride, was deposited as coating. A mole ratio of three or greater for the reactants, $H_2O/AlCl_6$, gave conversion efficiencies of 80 to 100 per cent for the aluminium chloride hydrolysis. Lower conversion efficiencies were achieved when less than stoichiometric proportions of the reactants were used.

The coatings obtained were uniform in thickness, relatively free of large voids, crack free, and showed good cohesion between the coating and the substrate. Coatings deposited at fluidized-bed temperatures of 700 to 750 F were porous, with a Knoop hardness of 100 to 300. At a fluid-bed temperature of about 1000 C, coating rates in the range 0.02 to 0.20 g of alumina per hr per g of initial bed material were achieved by varying the reactant feed rates. These coating rates correspond to a coating buildup in the range 1 to 20 microns per hr. Coatings deposited at about 1000 C at a coating rate of approximately 1 micron per hr were relatively dense (Figure 3), with a Knoop hardness of about 2000; for the same deposition temperature, and a coating rate of 20 microns per hr, the coating was more porous, with a Knoop hardness of only 600.

X-ray diffraction analysis of alumina coatings produced at temperatures in the range 750 to 1050 C revealed a finely crystalline alpha-phase alumina structure. There was some evidence of a glassy amorphous phase in coatings deposited at about 1000 C; this agrees with results on alumina coatings deposited at 1000 C, and reported by Dayton and Tipton.[8]

Acid-leach tests were made of UO_2 particles coated with 20 microns of alumina deposited at 1000 C. After an initial 6-hr leach, using 7.5 N nitric acid at 90 C to dissolve uncoated particles of fuel, a 6-hr test under the same conditions removed 0.007 per cent of the contained uranium. Alpha emission from the coated particles was measured by counting a monolayer of the particles in a zinc sulphide scintillation counter. The measurements indicated negligible contamination of the coatings.

Acid-leach testing of alumina-coated $(U,Th)O_2$ fuel particles with nitric acid was unsatisfactory, since traces of fluoride ion are needed in the nitric acid to dissolve the thoria and this also produces significant corrosion of the coating.

Beryllia compacts have been prepared by hot pressing Brush UOX grade beryllia, incorporating alumina-coated $(U,Th)O_2$ particles, at 1 tsi and 1500 C for 1 hr in a graphite die. Dense coatings 20 microns thick, deposited at 700 C, were used. In both cases the coatings remained intact. The stresses due to the greater thermal expansion of the $(U,Th)O_2$ fuel particle, compared with that of the alumina coating, were apparently not sufficient to fracture the coatings under the hot-pressing conditions. Significant densification of the 700 C coatings was observed.

BERYLLIA-COATED PARTICLES

Beryllia coatings have been deposited on UO_2 and $(U,Th)O_2$ particles by hydrolysis of beryllium chloride in equipment similar to that used for the alumina coatings. Because of the toxicity hazards the apparatus was located in a glove box as shown in Figure 4.

Preliminary coating runs at 1000 C produced coatings 3 to 14 microns thick in periods of up to 5 hr. Coating rates of 0.01 to 0.05 g of beryllia per hr per g of initial bed material have been obtained, corresponding to coating buildups of 1 to 7 microns per hr. Approximately 50-g beds of $(U,Th)O_2$ and UO_2 fuel particles in the size range -72+100 B.S.S. were used as the coating substrate. Conversion efficiencies of 70 to 100 per cent in the hydrolysis reaction were obtained with mole ratios of $H_2O/BeCl_2$ equal to or greater than 1.0. Approximately 15 to 40 per cent of the beryllia fed to the reactor as beryllium chloride was deposited as coating on the particles.

The beryllia coatings produced were uniform and showed good cohesion between the coating and the substrate. All the coatings deposited on

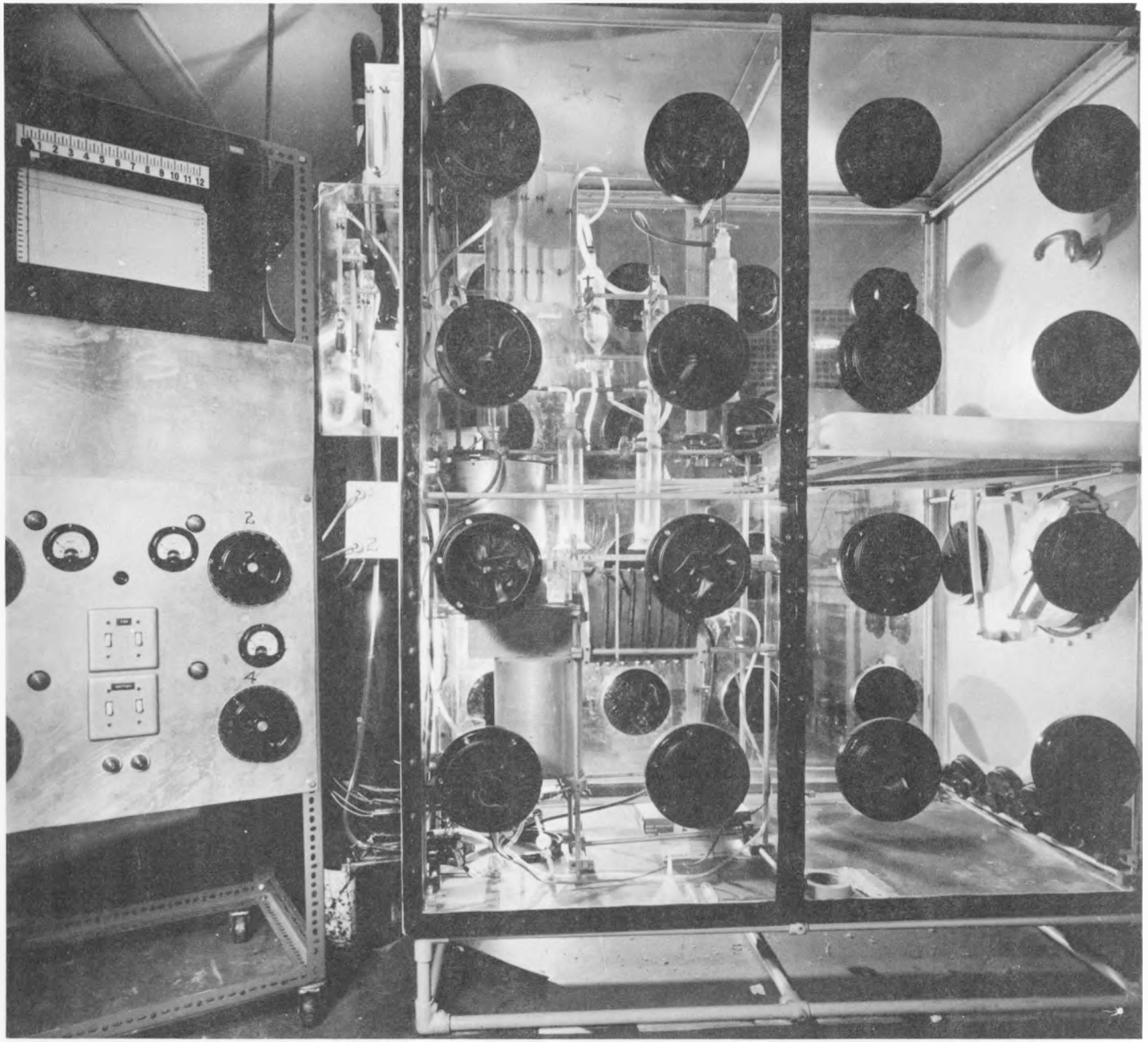

FIGURE 4. EQUIPMENT FOR BERYLLIA COATING RUNS

$(U,Th)O_2$ particles were porous, with Knoop hardnesses in the range 200 to 700, compared with about 1500 for hot-pressed beryllia. Marked surface protrusions of up to 15 microns existed on all coatings (Figure 5). A dense beryllia coating of 12 microns on UO_2 has been deposited at 1000 C and a coating rate of 3 microns per hr (Figure 6). The Knoop hardness of this coating was approximately 1250.

THE INCORPORATION OF COATED FUEL PARTICLES IN A BERYLLIA MATRIX

The incorporation of coated fuel particles in a beryllia matrix involves fabrication processes at temperatures which may be significantly above the coating deposition temperature. The temperature involved can affect the structure of the fuel particle, coating, and the matrix.

Since the thermal-expansion coefficients of urania and thoria are greater than those of beryllia and alumina at temperatures up to 1200 C,[9] heating the coated particle-matrix dispersion to the fabrication temperature may cause the coatings to crack due to the tensile forces generated in the coating. If fabrication is carried out in an oxidizing atmosphere, coatings which are permeable to oxygen at the fabrication temperature may also crack due to volume expansion of the fuel particle caused by its oxidation.

Cracks and void formation adjacent to local agglomerations of particles have been observed when dense, sintered fuel particles are incorporated into the matrix by cold pressing and sintering.[10] Dense coated fuel particles would probably cause these same faults. Suggestions for avoiding cracking have included the use of a burnout layer, for example, pyrolytic carbon, the use of an outer porous layer in the coating which shrinks during fabrication, or the use of a porous matrix which minimizes the problem.

The incorporation of alumina- and beryllia-coated particles in a beryllia matrix is at present under study at Lucas Heights, but until the variables which determine good coating deposition have been fully defined the problems involved will remain unresolved.

ACKNOWLEDGMENT

The authors gratefully acknowledge the support of the Analytical Chemistry Section, the Physical Metallurgy Group and the Ceramics Group in this work.

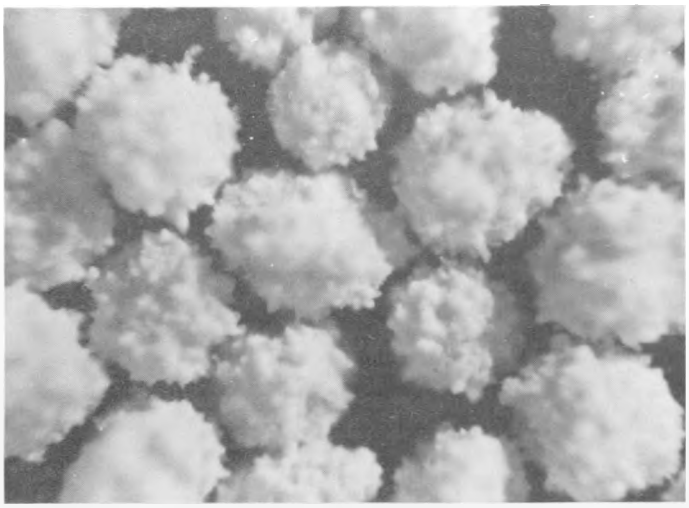

50X

FIGURE 5. BeO-COATED $(U,Th)O_2$
Coating temperature was 1000 C.

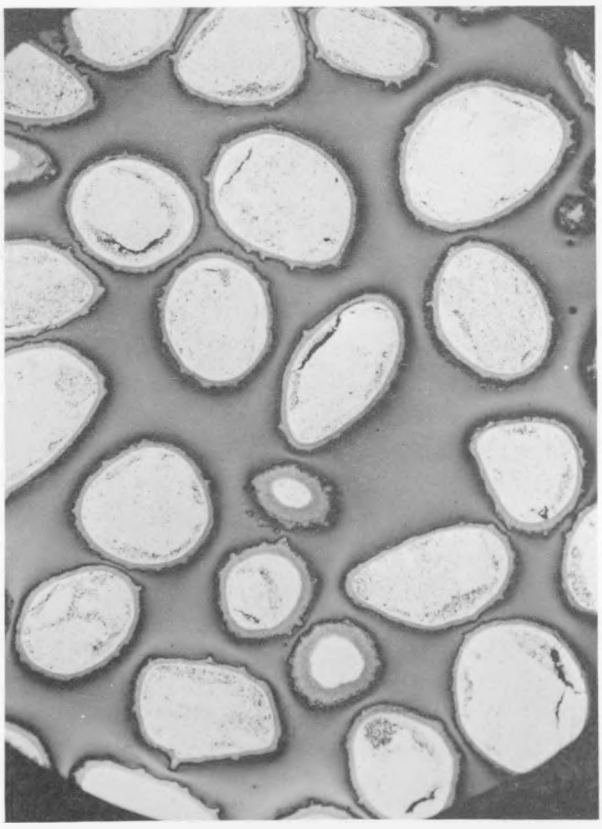

100X

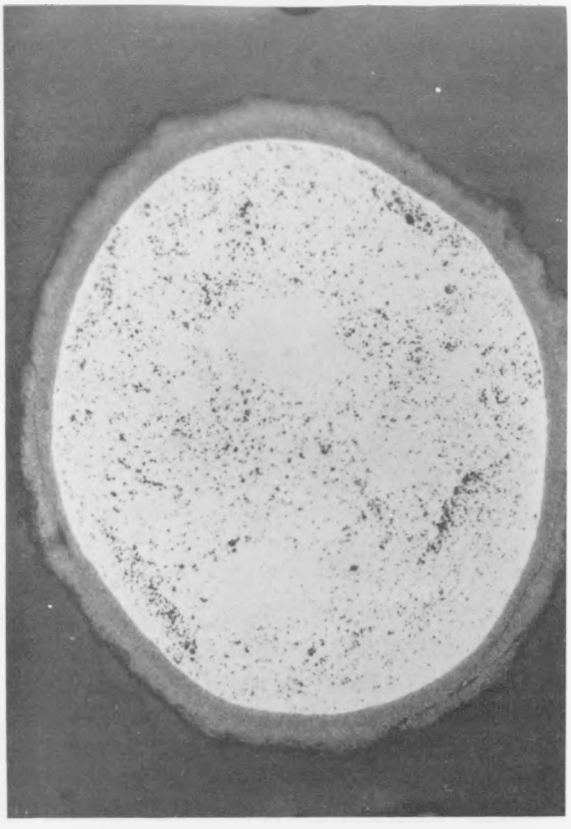

500X

FIGURE 6. 12-MICRON BERYLLIA COATING ON UO_2 DEPOSITED AT 1000 C

REFERENCES

1. B. S. Hickman, AAEC, Private Communication.
2. Progress on Ceramic Coated Fuel Particles at Battelle, BMI-1468, September, 1960.
3. K. A. Jones and K. D. Reeve, AAEC, Report in preparation.
4. H. J. Hedger and A. R. Hall, Preliminary Observations on the Use of the Induction-Coupled Plasma Torch for the Preparation of Spherical Powder. Powder Metallurgy, No. 8, 65, 1961.
5. F. R. Carter and E. J. Lee, AAEC, Work to be published.
6. T. B. Reed, Induction-Coupled Plasma Torch. Journal of Applied Physics, 32, No. 5, 821, May, 1961.
7. M. F. Browning, N. D. Veigel, T. E. Cook, W. S. Diethorn, J. M. Blocher, Alumina Coating of UO_2 Shot by Hydrolysis of Aluminum Chloride Vapor, BMI-1471, October, 1960.
8. R. W. Dayton and C. R. Tipton. Progress Relating to Civilian Applications During May 1961, BMI-1518, June, 1961.
9. G. Arthur, Ceramics - Properties, Nuclear Engineering, 6, 253, June, 1961.
10. K. D. Reeve, AAEC, Private Communication.

DISPERSED FUEL DEVELOPMENT WORK AT REACTOR FUEL ELEMENT DEVELOPMENT LABORATORIES, SPRINGFIELDS U.K.A.E.A.

By C. B. Greenough*

The Reactor Group, Reactor Fuel Element Laboratories
Springfields

The program of work at Reactor Fuel Element Laboratories, U.K.A.E.A. Reactor Group, is hinged essentially to the assumption that the elements will be first used in a reactor which is more akin to the Windscale Advanced Gas-Cooled Reactor than to the Dragon or Peach Bottom reactors. The chosen coolant is CO_2, because it has yet to be established that sufficient helium would be available for a large-scale reactor program in the U.K. The aim of the development work is therefore to produce fuels which

(i) Are resistant to an oxidizing atmosphere

(ii) Retain fission products very well indeed - we do not like the idea of 'dirty' coolant circuits

(iii) Have a large volume ratio of fuel:matrix, since we are interested in low-enrichment, nonbreeding, systems.

Two systems have been selected for study. The first is the same as that already being examined at other laboratories, viz., UO_2 particles in a BeO matrix, preferably without a BeO coating on the particle prior to incorporation into the matrix. The main worry in this system is irradiation damage in the BeO and possible mass transport of BeO by any moisture in the coolant. The second system is a new one, and uses a UC particle fuel with a coating of SiC to prevent diffusion of both gaseous and metallic fission products. The main worry here is that, although silicon carbide is an excellent refractory out-of-pile, there is little known on the effects of irradiation. Work is still in the preliminary stage, but fuel particles have already been made and coated for both systems which appear to be satisfactory. As yet, however, no irradiation tests have been carried out, and there is a long way to go before thoroughly proven fuel elements are available.

*Dr. Greenough spoke without notes but kindly prepared this summary of his presentation for inclusion in the Proceedings.

SOME ASPECTS OF HARWELL RESEARCH RELATING TO DISPERSED FUELS

By P. Murray

Metallurgy Division
A.E.R.E., Harwell

ABSTRACT

Harwell activities on dispersed fuels are concerned with both carbide and oxide systems. In recent studies attention has been given to the investigation of the uranium-carbon diagram both in the monocarbide and dicarbide region. It has been shown that hypostoichiometric uranium carbide exists as a metastable solid solution of uranium in uranium monocarbide, depending on the heat treatment conditions; studies of the effects of oxygen and nitrogen impurities on the relative stabilities of the sesquicarbide and dicarbide have cleared up many confusing observations and it is now possible to indicate which is the stable phase at high temperatures under the appropriate conditions. The irradiation behaviour of the bulk carbides and oxides is also being followed to high burn-up and the burn-up lengths in which discontinuous phenomena occur are beginning to be indicated. Broad indications are also being obtained of the relative diffusion of gases and other fission products in coated particles and of possible solutions to some of the problems. With oxides, the effects of irradiation on BeO as the structural material appear to be more significant than the behaviour of the dispersed fuel and, together with the behaviour of BeO under thermal conditions, represent the more important problems in this field.

1. Introduction

In the U.K. gas cooled reactor programme, attention has always been given to the advantages likely to arise from the use of higher operating temperatures and in the high temperature reactor field there is a change in concept in that an all non metallic fuel element is envisaged (c.f. the A.G.R. and E.G.C.R. "half way house"); here there are many research and development problems not least of which is that of developing fuel elements which retain fission gases and fission products at high temperatures. Harwell activities on dispersed fuels cover both the carbide and oxide systems and are also closely linked with the research proceeding on bulk ceramic fuels. In this paper, it is proposed to review the recent developments concentrating on the phase relations, properties and irradiation behaviour of the materials involved, both in bulk and in dispersed form.

2. Phase Studies

In dispersions based on carbides, the latter may be present either as the monocarbide, sesquicarbide or the dicarbide depending on the coating or matrix material.

Dealing first with the monocarbide, recent work has been concerned with the hypostoichiometric region. Williams and co-workers [1] noted that the lattice parameters of arc melted U-UC alloys varied with composition, decreasing with decreasing carbon content below the stoichiometric composition (4.8 wt.%C) to reach a minimum at about 3.8 wt.%C, and then increasing. Annealing at 1300°C resulted in a gradual reversion towards the parameter of pure UC. Since the uranium-carbon phase equilibrium diagram offers no explanation for these anomalies, the monocarbide existing only at the stoichiometric composition, it was originally thought that impurities might be responsible. Sintered carbides, being prepared at relatively low temperature should be free of UC_2, which is only observed above 1600°C, but

could contain traces of oxygen nitrogen or graphite. On the other hand cast UC should be relatively free from oxygen and nitrogen, but could contain metallic impurities adsorbed during arc melting and retained in metastable solid solution by the rapid cooling. Such impurities would presumably precipitate during subsequent low temperature annealing, giving the observed lattice parameter changes. An explanation of the composition dependence of the effect is however not obvious.

The recent work carried out by Buckley [2] was aimed at elucidating an explanation of these effects. Uranium-Carbon alloys with deliberate impurity additions were prepared by arc melting and the lattice parameters before and after annealing noted. Electron microscopical studies were undertaken in anticipation of detecting precipitated phases in the annealed carbide.

Preparation of Alloys

By solid state reaction

Mixtures of calcium-reduced uranium powder and from 1 to 5 wt.% Achesons 'Dag' graphite 621 were prepared and hot compacted at 800°C and 15 tons/in^2 pressure. The resulting pellets were then heated in vacuum at 1100°C for 50 hours to carburize the uranium.

By arc melting

30 gm. ingots of nominal composition similar to the above alloys were prepared by arc melting the appropriate mixtures of granular graphite and uranium powder on a water cooled copper hearth using a tungsten electrode. The ingots were re-melted to minimise segregation. Impurity was added to the constituents in the form of powdered intermetallic compounds, e.g. UN, U_6Fe, etc.

Dissolution of graphite in liquid uranium

Small samples of carbide were prepared by melting uranium in graphite

crucibles, or with graphite in thoria crucibles, in a resistance heated furnace which was specially constructed to enable the specimen to be quenched into water or oil. Specimen temperature prior to quenching were recorded by an optical pyrometer.

Metallography

X-ray diffraction patterns from the powdered alloys were obtained using a Straumanis type of Debye-Scherrer camera with copper radiation (Cu $K_{\alpha 1}$ = 1.54050Å, Cu $K_{\alpha 2}$ = 1.54434Å), and the unit cell dimensions determined from a circular Nelson-Riley plot. Specimens for metallographic examination were cleaved or cut with a diamond tipped saw, ground with fine diamond abrasive, and finally attack polished with chromic acid on alumina loaded laps. Shadowed "Formvar" replicas were examined using a Phillips electron microscope.

Results

Variation of metallographic structure and lattice parameter with composition

Uranium alloys containing less than 50 at.% carbon are two phase with the uranium forming a network round grains of the monocarbide. Occasionally globules of uranium trapped by advancing carbide dendrites are also seen within the carbide grains. With decreasing carbon content the volume of uranium increases at the expense of the carbide phase.

It soon became evident from preliminary lattice parameter measurements that the unit cell dimension of arc melted carbide is not significantly altered by small additions of Fe, W, Cu, etc. impurity, but is very sensitive to the carbon content of the alloy. Figure 1 summarises the observed lattice parameter-composition relation. The compositions quoted here were deduced from the relative areas of carbide and uranium phases in metallographic

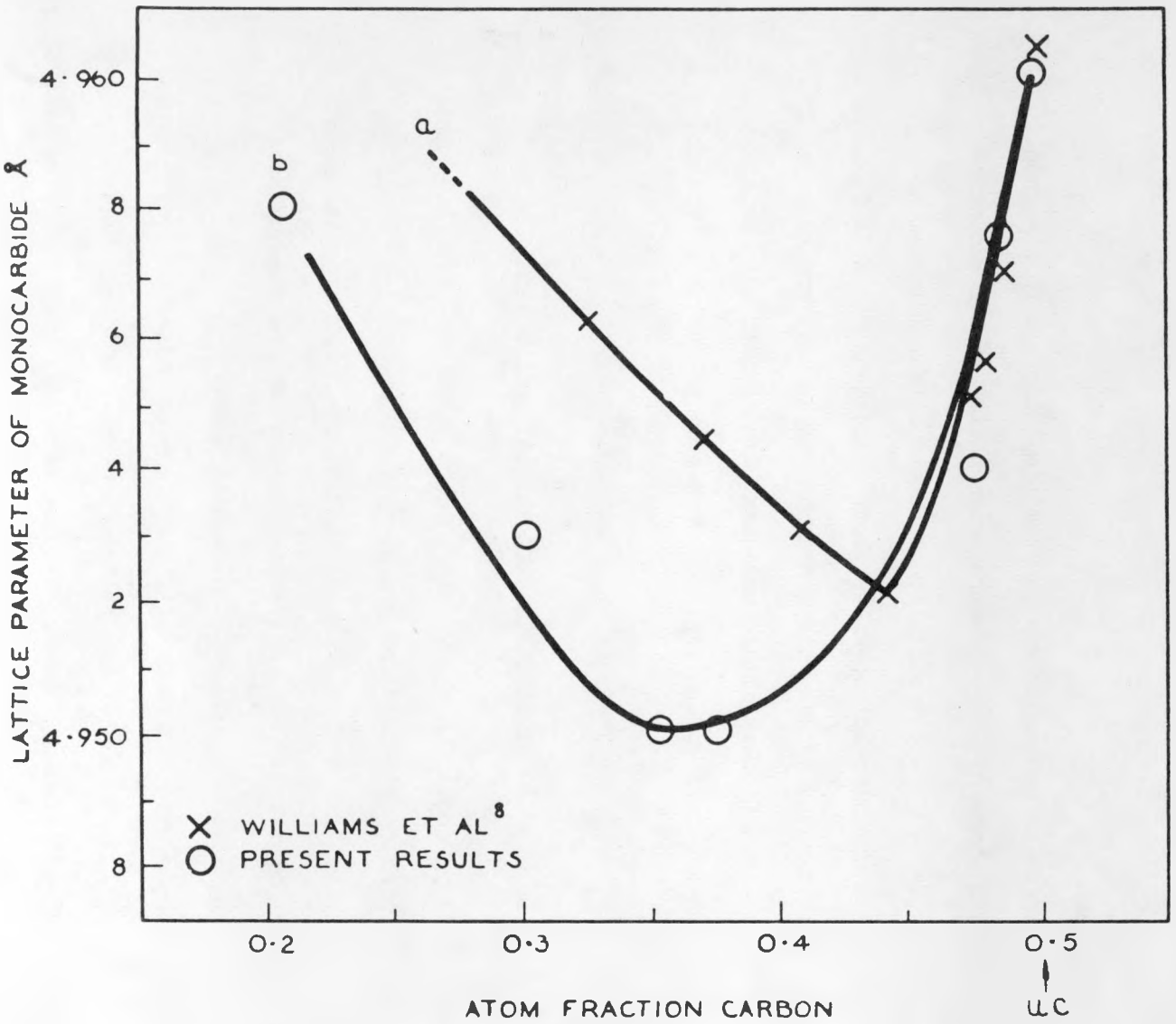

Figure 1

Variation in the lattice parameter of uranium-carbon alloys with composition

sections, assuming zero solid solubility. This 'visual' carbon content was usually substantially less than the nominal composition, presumably because of excessive volatalisation of carbon by the arc. The Williams' data, reproduced in curve 'a' uses nominal compositions, and lies to the carbon rich side of the present one.

Effect of high temperature heat treatment on an alloy of fixed composition

An alloy containing 47 wt.% carbon prepared by solid state reaction at 1100°C was annealed at various temperatures up to its melting point, and then quenched in oil. The lattice parameter of the resulting carbide decreased with increasing quenching temperature, reaching a minimum value 4.949Å at about 2000°C, and then at higher temperatures expanded again.

On subsequently annealing these quenched alloys or arc melted non-stoichiometric carbide at 1300°C in vacuum for periods up to 200 hours, the lattice parameters expanded to approach the value 4.959Å, and a precipitate of fine cubic particles appeared within the carbide grain. In resistance to abrasion, atmospheric oxidation, and chemical reagents the precipitate particles behave in an identical manner to the adjacent grain boundary α-uranium. Assuming that they are indeed α-uranium of density 19 gm. cm^{-2} in carbide of density 13.63 gm. cm^{-2}, the maximum observed volume of the precipitate corresponds to 1.25 at.% uranium in UC.

Discussion

The anomalous lattice parameter of non-stoichiometric uranium monocarbide is clearly a manifestation of the metastable retention of excess uranium atoms in the carbide crystal lattice. UC crystallises with a NaCl type structure with the relatively small carbon atoms occupying essentially interstitial positions in a face-centred cubic lattice of uranium atoms, and introduction of interstitial

uranium atoms into this lattice would create large strains and a unit cell expansion. A uranium rich solid solution can however also be formed by omitting carbon atoms, and this will give rise to a very much smaller strain and a slight unit cell contraction, in agreement with the experimental observations. Similar contractions in unit cell dimensions have previously been reported in several other carbide and nitride-metal systems e.g. NbC, TiC, TiN, but there is no parallel to the minimum in the UC parameter-quenching temperature or composition relation.

The retrograde solubility behaviour is believed to be unique in compounds, although several instances have been noted in primary metallic solid solutions. Buckley[2] has also predicted the shape of the solidus curve from thermodynamic considerations and in Fig.2 the necessary revision to the uranium-carbon phase diagram has been made with the Rundle liquidus on the left and the theoretical solidus on the right. Also plotted are the experimental solid solubilities deduced from the volume of precipitated uranium particles in carbide grains in the 47 at.% carbon alloy following quenching from temperatures in the region of 2000°C and annealing at 1200°C.

So far as the sesquicarbide and dicarbide are concerned, in the more recent work carried out by Livey, Henney and Hill [3] the annealing behaviour of arc cast or sintered material has been studied with special reference to the effects of impurities such as oxygen and nitrogen. The results of this work can be summarised as follows:

(a) When uranium is reacted to form carbide by arc melting or sintering in an inert atmosphere with excess carbon, the structure which usually results consists of the tetragonal phase "UC_2" containing a lamellar precipitate, which if present in sufficient quantity can be recognised as the cubic "UC type" phase. Under conditions of very rapid quench from the melt this precipitate is sometimes not observed but will appear on subsequent annealing.

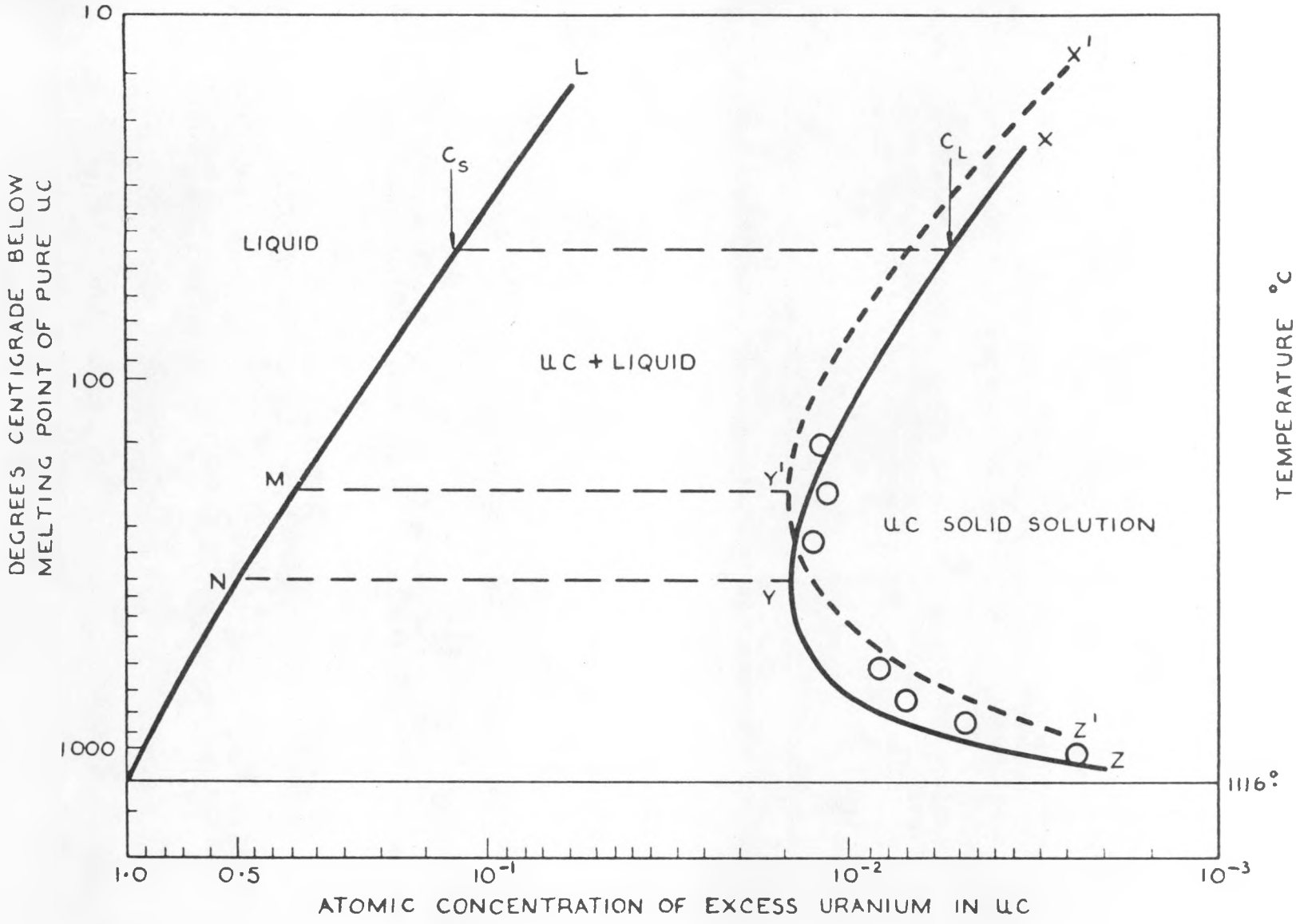

Figure 2

Revised uranium-carbon phase diagram in the region of the stoichiometric composition

(b) An argon arc melted structure might typically contain

$$0.017\%\ N_2 \qquad 0.20\%\ O_2$$

(c) The precipitate within the tetragonal phase appears to be a true equilibrium phase at high temperature since after annealing at high temperature in an "inert" atmosphere it remains after quenching, slow or intermediate cooling without apparent variation in quantity.

(d) On annealing at high temperature, a combination of lattice parameter measurements and chemical analysis suggests that the precipitate is principally a UC/UN solid solution in equilibrium with the tetragonal phase and graphite. In general the analysed nitrogen content can be accounted for by assuming it to exist completely in the precipitate as UC/UN.

(e) At 1750°C the equilibrium lattice parameter of the cubic phase was determined as $a = 4.935\text{Å}$. If this was assumed to be purely a UC/UN phase, this corresponds to 36 $^{m}/_{o}$ UC. The possibility of some oxygen being in the cubic phase however cannot be ruled out.

(f) The oxygen content of an annealed sample (1500° - 1750°C) of tetragonal phase plus cubic precipitate could typically be 4000 p.p.m. and the lattice parameter of the tetragonal phase at room temperature

$$a = 3.519\text{Å}$$

$$c = 5.98\text{Å}$$

(g) By annealing in a good vacuum (10^{-5} mm Hg) or in an inert atmosphere of sufficiently low oxygen potential at 1000°C - 1750°C, the above phases disappear and U_2C_3 plus carbon is formed. A temperature of 1500°C appears optimum for conversion and complete transformation is possible under these conditions.

(h) The formation of U_2C_3 is always associated with a fall in oxygen content (to $\leq$ 100 p.p.m.) and an increase in the lattice parameter of the tetragonal "UC_2" phase. The tetragonal phase in equilibrium with U_2C_3 was found to have parameters at room temperature,

$$a = 3.525 \pm 0.001\text{Å}$$

$$c = 6.000 \pm 0.001\text{Å}$$

and the U_2C_3 to have a lattice parameter of

$$a = 8.088 \pm 0.001\text{Å}$$

The lattice parameter of U_2C_3 was extremely consistent.

(i) The tetragonal "UC_2" was always found to be substoichiometric.

The following conclusions may be drawn from these results:-

1) The sesquicarbide U_2C_3 is the thermodynamically stable phase in the U-C binary system over the range 1000° - 1750°C.

2) The "carbide" phases - tetragonal and cubic - normally observed in the presence of excess graphite form part of the U-C-N-O system.

3) The tetragonal arrangement of uranium and carbon atoms ("UC_2") is stabilised by solution of oxygen, as evidenced by chemical analysis and a decrease in lattice parameter.

4) The cubic arrangement of uranium and carbon atoms is stabilised in the presence of the tetragonal structure and graphite by solution of nitrogen to form a UC/UN solid solution.

5) The oxygen content of the tetragonal phase in equilibrium with U_2C_3 is probably a variable depending on temperature and oxygen potential.

At 1500°C in a vacuum of 10^{-5} mm Hg U_2C_3 is readily formed from the tetragonal $UC_{1+x}O_y$ phase. At 1700° - 1750°C formation of U_2C_3 at this pressure becomes difficult and only partial transformation appears to take place ($\sim$10%).

This suggests that in this region of temperature the point is being reached at which a tetragonal phase very low in oxygen is in equilibrium with U_2C_3 and that the equilibrium temperature for a pure hypothetical tetragonal carbide phase with U_2C_3 is only a little higher. This could in fact be at the previously observed change over point (1820°C) for "UC_2" transforming from tetragonal ⟶ cubic.

Support for these conclusions has been obtained from the following experiments

1) A specimen of sintered uranium plus excess graphite, having a structure of "UC_2" with precipitate plus graphite, was partially transformed to U_2C_3 by annealing in a vacuum of 10^{-5} mm Hg. This was then re-annealed in a poor vacuum (10^{-2} mm Hg) at 1500°C for 20 hours and re-examined. This showed that conversion of the U_2C_3 back to "UC_2" with precipitate was complete.

2) U_2C_3 was formed directly by sintering "pure" UC ($a = 4.961\text{Å}$) and degassed graphite in vacuo (10^{-5} mm Hg) at 1500°C. Complete conversion to U_2C_3 was readily achieved.

3) The formation of U_2C_3 always begins at surfaces - cracks, porous areas, etc. - consistent with the removal of volatile impurities.

Although it has been postulated that stress is necessary for U_2C_3 formation, the conclusion that only a low oxygen potential combined with easy escape of oxygen impurity (i.e. vacuum treatment for best conditions) is necessary is not inconsistent with previously published data since in most cases, vacuum treatment was a component part of the method of preparation. A unique feature of U_2C_3 is the constancy of its lattice parameter, which fits in with these results in that it only forms at low oxygen content. The reported parameters are shown in Table 1.

The present work also suggests lattice parameter data for the tetragonal phase as shown in Table 2.

Confirmation of the lattice parameters in equilibrium with U_2C_3 is given by

TABLE I

Lattice Parameter Data on U_2C_3

Parameter Å	Reference
8.0870 ± 0.0005	Wilson
8.089 ± 0.001	Burdick et al
8.088 ± 0.001	Mallet et al
8.0885 ± 0.0005	Austin
8.088 ± 0.001	Livey et al

TABLE 2

Lattice Parameter Data for the Tetragonal Phase

Conditions	Parameter Å	
10^{-5} mm Hg	a = 3.525 ± 0.001	in equilibrium with U_2C_3
	c = 6.00 ± 0.01	
UO_2 present	a = 3.517	
	c = 5.98	

the work of Ferguson[4] who prepared a sample of "UC_2" for X-ray lattice expansion measurements. The prepared sample was found to consist of 50% $UC_{1.82}$ and 50% U_2C_3, the parameter of the $UC_{1.82}$ being

$$a = 3.5266 \pm 0.0005\text{Å}$$

$$c = 6.0023$$

These observations are providing a good understanding of dicarbide - sesquicarbide stability in terms of impurity content and are being extended to the systems containing the thorium carbides. Data[5] has also been obtained recently on the uranium-plutonium-carbon systems in the region between 50 and 60^a/o carbon i.e. on compositions between the monocarbide and sesquicarbide by metallographic and X-ray diffraction techniques. It is relivant to summarize the results of these studies since at some stage plutonium is likely to be considered as the fissile constituent in these highly enriched systems. Thus it has been found that:-

(a) Uranium-plutonium sesquicarbides form a complete range of solid solutions below 1600°C.

(b) Between the monocarbide and sesquicarbide compositions there is a two phase region in which plutonium will tend to concentrate in the sesquicarbide phase when the carbon concentration is below 55^a/o.

(c) Equilibrium is reached rapidly when the carbon content is below 50^a/o but extremely slowly above this concentration.

(d) The addition of plutonium stabilises the M_2C_3 phase in the ternary system.

3. Properties

Most attention has been paid to the thermal conductivity of the monocarbide

as a function of the carbon content, together with the determination of the effects of plutonium.

Room temperature thermal conductivity measurements[6] on specimens prepared by arc melting and hot pressing are accurate to ± 0.0015 cals/sec/°C/cm^2 and are given in Tables 3 and 4 and in Fig. 3.

(a) U-C The thermal conductivities of arc-cast specimens of U-C show that at carbon content below 4.8 at.% there is little change in thermal conductivity. This may be attributed to the similarity of the thermal conductivity of U-metal (0.0586 cals/sec/°C/cm^2/cm) to that of the carbide.

The effect of increase of carbon content on thermal conductivity is not yet completely clear. The thermal conductivity of UC_2 (and probably also of U_2C_3) is much lower than that of UC and thus a fall in conductivity with increase in carbon content is to be expected. There is some indication of this trend in both the arc cast specimens and in the hot pressed specimens.

When comparing the effect of method of fabrication on thermal conductivity it is necessary to consider the following points:-

(1) The second phase in the arc cast specimens in UC_2 whereas in the hot pressed specimens it is U_2C_3.

(2) The thermal conductivity values for the hot pressed specimens have not been corrected to theoretical density, and are therefore quite low relative to those for the arc cast specimens.

The measurement of thermal conductivity in the Schroder type apparatus appears to be particularly sensitive to the nature of the heat transfer surfaces and the manner in which this is affected by the average value of the porosity concentration and by the distribution of porosity. An example of the effect of porosity distribution is clearly seen if the two specimens of reaction sintered U-C containing 4.63 and 4.71 wt.% C are compared.

TABLE 3

The Thermal Conductivity of some Uranium Carbides

Method of Fabrication	Carbon content (wt.%)	Oxygen content (wt.%)	Density (g/cm^3)	Thermal Conductivity ($Cal/sec/^oC/cm^2/cm$)
Arc melted and cast	4.40	-	13.87	0.0522
	4.77	-	13.64	0.0516
	5.06	-	13.40	0.0576
	5.13	-	13.19	0.0464
	UC_2	-	11.51	0.0242
Hot pressed	4.91	-	13.08	0.0411
	5.05	0.19	12.49	0.0289
	5.06	0.24	12.62	0.0365
	4.85	0.17	12.35	0.0416
Reaction sintered	-	-	12.35	0.0351
	4.63	0.27	11.88	0.0328
	4.71	0.26	11.62	0.0403

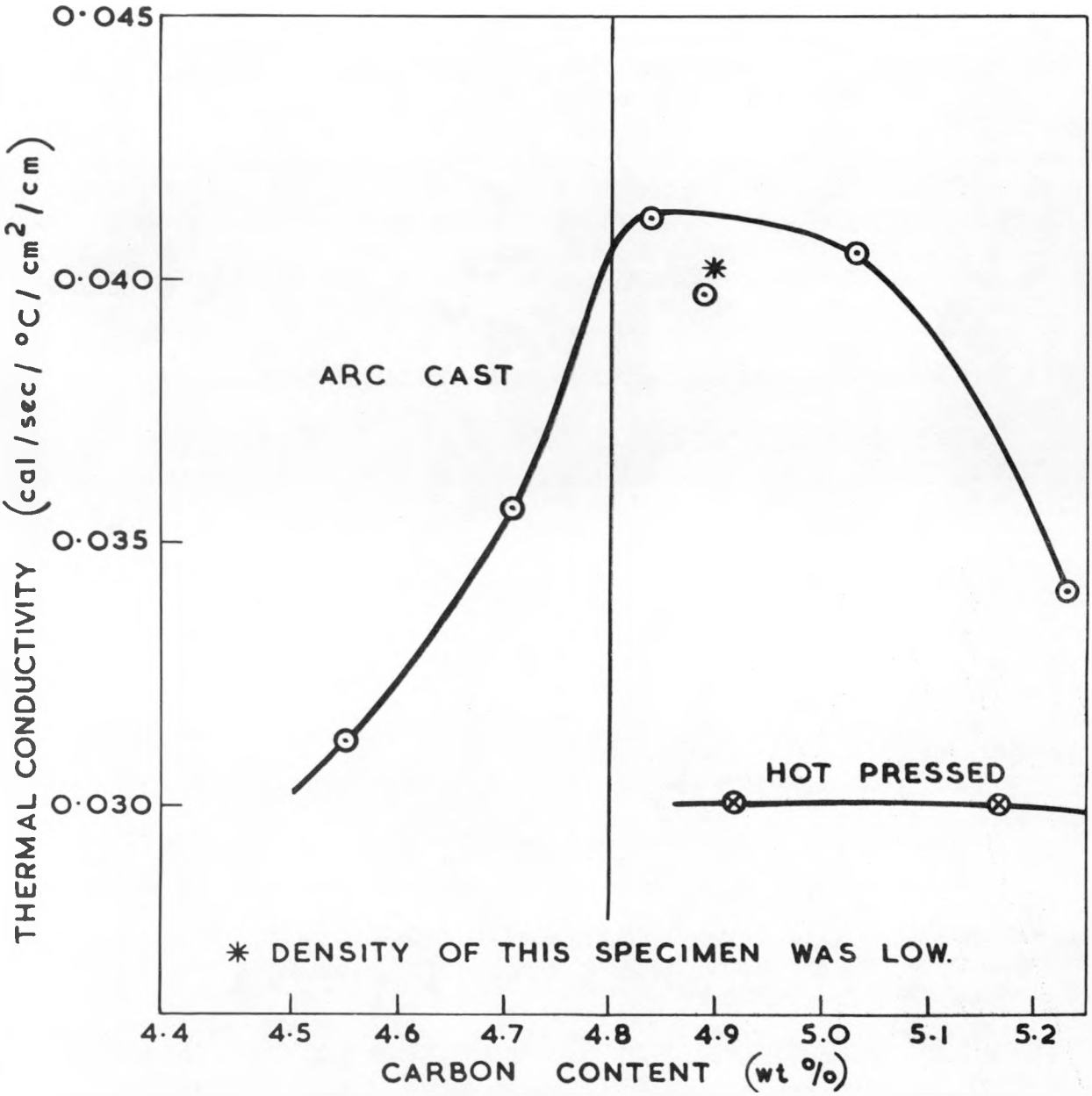

FIG. 3. THERMAL CONDUCTIVITY OF $(U_{85}Pu_{15})$ - C.

The carbon contents of these pieces are very similar and below 4.8 wt.% so that the small differences in uranium content will have little effect on conductivity. The oxygen contents and densities are also very similar. However these specimens have very different thermal conductivities namely 0.0328 and 0.0403 cals/sec/^{o}C/cm^{2}/cm. Careful examination of these specimens has shown that the specimen having the highest thermal conductivity also had the greatest ratio of internal to surface porosity. The low thermal conductivity specimen, on the other hand, had a much greater proportion of porosity at the surface.

Generally speaking the nature of the distribution of porosity in hot pressed specimens is similar from specimen to specimen. When the appropriate correction factors, which are certainly greater than those allowed by the Loeb relationship, are applied to the present results, it should be possible to discuss with some confidence the effects due to different manufacturing procedures.

(b) UPu-C The shape of the conductivity - carbon content plot in Fig. 3 shows that when the carbon content is below 4.8 wt.% the thermal conductivity is extremely sensitive to variations in carbon content. The rapid fall in conductivity as the concentration of free metal increases is believed to be due to the low conductivity of the UPu alloy which may be inferred from the low thermal conductivity of plutonium, 0.0098/cals/sec/^{o}C/cm^{2}/cm.

Over the composition range 4.8 - 5.0 wt.% C there appears to be very little variation of thermal conductivity. The low value of 0.0397 cals/sec/^{o}C/cm^{2}/cm is associated with an abnormally low density of 13.11 g/cm^{3}. Thus it may safely be concluded that over this composition range the thermal conductivity of $(U_{85}Pu_{15})C$ is 0.041 $\pm$ 0.0015 cals/sec/^{o}C/cm^{2}/cm.

The thermal conductivity values of the hot pressed specimens are approximately 75% of the values of the arc-cast material. However, the

hot-pressed material is generally of lower density and when the appropriate correction is applied these thermal conductivity values are increased. There is an additional reason for the lower densities of the hot pressed specimens. Metallographic examination of the hot pressed (UPu)C specimen having the lowest carbon content revealed the presence of ~ 30% of an M_2C_3 phase. This is in keeping with other observations which indicate that the effect of dissolved oxygen on microstructures is roughly equivalent to that of an equal volume of carbon. Thus the "equivalent total carbon" content of this specimen is 5.49 wt.%. It is clear that the thermal conductivity values for all of the hot pressed specimens, with one exception, are very similar and it is probable that this may result from the fact that the "equivalent carbon" contents are also very similar. A slight extrapolation of the curve for the arc cast materials indicates that there may be very little difference between the thermal conductivities of materials made by hot pressing or arc casting.

Although the range of oxygen contents found in the sample tested is quite wide it was not possible to make determinations on all samples. The accuracy of the measurements that were made is somewhat doubtful in view of the difficulties involved in preventing oxidation during the preparation of an analysis sample. The greatest range of oxygen contents in any series was that in the hot pressed (UPu)-C samples. Here, the dissolution of 0.57 wt.% O_2 has given a structure comparable to that of 5.49 wt.%C and the thermal conductivity is almost equal to that of a specimen of similar density and containing 5.52 wt.%C + 0.17 wt. % O_2 and a little higher than that of a specimen containing 5.50 wt. % C + 0.14 wt.% O_2. On the basis of this evidence it appears that even comparatively large oxygen contents do not materially affect the thermal conductivity of (UPu)-C in any other

sense than that they alter the effective C content. In order to confirm this it would be useful to have measurements of an arc-cast specimen of the same carbon content but with a range of oxygen concentrations.

With regard to the effect of plutonium on the thermal conductivity of U-C an assessment of the results from the arc-cast specimens show that a very substantial decrease in the conductivity of carbon-deficient alloys is observed. For compositions close to the stoichiometric one a 15% solution of PuC reduces the conductivity to 70 - 75% of that of UC in both hot pressed and arc-cast specimens. Making appropriate allowances for the accuracy of the value of the conductivity of PuC in Table 4 the decrease is somewhat more than twice that to be expected if there was a linear relationship between conductivity and composition between UC and PuC.

4. Irradiation behaviour of bulk carbides and oxides

As background data for the interpretation of experiments on dispersed oxide and carbide fuels, the irradiation behaviour of bulk materials including the effects of plutonium additions is being investigated at high burn up in the appropriate temperature ranges by Frost and his co-workers.[7] Preliminary data on UO_2, 10% PuO_2-UO_2, and 15% PuC-UC is summarised in Table 5 with special reference to fission gas release.

It will be noted that at high burn up, the gas release from the oxide is somewhat variable. Comparison with previous A.E.R.E. data on UO_2 irradiated to $\sim$ 2% burn up in the same range of centre temperatures

TABLE 4

The Thermal Conductivity of Pu-C and $(U_{85}Pu_{15})$-C

Method of Fabrication	Carbon content (wt.%)	Oxygen content (wt.%)	Density (g/cm^3)	Thermal conductivity ($Cal/sec/^oC/cm^2/cm$)
Arc melted and cast ($U_{85}Pu_{15}$-C)	4.55	0.042	13.67	0.0311
	4.71	0.049	13.55	0.0357
	4.84	-	13.24	0.0411
	4.88	-	13.12	0.0397
	5.03	0.135	13.30	0.0405
	5.23	0.19	13.23	0.0350
Hot pressed ($U_{85}Pu_{15}$-C)	4.92	0.57	13.21	0.0301
	5.17	-	13.04	0.0301
	5.50	0.14	13.08	0.0265
	5.50	-	13.21	0.0227
	5.52	0.17	13.04	0.0296
Hot pressed Pu_2C_3	7.03	-	12.32	0.0143
	-	-	12.08	0.0133

TABLE 5

High burn-up Oxide and Carbide Irradiation Results

Specimen number	Fuel composition	Burn-up MWD/Te fuel**	Estimated centre temp. °C (Ts=600°C)	Volume of Xe produced cm^3 ##	Total gas collected cm^3	Volume of Xe cm^3	% gas release	Ratio $\frac{Xe}{Kr}$
1	10V UO_2	9,000	880	2.93	$3.62.10^{-2}$	$3.62.10^{-4}$	* Not accurate	
4	"	12,000	1015	4.16	$8.07.10^{-2}$	$1.54.10^{-2}$	0.37	7.4
5	"	18,700	1275	5.53	0.409	0.31	5.53	6.3
7	Duplex UO_2	25,300	1030	0.935	$2.45.10^{-2}$	$9.55.10^{-4}$	0.10	(2.3)
8	"	44,200	1480	2.59	1.01	0.45	17	3.45
9	"	36,600	1250	2.25	$2.1.10^{-2}$	$1.26.10^{-5}$	≠ Kr not measurable	
10	"	53.300	1740	3.16	0.17	0.15	4.75	13
11	"	44,200	1530	2.64	$1.08.10^{-2}$	$4.3.10^{-3}$	-	6
18	"	44,200	1530	2.64	2.07	1.77	66	7.2
13	(15%PuC-UC) Mixed Carbide	19,000	600	1.28	$4.64.10^{-3}$	$3.4.10^{-4}$	$2.65.10^{-2}$	-
14	"	22,800	1020	1.13	$1.0.10^{-2}$	$1.32.10^{-5}$	1.1 & 10^{-3}	-
15	(10%PuO_2-UO_2) Mixed Oxide	12,700	1170	4.72	$2.7.10^{-2}$	$6.8.10^{-3}$	0.144	22.5
16	"	12,700	1170	4.72	0.25	Not available***		-
17	"	14,900	1050	5.39	0.457	0.278	5.2	23.5

*Argon leak from box during sampling.
**Design figures, precise figures await burn-up analysis.
***Hydrocarbon content too high for accurate analysis.

≠ Large air leak between sampling and analysis.
Calculated assuming that the $\frac{Xe}{Kr}$ ratios are respectively
U^{235}: 5.64/1 Pu^{239}: 18.8/1

where the gas release remains reasonably low ($\sim$ 2%) suggests that discontinuous processes leading to higher and more variable release are setting in between 2% and the 5% burn up in the present experiments. So far also no significant effects have been found when plutonium additions have been made up to the 10% level in the oxide case.

The monocarbide and mixed carbide (15% PuC) irradiation experiments have so far been carried out up to $\sim$ 2% burn up at centre temperatures up to $\sim$ 1100°C. No significant gas release has been found under these conditions and the present evidence would indicate that in this burn up range the diffusion coefficients for the rare gases are appreciably lower than the corresponding coefficients in bulk oxide. These experiments are being extended further both in terms of burn up and temperature and a programme of unrestrained swelling experiments on the bulk monocarbides is also under way. The higher carbides are also being included in these investigations.

5. Dispersed carbide fuels

The early Harwell work on dispersed carbide fuels for H.T.R. applications was concerned with the incorporation of uranium and thorium metal powders into finely ground graphite followed by cold pressing to obtain strong inserts. Heat treatment could then be carried out to form either the monocarbide or dicarbide dispersed in graphite. In the first experiments, small fuel sleeves were irradiated in graphite cans at 600°C. Two main types of fuel were investigated, the fuel loading being identical in both cases, viz. 50W/o of uranium (93% U_{235}).

(a) cold compacted uranium metal powder (20-30 microns diameter) and graphite, heat treated at 800°C to give the monocarbide dispersion.

(b) cold compacted uranium metal and graphite heat treated at 1450°C to give the dicarbide dispersion.

Irradiation was carried out to 1.7×10^{19} and 3.4×10^{19} fissions per c.c. of total fuel respectively. After a burn up of 1.7×10^{19} (corresponding to 2.4×10^{20} fissions per c.c. of uranium) small volume changes were noted (+0.25% to -0.7%) and in all cases were the resultant of increases in length and decreases in diameter. The xenon released into the can was approximately 10%. After irradiation to the higher burn up, the volume decrease was approximately 5% again mainly due to a decrease in diameter. Similar xenon release values were obtained.

A further series of irradiations were carried out on uranium/thorium/graphite sleeves of larger size, pre-heat treated to form the monocarbide dispersion and irradiated in fine grained graphite or impregnated fine grained graphite cans at mean temperatures of 900-1000°C to 2×10^{19} fissions per c.c. of total fuel. The heavy metal content was maintained at 18W/o in these experiments, the uranium being varied between 3.1 and 6.3W/o to give the required heat ratings. The main results from these series were that

(a) small volume changes occur, and there is a correlation between the volume change and the bulk density of the fuel compact. Thus, the more porous compacts were more stable dimensionally under irradiation.

(b) Fission gas release to the extent of about 10% occurs with this type of fuel under these irradiation conditions.

(c) The fuel rings showed little surface damage and were quite strong after irradiation.

Because of the fission gas release from this type of fuel, attention has been given (as in many other laboratories) to the coated particle concept and the fuel

compacts being considered at present consist of kernels of uranium and thorium dicarbide in solid solution coated with an impervious material to form nodules (coated particle), these being incorporated in a graphite matrix to form the compact. So far, there are essentially two types of carbon coated particles which have offered success as a retaining medium for gaseous fission products. The first is based on a pyrolytic coating of amorphous, layered carbon laid down at temperatures of about 1400°C in a fluidised bed process. The particles have a smooth exterior with an "onion skin" type of coating. The second type produced at higher temperatures (1700°C or above) consists of a columnar graphite coating with a "raspberry" appearance. Both types of coating are applied to spherical fuel particles of the dicarbide with a degree of porosity arbitrarily chosen in the 20-30% range. In certain cases, an oxide layer may be formed between the sphere and the coating but there is little information as to the effects of this intermediate layer. It is necessary that the fuel be stable thermodynamically in the presence of the coating at high temperatures and the practical way so far has been to use the highest carbide and allow for any instability (such as volume expansion on transformation to the sesquicarbides) by providing porosity in the kernel. Some degree of porosity is essential in any case because of the volume expansion at high burn up. As indicated previously more precise information is becoming available on the phase equilibria in the U-Th-C system at high temperatures and the effects of oxygen and nitrogen impurities in stabilising the dicarbides particularly.

Stability under thermal cycling conditions is dependent both on the phase stability of the dicarbide phase over the temperature range and the differential thermal expansion of the kernel and carbon coating. Pyrolytic carbon coatings have a very much lower expansion coefficient in the direction parallel to the surface of the kernel than that of the dicarbide and hence thermally induced stresses can be obtained leading to cracking of the coating. Two ways of overcoming

this are, firstly, to deposit the coating at a higher temperature than is likely to be realised in reactor operation and secondly to make the kernel sufficiently porous to take up part of the expansion of the dicarbide. Precise information on these effects is not available but there is some evidence that slow thermal cycling does not affect the stability of good quality coated particles.

Many experiments have been carried out by Bromley in the Chemical Engineering Division[8] on the diffusion of fission gases and fission products in graphite and carbon systems and the results can be generally classified into two groups depending on the diffusion rate at or above 1500°C. In the first group where diffusion is comparatively fast are the alkali and alkaline earth isotopes as well as some of the heavy rare earths; in the second group where the diffusion rate is much slower (by a factor of 100 in pyrolytic carbon) are the rare gases Kr and Xe, iodine and the trivalent metals. A similar distinction can be drawn in the case of coated particles from thermal annealing experiments carried out at Harwell in the Chemistry Division by Flowers and co-workers,[9] on the Xe^{133}, Ba^{140}, I^{131} and Kr^{95} release from lightly irradiated 3M pyrocarbon coated (U, Th)U_2 particles. After raising slowly to 1500°C during 6 hours and maintaining at 1500°C for two weeks, the fraction released together with the calculated "permeability coefficient" for the fission product are shown in Table 6.

These experiments indicate that pyrocarbon coated particles can effectively retain fission gases although the behaviour at high burn up with the associated stresses and cracking probability is being further investigated. The diffusion of barium, however, is much faster and extrapolation of these results to practical cases indicates appreciable γ active release from the present type of coated particles. It may be that other types of coating such as metallic carbides may be more effective than pyrocarbon. Thus, Long, Findlay and Laing[10] in their work on diffusion of xenon, barium, caesium and strongium from uranium monocarbide obtained coefficients of $\sim 10^{-16}$ cm^2/sec for the metals at 1400°C; these results indicate

a much slower movement of Ba, Cs and Zr in UC grains than in graphite.

6. Dispersed Oxide Fuels

Dispersed systems based on oxides such as UO_2-ThO_2 in BeO, are receiving more consideration for compact high temperature reactors; there are major differences with carbide dispersions and interesting comparisons may be drawn as follows:-

a) The data presently available on phase relations at high temperatures is extensive and sufficient to give confidence that such fuels approach the ideal case prior to irradiation. The BeO-UO_2-ThO_2 system is a two phase system consisting of BeO and UO_2-ThO_2 phases only at the temperatures of interest and it is relatively easy to obtain dense microstructures of UO_2-ThO_2 particles in a BeO matrix.

b) The need for coating individual fuel kernels with impervious oxides at present appears less imperative than in the corresponding graphite/carbide case provided that dense oxide matrices prove to be mechanically stable under irradiation.

c) There is an obvious need for a great deal more experimental data on the irradiation stability of dispersed oxide fuels. Nevertheless present evidence indicates that oxide based fuels could be developed which would have satisfactory dimensional stability at surface temperatures in the region of 1000°C to a burn up of $\sim 10^{21}$ fissions per c.c. of fuel.

d) Temperature gradients both within the fuel and the structural component of the fuel assembly will engender thermal stresses which could cause cracking. Analysis of these problems in terms of elastic behaviour and the mechanical properties indicate that fuel sections would need to be small to eliminate the possibility of cracking. Whether or not stress relaxation at high temperatures is aided or impeded under irradiation is an important topic needing investigation.

TABLE 6

Fission Product Release from Coated Particles

(Flowers, Gardner and Hyman)

Isotope	Fraction Released	t (secs)	P (cm^2/sec)
Xe^{133}	1.35×10^{-3}	1.5×10^{-6}	2.5×10^{-12}
Ba^{140}	0.79 ± 0.16	"	4×10^{-11}
I^{131}	~ 0.05	"	-
Zr^{95}	$< 10^{-5}$	"	-

e) The effects of irradiation on BeO either as the structural component or as the moderator in this type of system are less well defined than in the case of graphite, and the processes taking place are only just becoming understood.

In more detail, matrices of BeO can be prepared by sintering or hot pressing techniques to give permeability coefficients towards gases in the region of 10^{-10} cm^2/sec. So far as sintering is concerned, Livey and Hey[11] have recently carried out detailed studies on powders derived from the hydroxide, sulphate and oxalate, and have correlated the sintering and permeability changes in terms of the initial surface area and impurity contents of the powders. One important finding is that in certain powders derived from the hydroxide, reduction in surface area occurs quite rapidly at medium temperatures causing internal shrinkage and an increase in the permeability of the compact during the sintering cycle. Such effects are normally not found in other active powders and the characteristics necessary for achieving very high sintered densities on BeO are now well defined. Studies of the diffusion of fission product release from dispersed fuels based on such matrices have so far been confined to Xe^{133}, by both the "in pile" technique[12] and the "out of pile" technique.[13] The results obtained by Stubbs and Webster using the latter technique are given in Table 7.

Data on the Al_2O_3 based fuel developed for the Zenith high temperature reactor at Winfrith are included in this table for comparison with the $BeO-UO_2$ fuel. It will be seen that low release rates are obtained for the $BeO-UO_2$ fuel which are in the same range as the values quoted previously for coated carbide particles. More attention is now being given to the question of fission product release from this type of fuel.

In BeO itself, the irradiation induced growth of polycrystalline material arising from anisotropy, the way it is influenced by the temperature of irradiation and its effect on grain boundary cracking and "powdering" are of vital importance. The effects of irradiation on properties have been summarised by Clarke[14], the

TABLE 7. OUT-OF-PILE MEASUREMENTS OF Xe^{133} EMISSION FROM LIGHTLY IRRADIATED

Sample No.	P1	P2	P3	W99	W118	W130
Manufacture Code No.	IDFP-1	IDFP-2	IDFP-3	IDFS-1	IDFS-3/1	IDFS-6/1
Composition (by weight)	BeO UO_2	BeO UO_2	BeO UO_2	BeO UO_2	BeO UO_2	BeO UO_2
Molecular Ratio	4,000/1	4,000/1	4,000/1	80/1	11/1	26.8/1
UO_2 particle size (u)	< 50	< 50	< 50	150-180	100-150	150
Actual density (g/cm^3)						
% Theoretical density	92	92	92	98.8	98.5	93.3
Physical form	compacted pellet	compacted pellet	compacted pellet	compacted pellet	compacted pellet	compacted pellet
Weight of U^{235} (mg)	~ 4	~ 4	~ 4	1.0	3.6	3.7
Fractional ^{133}Xe)800°C	5.8×10^{-10}	2.4×10^{-10}	7.1×10^{-10}	7.0×10^{-9}	2.6×10^{-10}	8.2×10^{-10}
Release (sec^{-1}) 1000°C	2.0×10^{-9}	5.2×10^{-10}	1.0×10^{-9}			
after 24 hrs at 1200°C	3.6×10^{-9}			3.5×10^{-8}	1.4×10^{-10}	
Fractional ^{133}Xe) 800°C					3.5×10^{-10}	9.3×10^{-10}
Release (sec^{-1}))1000°C						
after 48 hrs at)1200°C					3.5×10^{-10}	
Effect of oxygen	not tested	not tested	not tested	not tested	not tested	not tested
Magnitude of 'burst' on heating	moderate	moderate	moderate	moderate	moderate	small
Remarks	*early expt.	*early expt.	*early expt.		coated with BeO skin (20μ)	coated with BeO skin (36 thou)

*Results of A. R. Palmer attached from Australian Atomic Energy Commission

SPECIMENS OF OXIDE DISPERSION TYPE FUELS (STUBBS AND WEBSTER)

W140	W104	W119	W126	W128	W48	W121	W123
IDFS-7/1	IDFS-2/1	IDFS-2/2	IDFS-4/1	IDFS-5/1		S3	
BeO	MgO 6.6%	MgO 6.6%	MgO 6.7%	ThO_2 37%	Al_2O_3 60.0%	Al_2O_3 52.9	Al_2O_3 53.8
UO_2	Al_2O_3 37.8%	Al_2O_3 37.8%	Al_2O_3 42.0%	Al_2O_3 18%	UO_2 30.9%	U_3O_8 39.2	UO_2 38.2
	SiO_2 50.0%	SiO_2 50.0%	SiO_2 55.7%	SiO_2 37%	SiO_2 7.1%	SiO_2 6.2	SiO_2 6.3
	UO_2 5.6%	UO_2 5.6%	UO_2 4.8%	UO_2 4%	MgO 1.3%	MgO 1.2	MgO 1.2
				MgO 4%	CaO 0.7%	CaO 0.6	CaO 0.6
10/1							
100-150							
	2.6	2.6	2.73	3.67			
97.0					99.9	99.5	99.5
compacted pellet	glass	glass	glass	glass	compacted pellet	compacted pellet	compacted pellet
2.9	0.86	0.91	0.67	1.1	3.8	3.0	621
	$\sim 2 \times 10^{-9}$	4.2×10^{-10}			1.38×10^{-9}	3.3×10^{-8}	2.2×10^{-10}
	$\sim 2 \times 10^{-9}$	3.5×10^{-10}	2.7×10^{-9}			8.3×10^{-8}	(at 500°C)
			3.2×10^{-9}				
		2.3×10^{-10}				1.9×10^{-8}	4.7×10^{-9}
		2.1×10^{-10}	2.7×10^{-9}			5.4×10^{-8}	(after full oxidation (at 500°C))
			1.4×10^{-9}				
	not tested	not tested	not tested	not tested	appreciable	appreciable	small
	θ small	θ small	θ small		moderate	marked	moderate
	θDe-vitrification would probably occur above 800°C			Experiment failed	early 'Zenith' pellet	Sandwich (Zenith type) U_3O_8 in centre	Actual 'Zenith' pellet (93V UO_2)

following being the main points.

(a) At temperatures up to 150°C, the macroscopic growth follows that calculated from the lattice parameter changes ($\frac{\Delta C}{C}$ being typically 3 to 5 $\frac{\Delta a}{a}$).

(b) In the dose range 10^{20} - 10^{21} nvt. (> 1 MeV) the theoretical growth begins to saturate and diverges from the macroscopic growth.

(c) Elastic moduli, thermal conductivity and crushing strength all begin to decrease appreciably in the dose range 10^{19} - 10^{20} nvt.

(d) At higher irradiation temperatures comparatively little work has been done, but the changes are considerably less. By increasing the irradiation temperature from 100° to 300°C the changes in properties at a given dose are reduced by about a factor of 3.

There is an indication that the nature of the damage is different at higher temperatures. At high doses agglomerates of defects are formed but the mechanism responsible for their formation is at present not clear. The suggestion that at high temperatures, irradiation may inhibit the growth of each agglomerate is important since the point defect concentration must be limited by the mutual interaction of point defects, thus leading to saturation. However, the relative thermal stability of defect agglomerates allows a mechanism by which irradiation damage effects can continue to accrue long after the point defect concentration has achieved saturation. If, however, the agglomerates themselves are broken up by irradiation at high temperatures then a much lower saturation of damage might occur. Annealing mechanisms of damage are complex but there is a strong indication of a dose effect. Thus up to 10^{19} nvt., damage is annealed out at 200°C whereas at $\sim 10^{20}$ nvt. (or above), temperatures in the region of 1000°C are needed to produce annealing of a comparable degree.

The weight of evidence suggests that "powdering" on irradiation at 100°C is a function of the irradiation growth at least up to doses of 5 x 10^{20} nvt., the actual

dose depending also on the method of fabrication. With high bulk density material it occurs at $\sim 10^{20}$ nvt. whereas low bulk density ($\sim$ 2.7 gm/cc) can be irradiated at 100°C to $> 10^{21}$ nvt. without cracking or powdering. There is also evidence of a favourable effect of temperature so far as this phenonemon is concerned but at higher temperatures the processes are more complex and require further investigation.

7. Conclusions

The following conclusions can be drawn from these recent results.

a) The phase studies have shown that hypostoichiometric UC exists as a solid solution of uranium in uranium monocarbide depending on the heat treatment conditions.

b) The studies of the effects of oxygen and nitrogen on the relative stabilities of the sesquicarbide and dicarbide have cleared up many confusing observations and it is now possible to indicate which is the stable phase under the appropriate conditions. Again, this is important practically since thermodynamic (and volume) stability of the fissile phase is essential to the successful irradiation behaviour of dispersed fuels based on carbides.

c) The approach of studying the irradiation behaviour of the bulk fuels (in so far as fission gas and fission product release characteristics are concerned) is beginning to indicate the burn up ranges in which discontinuous phenomena are likely to occur.

d) Broad indications are being obtained of the relative diffusion of gases and other fission products in the coated particle case and of possible solutions to some of the problems.

e) With oxides, the difficulties do not appear to lie with the dispersed fuel although much more detailed work at high burn up is required. The effects of

irradiation on BeO as the structural material are more significant and together with the behaviour under thermal stresses represent the important problems in this field.

8. References

1. J. Williams and co-workers, J. Nuc. Matls., 1961
2. S. N. Buckley, A.E.R.E.-R.3872, November, 1961
3. D. T. Livey, J. Henney and N. A. Hill. Paper to I.A.E.A. Panel on a review of carbide data in the light of recent phase studies
4. I. F. Ferguson et alia A.E.R.E.-M.819
5. J. T. Dalton, Metallurgy Division, A.E.R.E. - Unpublished results
6. G. A. Keig and L. E. Russell, Metallurgy Division, A.E.R.E. - Unpublished results
7. B. R. T. Frost and co-workers, Metallurgy Division, A.E.R.E. - Unpublished results
8. J. Bromley. Chemical Engineering Division, A.E.R.E. - Unpublished results
9. Flowers, Gardner and Hyman, Chemistry Division, A.E.R.E. - Unpublished results
10. Long, Findlay and Laing, Chemistry Division, A.E.R.E. - Contribution to Libby/ Cockcroft meeting on UO_2 and UC, A.E.R.E., October 1962
11. D. T. Livey and A. W. Hey, A.E.R.E.-R.3870, 1962
12. A. R. Palmer, A.E.R.E.-R.4062, 1962
13. F. J. Stubbs. "Diffusion Studies in Dispersed Fuels." Ceramics in Nuclear Science - Meeting of the British Ceramic Society at A.E.R.E., November, 1961 - in the press
14. F. J. P. Clarke, A.E.R.E.-R.3971, 1962

DISCUSSION

Question, W. P. Chernock (CE): "In the high burnup irradiations of UO_2, is the quoted temperature at the beginning or the end of the irradiation?"

Reply, P. Murray (UKAEA): "This is the calculated temperature at the beginning of the irradiation."

Question, W. P. Chernock (CE): "Do you think this temperature is representative of when the fission gas release was measured?"

Reply, P. Murray (UKAEA): "We feel it is below that at which structural changes in the UO_2 occur."

Question, C. W. Kuhlman (UNC): "How much nitrogen is required to stabilize the uranium sesquicarbide?"

Reply, P. Murray (UKAEA): "0.2 per cent."

THE PREPARATION OF GRAPHITE-MATRIX FUEL COMPACTS CONTAINING COATED CARBIDE PARTICLES

By D. W. Savage

Chemical Engineering Division
A.E.R.E., Harwell

INTRODUCTION

The object of the work is to study the preparation of ceramic fuel compacts suitable for use in a high-temperature nuclear reactor where maximum temperatures might be in the region of 1500 C. This paper is restricted to a consideration of coated carbide fuel in a highly graphite matrix.

The choice of coated-particle size and coating thickness depends on a number of factors. To give the coatings a reasonable chance of retaining fission products, the coating thickness must be at least as great as the fission-fragment recoil distance in the coating material. This would automatically ensure protection of the matrix from fission-fragment recoil damage. Having established a minimum coating thickness, the carbide core size is limited from below by the ratio of fuel atoms to carbon atoms in the fuel compact, and by the volume packing of particles which can be achieved - about 58 per cent in a random array. On the other hand, particle core size is limited from above by nuclear physics considerations which govern the allowable flux depression through a particle. These factors indicate that for HTR's such as the DRAGON reactor we could well be restricted to particle core sizes in the range 200 to 500 microns, and also, that we should aim to obtain volume packings in the region of 50 per cent or even higher. Coatings thicker than the minimum may be necessary, especially with the larger core sizes, to give a coating strength sufficient to withstand the pressure of fission gases generated within the particles. It is unlikely that very thick coatings could be employed, on account of their poor stability under thermal cycling and irradiation conditions. In our initial studies we have been using pyrolytic-carbon coatings up to 100 microns in thickness, but we are extending the work to silicon carbide and

other coatings.

The principal requirements of the matrix are high thermal conductivity and reasonable strength, both of which call for a high density of the matrix material. An increase in thermal conductivity for a given dimension is one of the most powerful methods of reducing diffusion in the fuel, as it leads to a reduction in the temperature at the axis of the fuel element.

At the moment, it is not clear what will be the eventual size and shape of an economic design of HTR fuel element suitable for a Civil Power Station reactor. We have adopted a dual approach; the short squat fuel element, to which forming by pressing is applicable, and the type of fuel element which might extend over the whole length of the reactor core, a type suited to extrusion forming. We would hope ultimately to be able to produce a process for a fuel element in which there are at least two barriers to the diffusion of fission products. Coatings on fuel particles might constitute one barrier and either the matrix itself or an outer unfuelled zone of the matrix or other matrix or other material might provide a second line of defense. In any case it seems desirable that the second diffusion product barrier should be integral with the fueled zone; this would make possible the design of an HTR fuel element which eliminates gas gaps, and hence give thermal properties allowing lower fuel temperatures than are envisaged in some present-day HTR experiments.

METHOD OF APPROACH

In considering possible methods of manufacture we have tried to bear in mind economy of manufacture, especially in the number of handling operations involving enriched material, and the applicability of the method to large-scale production.

The approach adopted in Chemical Engineering Division at Harwell has been to use the knowledge and experience of graphite manufacture which has been gained on the Harwell Experimental Graphite Plant. The sequence of operations in graphite manufacture - mixing of grist and binder, forming by extrusion, slow baking and heat treatment - have been followed as closely as possible and modifications made at various stages to prevent damage to the relatively large and fragile coated particles.

Although a high thermal conductivity of the matrix is required, which implies a graphite structure, it was known at the outset that the final heat-treatment temperature might have to be limited to 1800 to 2000 C in order to prevent uranium diffusion into the coatings. The matrix would therefore

be no more graphitic in character than the starting materials, and hence our studies have been limited to graphite grists. In the case of binder materials, owing to this limitation on heat-treatment temperature, there was no apparent reason for using a graphitizable rather than a nongraphitizable binder, and consequently we are considering thermosetting binders such as phenolformaldehyde, furfuryl alcohol, and certain other resins as well as pitch.

It seems likely that an optimum grist size distribution in relation to the coated-particle size and volume packing will exist. We have not explored this point fully yet, but we have learned that a high proportion of the grist, 30 or 40 per cent by weight, should be very fine material with a mean size in the region of 1 micron, and the binder content should be in the region of 20 to 30 per cent by weight.

The requirement in the mixing stage is to produce a good dispersion of the coated particles within the matrix material, and at the same time to ensure that the binder is well distributed over the fine grist particles. In general, a mixing action capable of achieving this second requirement, without the use of excessive solvent for the binder, tended to break the coated particles. Our standard sigma-blade dough mixer used for the hot mixing of pitch and grist, broke coated particles very quickly by trapping them between the mixer blades and the casing, and other mixers capable of handling pastes broke particles in a similar manner. To overcome this problem a two-stage mixing process was developed. In the first stage, the graphite grist and binder were mixed in the sigma-blade dough mixer. The coated particles were then added to the grist/binder mix in a second mixer in the presence of a small amount of solvent for the binder. This mixer had a simple mechanical precessing stirrer which rotated very slowly and had large clearances at the wall. Scraper blades, spring loaded against the sides of the mixer, eliminated dead volume and gave some volume blending. The solvent was subsequently evaporated from the mix before forming.

At the forming stage, the molding pressure for pressing was limited to about 3500 psi. The force necessary to extrude a pitch binder mix containing coated particles at 130 C, namely 4000 to 5000 psi, did not damage the particles. The green extrusions and pressings were packed tightly in coarse coke grist within metal or graphite pots, and baked slowly to 850 C.

SOME RESULTS

The results we have available so far apply to compacts in which a pitch binder was used, with a grist of -120 B.S.S. mesh graphite plus a high percentage of very fine graphite having an average particle size of 1 micron.

Pressings in the form of right cylinders 1-3/4 in. in diameter and about 1 in. long were formed using single-ended pressing and a compaction pressure of 3500 psi. Pressings with up to 50 per cent by volume of coated particles maintained their shape and were crack-free after slow baking to 850 C and heat treatment to 2000 C. However, the matrix density obtained depended on the volume proportion of particles. For low volume loadings of 1 per cent, the final matrix density was about 1.74 g/cm^3, when the volume loading was increased to 30 per cent the matrix density fell to around 1.68 g/cm^3, and for 50 per cent by volume of coated particles the matrix density was only 1.53 g/cm^3.

In the case of 3/4 in.-diameter extrusions, rather higher matrix densities were obtained, but again the matrix density fell as the volume loading of coated particles was increased. The extrusions with up to 30 per cent by volume of coated particles were sound after baking and heat treatment; those with 50 per cent particles were sound but had a poor surface texture. For volume loadings up to 30 per cent a matrix density of 1.78 g/cm^3 was obtained, and with 50 per cent particles the density was 1.75 g/cm^3.

The difference between the densities of pressings and extrusions was mainly due to differences in behavior at the baking stage. In the case of extrusions a shrinkage generally occurred, but pressings tended to expand, especially in the axial direction. To prevent this axial expansion, we are currently looking into methods of supporting pressings during baking in order to constrain the pressings in the lengthwise direction.

Microscopic examination of sections of pressings and extrusions revealed less than 0.1 per cent of broken coatings and a random distribution of coated particles. In locations where broken coatings were found, there appeared to have been direct particle-particle contacts.

The thermal conductivity of pressings containing dummy fuel particles, i.e., carbon balls coated with pyrolytic carbon, was measured at room temperature and at temperatures up to 1000 C. The addition of the dummy fuel particles caused a reduction in the thermal conductivity of the compact. With 50 per cent by volume of particles and a matrix density of 1.5 g/cm^3,

the room-temperature radial thermal conductivity was about 0.08 cal/sec/cm/C, compared with 0.12 cal/sec/cm/C for the matrix material alone. The thermal conductivity at 1000 C was about 75 per cent of the room-temperature value.

CONCLUSIONS

The main conclusion to be drawn from these results is that although we can obtain a high volume packing of 50 per cent by conventional techniques of pressing and extruding, the matrix density of pressings at this high loading is rather low. We feel that this is partly due to the difficulty of preventing expansion occurring at the baking stage. However, the matrix density of the extruded artifacts is more encouraging. The hot-pressing process for producing small-size fuel compacts, which has received attention in the U.S.A., is an alternative approach, and we have begun some hot-pressing work at Harwell.

We are also devoting some attention to methods of coating individual coated particles with a thin layer of binder and grist to give them extra protection during fabrication, and ensure a more uniform spacing of particles in the compact.

ACKNOWLEDGMENT

The author is grateful to Mr. F. Roberts and Dr. K. W. Carley-Macauly for assistance in the preparation of this paper.

* * *

DISCUSSION

Question, W. D. Manly (ORNL): "You stated that you have two sources of fission-product retention in these elements. What is the second?"

Reply, D. W. Savage (UKAEA): "We would hope eventually to be able to produce a fuel element having two consecutive barriers to fission-product diffusion. In the elements described in the paper the graphite matrix was the only barrier in addition to the fuel-particle coatings, but we do not know how effective a barrier it is."

Question, W. D. Manly (ORNL): "Why are you using such a high fuel loading?"

Reply, D. W. Savage (UKAEA): "In order to satisfy the over-all heavy metal-to-carbon atom ratio. The reactor design limits the amount of carbon available in the fuel compacts."

Question, W. H. Duckworth (BMI): "What benefit did you achieve in your high-temperature heat treatment?"

Reply, D. W. Savage (UKAEA): "Our results are not yet available."

CARBON-COATED PARTICLES FOR DISPERSION FUELS

By A. Auriol and C. David
Battelle Memorial Institute, Geneva

G. Kurka and E. LeBoulbin
C.E.A., Department de Metallurgie, Grenoble

SUMMARY

The main results obtained on carbon-coated fuel particles at the C.E.A., France, and at B.M.I., Geneva, under contract with the C.E.A. are presented.

These concern:

(1) The preparation of spheroidal particles of UO_2 coated with pyrolytic carbon.

(2) The properties of the coatings.

(3) The high-temperature behavior of the particles.

1. PREPARATION OF THE PARTICLES

A ceramic-grade UO_2 powder is compacted into pellets 15 to 30 mm in diameter. These pellets are crushed in a mortar, screened to obtain particles of the desired size, and spheroidized in a tumbling barrel. Then the spheroids are disposed in a layer about 2 cm thick and sintered in hydrogen at 1650 C.

The density of the particles is about 10.6 g/cm^3, and their appearance is shown in Figure 1.

2. Deposition Procedure of Pyrolytic Carbon

The particles are carbon coated in a fluidized-bed reactor by cracking at elevated temperature of a gaseous hydrocarbon diluted in an inert gas.

The temperatures of cracking fall in the range from 1100 to 1800 C, and the partial pressures of hydrocarbon in the range from 1/3 to 1/20 atm.

Fig. 1 Spheric UO_2 particles
100 x

The selected hydrocarbons are acetylene at low temperatures (up to 1400 C) and methane at higher temperatures.

Deposition Kinetics

The main factors controlling the deposition speed are the temperature and the partial pressure of hydrocarbon.

(a) Influence of Temperature. Temperature and deposition are not related by a simple law. The effect of temperature is less marked as temperature increases from 1000 to 1400 C (Figure 2) to become nil, with methane, in the range of from 1400 to 1600 C (Table I); above, the deposition speed increases again with temperature.

(b) Influence of Partial Pressure. At 1600 C, in the case of methane, deposition speed is nearly proportional to partial pressure (Figure 3). The results obtained with C_2H_2 at 1200 C show that this law is no longer valid (Table II), but the results did not allow, after correction for depletion of the reactants, a definite relation to be formulated.

II. PROPERTIES OF THE PYROLYTIC CARBON COATING

1. Microstructure

The appearance of coatings deposited below 1400 C at partial pressures greater than 0.05 atm on particles 150 to 400 microns in diameter is shown in Figures 4 and 5. The coating is compact without any cracks; it does not present any apparent microstructure under polarized light, but successive layers are often observed. At higher temperatures this same type of microstructure is observed at high partial pressure (Figure 6), but at low rates of deposition there appears a "conic regenerated" type of structure as shown in Figure 7. At 1600 C the transition between the two types takes place at 0.2 to 0.33 atm of CH_4 on particles 400 microns in diameter (Figures 6 to 9), but it is strongly dependent on the size of the particles.

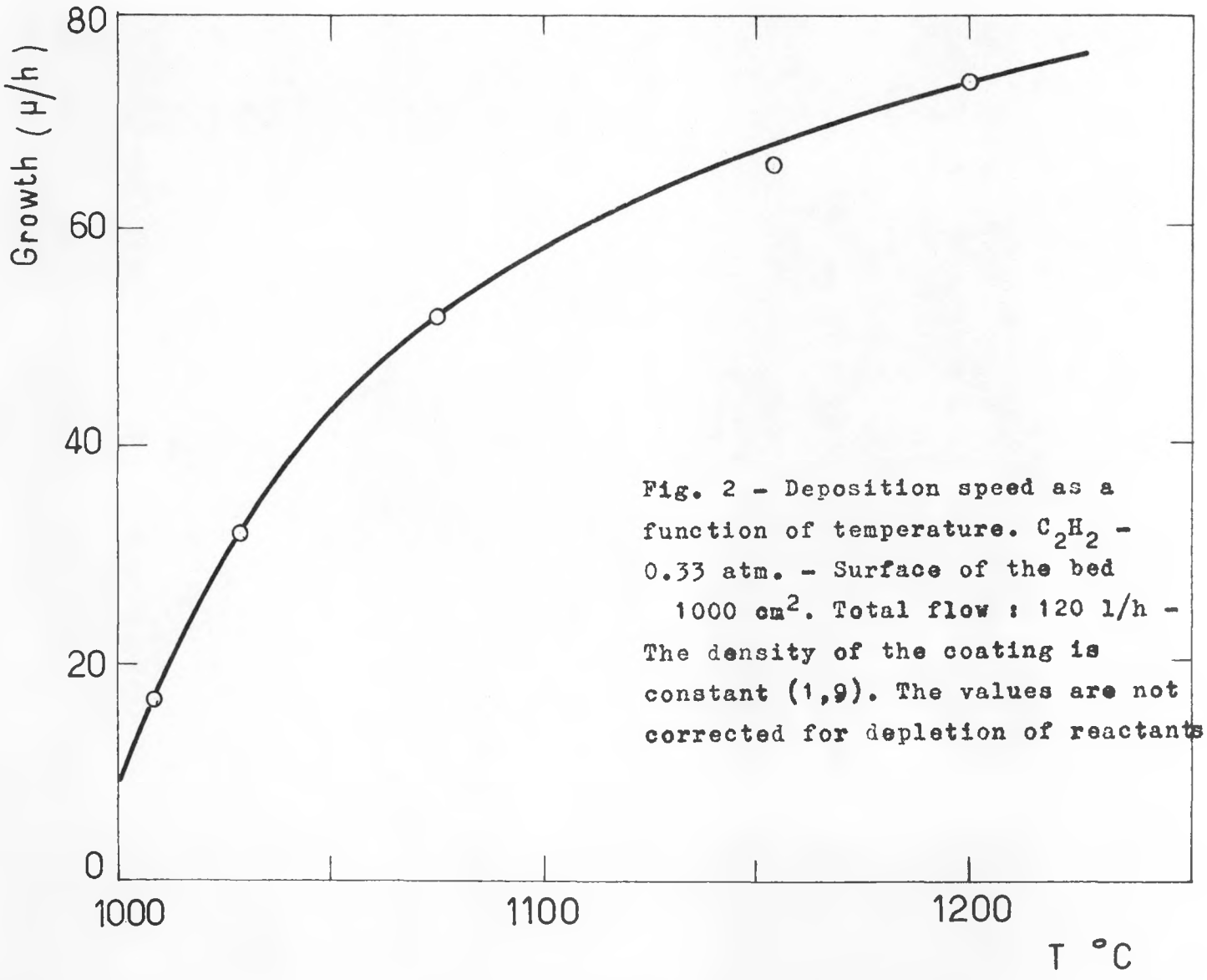

Fig. 2 - Deposition speed as a function of temperature. C_2H_2 - 0.33 atm. - Surface of the bed 1000 cm^2. Total flow : 120 l/h - The density of the coating is constant (1,9). The values are not corrected for depletion of reactants

Table I

Temperature, C	Weight Deposited, g/hr
1400	2.5
1500	2.5
1600	2.7

Conditions:
CH_4 = 0.07 atm
Surface of the bed = ~800 cm^2
Total flow = 160 liters/hr.

Table II

Partial Pressure, atm	Total Flow, liters/hr	Surface of the Bed, cm^2	Deposition Growth, μ/hr
0.05	240	1000	9
0.1	330	1500	16.5
0.17	250	1500	22.5
0.2	120	2750	31
0.33	120	2000	74

Conditions:
C_2H_2 at 1200 C.

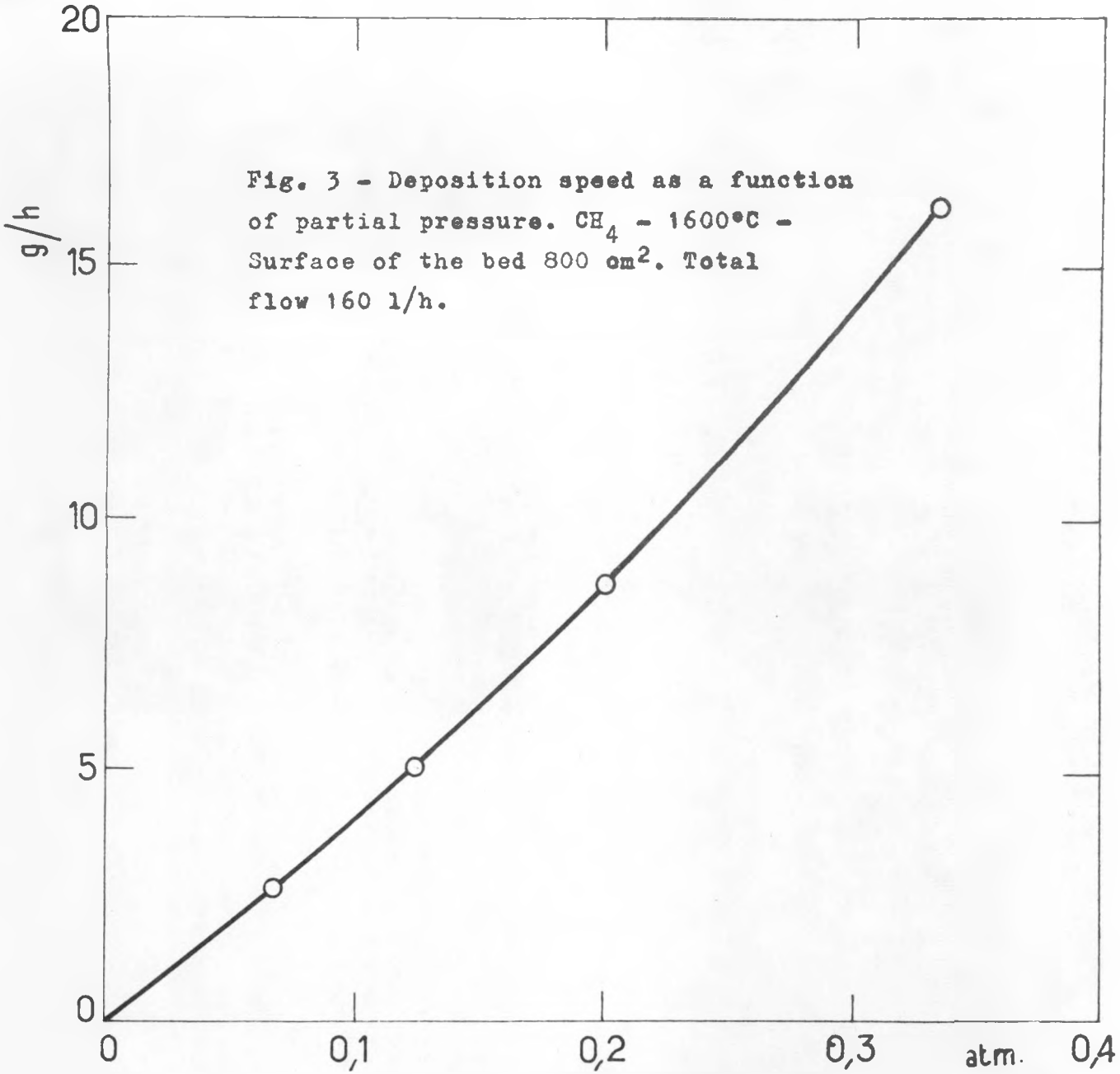

Fig. 3 - Deposition speed as a function of partial pressure. CH_4 - 1600°C - Surface of the bed 800 cm^2. Total flow 160 l/h.

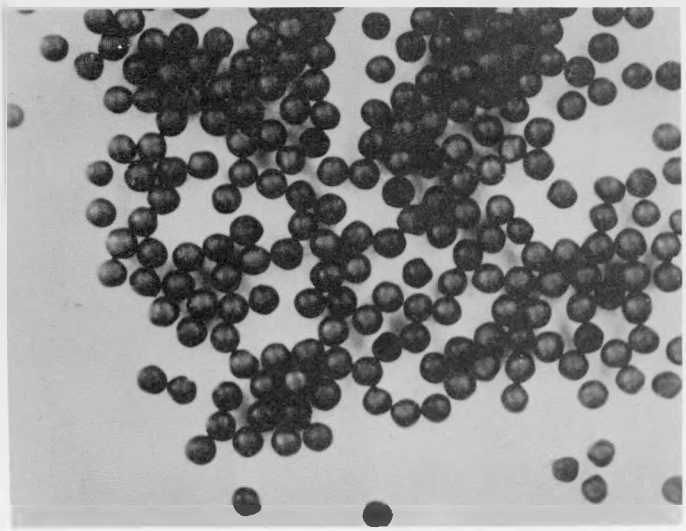

Fig. 4
Carbon coated UO_2 particles
15 ×

Fig. 5
UO_2 particles coated at 1200°C - 0.33 atm. of C_2H_2
200 ×

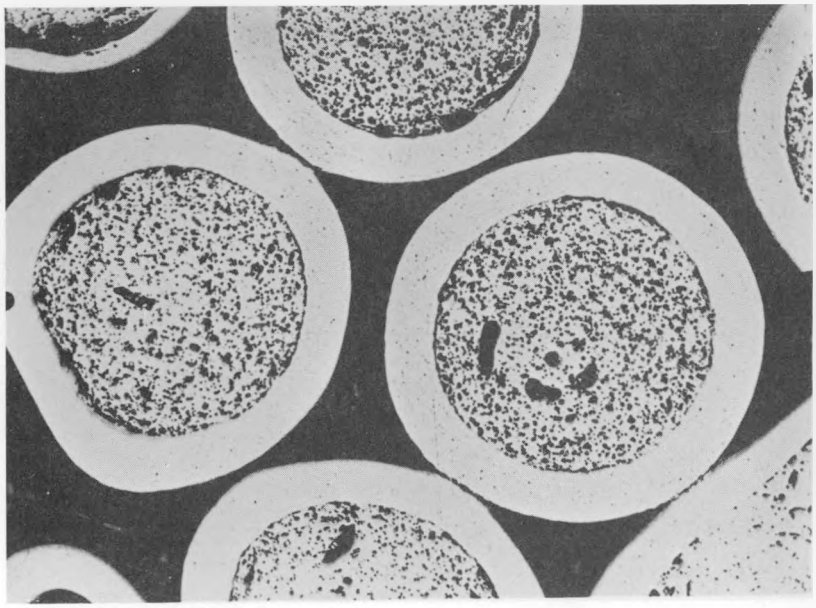

Normal light

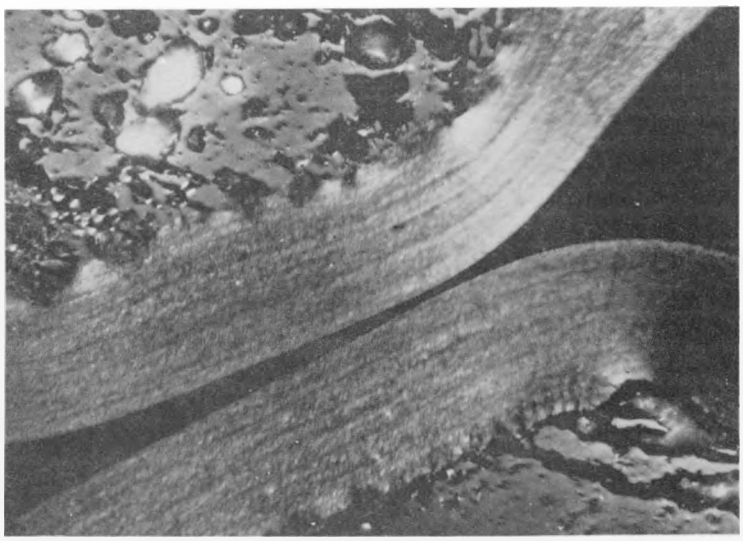

Polarized light

Fig. 6

UO_2 particles coated at 1600°C - 0.33 atm. of CH_4

500 ×

Fig. 7

UO_2 particle coated at 1600°C - 0.07 atm. of CH_4

500 ×

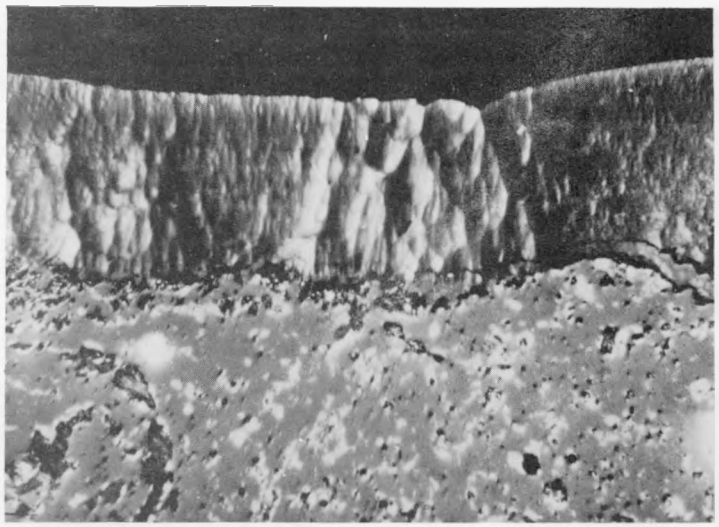

Polarized light

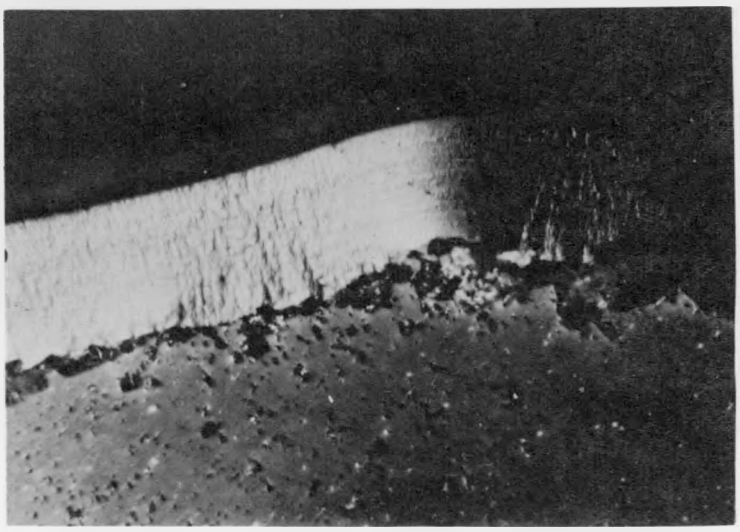

Polarized light

Fig. 8

UO_2 particle coated at 1600°C - 0.2 atm. of CH_4

500 ×

Fig. 9

UO_2 particle coated at 1600°C - 0.12 atm. of CH_4

500 ×

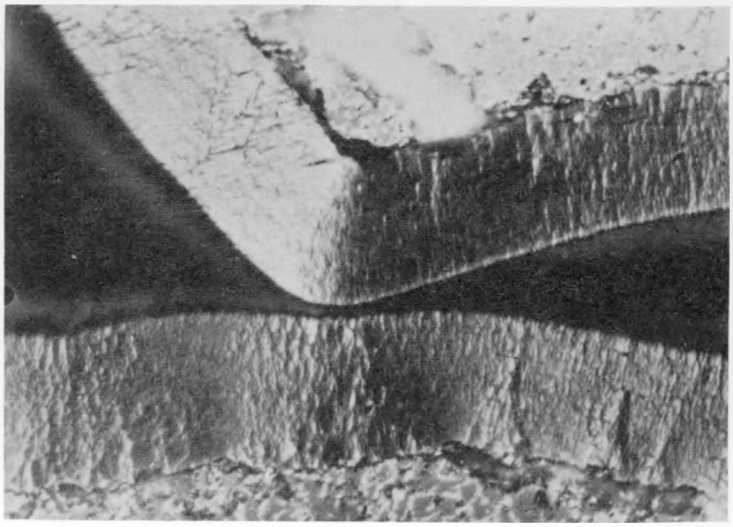

Polarized light

2. Crystallography

The values of the parameters $\frac{c}{2}$ and L_c measured on coatings as deposited are shown in Table III.

The preferred orientation has been measured by the method of Bacon (1) on samples prepared in the following way. The particles, coated with a thin layer of pyrolytic carbon, are crushed, and the coating is separated by dissolution of the substrate; the resulting flakes about 30 microns in diameter are then laid flat and stuck on the two sides of a thin plastic sheet.

Preliminary results show that the degree of preferred orientation of coatings deposited at 1600 C from CH_4 is similar to that of a massive deposit obtained on a wall at the same temperature. It seems that this preferred orientation is slightly more pronounced for coatings showing the "conic regenerated" microstructure.

3. Density

The density of the carbon layer was measured by flotation in mixtures of bromoform and butyl alcohol. It is strongly dependent on temperature in the range of 1300 to 1800 C; at constant partial pressure a minimum value is reached with methane at about 1500 C (Table IV). The density of a deposit produced from C_2H_2 (1200 C, 0.33 atm) was found to be rather heterogeneous, varying from 1.85 to 2.01 g/cm^3 with an average value of 1.90.

The influence of partial pressure has not been clarified and changes with temperature.

4. Permeability

The coated particles are etched with 1/2 M HNO_3 at 80 C for testing roughly the permeability of the coating and to separate the defective particles. Only coatings without an apparent microstructure have been studied.

The dissolution seems to take place in three stages:

Firstly, the defective particles are quickly disintegrated (about 1 hr); they represent a small fraction of the uranium coated in a single operation (100 G), at the maximum 1 per cent.

In the second stage, the acid leaching appears to proceed very slowly, due to a slow penetration of the acid through

Table III

Deposition Temperature, C	Hydrocarbon	Partial Pressure, atm	$\frac{C}{2}$, Å	L_c, Å
1200	C_2H_2	0.16	3.51	21
1400	CH_4	0.07	3.49	21
1500	CH_4	0.07	3.46	28
1600	CH_4	0.07	3.43	40
1600	CH_4	0.1	3.42	62

Table IV

Deposition Temperature, C	Hydrocarbon	Partial Pressure, atm	Surface of the Bed, cm^2	Density, g/cm^3
1200	C_2H_2	0.07	2000	1.94
1200	C_2H_2	0.33	1000	1.9
1400	CH_4	0.07	800	1.49
1400	CH_4	0.2	5000	1.68
1500	CH_4	0.07	800	1.36
1600	CH_4	0.07	800	1.41
1600	CH_4	0.12	800	1.50
1600	CH_4	0.2	800	1.45
1600	CH_4	0.33	800	1.46
1700	CH_4	0.17	3300	1.66

certain coating flaws. The acid leaching of 1 g of coated particles involving about 5000 granules shows that 2 to 10 of these exhibit the flaws. This second stage, in our operating conditions, extends over a period of 10 to 100 hr.

When all these faulty particles have been eliminated the proportion of uranium dissolved during attacks of more than 5 hr reaches the limit of analytical detection, corresponding to about 10^{-5}. In one particular case, operating on an important quantity, the result was under the limit of analytical detection of 2.10^{-6}.

The results of the third stage of attack, the only one which is significant for the permeability, have been found independent of the deposition conditions.

III. HIGH-TEMPERATURE BEHAVIOR OF COATED PARTICLES

1. Procedure

The heat treatments are carried out in an induction furnace in purified argon atmosphere, or in vacuum, the samples being heated in graphite crucibles. The treatment duration is always 5 hr, and the temperature ranges from 1000 to 2200 C.

2. Thermodynamic Provisions

The reaction $UO + 3C \rightleftharpoons UC + 2CO$ is foreseen to take place beyond 1400 C. The equilibrium pressures of CO, according to the free-energy values given by Glassner[2] for UO_2 and by Alcock and Grieveson[3] and Huber et al.[4] for UC, are 0.15 atm at 1800 C and 6 atm at 2200 C. If the pyrolytic-carbon coatings are gas-tight, the carburization of UO_2 is expected not to be complete: the reaction does not proceed as the CO pressure reaches the equilibrium pressure at the temperature considered. Hence the examination of the UO_2 particle carburization is a qualitative evaluation of the carbon-coating tightness. If this coating is faulty

or porous, the reaction can proceed until complete carburization to UO_2 is attained, because the gas can be released.

3. Results

The UO_2 particles coated either at 1100 or at 1600 C with a layer over 40 microns thick appear to be quite stable up to about 1800 C. Their carburization induces stresses which result in cracks near the surface of contact (Figure 10). The scraps created in this manner generally flake off during polishing for microscopic examination, so that the voids between the substrate and the coating do not only result from consumption of carbon. The increasing importance of this phenomenon as a function of temperature is shown in Figures 11 to 14.

At 1900 C most of the particles are ruptured. Figure 15 exhibits a completely carbonized particle. In Figure 16 the number of damaged particles is reported as a function of treatment temperature, as determined by leaching tests with HNO_3. Distinction may be made, by microscopic examination between two kinds of aspects:

(a) Particles which burst during heating or high-temperature treatment, and which are completely carburized with consumption of carbon because of the release of CO (Figure 15).

(b) Particles which burst by thermal shock during cooling and which are not carburized (Figure 17).

Long-period leachings where the third stage of attack has been reached show that the tightness of the coating is not significantly affected by high-temperature treatment (Table V). The effect of coating thickness on the behavior of the particles is also apparent from this table.

CONCLUSION

UO_2 particles have been studied first on account of their sphericity and also because the reaction of UO_2 and carbon with release of CO provides a simple means to study the gas impermeability of carbon coatings at elevated temperature. These particles seem not to be damaged by heating up to 1700 C.

Work is now in progress on carbide particles, and different approaches to the study of fission-product diffusion are being considered.

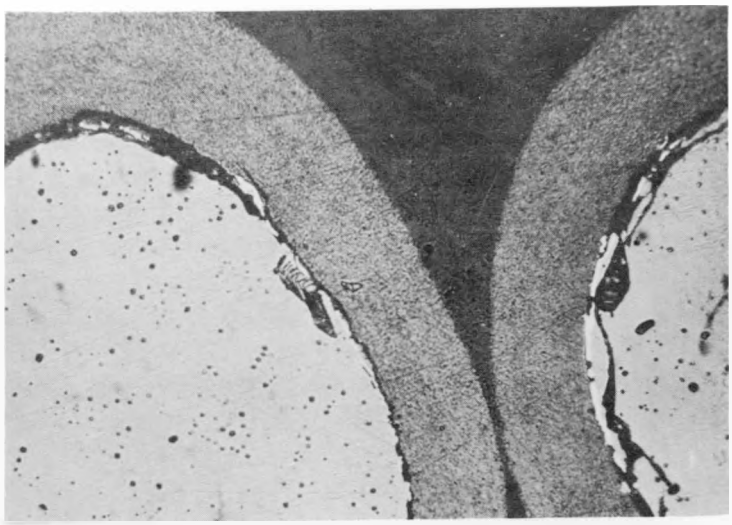

Fig. 10

PyC coated UO_2 after heat treatment. See the cracks and carbide phase at the surface of contact (UC = white zone)

400 ×

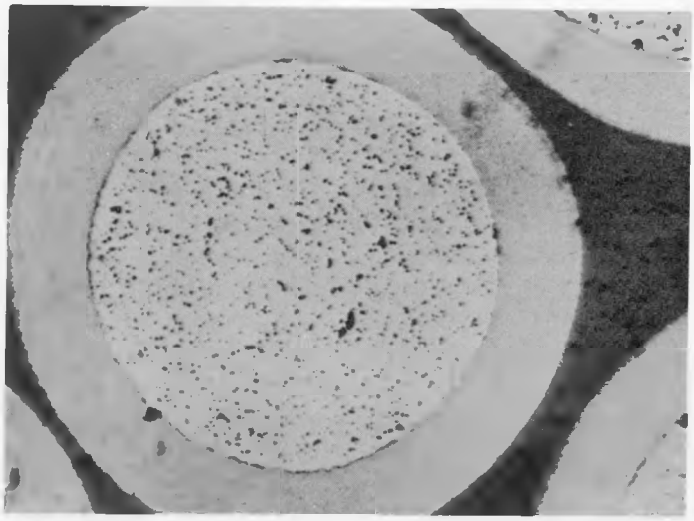

Fig. 11

UO_2 - PyC
heat treated at 1500°C

300 ×

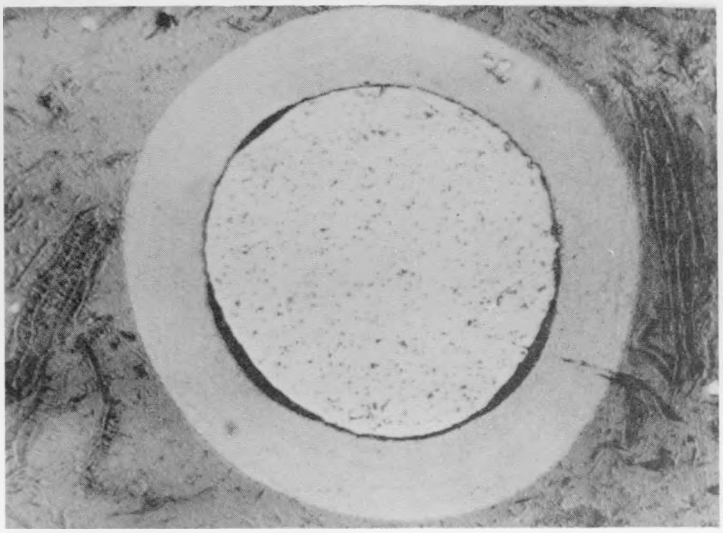

Fig. 12

UO_2 - PyC
heat treated at 1700°C

300 ×

Fig. 13

UO_2 - PyC
heat treated at 1800°C

300 ×

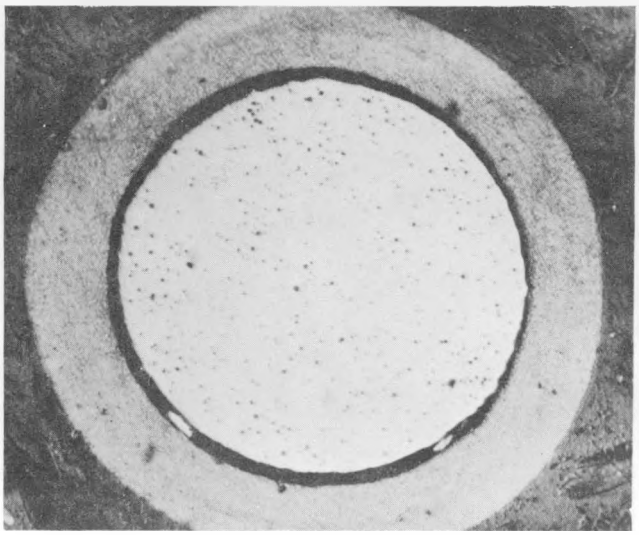

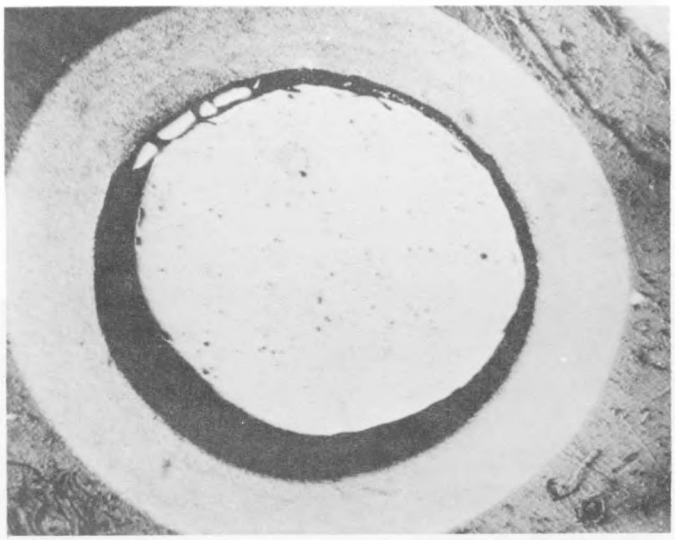

Fig. 14

UO_2 - PyC
heat treated at 1900°C

300 ×

Fig. 15

UO_2 - PyC
heat treated at 1900°C
a completely carburized particle

400 ×

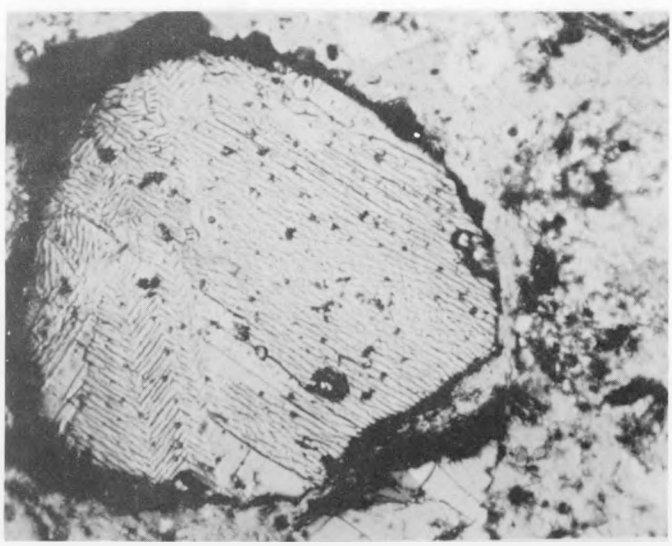

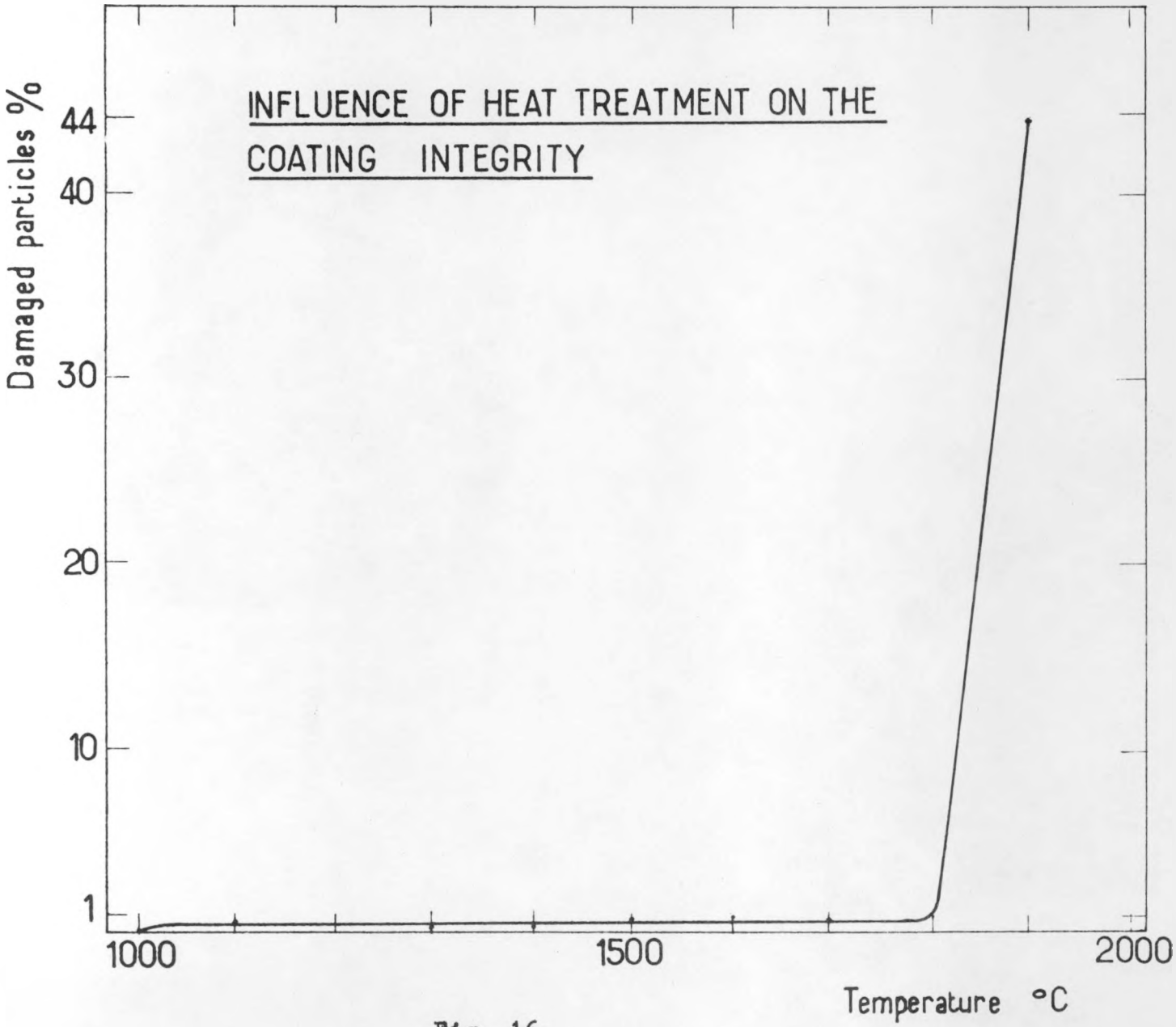
INFLUENCE OF HEAT TREATMENT ON THE
COATING INTEGRITY
Damaged particles %
44
40
30
20
10
1
1000
1500
2000
Temperature °C

Fig. 16

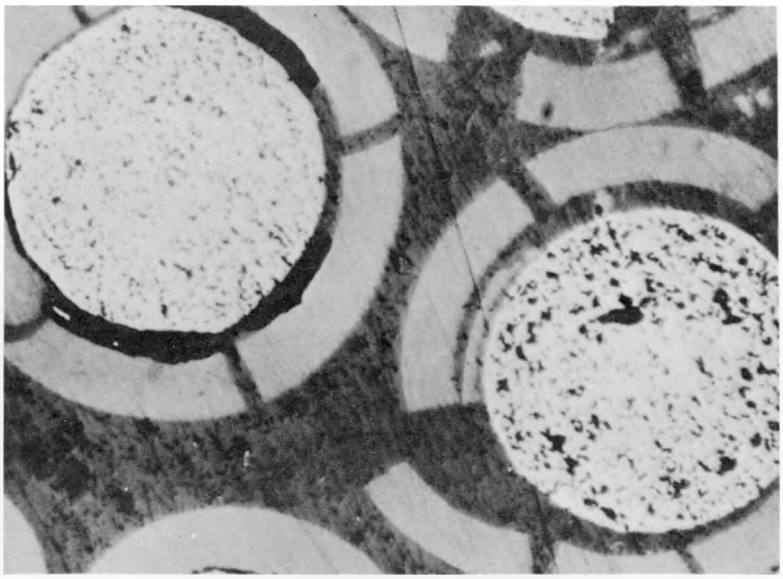

Fig. 17

Heat treated at 1800°C
Effect of thermal shock
during cooling

200 ×

Table V

Deposition Temperature, C	Partial Pressure, atm	Thickness, μ	Proportion of Uranium Dissolved During Acid Leaching							
			As Deposited		Heat Treated at 1500 C in Argon		Heat Treated at 1800 C in Argon		Heat Treated at 1500 C in Vacuum	
			First Attack	Last Attack	First Attack	Last Attack	First Attack	Last Attack	First Attack	Last Attack
1700	0.17	20	0.16 %	3.10^{-5}	--	--	45 %	5.10^{-5}	7 %	6.10^{-5}
1600	0.17	20	1.3 %	3.10^{-5}	--	--	100 %	--	7 %	6.10^{-5}
1600	0.1	30	1 %	3.10^{-5}	1 %	5.10^{-5}	10 %	5.10^{-5}	3 %	--
1600	0.1	40	0.08 %	3.10^{-5}	1 %	5.10^{-5}	1 %	5.10^{-5}	--	--

Notes:

All attacks: 5 hr in 1/2 M HNO_3 at 80 C

Last attack corresponds to the third stage, when all faulty particles have been eliminated.

REFERENCES

(1) G. E. Bacon, J. Applied Chem. (November, 1956), p 477.

(2) A. Glassner, ANL-5750.

(3) C. B. Alcock and P. Grieveson, Symposium on the Thermodynamics of Nuclear Materials, Vienna (May, 1962), Paper SM-26/6.

(4) E. J. Huber and C. E. Holley, Symposium on the Thermodynamics of Nuclear Materials, Vienna (May, 1962), Paper SM-26/26.

FUEL FOR THE BBC-KRUPP REACTOR

By C. B. von der Decken*

Brown Boveri/Krupp
Julich, Kernforschungsanlagen
West Germany

Dr. von der Decken discussed the fuel-element design for the BBC-Krupp Reactor. The elements are 2-1/2-in. spheres of graphite each containing a cylindrical insert of graphite impregnated with UC_2. Low-burnup tests with these elements have shown no half-life dependence for the release of fission gases, with approximately 20 per cent of the long-lived gases and 10 to 15 per cent of the short-lived gases released at 1000 C. Other fission products had release fractions on the order of 10^{-3} to 10^{-4}. No change in release was observed when the permeability of the graphite shell was varied between 10^{-6} and 10^{-4} cm^2/sec. The release did exhibit a temperature dependence, and it was found to be dependent upon the particle size in the fuel compact, the release fractions decreasing with increasing particle size. A half-life dependency was observed when the fuel compact was coated with pyrolytic carbon.

*Dr. von der Decken spoke without notes. This short summary of his remarks is based on reports of BMI participants at the meeting.

STUDIES ON COATED PARTICLES AT NUKEM

By L. Schäfer*

Nukem Nuklear-Chemie und -Metallurgie G.M.B.H.
Wolfgang bei Hanau (Main)

Dr. Schäfer described the accidental formation of spherical uranium carbide (UC) particles during skull-melting experiments by means of centrifugal casting. Efforts to repeat this work have been unsuccessful in so far as only a low yield could be obtained. Further attempts to increase the yield have not been made.

NUKEM has coated fuel pellets with pyrolytic carbon for the AVR reactor. Such a fuel pellet consists of a mixture of UC_2 and graphite and is supported in the center of a graphite ball. The ball is inpregnated with an organic agent for fission-gas retention. In order to prevent the organic agent from reacting with the UC_2 in the fuel pellet, the pellet is coated before being inserted in the ball.

Coating was carried out in an inductively heated furnace at 1400 C, using methane. The pyrolytic carbon deposited was of the columnar type, and had a thickness of 100 microns and a density of 2.1 g/cm^3. The permeability of the coated pellet was 2×10^{-6} cm^2/sec as compared to 1.2×10^{-2} cm^2/sec for the uncoated pellet. The coated pellet proved to be resistant against the organic agent used for impregnation of the graphite ball.

Attempts are also being made to improve the thermal conductivity of UO_2 compacts to be used in a fast breeder reactor. The approach is to provide a network of molybdenum in the compact which would serve as heat-transfer "streets". The initial experiments, using molybdenum carbonyl to form the molybdenum, were not successful, probably because of the formation of a molybdenum carbide. However, UO_2 granules coated with powdered molybdenum cold pressed into a compact and sintered exhibited a thermal conductivity twice that of a similar compact without the molybdenum.

*Dr. Schäfer spoke without notes. This summary of his presentation is based on reports of BMI participants at the meeting.

BIBLIOGRAPHY

ON CERAMIC COATED-PARTICLE NUCLEAR FUELS

Foreword

This bibliography has been prepared to provide people having an interest in ceramic coated particles with a comprehensive listing of unclassified literature sources in this area. The initial bibliography was compiled from Nuclear Science Abstracts. The resulting draft was reviewed by scientists working in this field, many of whom provided additional references. The reviewers were: Mr. R. F. Kirkpatrick and Mr. Jack Conner, U. S. Atomic Energy Commission, Washington D. C.; Dr. W. O. Harms, Oak Ridge National Laboratory; Dr. Walter Goeddel, General Atomic; Mr. Hugh E. Voress, Division of Technical Information Extension, Oak Ridge, Tennessee; Dr. Clarence Brown, Nuclear Materials and Propulsion Operation, Cincinnati, Ohio; Dr. L. D. Stoughton, National Carbon Company, New York, New York; Dr. Z. M. Shapiro, Nuclear Materials and Equipment Corporation, Apollo, Pennsylvania; and J. H. Oxley, J. Blocher, M. F. Browning, W. Duckworth, M. C. Brockway, K. Smalley, W. H. Goldthwaite, N. E. Miller, R. F. Dickerson, R. J. Burian, B. Dunnington, D. Sunderman, T. Elleman, C. W. Townley, and R. L. Ritzman, Battelle Memorial Institute. Their assistance is appreciated.

Open Literature

1. T. Adamski and Fr. Mucha, Coating of Some Materials With Carbon by Pyrolysis of Hydrocarbons in a Fluidized Bed, Report PAN-232/IV, Polish Academy of Nuclear Sciences, Institute of Nuclear Research, Warsaw, May 1961.

2. J. M. Blocher, Jr., and J. H. Oxley, Chemical Vapor Deposition Opens New Horizons in Ceramic Technology, American Ceramic Society Bulletin, 41 (2): 81-84 (February 1962).

3. R. A. Ewing, T. S. Elleman, and R. B. Price, Separation of Coated Fuel Particles from a Graphite Matrix, Trans. American Nuclear Society, 4 (1): 152-153 (June 1961).

4. W. V. Goeddel and G. R. Tully, Jr., The Use of Graphite in High-Temperature Nuclear Fuel Elements, Proceedings of the Fifth Conference on Carbon, in press.

5. J. H. Oxley and J. M. Blocher, Jr., Coated Powders Provide Unique Materials, Battelle Technical Review, 8 (7): 9-13 (July 1959).

6. J. H. Oxley, A. C. Secrest, N. D. Veigel, and J. M. Blocher, Jr., Kinetics of Carbon Deposition in a Fluidized Bed, A. I. Ch. E. Journal, 7 (3): 498-501 (September 1961).

7. J. H. Oxley, M. F. Browning, N. D. Veigel, and J. M. Blocher, Jr., Microminiaturized Fuel Elements by Vapor Deposition Techniques, Ind. Chem., Prod. Research and Development, 1: 102-7 (June 1962).

8. W. E. Parker and M. J. Smith, Development of Graphite Matrix Fuel Elements, Trans. Am. Nuclear Soc., 4 (2): 343 (November 1961).

9. F. K. Pittman, "Nuclear Power-1961", A Forum Report Nuclear Frontiers - 1960, Proceedings of the 1960 Annual Conference of Atomic Industrial Forum, p 7.

10. G. E. Raines, C. W. Townley, S. D. Beck, and W. H. Goldthwaite, In-Pile Fission Gas Release Behavior of Al_2O_3 Coated Particles, Trans. American Nuclear Society, 4 (1): 60 (June 1961).

11. Reactor Core Materials, 4 (4): 6-9 (November 1961).

12. Reactor Materials, 5 (1): 10-14 (February 1962); 5 (2): 12-17 (May 1962); 5 (3): 8-14 (August 1962).

13. S. T. Robinson, The Pebble Bed Reactor, Gas-Cooled Reactors, A Symposium of the Franklin Institute at The American Nuclear Society, Delaware Valley Section, 1960, Philadelphia, Journal of the Franklin Institute 1960, Monograph No. 7, 87-108.

14. A. K. Smalley, W. C. Riley, and W. H. Duckworth, Al_2O_3-Clad UO_2 Ceramics for Nuclear Fuel Applications, American Ceramic Society Bulletin, 39 (7): 359-361 (July 1960).

15. L. D. Stoughton, Ceramic Coatings for Peach Bottom Reactor Fuel Elements, Atomics, 14: 16-20 (July 1961).

16. L. D. Stoughton, Development of Spherical Uranium-Graphite Fuel Elements, Gas-Cooled Reactors, A Symposium of the Franklin Institute at The American Nuclear Society, Delaware Valley Section, 1960, Philadelphia, Journal of the Franklin Institute 1960, Monograph No. 7, 200-226.

17. C. W. Townley, N. E. Miller, T. S. Elleman, and D. N. Sunderman, Improved Techniques for the Measurement of Short-Lived Fission Gases, ANS Trans., 193 (June 1962); Nuclear Sci. and Engr., 13 (3): 297 (1962).

18. Staff Article: Capsule Cure for Atomic Power Ills, Chemical Week, pp 59-62, (November 5, 1960).

19. Staff Article: Improved Fuel Elements, Metal Progress, p 93 (April 1961).

20. Staff Article: Coated Particle Fuels – Promise and Problems, Nucleonics, 19 (3): 96-98 (March 1961).

Topical Reports

21. G. L. Allen, The Formation and Properties of Pyrolytic Carbon, GAMD-798, General Atomic Div., General Dynamics Corp., May 19, 1959.

22. E. E. Anderson, P. E. Gethard, and L. R. Zumwalt, Recent Data Obtained on Fission Products Released From (Th, U)C_2-Particle-Graphite Fuels, GA-3119, General Atomic Div., General Dynamics Corp., May 22, 1962.

23. E. E. Anderson, P. E. Gethard, L. R. Zumwalt, Use of the King Furnace in Fission Product Retention Studies of Graphite Reactor Fuels, TID-7622, p 171, Nuclear Reactor Chemistry, Second Conference, Gatlinburg, Tennessee, October 10-12, 1961.

24. E. E. Anderson, P. E. Gethard, and L. R. Zumwalt, Steady-State Release Fraction of Krypton and Xenon Fission Products at High Temperatures From (U, Th)C_2-Graphite Fuel Matrix in Out-of-Pile Experiments, GA-3211, General Atomic Div., General Dynamics Corp., June 15, 1962.

25. Battelle Memorial Institute, Progress on Ceramic Coated Fuel Particles at Battelle, BMI-1468, September 16, 1960.

26. Battelle Memorial Institute, Chemical Vapor Deposition, Report DMIC-170 (June 4, 1962).

27. J. M. Blocher, Jr., M. F. Browning, A. C. Secrest, V. M. Secrest, J. H. Oxley, Preparation of Ceramic Coated Nuclear Fuel Particles, TID-7622, p 57, Nuclear Reactor Chemistry, Second Conference, Gatlinburg, Tennessee, October 10-12, 1961.

28. J. M. Blocher, N. D. Veigel, J. H. Oxley, V. M. Secrest, and E. E. Rose, Fluidized-Bed Coating of UO_2 Powder With Niobium and Other Elements, BMI-1440, Battelle Memorial Institute, May 25, 1960.

29. H. C. Brassfield, Production of Pebble-Type Fuel Elements, APEX-377, General Electric Company, Aircraft Nuclear Propulsion Department, June 1955.

30. M. F. Browning, N. D. Veigel, T. E. Cook, W. S. Diethorn, and J. M. Blocher, Alumina Coating of UO_2 Shot by Hydrolysis of Aluminum Chloride Vapor, BMI-1471, Battelle Memorial Institute, October 25, 1960.

31. R. J. Burian, R. L. Ritzman, J. E. Gates, and R. F. Dickerson, Evaluation of Irradiated Alumina-Coated UO_2 Particles Dispersed in Graphite Spheres, BMI-1572, Battelle Memorial Institute, March 22, 1962.

32. G. B. Engle, Development of Carbon-Coating Process for (Th, U)C_2 Fuel Particles, GA-2301, General Atomic Div., General Dynamics Corp., October 10, 1961.

33. G. B. Engle, F. D. Carpenter, W. V. Goeddel, and D. L. Menken, Metallography of Carbide Fuel Compounds, GA-2067, General Atomic Div., General Dynamics Corp., March 14, 1961.

34. G. B. Engle, C. S. Luby, and J. C. Bokros, Evaluation of (Th, U)C_2, Carbon-Coated (Th, U)C_2 Particles, and Carbon Coatings, GA-3067, General Atomic Div., General Dynamics Corp., April 26, 1962.

35. C. K. H. DuBose and R. J. Gray, Metallography of Pyrolytic Carbon Coated and Uncoated Uranium Carbide Spheres, ORNL-TM-91, Oak Ridge National Laboratory, March 21, 1962.

36. Leslie M. Ferris, Chemical Processing of Coated Particle Fuels, ORNL-TM-193, presented at Coated Particle Working Group Meeting, ORNL, May 7-8, 1962, Oak Ridge National Laboratory, April 3, 1962.

37. A. P. Fraas, et al., Design Study of a Pebble-Bed Reactor Fuel Plant, CF-60-12-5, Oak Ridge National Laboratory, December 14, 1960.

38. General Atomic Div., General Dynamics Corp., A Review of Fuel Element Research and Development for the High-Temperature Helium Gas-Cooled Reactors, GA-2283, presented at the 6th Nuclear Congress Organized by the C. N. E. N. in Rome, Italy, June 13-18, 1961, June 8, 1961.

39. A. F. Gerds and A. K. Smalley, High-Temperature Compatibility of Al_2O_3-, BeO-, and Metal-Coated UO_2 Particles With Graphite and Coke, BMI-1479, Battelle Memorial Institute, November 28, 1960.

40. W. V. Goeddel, Coated Fuels Irradiation Tests, A Materials Summary, GAMD-2729, General Atomic Div., General Dynamics Corp., October 10, 1961.

41. W. V. Goeddel, Thermal Stability Testing of Graphite-Matrix Fuel Compacts Containing Pyrolytic-Carbon Coated Carbide Particles With Comments on the Amoeba Effect, GAMD-2675, General Atomic Div., General Dynamics Corp., September 26, 1961.

42. W. V. Goeddel, Procedures for the Preparation of Graphite-Matrix Fuel Compacts Containing Carbon-Coated (Th, U)C_2 Fuel Particles, GAMD-2221, General Atomic Div., General Dynamics Corp., April 27, 1961.

43. W. V. Goeddel, The Development and Evaluation of Graphite-Matrix Fuel Compacts for the HTGR, GA-2289, General Atomic Div., General Dynamics Corp., August 8, 1961.

44. W. V. Goeddel and G. R. Tully, Jr., The Use of Graphite in High-Temperature Nuclear Fuel Elements, GA-2304, General Atomic Div., General Dynamics Corp., September 15, 1961.

45. A. H. Kibbey, L. M. Ferris, U-Th Recovery From Pyrolytic Carbon-Coated Carbide Fuel Particles by Electrolysis in Nitric Acid, ORNL-TM-384, Oak Ridge National Laboratory, September 26, 1962.

46. A. Levy and J. F. Foster, The Compatibility of Gas Coolants and Ceramic Materials in Coated-Particle Nuclear Fuels, BMI-1530, Battelle Memorial Institute, July 18, 1961.

47. C. S. Luby, Apparatus and Procedure for Coating Thorium-Uranium Carbides With Carbides With Carbon at 1000 to 1400 C, GA-2241, General Atomic Div., General Dynamics Corp., May 25, 1961.

48. W. J. McDowell, Coating of UO_2 Particles With BeO by Solution Methods, ORNL-TM-220, Oak Ridge National Laboratory, May 9, 1962.

49. D. L. Morrison, R. H. Barnes, T. S. Elleman, D. N. Sunderman, Post-Irradiation Release of Xenon-133 From Single-Crystal Alpha Alumina, BMI-1592, Battelle Memorial Institute, August 23, 1962.

50. Oak Ridge National Laboratory, Conceptual Design of the Pebble Bed Reactor Experiment, ORNL-TM-201, May 17, 1962.

51. Oak Ridge National Laboratory, GCRP Semiannual, ORNL-3372, Period Ending September 30, 1962.

52. J. H. Oxley, R. B. Landrigan, A. C. Secrest, C. F. Powell, and J. M. Blocher, Jr., Coating and Preparation of Uranium and Thorium Carbide Powders, BMI-X-160, Battelle Memorial Institute, August 2, 1960.

53. S. J. Paprocki, D. L. Keller, and W. M. Pardue, Study of Experimental Fuel Bodies Made From Alumina-Coated UO_2 Particles, BMI-1586, Battelle Memorial Institute, July 16, 1962.

54. L. P. Pepkowitz, B. L. Vandra, and F. J. Shipko, Development of Protective Metal Coatings for U and UO_2 Particles, TID-7622, Nuclear Reactor Chemistry Second Conference, Gatlinburg, Tennessee, October 10-12, 1961, p 98, Nuclear Materials and Equipment Corporation, Apollo, Pennsylvania.

55. A. E. Powers, Conductivity in Aggregates, KAPL-2145, Knolls Atomic Power Laboratory, March 6, 1961.

56. G. E. Raines and W. H. Goldthwaite, In-Pile Fission-Gas-Release Behavior of Alumina-Coated UO_2 Particles Irradiated High Burnup, BMI-1552, Battelle Memorial Institute, November 6, 1961.

57. Sanderson and Porter, The Pebble Bed Reactor Program, Current Fuel Element Developments and Their Effects on the Pebble Bed Reactor Program, TID-6809, May 10, 1960.

58. Sanderson and Porter, Fuel Element Development Program for the Pebble Bed Reactor, Topical Report on Sub-Surface Coatings for Fueled Graphite Spheres, NYO-9060, June 30, 1960.

59. A. K. Smalley, M. C. Brockway, and W. H. Duckworth, Improved Techniques for Dispersing Coated Fuel Particles in Ceramic Bodies, BMI-1579, Battelle Memorial Institute, May 22, 1962.

60. A. K. Smalley, W. C. Riley, and W. H. Duckworth, Alumina-Clad UO_2 for Fuel Applications, BMI-1321, Battelle Memorial Institute, February 18, 1959.

61. USAEC Division of Reactor Development, Nuclear Fuels and Materials Development, TID-11295, February 1961.

Progress and Final Reports

62. Aerojet General Nucleonics, The Army Gas Cooled Reactor Systems Program, A Preliminary Study of a 1000 KW(e) Mobile Nuclear Power System, AGN-TM-390, December 1960.

63. Aerojet-General Nucleonics, Army Gas-Cooled Reactor System Program, Monthly Progress Report for November, 1960, IDO-28566, December 30, 1960.

64. Aerojet-General Nucleonics, Army Gas Cooled Reactor System Program, Monthly Progress Report for January, 1961, IDO-28569, February 28, 1961.

65. Aerojet-General Nucleonics, Army Gas Cooled Reactor Systems Program, Semi-Annual Progress Report, January 1-June 30, 1961, IDO-28573, August 10, 1961.

66. Ill. Inst. of Tech., Armour Research Foundation, Modified Graphite Technology Final Report, C. W. Boquist and S. W. Bradstreet, LAR-49, January 5, 1961, changed from Official Use Only March 15, 1961.

67. W. V. Goeddel (Ed.), Coated Fuel Particle Newsletter, GAMD 2646, Part I, April-June 1961; Part II, July 1961; Part III, August-September 1961; Part IV, October 1961, Part V, November 1961; Part VI, October-December 1961; Part VII, January 1962; Part VIII, February 1962; Part IX, May-July 1962.

68. W. V. Goeddel (Ed.), Summary of Coated Particle Fuel Development at General Atomic for the Period October 1961 to April 1962, GA-3109, April 26, 1962.

69. National Carbon Company, Fuel Cycle Development Monthly Newsletter, ORO-494, August 1961 (September 20, 1961).

70. National Carbon Company, Fuel Cycle Development Monthly Newsletter, ORO-474, June 1961 (September 8, 1961).

71. National Carbon Company, Fuel Cycle Development Program Monthly Newsletters: ORO-493, July 1961 (August 29, 1961); ORO-494, August 1961 (September 20, 1961); ORO-515, September 1961 (October 29, 1961).

72. P. Marien (Ed.), First Semi-Annual Report for Period July 1, 1960, to December 31, 1960, (United Kingdom Atomic Energy Authority, Research Group, Atomic Energy Establishment), NP-10477, June 1961, Project Dragon (DP-34).

73. European Nuclear Energy Agency, Paris, OEEC High-Temperature Reactor Project Dragon, Second Annual Report, April 1, 1960-March 31, 1961, NP-10483, April 1, 1960-March 31, 1961.

74. Nuclear Materials and Equipment Corp., Final Report on Corrosion and Radiation Damage Resistant Fuel Material, November 15, 1959, through November 14, 1960, NYO-9187.

75. Nuclear Science and Engineering Corp., R. C. Koch, G. L. Grandy, I. J. Gruverman, R. F. Weise, and C. R. Wilson, Final Report on In-Pile Loop Test for the Pebble Bed Reactor Fuel Element Development Program, NSEC-47, April 28, 1961.

Series of Battelle Memorial Institute Progress Reports

R. W. Dayton and C. R. Tipton, Jr., Progress Relating to Civilian Applications During ....., USAEC Report BMI-....., dated.....

76.	June, 1959	BMI-1357	July 1, 1959
77.	July, 1959	BMI-1366	Aug. 1, 1959
78.	August, 1959	BMI-1377	Sept. 1, 1959
79.	September, 1959	BMI-1381	Oct. 1, 1959
80.	October, 1959	BMI-1391	Nov. 1, 1959
81.	November, 1959	BMI-1398	Dec. 1, 1959
82.	December, 1959	BMI-1403	Jan. 1, 1960
83.	January, 1960	BMI-1409	Feb. 1, 1960
84.	February, 1960	BMI-1423	Mar. 1, 1960
85.	March, 1960	BMI-1430	Apr. 1, 1960
86.	April, 1960	BMI-1434	May 1, 1960
87.	May, 1960	BMI-1442	June 1, 1960
88.	June, 1960	BMI-1448	July 1, 1960
89.	July, 1960	BMI-1455	Aug. 1, 1960
90.	August, 1960	BMI-1464	Sept. 1, 1960
91.	September, 1960	BMI-1469	Oct. 1, 1960
92.	October, 1960	BMI-1473	Nov. 1, 1960
93.	November, 1960	BMI-1480	Dec. 1, 1960
94.	December, 1960	BMI-1489	Jan. 1, 1961
95.	January, 1961	BMI-1496	Feb. 1, 1961
96.	February, 1961	BMI-1504	Mar. 1, 1961
97.	March, 1961	BMI-1509	Apr. 1, 1961
98.	April, 1961	BMI-1514	May 1, 1961
99.	May, 1961	BMI-1518	June 1, 1961

100.	June, 1961	BMI-1524	July 1, 1961
101.	July, 1961	BMI-1534	Aug. 1, 1961
102.	August, 1961	BMI-1541	Sept. 1, 1961
103.	September, 1961	BMI-1546	Oct. 1, 1961
104.	October, 1961	BMI-1549	Nov. 1, 1961
105.	November, 1961	BMI-1557	Dec. 1, 1961
106.	December, 1961	BMI-1561	Jan. 1, 1962
107.	January, 1962	BMI-1565	Feb. 1, 1962

Change in authors to: R. W. Dayton and R. F. Dickerson

108.	February, 1962	BMI-1569	Mar. 1, 1962
109.	March, 1962	BMI-1574	Apr. 1, 1962
110.	April, 1962	BMI-1577	May 1, 1962
111.	May, 1962	BMI-1581	June 1, 1962
112.	June, 1962	BMI-1583	July 1, 1962
113.	July, 1962	BMI-1589	Aug. 1, 1962

Series of General Atomic Progress Reports

General Atomic Div., General Dynamics Corp., Quarterly Progress Reports for the Period Ending....., on the 40-MW(E) Prototype High-Temperature Gas-Cooled Reactor Research and Development Program, USAEC Report GA-.....

114. GA-1640, Period ending June 30, 1960.
115. GA-1774, Period ending Sept. 30, 1960.
116. GA-1982, Period ending Dec. 31, 1960.
117. GA-2204, Period ending Mar. 31, 1961.
118. GA-2493, Period ending June 30, 1961.
119. GA-2747, Period ending Sept. 30, 1961.
120. GA-2861, Period ending Dec. 31, 1961.
121. GA-3132, Period ending Mar. 3, 1962.
122. GA-3396, Period ending June 30, 1962.

Oak Ridge National Laboratory Quarterly Progress Reports

123. ORNL-3061, Progress Report on Homogeneous Reactor Program for Period From August to November 30, 1960 (Mar. 6, 1961).

124. ORNL-3102, Gas Cooled Reactor Project Quarterly Progress Report for Period Ending March 31, 1961 (May 26, 1961).

125. ORNL-3166, GCR, Period Ending June 30, 1961 (Aug. 28, 1961).

126. ORNL-3210, GCR, Period Ending Sept. 30, 1961 (Feb. 5, 1962).

127. ORNL-3254, GCR, Period Ending Dec. 31, 1961 (Apr. 6, 1962).

128. ORNL-3302, GCR, Period Ending Mar. 31, 1962 (July 16, 1962).

Sanderson and Porter Progress and Summary Reports

129. NYO-2706, Sanderson and Porter, Progress Report on Fuel Element Development Program for the Pebble Bed Reactor, Phase I, May 1, 1959, to Oct. 31, 1959.

130. NYO-9058, Sanderson and Porter, Quarterly Progress Report on Fuel Element Development Program for the Pebble Bed Reactor, Feb. 1 to Apr. 30, 1960.

131. NYO-9061, Sanderson and Porter, Quarterly Progress Report on Fuel Element Development Program for the Pebble Bed Reactor, May 1 to July 31, 1960.

132. NYO-9062, Sanderson and Porter, Progress Report on Fuel Element Development Program for the Pebble Bed Reactor, Phase II, Summary Report, November 1, 1959, to October 31, 1960.

133. NYO-9063, Sanderson and Porter, Quarterly Progress Report on Fuel Element Development Program for the Pebble Bed Reactor, Nov. 1, 1960, to Jan. 31, 1961.

134. NYO-9064, Sanderson and Porter, Final Report on Fuel Element Development Program for the Pebble Bed Reactor, Apr. 30, 1961.

135. TID-6845, Sanderson and Porter, Progress Report on the Fuel Element Development Program for the Pebble Bed Reactor, June 1960.

136. TID-6846, Sanderson and Porter, Progress Report on Fuel Element Program for the Pebble Bed Reactor, May 1960.

Patents

137. Huddle, R. A. U., Improvements in or Relating to Nuclear Fuel Materials, British Patent 878,927 (to United Kingdom Atomic Energy Authority), Oct. 4, 1961.